

Exploring the Role of Tumour Microenvironment in the Behaviour of Breast Ductal Carcinoma *in Situ*

Michael Salah Shawky Toss

MB.BCH, MSc

Thesis submitted to the University of Nottingham for the Degree of Doctor of Philosophy

March 2020

School of Medicine

ACKNOWLEDGMENT

I am very grateful to the ***GOD ALMIGHTY*** for without His graces and blessings, this study would not have been possible.

I would like to express my sincere gratitude to Professor Emad Rakha for his supervision and the continuous and endless support of my PhD study and related research, for his patience, motivation, and immense knowledge. His guidance helped me in all the time of research and writing of this thesis. I could not have imagined having a better supervisor and mentor for my PhD study.

I gratefully acknowledge Dr. Andrew Green for his advice, supervision, and crucial contribution. His truly scientist intuition has made him as a constant supporter with limitless ideas and passions in science, I am grateful in every possible way and hope to keep up our collaboration in the future.

Very special thanks to Professor Ian Ellis. I am much indebted to him for his invaluable advice in scientific discussions, using his precious times to guide me with his fruitful ideas.

My sincere thank also goes to Dr. Kylie Gorringe, Dr. Ioannis Roxanis and Dr. Karuna Mittal, who provided me with fruitful collaborative work. Without their precious support it would not be possible to conduct this research.

Many thanks are due to Mr. Christopher Nolan and Mrs. Maria Diez Rodrigeuz for their invaluable assistance and to all members of Breast Cancer Research Group for their kind help and advice.

Immeasurable appreciation and deepest gratitude to Miss Catherine Douglas Morgan and Miss Holly Nichollas for all their spiritual support throughout my study. Without their invaluable help, I would never achieve any progress.

Thank to my parents who give me all the support and encouragement in my life.

I would like to thank everybody who was important to the successful realisation of thesis, as well as expressing my apology that I could not mention personally one by one.

This study was under the financial support of the Ministry of Higher Education Egypt; to whom I am indebted. Many thanks go to my colleagues in Pathology Department, South Egypt Cancer Institute, Assiut University, Egypt, for their spiritual support.

DEDICATION

Words fail me to express my appreciation to my wife, Mariam, whose dedication, love and persistent confidence in me, has taken the load off my shoulder. Your encouragement when the times got tough are much appreciated and duly noted. It was a great comfort and relief to know that you are willing to provide everything you can give even though I know that you have struggled a lot.

To my son, George, I will not be this stronger without you as my inspiration. You are the reason why I keep pushing; I keep facing all the struggles, pains and hardships. I love you all so much!

DECLARATION

I declare that this thesis is the result of my own work and has not in this, or any other form, been presented to this, or any other University in support of an application for any degree other than for which I am now a candidate.

Michael Toss

March 2020

APPROVAL

This work has been approved by Nottingham Research Ethics Committee 2, Reference number: REC:C20313

Under the title: Development of a molecular genetic classification of breast cancer.

ABBREVIATIONS

ACTB	Beta actin
ADH	Atypical ductal hyperplasia
AIDS	Acquired immune deficiency syndrome
ALH	Atypical lobular hyperplasia
BC	Breast cancer
BCS	Breast conserving surgery
BCSS	Breast cancer specific survival
BM	Basement membrane
CA	Centrosome amplification
CAFs	Cancer associated fibroblast
CAS	Centrosomal amplification score
CC-DCIS	Comedo-carcinoma in situ
CCNB1	Cyclin B1
CD	Cluster of differentiation
CGH	Comparative genomic hybridisation
CI	Confidence interval
CIN	Chromosomal instability
CISH	Chromogenic in situ Hybridisation
CNV	Copy number variation
COL11A1	Collagen (XI) alpha-1 chain
COMET	Comparison of Operative versus Medical Endocrine Therapy for Low-Risk DCIS
CPI	Collagen Prognostic Index
CTLs	Cytotoxic CD8+ T-cell lymphocytes
CTLA4	Cytotoxic T lymphocytes associated molecule 4
CTSA	Cathepsin A
CTSV	Cathepsin V
DAB	Diaminobenzidine
DC	Discovery cohort
DCIS	Ductal carcinoma in situ
DCs	Dendric cells
DIN	Ductal intraepithelial neoplasia
DNA	Deoxyribonucleic acid
ECM	Extracellular matrix
ECs	Endothelial cells
EMT	Epithelial mesenchymal transition
EndMT	Endothelial to mesenchymal transition
EORTC	European Organisation for Research and Treatment of Cancer
EPC	Encapsulated papillary carcinoma
ER	Oestrogen receptor
ET	Endocrine therapy
FEA	Flat epithelial atypia
FFPE	Formalin fixed paraffin embedded

FGA	Fraction of the genome altered
FISH	Fluorescent in situ hybridisation
GAPDH	Glyceraldehyde 3-phosphate dehydrogenase
GATK	Genome Analysis Tool Kit
GSTM1	Glutathione S-Transferase Mu 1
GUS	Glucuronidase reporter system
HER2	Human epidermal growth factor receptor 2
HR	Hazard ratio
IBC	Invasive breast carcinoma
ICC	Inter-class correlation coefficient
iCTRs	Individually distinguishable centrosomes
IHC	Immunohistochemistry
IL	Interleukin
IMS	Industrial Methylated Spirit
JPEG	Joint Photographic Experts Group
LCIS	Lobular carcinoma in situ
LGMN	Legumain
LOH	Loss of heterozygosity
LORD	LOw Risk DCIS trial
LORIS	LOw RISk DCIS trial
LRFI	Local recurrence free interval
mCTRs	Megacentrosomes
MDSCs	Myeloid derived suppressor cells
MECs	Myoepithelial cells
METABRIC	Molecular Taxonomy of Breast Cancer International Consortium
MMP	Matrix metalloproteinase
MYBL2	MYB like protein 2
NCCN	National Comprehensive Cancer Network
NHS	National Health System
NICE	National Institute for Health and Care Excellence
NPV	Negative predictive value
NSABP	National Surgical Adjuvant Breast and Bowel Project
NTAI	Number of telomeric allelic imbalances
OR	Odds ratio
P4HA2	Prolyl-4-Hydroxylase A Subunit 2
PBS	Phosphate buffer saline
PD1	Programmed cell death 1
PDL1	Programmed cell death ligand-1
PPV	Positive predictive value
PR	Progesterone receptor
PSR	Picrosirius red
ROIs	Regions of interest
RPLP0	Ribosomal Protein Lateral Stalk Subunit P0
RT	Radiotherapy

RT-PCR	Reverse transcriptase polymerase chain reaction
SEER	Surveillance Epidemiology and End Results
SLNB	Sentinel lymph node biopsy
SMA	smooth muscle actin
SNP	Single nucleotide polymorphism
SPC	Solid papillary carcinoma
STK15	serine/threonine kinase 15
TACS	Tumour associated collagen signature
TAMs	Tumour associated macrophages
TBS	Tris Buffered Saline
TDLU	Terminal duct lobular unit
TGF-β	Tumour Growth Factor beta
Th	T helper cells
TILs	Tumour infiltrating lymphocytes
TMA	Tissue microarray
TME	Tumour microenvironment
TNBC	Triple negative breast cancer
Treg	Regulatory T cells
UDH	Usual ductal hyperplasia
UK/ANZ	The United Kingdom, Australia and New Zealand
VD	Validation cohort
VN	Van Nuys
VNPI	Van Nuys Prognostic Index
WB	Western Blot
WHO	World Health Organisation

ABSTRACT

Background:

Breast ductal carcinoma in situ (DCIS) accounts for more than 20% of screen-detected breast cancer. To date, predictors of DCIS behaviour are not well defined. Tumour microenvironment (TME) plays a role in tumour progression; therefore, the aim of the current study was to characterise a large cohort of DCIS with long term follow-up data and to decipher the role of TME in DCIS outcome.

Patients and methods:

This study includes 1,488 cases comprises pure DCIS (n=1,249) and DCIS associated with synchronous invasive carcinoma (n=239). Clinicopathological and outcome data was collected. All cases were histologically reviewed, and representative tumour blocks were retrieved. Tissue microarrays (TMAs) were constructed followed by molecular characterisation for oestrogen receptor (ER), progesterone receptor (PR), human epidermal growth factor receptor 2 (HER2) and Ki67. Tumour infiltrating lymphocytes (TILs) were assessed using novel method and their association with local recurrence was investigated. Mining for biomarkers that regulate remodelling and degradation of the surrounding stroma and have potential prognostic values in DCIS was performed. This includes prolyl-4-hydroxylase A subunit 2 (P4HA2), cathepsin A (CTSA), cathepsin V (CTSV), legumain (LGMN) and Collagen (XI) alpha-1 chain (COL11A1). The expression of these biomarkers was evaluated in the TMA using immunohistochemistry and their prognostic value was analysed. In addition, image analysis assessment of the geometric characterisation of collagen surrounding DCIS was performed and collagen prognostic index (CPI) was developed. Moreover, the role of hypoxia and centrosome amplification (CA) has been investigated.

Results:

There was a significant increase in the rate of breast conserving surgery (BCS) and the use of radiotherapy (RT) in DCIS management with time, along with a decline in the rate of re-excisions. Large size, high grade, and omission of adjuvant RT were independent predictors of the development of ipsilateral local recurrence. The highest proportion (60%) of cases were of Luminal A subtype, and the lowest attribution (11%) was for HER2 positive tumours. HER2 positive and Triple Negative subtypes were of larger tumour size, higher grade, and more frequently treated with mastectomy.

Dense TILs were associated with adverse clinicopathological parameters and high recurrence rate. DCIS associated with synchronous invasive carcinoma showed higher TILs density than pure DCIS.

The assessment of the selected biomarker panel revealed a significant difference in their protein expression between pure DCIS and those associated with invasion. An independent association between high expression of P4HA2, CTSA, CTSV, LGMN and COL11A1 with the development of local recurrence was observed.

DCIS with high CPI and harbouring higher structural and/or numerical centrosomal aberrations were associated poor outcome.

Conclusions

This study shows that TME plays a key role in DCIS behaviour and outcome. In addition to the conventional clinicopathological variables, dense TILs, high expression of P4HA2, CTSA, CTSV, LGMN, COL11A1, high CPI and centrosomal aberrations were independent predictors of DCIS outcome. These variables could potentially be used in combination to refine the prognostic stratification of DCIS patients in routine practice.

STUDY RELATED PUBLICATIONS

Peer-Reviewed Publications

1- **Michael S Toss**, Asima Abidi, Dorothea Lesche, Chitra Joseph, Sakshi Mahale, Hugo Saunders , Tanjina Kader, Islam M Miligy, Andrew R Green, Kylie L Gorringe, and Emad A Rakha. **"The prognostic significance of immune microenvironment in breast ductal carcinoma in situ".**
British Journal of Cancer (2020)

2- Karuna Mittal, **Michael S. Toss**, Guanhao Wei, Jaspreet Kaur, Da Hoon Choi, Brian D. Melton, Remus M. Osan, Islam M. Miligy, Andrew R Green, Emiel A. M. Janssen, Håvard Soiland, Keerthi, Gogineni, Upender Manne, Padmashree Rida, Emad A. Rakha, Ritu Aneja. **"A quantitative centrosomal amplification score predicts local recurrence of ductal carcinoma in situ''**.
Clinical Cancer Research (2020)

3- Abrar I. Aljohani, **Michael S. Toss**, Sasagu Kurozumi, Chitra Joseph, Mohammed A. Aleskandarany, Islam M. Miligy, Rokaya El Ansari, Nigel P. Mongan, Ian O. Ellis, Andrew R. Green, Emad A. Rakha. **"The prognostic significance of wild-type isocitrate dehydrogenase 2 (IDH2) in breast cancer"**
Breast Cancer Research and Treatment (2020)

4- Sergey Klimov, Islam M. Miligy, Arkadiusz Gertych, Yi Jiang, **Michael S. Toss**, Padmashree Rida, Ian O. Ellis, Andrew Green, Uma Krishnamurti, Emad A. Rakha and Ritu Aneja. **"A whole slide image-based machine learning approach to predict ductal carcinoma in situ (DCIS) recurrence risk".**
Breast Cancer Research (2019)

5- **Michael Toss**, Islam Miligy, Kylie Gorringe, Karuna Mittal, Ritu Aneja, Ian Ellis, Andrew Green, Emad Rakha. **"Prognostic significance of cathepsin V (CTSV/CTSL2) in breast ductal carcinoma in situ"**.
Journal of Clinical Pathology (2019)

6- **Michael S Toss**, Islam M Miligy, Kylie L Gorringe, Abdulbaqi AlKawaz, Karuna Mittal, Ritu Aneja, Ian O Ellis, Andrew R Green, Ioannis Roxanis and Emad A Rakha. **"Geometric characteristics of collagen have independent prognostic significance in breast ductal carcinoma in situ: An image analysis study".**
Modern Pathology (2019)

7- **Michael S Toss,** Islam M Miligy, Kylie L Gorringe, Mohammed A Aleskandarany, Abdulbaqi Alkawaz, Karuna Mittal, Ritu Aneja, Ian O Ellis, Andrew R Green and Emad A Rakha. **"Collagen (XI) alpha-1 chain is an independent prognostic factor in breast ductal carcinoma in situ".**
Modern Pathology (2019)

8- I. M. Miligy, **Toss M. S.,** K. L. Gorringe, A. H. Lee, I. O. Ellis, A. R. Green and E. A. Rakha. **"The clinical and biological significance of HER2 over-expression in DCIS: A large study from a single institution".**
British Journal of Cancer (2019)

9- Islam M Miligy, **M S Toss**, Hazem Khout, Whisker L, Burrell HC, Ian O Ellis1, Andrew R Green, Macmillan RD and Emad A Rakha. **"Surgical Management of Ductal Carcinoma in Situ (DCIS) of the Breast; a large retrospective study from a single institution".**
The Breast Journal (2019)

10- **Toss MS,** Billingham K, Egbuniwe IU, Moreno F, Abass A, Rakha EA. **"Breast Tumours Resembling the Tall Cell Variant of Thyroid Papillary Carcinoma: Are They Part of the Papillary Carcinoma Spectrum or a Distinct Entity?".**
Pathobiology (2019)

11- **Toss, M. S**., Miligy, I. M., Haj-Ahmad, R., Gorringe, K. L., AlKawaz, A. , Mittal, K. , Ellis, I. O., Green, A. R. and Rakha, E. A. "**The prognostic significance of lysosomal protective protein (Cathepsin A) in breast ductal carcinoma in situ".**
Histopathology (2019)

12- **Toss, M. S.,** I. Miligy, A. Al-Kawaz, M. Alsleem, H. Khout, P. C. Rida, R. Aneja, A. R. Green, I. O. Ellis and E. A. Rakha. **"Prognostic significance of tumor-infiltrating lymphocytes in ductal carcinoma in situ of the breast."**
Modern Pathology (2018)

13- **Toss, M. S.,** I. M. Miligy, K. L. Gorringe, A. AlKawaz, H. Khout, I. O. Ellis, A. R. Green and E. A. Rakha. **"Prolyl-4-hydroxylase Alpha subunit 2 (P4HA2) expression is a predictor of poor outcome in breast ductal carcinoma in situ (DCIS)".**
British Journal of Cancer (2018)

14- **Toss, M. S.,** I. M. Miligy, K. L. Gorringe, L. McCaffrey, A. AlKawaz, A. Abidi, I. O. Ellis, A. R. Green and E. A. Rakha. **"Legumain is an independent predictor for invasive recurrence in breast ductal carcinoma in situ."**
Modern Pathology (2018)

15- Ali, R., A. Al-Kawaz, **M. S. Toss**, A. R. Green, I. M. Miligy, K. A. Mesquita, C. Seedhouse, S. Mirza, V. Band, E. A. Rakha and S. Madhusudan. **"Targeting PARP1 in XRCC1-Deficient Sporadic Invasive Breast Cancer or Preinvasive Ductal Carcinoma In Situ Induces Synthetic Lethality and Chemoprevention."**
Cancer Research (2018)

16- Miligy, I. M., K. L. Gorringe, **M. S. Toss**, A. A. Al-Kawaz, P. Simpson, M. Diez-Rodriguez, C. C. Nolan, I. O. Ellis, A. R. Green and E. A. Rakha. **"Thioredoxin-interacting protein is an independent risk stratifier for breast ductal carcinoma in situ".**
Modern Pathology (2018)

17- Rakha, E. A., I. M. Miligy, K. L. Gorringe, **M. S. Toss**, A. R. Green, S. B. Fox, F. C. Schmitt, P. H. Tan, G. M. Tse, S. Badve, T. Decker, A. Vincent-Salomon, D. J. Dabbs, M. P. Foschini, F. Moreno, Y. Wentao, F. C. Geyer, J. S. Reis-Filho, S. E. Pinder, S. R. Lakhani and I. O. Ellis. **"Invasion in breast lesions: the role of the epithelial-stroma barrier".**
Histopathology (2018)

18- **Toss, M.,** I. Miligy, A. M. Thompson, H. Khout, A. R. Green, I. O. Ellis and E. A. Rakha. **"Current trials to reduce surgical intervention in ductal carcinoma in situ of the breast: Critical review".**
Breast (2017)

19- **Toss, M. S**., S. E. Pinder, A. R. Green, J. Thomas, D. A. Morgan, J. F. Robertson, I. O. Ellis and E. A. Rakha. **"Breast conservation in ductal carcinoma in situ (DCIS): what defines optimal margins?"**
Histopathology (2017)

Conference Presentations

1- Targeting PARP1 in XRCC1 deficient sporadic invasive breast cancer or pre-invasive ductal carcinoma in situ for synthetic lethality and chemoprevention **(25th Biennial Congress of the European Association for Cancer Research, Amsterdam, The Netherlands, June 2018).**
Poster presentation

2- Legumain (LGMN) is associated with invasive recurrence in breast ductal carcinoma in situ (DCIS) **(Pathological Society Meeting June 2018, Maastricht, The Netherlands)**
Poster presentation

3- Targeting Protein for Xenopus Kinesin-Like Protein 2 (TPX2) Expression is Associated with Poor Outcome in Breast Ductal Carcinoma in situ (DCIS) (**Pathological Society Meeting January 2018, London, United Kingdom)**
Poster presentation

4- Characterisation of HER2 Status in DCIS Using Immunohistochemistry (IHC) and Chromogenic in situ Hybridisation (CISH) (**Pathological Society Meeting January 2018, London, United Kingdom)**
Poster presentation

5- Lysosomal Protective Protein/Cathepsin A (CTSA) is an Independent Prognostic Factor in Breast Ductal Carcinoma in situ (DCIS) (**Pathological Society Meeting January 2018, London, United Kingdom)**
Poster presentation

6- Prolyl-4-hydroxylase a subunit 2 is associated with poor outcome in breast ductal carcinoma in situ (DCIS) (**UK Interdisciplinary Breast Cancer Symposium January 2018, Manchester, United Kingdom)**
Poster presentation

7- Tumour-infiltrating lymphocytes is an independent prognostic factor in breast ductal carcinoma in situ (DCIS) (**UK Interdisciplinary Breast Cancer Symposium January 2018, Manchester, United Kingdom)**
Poster presentation

8- Aurora Kinase A (AURKA) is an independent predictor of recurrence in breast ductal carcinoma in situ (DCIS) (**UK Interdisciplinary Breast Cancer Symposium January 2018, Manchester, United Kingdom)**
Poster presentation

9- Thioredoxin-Interacting Protein (TXNIP) is an independent prognostic factor in breast ductal carcinoma in situ (DCIS) (**UK Interdisciplinary Breast Cancer Symposium January 2018, Manchester, United Kingdom)**
Poster presentation

10- Legumain (LGMN) is associated with invasive recurrence in breast ductal carcinoma in situ (DCIS) **(Nottingham Breast Cancer Research Centre March 2018)**
Oral presentation

11- Tumour-infiltrating lymphocytes is an independent prognostic factor in breast ductal carcinoma in situ (DCIS) **(Nottingham Breast Cancer Research Centre Weekly Seminar)**
Poster presentation

CONTENTS

CHAPTER 1: GENERAL INTRODUCTION 1

1.1 Breast Ductal Carcinoma in situ (DCIS) 2
1.1.1 Definition and historical background 2
1.1.2 Incidence and epidemiology 3
1.1.3 Risk factors 4
1.1.4 Pathogenesis and cytogenetics 4
1.1.5 Clinical presentation and diagnosis 5
1.1.6 Bilaterality, multifocality and multicentricity 8
1.1.7 Pathology of DCIS 10
1.1.7.1 Gross pathology 10
1.1.7.2 Histological features and classifications 10
1.1.8 DCIS histological patterns 11
1.1.9 Rare morphological variants of DCIS 13
1.1.9.1 Solid and encapsulated papillary carcinoma 13
1.1.9.2 Cystic hypersecretory DCIS 14
1.1.9.3 Apocrine DCIS 14
1.1.9.4 Clear and signet ring cell DCIS 15
1.1.9.5 Spindle cell DCIS 16
1.1.9.6 Paget's disease 16
1.1.9.7 DCIS with microinvasion 16
1.1.10 DCIS grading 17
1.2 Molecular classification of DCIS 23
1.3 Oncotype DX DCIS 25
1.4 Genetic features of DCIS and its progression to invasive carcinoma 27
1.4.1 Progression to invasive carcinoma 28
1.5 Management 30
1.6 Prognostic and predictive factors 32
1.6.1 Predictive factors of DCIS recurrence 33
1.6.2 Predictive factors for DCIS progression to IBC 35
1.7 DCIS outcome and risk assessment 36
1.8 Tumour microenvironment; components and role in carcinogenesis 38
1.8.1 Tumour immunity 39
1.8.1.1 Tumour antigens and tumour surveillance from the immune system 40
1.8.1.2 Tumour associated macrophages and tumour growth 43

1.8.1.3 Role of myeloid derived suppressor cells and T regulatory cells....44
1.8.2 Cancer associated fibroblasts 45
1.8.3 Extracellular matrix and tumour progression 45
1.8.4 Tumour vasculature and angiogenesis 46
1.9 Tumour microenvironment of breast cancer 46
1.9.1 Immune response in breast cancer....47
1.9.1.1 Tumour associated macrophages 47
1.9.1.2 Humoral and cell-mediated immunity 48
1.9.1.3 Immune checkpoint proteins 49
1.9.2 Cancer associated fibroblasts and breast cancer....50
1.9.3 Extracellular matrix in breast cancer 51
1.9.4 Endothelial cells and angiogenesis in breast cancer 52
1.9.5 Myoepithelial cells and breast cancer....53
1.9.6 Effects of breast cancer on tumour microenvironment....57
1.9.6.1 Degradation of basement membranes and invasiveness to surrounding tissues....58
1.9.6.2 Epithelial mesenchymal transition and its role in tumour progression....58
1.10 Hypothesis and aims of the thesis 60

CHAPTER 2: Patients and methods 63

2.1 Patient cohort and data collection 64
2.1.1 Pure DCIS cohort identification....64
2.1.2 Mixed DCIS and IBC cohort identification 66
2.2 TMA Construction 67
2.1.3 Collection of the study cohort and preparation of the donor blocks....68
2.1.4 Slide digitalisation and image acquisition 69
2.1.5 TMA construction of pure DCIS cases 70
2.2.1.1 Construction protocol 70
2.2.1.2 Digital images marking....70
2.2.1.3 Recipient blocks construction....71
2.2.1.4 TMA layout design....73
2.2.1.5 Coring process....75
2.2.1.6 TMA blocks' annealing and sectioning 76
2.1.6 TMA construction of mixed cohort 78
2.3 Literature-based selection of biomarkers 79
2.4 Validation of antibody specificity....81

2.4.1 Preparation of samples, electrophoresis and transfer 81
2.5 Immunohistochemistry 83
2.1.7 Optimisation 83
2.1.8 IHC technique 84
2.1.9 Assessment of immunoreactivity 88
2.1.10 Determination of the cut-off points 90
2.6 Chromogenic in situ Hybridisation 92
2.7 Conventional statistical approach 93
2.1.11 Correlation with clinicopathological parameters 94
2.1.12 Univariate analysis with outcome 95
2.1.13 Multivariate analysis with outcome 95

Chapter 3: Clinicopathological characterisation of DCIS 96

3.1 Introduction 97
3.1.1 Incidence of DCIS 97
3.1.2 Treatment of DCIS 97
3.1.3 Factors affecting DCIS outcome 98
3.2 Hypothesis and aims 99
3.3 Patients and methods 99
3.4 Results 100
3.4.1 Data analysis 100
3.4.1.1 Correlation between clinicopathological factors associated with the selection of type of primary surgery 103
3.4.1.2 Factors affecting re-excision 105
3.4.1.3 Clinicopathological factors associated with presence of residual tumour in the re-excision specimens 112
3.4.1.4 Clinicopathological factors and their association with offering postoperative radiotherapy 117
3.4.2 Axillary lymph node surgery 120
3.4.3 Factors influencing the development of local recurrence 120
3.5 Discussion 125

Chapter 4: Molecular characterisation of DCIS 136

4.1 Introduction 137

4.2 Clinicopathologic parameters as prognostic factors 138

4.3 Gene expression profiling-derived classes and signatures 140

4.3.1 Molecular Classes 141

4.3.1.1 Historical background 141

4.3.1.2 Importance of molecular classification..... 141

4.3.1.3 Surrogate molecular subtypes for DCIS..... 142

4.3.1.4 Oestrogen receptor 142

4.3.1.5 Progesterone receptor 147

4.3.1.6 Human epidermal growth factor receptor 2..... 148

4.3.1.7 The proliferation marker "Ki67"..... 149

4.4 Hypothesis and aims 150

4.5 Patients and methods.....151

4.5.1 Study cohort..... 151

4.5.2 IHC and CISH 151

4.5.2.1 IHC..... 151

4.5.2.2 CISH..... 152

4.5.3 Statistical analysis 153

4.6 Results 154

4.6.1 ER distribution among study cohort..... 155

4.6.2 Association between ER and other clinicopathological factors 155

4.6.3 Association between ER status and DCIS outcome..... 157

4.6.3.1 Outcome of ER-positive DCIS based on nuclear grade159

4.6.3.2 Contralateral breast cancer and ER status 160

4.6.3.3 The association between overall risk of developing a recurrent IBC event either ipsilateral or contralateral after primary diagnosis of DCIS and ER status 160

4.6.3.4 Overall survival 161

4.6.4 Assessment of HER2 status..... 162

4.6.5 Correlation with clinicopathological parameters and molecular biomarkers 166

4.6.6 Characteristics of DCIS by surrogate molecular subtypes 166

4.6.7 Associations with the outcome..... 169

4.7 Discussion 172

Chapter 5: The prognostic significance of tumour infiltrating lymphocytes in DCIS 186

5.1 Introduction 187
5.2 Tumour infiltrating lymphocytes 187
5.2.1 TILs subpopulations and immune checkpoint proteins ... 188
5.3 Hypothesis and aims 189
5.4 Materials and methods 190
5.4.1 Evaluation of TILs and their prognostic significance 190
5.4.1.1 Study cohort 190
5.4.1.2 TILs scoring 193
5.4.2 Assessment of immune cell subpopulation and checkpoint proteins 199
5.4.2.1 IHC of immune cell markers and checkpoint proteins 199
5.4.2.2 Immunoscoring 201
5.4.2.3 DNA extraction, targeted sequencing library preparation, enrichment, and sequencing 201
5.4.2.4 Copy number and variant data analysis 203
5.4.2.5 Statistical analysis 204
5.5 Results 207
5.5.1 Training set 207
5.5.2 Validation set 212
5.5.3 Association of TILs density with other clinicopathological parameters 213
5.5.4 Outcome analysis 216
5.5.5 Patterns of expression and distribution of various inflammatory cells and immune checkpoints 220
5.5.6 Association between immune cells subpopulations and other clinicopathological parameters 228
5.5.7 Copy number variation and TP53 mutations 233
5.5.8 Outcome analysis 236
5.6 Discussion 243

Chapter 6: The role of extracellular matrix remodelling proteins in DCIS behaviour 255

6.1 Introduction 256
6.2 Tumour cell intrinsic factors involved in DCIS progression 257

6.2.1 Molecular features of DCIS and its progression 257
6.3 Extrinsic factors and DCIS progression.....259
6.4 Identification of progression drivers 260
6.4.1 Prolyl-4-Hydroxylase A Subunit 2..... 263
6.4.2 Lysosomal Protective Protein (Cathepsin A)..... 263
6.4.3 Cathepsin V 264
6.4.4 Legumain 265
6.4.5 Collagen (XI) alpha-1 chain..... 266
6.5 Hypothesis and aims 267
6.6 Patients and methods.....268
6.6.1 Study cohort..... 268
6.6.2 Analysis of biomarkers mRNA expression in breast cancer 269
6.7 Results 269
6.7.1 Antibodies specificity..... 269
6.7.2 Biomarkers distribution and localisation 270
6.7.2.1 P4HA2..... 270
6.7.2.2 CTSA..... 273
6.7.2.3 CTSV..... 274
6.7.2.4 LGMN..... 277
6.7.2.5 COL11A1 280
6.7.3 Association of the studied biomarkers and clinicopathological parameters 283
6.7.3.1 P4HA2..... 283
6.7.3.2 CTSA..... 288
6.7.3.3 CTSV..... 292
6.7.3.4 LGMN..... 297
6.7.3.5 COL11A1 302
6.7.4 Association of the studied biomarkers and DCIS recurrence 307
6.7.4.1 P4HA2..... 307
6.7.4.2 CTSA..... 314
6.7.4.3 CTSV..... 317
6.7.4.4 LGMN..... 322
6.7.4.5 COL11A1 327
6.8 Discussion 336

Chapter 7: Geometric characteristics of collagen in DCIS.....357

7.1 Introduction.....358
7.1.1 Collagen.....358
7.2 Hypothesis and aims.....359
7.3 Patients and methods.....360
7.3.1 Study cohort.....360
7.3.2 Histochemical collagen staining.....360
7.3.3 Image acquisition.....361
7.3.4 Image analysis.....361
7.3.5 Calculation of Collagen Prognostic Index score.....364
7.4 Results.....366
7.4.1 Distribution of CPI.....366
7.4.2 Significance of CPI.....370
7.4.3 Outcome analysis.....377
7.5 Discussion.....385

Chapter 8: Hypoxia Driven Centrosome Amplification in DCIS.....393

8.1 Introduction.....394
8.1.1 Role of centrosome amplification in carcinogenesis.....394
8.2 Hypothesis and aims.....396
8.3 Materials and methods.....397
8.3.1 Study cohort.....397
8.3.2 Immunofluorescence staining and imaging.....401
8.3.3 Centrosome scoring.....402
8.3.4 Centrosomes categorisation.....403
8.3.5 Algorithm-based analytics.....405
8.3.5.1 Quantitation of numerical CA.....405
8.3.5.2 Quantitation of structural CA.....407
8.3.6 Statistical analysis.....409
8.4 Results.....411
8.4.1 CAS and DCIS recurrence.....411
8.4.2 CAS and RT benefit.....424
8.4.3 Clinical significance of CAS total.....425

8.4.4 Comparison between CAS and VNPI in recurrence prediction 432
8.4.5 Comparison between CAS in pure DCIS and DCIS co-exist with IBC 433
8.5 Discussion 435

Chapter 9: General Discussion..... 440

9.1 Background 441
9.2 Hypothesis, aims and methods of the study 443
9.3 Cardinal findings of the study.....445
9.3.1 Clinical characterisation of DCIS 445
9.3.2 Molecular Taxonomy of DCIS..... 446
9.3.3 Effect of ECM changes 447
9.3.4 Prognostic significance of TILs 448
9.3.5 Centrosome amplification and recurrence..... 449
9.4 Tumour microenvironment and DCIS progression .450
9.5 Clinical applicability.....451
9.6 Final conclusions 453
9.7 Strengths of the study.....453
9.8 Potential limitations and weakness 455
9.9 Suggestions and future investigations.....456

References 459

LIST OF TABLES

Table 1-1 Holland's classification system for DCIS 18
Table 1-2 Van Nuys pathological classification system for DCIS 19
Table 1-3 Cytonuclear grading of DCIS.....20
Table 1-4 Modified grading system for DCIS.....21
Table 1-5 Scheme of new pathological grading system of DCIS 22
Table 1-6 Nuclear and proliferation index grading system ..22
Table 1-7 Molecular subtypes of DCIS 24
Table 1-8 Oncotype DX DCIS assay genes and score.....26
Table 1-9 Modified Van Nuys Prognostic Index 34
Table 1-10 Markers of normal myoepithelial cells.....54
Table 1-11 Tumour suppressor genes expressed by myoepithelial cells 55
Table 1-12 Current and proposed profile of DCIS reporting 59
Table 2-1: Clinicopathological characteristics of pure DCIS cohort.....66
Table 2-2: Specificity of the selected antibodies for the project 83
Table 2-3: Optimum conditions of the selected antibodies..87
Table 2-4: Antibodies used, their expression localisation and cut-offs 91
Table 3-1: Clinicopathological parameters of pure DCIS cohort 102
Table 3-2: Clinicopathological factors associated with the selection of type of primary surgery for DCIS management104
Table 3-3: Detailed surgical management of the DCIS.....105
Table 3-4: Clinicopathological factors associated with re-excision after primary treatment with breast conserving surgery 108

Table 3-5: Clinicopathological factors associated with the choice of type of DCIS re-excision 110
Table 3-6: Clinicopathological factors associated with presence of residual tumour tissue in the re-excision specimens 113
Table 3-7: Multivariate logistic regression model analysis 115
Table 3-8: Univariate survival analysis of various clinicopathological parameters and all recurrences 122
Table 3-9: Univariate survival analysis of various clinicopathological parameters and invasive recurrence only 123
Table 3-10: Multivariate Cox regression analysis between various clinicopathological parameters and DCIS recurrence 124
Table 4-1: Clinicopathological features of the pure DCIS cohort included in the study 154
Table 4-2: Correlation between ER expression and the clinicopathological variables of pure DCIS cases 156
Table 4-3: HER2 status in pure DCIS cases using IHC and CISH 162
Table 4-4: HER2 status in DCIS cases mixed with invasion using IHC and CISH 165
Table 4-5: Final HER2 status of DCIS and invasive component of DCIS cases mixed with invasion 165
Table 4-6: Comparison between HER2 status in pure DCIS cases using IHC and CISH 165
Table 4-7: HER2 status of DCIS cases mixed with invasion using IHC 165
Table 4-8: Comparison between HER2 status of the DCIS component in cases mixed with invasion using IHC and CISH 165

Table 4-9: Comparison between HER2 status of the invasive component in DCIS cases mixed with invasion using IHC and CISH..... 166
Table 4-10: HER2 status of DCIS and invasive component in DCIS cases mixed with invasion using CISH 166
Table 4-11: Association between final HER2 status and the clinicopathological parameters of pure DCIS cohort 167
Table 4-12: Characteristics of DCIS by surrogate molecular subtypes. 168
Table 4-13: Univariate analysis for predictors of local recurrence in pure DCIS patients treated with breast conserving surgery 170
Table 4-14: Multivariate Cox proportional hazards for factors associated with local recurrence in pure ductal carcinoma in situ patients..... 171
Table 5-1: Clinicopathological characteristics of the training and validation sets for TILs assessment 192
Table 5-2: Methods and parameters of TILs assessment .. 196
Table 5-3: Different antibodies used for immune cells characterisation and their staining protocols..... 200
Table 5-4: Cut-off points of mean TILs count/DCIS duct .. 206
Table 5-5: TILs Inter-rater concordance results in the training set 207
Table 5-6: Distribution of TILs in the training set 209
Table 5-7: Correlation between Touching TILs and TILs at other topographic areas (training set) 209
Table 5-8: Frequency of TILs density in different topographic areas and their association with recurrence in the training set 210
Table 5-9: Correlation between TILs density and clinicopathological parameters in the validation set 215

Table 5-10: Cox regression analysis of TILs association with LRFI* 220
Table 5-11: Distribution of various TILs and immune check point proteins in the pure DCIS cohort 222
Table 5-12: Correlation between immune cell markers, immune checkpoints with the clinicopathological parameters in pure DCIS cohort 229
Table 5-13: Univariate survival analysis between overall TILs and various immune cell markers with the local recurrence free interval in DCIS patients treated with breast conserving surgery 239
Table 5-14: Multivariate survival analysis of variables (with and without immune cell markers) predicting outcome 240
Table 6-1: Correlation between P4HA2 expression with different clinicopathological parameters in the pure DCIS cohort 284
Table 6-2: Correlation between P4HA2 expression with different clinicopathological parameters in the pure DCIS cohort using continuous data. 286
Table 6-3: Correlation between *P4HA2* mRNA level and the clinicopathologic parameters in the METABRIC series. 287
Table 6-4: Correlation between CTSA expression with clinicopathological parameters in the pure DCIS cohort 289
Table 6-5: Correlation between *CTSA* mRNA and the clinicopathologic parameters in the METABRIC series. 291
Table 6-6: Correlation between CTSV expression with clinicopathological parameters in the pure DCIS cohort. 293
Table 6-7: Correlation between CTSV expression and clinicopathological parameters in the pure DCIS cohort using continuous data 295
Table 6-8: Correlation between *CTSV* mRNA level and the clinicopathological parameters in the METABRIC series 296

Table 6-9: Correlation between LGMN expression with different clinicopathological parameters in the pure DCIS cohort. 298
Table 6-10: Correlation between LGMN expression and different clinicopathological parameters in the pure DCIS cohort using continuous data. 300
Table 6-11: Correlation between *LGMN* mRNA level and the clinicopathological parameters in the METABRIC series. 301
Table 6-12: Correlation between COL11A1 expression with different clinicopathological parameters in the pure DCIS cohort. 303
Table 6-13: Correlation between COL11A1 expression and different clinicopathological parameters in the pure DCIS cohort using continuous data. 305
Table 6-14: Correlation between *COL11A1* mRNA level and the clinicopathological parameters in the METABRIC series. 306
Table 6-15: Multivariate survival analysis of P4HA2 and other variables predicting ipsilateral local recurrence in patients treated by BCS in pure DCIS cohort 313
Table 6-16: Multivariate survival analysis of CTSA and other variables predicting ipsilateral local recurrence in patients treated by BCS 316
Table 6-17: Multivariate survival analysis of CTSV and other variables predicting ipsilateral local recurrences in patients treated by BCS. 320
Table 6-18: Multivariate survival analysis of COL11A and other variables predicting ipsilateral local recurrences in patients treated by BCS 334
Table 7-1: Scores of collagen directionality, dispersion, density and collagen prognostic index 365
Table 7-2: Distribution of CPI and its parameters scores .. 368

Table 7-3: Correlation between CPI and clinicopathological parameters 372
Table 7-4: Correlation between CPI scores (continuous values) and different clinicopathological parameters 373
Table 7-5: Correlation between CPI parameters and different clinicopathological parameters 374
Table 7-6: Correlation between different CPI parameters and clinicopathological parameters using continuous data. 376
Table 7-7: Multivariate survival analysis of CPI and other variables predicting ipsilateral local recurrence 383
Table 8-1: Clinicopathological features of study cohort 399

LIST OF FIGURES

Figure 1-1: Mammographic features of DCIS..... 7
Figure 1-2: Diagnostic criteria used for breast intraductal proliferations 11
Figure 1-3 Morphological patterns of DCIS.....13
Figure 1-4 Van Nuys grading system of DCIS.....19
Figure 1-5 Examples of DCIS nuclear grades 20
Figure 1-6: Model of progression from normal breast duct to invasive carcinoma 28
Figure 1-7 Nomogram for DCIS recurrence.....35
Figure 1-8 Tumour microenvironment and its role in carcinogenesis 39
Figure 1-9 Tumour associated inflammatory cells 42
Figure 1-10 Role of Myoepithelial cells in breast cancer.....55
Figure 1-11 Myoepithelial cells in normal breast duct and DCIS 56
Figure 2-1: Marking of scanned images for TMA construction 71
Figure 2-2: Agarose embedding block.....73
Figure 2-3: TMA layouts.....75
Figure 2-4: TMA construction process 76
Figure 2-5: Final TMA blocks and stained slides.....77
Figure 3-1: Annual Frequency of DCIS 101
Figure 3-2: DCIS Clinical Presentation.....101
Figure 3-3: Re-excision Rates of DCIS. 106
Figure 3-4 Van Nuys Prognostic Index rate change over study period 117
Figure 3-5: The annual clinical rates of DCIS 119
Figure 3-6: Kaplan Meier Curves showing the association between DCIS treatment and recurrence 121

Figure 4-1: Immunohistochemistry of the biomarkers used in DCIS molecular characterisation. 152
Figure 4-2: HER2 expression in pure DCIS cases 163
Figure 4-3: The rate of HER2 positivity over years 164
Figure 5-1: Schematic distribution of study cohorts 193
Figure 5-2: Parameters of TILs assessment 198
Figure 5-3: Touching TILs density around DCIS 211
Figure 5-4: Kaplan-Meier curves showing association between TILs density within different topographic areas and LRFI in training set 213
Figure 5-5: Association between touching TILs density with LRFI 219
Figure 5-6: Photomicrograph for immune cells and checkpoint proteins in DCIS 223
Figure 5-7: Distribution of CD20, CD3, CD4 and CD8 in DCIS 224
Figure 5-8: Correlation Matrix showing the correlation between TILs subtypes, overall TILs, and other associated biomarkers 226
Figure 5-9: Bar charts showing the difference between expression of various immune cells and checkpoint proteins in pure DCIS and DCIS coexisting with invasive disease 227
Figure 5-10: Violin plots showing the association between various clinicopathological parameters, *TP53* mutation with the fraction of genomic altered and with number of telomeric allelic imbalances 234
Figure 5-11: Violin plots showing the association between TP53 variants TILS 235
Figure 5-12: Kaplan Meier Curves showing the association between TILs and LRFI 238
Figure 5-13: Kaplan Meier curves showing the association between TILs and PDL1 and local recurrence free interval . 242

Figure 6-1: Factors contributing to the progression of DCIS to invasive cancer 260
Figure 6-2: Flowchart demonstrating the identification of the study biomarkers..... 262
Figure 6-3: Western Blot of the antibodies used in the study 270
Figure 6-4: Patterns of P4HA2 expression..... 272
Figure 6-5: Patterns of CTSA expression 273
Figure 6-6: Patterns of CTSV expression 276
Figure 6-7: Violin plots show the difference between CTSV expression in pure DCIS, DCIS component in mixed cases and invasive component in mixed cases..... 276
Figure 6-8: Patterns of LGMN expression..... 279
Figure 6-9: Bar chart showing differences of legumain expression between pure DCIS and DCIS-mixed both in tumour cells and surrounding stroma 279
Figure 6-10: Patterns of COL11A1 expression 282
Figure 6-11: Violin plots showing differences of COL11A1 expression between pure DCIS and DCIS-mixed 282
Figure 6-12: Violin plots showing the associations between CTSA expression and other clinicopathological parameters in pure DCIS cohort..... 290
Figure 6-13: Kaplan Meier curves show the association between P4HA2 and outcome 310
Figure 6-14: Kaplan Meier curve shows association between high P4HA2 expression and ipsilateral local invasive recurrences in BCS treated patients. 311
Figure 6-15: Kaplan Meier curves show association between post-operative adjuvant radiotherapy (RT) and recurrence within low and high P4HA2 expression groups 311
Figure 6-16: Forest plots showing the univariate analysis results of association between different clinicopathological

parameters and ipsilateral tumour recurrence for patients treated with breast conserving surgery in pure DCIS cohort 312
Figure 6-17: Kaplan Meier curves show the association between CTSA and outcome 315
Figure 6-18: Kaplan Meier curves show the association between epithelial CTSV and outcome 318
Figure 6-19: Kaplan Meier curves show the association between stromal CTSV and outcome 319
Figure 6-20: Kaplan Meier curves show the association between LGMN and outcome 324
Figure 6-21: Forest plots showing the hazard ratio of the different clinicopathological parameters and ipsilateral tumour recurrence for patients treated with breast conserving surgery in pure DCIS cohort 325
Figure 6-22: Kaplan Meier curves show the association between DCIS risk and local recurrence free interval in patients treated with breast conserving surgery 326
Figure 6-23: Kaplan Meier curves show the association between epithelial COL11A1 and outcome 330
Figure 6-24: Kaplan Meier curves show the association between stromal COL11A1 and outcome 331
Figure 6-25: Kaplan Meier curves showing that radiotherapy is associated with better outcome in patients treated with breast conserving surgery and have low stromal COL11A1 expression 332
Figure 6-26: Kaplan Meier curves showing the association between DCIS risk and local recurrence free interval in patients treated with breast conserving surgery 333
Figure 7-1: Diagram shows the different parameters assessed to evaluate the collagen characteristics surrounding DCIS . 364

Figure 7-2: Schematic representation of evaluation of collagen around DCIS ducts..... 366
Figure 7-3: Example of collagen fibre arrangement..... 368
Figure 7-4: Violin plots comparing the distribution of CPI parameters between pure DCIS and DCIS co-existing with invasive carcinoma 370
Figure 7-5: Kaplan Meier curves show that the poor collagen prognostic index group is associated with shorter ipsilateral local recurrence free interval..... 379
Figure 7-6: Kaplan Meier curves show that poor collagen prognostic index group is associated with shorter ipsilateral local recurrence free interval..... 380
Figure 7-7: Kaplan Meier curves show the association between collagen geometrics and outcome 381
Figure 7-8: Forest plots showing the univariate analysis results of association between different clinicopathological parameters and the ipsilateral tumour recurrence 382
Figure 8-1: A schematic summarising the role of hypoxia in CA at different stages of the centrosome cycle..... 396
Figure 8-2: Diagram describing the flow of patients through the study..... 398
Figure 8-3: Association between conventional clinicopathological parameters and DCIS recurrence in the whole study cohort 400
Figure 8-4: Schematic depicting semi-automated workflow to quantify CA..... 402
Figure 8-5: Representative immunographs of normal and normal adjacent breast tissue sections for centrosomes 404
Figure 8-6: Schematic depicting the high and low severity and frequency of numerical and structural centrosome amplification. 406

Figure 8-7: Representative confocal micrographs of DCIS tissue sections immunolabeled for centrin-2 (red), γ-tubulin (green) and nuclei (blue) in split form 409
Figure 8-8: Graphical checks of the proportional hazard assumption 410
Figure 8-9: DCIS cases in the DC with ipsilateral recurrence exhibit higher CAS than recurrence-free cases 412
Figure 8-10: DCIS cases in the DC with local recurrence exhibit higher frequency and severity of both numerical and structural CA 413
Figure 8-11: Representative confocal micrographs of DCIS tissue sections from VC immunolabeled for γ-tubulin (red) and Hoechst (blue) in recurrence and recurrence free samples. 414
Figure 8-12: Grade matched DCIS cases with local recurrence exhibit higher CAS than grade-matched cases without recurrence 415
Figure 8-13: Recurrent DCIS cases treated with BCS in the DC exhibit higher CAS than recurrence-free cases 416
Figure 8-14: In the DC and VC, higher CAS is associated with poorer LRFI 418
Figure 8-15: Higher CAS is associated with poorer LRFI for DCIS patients treated with BCS in the DC 419
Figure 8-16: Higher severity and frequency of numerical and structural CA are associated with poor LRFI in the DC..... 420
Figure 8-17: Fitted normal and kernel density curves on the histogram are estimated based on the bootstrap sample mean and standard deviation 421
Figure 8-18: Higher CAStotal is associated with LRFI 422
Figure 8-19: Estimated 10-year risk of local recurrence as a continuous function using CAStotal 423
Figure 8-20: Higher CAS is associated with poor LRFI for DCIS patients treated with surgery 427

Figure 8-21: Higher CAS is associated with poor LRFI for DCIS patients in the VC treated with surgery alone 428
Figure 8-22: DCIS cases who recurred as IBC exhibited higher CAStotal compared to the patients who recurred as DCIS.. 428
Figure 8-23: Distribution of the CAStotal according to clinical and pathologic characteristics in DC 429
Figure 8-24: Distribution of the CAStotal according to clinical and pathologic characteristics in VC 430
Figure 8-25: Forest plot representing estimates of 10-year recurrence rates within high grade DCIS patient subgroups 431
Figure 8-26: Comparison of the stratification of DCIS patients by CAStotal and VNPI..... 432
Figure 8-27: DCIS cases in the mixed DCIS cohort exhibit higher CAS when compared with CAS of pure DCIS samples 434
Figure 9-1: The tumour microenvironment orchestra and DCIS progression..... 452

1 CHAPTER 1: GENERAL INTRODUCTION

1.1 Breast Ductal Carcinoma *in situ* (DCIS)

1.1.1 Definition and historical background

Breast ductal carcinoma *in situ* (DCIS) is a heterogeneous group of diseases which refers to proliferation of malignant epithelial ductal cells within the confinement of the ducto-lobular system of the breast surrounded by intact myoepithelial layer and basement membrane without invasion into the surrounding stroma [1]. It was first described in the early twentieth century by a group of surgeons as a transitional phase between hyperplastic changes and invasive disease wherein pathologists identified their different characteristics features and patterns [2]. Early descriptions of DCIS outlined the major morphological patterns of the disease that are recognised nowadays. This includes micropapillary and cribriform types which were described as laciform and cartwheel patterns, respectively [2, 3]. The comedo type DCIS was firstly described by Bloodgood and classified as comedocarcinoma. Since then, there have been a plethora of studies that have been performed on DCIS to clarify its genotypic and phenotypic characteristics, relation with invasive breast carcinoma (IBC) and methods of detection and management.

1.1.2 Incidence and epidemiology

Several decades ago, the diagnosis of DCIS was infrequent and represented about 1-2% of newly diagnosed breast cancer (BC) [4]. In 1975, data from National Cancer Institute's Surveillance Epidemiology and End Results (SEER) programme showed less than 3% of BC patients had pure DCIS [5]. After introduction of mammography in BC screening programmes in early 1990s, the incidence of DCIS has increased dramatically. In the USA the age adjusted incidence of DCIS increased from 2.4 per 100,000 women in 1973 to 16 per 100,000 women in 1992 and 32.5 per 100,000 women in 2004 [6, 7]. According to the last cancer statistics published by SEER, approximately 63,000 DCIS cases will be diagnosed by end of 2019 in US with similar figure in the UK [8]. Currently, DCIS represents about 20-25% of mammographic screen detected BC [9]. This increase in incidence of DCIS is observed in all ethnic groups [10]. Although DCIS is less common than IBC, its incidence increases with age like invasive disease. The mean age of DCIS diagnosis in multiple studies was between 50 and 59 years, similar to the mean age of IBC [11-13]. DCIS is unlikely to be diagnosed in patients less than 30 years old and the incidence is approximately doubled comparing patients with age group 40-50 years with those between 70 and 80 years [14]. However, DCIS of

younger women is usually more aggressive with a higher incidence of recurrence and progression to IBC [15-18].

1.1.3 Risk factors

Risk factors for developing DCIS are similar to those of IBC including family history of BC, early menarche, late menopause, nulliparity, long term usage of hormonal replacement therapy and obesity [14]. One of the strongest risk factors for DCIS development is high breast tissue density as detected by mammography [19-21]. *BRCA1* and *BRCA2* mutations are risk factors for both IBC and DCIS [22, 23]. *BRCA* mutation was detected in 13% of DCIS diagnosed before the age of 50 [24].

1.1.4 Pathogenesis and cytogenetics

The pathogenesis of DCIS is complex and shares multiple features as IBC [25]. Chromosomal abnormalities with loss of heterozygosity (LOH) are observed in 70% of high-grade DCIS [26]. The frequency of aneuploidy in DCIS ranges from 21-71% [27, 28]. Higher grade DCIS with comedo type necrosis has higher rate of Deoxyribonucleic acid (DNA) aneuploidy.

Oncogene overexpression such as human epidermal growth factor receptor2 (*HER2*) is detected in DCIS. *HER2* gene amplification is seen in 40-48% of DCIS [29, 30] with higher rate of amplification in comedo than non-comedo type DCIS

[30]. DCIS also shows loss of tumour suppressor genes, such as *TP53* and *p16*, and overexpression of proliferation markers such as Ki67 [31]. Loss of heterozygosity (LOH) commonly occurs in chromosomes 17p, 11p and 16q [32-34]. Interestingly, the molecular profile of DCIS is usually similar to the adjacent IBC [35, 36] which highlight the potential role of other factors such as myoepithelial cells and surrounding tumour microenvironment (TME) in the process of progression from DCIS into invasive disease.

1.1.5 Clinical presentation and diagnosis

The majority of DCIS cases are diagnosed at early asymptomatic stage with introduction of mammography in the screening programme while the remaining percentage is usually presented as a breast lump, nipple discharge or Paget's disease of the nipple [37, 38]. Approximately 10-15% of DCIS are discovered incidentally in biopsies performed for other indications [11]. Mammography shows high sensitivity (about 80-90%) in detection of DCIS. Age and breast tissue density may play role in the sensitivity of mammography [39]. Mammography also can detect the extent of the lesion especially those with comedo necrosis rather than cribriform or micropapillary types which usually grow in creeping fashion within the ducts in which the mammogram underestimate their size [40]. Moreover, the size of DCIS determined by

mammographic measurement is significantly smaller in women examined annually (mean, 1.6 cm) than in those examined on a biennial (mean, 2.3 cm) or triennial (mean, 3.5 cm) schedule. Comedo-type DCIS is significantly more frequent in the biennial (74%) than in the annual (47%) screening group. Tumour size and nuclear grade are inversely related with the mean sizes for low-, intermediate- and high-grade lesions determined to be 1.2 cm, 1.9 cm, and 2.8 cm, respectively. The frequency of microinvasion tends to increase with longer intervals between examinations, but these differences are not statistically significant [41].

Calcifications alone are more likely to be the mammographic indicator of DCIS in women younger than 50 years, whereas co-existent soft-tissue abnormalities are evident more often in women older than 50, a distinction that probably results from variation in overall breast density in these age groups rather than from intrinsic tumour differences [42].

Calcifications associated with DCIS are generally described as linear "casts" or as granules on mammography (**Figure 1-1**). Round or oval, well-circumscribed calcifications are less frequent features of DCIS. Predominantly linear, granular, or mixed types of calcifications occur with approximately equal frequency. Calcifications may be clustered, dispersed, or

dispersed around clustered foci. Branching calcifications with linear patterns that outline the distribution of one or more ducts may be observed. The type of calcifications is not related to age at diagnosis or to the size of the area involved mammographically. The level of suspicion for DCIS is a function of the character and the number of calcifications. The majority of DCIS have five or more calcifications [42].

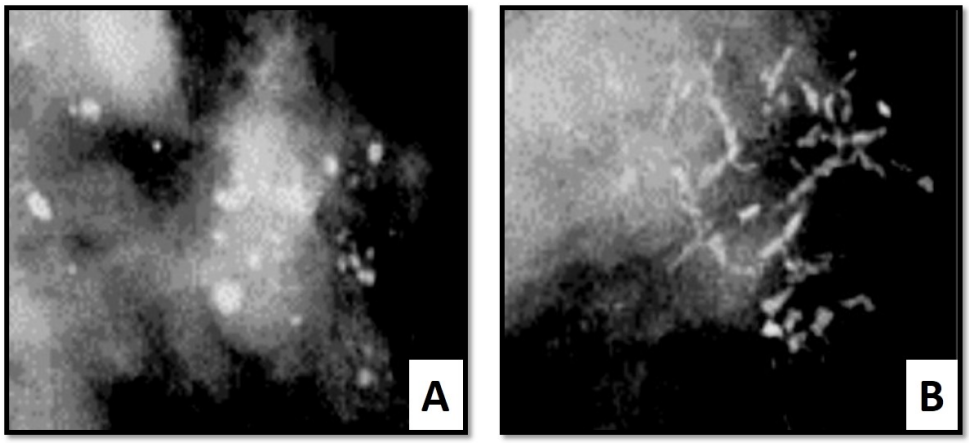

Figure 1-1: Mammographic features of DCIS.

A) Clustered round, punctate calcifications and B) branching linear calcifications

Occasionally, in less than 10% of mammographically detected lesions, DCIS shows unusual mammographic presentations with a configuration mimicking a benign lesion or invasive carcinoma [43].

Although rarely used, magnetic resonance imaging was shown as effective method to detect DCIS especially in cases lacking calcifications. Lesions usually detected through contrast

enhancement in the breast parenchyma after injection of a gadolinium contrast agent when compared to the pre-injection image [44].

Final confirmed diagnosis of DCIS is through histopathological examination of obtained biopsies from lesion either through needle core biopsy, vacuum assisted core biopsy, incisional or excisional biopsy. No definite cytological features can differentiate DCIS from IBC in fine needle aspiration cytology specimens or nipple discharge smears.

1.1.6 **Bilaterality, multifocality and multicentricity**

Limited data describing the frequency of DCIS bilaterality is available. About 10-20% of DCIS presented bilaterally, either in the form of concurrent contralateral disease or subsequent episode of DCIS as reported by Cancer Registration Statistics, England (www.cancerresearchuk.org).

There is no uniformly accepted definition of multicentricity in DCIS. Carcinoma was considered as multicentric when they were separate from the clinically detected lesion. Lagios *et al*. defined multicentricity as "the presence of independent foci of carcinoma within the breast which are separate from the clinically or mammographically evident lesion, that is, the reference tumour" [45]. Others defined DCIS as multicentric if it is detected in more than one quadrant or if it is 5 cm from

the index lesion [46, 47]. In practical terms, multicentricity refers to foci of DCIS in distinctly different regions of the breast, usually in two or more quadrants.

Multicentricity should be distinguished from intraepithelial extension within ducts and lobules of a single carcinomatous focus typically limited to one region or quadrant. The latter condition is commonly referred to as multifocality. One commonly employed criterion for establishing the presence of multifocality depends the number of histologic sections that show tumour. Unifocal DCIS is considered when the tumour is seen in only one section of two or more obtained from different blocks, while if the tumour is detected in sections from two or more different blocks, it is considered as multifocal [48]. Silverstein *et al*. considered DCIS to be multifocal when separate foci more than 2cm from primary site were found in [49]. The frequency of multifocal DCIS differs between studies based on the applied definition. Multicentricity was reported in 33% and 37% of mastectomies performed for various histological types of DCIS [6, 47]. When classified on the basis of the predominant growth pattern, micropapillary DCIS was more often multicentric (86%) than papillary (33%) or comedo (42%) subtypes [46].

1.1.7 Pathology of DCIS

1.1.7.1 Gross pathology

Grossly, DCIS may show unremarkable changes within the excised specimens. Classically, DCIS does not produce a lesion that is clearly recognisable on macroscopic examination. However, exceptions include cases of high-grade DCIS with comedo necrosis where widened duct spaces with "soft centres" can be observed and some cases of solid papillary DCIS, which may result in a mass lesion of variable size with a circumscribed margin [1]. Dilated ducts with intraluminal necrotic materials or gritty mass may be also seen [50].

1.1.7.2 Histological features and classifications

Diagnostic criteria for DCIS depend, in part, on the degree of cytological atypia, but in general include cytonuclear and architectural features, clonality of the cell population and extent of the lesion. These criteria differentiate between DCIS and other mimicking lesions such as usual ductal hyperplasia (UDH) and atypical ductal hyperplasia (ADH) of the breast as illustrated in **Figure 1-2**.

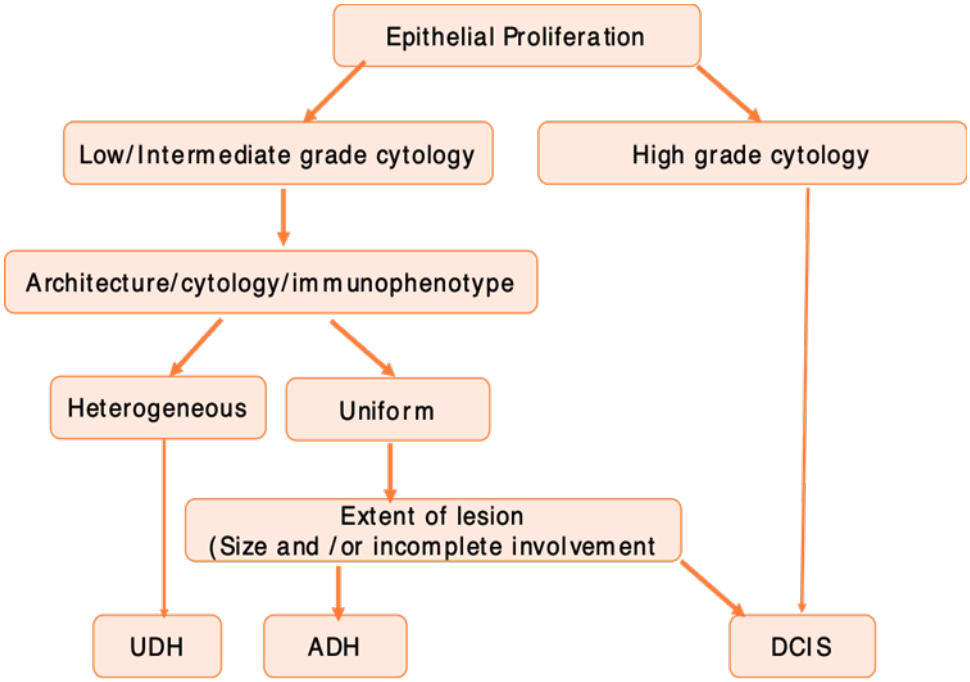

Figure 1-2: Diagnostic criteria used for breast intraductal proliferations

Histologically DCIS can by classified according to the morphological pattern or according to the grade. Some classification systems combine both features in their scheme. Despite the prevalence of DCIS, there is no consistent accepted histological classification system, but, a growing consensus admits the importance of grade over morphology.

1.1.8 DCIS histological patterns

DCIS shows proliferation of malignant epithelial cells within the breast ducts in different patterns [50]. Most lesions show a mixture of patterns, within the same lesion [25]. Allred classified DCIS into two groups: the more aggressive comedo large cell group and the less aggressive non-comedo small cell

group [51]. Poller *et al*. classified lesions simply into DCIS without necrosis, non-pure comedo DCIS and pure comedo DCIS which showed correlation with proliferation index and HER2 expression (Nottingham classification system, 1994) [52]. World Health Organisation (WHO) classification of the tumours of the breast, 5th edition, describes different patterns of DCIS which include solid, cribriform, clinging, micropapillary, papillary and comedo types (**Figure 1-3)** beside some unusual patterns such as apocrine, signet ring cell, neuroendocrine, spindle, and clear cell types [53].

Comedo-carcinoma *in situ* (CC-DCIS) is a distinctive type of high-grade DCIS. CC-DCIS is the only DCIS that is observed grossly; therefore, it was over-diagnosed before the advent of mammography. The term comedo refers to a yellowish creamy necrotic material secreted from the ducts that resemble comedones. Histologically, this subtype is characterised by enlarged ducts filled with central acellular necrosis with nuclear debris surrounded by up to a few layers of highly atypical epithelial cells and multiple mitotic figures. Necrosis usually occupies more than 90% of the duct cross section. The necrotic material calcifies and appears as large stringy branching calcifications on a mammogram [54].

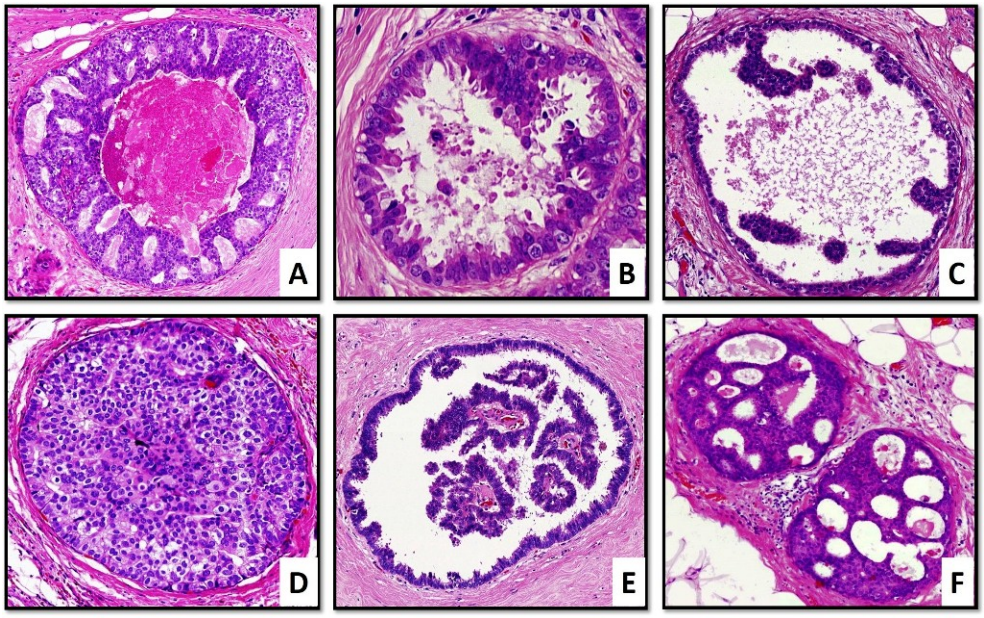

Figure 1-3 Morphological patterns of DCIS.

(A) Comedo, (B) Clinging, (C) Micropapillary, (D) Solid, (E) Papillary, and (F) Cribriform type

1.1.9 Rare morphological variants of DCIS

A great proportion of DCIS accommodates more than one morphological variant. The majority of these morphological variants are well recognised by pathologists including comedo, solid, clinging, cribriform, micropapillary and papillary. However, some patterns are rare such as:

1.1.9.1 Solid and encapsulated papillary carcinoma

Although solid papillary (SPC) and encapsulated papillary carcinoma (EPC) have been regarded as variants of DCIS, recent studies have shown that the immunohistochemical markers for myoepithelial cells (MECs) are deficient in some

lesions around the periphery of the tumour [1]. Rakha *et al.* have proposed considering those lesions with obvious MECs as DCIS and those without as a special type of invasive carcinoma. In their study, these lesions were associated with a low incidence (3%) of stromal or skeletal muscle invasion, lymph node metastasis and rare development of regional or distant recurrence. Therefore, they inferred that these lesions are characterised by indolent behaviour and good prognosis. They emphasised that treatment of these lesions is adequate by local excision without adjuvant chemotherapy similar to the conventional DCIS [55].

1.1.9.2 Cystic hypersecretory DCIS

In cystic hypersecretory DCIS, the lesion is formed of cysts lined by inconspicuous flat cells or a single layer of cuboidal to columnar cells. Generally, the cells in such lesions have uniform cytologically bland nuclei and scant cytoplasm. Atypical features such as epithelial crowding, hyperchromasia, occasional mitotic figures, and enlargement of nuclei, which may contain nucleoli are uncommon [56].

1.1.9.3 Apocrine DCIS

Scott *et al.* suggested that distinguishing apocrine DCIS from atypical apocrine proliferations is challenging and the difficulty is in defining accurate grade [57]. Many morphological variants of apocrine DCIS have been described including solid,

cribriform, and comedo subtypes but it is the characteristic cellular features of large cells with abundant eosinophilic cytoplasm with enlarged nuclei and prominent nucleoli that can define this entity. Nuclear grading of apocrine DCIS is essentially difficult as classic apocrine cells are enlarged with prominent nucleoli leading some to suggest that the diagnosis and grading of apocrine DCIS particularly should rely not only on nuclear grade and the presence or type of necrosis but also on lesion size [58].

1.1.9.4 Clear and signet ring cell DCIS

Clear cell DCIS is a poorly defined variant typically encountered with solid and comedo patterns. Some clear cell DCIS are composed of cells with an arrangement described as "mosaic" because of the appearance created by sharply defined cell borders. The presence of a monomorphic clear cell population is highly suggestive of DCIS.

Signet ring cells, usually associated with lobular carcinoma, also occur in DCIS, most often in the papillary and cribriform types. The presence of signet ring cells with cytoplasmic mucin demonstrated with the mucicarmine, periodic acid-Schiff, or Alcian blue stains is strong evidence for a diagnosis of DCIS. Signet ring cells have eccentric nuclei that are often indented

along the nuclear border, which abuts on the cytoplasmic mucin vacuole.

1.1.9.5 Spindle cell DCIS

Spindle cell DCIS may express neuroendocrine markers such as chromogranin, synaptophysin, and neuron-specific enolase. The swirling growth pattern of cells in spindle cell DCIS mimics "streaming" that is characteristically found in UDH. Spindle cell DCIS often co-exists with cribriform pattern [59].

1.1.9.6 Paget's disease

Paget's disease of the nipple is defined by the presence of malignant epithelial cells within the squamous epithelium of the nipple and areola. Patients usually present by an eczematous change in the nipple and areola area and are commonly associated with high-grade DCIS with or without invasive disease in the underlying dermis. This variant of *in situ* disease is usually HER2 positive [1].

1.1.9.7 DCIS with microinvasion

DCIS with microinvasion is defined by malignant epithelial cells that have breached the basement membrane (BM) and invaded the adjacent stroma to a depth of 1mm or less. This can be in the form of a single cell or clusters of cells and can occur singly in an area of DCIS or at different points along the affected duct. Multiple foci of microinvasion are present when

the size of the individual foci cannot be added together, and the lesion is still staged as T1mic. Although it may be identified in association with all grades of DCIS, it is most commonly seen with high-grade lesions [60]. Exact clear diagnosis may be questionable in cases of high-grade DCIS with extensive cancerisation of lobules or cases with a prominent stromal lymphocytic infiltrate or marked stromal distortion. These difficulties can be resolved by the application of combinatorial cytokeratin stains to highlight the epithelial cells and myoepithelial markers to demonstrate the presence of malignant cells beyond the boundaries of the duct space. Microinvasion particularly in association with high grade DCIS will often necessitate a sentinel lymph node biopsy and up to 20% in cases with lymph node metastases, predominantly micrometastases or isolated tumour cells [61].

1.1.10 **DCIS grading**

Several grading systems for DCIS are available and all of them are subjective. In 1994 Holland *et al.* classified DCIS into well, intermediate and poorly differentiated tumours depending on cytonuclear features, growth patterns and calcifications **(Table 1-1**).

Table 1-1 Holland's classification system for DCIS

	Well differentiated	**Moderately differentiated**	**Poorly differentiated**
Nuclei	Monomorphic	Slightly pleomorphic	Markedly pleomorphic
Nucleoli	Inconspicuous	Conspicuous	Prominent
Mitosis	Rare	Occasional	Often
Chromatin	Fine and uniform	Fine to coarse	Coarse and clumped
Cell Polarisation	Marked	Present	Absent
Central necrosis	Absent or minimal	variable	Present and often marked
Individual cell necrosis	Absent	Focal	Marked
Growth pattern	Clinging, cribriform or micropapillary and rarely solid	Any pattern	Mostly solid and clinging
Calcification	Laminated, psammoma-like and rarely amorphous	Laminated and amorphous	Amorphous

The Van Nuys (VN) classification system provides a scheme for risk stratification of patients with DCIS for different treatment approaches. This system includes tumour size, grade, and resection margins distance. It was later modified by addition of patient age. Grading in this system is a combination between nuclear grade and presence of necrosis (**Table 1-2** and **Figure 1-4**) [62].

Table 1-2 Van Nuys pathological classification system for DCIS

	Grade 1	**Grade 2**	**Grade 3**
Pathological classification	Non high-grade DCIS (nuclear grade 1 or 2) without necrosis	Non high-grade DCIS (nuclear grade 1 or 2) with necrosis	High grade lesions (nuclear grade 3) with or without necrosis.

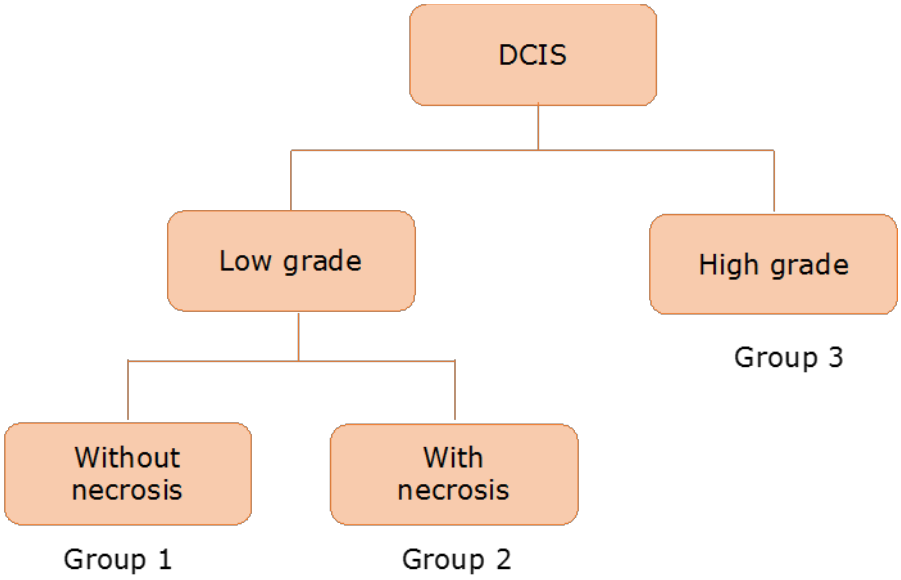

Figure 1-4 Van Nuys grading system of DCIS

Although the cytonuclear grading for DCIS developed in 1997 by Consensus Committee Recommendations and confirmed in 2005 by the National Pathology Co-ordinating Group [63, 64] it remains subjective, but is still the standard and most widely used for DCIS grading and it is recommended also in the WHO classification of the tumour of the breast [53, 65]. Summary of

different features of this grading system is addressed in **Table 1-3** and examples of these grades are shown in **Figure 1-5**.

Table 1-3 Cytonuclear grading of DCIS

	Low	**Intermediate**	**High**
Pleomorphism	Mild	Moderate	Marked
Size	x1.5-2 the size of RBC or the size of normal duct epithelial cell nucleus	x2.5 the size of RBC or the size of normal duct epithelial cell nucleus	More than 2.5 the size of RBC or the size of normal duct epithelial cell nucleus
Chromatin pattern	Fine dispersed diffuse chromatin	Intermediate	Dense clumped irregularly distributed
Nucleoli	Rarely conspicuous	Occasionally	Prominent and/or multiple
Mitosis	Few if any	Intermediate	Numerous
Orientation	Polarised towards the lumens	Degree of polarisation seen	No polarisation

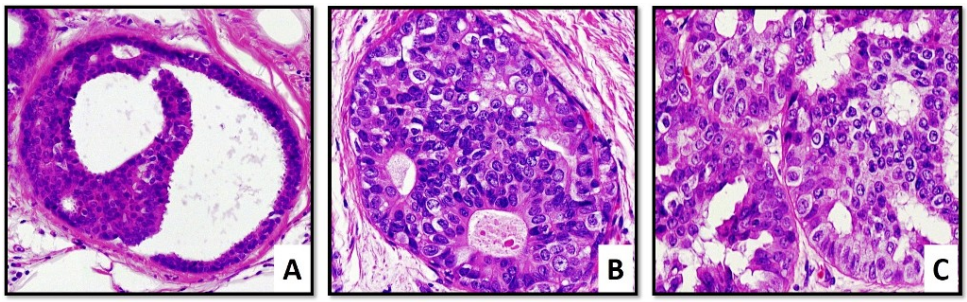

Figure 1-5 Examples of DCIS nuclear grades

(A) Low (B) Intermediate (C) High

Another grading system of DCIS based on degree of differentiation along with the nuclear features, comparable to that used for grading IBC [51, 66]. Main criteria of that classification are summarised in **Table 1-4.**

Table 1-4 Modified grading system for DCIS

Features	Score 1	Score 2	Score 3
Gland/Papillae	More than 75%	10-75%	Less than 10%
Mitosis	No	1-2	More than 2
Nuclear grade	Low	Intermediate	High
Central necrosis	Less than 10%	10-50%	More than 50%
Total score (range from 4-12) - Low grade lesions; scores 4-7 - Intermediate grade lesions; scores 8 and 9 - High grade lesions; scores 10-12			

In 2010, Pinder *et al.* published a new classification scheme for DCIS correlating it with the incidence of ipsilateral tumour recurrence which identified a subgroup of high-grade DCIS with worse prognosis compared to the classic classification system which depends on cytonuclear features only (**Table** 1-5) [67].

Table 1-5 Scheme of new pathological grading system of DCIS

Grade	Pathological features
Low/Intermediate grades	Lesions with low/intermediate grade cytonuclear features only
High grade	Lesions with high grade cytonuclear features and, Non-solid architecture or less than 50% of ducts show central necrosis
Very high grade	Lesions with high grade cytonuclear features and, Solid architecture or extensive (more than 50% of ducts) show confluent central comedo necrosis

Nuclear grade and proliferation index (N+P) grading system is another system for DCIS grading (**Table 1-6**) which showed comparable results to the classic VN grading system when correlated with different clinicopathological parameters [68].

Table 1-6 Nuclear and proliferation index grading system

Grade	Features
I	Nuclear grade 1 or 2 + Proliferation index less than 25%
II	Nuclear grade 3 **or** proliferation index 25% and more
III	Nuclear grade 3 **and** proliferation index 25% and more

Although there are many grading systems for DCIS, the reproducibility and reliability of them are different between pathologists and their expertise in breast pathology, hence working on finding a universal objective scheme for grading

may provide a more convenient method for prediction of DCIS behaviour and understanding its natural history [69].

Low and high-grade DCIS are rarely found together, and low-grade DCIS rarely proceeds to high grade DCIS [54, 70].

Tavassoli and Devilee proposed an alternate grading system for atypical and malignant intraductal proliferations including DCIS. In this system, the term ductal intraepithelial neoplasia (DIN) evolved and a numerical and alphabetical designation employed to specify lesion severity, such as low-grade DCIS is named DIN IC, intermediated grade DCIS is termed DIN II, and high grade DCIS is referred to as DIN III. Although this system has many advantages, it has not been widely accepted in clinical practice [71].

1.2 **Molecular classification of DCIS**

Routine histological classification of DCIS has remained for a long period the gold standard as a prognostic and predictive factor for their behaviour. Recently, with the breakthrough in molecular studies, new classification methods have been developed depending on the molecular signatures of the tumours with ongoing updates and modification upon them [72, 73].

Although molecular classification of DCIS lesions are not widely used in routine practice as the invasive carcinoma classification, they share frequent molecular, genotypic, phenotypic and transcriptomic similarities [73]. Main basic molecular subtypes of DCIS are summarised in **Table 1-7** which rely mainly on oestrogen receptor (ER), progesterone receptor (PR), HER2 and the proliferating marker Ki67 expression.

Table 1-7 Molecular subtypes of DCIS

Molecular type	**Main molecular features by IHC**
Luminal A	ER+/PR+, HER2– and low Ki67 (less than 14%)
Luminal B	ER+/PR+, HER2–/+ and high Ki67 (more than or equal 14%)
HER2 enriched	ER-/PR-, HER2+
Triple negative	Triple negative (ER, PR and HER2)

Using genomic criteria, DCIS can be classified into three groups: 1) group with high level of amplified genes such as *FGFR1, CyclinD1, HER2 and BMP7/BCAS1* besides *TP53* mutation, 2) group with chromosome 1q gain and 16q loss (most lesions in this group are of luminal type) and, 3) group with copy number aberrations [74, 75]. Comparative genomic hybridisation (CGH) studies showed that high-grade DCIS with

amplified *HER2* usually have chromosome 17q gain and low-grade lesions of luminal types usually have chromosome 16q losses [74]. Molecular analysis of DCIS is playing important roles in prediction of its behaviour. Although there is a marked molecular heterogeneity between DCIS lesions, identifying new biomarkers and molecular signatures for these lesions will help in clarifying the dilemma of DCIS and hence their natural history [76].

1.3 **Oncotype DX DCIS**

Oncotype DX DCIS is a multigene reverse transcriptase polymerase chain reaction (RT-PCR) assay to stratify patients into risk groups in order to predict recurrence rate independently from other clinicopathological parameters [77]. The results of the assay are given in a numerical value from 0-100 which are categorised into three risk groups for recurrence (low, intermediate and high). Genes involved in the analysis and score categories are summarised in **Table 1-8.** The Oncotype DX DCIS assay has some limitations including high cost and requiring further validation studies for application in routine practice [78].

Table 1-8 Oncotype DX DCIS assay genes and score

Genes included in Oncotype DX DCIS			
Proliferation genes	Hormone receptor	Metabolism of carcinogens	Reference group
Ki67	*PR*	*GSTM1*	*ACTB (β-actin)*
STK15			*GAPDH*
Survivin			*RPLPO*
CCNB1 (cyclin B1)			*GUS*
MYBL2			*TFRC*
Scores and risk groups of Oncotype DX DCIS			
Low risk group (score less than 39)			
Intermediate risk group (scores 39-54)			
High risk group (score 55-100)			

Certainly, the impact of molecular test costs and their application to a wide spectrum of patients with DCIS need to be analysed in order to maximise their effect on patient management [79]. It will be better to stratify patients with DCIS using a combination of pathologic examination, immunohistochemical studies and molecular analysis. For this reason, identification of ways to minimise the consequence of overdiagnoses has led to new research aiming at recognising potential low risk DCIS and whether surgical treatment is necessary for all patients with DCIS.

1.4 Genetic features of DCIS and its progression to invasive carcinoma

Many studies have been conducted to investigate the genetic alterations underpinning the development of DCIS and its progression to invasive carcinoma [80]. These studies have modified the original model of BC development proposed by Wellings and Jensen [81]. In the latter model, BC develops over a long period of time from a normal terminal duct lobular unit (TDLU) through UDH to ADH to low grade DCIS then high-grade DCIS and ultimately IBC by the accumulation of random genetic alterations [81], **(Figure 1-6)**. The current hypothesis proposes two models; with low-grade DCIS being the precursor of low-grade invasive carcinoma and high-grade DCIS being the precursor of high-grade IBC [82]. To support this view low grade *in situ* and invasive lesions and many of their supposed precursor lesions: flat epithelial atypia (FEA), ADH, atypical lobular hyperplasia (ALH), and lobular carcinoma *in situ* (LCIS) are predominantly ER positive, HER2 negative lesions and are frequently characterised by the shared deletion of 16q and 1q gain [1]. In contrast, high-grade *in situ* and invasive lesions are more frequently ER negative, HER2 amplified, infrequently harbour 16q deletions but rather have more frequent alterations (regions of gains and losses)

and areas of amplifications as determined by CGH and Fluorescent *in situ* hybridisation (FISH) studies. The evolution of intermediate grade disease is less clear and currently no specific genetic alteration can predict with certainty the progression from DCIS to invasion [1].



Figure 1-6: Model of progression from normal breast duct to invasive carcinoma

1.4.1 Progression to invasive carcinoma

The molecular subtypes revealed by comprehensive gene expression profiling of IBC [83] are present at the DCIS stage [74] suggesting the existence of distinct tumour progression pathways for each tumour subtype. Either cell of origin or tumour subtype-specific genetic and / or epigenetic events, or a combination of both, are possible explanations of the existence of distinct molecular subtypes from the early stages of BC development [84] and the respective maintenance of the phenotypic characteristics from DCIS to invasive cancer and from IBC to metastasis in the majority of cases [85].

Phenotypic and genomic analysis comparing DCIS and IBC demonstrate strong similarities between these lesions but

have failed to identify tumour specific signatures [86, 87]. These results support the hypothesis that the progression from DCIS to invasive cancer may not be necessarily determined by specific genetic alterations or their consequences on gene expression profile. An alternative explanation for the lack of a genetic aberration that could be considered a common denominator in the progression from DCIS to invasive cancer is that there are multiple genetic or epigenetic aberrations that might drive progression, and that in each case, specific aberrations occur [80]. In addition, molecular changes in the TME may play a role in the progression from *in situ* to invasive disease [80]. Distinct epigenetic alterations in all cell types during breast tumourigenesis, including tumour epithelial and stromal cells [88]. Epigenetic changes observed in both the stroma and tumour cells may also be different depending on the tumour subtype, putting forward the concept of co-evolution of tumour epithelial and stromal components.

The identification of novel genetic alterations and molecular pathways underlying the progression from DCIS to IBC may help to establish biomarkers that have the potential to distinguish low-risk patients who do not require aggressive treatment and high-risk patients who are likely to progress to IBC [89]. In clinical practice, a proportion of patients presents

with extensive involvement of the breast with DCIS without invasion [90]. Although it cannot be excluded that these cases would progress over time, the DCIS growth pattern suggests that these cases have a limited invasive potential. On the other hand, other patients have a limited amount of DCIS adjacent to an invasive component or multiple foci of invasion, suggesting a high invasive potential. These differences in biological behaviour of DCIS display different alterations at the molecular level [90].

1.5 **Management**

Traditionally, mastectomy was the standard treatment for DCIS. The frequency of mastectomy has increased again recently especially in young patients, those with extensive disease or if radiotherapy (RT) is contraindicated [91]. Currently, the main treatment of DCIS is breast conservative surgery (BCS) followed by RT. Four major clinical trials show the benefit of RT in decreasing the recurrence rate of DCIS (invasive recurrence represents about half DCIS recurrences) by 50% [92-96]. RT showed significant reduction of DCIS recurrence rate after BCS in all DCIS patients whatever the grade, size or resection margins width [97-100]. Whatever the plan for RT after BCS in DCIS, recently published guidelines recommend at least 2mm free resection margins [101, 102].

The value of systemic endocrine therapy (ET) in hormonal receptor positive DCIS patients is not fully clear and some of ongoing studies show promising results in decreasing the recurrence rate in those patients [103-105]. The benefit of adjuvant Tamoxifen in DCIS patients treated with lumpectomy was investigated in two clinical trials, the United Kingdom, Australia and New Zealand DCIS (UK/ANZ DCIS) trial [106] and the National Surgical Adjuvant Breast and Bowel Project (NSABP) B-24 trial [96]. A meta-analysis of the two trials [107] reported an overall reduction in both ipsilateral and contralateral *in situ* recurrence risk and lower risk of contralateral invasive disease with Tamoxifen treatment [108].

While the reporting of ER status is variable in clinical practice, it is recommended by the National Comprehensive Cancer Network (NCCN) that this will likely be a mandatory additional requirement [109]. The evaluation of ER in addition to providing prognostic information has predictive utility. Therefore, the National Institute for Health and Care Excellence (NICE) has updated the recommendations for adjuvant ET for DCIS to offer it after BCS for women with ER-positive DCIS if RT is recommended but not received; and to consider ET after BCS for women with ER-positive DCIS if RT is not recommended [110]. The evidence base for this having

been extrapolated from invasive cancer data. Although the concept of ET for ER-positive DCIS patients who require RT but cannot or choose not to receive it, is obvious as these patients are usually at high risk of disease progression and/or recurrence, this is a relatively small group. In reality, most women who receive ET for DCIS also receive RT and are low risk. Moreover, clinical application of these recommendations means that ER testing would be necessary for all DCIS in order to be considered for management decision. The effect of implementation of such recommendation on clinical practice and the effect on overall patient mortality and morbidity, therefore, should be investigated.

The most recent approach for management of DCIS is active surveillance in patients with very low probability for disease progression. Four clinical trials are now in patients' recruitment stage to compare active surveillance against surgical management in low risk patients and the preliminary results for this are awaited [111-113].

1.6 **Prognostic and predictive factors**

The prognostic and predictive factors for DCIS can be addressed in two separate ways: predictive factors for DCIS recurrence and predictive factors for progression to IBC.

1.6.1 Predictive factors of DCIS recurrence

Although DCIS is a non-fatal disease with mortality rate about nil, half of recurrences of DCIS are invasive disease which are potentially fatal [114], therefore recognition of patients who are at high-risk for recurrence is essential to avoid tumour progression. Current thesis, similar to other studies, focused on identification of potential predictors of DCIS recurrence, mainly as invasive disease, as this reflects the clinical needs for personalised patient management. Recurrence as new *in situ* disease carries extremely low risk of mortality, thus it is not clinically relevant as invasive recurrence.

Some clinicopathological features are associated with increasing risk of DCIS recurrence such as age <40 years old [115], symptomatic patients comparing with screen detected lesions [116] and high mammographic density [117]. Wang *et al.* addressed in his meta-analysis of the predictive factors for DCIS recurrence pathological features associated with increased risk of recurrence such as tumour multifocality, tumour size, comedo necrosis, high nuclear grade and margin status [116]. Omission of RT especially in high-risk patients, is a strong predictive factor for tumour recurrence. Van Nuys prognostic index (VNPI) for DCIS is one of widely used schemes for risk stratification of DCIS patient according to risk of recurrence and hence for adequate management

approaches (**Table 1-9**). However, it shows limitations and lack of validation in some studies [118, 119]. Rudolf *et al.* combined 10 clinicopathological parameters (**Figure 1-7**) to develop a nomogram for prediction of DCIS recurrence which has been validated in other studies [120, 121]. Molecular subtypes play role also in rate of recurrence. Lesions negative for ER, positive for HER2 or showing high proliferation index are more susceptible for recurrence [122]. Lastly, new genomic and transcriptomic studies such as Oncotype DX and copy number variations (CNV) may show significant predictive value for recurrence risk after DCIS and risk stratification of the patients [77].

Table 1-9 Modified Van Nuys Prognostic Index

Score	**1**	**2**	**3**
Tumour size (mm)	≤15	16-40	≥41
Margin width (mm)	≥10	1-9	<1
DCIS grade	Non-high nuclear grade, No comedo necrosis	Non-high nuclear grade, Comedo necrosis present	High nuclear grade With or without comedo necrosis
Age	>60	40-60	<40
VNPI Score and suggested treatments			
Score		**Treatment option**	
Low (score 3, 4, 5)		Excision alone	
Intermediate (score 7, 8, 9)		Excision plus RT	
High (score 10, 11, 12)		Mastectomy	

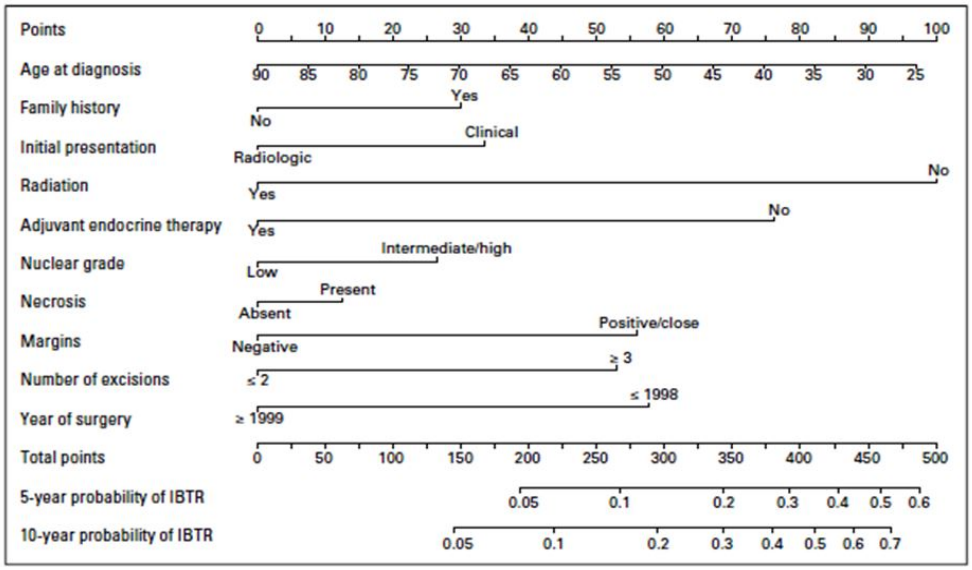

Figure 1-7 Nomogram for DCIS recurrence [120]

1.6.2 Predictive factors for DCIS progression to IBC

Although the natural history of DCIS is not clear as almost all patients are treated surgically after diagnosis [14], some reports show that about 15-50% of DCIS cases will progress to IBC if left untreated within a period of 10 years [123, 124]. Other studies report that low-grade DCIS will progress to low-grade invasive tumour and high-grade DCIS will progress to high-grade invasive tumour in most cases [73]. High-grade lesions, lesions with comedo necrosis, with high mitotic rate and high proliferative index, HER2+ subtypes and with mutated *TP53* are more likely to progress to invasive disease than others [125].

1.7 **DCIS outcome and risk assessment**

Until now, reproducible and robust methods using clinicopathological features to distinguish patients of low risk of local recurrence following BCS alone have not been well established and it is necessary to improve personalised treatment decisions to reduce both over- and under-treatment. Moreover, clinicopathological criteria alone are deficient to clearly and reliably identify individuals with a low recurrence risk [126].

The process of recurrence in DCIS is not well understood, especially progression to invasive recurrence. It is assumed that all ipsilateral recurrences arise as a result of residual carcinoma cells inadvertently left behind after surgery and re-establishing a local tumour. In contrast, contralateral recurrences are assumed to be independent primary tumours. Clinical trial data shows that 10 years after diagnosis of DCIS, there are 4-5 fold as many ipsilateral recurrences (19-31%) compared with contralateral tumours (4-7%) when treated with surgery alone [93, 96, 106].

On the assumption that ipsilateral recurrences are derived from residual primary tumour cells and therefore share a genetic common ancestor (i.e. primary and recurrence are clonally related), biomarker studies mostly seek tumour-

intrinsic features to predict recurrence. These studies have generally been unsuccessful in identifying robust predictors. One reason for this could be that some recurrences are in fact independent primary tumours. Such cases will "contaminate" tumour-intrinsic biomarker studies, reducing the power to detect predictive features.

The ipsilateral recurrence rate after DCIS suggest that women with recurrences have inadequate treatment and/or a breast tissue environment favouring tumour development. Patient management in the latter situation should focus on prevention of new tumours rather than aggressive treatment of the current primary. To solve this clinically significant dilemma the clonal relationship between recurrence and original DCIS needs to be established.

1.8 Tumour microenvironment; components and role in carcinogenesis

Carcinogenesis is a multiplex process with interactions between the growing tumour cells and the surrounding TME [127]. This theory refers to the soil (stroma) and seed (tumour cells) theory which means that a proper microenvironment is essential for tumour growth through crosstalk between both components [128]. The cells within the stroma are relatively genetically stable, in comparison with the tumour cells, and hence they may be targets for therapeutic agents for cancer such as cancer immunotherapy [127]. **Figure 1-8** summarises some of these roles and interactions between both components.

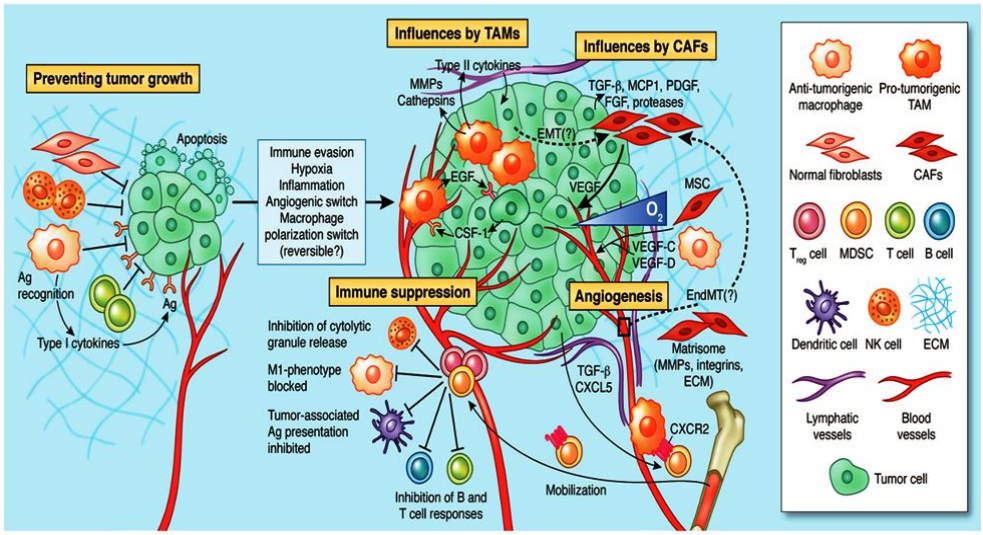

Figure 1-8 Tumour microenvironment and its role in carcinogenesis

Immune system attacks the tumour cells to get rid of it. Tumour antigens play a role during this process, which are recognised by cytotoxic immune cells. Fibroblasts and macrophages within the tumour microenvironment also contribute to this defence mechanism. However, these cells may play also role in tumorigenesis. Tumour associated macrophages promote primary tumour growth, angiogenesis and invasion by secreting proteases, cytokines and growth factor. T regulatory lymphocytes disrupt immune surveillance. Cancer associated fibroblasts secrete extracellular matrix proteins and basement membrane components, regulate differentiation, modulate immune responses, angiogenesis, and contribute to deregulated homeostasis [127].

1.8.1 **Tumour immunity**

Evidence supporting interactions between inflammation and carcinogenesis are derived from relative increased risk of tissue harbouring chronic inflammation to develop cancer, such as hepatocellular carcinoma in context of chronic hepatitis or colorectal cancer in top of ulcerative colitis, and from the tumour infiltrating inflammatory cells (tumour immunity) and their role in tumour regression or progression [129]. A meta-analysis done in 2008 showed that about 15% of tumours are due to infectious causes and concurrent

inflammation [130]. Along with this, impaired immunity is associated also with increased risk of tumour as noticed in patients with acquired immune deficiency syndrome (AIDS) who have high risk for malignant tumours especially Kaposi sarcoma, lymphoma and multiple myeloma [129].

1.8.1.1 Tumour antigens and tumour surveillance from the immune system

There are two types of tumour antigens that may elect immune response against cancer cells. They are tumour specific antigens (specific for tumour cells only) and tumour associated antigens (present in both tumour cells and normal cells) [131]. Examples of these antigens are products of mutated genes, such as *TP53*, overexpressed or aberrantly expressed cellular proteins, such as overexpressed tyrosinase in melanoma cells, products of oncogenic viruses genes, oncofoetal proteins, such as carcinoembryonic antigen and alpha fetoprotein, abnormal cell surface glycolipids and glycoproteins, such as CA-125 and CA19-9, and cell type specific differentiation antigens, such as CD20 in B cell lymphoma [131].

The adaptive immune system of the body is activated against these antigens as an immune response, known as "tumour immunity". The main components of this response are cytotoxic CD8+ T-cell lymphocytes (CTLs), natural killer cells

which recognise cells escaping from T cells and along with CTLs; they play the main role in anti-tumour mechanisms. Tumour associated macrophages (TAMs) also play a role in host defence mechanisms against tumour. In contrast, humoral immunity plays a minor role in tumour immunity. However, in some tumours such as B cell lymphomas, using anti CD20 monoclonal antibody is widely used as a therapeutic agent. Roles of inflammatory cells in cancer are summarised in **Figure 1-9**.

However, there are various mechanisms that the tumour follows to escape from this immune response, tumour evasion of the immune system or Immune Surveillance. Some tumours show "selective outgrowth of antigen-negative subclones'' with elimination of marked immunogenic clones. This theory is supported by experiments in which tumours arising in immunocompromised mice express antigens that are recognised, with consequent elimination of the tumours by the immune system in normal mice, whereas similar tumours arising in immunocompetent mice are non-immunogenic. Another mechanism is the loss or reduced expression of histocompatibility molecules' and hence they escape the attack by CTLs. Some other tumours produce "immunosuppressive'' proteins. For example, Tumour Growth

Factor beta (TGF-β), secreted by many tumours, is a potent immunosuppressant [132].

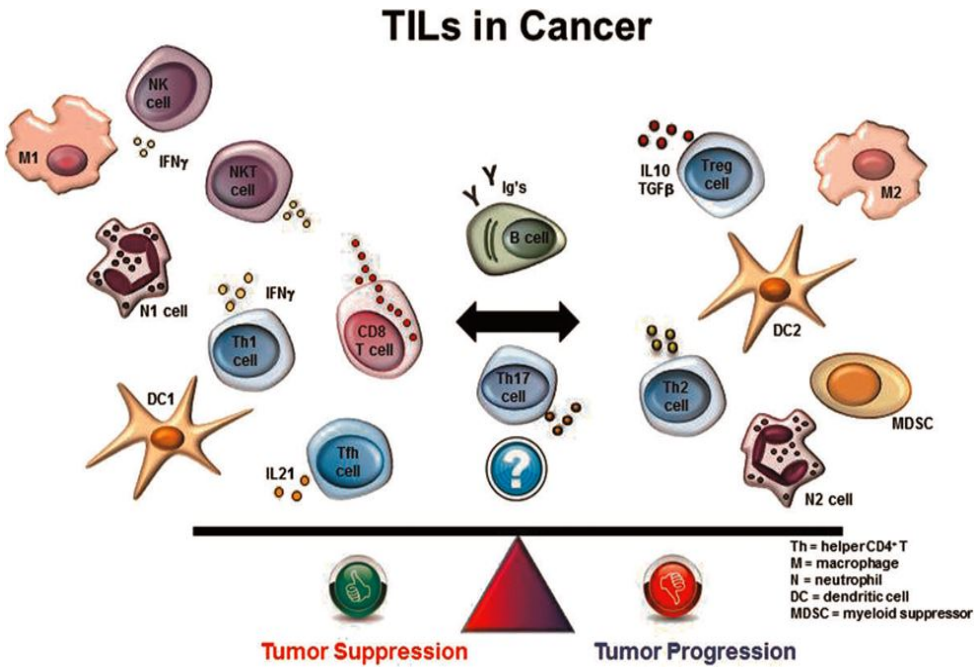

Figure 1-9 Tumour associated inflammatory cells

The cellular crosstalk between different leukocyte subsets and their predominant contribution to either pro- or antitumour activities, including myeloid lineage leukocytes, TAMs with either protumourigenic (M2) or antitumorigenic (M1) properties, helper T-cell subsets, cytotoxic T cells, Treg cells, B cells, dendritic cells and myeloid derived suppressor cells are shown [133]

In other cases, the immune response induced by the tumour may inhibit tumour immunity: co-option of the immune checkpoints [132]. For instance, recognition of tumour cells may lead to engagement of the T cell inhibitory receptor, CTLA-4, or activation of regulatory T cells (Treg) that suppress immune responses. Another example is the PD1/PDL1 pathway in immune response suppression which has promising applications in cancer immunotherapy [134].

Antigen masking is another mechanism for evasion of immune response against tumours. Many tumour cells produce a thicker coat of external glycocalyx molecules, such as sialic acid–containing mucopolysaccharides, than normal cells which block access of immune cells to antigen-presenting molecules. Lastly, "Downregulation of co-stimulatory molecules'' by the tumour cells play a role in tumour surveillance from the host immune system. Co-stimulatory molecules are required to initiate strong T cell responses [131]. Cancer immunoediting theory is the process that defines the interaction between tumour cells and the immune system and usually follows three phases which are elimination, equilibrium and escape [135]. Therapies that reactivate host anticancer immune response show promising results in treating melanoma and lung cancer [136].

1.8.1.2 Tumour associated macrophages and tumour growth

TAMs are an important component of the tumour TME and play important role in tumourigenesis [127]. Although macrophages may play role in tumour immunity, as previously mentioned, they have evident roles in tumour progression especially as a driver for invasive phenotypes [137, 138]. In gliomas, TAMs play an important role in tumour cells invasion through paracrine effect involving tumour derived colony

stimulating factor 1 and macrophage derived epidermal growth factor beside their secretion of cathepsins (proteases) [139, 140]. The dual reverse functions of the macrophages and their switch from tumour suppressors to tumour promotors are not fully understood and may be due to their plasticity from classically activated M1 cells to alternatively activated M2 cells with production of type II cytokines which have tumorigenic activities. Hypoxia may also play role in this transition [141, 142].

1.8.1.3 Role of myeloid derived suppressor cells and T regulatory cells

As mentioned before, immunosuppressive protein secretion is one of the methods that a tumour uses to evade the host immune system. Myeloid derived suppressor cells (MDSCs) and Treg are among cells which help in immunosuppression. MDSCs are present in normal tissues and are mobilised to malignant tissues during tumourigenesis. Beside their role in immunosuppression, through disruption of the tumour antigens presentation to cytotoxic cells, alternative activation of macrophages and inhibition of natural killer cells, they play also role in tumour vascularisation [143-146]. Treg are T lymphocytes which play role normally in immune response homeostasis through actions on T and B effector lymphocytes [147]. They play a promoting effect during tumourigenesis

and they have a poor prognostic impact in various types of cancer [148, 149]. In contrast, they are associated with good survival in colorectal carcinoma [150]. They share similar functions to MDSCs but their heterogenic roles in carcinogenesis is not fully understood [151].

1.8.2 **Cancer associated fibroblasts**

Fibroblasts are the cornerstone in homeostasis of the body tissues through extracellular matrix (ECM) production, BM deposition, epithelial cell differentiation and immune response modulation [152]. Cancer associated fibroblasts (CAFs) are different from normal fibroblasts as seen in a model when they induce prostatic neoplasia when injected into mice in contrast to the normal cells [153, 154]. The exact origin of CAFs is unclear and they may be derived through endothelial to mesenchymal transition (EndMT) or from epithelial mesenchymal transition (EMT) [155, 156]. Activated CAFs produce growth factors which support the tumour vasculature and maintenance [157]. CAFs additionally produce pro-inflammatory factors that promote tumourigenesis [158].

1.8.3 **Extracellular matrix and tumour progression**

ECM limits the progression of tumours in their early stages and on the other hand can promote their progression in late stages [127, 159]. Matrisome is the term applied for the protein

composition of ECM surrounding certain tumours [160] which plays a vital role in the metastatic potential of a given tumour.

1.8.4 **Tumour vasculature and angiogenesis**

Angiogenesis is one of the hallmarks of carcinogenesis [161]. Tumour vascularisation requires co-operation of multiple TME cell types, including vascular endothelial cells, pericytes and BM derived precursor cells, which are often regulated by hypoxia with contribution of TAMs, CAFs and mesenchymal stem cells [162-164]. Lymphangiogenesis is another mode of vascularisation in tumours, and lymphatic vessels represent an alternate route for cancer cell dissemination [165]. Activated macrophages produce vascular growth factors and receptors, which correlates with peritumoural inflammation and lymphangiogenesis in human cervical cancer [166].

1.9 **Tumour microenvironment of breast cancer**

Growth of BC cells requires adequate crosstalk signalling between the tumour parenchymal cells and the components of the TME for maintenance of its growth and progression [128]. Studies aiming to clarify the role of TME in progression from DCIS into IBC continue with promising results [167]. In the following sections the components of TME in BC and their roles in DCIS and IBC will be highlighted.

1.9.1 **Immune response in breast cancer**

BC parenchyma is usually infiltrated by immune cells which represent both innate and adaptive immunity. These cells have contribution to either pro- or anti-tumour activities (**Figure 1-9**). The myeloid lineage leukocytes, such as TAMs, and MDSCs, play a central role in shaping the TME towards either tumour suppressor milieu or tumour-promoting milieu. In 2014, the international tumour infiltrating lymphocytes (TILs) Working Group recommended an evaluation scheme for TILs in routinely stained sections of IBC tissues based on meta-analysis of numerous studies about intratumoral and stromal TILs evaluation using either immunohistochemistry techniques or routinely H&E stained sections [133]. These recommendations are applied on IBC and recently was recommended for DCIS and other solid tumours Reference not added here.

1.9.1.1 Tumour associated macrophages

Studies on TAMs in BC reveal their role in tumour invasion through paracrine signalling effect in addition to production of proteolytic enzymes which may play a role in progression form DCIS into invasive disease [168]. Removal of macrophages from mice reduce the rate of progression and almost ablate its ability to invade, so there is a strong relation between increased density of macrophages with the tumour and the

poor prognosis [138]. Macrophages usually accumulate within the hypoxic areas in BC tissue which in turn alternatively activate them to produce M2 cells and promote their pro-tumourigenic actions [142]. Moreover, they help in angiogenesis and provide a nutritional source for the tumour and hence promoting progression [142]. Although assessment of macrophages is not recommended by the recent guidelines of the International Working Group, they mentioned that evidence is developing to support their importance in tumour behaviour [133].

1.9.1.2 Humoral and cell-mediated immunity

The better prognosis of some IBC types, such as medullary carcinoma, gives a clue for the role of dense TILs in the anti-tumour response [169]. Dense infiltration of tumour tissue by CTLs is associated with better prognosis [170]. The role of CD4+ T helper cells is more complicated due to diversity of these cells. Th1 cells, which produce interferon-γ, are associated with good prognosis in contrast to Th2 cells which are associated with poorer outcome due their inhibitory effect on the anti-tumour immune response [171, 172]. The CD4+/FOXP3+ Treg role is alternating between a good or bad prognostic factor in studies and is related to ER status within the tumours [148, 173, 174]. Th17 cells, producers of the pro-inflammatory interleukin 17 cytokine family, appear to have

variable effects depending on the surrounding cytokine milieu, which may in part be linked with the organ site and tumour type [175]. Role of humoral immune cells (B lymphocytes) is not so clear in BC [176]. A study comparing immune cells densities in DCIS and IBC concluded that lymphocytes may play role in early stages of BC development which need further investigation [177]. Similar results are reported with correlation of dense inflammatory cells in DCIS with poor prognosis or association with a high Oncotype DX score [77, 178].

1.9.1.3 Immune checkpoint proteins

BC cells produce proteins which inhibit the host anti-tumour response directly or indirectly through activation of Tregs [132]. In other words, they co-opt the immune check points in the body so that they recognise tumour cells as normal host cells. Example of these proteins are Cytotoxic T lymphocytes associated molecule 4 (CTLA4) and programmed cell death ligand-1 (PDL1) which bind to CD86 and PD1 receptors on T cells, respectively leading to their inactivation and tumour immune surveillance [179, 180]. Recently, multiple studies are carrying on the role PD1/PDL1 pathway in BC and its association with Treg lymphocytes and clinical application in cancer immunotherapy [136, 179, 181-184]. In DCIS, one study showed that lesions showing high PDL1 expression in

TILs are triple negative and involving younger patients which may reflect their poor prognostic effects [178].

1.9.2 **Cancer associated fibroblasts and breast cancer**

CAFs are one of the most important components of the BC TME [185]. CAFs are distinct from normal fibroblasts which are mainly in increased expression of fibroblastic markers such as, fibroblast-specific protein 1 and fibroblast-activating protein, and matrix metalloproteinase 3 (MMP3) along with cytokines and growth factors [185]. Lesions surrounded by CAFs are more liable to invade and metastasise [186]. Using an integrative strategy with 3D cell culture of tumour spheroid, clinical samples and xenograft mouse models showed that the Tiam-1 osteopontin pathway in CAFs mediates invasive behaviour of the BC cells and inhibition of this interaction could prevent their metastatic potential [187]. Malignant epithelial cells acquire a mesenchymal phenotype when cultured with CAFs, supported with an increase in mesenchymal cells markers and a decrease in epithelial cell markers, through actions of TGF-β [186]. Another mechanism for such actions, supported through study of murine BC models, is the modulation of the immune TME including TAMs, Treg cells and MDSCs which enhances tumour growth and angiogenesis

[188]. Studies on CNV between normal stromal cells and CAFs show that the tumour associated stromal cells acquire copy number gain in genes related to tumour invasion and proliferation and this supports their role in tumorigenesis and progression [189, 190]. Paracrine signalling by interleukin 6 between DCIS cells and CAFs is thought to be a crucial factor in the initiation of DCIS progression to IBC through activation of JAK/STAT pathway [191]. Furthermore, secretion of the chemokine CXCL12 by CAFs may promote angiogenesis and increase cancer cell proliferation [192].

1.9.3 Extracellular matrix in breast cancer

ECM plays an important role in BC. Analysis of the Matrisome has resulted in the classification of IBC tumours into four groups according to ECM signatures and their relationship with the tumour behaviour. For example, tumours with high expression of protease inhibitors (e.g. serpin family members) in their ECM are associated with good prognosis, while tumours with high expression of integrins and MMPs correlate with poor prognosis and risk of recurrence [159]. Assessment of the ECM by picrosirius red staining revealed that the ECM deposited in the presence of CAFs was not only more abundant, referred to as ECM stuffiness, but also more aligned [193]. These data suggests that the aligned ECM deposited by the CAFs could be used by tumour cells as tracks to invade

and disseminate [186, 193]. Moreover TME can contribute to tumour resistance to therapy through different mechanisms such as; dense ECM or limited blood flow may limit drug delivery to tumour cells, activation of survival pathways through ECM-epithelial cells interactions may lead to acquirement of resistance through genetic changes, secretion of pro-survival factors by stromal cells [194]. A study showed that tumour associated collagen signature-3 (TACS-3) is correlated with poor outcome in IBC. TACS-3 is characterised by bundles of straightened and aligned collagen fibres that are oriented perpendicular to the tumour boundary [195, 196]. Myxoid stroma also around DCIS may play role in increased incidence of tumour recurrence [197, 198].

1.9.4 **Endothelial cells and angiogenesis in breast cancer**

Endothelial cells (ECs) line the inner wall of blood vessels and play a role in controlling the diffusion of nutrients into tissues from blood, maintaining flow of blood and also regulating the migration of leukocytes [199]. Unlike normal ECs, tumour ECs are irregular in shape, size and comparatively long, participate in intussusceptive angiogenesis, the process where trans-vascular extension of the vessel wall in the lumen split the vessel into two halves and it is a rapid process than sprouting

to increase the vessel density in TME [199]. These abnormalities may lead to tumour hypoxia which induces various vascular growth factor mediated angiogenesis to support growth and metastasis of cancer cells [200]. ECs are also a main source of mesenchymal stem cells.

1.9.5 **Myoepithelial cells and breast cancer**

The ducto-lobular system of the breast is lined by two cell layers: the inner epithelial and the outer myoepithelial. MECs are spindle shaped cells oriented parallel to the long axis of the ducts and form a continuous layer around the luminal inner cells. They have contractile functions and ultra-structurally they contain smooth muscle filaments to help milk ejection through breast ducts [201]. They also express intermediate filaments like epithelial keratins and form desmosomes, gap junctions with cadherin mediated interactions between each other besides hemi-desmosomes formation with the BM [202-205] (**Table 1-10 and Figure 1-10**).

Table 1-10 Markers of normal myoepithelial cells

Some of normally expressed myoepithelial protein markers	
CK5	P-cadherin
CK14	α1 Integrin
Vimentin	α6 integrin
α-Smooth muscle actin	β4 integrin
Calponin	Connexin-43
Maspin	Laminin

MECs are not only participate in the milk ejection process but they have diverse functions. They play a role in regulation of normal breast tissue morphogenesis through paracrine signalling and formation of normal basement membrane components [205]. MECs under normal conditions are tumour suppressors through different mechanisms apart from being normal physical barrier against tumour cells invasion beyond the breast ducts [185, 206]. MECs express many ECM structural proteins (such as fibronectin and collagen), proteinase inhibitors (Maspin), angiogenic inhibitors (thrombospondin-1) and accumulate ECM rather than degrade it [207]. Moreover, myoepithelial cells express tumour suppressor genes (**Table 1-11)** [208].

Table 1-11 Tumour suppressor genes expressed by myoepithelial cells

Tumour Suppressor gene	Function
α-Smooth muscle actin	Cytoskeletal structure; suppress cell growth and motility
Cytokeratin- 5	Cytoskeletal structure; regulates cell growth
α6 integrin	ECM receptor
Caveolin-1	Regulation of cell growth
Connexin-43	Gap junction protein
Maspin	Protease inhibitor
TIMP-1	Protease inhibitor
Relaxin	Hormone-regulation, cell growth
Activin	Hormone regulation

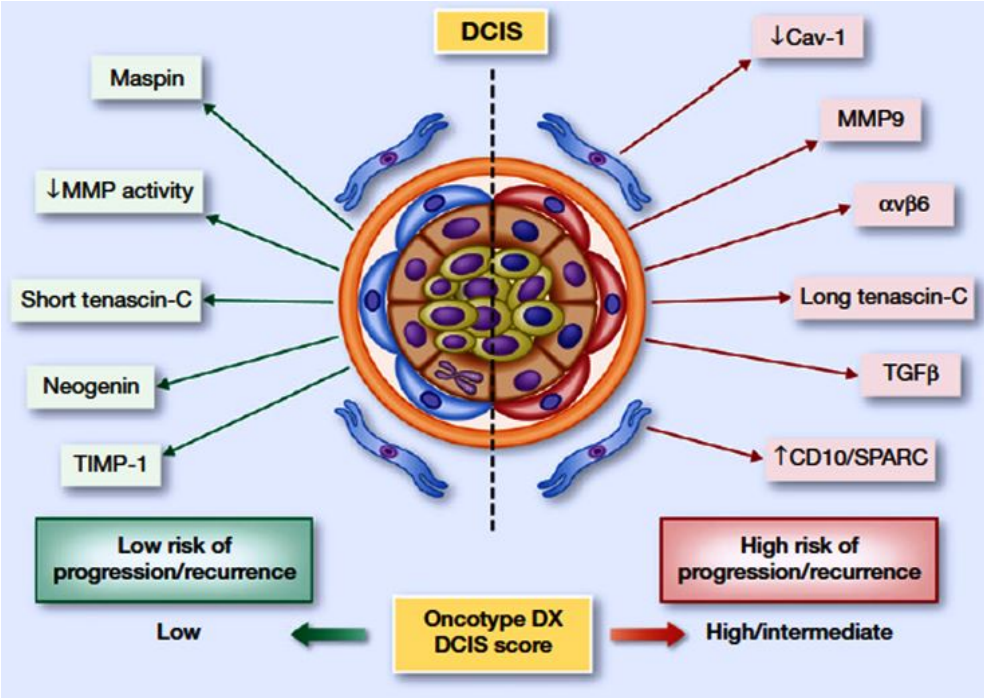

Figure 1-10 Role of Myoepithelial cells in breast cancer [204]

Other studies show that myoepithelial conditioned media inhibits the growth of BC cell lines through G_2/M cell cycle arrest [209]. Proteases inhibitors produced by MECs inhibit

tumour invasion beside their function in growth and angiogenesis suppression as well [210]. Although MECs have tumour suppressor functions and they remain intact in DCIS, they appear to be distinct genetically from the those lining normal ducts **(Figure 1-11)** and secrete many chemokines which were implicated in the induction of tumour cell growth and metastasis [211, 212]. Gudjonsson *et al.* showed that 20% of carcinomas in which MECs were present expressed little or no laminin-1, and that purified cancer MECs were unable to polarise luminal cells in three-dimensional collagen assays [213].

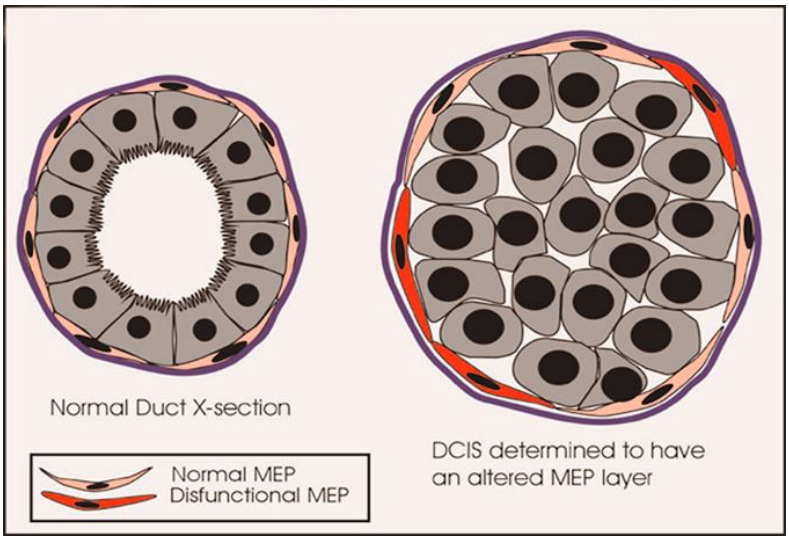

Figure 1-11 Myoepithelial cells in normal breast duct and DCIS

In the normal breast MECs are located between the luminal cells and the BM. In DCIS the myoepithelial layer is still present. Recently it was showed that there appears to be molecular differences between MECs present in normal breast versus DCIS lesions [211]

The exact mechanism of how tumour cells of DCIS invade the myoepithelial layer and the BM to the surrounding stroma is

not fully understood and two main theories are proposed; the first depends on proteolytic enzyme action and degradation of these barrier layers to invade while the other one suggests that a genetic defect in the MECs due to genetic abnormalities (mutations), inflammation or any physical or chemical injury leading to partial disruption of the myoepithelial layer and hence the tumour cells make their way to the surrounding stroma [214, 215].

1.9.6 **Effects of breast cancer on tumour microenvironment**

The previous sections demonstrate briefly the roles of TME elements in BC tumorigenesis and progression. However, the tumour cells themselves interact with the TME in several ways to modulate the host immune response and to invade the surrounding BM and stroma to invade the involved tissue parenchyma. The following sections discuss, in short, some of these interactions that help invasion of the tumour cells to surrounding stroma which play a main role in progression from DCIS to IBC and from localised invasive disease to metastatic behaviour.

1.9.6.1 Degradation of basement membranes and invasiveness to surrounding tissues

One of the hallmarks of any malignant tumour is its ability to invade the resting BM and the surrounding tissues [161]. Epithelial malignant cells express numerous proteolytic enzymes such as MMPs and cathepsins that facilitate the degradation and invasion of the surrounding tissues [216, 217]. Recent studies on CNV showed a significant difference between these genes between normal, DCIS and IBC epithelial cells [218-220].

1.9.6.2 Epithelial mesenchymal transition and its role in tumour progression

The recent breakthrough in understanding the mechanisms of EMT helps in clarifying the metastatic capability and also the unusual phenotype of some tumours [221]. EMT also plays role in formation of the tumour surrounding stroma [156]. In DCIS, some studies showed the role of EMT in tumour progression to invasive disease [222]. The EMT gene profile is highly expressed in IBC cases with DCIS rather than pure DCIS cases which may implicate their role in disease progression [222].

Lastly, despite the importance of DCIS TME, which has been addressed earlier, the current practice does not include any note on stroma during reporting of DCIS cases. The current

and proposed pathological profiles of DCIS [185] are summarised in **Table 1-12**.

Table 1-12 Current and proposed profile of DCIS reporting

Current profile	**Proposed profile**
Clinicopathological factors: - Age - Morphological factors: Grade, size, necrosis, margin status - Hormonal profile: ER/PR expression Stromal factors: - None	Clinicopathological factors: - Age - Morphological factors: Grade, size, necrosis, margin status - Hormonal profile: ER/PR expression - Basal-like phenotype - Oncotype DX DCIS Stromal factors: - Measurement of stromal stiffness - TILs - Myxoid stroma - Stromal protein expression

1.10 **Hypothesis and aims of the thesis**

The hypothesis of this thesis is:

There is a dynamic interaction between malignant epithelial cells of DCIS and the different components in the surrounding TME which plays a role in DCIS progression and recurrence especially the invasive recurrence. Molecular characterisation of the DCIS microenvironment can facilitate prediction of DCIS behaviour and further our understanding of the molecular events underlying DCIS progression and recurrences. Scrutinising the expression patterns of these biomarkers will explain at the translational level DCIS heterogeneity and act as useful prognostic or predictive tool and the intention is to design the simplest robust system for DCIS prognosis suitable for use in routine clinical laboratories.

Therefore, this thesis aims to:

Characterise the phenotypic and molecular features of DCIS microenvironment and correlate them with the clinical outcome in order to predict DCIS behaviour in routine clinical practice. The ability to distinguish patients with DCIS at high or low risk of recurrence, particularly invasive recurrence, would facilitate personalised patient management.

In this context, the thesis aimed to determine the clinicopathological and molecular characteristics of DCIS TME associated with recurrence in women with DCIS.

The specific aims of this thesis are:

1- Collect a large series of DCIS diagnosed in Nottingham over 20 years' period with linked clinical information and follow up and outcome data.
2- Construct Tissue Microarrays (TMAs) from representative sections of pure DCIS lesions and a control group of DCIS associated with synchronous IBC.
3- Correlate the clinicopathological characteristics of the study population with patients' outcome.
4- Characterise the DCIS cohort according to the molecular classification of BC.
5- Assess the role of TILs and immune checkpoint proteins in DCIS.
6- Perform quantitative assessment to study the expression pattern of novel selected biomarkers that related to ECM remodelling and degradation to assess the likely predictive biomarkers that might predict the risk of invasive/non-invasive progression/recurrence of DCIS.

7- Perform quantitative assessment of the geometric characteristics of collagen surrounding DCIS and their prognostic impact.

8- Assess the role of hypoxia in DCIS behaviour and study the underlying mechanisms that hypoxia, as a TME factor, could affect DCIS behaviour mainly through its association with centrosomal aberrations and genomic instability.

2 CHAPTER 2: Patients and methods

2.1 **Patient cohort and data collection**

2.1.1 Pure DCIS cohort identification

A cohort of pure DCIS cases that were diagnosed between 1987-2017 at the Nottingham Breast Institute was identified (n=1,249). Cases associated with invasive or micro-invasive carcinoma were excluded. Cases with multiple specimens or who underwent multiple operations to excise the primary tumour, were considered to have a single primary tumour surgical episode and the size of any residual DCIS identified in the re-excision specimens was added to the size of tumour in the originally excised specimen to estimate the final tumour size. Clinicopathological data including age at diagnosis, mode of DCIS presentation either screen-detected or symptomatic, size of the lesion, nuclear grade, presence of comedo type necrosis, DCIS morphological type and associated Paget's disease, were retrieved from patient records. Management options including primary operation type (BCS vs mastectomy), margin status, re-excision surgery and its type, presence of residual DCIS in the re-excised specimens and the final operation together with RT data were also retrieved. None of the cases included in this thesis received ET.

Resection margin status data was further categorised based on recent recommendations for DCIS; i.e. positive margin

including tumour on ink and less than 2mm free margins, and negative margin (≥2mm) [101, 102]. For comparison purposes, the cohort was further split into two groups; those diagnosed between 1987-2008 (n=803) and 2009-2017 (n=446). This was based on the local institutional guideline change with regard to margin of excision, in 2008, with acceptable free margin after BCS in DCIS of 5mm instead of 10mm [223]. Although, the service currently follows the new guidelines published in 2016 that recommend 2mm as optimal free margin in DCIS, cases managed in 2016 and 2017, were included in the latter group to avoid bias in statistical analysis. VNPI was assessed for all cases treated with BCS after the first operation and the risk score was estimated.

Data on local ipsilateral tumour recurrence including type of recurrence, and local recurrence free interval (LRFI) were also collected. LRFI was estimated (in months) and defined as any event of ipsilateral tumour recurrence (either as DCIS or invasive disease) that occurred after 6 months from the first DCIS surgery. Any operation within the first 6 month of the primary operation due to positive or close surgical margins was considered as re-excision of residual primary tumour and not as a recurrence event. Contralateral breast carcinoma either DCIS or invasive were not considered as recurrence and were censored at the time of occurrence of the contralateral event.

Data collection and validation was performed mainly by the author.

Frequencies for clinical and pathological parameters of pure DCIS cases are included in **Table 2-1**.

Table 2-1: Clinicopathological characteristics of pure DCIS cohort

Clinicopathological parameter	Number (%)
Age at diagnosis (Years)	
≤ 50	266 (21)
> 50	983 (79)
DCIS Presentation	
Screening	748 (60)
Symptomatic	501 (40)
DCIS Size (mm)	
≤ 20	632 (51)
> 20	610 (49)
DCIS Grade	
Low	156 (13)
Intermediate	333 (27)
High	760 (60)
Comedo type necrosis	
Present	840 (67)
Absent	409 (33)
Management*	
BCS	642 (51)
Mastectomy	606 (49)
Radiotherapy**	
Yes	263 (41)
No	379 (59)
Recurrence	
DCIS recurrence	35 (3)
Invasive recurrence	62 (5)
No	1150 (92)

*Final operation type
**For patients treated with BCS
BCS: Breast conserving surgery

2.1.2 Mixed DCIS and IBC cohort identification

Another cohort of 239 cases of DCIS associated with co-existing synchronous IBC was also identified. These cases were

used as comparable cohort for the study targets between pure DCIS cases and DCIS associated with IBC. These cases were diagnosed within the period from 2000-2007 as cases before 2000 were already included in other studies and most of their blocks were unavailable. Selection of these cases was random and depended on the availability of tissue formalin fixed paraffin embedded (FFPE) blocks and the burden of both tumour (the invasive and DCIS) components within the blocks.

2.2 **TMA Construction**

The TMA technique brings revolutionary changes in high-throughput analysis by being able to handle up to several hundred samples in one slide with subsequent application of techniques such as immunohistochemistry (IHC) to allow a diverse range of biomarkers to be studied [224]. Using TMAs saves a considerable amount of tissue, time, and reagents, while attaining more standardised laboratory conditions across samples [225]. TMAs can make working with and evaluation of IHC and other staining protocols faster and easier [226, 227]. The steps of the TMA production included: collection of the study cohort to be arrayed, preparation of the recipient array blocks, designing the array grids, construction of the individual array blocks, and preparation of the array block for sectioning [228]. The initial tasks of preparing donor blocks and TMA

design are the most critical parts of TMA construction and are therefore quite time consuming. TMA construction was performed mainly by the author.

2.1.3 Collection of the study cohort and preparation of the donor blocks

Searching for DCIS cases was done through different data storage pathology systems. Pulling and reviewing slides for both DCIS cohorts was executed to select suitable cases for TMA construction. Using light microscopy, H&E stained tissue sections were thoroughly scanned to select the most appropriate area of tumour, avoiding necrotic tumour zones.

A representative FFPE tumour block (donor) for each of patient's specimen was retrieved from the tissue block archives. Priority was given to blocks containing viable tumour tissue with acceptable tumour burden and that had not been frequently sectioned for previous studies (not less than 4mm in depth). A fresh full-face section of 4μm thickness was cut from each block and stained with H&E and each slide was further reviewed by the author using light microscopy to confirm the presence of the tumour and to identify the most representative areas suitable for array sampling. In cases where the block did not contain tumour, insufficient tumour, or was thinner than 4mm, an alternative archive block for the

patient was retrieved. Some cases were omitted from the arrays because either block was thin or contained no/insufficient tumour with no alternative blocks in the archive to ensure that we do not deplete the patient's diagnostic materials. The total final number of blocks that were used in the pure DCIS TMA construction was 1042 blocks representing 778 pure DCIS cases. Some cases (n=264) were presented by more than one block thus the TMA contained 2 or 3 cores for these cases. However, the cases with more than one core was considered as a single case in the final analysis and the average expression of a certain marker used in this thesis was considered for these cases. Although the number of cases included in the TMA was different from the cases' number originally identified, this did not introduce any bias during data analysis, as the exclusion was random, and various comparison statistical tests showed no significant difference between cohorts. For the mixed cohort, 239 blocks containing both components were used for the TMA construction.

2.1.4 Slide digitalisation and image acquisition

High resolution digital slide scanning was achieved with the Pannoramic digital slide scanner (250 Flash III, 3DHISTECH®, Budapest, Hungary), at 20x magnification. This was followed by viewing the images using Pannoramic Viewer software v

1.15.4 (3D HISTECH®, Budapest, Hungary) to check the quality of the scanning.

2.1.5 TMA construction of pure DCIS cases

2.2.1.1 Construction protocol

The most suitable FFPE block from each case was selected based on those harbouring an abundant amount of DCIS and a suitable tissue thickness for arraying. The selected blocks were divided into two sets; 1) blocks which contained only one area of DCIS sufficient to be arrayed and 2) all other blocks which could be arrayed more than once. To increase the probability of tumour sampling with area of surrounding stroma, a TMA core diameter of 2mm was used for those blocks with only one sampling area and a 1mm core diameter was used for the other groups.

2.2.1.2 Digital images marking

Using the Pannoramic Viewer software v 1.15.4 (3D HISTECH®, Budapest, Hungary), all scanned H&E images were marked for TMA cores. A maximum number of suitable cores for each image were marked (**Figure 2-1**).

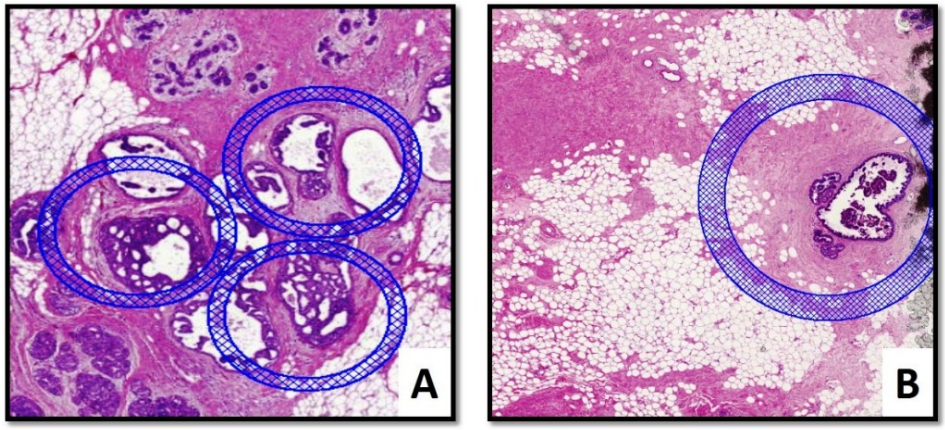

Figure 2-1: Marking of scanned images for TMA construction

(A) 1 mm cores in cases with more abundant tumour tissue. (B) 2mm core in cases with scanty tumour tissue

2.2.1.3 Recipient blocks construction

Two types of recipient blocks were used in the construction. The first one was the ordinary paraffin wax-based blocks used in cases of 1mm tissue core diameter. These blocks were prepared by freshly poured empty paraffin blocks (5-10mm deep) into which the tissue array cores were extruded into. The recipient block was prepared by pouring molten (56-58°C) regular paraffin wax into a mould then a histopathological tissue cassette was placed on top [228]. The complex was cooled on ice until hardened. The wax was checked for presence of air bubbles, striations or stress marks, fault line and that wax covered the entire base of the cassette without surplus wax on the edges or back of the cassette [229]. The block was trimmed smooth to ensure a flat surface using a microtome [229].

The other one was an agarose-based block (**Figure 2-2**) and was used in construction of cases with 2mm tissue core diameter to avoid curling of the cores during cutting. Agarose based blocks were constructed by another PhD student from our group using 2-Hydroxyethylagarose (SIGMA-ALDRICH, Cat No. A4018, Lot No. SLBB4989) and empty embedding cassette (Leica, one-piece tissue cassette, Cat No. 380267). The agarose layer was prepared by filling the empty cassettes with molten 2% agarose in distilled water. It was left to solidify in a moist chamber (Petri dish) at room temperature for 15 minutes. The covered agarose cassettes were kept in the moist chamber until transferred to tissue fixation and processing machine to avoid unfavourable shrinkage. Following this, the agarose layers were removed from the embedding cassettes and were embedded on other cassettes and coated with paraffin wax similar to human tissue embedding. The thickness of the agarose-paraffin block between the surface of the embedding cassette and the top surface of the paraffin wax was 4mm.

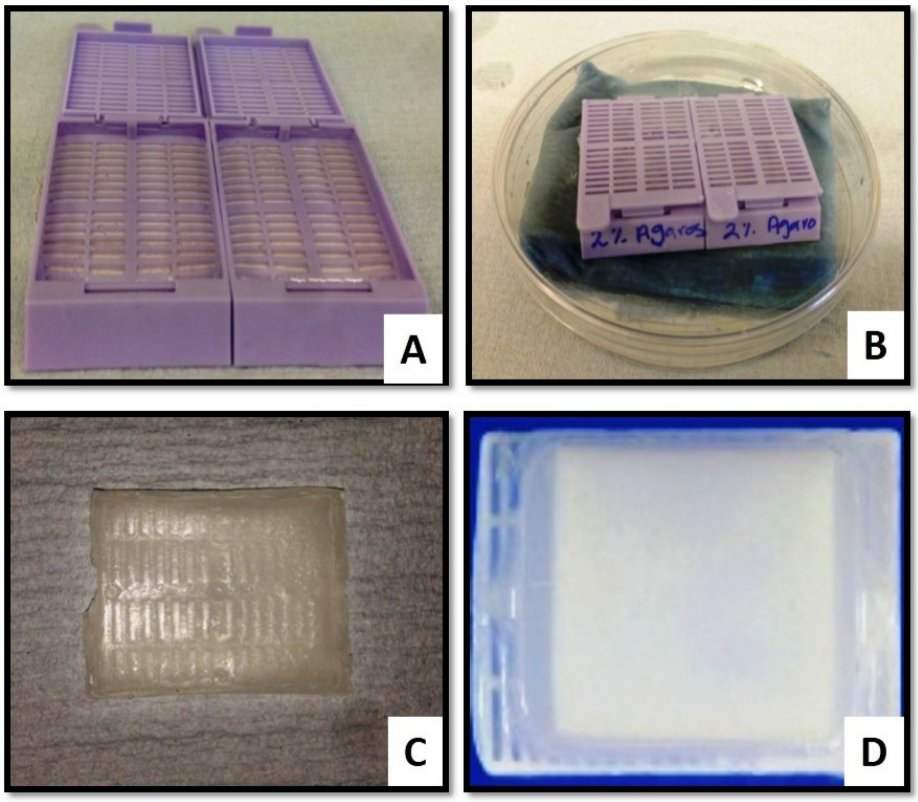

Figure 2-2: Agarose embedding block

(A) Tissue cassettes filled with 2% Agarose, (B) Agarose left in moisture petri dish to solidify. (C) The Agarose layer after fixation and processing, (D) Agarose-paraffin block containing the agarose layer embedded in the paraffin block

2.2.1.4 TMA layout design

Block layout design was performed using the TMA GRAND MASTER 2.4-UG-EN software (3D HISTECH®, Budapest, Hungary). Creation of a new layout followed by insertion of a new layout name was performed. Block size was inserted as a standard of 24x35mm. Core size was set up to 1mm or 2mm accordingly. Six replicate blocks were prepared where possible. Blocks were distinguished by version number added to the block later.

For 1mm core cases, each array was designed to contain 70 samples, with a 1mm gap between each core, arranged in 2 groups (subarrays). The first group representing the upper half of the block contained 42 cores (6 rows, 7 columns), while the second/lower half of the block held 28 cores (4 rows, 7 columns). Cores in each sub-array were arranged at a centred distance and the subarrays were separated by a single gap for orientation and macroscopic identification of the TMA block. Additional orientation cores from normal kidney, liver and tonsil tissues were included outside of the geometric margin of the array on the top and bottom left-hand side. The orientation cores served as positive internal experimental controls.

For cases with a 2mm core diameter, a layout of 30 recipient cores was constructed in 6 consecutive rows with 1mm gap between each core with only 3 cores for orientation tissues in the bottom left hand side. **Figure 2-3** shows the layouts used for the pure DCIS cohort TMA construction.

Great care was taken during documentation of both the donor block and the TMA position of each individual core. An array map grid was produced for each array block. Each grid contained a unique identifier and was arranged in the same sequence corresponding to its position in the array block.

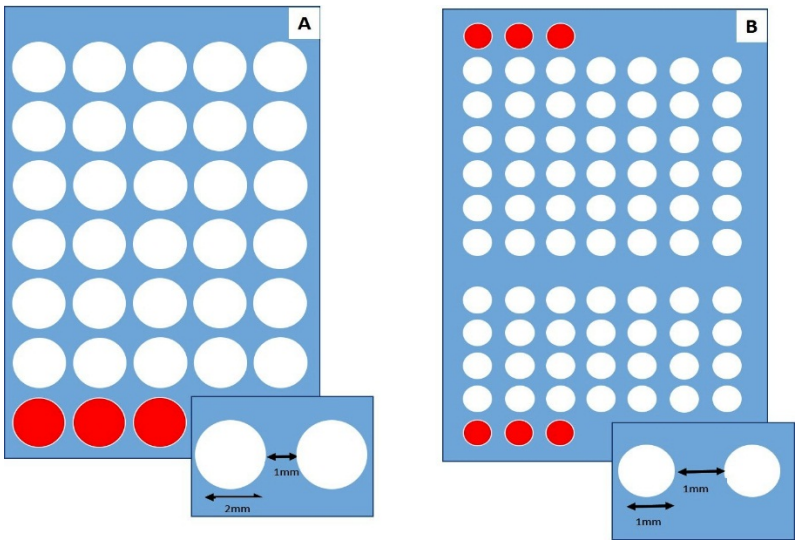

Figure 2-3: TMA layouts

A) Layout of 2mm core diameters recipient block, and B) Layout of 1mm core diameters recipient block

2.2.1.5 Coring process

The automated TMA arrayer was loaded each time by 60 donor blocks and 2 recipient blocks (only one recipient block was loaded during construction cases with only one available core). Labelling the donor blocks with a pseudoanonymised identifier while the recipient blocks were labelled with DCIS1, DCIS2,… DCIS17). Matching and overlying of the scanned and marked images with their related donor blocks was performed using the software before the cores from the donor blocks were automatically sampled and embedded into recipient blocks. To secure the functionality of agarose, holes at least 2mm away from the agarose tissue edges were created. **Figure 2-4** summarises the process of TMA construction.

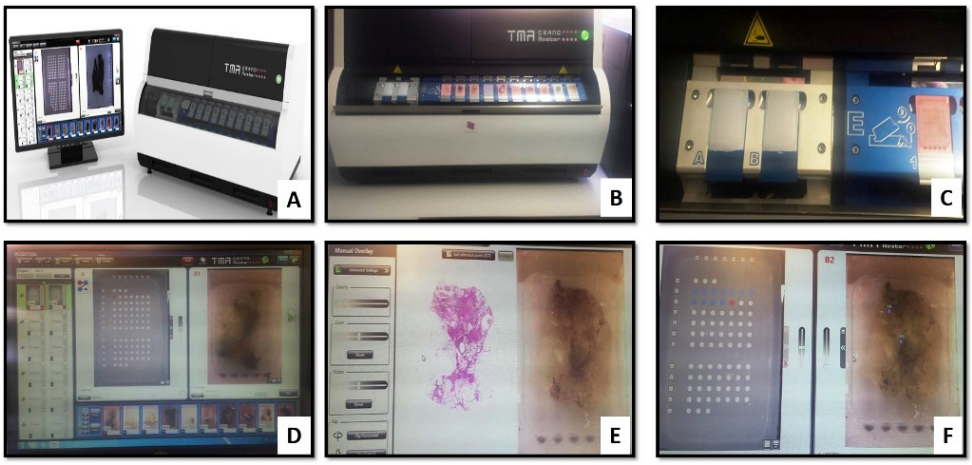

Figure 2-4: TMA construction process

A) TMA machine and screen, B) Loaded machine with donor and recipient blocks, C) Blank recipient blocks loaded in TMA machine, D) Screen showing images of donor block (right one in the screen and recipient block (left one) mapped with selected layout , E) Matching the scanned images with the relevant donor block, F) Marked suitable sites for coring in donor block

2.2.1.6 TMA blocks' annealing and sectioning

After construction of the TMA blocks, they were annealed to promote adherence of the tissue cores to the walls of the holes in the array block and making the wax flexible to handle. This is important because levelling maximises the number of sections containing all the samples in the array. The blocks were placed facing upward in an oven at 37°C for 3 hours. A clean glass microscope slide was used to level the face surface of the block where the glass slide was placed on top of the block, applying gentle but even pressure to push all the cores on the array to the same level. The blocks were left to cool at room temperature for 3 hours. This cycle of annealing was repeated 3 times. After annealing the blocks, they were kept

at 4°C overnight before sectioning. The agarose-based blocks were annealed through placing the blocks facing upwards within a metal mould over a hot surface at 60°C to allow melting the paraffin wax around the agarose gel without losing the cores. Blocks were allowed to cool and kept overnight at 4°C.

Using a microtome, 4µm sections were cut from TMA blocks onto permanent positive charged glass slides (Surgipath, X-tra™ Adhesive, Peterborough, UK), using the standard microtome sectioning technique. The initial section from each block was stained in H&E for quality control purposes to ensure histology and efficient construction steps (**Figure 2-5**).

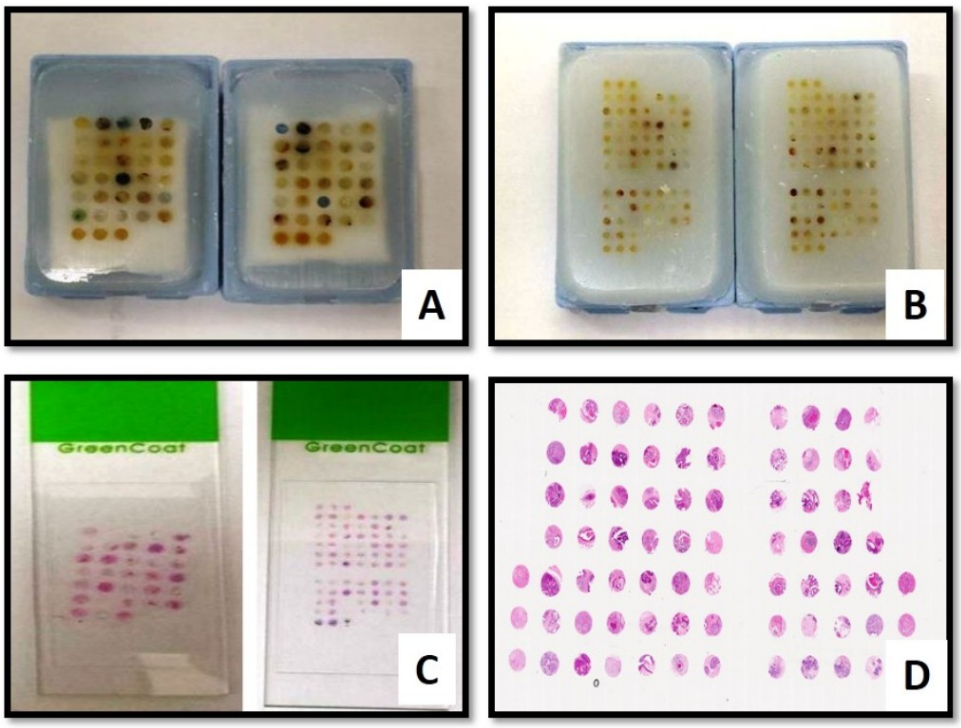

Figure 2-5: Final TMA blocks and stained slides

A and B) Constructed TMA blocks. C) H&E stained sections and E) Scanned section with Nanozoomer scanner (x20)

2.1.6 TMA construction of mixed cohort

The protocol used in TMA construction of the mixed cases was quite similar to the pure DCIS cohort. Marking the images was done using two different circle colour where 1mm diameter was used to mark the DCIS area and 0.6 mm diameter was used for the invasive areas. The latter was used as 0.6mm compared to the routine practice of invasive TMA construction in our research group. Both components were constructed in separate recipient blocks. The DCIS blocks had the same layout of the pure cases (i.e. 70 cores per block plus 6 orientation cores), while the invasive component was constructed using different layout. This layout was designed to contain 150 samples, with a 0.8mm gap between each core, arranged in 3 groups (subarrays). The first group representing the upper half of the block contained 60 cores (6 rows, 10 columns), the middle group contained 50 cores (5 rows, 10 columns), while the third/lower half of the block held 40 cores (4 rows, 10 columns). Cores in each subarray were arranged at a centred distance and the subarrays were separated by a single gap for orientation and macroscopic identification of the TMA block. Additional orientation cores from normal kidney, liver and tonsil tissues were included outside of the geometric margin of the array on the top and bottom left-hand side as usual. The remaining process in term of coring, annealing of

the blocks, sectioning and staining are similar to the pure DCIS and as described earlier.

2.3 **Literature-based selection of biomarkers**

A plethora of studies have been conducted to unravel the diverse molecular and biological nature of DCIS and its progression to invasive carcinoma. As it was hypothesised that there is a role for the TME and the biomarkers responsible for ECM remodelling and degradation in DCIS behaviour, the literature was mined to identify novel biomarkers to study their role in DCIS outcome and progression. A thorough review of literature was performed regarding different proteins and molecular markers closely relevant to ECM remodelling, degradation and EMT in published studies that used different techniques and tissue platforms. Studies conducted using gene microarrays, *in-vitro* studies utilising *in situ* and BC cell lines, *in-vivo* animal models for inoculates from BC cell lines of varying malignant/aggressive potentials [190, 193, 211, 230, 231].

The human proteome is composed of approximately 20,500 different proteins resulting from translation of protein-coding genes [232]. Following translation, many proteins are subject to post-translational modifications. The development of cancer is driven by the acquisition of somatic genetic alterations,

including single base substitutions, translocations and CNVs [233, 234]. The genomic instability of cancer cell genome fuels this diversity in cellular proteome.

A powerful way to discover key genes playing causal roles in oncogenesis is to identify genomic regions that undergo frequent alteration in human cancers. CNVs are extremely common in cancer [235, 236]. Therefore, proteins involved in tumour progression are anticipated to be highly diverse, integrated in complex inter-related networks of proteins and molecular pathways. Bearing in mind that some proteins may play a key role in carcinogenesis and tumour progression makes these proteins "master regulatory" proteins. Therefore, a panel of molecular markers of potential role in DCIS progression has been proposed and subject to scrutiny.

Accordingly, the rationale behind choosing certain biomarker out of myriads in literature while omitting others, were based on: A) molecules used to determine the hormonal status of the patients; ER and PR; B) a well-known oncogene used for characterisation of IBC (HER2); C) molecules reflecting the proliferative fraction of the tumour e.g. Ki67; D) proteins that are commonly altered in carcinogenesis e.g. p53 and, E) molecules that might have a role in tumour progression or being involved in the stromal modification and degradation e.g.

Prolyl-4-Hydroxylase A Subunit 2 (P4HA2), Lysosomal protective protein (Cathepsin A), Cathepsin V (CTSV/CTSL2), Legumain (LGMN) and Collagen (XI) alpha-1 chain (COL11A1).

2.4 **Validation of antibody specificity**

Western blotting (WB) was performed to determine the specificity of the antibodies used in IHC, and it was performed by the author. A mixture of cell lysates from 6 cell lines: MCF-7, MD-MBA-231, 293, SKBR3, HeLa, and Jurkat that were obtained from the American Type Culture Collection; Rockville, MD, USA was used to reflect the expression of the selected proteins.

2.4.1 **Preparation of samples, electrophoresis and transfer**

Cell line lysate was prepared in a maximum volume of 30 µl (19.5µl of lysate, 7.5µl of NuPAGE LDS sample buffer (4x), and 3µl of reducing agent, 10x), all reagents were from Novex Life Technologies. This mixture was heated for 5 minutes at 100 °C and left to cool on ice. The prepared sample was loaded onto 10% SDS–NuPAGE (4-12%) or (3-8% Tris-Acetate gels for detection of high molecular weight proteins) (Novex Life Technologies) in 20x MOPS running buffer (Novex Life Technologies) or Tris-Acetate SDS Running buffer 20x (for high

molecular weight proteins). The pre-stained Thermo Scientific PageRuler Plus Protein Ladder 26619, was used as a molecular weight standard (Hi-Mark prestained protein standard for detection of high molecular weight proteins) and gels were run at 150 volts for 90 minutes. Proteins were transferred to a Hybond-P PVDF nitrocellulose membrane by wet transfer and electro-blotting at 30 volts for 1 hour in transfer buffer. For blocking, the membranes were incubated in Phosphate Buffered Saline (PBS, Sigma) containing 0.1% Tween-20 (Sigma, P 2287, Polyethylene glycol sorbitan monolaurate, Polyoxyethylene sorbitan monolaurate, Polysorbate 20) and 5% non-fat dry milk (Marvel dried skimmed milk, UK) for 60 minutes. The membrane was washed three times with PBS Tween-20 and incubated with the primary antibody overnight at 4°C using the optimal concentration as instructed by the manufacturer (**Table 2-2**).

Membranes were washed with PBS Tween-20 (3 x 5 minutes) and incubated with the secondary antibody; fluorescent secondary antibody was used (anti mouse or anti rabbit, Licor Biosciences). The membrane was washed three times with PBS Tween-20. For fluorescence, the membrane was visualised using Odyssey Infrared Imaging System (LI-COR Biosciences, Nebraska, USA). Mouse β-Actin (A5441, Sigma-Aldrich; Clone AC-15; Sigma, UK) or Rabbit β-Actin (SAB5600204, Sigma-

Aldrich; Clone RM112; Sigma, UK) were used as a house-keeping protein at concentration of 1:15000, according to the primary antibody species.

Table 2-2: Specificity of the selected antibodies for the project

Antibody	Molecular Weight (KDa)	Concentration	Supplier
P4HA2	61	1:500	Abcam
COL11A1	180	1:250	DMXT invasion
CTSV	37	1:500	Abcam
CTSA	51	1:300	Abcam
LGMN	55	1:500	Abcam
B-actin	42	1:15000	Sigma

2.5 **Immunohistochemistry**

2.1.7 Optimisation

Optimisation of the staining conditions for each antibody (**Table 2-3**) was performed by changing several variables in the staining protocol until the optimal result was obtained. These variables include: 1- dilution of the antibody, starting with the dilution recommended by the manufacturer plus dilutions above and below (e.g. in case of recommended 1: 100 dilution, I tried 1:100, 1:50, 1:25, 1:150, 1:200). 2- Antigen retrieval solution: microwave pre-treatment in citrate buffer at pH 6.0, or water bath pre-treatment in EDTA buffer (AR9640, Bond^{TM} Epitope Retrieval Solution 2), pH 9.0. 3- The primary antibody incubation time started with the duration

recommended by the manufacturer, then change the period according to the obtained results of staining.

Ideally, an antibody with specific staining of the cells showing immunoreactivity within the specific cellular location (membranous, cytoplasmic, or nuclear) with no or minimal background staining would allow the most accurate evaluation of its protein expression status. This was obtained through finding the optimum antibody concentration by applying serial dilutions of the antibody to sequential sections of DCIS tissue. All the staining procedures including optimisation were performed by the author except ER staining was performed by the Histopathology Department, Queen's Medical Centre, Nottingham.

2.1.8 IHC technique

IHC was performed on 4µm full face tissue or TMA sections mounted on permanent positive charged glass slides (Surgipath, X-tra™ Adhesive, Peterborough, UK). Unless otherwise stated, for antibodies studied, sections were stained using Novolink™ Polymer Detection System (RE7150-K). To confirm adhesion of tissue sections with the slide surface, sections were placed on a hot plate (60 °C) for 10 minutes and left to cool. Slides were dewaxed in xylene (Genta Medica, York, UK) twice for 5 minutes, rehydrated thrice in Industrial

Methylated Spirit (IMS) or methanol (2 minutes/each) followed by 5 minutes in running tap water. Heat induced retrieval of antigen epitopes was performed, when required, by Whirlpool JT359 microwave (1000 W) treatment of the slides in 1 litre of 10mM sodium citrate buffer (pH 6.0), using full power for 20 minutes. COL11A1 was pre-treated by heated steamer or water bath in EDTA Buffer, pH 9.0. Slides were cooled for 10 minutes under continuous stream of tap water and were rinsed with Tris Buffered Saline (TBS) (0.05 mol/L Tris HCL, 0.15 mol/L NaCl; pH 7.6). Endogenous peroxidase activity was blocked by incubation of the slides in peroxidase block (RE7101, 3-4% hydrogen peroxide) for 5 minutes, protein block (RE7102, 0.4% casein in phosphate-buffered saline, with stabilisers, surfactant, and 0.2% Bronidox L as a preservative) for 5 minutes and primary antibodies, optimally diluted using Leica antibody diluent (AR9352) were added. Each of these steps was followed by washing 3×5 minutes with 0.1% TBS-Tween 20. Post primary block (RE7111, Rabbit anti mouse IgG (<10µg/mL) in 10% animal serum in TBS/0.09% ProClin™ 950) was incubated for 30 minutes followed by 3×5 minutes washing with TBS-Tween 20 0.1% and then Novolink Polymer (RE7112, Anti-rabbit Poly-HRP-IgG (<25µg/mL) containing 10% animal serum in TBS/0.09% ProClin™ 950) was added for 30 minutes and followed by the same washing. 3,3'-

Diaminobenzidine (DAB) working solution [(DAB chromogen, RE7105, 1.74% w/v 3,3' - diaminobenzidine, in a stabiliser solution) and DAB substrate buffer (RE7143, buffered solution containing ≤0.1% hydrogen peroxide and preservative) of a ratio 1:20] was added for 5 minutes, 3×5 minutes washing was followed by counterstaining with Meyer's Haematoxylin (RE7107, <0.1% haematoxylin) for 6 minutes. The slides were dehydrated with alcohol and cleared with xylene (Genta Medica, York, UK). Finally, slides were mounted with Distyrene, a Plasticiser, and Xylene.

For ER, sections were stained using the Ventana Benchmark® ULTRA system (Tucson, Arizona, USA) with the Ventana anti-ER (SP1) rabbit monoclonal primary antibody as per the recommended protocol. The primary antibody was applied for 16 minutes at 37°C followed by the OptiView HQ Linker for 8 minutes and the OptiView HRP Multimer for 8 minutes.

Tissue sections used as negative as well as positive controls were included with every staining run during staining of each antibody. A negative control was obtained by omitting the primary antibody and incubating slides in antibody diluent only. Additionally, tissues with known reactivity to each antibody according to the supplier's data sheet were used as a positive control (**Table 2-3**).

Table 2-3: Optimum conditions of the selected antibodies

Antibody	Supplier	Species	Clone	Dilution	Pre-treatment	Incubation time	Positive control
ER	Ventana	Rabbit Monoclonal	SP1	N/A	N/A	16 minutes	Internal/normal breast ducts
PR	Agilent	Mouse Monoclonal	PgR636	1:150	Microwave	30 minutes	Internal/normal breast ducts
HER2	DAKO	Rabbit Polyclonal	-	1:400	N/A	30 minutes	BC tissue
Ki67	DAKO	Mouse Monoclonal	MIB-1	1:100	Microwave	1 hour	Tonsil tissue
p53	Leica Novocastra	Mouse Monoclonal	DO7	1:50	Microwave	30 minutes	BC tissue
CK5/6	Ventana	Mouse Monoclonal	D5/16B4	N/A	N/A	20 minutes	Internal myoepithelial cells surrounding breast ducts
HIF1α	Abcam	Rabbit Monoclonal	EPR16897	1:1000	Microwave	1 hour	Internal/ tumour cells surrounding necrosis
P4HA2	Abcam	Mouse Monoclonal	CL0351	1:100	Microwave	16 hours	Testis
COL11A1	DMXT invasion	Mouse Monoclonal	1E8.33	1:150	Water Bath	1 hour	Fibroblasts surrounding BC tissue
CTSV	Abcam	Mouse Monoclonal	BV55-1	1:100	Microwave	1 hour	Skin
CTSA	Abcam	Rabbit Polyclonal	-	1:200	Microwave	16 hours	Liver
LGMN	Abcam	Rabbit Polyclonal	-	1:150	Microwave	16 hours	Kidney

2.1.9 Assessment of immunoreactivity

Prior to application of each primary antibody to the TMA using IHC, the staining of 10 full face sections was performed from FFPE of pure DCIS and IBC tissues mixed with DCIS with each primary antibody to assess homogeneity of immunoreactivity in terms of staining intensity and distribution. For all the studied biomarkers, only those were proceeded to be applied to TMAs when even staining distribution across the tissue was ensured. Therefore, all candidate biomarkers were studied on TMA sections except Ki67, which showed heterogeneous distribution of staining positivity, and poor concordance between Ki67 assessed on TMA and full-face sections. Accordingly, Ki67 was assessed on three replicates of the TMA to compensate for the discrepancy and the final score was taken as average. Previous studies have validated the use of one TMA core to study the expression of tumour markers in a large series [237].

High resolution digital images (0.45μm/pixel) of stained slides were obtained using a NanoZoomer slide scanner (Hamamatsu Photonics, Welwyn Garden City, UK) and accessed using Xplore viewing software viewer (Philips). Immunoreactivity was manually assessed at 20x magnification using a minimum of a 24” high resolution screen (1920x1080).

Each TMA core was assessed whether DCIS/invasive tumour occupied >15% of the total area of the core. If this was the case, the core was eligible for scoring. Histo-score (H-score) [238], was the main scoring system used taking into consideration the intensity (0=negative, 1=weak, 2=moderate and 3=strong staining) and the percentage of stained tumour cells (0-100%). The intensity was multiplied by the percentage and added together to obtain the final H-score with a range from 0-300. As the studied markers showed reactivity with the surrounding stromal fibroblasts, scoring of expression within the specialised stroma surrounding DCIS (i.e. equivalent to 2-high power fields of the surrounding stroma) [239] was assessed as percentage of positive cells. Determination of the expression intensity within the scanty cytoplasm of the slender shaped fibroblasts was challenging; thus, staining intensity was not scored. Cases with multiple cores were scored and the average score (in either tumour epithelial cells of the stroma) was used as the final score for analysis. All cases were scored blindly without prior knowledge of patients' pathological or outcome data.

Scoring TMA cores stained by HER2 was performed using HercepTest according to the manufacturer's recommendation; DAKO protocol (DAKO Corporation, Glostrup, Denmark). Each core was placed into one of four categories (0, 1+, 2+, or 3+).

Tumours with complete absence of membrane staining, or in which membrane staining was observed in <10% of the tumour cells were scored as 0. Those with faint/barely perceptible, incomplete membranous staining detected in >10% of tumour cells were classified as 1+. Tumours with either weak to moderate complete membranous staining in greater than 10% of the tumour cells were classified as 2+. While those with strong, complete membranous staining in greater than 10% of the tumour cells were classified as 3+.

2.1.10 Determination of the cut-off points

Cut-off values for the dichotomisation of biomarkers were individually assessed and determined by several methods 1) Using cut-offs from previous studies that assessed large number of data if available 2) Using either the mean or median according to the distribution of data whether normally or not normally distributed respectively or 3) Using non-commercial research tool; X-tile software (version 3.6.1, 2003-2005, Yale University, USA http://x-tile.software.informer.com). This software randomly divides the total patient cohort into two separate equal training and validation sets by producing separate lists of 'censored' and 'uncensored' observations, ranked by patients' follow up time. Those patients developed ipsilateral local recurrence were considered as an event (uncensored), while patients did not develop local recurrence

or lost follow-up during this study were censored during the analysis at the time of that event. The optimal cut-points were determined by locating the brightest pixel on the X-tile plot diagram of the training set. Statistical significance was tested by validating the obtained cut-point to the validation set [240] with corrected *p* value and relative risk against LRFI [240, 241]. Information regarding the stained antibodies in this study, their expression and their cut-offs are listed in **Table 2-4**.

Table 2-4: Antibodies used, their expression localisation and cut-offs

Abs.	Stained series	IHC localisation	Cut-off values	Method
ER	Pure DCIS	Nuclear	Positive (≥1%)	[242]
PR	Pure DCIS	Nuclear	Positive (≥1%)	[242]
HER2	Pure and mixed DCIS	Membranous	Positive (≥10% strong complete staining)	[243]
Ki67	Pure DCIS	Nuclear	Positive (≥14%)	[244]
p53	Pure DCIS	Nuclear	Inactivating mutation (0), Normal (1-50%), Missense mutation (>50%)	[245]
P4HA2	Pure and mixed DCIS	Cytoplasmic	Tumour epithelial cells >40 (H score) Stromal fibroblasts >60%	X-Tile
COL11A1	Pure and mixed DCIS	Cytoplasmic	Tumour epithelial cells >120 (H score) Stromal fibroblasts >15 %	X-Tile
CTSV	Pure and mixed DCIS	Cytoplasmic	Tumour epithelial cells >60 (H score) Stromal fibroblasts >65%	X-Tile
CTSA	Pure and mixed DCIS	Cytoplasmic	Tumour epithelial cells >125 (H score)	X-Tile
LGMN	Pure and mixed DCIS	Cytoplasmic	Tumour epithelial cells >60% Stromal fibroblasts >5%	X-tile [246]

2.6 **Chromogenic *in situ* Hybridisation**

HER2 gene amplification was determined by chromogenic *in situ* hybridisation (CISH) using the ZytoDot 2C SPEC ERBB2/CEN 17 Probe Kit, (ZytoVision®, Germany). TMA sections were deparaffinised and incubated for 10 minutes (at 70°C on thermal plate) followed by dewaxing in xylene (twice, each 5 minutes), and then gradient ethanol (each 5 minutes). Incubation of the slides with hydrogen peroxide, H_2O_2 (3%, for 5 minutes), followed by washing in distilled water. Treatment of the slides by pre-heated pre-treatment solution EDTA (PT2) for 15 minutes, was performed, followed by immediate transfer into distilled water (twice, 2 minutes each). Enzymatic digestion was carried out by drop-wise application of pepsin solution (ES1) to the tissue sections and incubation for 5 minutes at room temperature in a humidity chamber. After a wash in distilled water, slides were dehydrated with graded ethanol followed by air drying. A ready to use DNA probe (ZytoDot 2C SPEC ERBB2/CEN 17 Probe, PD12) was applied to the slides (10µl per slide) and cover-slipped (22x22mm) then sealed with a layer of rubber cement. The sections were denatured on a thermal plate (80°C for 5 minutes), and hybridisation was carried out overnight at 37°C in a humidity chamber. After

hybridisation, the cover slip was removed, and slides were washed twice (each 5 minutes) with wash buffer SSC (WB1) (1st wash at RT, and the 2nd heated to 75°C). After two washes in distilled water (1 minute each), slides were immersed into 1x Wash Buffer TBS (prepared using WB5). The HER2 probe was detected by sequential incubation with anti-digoxigenin DIG/DNP-Mix (AB14) for 15 minutes (at 37°C in a humidity chamber), peroxidase polymer horseradish peroxidase HRP/AP-Polymer-Mix (AB13) for 15 minutes (at 37°C in a humidity chamber), AP-Red Solution B (SB6b) for 15 minutes at room temperature and HRP-Green Solution A (SB7a) for 15 minutes at room temperature. Counter-staining was achieved by Nuclear Blue Solution (CS2) for 2 minutes followed by washing and dehydration in absolute ethanol followed by xylene. Covering the slides using Alcoholic Mounting Solution (MT4) and air-dry slides for 30 minutes was the final step.

2.7 **Conventional statistical approach**

Statistical analysis was performed using Statistical Package for Social Sciences (SPSS) version 24 statistical software (SPSS Inc., Chicago, IL, USA). For all statistical tests, a *p*-value <0.05 (two sided) was considered significant. The following statistical methods were used:

2.1.11 Correlation with clinicopathological parameters

Analysis of continuous variables was performed using the appropriate statistical test according to distribution pattern of data (e.g. Student t-test and Analysis of variance 'ANOVA' for normally distributed data while the Mann Whitney and Kruskal Wallis tests were used when the data was not normally distributed). Chi-squared analyses were used for inter-relationships between categorical variables. Regression analysis model was used when comparison with several parameters was indicated. Correlation between continuous variables was performed using Spearman or Pearson tests.

Although large number of data analysis and multiple comparisons were carried out in this thesis, the author did not use multiple comparison correction test (e.g Bonferroni correction) throughout the thesis. There is a debate on the value of using these correction methods among statisticians [247, 248]. The author used various statistical tests and analysed the data using continuous and categorical variables to ensure the reproducibility and reliability of the results. Multivariate Cox regression analysis was also applied for multivariate correlation analysis.

2.1.12 Univariate analysis with outcome

Survival estimates for patient LRFI was analysed by Kaplan-Meier curves with significance determined by the log rank test.

2.1.13 Multivariate analysis with outcome

Multivariate analysis was performed by Cox regression proportional hazard analysis to test for confounders and prognostic or predictive independency of the studied biomarker from standard prognostic/predictive factors.

All statistical analyses were performed by the author unless stated otherwise.

3 Chapter 3: Clinicopathological characterisation of DCIS

3.1 Introduction

3.1.1 Incidence of DCIS

DCIS represents about 10% of BC [249]. DCIS is a heterogenous group of diseases. Such heterogeneity is reflected in tumour morphology, molecular profiles, response to treatment and behaviour. Ideally the management approach needs to be designed accordingly to decrease the risk of progression and/or recurrence without over-treatment [223, 250].

3.1.2 Treatment of DCIS

Mastectomy was long considered the standard management for DCIS and remains so in certain situations (e.g. extensive disease, those with failed breast conservation, or where there are contraindications to RT in high-risk patients) [91, 251]. It provides an effective and near total cure rate; however, for most women it is an aggressive over-treatment of a lesion with low mortality risk with potential increased psychosocial morbidity and health economic costs [223]. BCS with or without RT, is offered when DCIS can be removed with an acceptable cosmetic outcome and considered equivalent to mastectomy in terms of overall or BC specific survival [249]. However, studies report women treated with BCS have up to 10-15% risk of recurrence within 10 years and half of these

recurrences are invasive disease with a subsequent mortality risk [5, 252]. RT following BCS decreases the risk of recurrence to less than 10% at 10 years although clear guidelines for its indications in specific risk groups continue to be debated [93, 94, 97, 99, 100]. The role of ET in DCIS management and prevention is still debated. Over- or under-treatment of DCIS remains a problem and numerous trials have been performed to assess more personalised therapy but have so far been inconclusive [111, 112].

3.1.3 Factors affecting DCIS outcome

Various factors affecting outcome of treated DCIS have been analysed and different risk groups can be stratified accordingly, aiding treatment decisions [253]. Age at diagnosis, clinical presentation, nuclear grade and tumour size, resection margin status are well recognised factors used for this purpose. The VNPI is a popular risk assessment tool combining patient age, lesion size, nuclear grade and margin status for treatment decisions as described in **Chapter 1** [62, 254].

Optimal extent of free surgical resection margins after BCS is still controversial. A UK survey in 2007 identified that approximately half of surgeons aim for a free margin of more than 2mm [10]. In 2016, the Society of Surgical Oncology, American Society for Radiation Oncology and American Society

of Clinical Oncology consensus guideline on margins for BCS with whole-breast irradiation in DCIS suggest a 2mm free surgical margin [102]. Positive or close margins are the main indication for surgical re-excision or completion mastectomy after primary surgery for DCIS [255-257].

3.2 **Hypothesis and aims**

In this chapter, it is hypothesised that different clinicopathological factors of DCIS are important predictors of DCIS outcome. Therefore, the aim was to collect a large cohort of DCIS treated in a single institution and correlate their clinicopathological characteristics with patient outcome.

3.3 **Patients and methods**

Pure DCIS cases diagnosed between 1987-2017 at the Nottingham Breast Institute were identified (n=1,249). Clinicopathological characteristics together with patient outcome data was collected (**Chapter 2**). Chi-square test and the multivariate logistic regression model were used to correlate between different clinicopathological factors with primary operation preference, re-excision, type of re- excision, RT and presence of residual tumour tissue in the re-excised specimens.

3.4 **Results**

3.4.1 **Data analysis**

The annual number of cases within the study period is described in **Figure 3-1**. 945 women (75%) were diagnosed within the screening age group (50-70 years). The number of cases diagnosed through screening method showed steady increase throughout the study period as shown in **Figure 3-2**. High nuclear grade was observed in 61% of cases, while comedo type necrosis was recorded in two thirds of cases (67%). Solid DCIS was the predominant histological type, either in pure form or mixed with other morphological types and represented 58% of cases. Paget's disease was observed in 56 cases (9%). **Table 3-1** summarises various clinicopathological parameters of DCIS diagnosed prior and after 2008.

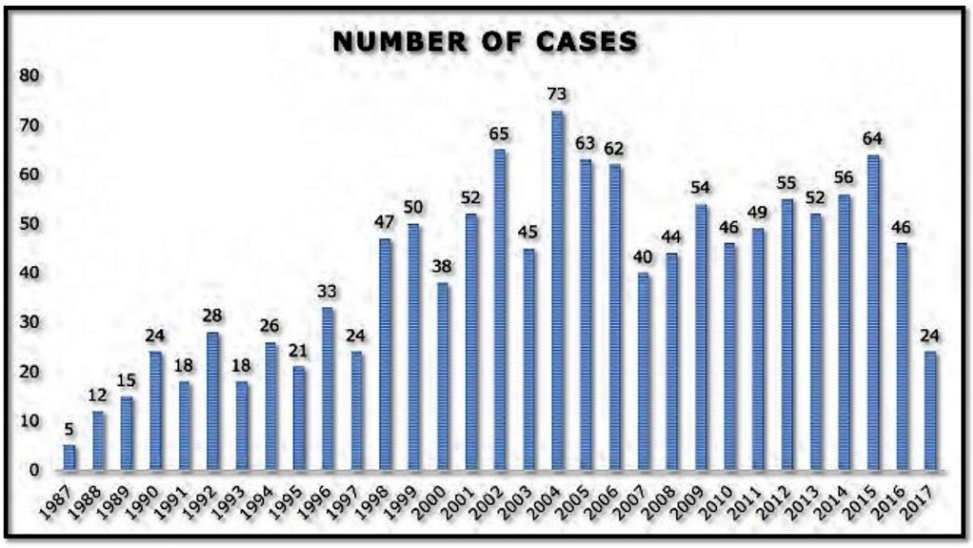

Figure 3-1: Annual Frequency of DCIS

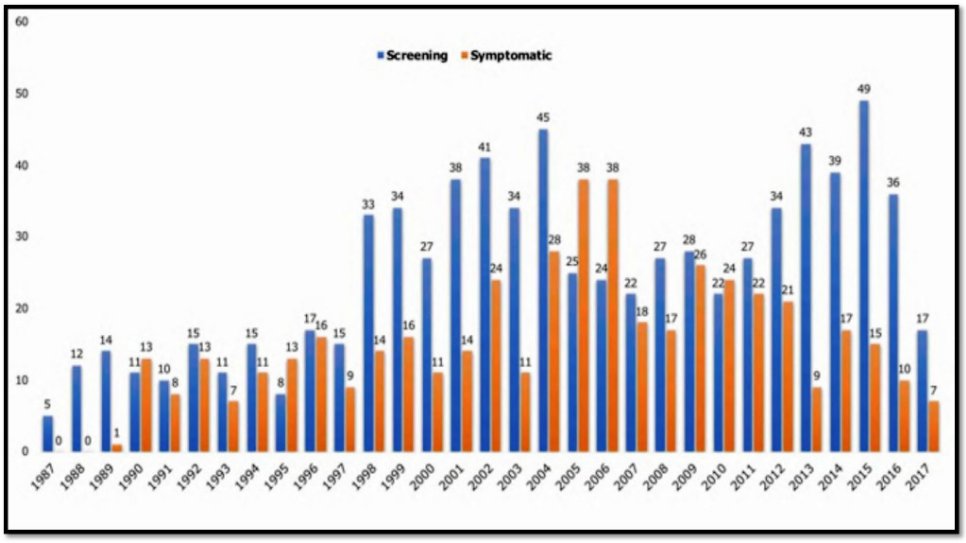

Figure 3-2: DCIS Clinical Presentation

The proportion of screen detected DCIS showed steady rise over the years compared to symptomatic DCIS

Table 3-1: Clinicopathological parameters of pure DCIS cohort

Parameter	Total (n=1249) N (%)	DCIS Diagnosed 1987-2008 (n=803) N (%)	DCIS diagnosed 2009-2017 (n=446) N (%)	X^2 *P*-value
Age*				
<40	32 (3)	24 (3)	8 (2)	11.9
40 to 60	688 (55)	467 (58)	221 (49)	**0.003**
>60	529 (42)	312 (39)	217 (49)	
Presentation				
Symptomatic	501 (40)	351 (44)	150 (34)	11.8
Screening	748 (60)	452 (56)	296 (66)	**0.001**
DCIS Site**				
Localised	929 (85)	590 (88)	339 (81)	11.5
Diffuse	160 (15)	79 (12)	81 (19)	**0.001**
Tumour Size*				
<16mm	457 (37)	308 (39)	149 (34)	3.6
16 to 40mm	484 (39)	304 (38)	180 (40)	0.160
>40mm	301 (24)	184 (23)	117 (26)	
Tumour Grade				
Low	156 (12)	109 (14)	47 (11)	16.8
Intermediate	333 (27)	185 (23)	148 (33)	**<0.0001**
High	760 (61)	509 (63)	251 (56)	
Comedo necrosis				
No	409 (33)	280 (35)	129 (29)	4.6
Yes	840 (67)	523 (65)	317 (71)	**0.032**
Solid DCIS				
No	529 (43)	406 (51)	123 (28)	62.3
Pure	291 (23)	164 (20)	127 (28)	**<0.0001**
Mixed with other types	429 (34)	233 (29)	196 (44)	
Cribriform DCIS				
No	649 (52)	444 (56)	205 (46)	12.1
Pure	114 (9)	75 (9)	39 (9)	**0.002**
Mixed with other types	486 (39)	284 (35)	202 (45)	
Papillary DCIS				
No	1127 (90)	729 (91)	398 (89)	0.8
Pure	42 (3)	26 (3)	16 (4)	0.663
Mixed with other types	80 (7)	48 (6)	32 (7)	
Micropapillary DCIS				
No	916 (73)	594 (74)	322 (72)	1.3
Pure	79 (7)	53 (7)	26 (6)	0.520
Mixed with other types	254 (20)	156 (19)	98 (22)	
Paget's Disease				
No	550 (91)	390 (90)	160 (92)	0.7
Yes	56 (9)	43 (10)	13 (8)	0.361
Management***				
Mastectomy	424 (34)	292 (36)	132 (30)	5.9
BCS	824 (66)	510 (64)	314 (70)	**0.015**
Margin width†				
Positive (Tumour on ink)	317 (40)	240 (50)	77 (26)	72.5
<2mm	88 (11)	36 (8)	52 (16)	**<0.0001**
≥2mm	382 (49)	202 (42)	180 (58)	
Re excision†				
Yes	414 (50)	298 (58)	116 (37)	35.9
No	410 (50)	212 (42)	198 (63)	**<0.0001**

Type of re-excision†				
Re excision	232 (56)	159 (53)	73 (63)	3.1
Mastectomy	182 (44)	139 (47)	43 (37)	0.078
Residual Tumour†				
No	196 (47)	150 (50)	46 (40)	3.8
Yes	218 (53)	148 (50)	70 (60)	0.051
Management****				
Mastectomy	606 (49)	431 (54)	175 (39)	24.1
BCS	642 (51)	371 (46)	271 (61)	**<0.0001**
Radiotherapy§				
Yes	263 (41)	92 (25)	171 (63)	127.1
No	379 (59)	279 (75)	100 (37)	**<0.0001**
VNPI†				
Low risk	195 (25)	105 (22)	90 (29)	7.1
Moderate risk	470 (60)	288 (61)	182 (59)	**0.030**
High risk	118 (15)	81 (17)	37 (12)	

DCIS: Ductal carcinoma *in situ;* N: Number; X^2: Chi square, P values in **bold** are significant

*Age and size were categorised according to Van Nuys Prognostic Index (VNPI)

** Site; Localised: DCIS is involving one quadrant, diffuse: DCIS is in more than one quadrant

*** Management of DCIS as a first operation

†Refers to patients treated primarily with BCS (first operation)

**** Management of DCIS as a final operation

§Refers to patients treated finally by BCS (final operation)

3.4.1.1 Correlation between clinicopathological factors associated with the selection of type of primary surgery

As regard to DCIS management, 824 (66%) cases were treated primarily with BCS, while mastectomy was performed in 424 cases (34%). The former was the first choice for those who were asymptomatic and diagnosed through routine mammographic screening (p<0.0001), with localised DCIS lesions (i.e. involving one quadrant of breast) (p<0.0001), DCIS size <16mm (p<0.0001), low nuclear grade (p<0.0001), with no associated comedo type necrosis, solid , cribriform or micropapillary DCIS (p<0.0001, p=0.043, p=0.017 and p=0.043, respectively) (**Table 3-2**).

Table 3-2: Clinicopathological factors associated with the selection of type of primary surgery for DCIS management

Parameter	DCIS Diagnosed 1987-2008 N (%)		X^2 P-value	DCIS diagnosed 2009-2017 N (%)		X^2 P-value	Total N (%)		X^2 P-value
	BCS (n=510)	**Mastectomy** (n=292)		**BCS** (n=314)	**Mastectomy** (n=132)		**BCS** (n=824)	**Mastectomy** (n=424)	
Age*									
<40	13 (3)	11 (4)	0.9	5 (2)	3 (2)	1.8	18 (56)	14 (44)	2.6
40 to 60	297 (58)	170 (58)	0.610	150 (48)	71 (54)	0.412	447 (65)	241 (35)	0.271
>60	200 (39)	111 (38)		159 (50)	58 (44)		359 (68)	169 (32)	
Presentation									
Symptomatic	204 (40)	146 (50)	7.6	84 (27)	66 (50)	22.5	288 (58)	212 (42)	26.4
Screening	306 (60)	146 (50)	**0.006**	230 (73)	66 (50)	**<0.0001**	536 (72)	212 (28)	**<0.0001**
Site									
Localised	365 (92)	224 (82)	51.7	250 (85)	89 (71)	10.5	615 (66)	313 (34)	48.6
Diffuse	30 (8)	49 (18)	**<0.0001**	45 (15)	36 (29)	**0.005**	75 (47)	85 (53)	**<0.0001**
Size*									
<16mm	256 (50)	52 (18)	96.9	133 (42)	16 (12)	78.1	389 (85)	68 (15)	162.5
16 to 40mm	175 (35)	129 (44)	**<0.0001**	134 (43)	46 (35)	**<0.0001**	309 (64)	175 (36)	**<0.0001**
>40mm	75 (15)	109 (38)		47 (15)	70 (53)		122 (41)	179 (59)	
Grade									
Low	92 (18)	17 (6)	39.1	41 (13)	6 (5)	18.3	133 (85)	23 (15)	58.6
Intermediate	133 (26)	51 (17)	**<0.0001**	116 (37)	32 (24)	**<0.0001**	249 (75)	83 (25)	**<0.0001**
High	285 (56)	224 (77)		157 (50)	94 (71)		442 (58)	318 (42)	
Comedo necrosis									
No	215 (42)	64 (22)	33.5	109 (35)	20 (15)	17.3	324 (79)	84 (21)	48.4
Yes	295 (58)	228 (78)	**<0.0001**	205 (65)	112 (85)	**<0.0001**	500 (60)	340 (40)	**<0.0001**
Solid DCIS									
No	273 (54)	132 (45)	6.3	95 (31)	28 (21)	4.3	368 (70)	160 (30)	7.1
Pure	103 (20)	61 (21)	**0.043**	89 (28)	38 (29)	0.115	192 (66)	99 (34)	**0.030**
Mixed with other types	134 (26)	99 (34)		130 (41)	66 (50)		264 (62)	165 (38)	
Cribriform DCIS									
No	274 (54)	169 (58)	8.1	143 (46)	62 (47)	4.2	417 (64)	231 (36)	12.1
Pure	59 (12)	16 (6)	**0.017**	33 (10)	6 (5)	0.120	92 (81)	22 (19)	**0.002**
Mixed with other types	177 (35)	107 (36)		138 (44)	64 (48)		315 (65)	171 (35)	
Papillary DCIS									
No	458 (90)	271 (93)	4.7	270 (86)	128 (97)	11.7	728 (65)	399 (35)	12.6
Pure	21 (4)	4 (1)	0.095	15 (5)	1 (1)	**0.003**	36 (88)	5 (12)	**0.002**
Mixed with other types	31 (6)	17 (6)		29 (9)	3 (2)		60 (75)	20 (25)	
Micropapillary DCIS									
No	391 (76)	202 (69)	6.3	236 (75)	86 (65)	5.9	627 (69)	288 (31)	9.6
Pure	33 (7)	20 (7)	**0.043**	14 (5)	12 (9)	0.052	47 (60)	32 (40)	**0.008**
Mixed with other types	86 (17)	70 (24)		64 (20)	34 (26)		150 (59)	104 (41)	

DCIS: Ductal carcinoma in situ; N: Number; X2: Chi square, BCS: Breast conserving surgery, P values in **bold** are significant
*Age and size according to VNPI

3.4.1.2 Factors affecting re-excision

After primary BCS, 306 (37%) cases showed positive margins (tumour on ink), while 75 cases (9%) showed close margins <2mm. Margin >10mm was observed in 20% of cases. Over the entire study period, half of the DCIS cases treated primarily with BCS (n=414) underwent re-excision. The re-operation was either in the form of further conservative surgery (n=232) or completion mastectomy (n=182) (**Table 3-3**).

Table 3-3: Detailed surgical management of the DCIS

Surgical management				
Primary operation	**Mastectomy** (n=424) 34%		**BCS** (n=824) 66%	
Re excisions		Yes (n=414)		No re-excision (n=410)
		Mastectomy 182	Re-excision 232	
Final operation	**Mastectomy** (n=606) 49%		**BCS** (n=642) 51%	

BCS: Breast conserving surgery; n: number

Several factors influenced lower rates of re-excision, including older patients age (p=0.028), asymptomatic disease presentation (p<0.0001), lesions localised to one breast quadrant (p=0.003), smaller DCIS size (p<0.0001), negative resection margins ≥2mm (p<0.0001) and lower VNPI (p<0.0001). Moreover, absence of solid and/or micropapillary DCIS either in pure form or with other morphological types was associated with a lower rate of re-excision (p<0.0001). **Figure 3-3** shows the rate of re-excision as regard to margin status, DCIS grade and VNPI. It is noteworthy that 196 (47%) of those

who underwent re-excision were of low and intermediate grade. Moreover, 10% of low risk VNPI cases had a second operation. **Table 3-4** and **Table 3-5** show the detailed association between re-excision and type of re-excision with various clinicopathological variables.

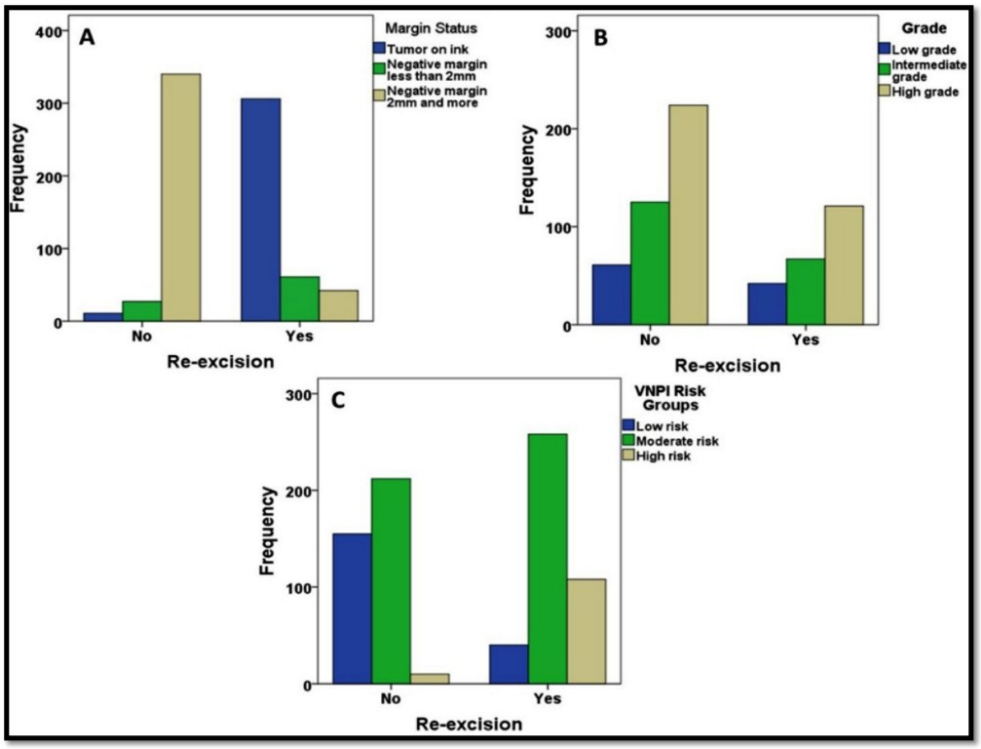

Figure 3-3: Re-excision Rates of DCIS.

Frequency of re-excision after primary breast conserving surgery in relation to: A) margin status, B) tumour grade and C) Van Nuys Prognostic Index (VNPI) Risk Groups. A considerable percentage of low and intermediate grade as well as low risk DCIS underwent re-excision.

Completion mastectomy was more likely to be recommended for women <40 years old (p=0.018), with symptomatic DCIS (p<0.0001), multiple DCIS lesions or involving more than one breast quadrant (p=0.005), with DCIS > 4cm in maximum diameter (p<0.0001), positive or close resection margin

<2mm (p<0.0001) and high-risk DCIS defined by VNPI (p<0.0001).

Table 3-4: Clinicopathological factors associated with re-excision after primary treatment with breast conserving surgery

Parameter	DCIS Diagnosed 1987-2008 N (%)		X^2 P-value	DCIS diagnosed 2009-2017 N (%)		X^2 P-value	Total		X^2 P-value
	No (n=212)	**Yes** (298)		**No** (198)	**Yes** (116)		**No** (410)	**Yes** (414)	
Age*									
<40	3 (2)	10 (3)	6.7	3 (2)	2 (2)	0.1	6 (2)	12 (3)	7.2
40 to 60	113 (53)	184 (62)	**0.034**	95 (48)	55 (47)	0.987	208 (51)	239 (58)	**0.028**
>60	96 (45)	104 (35)		100 (50)	59 (51)		196 (47)	163 (39)	
Presentation									
Symptomatic	65 (31)	139 (47)	13.2	41 (21)	43 (37)	9.9	106 (26)	182 (44)	29.7
Screening	147 (69)	159 (53)	**<0.0001**	157 (79)	73 (62)	**0.002**	304 (74)	232 (56)	**<0.0001**
Site									
Localised	157 (92)	208 (92)	1.6	169 (89)	81 (77)	10.9	326 (80)	289 (70)	11.5
Diffuse	13 (8)	17 (8)	0.459	21 (11)	24 (23)	**0.004**	34 (20)	41 (30)	**0.003**
Size*									
<16mm	133 (64)	123 (41)	37.1	112 (56)	21 (18)	47.8	245 (60)	144 (35)	69.1
16 to 40mm	66 (32)	109 (37)	**<0.0001**	69 (35)	65 (56)	**<0.0001**	135 (33)	174 (42)	**<0.0001**
>40mm	10 (4)	65 (22)		17 (9)	30 (26)		27 (7)	95 (23)	
Grade									
Low	34 (16)	58 (20)	0.9	27 (14)	14 (12)	1.6	61 (15)	72 (17)	0.9
Intermediate	57 (27)	76 (25)	0.610	68 (34)	48 (41)	0.459	125 (35)	124 (30)	0.614
High	121 (57)	164 (55.0)		103 (52)	54 (47)		224 (55)	218 (53)	
Comedo necrosis									
No	81 (38)	134 (45)	2.3	62 (31)	47 (40)	2.7	143 (35)	181 (44)	6.7
Yes	131 (62)	164 (55)	0.128	136 (68)	69 (60)	0.098	267 (65)	233 (56)	**0.009**
Solid DCIS									
No	98 (46)	175 (59)		59 (30)	36 (31)		157 (38)	211 (51)	
Pure	55 (26)	48 (16)	9.8	67 (34)	22 (19)	9.1	122 (30)	70 (17)	22.1
Mixed with other types	59 (28)	75 (25)	**0.007**	72 (36)	58 (50)	**0.011**	131 (32)	133 (3)	**<0.0001**
Cribriform DCIS									
No	108 (51)	166 (56)		97 (49)	46 (40)		205 (50)	212 (51)	
Pure	27 (13)	32 (11)	1.2	23 (12)	10 (9)	4.5	50 (12)	42 (11)	0.9
Mixed with other types	77 (36)	100 (33)	0.543	78 (39)	60 (51)	0.103	155 (38)	160 (38)	0.646

Papillary DCIS									
No	188 (89)	270 (91)		168 (85)	102 (88)		356 (87)	372 (90)	
Pure	10 (5)	11 (4)	0.5	13 (7)	2 (2)	3.9	23 (6)	13 (3)	3.2
Mixed with other types	14 (6)	17 (5)	0.766	17 (8)	12 (10)	0.141	31 (7)	29 (7)	0.204
Micropapillary DCIS									
No	175 (83)	216 (73)		160 (81)	76 (65)		335 (82)	292 (71)	
Pure	6 (3)	27 (9)	10.1	7 (4)	7 (6.0)	9.2	13 (3)	34 (8)	16.8
Mixed with other types	31 (14)	55 (18)	**0.006**	31 (15)	33 (29)	**0.010**	62 (15)	88 (21)	**<0.0001**
Margin width									
Positive (tumour on ink)	0 (0)	232 (78)		0 (0)	74 (65)		0 (0)	306 (75)	
<2mm	4 (2)	27 (9)	318.7	10 (5)	34 (31)	225.1	14 (4)	61 (15)	543.7
≥ 2mm	178 (98)	37 (13)	**<0.0001**	186 (95)	5 (4)	**<0.0001**	364 (96)	42 (10)	**<0.0001**
VNPI									
Low risk	73 (40)	32 (11)		82 (42)	8 (7)		155 (41)	40 (10)	
Moderate risk	103 (57)	185 (63)	108.9	109 (56)	73 (65)	71.3	212 (56)	258 (63)	168.9
High risk	5 (3)	76 (26)	**<0.0001**	5 (2)	32 (28)	**<0.0001**	10 (3)	108 (27)	**<0.0001**

DCIS: Ductal carcinoma in situ; N: Number; X2: Chi square, P values in **bold** are significant
VNPI: Van Nuys Prognostic Index
*Age and size according to VNPI

Table 3-5: Clinicopathological factors associated with the choice of type of DCIS re-excision

Parameter	DCIS Diagnosed 1987-2008 N (%)		X^2 P-value	DCIS diagnosed 2009-2017 N (%)		X^2 P-value	Total N (%)		X^2 P-value
	BCS (n=159)	**Mastectomy** (n=139)		**BCS** (n=73)	**Mastectomy** (n=43)		**BCS** (n=232)	**Mastectomy** (n=182)	
Age*									
<40	2 (1)	8 (6)	4.6	0 (0)	2 (15)	4.6	2 (1)	10 (5)	7.9
40 to 60	101 (64)	83 (60)	0.098	38 (52)	17 (39)	0.099	139 (60)	100 (55)	**0.018**
>60	56 (35)	48 (34)		35 (48)	24 (46)		91 (39)	72 (40)	
Presentation									
Symptomatic	60 (38)	79 (57)	10.9	20 (27)	23 (54)	7.9	80 (34)	102 (56)	19.2
Screening	99 (62)	60 (43)	**0.001**	53 (73)	20 (46)	**0.005**	152 (66)	80 (44)	**<0.0001**
Site									
Localised	98 (93)	110 (92)	16.7	55 (82)	26 (68)	2.9	153 (89)	136 (86)	10.7
Diffuse	7 (7)	10 (8)	**<0.0001**	12 (18)	12 (32)	0.233	19 (11)	22 (14)	**0.005**
Size*									
<16mm	94 (59)	29 (21)	61.6	19 (26)	2 (5)	18.7	113 (49)	31 (17)	73.8
16 to 40mm	54 (34)	55 (40)	**<0.0001**	44 (60)	21 (49)	**<0.0001**	98 (42)	76 (42)	**<0.0001**
>40	11 (7)	54 (39)		10 (14)	20 (46)		21 (9)	74 (41)	
Grade									
Low	32 (20)	26 (19)	0.1	10 (14)	4 (9)	0.6	42 (18)	30 (16)	0.2
Intermediate	40 (25)	36 (26)	0.952	29 (40)	19 (44)	0.754	69 (30)	55 (31)	0.911
High	87 (55)	77 (55)		34 (46)	20 (47)		121 (52)	97 (53)	
Comedo necrosis									
No	75 (47)	59 (42)	0.7	27 (37)	20 (46)	1.1	102 (44)	79 (43)	0.1
Yes	84 (53)	80 (58)	0.413	46 (63)	23 (54)	0.313	130 (56)	103 (57)	0.909
Solid DCIS									
No	87 (55)	88 (63)		24 (33)	12 (28)		111 (48)	100 (55)	
Pure	29 (18)	19 (14)	2.3	14 (19)	8 (19)	0.4	43 (2)	27 (15)	2.2
Mixed with other types	43 (27)	32 (23)	0.306	35 (48)	23 (53)	0.824	78 (50)	55 (30)	0.333
Cribriform DCIS									
No	90 (57)	76 (54)		30 (41)	16 (37)		120 (52)	92 (50)	
Pure	20 (13)	12 (9)	1.9	8 (11)	2 (5)	1.9	28 (12)	14 (8)	2.7
Mixed with other types	49 (31)	51 (37)	0.389	35 (48)	25 (58)	0.388	84 (36)	76 (42)	0.251

Papillary DCIS									
No	142 (89)	128 (92)		65 (89)	37 (86)		207 (89)	165 (91)	
Pure	9 (6)	2 (1)	3.9	2 (3)	0 (0)	2.1	11 (5)	2 (1)	5.1
Mixed with other types	8 (5)	9 (7)	0.141	6 (8)	6 (14)	0.356	14 (6)	15 (8)	0.080
Micropapillary DCIS									
No	121 (76)	95 (68)		51 (70)	25 (58)		172 (74)	120 (66)	
Pure	15 (9)	12 (9)	3.6	5 (7)	2 (5)	2.6	20 (9)	14 (8)	5.1
Mixed with other types	23 (15)	32 (23)	0.165	17 (23)	16 (37)	0.269	40 (17)	48 (26)	0.079
Margin width									
Positive (Tumour on ink)	108 (69)	124 (89)		42 (58)	32 (78)		150 (66)	156 (87)	
<2mm	21 (13)	6 (4)	19.9	25 (35)	9 (22)	6.918	46 (20)	15 (8)	24.9
≥ 2mm	28 (18)	9 (7)	**<0.0001**	5 (7)	0 (0)	0.075	33 (14)	9 (5)	**<0.0001**
VNPI (1st operation)									
Low risk	25 (16)	7 (5)		7 (10)	1 (2)		32 (14)	8 (5)	
Moderate risk	109 (70)	76 (55)	31.8	48 (67)	25 (61)	4.8	157 (69)	101 (56)	30.9
High risk	21 (14)	55 (40)	**<0.0001**	17 (23)	15 (37)	0.190	38 (17)	70 (39)	**<0.0001**

DCIS: Ductal carcinoma in situ; N: Number; X2: Chi square, BCS: Breast conserving surgery, P values in **bold** are significant
VNPI: Van Nuys Prognostic Index
*Age and size according to VNP

3.4.1.3 Clinicopathological factors associated with presence of residual tumour in the re-excision specimens

Residual tumour tissue was detected in 218/414 cases (53%) who had re-excision surgery. Presence of residual tumour tissue in the re-excised specimens was associated with DCIS presenting symptomatically (p<0.0001), larger tumour size (p<0.0001), DCIS with cribriform morphology (p=0.018), positive or close margins <2mm (p=0.015) and high risk VNPI (p<0.0001). Patients who underwent a second re-excision operation showed a higher rate of residual tumour tissue than those who had completion mastectomy (p<0.0001). **Table 3-6** shows the different factors associated with the presence of residual tumour tissue in the specimens obtained after the second operation.

Multivariate logistic regression analysis showed that symptomatic DCIS, extent of the lesion, DCIS size, presence of comedo type necrosis and surgical margin status were the common independent factors affecting the rate of re-excision, type of re-excision and/or presence of residual tumour in the re-excised specimens. **Table 3-7** summarise the multivariate logistic regression results.

Table 3-6: Clinicopathological factors associated with presence of residual tumour tissue in the re-excision specimens

Parameter	DCIS Diagnosed 1987-2008 N (%)		X^2 P-value	DCIS diagnosed 2009-2017 N (%)		X^2 P-value	Total N (%)		X^2 P-value
	No (n=150)	**Yes** (n=148)		**No** (n=46)	**Yes** (n=70)		**No** (n=196)	**Yes** (218)	
Age*									
<40	3 (2)	7 (5)	3.2	0 (0)	2 (2)	1.5	3 (2)	9 (4)	3.4
40 t0 60	89 (59)	95 (64)	0.205	21 (46)	34 (49)	0.462	110 (56)	129 (59)	0.182
>60	58 (39)	46 (31)		25 (54)	34 (49)		83 (42)	80 (37)	
Presentation									
Symptomatic	55 (37)	84 (57)	12.1	7 (15)	36 (51)	15.6	62 (32)	120 (55)	22.9
Screening	95 (63)	64 (43)	**0.001**	39 (85)	34 (49)	**<0.0001**	134 (68)	98 (45)	**<0.0001**
Site									
Localised	105 (95)	103 (90)	1.8	33 (75)	48 (79)	2.5	138 (89)	151 (86)	0.6
Diffuse	6 (5)	11 (10)	0.403	11 (25)	13 (21)	0.281	17 (11)	24 (14)	0.719
Size*									
<16mm	82 (55)	41 (28)	37.1	11 (24)	10 (14)	9.2	93 (48)	51 (23)	47.9
16 to 40mm	54 (36)	55 (37)	**<0.0001**	30 (56)	35 (50)	**0.010**	84 (43)	90 (41)	**<0.0001**
>40	13 (9)	52 (35)		5 (10)	25 (36)		18 (9)	77 (36)	
Grade									
Low	33 (22)	25 (17)	1.2	5 (11)	9 (13)	0.9	38 (19)	34 (16)	1.9
Intermediate	37 (25)	39 (26)	0.538	17 (37)	31 (44)	0.616	54 (28)	70 (32)	0.378
High	80 (53)	84 (57)		24 (52)	30 (43)		104 (53)	114 (52)	
Comedo necrosis									
No	76 (51)	58 (39)	3.9	18 (39)	29 (41)	0.1	94 (48)	87 (40)	2.7
Yes	74 (49)	90 (61)	0.46	28 (61)	41 (59)	0.805	102 (52)	131 (60)	0.099
Solid DCIS									
No	84 (56)	91 (62)		19 (41)	17 (24)		103 (53)	108 (50)	
Pure	27 (18)	21 (14)	1.1	11 (24)	11 (16)	7.1	38 (19)	32 (14)	3.4
Mixed with other types	39 (26)	36 (24)	0.566	16 (35)	42 (60)	**0.029**	55 (28)	78 (36)	0.178
Cribriform DCIS									
No	85 (57)	81 (55)		19 (41)	27 (39)		104 (53)	108 (50)	
Pure	21 (14)	11 (7)	4.6	6 (13)	4 (6)	2.3	27 (14)	15 (7)	7.9
Mixed with other types	44 (29)	56 (38)	0.098	21 (46)	39 (56)	0.313	65 (33)	95 (43)	**0.018**

Papillary DCIS									
No	132 (88)	138 (93)		42 (92)	60 (86)		174 (89)	198 (91)	
Pure	9 (6)	2 (1)	4.6	2 (4)	0 (0)	5.8	11 (6)	2 (1)	8.3
Mixed with other types	9 (6)	8 (6)	0.099	2 (4)	10 (14)	0.055	11 (5)	18 (8)	**0.016**
Micropapillary DCIS									
No	114 (76)	102 (69)		32 (70)	44 (63)		146 (75)	146 (67)	
Pure	14 (9)	13 (9)	2.9	4 (9)	3 (4)	2.3	18 (9)	16 (7)	5.5
Mixed with other types	22 (15)	33 (22)	0.236	10 (21)	23 (33)	0.318	32 (16)	56 (26)	0.064
Margin width									
Positive (Tumour on ink)	107 (72)	125 (85)		24 (52)	50 (75)		131 (68)	175 (82)	
<2mm	19 (13)	8 (5)	9.2	18 (39)	16 (24)	9.5	37 (19)	24 (11)	12.3
≥ 2mm	22 (15)	15 (10)	0.057	4 (6)	1 (1)	**0.023**	26 (13)	16 (7)	**0.015**
Type or re-excision									
Re excision	113 (75)	74 (50)		37 (80)	46 (66)		150 (76)	120 (55)	
Completion Mastectomy	37 (25)	74 (50)	20.4 **<0.0001**	9 (20)	24 (34)	2.9 0.086	46 (24)	98 (45)	21.0 **<0.0001**
VNPI**									
Low risk	22 (15)	10 (7)		3 (7)	5 (8)		25 (13)	15 (7)	
Moderate risk	100 (69)	85 (57)	22.5	36 (78)	37 (55)	9.1	136 (71)	122 (57)	23.9
High risk	23 (16)	53 (36)	**<0.0001**	7 (15)	25 (37)	**0.028**	30 (16)	78 (36)	**<0.0001**

DCIS: Ductal carcinoma *in situ*; N: Number; X^2: Chi square, P values in **bold** are significant
*Age and size according to VNPI
**VNPI: Van Nuys Prognostic Index, after the primary operation

Table 3-7: Multivariate logistic regression model analysis

The tables shows the association between the various clinicopathological parameters and; a) selection of type of primary surgery for DCIS management (BCS versus mastectomy), b) re-excision after primary treatment with BCS, c) type of the re-excision surgery either another conservative operation or completion mastectomy and, d) presence of residual tumour tissue in the re excision specimens

A)

Parameter	DCIS Diagnosed 1987-2008			DCIS Diagnosed 2009-2017			Whole Cohort		
	HR	95%CI	p-value	HR	95%CI	p-value	HR	95%CI	p-value
Patient age	2.1	0.6-6.8	0.261	2.2	0.2-22.5	0.512	2.3	0.8-6.3	0.121
DCIS presentation	0.7	0.4-1.1	0.134	1.1	0.5-2.6	0.823	0.8	0.5-1.2	0.275
DCIS site (extent)*	2.2	1.1-4.4	**0.030**	0.9	0.3-2.2	0.773	1.7	0.9-2.8	0.058
DCIS size	1.2	0.6-2.2	0.632	1.8	0.7-4.5	0.219	1.2	0.7-1.8	0.527
DCIS Nuclear grade	1.8	1.1-3.2	**0.042**	0.9	0.1-6.1	0.923	1.5	0.9-2.5	0.082
Comedo necrosis	1.7	0.9-2.9	0.075	6.4	1.8-23.1	**0.004**	2.3	1.4-3.8	**0.001**
DCIS Histological type	1.5	0.9-2.4	0.076	0.6	0.2-1.5	0.279	1.2	0.8-1.8	0.381
Presence of Paget's Disease	2.5	1.1-6.2	**0.045**	0.5	0.1-2.4	0.402	1.8	0.8-3.9	0.130

p values in **bold** are significant. HR; hazard ratio, CI; confidence interval

*DCIS extent refers to either localised DCIS involving one quadrant or diffuse that involves more than one breast quadrant.

B)

Parameter	DCIS Diagnosed 1987-2008			DCIS Diagnosed 2009-2017			Whole Cohort		
	HR	95%CI	p-value	HR	95%CI	p-value	HR	95%CI	p-value
Patient age	2.2	0.1-68.3	0.661	0.5	0.2-1.3	0.155	0.9	0.1-8.6	0.974
DCIS presentation	1.2	0.5-2.9	0.646	0.2	0.1-0.9	**0.041**	1.2	0.6-2.2	0.635
DCIS site (extent)	0.1	0.01-0.2	**0.001**	1.4	0.2-6.7	0.711	0.2	0.1-0.5	**0.002**
DCIS size	1.5	0.3-8.1	0.644	2.1	0.3-13.7	0.439	2.8	1.1-6.9	**0.026**
DCIS Nuclear grade	0.4	0.1-1.2	0.114	1.7	0.2-14.7	0.649	0.6	0.2-1.5	0.280
Comedo necrosis	0.6	0.2-1.6	0.336	0.3	0.1-1.3	0.103	0.4	0.2-0.9	**0.046**
DCIS Histological type	1.2	0.5-2.8	0.605	1.6	0.5-4.9	0.409	1.4	0.8-2.4	0.282
Margin status	0.1	0.07-0.2	**<0.0001**	0.1	0.03-0.2	**<0.0001**	0.1	0.02-0.2	**<0.0001**

p values in **bold** are significant

C)

Parameter	DCIS Diagnosed 1987-2008			DCIS Diagnosed 2009-2017			Whole Cohort		
	HR	95%CI	p-value	HR	95%CI	p-value	HR	95%CI	p-value
Patient age	1.5	0.8-2.9	0.233	1.6	0.6-4.4	0.351	1.5	0.9-2.5	0.143
DCIS presentation	2.3	1.2-4.5	**0.014**	1.9	0.6-6.1	0.230	2.4	1.4-4.1	**0.001**
DCIS site (extent)	0.5	0.1-1.8	0.289	0.8	0.3-2.7	0.758	0.6	0.2-1.3	0.158
DCIS size	10.4	3.9-27.8	**<0.0001**	5.2	1.5-18.5	**0.010**	9.7	4.4-21.5	**0.0001**
DCIS Nuclear grade	1.1	0.4-3.0	0.929	3.1	0.8-11.9	0.084	1.3	0.5-3.2	0.590
Comedo necrosis	1.6	0.7-3.5	0.262	0.2	0.1-0.8	**0.028**	0.9	0.5-1.8	0.896
DCIS Histological type	1.3	0.7-2.4	0.491	0.8	0.3-2.6	0.748	0.9	0.5-1.6	0.856
Margin status	0.2	0.1-0.6	**0.002**	1.1	3.6-7.3	**<0.0001**	0.3	0.1-0.7	**0.005**

p values in **bold** are significant

D)

Parameter	DCIS Diagnosed 1987-2008			DCIS Diagnosed 2009-2017			Whole Cohort		
	HR	95%CI	p-value	HR	95%CI	p-value	HR	95%CI	p-value
Patient age	0.7	0.1-5.4	0.731	0.9	0.3-2.2	0.771	1.2	0.7-2.1	0.490
DCIS presentation	1.8	0.9-3.6	0.082	4.4	1.3-14.6	**0.017**	2.1	1.2-3.7	**0.007**
DCIS site (extent)	1.1	0.3-4.3	0.845	0.2	0.1-0.8	**0.023**	0.6	0.3-1.4	0.262
DCIS size	4.1	1.6-10.9	**0.004**	4.7	1.1-19.7	**0.034**	4.2	1.9-9.4	**0.0002**
DCIS Nuclear grade	0.7	0.2-2.2	0.596	1.2	0.3-4.1	0.794	0.7	0.4-1.4	0.297
Comedo necrosis	2.3	0.9-5.2	0.051	0.9	0.3-3.9	0.950	2.0	1.1-3.9	**0.042**
DCIS Histological type	1.3	0.7-2.6	0.359	2.1	0.7-5.6	0.162	1.8	1.1-2.9	**0.030**
Margin status	2.2	0.6-9.1	0.257	0.3	0.1-4.5	0.442	1.3	0.5-3.4	0.626
Type of re-excision*	4.8	2.4-9.5	**0.0001**	2.5	0.8-7.9	0.119	3.3	1.9-5.7	**0.0001**

p values in **bold** are significant

*Type of re-excision either another conservative surgery or completion mastectomy.

VNPI was assessed for all cases treated with BCS after the first operation (n=824) and risk score calculated (mean score was 7.7±1.7, range 4-12). Low risk DCIS was observed in 195 cases (25%), 470 (60%) cases assigned as moderate risk while 118 (15%) cases were high risk DCIS. VNPI could not be assessed in 41 (5%) cases due to one or more of the index parameters were missing. **Figure 3-4** shows that the rate of low risk DCIS increased over years of the study compared with the high and intermediate risk groups that showed lower rates after 2000s.

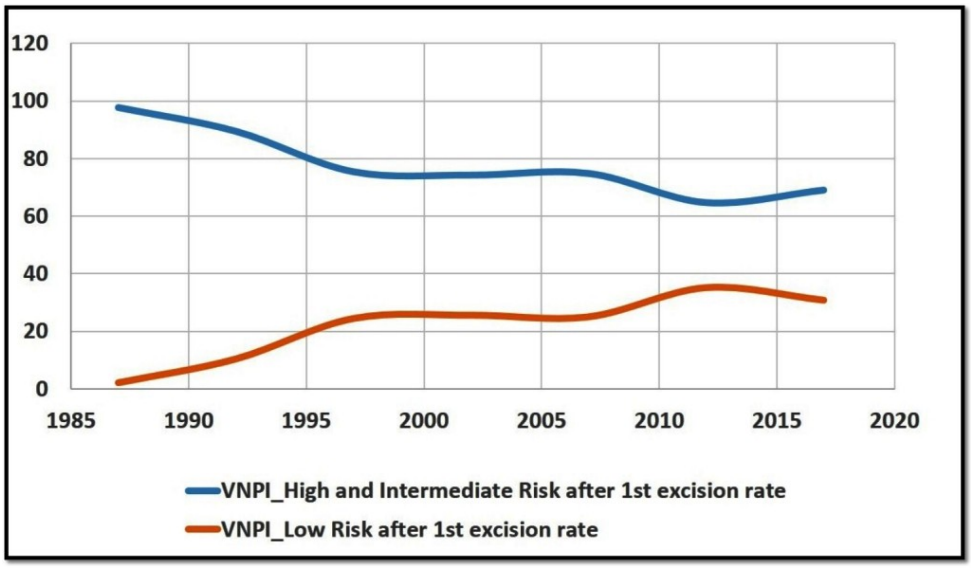

Figure 3-4 Van Nuys Prognostic Index rate change over study period

3.4.1.4 Clinicopathological factors and their association with offering postoperative radiotherapy

263 out of 642 patients (41%) treated with BCS as a final surgery received post-operative adjuvant RT. Its use was

associated with aggressive DCIS features including tumour size >40mm (p<0.0001), higher tumour grade (p<0.0001), presence of comedo type necrosis (p<0.0001), positive or close surgical margins (p=0.008), and moderate and high-risk DCIS based on final VNPI (p<0.0001).

Management of DCIS showed significant changes with acceptance of smaller margins, improving quality of imaging detection of DCIS and more frequent use of local RT. **Figure 3-5** shows details of the trends of primary and final BCS, RT rate, re-excision rate and local recurrence rate. As the most significant change in the margin status was introduced in 2008, this time point was used to compare the old and recent series of DCIS in this study. After 2008, a significant reduction in the rate of mastectomy as the first operative choice for DCIS management was observed (p=0.015), along with a marked decrease in the rate of re-excision to 37% vs 58% prior to 2008 (p<0.0001) and an increase in the presence of residual DCIS in excised specimens (p=0.04). Re-excision rate in 2017 was 23%.

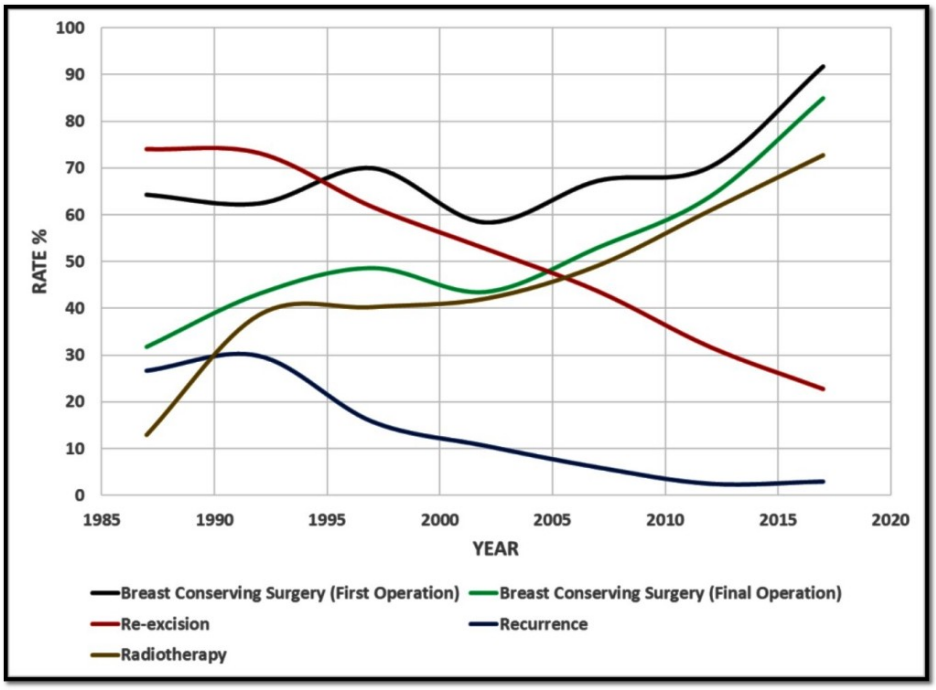

Figure 3-5: The annual clinical rates of DCIS

A) Breast conserving surgery (BCS); shows the higher rates of BCS as a primary surgical choice over the years, B) Shows the comparable rates of final BCS after re-excisions. Obviously over the last 10 years the rates of BCS exceed the rates of mastectomy. C) Post-operative adjuvant radiotherapy; a significant increase of radiotherapy use post-operatively after 2000 is observed. D) Re-excision and E) Recurrence after primary BCS; A significant decrease in both is observed over the last 10 years

The change in surgical practice after 2008, with acceptance of narrower surgical margins, was not hazardous in context of the ipsilateral local recurrence rate. In contrast, the 5-year recurrence rate decreased from 5.4% for DCIS managed between 1987-2008 to 2.2% for those after 2008. The same was observed in the 10-year recurrence rate which was 8.8% in the former and dropped to 2.5% in the latter. However, these differences did not show a statistically significant difference (p=0.223 and 0.225, respectively).

3.4.2 Axillary lymph node surgery

Axillary lymph node sampling was performed for 559 patients (45%) while axillary clearance was performed in four cases (0.3%) which were of high tumour grade and showed comedo type necrosis. None of the cases included in the pure DCIS cohort showed lymph node metastasis with the primary diagnosis of DCIS. Axillary lymph node sampling was carried out for 70% of patients treated with mastectomy compared to 30% of patients treated with BCS ($p<0.0001$). Symptomatic presentation ($p<0.0001$), lesions involving more than one quadrant ($p=0.006$), DCIS size >20mm ($p<0.0001$), high nuclear grade ($p<0.0001$) and presence of comedo type necrosis ($p<0.0001$) were associated with increased rate of axillary lymph node sampling.

3.4.3 Factors influencing the development of local recurrence

Within the median follow up period of 103 months, 97 cases were reported to develop recurrence. Recurrence as DCIS occurred in 36% (n=35) of recurrent cases while approximately two thirds (n=62; 64%) recurred as invasive disease.

Patients treated with BCS alone had the worst prognosis in terms of tumour recurrence compared to patients treated with

either mastectomy or BCS with adjuvant RT either for all recurrences (HR=2.3, 95%CI=1.8-2.9, p<0.0001); or invasive recurrences (HR=2.1, 95%CI=1.5-2.8, p<0.0001); **Figure 3-6.**

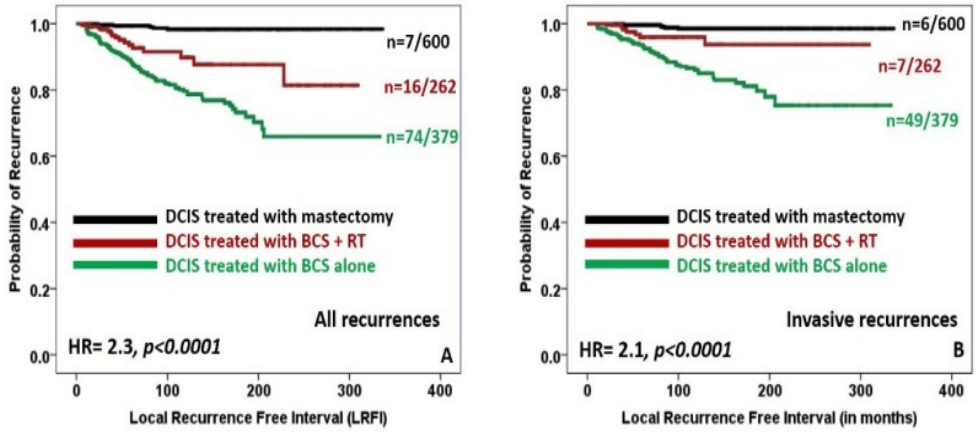

Figure 3-6: Kaplan Meier Curves showing the association between DCIS treatment and recurrence

A) All recurrences and B) Invasive recurrences

Table 3-8 and **Table 3-9** detail the univariate survival analysis showing the association between various clinicopathological parameters and DCIS recurrences, in patients treated with BCS, either all recurrences or invasive recurrence, respectively.

Multivariate analysis showed that higher nuclear grade and larger tumour size are the independent parameters for shorter recurrence free interval in DCIS either for all recurrences or for invasive recurrences (**Table 3-10**)

Table 3-8: Univariate survival analysis of various clinicopathological parameters and all recurrences

Clinicopathological factor	Hazard Ratio (HR)	95% confidence interval		*p*-value
		Lower	**Upper**	
Age at Diagnosis	2.4	1.4	3.9	**0.001**
DCIS Presentation	2.2	1.4	3.5	**0.001**
DCIS Extent	1.9	0.8	4.5	0.136
DCIS Size	2.0	1.3	3.3	**0.004**
DCIS Grade	1.7	1.2	2.4	**0.002**
Comedo type Necrosis	1.1	0.6	1.6	0.974
Solid type DCIS	0.9	0.6	1.5	0.766
Cribriform type DCIS	1.9	1.2	3.1	**0.005**
Papillary type DCIS	2.1	1.2	3.6	**0.008**
Micropapillary type DCIS	0.6	0.3	1.2	0.185
Margin status	2.5	1.2	5.3	**0.015**
Re-excision	1.3	0.8	2.1	0.212
Presence of Residual tumour	0.9	0.5	1.9	0.852
VNPI	1.9	1.2	3.2	**0.008**

Significant p values are in **bold**
DCIS; ductal carcinoma in situ, VNPI; Van Nuys Prognostic Index

Table 3-9: Univariate survival analysis of various clinicopathological parameters and invasive recurrence only

Clinicopathological factor	Hazard Ratio (HR)	95% confidence interval		*p*-value
		Lower	**Upper**	
Age at Diagnosis	2.6	1.1	6.0	**0.032**
DCIS Presentation	1.9	1.1	3.5	**0.018**
DCIS Extent	1.4	0.4	4.7	0.559
DCIS Size	2.3	1.3	4.1	**0.006**
DCIS Grade	1.9	1.2	3.0	**0.003**
Comedo type Necrosis	1.3	0.8	2.3	0.319
Solid type DCIS	1.0	0.6	1.8	0.976
Cribriform type DCIS	1.6	0.6	2.4	0.071
Papillary type DCIS	1.4	0.6	3.0	0.385
Micropapillary type DCIS	0.7	0.3	1.5	0.391
Margin status	1.7	0.8	2.8	0.119
Re-excision	1.0	0.6	1.8	0.874
Presence of Residual tumour	0.8	0.3	2.1	0.727
VNPI	2.8	1.5	5.5	**0.001**

Significant p values are in **bold**
DCIS; ductal carcinoma in situ, VNPI; Van Nuys Prognostic Index

Table 3-10: Multivariate Cox regression analysis between various clinicopathological parameters and DCIS recurrence

All Recurrences				
Clinicopathological factor	**Hazard Ratio (HR)**	**95% confidence interval**		***p*-value**
		Lower	**Upper**	
Age at diagnosis	1.7	0.9	3.0	0.106
DCIS Presentation	1.7	0.9	2.9	0.062
DCIS size	1.9	1.1	3.4	**0.023**
DCIS grade	1.8	1.2	2.9	**0.008**
Margin status	0.8	0.6	1.1	0.115
VNPI	0.7	0.4	1.5	0.420
Invasive Recurrences				
Age at diagnosis	2.1	0.8	5.7	0.128
DCIS Presentation	1.4	0.7	2.9	0.296
DCIS size	2.1	1.1	3.9	**0.043**
DCIS grade	1.7	1.1	3.0	**0.047**
VNPI	1.4	0.6	3.3	0.456

Significant p values are in **bold**
DCIS; ductal carcinoma in situ, VNPI; Van Nuys Prognostic Index

3.5 **Discussion**

Currently, after introduction of mammographic screening programme for all women, the incidence of DCIS has dramatically increased and accounts for 20-25% of screen detected BC [7]. Variability in the figures of screen detected versus symptomatic DCIS diagnosis is related to cancer centres' registration strategies, variable target screening age range between countries and time intervals between each screening, reporting of the discovered DCIS and women compliance to the screening programme [117]. For instance, the targeted screening age in the USA ranges from 40 to 84 years old while in UK and Australia it ranges between 50 to 69, with current trends to expand it [37]. In the current series, 60% of cases were screen detected and the remaining presented symptomatically either with a mass forming lesion, nipple discharge or Paget's disease of the nipple. These figures are comparable to findings of the National Cancer Intelligence Network in 2007 where 62% of DCIS were screen detected [258].

Prior to the early 1990's, the standard treatment for DCIS was mastectomy. However, BCS with adjuvant RT showed comparable outcome to mastectomy in terms of LRFI and overall survival and as a result, the rate of mastectomies has

declined and BCS predominates [20, 259]. In Nottingham, over a 30-year period, approximately two thirds of cases were treated with BCS as a first surgical modality. Mastectomy was the preferred option for patients with symptomatic DCIS, high tumour grade, larger sized tumours (>40mm), showing comedo necrosis and tumours involving more than one quadrant of the breast. There was not only an increase in the rates of initial BCS but also a significant decline in the re-excision, final mastectomy and ipsilateral local recurrences rates. Although the change in local practice occurred at certain points of time such as in 2008 in which margin width of 5mm was accepted instead of 10mm, and a recent change of practice in 2016 in which 2mm margin was adopted [102], the frequency of BCS, re-excision rates and local recurrence rates appear to show gradual change over time rather than sudden transition at a certain time point. This may reflect the impact of several factors including the improvement of imaging quality with better assessment of DCIS size and extent, quality of surgery, and the growing use of local RT.

Sentinel lymph node biopsy (SLNB) is not routinely performed as a part of the surgical management of DCIS and current practice guidelines recommend offering SNLB for patients scheduled to be treated by mastectomy as they are usually at a higher risk to harbour invasive foci within their DCIS [260].

For BCS, SLNB might be performed if the lesion is >5cm or forming a mass [261] although positive SLNB rarely changes the adjuvant regimen therapy in these patients [262]. Approximately half of cases in the current series had axillary lymph node sampling which was targeted mainly for patients treated with mastectomy. Symptomatically presented young patients treated with BCS for a large size high grade DCIS, with comedo necrosis also underwent SLNB. There were four patients who underwent axillary clearance and those presented symptomatically before 1995, older than 60 years old and had large sized high-grade tumours showing comedo necrosis and managed by mastectomy. It can therefore be postulated that such aggressive features were convenient for the surgeons to follow such aggressive approach in treatment.

The results describe the radiological and pathological indications for attempting BCS and the factors associated with the decision to perform additional therapeutic operations. The predominant factor in deciding BCS as the surgical modality is the extent of the disease. Patient choice might also be a contributing factor as evidenced by the NHS Breast Screening Programme where patient choice accounts for about 11% of mastectomies for DCIS [263]. Recently, in the UK and US, mastectomy rates have increased particularly in young women perceived at high risk of further BC events [91, 264]. In a

report on 8,000 DCIS cases included in the Sloane Project and treated between 2003 and 2012, the rate of attempted BCS was 79% and successful BCS was 68% [263, 265]. Achieving success at BCS for DCIS remains a challenge and it continues to be the case that a woman with DCIS is at least as likely to have a mastectomy as a woman with IBC. Re-excision rates after BCS as a treatment for DCIS are higher than re-excisions for IBC. Furthermore, invasive disease accompanying DCIS has a higher re-operation rate than invasive disease alone [266, 267].

The need to perform further surgery, re-excision or completion mastectomy, is governed predominantly by what is regarded as a minimum free resection margin. Young patient age, symptomatic presentation, lesions involving more than one breast quadrant, DCIS size >40mm, and presence of comedo necrosis are associated with positive surgical margin. Positive resection margin is likely due to radiological under-estimation of DCIS size which occurs in over 50% of cases [265, 268]. Other studies [266, 268-274] have shown that diffuse DCIS growth patterns such as micropapillary and cribriform types, high nuclear grade DCIS with comedo type necrosis and high risk VNPI are factors associated with increased rate of re-excisions.

Approximately half of the DCIS patients who underwent re-excision, due to positive or close surgical margins, were of low and intermediate grade. This might change the pending outcome of recent trials of more conservative management of low risk DCIS [112, 275].

In this study, half of the re-excised specimens were free of residual tumour tissue, although some cases were reported to have tumour on ink after the primary excision. Such finding perhaps reflects the inconsistency in pathological evaluation. However, the presence of residual DCIS was associated with adverse clinicopathological parameters such as symptomatic presentation, tumour size, DCIS with cribriform and micropapillary architecture. Some studies have tried to establish a margin index based on tumour size and the closest surgical margin to show the association with presence of residual tumour tissue after re-excision, but this did not show a significant association [276, 277]. Another study concluded that the extent of margin involvement as well as the number of involved ducts in that margin are key factors for predicting presence of residual DCIS in the re-excision specimen [257]. In this study, it was shown that after 2008, there was an increased rate of residual tumour in the re-excision specimen and this might reflect a better overall strategy for further surgery.

Determining the optimal free margin for BCS is challenging particularly in pure DCIS. The Society of Surgical Oncology-American Society for Radiation Oncology published new guidelines for the optimal surgical margin in invasive disease and defined negative margin as 'no tumour on ink' because there is no evidence that wider clear margins reduce the ipsilateral local recurrence [278]. The same group has published consensus guidelines suggesting a 2mm free margin as a standard for adequate surgical resection of DCIS [102]. Systematic review and meta-analysis of 20 studies showed that negative surgical margin minimises the risk of ipsilateral local recurrence by 50% compared to involved margins. A 2mm margin minimises the risk of recurrence compared to narrow negative margins [102, 279-282]. However, the agreement on the previous recommendations is different and the choice of optimal margins depends mainly on the surgeons' practice and the pathologists' methods of margin assessment which is currently supported by NICE guidelines [283]. Adopting close margins of excision is a means of reducing reoperation rates, as it has been shown in invasive disease [284], however, planning a wider macroscopic margin in higher risk cases but tailoring the scrutiny of margin analysis to the risk factors should be performed. The current results show that the change in surgical practice with narrow

free margin in patients treated conservatively did not increase the recurrence rate. This reflects better risk assessment, modest use of adjuvant RT and individualised management for patients based on constellation of all clinicopathological factors.

Some trials have shown a 50% reduction in the recurrence rate using adjuvant RT after conservative DCIS surgery [92, 93, 95, 98, 285]. However, they could not identify a specific group of patients where RT could be safely avoided and hence the continued debate over RT indication after BCS remains. In routine practice, approximately 30-50% of BCS treated patients receive adjuvant RT [286]. A common local practice before 2008 was not to offer further treatment for patients with clear surgical margin of 10 mm or more. However, in the current series, 41% of BCS treated patients were offered post-operative RT regardless of their margin status. Outcome analysis of previous studies has shown that selective RT was introduced and then it was recommended after BCS to those with high grade DCIS, women <50 and lesions >30mm following a multidisciplinary team discussion [223]. Patients who undergo mastectomy are not offered RT regardless of their age, tumour grade or lesion size.

The current study reports a local recurrence rate of 7.5% regardless of the management modality and 14.5% following BCS, which is close to the reported figures with a range between 7 and 12% [287]. Most of the previous trials reported that half of the local recurrences are invasive [96, 288-290]. In this series, approximately 64% of the recurrences were invasive.

Although factors of aggressive DCIS such as young patient age, symptomatic presentation, high grade, comedo necrosis and close surgical margins are associated with poor outcome, their results were inconsistent between various studies depending on the included sample size, local surgical management practice and DCIS pathological evaluation. This study showed that DCIS size, high nuclear grade and absence of adjuvant RT are the key independent factors that were associated with poor outcome in terms of shorter LRFI in BCS treated DCIS. Papillary DCIS was associated with shorter LRFI in this series which may be related to incomplete excision of these lesions which show extendable growth pattern.

An increased recurrence rate associated with high grade DCIS might reflect the natural history of the disease rather than being truly predictive of recurrence [67].

In a study by Ringberg *et al.* patients with low or intermediate grade DCIS had approximately half the risk of an ipsilateral breast event compared to patients with high grade DCIS [291]. Although there is a great acceptance that low grade tumours are associated with a lower risk of recurrence, few studies have examined the long natural history of low-grade DCIS. A unique study in the USA followed 28 women with low grade DCIS after biopsy alone, over a 30 year period [292]. After the follow up period, 11 out of the 28 women developed an ipsilateral IBC. All of the invasive recurrences were in the same quadrant as the initial biopsy. Eight women developed recurrence within 12 years after diagnosis and the remaining three had invasive recurrences at 23 and 29 years respectively. The authors concluded that the long natural history of low-grade DCIS marked it as a distinct lesion, with a different behaviour to higher grade DCIS. They showed that women with low grade DCIS who did not receive definite treatment remained at risk of recurrence for a prolonged period after the diagnosis, particularly in the first 15 years. Analysis of risk factors in the European Organisation for Research and Treatment of Cancer (EORTC) study was performed on 76% of study population [289]. Patients with low grade DCIS had a significantly lower risk of DCIS recurrence compared to patients with an intermediate or high-

grade tumour. However, there was no significant difference in the incidence of invasive recurrences at 10 years. The above data suggest that the risk of recurrence in patients with low grade DCIS continues to rise beyond 5 years of follow up. Thus, sufficient follow up time is necessary for evaluating the outcome of patients with low grade DCIS. This should be taken into consideration for management decision making in patients with low grade DCIS [293].

Although the definition of young age varied among the studies, it was shown to be significantly associated with an increased risk of local recurrence [67, 96, 294]. In a study of 615 patients treated with BCS for DCIS, multifocality defined as the presence of more than one distinct focus of DCIS with at least 5mm of intervening healthy tissue confined to a single quadrant of the breast, was identified in 42% of patients. In a multivariate analysis, multifocality was a predictor of local recurrence. In addition, omission of RT, margin width <4mm and high nuclear grade were also predictors of local recurrence.

VNPI assesses DCIS risk for optimal management based on the previously described four clinicopathological parameters [62]. Several studies have attempted to validate its value [118, 119, 254, 295]. VNPI risk groups in the current series

were categorised after the first operation and showed high correlation with the final treatment decisions. However, VNPI assessed after the final operation showed no association with tumour recurrence. Our findings were concordant with other studies which tried to verify using this index to predict tumour recurrence [119, 295]. Taken together, VNPI would be a reasonable risk index for choosing the management approach but might not be a powerful index for predicting tumour recurrence. So, other nomograms were developed in order to provide a risk index for tumour recurrence, but they need more validation [120, 296, 297].

In conclusion, this study showed the interplay between different clinicopathological factors and patient outcome and that some indices like VNPI may be helpful in deciding treatment but not predicting patients' outcome. Surgical margins should be thoroughly examined to eliminate their effect on later development of local recurrence.

4 Chapter 4: Molecular characterisation of DCIS

4.1 **Introduction**

Robust prognostic and predictive tools have the ability to identify the risk of disease progression and outcome and hence adjuvant therapy following local surgery could be personalised and justified for cost and benefit effectiveness [298]. To be applicable, prognostic factors must show a considerable separation in the outcome of the identified groups with adequate numbers of patients in each group. Nevertheless, for precision medicine, no single prognostic factor satisfies all these criteria [299]. In addition, the reliability of such prognostic factors using routine techniques of tissue and imaging diagnostic tools, rather than sophisticated ones, besides cost limits are practically inhibitive.

Predictive factors, which predict whether a tumour is likely to respond to a certain treatment are complimentary to prognostic factors and used to select the most appropriate additional therapy for a patient when needed. Contrary to predictive factors for ET which are well established, those predictive of chemosensitivity are less well defined. It is difficult to recognise those patients who are more likely to respond to a particular chemotherapy regimen based on traditional prognostic/predictive factors such as lymph node status and tumour size alone [300, 301].

In DCIS, there is a current inability to predict patients' risk to develop invasive cancer precisely; therefore, the standard care for patients diagnosed with DCIS was long been considered as surgical removal of the tumour either through mastectomy or BCS followed by postoperative RT [302]. Even with RT, some risk of invasive progression remains, and therefore current management is to eradicate DCIS in order to prevent this occurrence. However, DCIS is morphologically, molecularly and biologically heterogeneous disease [122] where some cases will behave indolently and not progress to invasive carcinoma during the patient's lifetime, while others will follow an aggressive course. The events orchestrating the progression of DCIS to invasive carcinoma have not been fully identified yet [167].

4.2 Clinicopathologic parameters as prognostic factors

Certain clinical and pathological features of DCIS may be prognostic of local and/or invasive recurrence following surgical excision [303], as described in **Chapter 3**. For instance, some studies have suggested that tumour size is a strong predictor of local recurrence [304, 305]. Nuclear grade and margin status are other factors that appear to influence recurrence in DCIS [54, 252, 306], though certainly there is a

study that disproves these findings [307]. Two major clinical tools that aid in risk stratification and treatment planning; the VNPI and the DCIS nomogram introduced by Rudloff *et al.* utilise both 10 various parameters including clinical and pathologic features such as tumour size, necrosis, and margin status [120, 303, 308]. Furthermore, the newly described genetic signatures such as Oncotype DX DCIS for prediction of recurrence show controversial results and need further validation [77, 78, 120, 296, 308, 309]. Currently, no single factor or combination of factors are able to reliably predict the behaviour of a DCIS lesion, leading to potential over- or under-treatment of an individual patient and accompanying morbidity, potential mortality, financial and social cost.

While the current ability to accurately predict recurrence on the basis of these parameters is limited, clearly the paradigm that one approach fits all in patients with DCIS is changing [79].

Research efforts have focussed on classifying patients who may be managed conservatively and those who are at higher risk for disease progression and thus may require adjuvant therapy [79]. Currently, there are several studies that propose watchful waiting for low risk DCIS, however the inclusion criteria of these trials are very restricted, and the outcome is not clarified yet. The ideal classification scheme would be

clinically useful and easy to adapt with the ability to stratify patients into prognostic groups. While not consistently identified in all studies, certain histopathological parameters and expression of various markers have been variably shown to affect the risk of recurrence in pre-malignant breast lesions [310]. Improved molecular characterisation of DCIS will offer additional, perhaps more definitive, prognostic information and may provide the opportunity for personalised therapeutic options for patients with DCIS.

4.3 Gene expression profiling-derived classes and signatures

The developments of gene expression profiling studies and related prognostic signature studies have dramatically unravelled the molecular heterogeneity and diversity in BC in general and DCIS in particular [311]. Moreover, they have contributed to the current understanding of BC molecular intricacy and led to the identification of distinct subtypes. Importantly, molecular subtyping and prognostic signatures that have arisen from gene expression profiling studies will have important impacts on future drug discoveries and improving clinical management [312].

4.3.1 Molecular Classes

A biomarker is defined as "a detectable substance that is objectively measured and evaluated as an indicator of normal biological processes, pathogenic processes, or pharmacologic responses to a therapeutic intervention" [313].

4.3.1.1 Historical background

A new classification system of biological BC subtypes was adopted at the 12th St. Gallen International Breast Cancer Conference 2011 [314]. The intrinsic molecular subtypes based on gene expression analyses [311, 315] are for practical purposes approximated using clinicopathological criteria [316]. Systemic therapy recommendations for IBC according to the subtype classification were also proposed [317].

4.3.1.2 Importance of molecular classification

A clinically useful histopathological classification system for DCIS predicting prognosis however is still missing. Survival is excellent after a primary diagnosis of DCIS, but the risk of recurrence is considerably high [318]. Hence, identification of biomarkers to aid in individualised treatment decisions regarding surgery and RT is needed. Kerlikowske *et al.*, [31] used IHC for biomarkers including Ki67 showing that biomarkers were better than histopathological criteria for identifying risk groups for subsequent invasive cancer and

Solin *et al.*, [78] used a 12-gene array Oncotype DX DCIS to identify risk groups after BCS without postoperative RT.

4.3.1.3 Surrogate molecular subtypes for DCIS

The different subtypes are defined as follows;

- Luminal A (ER and/or PR positive, HER2 negative and Ki67 <14%)
- Luminal B/HER2- (ER and/or PR positive, HER2 negative and Ki67 ≥14%),
- Luminal B/HER2+ (ER and/or PR positive, HER2 positive),
- HER2+/ER- (non-luminal) (ER and PR negative and HER2 positive),
- Triple Negative DCIS, (ER, PR and HER2 negative).

The IHC surrogate definitions are based on the 2011 St. Gallen guidelines [314].

4.3.1.4 Oestrogen receptor

Although there are a very large pool of potential biomarkers, only three are used in routine clinical practice worldwide: ER, PR and HER2 [319]. ER was one of the first biological markers studied in depth. It was identified by Ellwood Jensen in the late 1950s [320], and ER status has been used since the mid-1970s, as one of the most valuable markers in BC, both to predict responsiveness of the invasive tumour to ET [321] and as a prognostic factor for early recurrence and long-term outcome [313].

In a review study that examined ER expression rate in DCIS, the mean ER expression rate was 70-75% [321]. Two studies have revealed ER expression to be inversely related to the nuclear grade of DCIS, for example, ER expression is higher in well-differentiated tumours than in poorly differentiated lesions [322, 323]. Some studies have identified an association between ER negative DCIS and risk of local recurrence [31, 324].

4.3.1.4.1 Oestrogen receptor status in clinical settings

The management of DCIS continues to be a challenge. Although DCIS is predominantly associated with a low risk of mortality [318, 325], it is well documented that it could progress into IBC, which is associated with increased risk of death [93, 96]. Furthermore, the psychological impact of a recurrence, in-situ or invasive disease, must not be underestimated. Lack of a robust tool to identify low risk DCIS results in recommendations that all women with DCIS undergo treatment, especially results of the clinical trials that provide no active treatment to low risk DCIS are not published yet [111, 112].

Most DCIS patients will be treated with BCS followed by RT, because of its proven efficacy to reduce local recurrence risk [92, 106, 289]. RT may be omitted for women at low risk of recurrence, however clinical and pathological features have not

reliably identified patients at low risk of recurrence following BCS alone, leading to variability in treatment and outcomes of women with DCIS [326].

Data on adjuvant ET in DCIS continues to evolve and its use has become more common in the US, with approximately 60% of all DCIS cases having BCS receiving it in recent years [327]. Adjuvant ET for hormone receptor–positive DCIS tumours, with Tamoxifen or aromatase inhibitors (anastrozole), may improve local control in hormone-responsive disease [106, 108, 328-330] and reduce the risk of BC recurrence without showing survival benefit [96, 106]. Data on outcome by the ER status of the DCIS is absent in most randomised trials. However, a sub-study of 732/1799 (41%) of patients in NSABP B-24 trial reported that Tamoxifen significantly decreased BC recurrence in ER positive but not ER negative DCIS [105].

NICE has updated the recommendations for adjuvant ET for DCIS to offer it after BCS for women with ER-positive DCIS if RT is recommended but not received; and to consider ET after BCS for women with ER-positive DCIS if RT is not recommended [110]. The American Society of Clinical Oncology/College of American Pathologists also recommended testing of DCIS for ER to determine the potential benefit of ET to reduce risk of future BC [331]. Clinical application of these

recommendations means that ER testing would be necessary for all DCIS in order to be considered for management decision. However, DCIS is not routinely stained with ER and the impact of ET on the outcome of DCIS, and whether this impact is limited to ER-positive DCIS, remains to be defined. Furthermore, routine measurement of ER would increase the burden on the pathology service. The effect of implementation of such recommendation on clinical practice and the effect on overall patient mortality and morbidity should be investigated.

4.3.1.4.2 Literature review of clinical trials of ET for DCIS

Four clinical trials reported in literature evaluated the response of DCIS patients to ET following BCS and RT with or without comment on ER status, two of Tamoxifen versus placebo [330, 332] and two comparing the difference of clinical benefit between Tamoxifen and anastrozole [108, 329]. None of these trials included DCIS grade as a criterion for inclusion into assessment.

In the NSABP B-24 trial, all women with DCIS received RT before being randomly assigned to Tamoxifen or matching placebo. After a median follow-up of 6 years, a significant 37% reduction in BC recurrence was observed with Tamoxifen compared with placebo. BC events were lower in the Tamoxifen group (6.0%) compared to the placebo arm (9.3%) in the ipsilateral breast. The cumulative incidence of all IBC events in

the Tamoxifen group was 2.1% in the ipsilateral breast at 5 years which was lower than that in the placebo arm (4.2%) [330].

Retrospective evaluation of ER and PR in 732/1804 patients from this B-24 trial was done. 449 tumours had ER & PR measured at a central lab while the remaining 283 tumours had results from the enrolling institutions. 76% of DCIS were ER positive. 24% of DCIS tumours were ER negative. Benefit of Tamoxifen by receptor status at 10 years was evaluated with overall follow-up of median 14.5 years. Patients with ER-positive DCIS treated with Tamoxifen showed significant 51% reduction in subsequent BC at 10 years and overall follow-up, which was independent of other confounding prognostic factors. No significant benefit was observed in ER-negative DCIS [105].

In the UK/ANZ DCIS trial, 1578 women with DCIS were randomly assigned to receive Tamoxifen with or without RT. After a median of 13 years of follow-up, Tamoxifen significantly reduced all new BC events by 29%, with a significant impact on ipsilateral DCIS recurrence and contralateral tumours, but no effect on ipsilateral invasive recurrence [106, 332]. ER was not an entry criterion and there was no analysis of the invasive recurrence by ER status of the initial DCIS.

Overall the evidence from the former studies is that Tamoxifen significantly decreases BC recurrence. Based on the sub-study on B-24 this would appear to be limited to ER-positive DCIS and not ER-negative DCIS.

These findings would be supported by the BC prevention studies of Tamoxifen [333] and aromatase inhibitors [334, 335] versus placebo which have reported a significant reduction in ER-positive BC (both invasive and DCIS) but no significant reduction in ER-negative disease.

In the observational study of prospective artificially randomised cohort [336], low dose Tamoxifen showed 30% reduction of any type of recurrence in women with high risk ER-positive DCIS. However, when ipsilateral invasive recurrence was considered the difference was not significant.

In NSABP B-35, 3104 patients were enrolled and randomised to either Tamoxifen or anastrozole. Within the median follow-up period of 9 years, 212 BC free interval events occurred: 122 in the Tamoxifen group and 90 in the anastrozole group.

4.3.1.5 Progesterone receptor

PR is considered as an additional marker to ER in IBC where it is weakly prognostic as regard to LRFI and also a predictor of response to ET [321]. In previous studies, the mean PR expression rate in DCIS was 60%. Similar to ER, an inverse

relationship was observed between PR expression and nuclear grade, for example, patients with high-grade DCIS were less likely than patients with non-high grade DCIS to have PR-positive disease [337, 338]. A direct positive relationship was observed between PR and ER expression [339]. Few studies have showed a significant correlation between PR-negative DCIS and local recurrence [340, 341].

4.3.1.6 Human epidermal growth factor receptor 2

4.3.1.6.1 HER2 protein expression

One of the interesting aspects of DCIS is that the expression of HER2 is linked to initiation and progression of BC [78]. Therefore, its frequent overexpression is commonly seen in high grade DCIS with or without necrosis which suggests that HER2 plays a role in tumour initiation and progression [342]. HER2 is a member of the type I receptor tyrosine kinase family. The major role of HER2 is to serve as a co-receptor in the dimerisation and activation of other HERs. The amplification of the gene *HER2* results in a 50 to 100-fold increase in the number of surface HER2 receptors on cancer cells compared to normal mammary cells [343]. The expression of HER2 in DCIS is linked to recurrence following surgical excision without RT [304]. However, HER2 expression as an independent risk factor for recurrence remains controversial [344].

IHC staining is the predominant method of determining HER2 status in BC specimens due to its relative ease to perform with rapid turnaround time and lower cost [345]. However, commercially available antibodies have shown wide variation in sensitivity and specificity for FFPE tissue samples, in which tissue fixation and pre-treatment have a substantial effect on staining [346].

4.3.1.6.2 *HER2* gene amplification

HER2 gene amplification is primarily detected by FISH to detect the signals. This method is expensive and requires expertise with fluorescent microscopy using appropriate filters [347]. CISH offers an alternative method, and whilst it utilises *in situ* hybridisation technology of FISH, it takes advantage of a chromogenic signal detection that is assessed using light microscopy and therefore is a cheaper alternative. CISH is able to detect *HER2* gene amplification and to minimise, if not eliminate, the borderline category with IHC [348].

4.3.1.7 The proliferation marker "Ki67"

Ki67 protein was first defined by Gerdes and colleagues, who developed a prototype monoclonal antibody Ki67 through immunising mice with the nuclei of the Hodgkin lymphoma cell line L428 [349]. Detailed cell cycle analysis reveals that the antigen is present in the nuclei of cells in all active cycling/proliferative phases (G1, S, and G2) as well as in M

phase, while quiescent or resting cells in the G0 phase did not express it. Therefore, it has been used as a biomarker to assay the growth fraction of a given cell population [350, 351]. The nuclear antigen Ki67 is commonly used to assess the proliferation rate of BC, which is a key element of progression of the disease [352]. Variable mean Ki67 expression is observed, and attributable to several factors such as tumour grade and HER2 status [353, 354]. In addition, Ki67 is a predictor of local recurrence, either independently or in combination with other factors [31, 355].

4.4 **Hypothesis and aims**

It is hypothesised that classification of DCIS according to the molecular classification of BC might help in patient risk stratification and that identification of biomarkers to aid in individualised treatment decisions regarding surgery and RT is needed. Therefore, implementing well-established biomarkers for IBC; ER, PR, HER2 and Ki67 to classify DCIS tumours was aimed.

Also, in this chapter, a large retrospective cohort of DCIS treated in a single institution was used to address the outcome of ER-positive DCIS, especially invasive recurrence to consider the utility of routine ER testing in these patients. Also, the

randomised studies reporting on adjuvant ET and clinical outcomes of DCIS after BCS were reviewed.

4.5 Patients and methods

4.5.1 Study cohort

This retrospective study was conducted on a consecutive series of primary pure DCIS (**Chapter 2**). 778 cases of pure primary DCIS with available FFPE tumour blocks were included in the TMA construction together with a series of 239 cases diagnosed as synchronous DCIS and invasive tumours (mixed DCIS and IBC) collected for comparison.

4.5.2 IHC and CISH

4.5.2.1 IHC

The IHC staining and evaluation of ER, PR, HER2 and Ki67 was performed using the TMA sections. Positive and negative controls were included in every assay, where internal control of breast tissue was used as a positive control for ER and PR, BC tissue for HER2 and tonsil tissue for Ki67. MIB1 antibody was used for evaluation of Ki67 expression. Nuclear staining was assessed for ER, PR and Ki67 and membrane staining for HER2 (**Chapter 2**), as demonstrated in **Figure 4-1**. HER2 status was assessed using HercepTest scoring method [356]. HER2 status was considered negative if the

immunohistochemical score was 0 or 1+, equivocal if the score was 2+, and positive if the score was 3+.

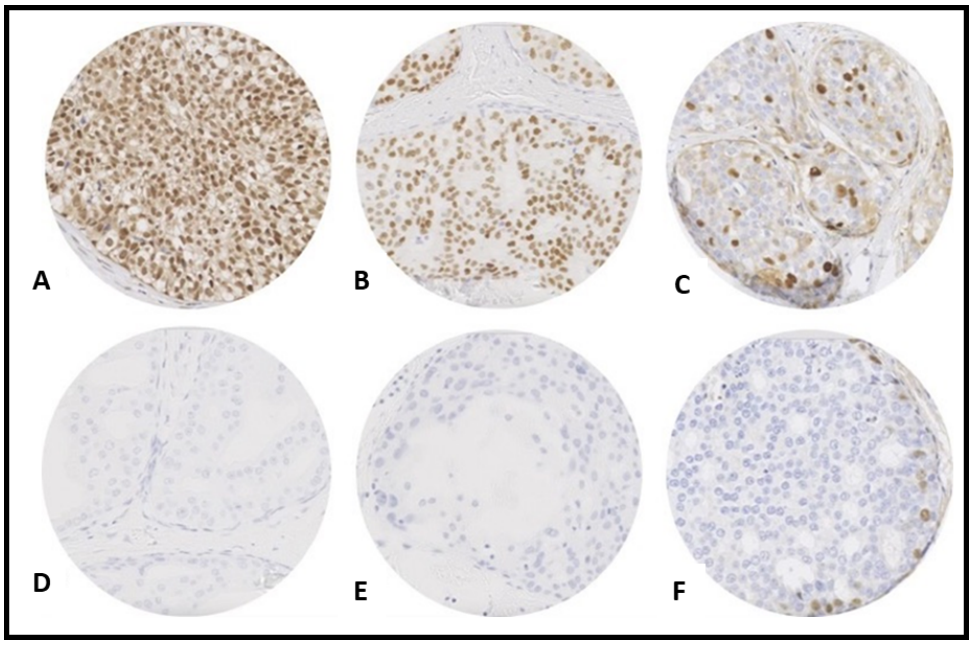

Figure 4-1: Immunohistochemistry of the biomarkers used in DCIS molecular characterisation.

ER positive (A), PR positive (B). Ki67 high proliferative index (C), ER negative (D), PR negative (E) and Ki67 low proliferative index (F).

4.5.2.2 CISH

CISH was performed according to the recommended method (**Chapter 2**). *HER2* gene amplification was determined by CISH using the ZytoDot 2C SPEC *ERBB2/CEN17* Probe Kit, (ZytoVision®, Germany). Interpretation of CISH was performed using a Nikon microscope equipped with a x63 objective lens. At least 20 malignant, non-overlapping cell nuclei were scored to assess *HER2* gene copy number. Chromosome 17 (represented by the red signals) was used as an internal control particularly in the low *HER2* gene copy

number cases as per the recommended protocol. *HER2* gene amplification was defined as six or more signals per nucleus or when clusters (clumps of aggregated green signals) were identified in the cell nuclei in more than 50% of tumour cells [357]. If the average copy number was ≥4 to <6 per nucleus (equivocal), another 20 tumour cells were enumerated, and the final average copy number of the case was calculated from the total of 40 cells.

For ER and PR, a 1% cut-off value was used to dichotomise cases into positive and negative [358]. For Ki67 the cut-off for differentiating low and high proliferative groups was 14% [317].

4.5.3 Statistical analysis

Association between final HER2 status and clinicopathological parameters using categorised data in the pure DCIS cohort was evaluated using Chi-squared test. Survival rates were determined using the Kaplan–Meier method and compared by the log-rank test. Multivariate survival analyses using Cox proportional hazard regression model was used to evaluate the associations between independent variables and local recurrence. Multivariable hazards ratio and their corresponding 95% CI were initially performed for each marker alone and then for the combination of biomarkers. All tests were 2-tailed

and a *p* value of less than 0.05 was considered as statistically significant.

4.6 **Results**

A total of 651 pure DCIS cases were suitable for analysis. The clinicopathological characteristics of pure DCIS cases, the frequency of ER and PR positivity and the proliferation index are detailed in **Table 4-1**.

Table 4-1: Clinicopathological features of the pure DCIS cohort included in the study

Parameter	Total (n=651) n (%)
Age, years	
<40	22 (3)
40 to 60	379 (59)
>60	250 (38)
Presentation	
Screening	337 (52)
Symptomatic	314 (48)
DCIS Size (mm)	
<16	224 (35)
16 to 40	247 (38)
>40	175 (27)
Nuclear Grade	
Low	87 (14)
Intermediate	167 (25)
High	397 (61)
Comedo necrosis	
Yes	416 (64)
No	233 (36)
ER Status	
Positive	428 (75)
Negative	142 (25)
PR Status	
Positive	302 (46)
Negative	349 (54)
Ki67 Index	
High (≥14%)	110 (23)
Low (<14%)	361 (77)

DCIS: Ductal carcinoma *in situ*; ER: Oestrogen receptor; PR: Progesterone receptor

4.6.1 ER distribution among study cohort

A total of 643/1249 (51%) cases were available for ER measurement and subsequent analyses. 475/643 (74%) DCIS cases showed positive expression of ER. There was a trend towards an increase in ER positivity and a decrease HER2 positivity over the period of the study.

Within these patients 300 (47%) patients were treated by BCS, and 100 (33%) of those patients were offered RT.

4.6.2 Association between ER and other clinicopathological factors

ER positivity was associated with features of good prognosis including smaller tumour size (<40mm), low nuclear grade, absence of comedo necrosis, positive PR status and lack of HER2 overexpression (all $p<0.0001$). Most ER-positive DCIS patients were treated with BCS (81%; $p<0.0001$), without adjuvant RT (84%; $p=0.039$) compared to ER-negative cases ($p<0.0001$). **Table 4-2** summarises the correlations between ER expression and other clinicopathological parameters.

Table 4-2: Correlation between ER expression and the clinicopathological variables of pure DCIS cases

Parameter	ER Expression		
	Negative (n=168) n (%)	**Positive (n=475) n (%)**	**χ^2 (*p* value)**
Age (years)*			
<40	6 (26)	17 (74)	0.077
40 to 60	94 (27)	260 (73)	(0.962)
>60	68 (26)	198 (74)	
Presentation			
Screening	96 (29)	240 (71)	2.178
Symptomatic	72 (23)	235 (77)	(0.140)
Localisation			
Localised	118 (26)	333 (74)	0.764
Diffuse	27 (31)	61 (69)	(0.382)
Size*			
<16mm	42 (20)	168 (80)	17.272
16 to 40mm	57 (23)	191 (77)	(<**0.0001**)
>40mm	68 (37)	114 (63)	
Grade			
Low	6 (7)	80 (93)	25.194
Intermediate	10 (6)	158 (94)	**(<0.0001)**
High	152 (39)	237 (61)	
Comedo necrosis			
Yes	145 (35)	267 (65)	48.844
No	23 (10)	208 (90)	(**<0.0001**)
Associated Paget's			
Yes	16 (55)	13 (45)	7.962
No	95 (30)	225 (70)	(**0.005**)
Management+			
Mastectomy	110 (32)	232 (68)	13.617
BCS	58 (19)	242 (81)	(**<0.0001**)
Radiotherapy**			
Yes	26 (26)	74 (74)	4.275
No	32 (16)	168 (84)	**(0.039)**
PR Status			
Positive	4 (1)	338 (99)	274.791
Negative	154 (63)	92 (37)	**(<0.0001)**
HER2 Status***			
Negative	73 (16)	374 (84)	84.379
Positive	63 (59)	44 (41)	**(<0.0001)**

DCIS: Ductal carcinoma in situ, N: Number, X2: Chi square, p value in bold: significant.
ER: Oestrogen receptor, BCS: Breast conserving surgery, PR: Progesterone Receptor.
*Age and size: categorised according to the Van Nuys Prognostic Index (VNPI),
+Management is according to the final operation
**Radiotherapy status is for cases treated with BCS,
***HER2 final status is achieved using combination of IHC and chromogenic in situ hybridisation (CISH).

4.6.3 Association between ER status and DCIS outcome

Ipsilateral recurrence developed in 12% of patients (37/300) within 5 years and in 19% of patients (56/300) within 10 years. Of all ipsilateral recurrences, 55% (31/56) were invasive. The recurrence rate was similar between ER negative and ER positive DCIS within 5 years (p=0.940); and within 10 years (p=0.664). Similar results were observed when the analysis was confined for invasive recurrences (p=0.395 for 5-year recurrence and p=0.337 for 10-year recurrence).

It is noteworthy that 94% of the overall invasive recurrences have the same ER status of their primary DCIS. 25/26 ER positive DCIS patients developed ER positive invasive recurrence (96%), whereas 7/8 ER negative DCIS patients developed ER negative invasive carcinoma (88%). The single case that was ER positive DCIS and recurred as ER negative invasive recurrence, was intermediate and high-grade DCIS, while the recurrence was high grade invasive carcinoma associated with high grade DCIS only. The discrepant case that was ER negative DCIS and recurred as ER positive invasive recurrence, was high grade DCIS with triple negative profile, where the recurrence was invasive lobular carcinoma, which could be a new primary rather than recurrence from the primary tumour.

In the ER positive DCIS treated with BCS, 28 patients developed local recurrence within 5 years of which 54% (15/28) were invasive recurrences (7 cases followed intermediate grade DCIS and 8 cases followed high grade DCIS). Within 10 years follow-up, 44 patients developed ipsilateral local recurrence with 59% (26/44) invasive recurrence rate (11 cases followed intermediate grade DCIS and 13 cases followed high grade DCIS). 2 low grade ER positive DCIS recurred as invasive disease within 10 years follow-up, and both recurrences were grade 1-2 ER-positive invasive carcinoma associated with low grade DCIS.

Seven patients died from ipsilateral IBC recurrence (2% of the whole BCS cohort, 13% of the recurrent cases). These patients had median age of 56 years, initially presented with intermediate to high grade DCIS, with comedo necrosis and 6 cases were treated with BCS only without postoperative adjuvant RT. The ER status was positive in 5 cases. The invasive recurrence was of no special type, grade 2 and 3 with more than half of the recurrences (4/7) developed within five years.

4.6.3.1 Outcome of ER-positive DCIS based on nuclear grade

ER positivity was seen in 82/88 (93%) low grade DCIS. Approximately two-thirds 51/82 (62%) of them were treated by BCS with or without RT, while the remaining were treated with mastectomy. The invasive recurrence in this subgroup was nil within 5 years and occurred in 2 patients (2 out of 4 recurrences) within 10 years, which were grade 2 ER positive invasive carcinoma and the 10-years survival rate was 100%. In the recurrent low-grade group, no cases received postoperative RT.

ER positivity was seen in 155/165 (94%) intermediate grade DCIS. Approximately half 80/165 (49%) of them were treated by BCS with or without RT. The proportion of recurrences that were invasive in this group was 7/13 (54%) and 11/19 (58%) at 5 and 10 years follow up, respectively. 9 recurrence were grade 2 IBC while 2 cases were of grade 3, and all cases were ER positive. Only one cases died from BC within 10 years from diagnosis of the recurrent event.

ER positivity was seen in 191/330 (58%) high grade DCIS. Approximately half 103/191 (54%) of them were treated by mastectomy. The proportion of recurrences that were invasive in this group was 18/27 (67%), which were grade 3 invasive carcinoma in 8 cases and grade 2 in 10 cases. 13/18 (72%)

cases were ER positive IBC, while one case was ER negative and ER status was not available in 4 cases.

4.6.3.2 Contralateral breast cancer and ER status

Contralateral BC was identified in 55/643 cases (9%); of which 37 cases were invasive disease (representing 6% of the overall cases and 67% of the contralateral events). In patients initially treated for ER-positive DCIS, 30 cases had invasive contralateral disease. The primary DCIS in those cases were high grade in 14 patients (47%), intermediate grade in 11 (34%) and low grade in 5 cases (17%). 90% (27/30) of the contralateral invasive disease cases were ER-positive. The three discrepant cases that developed ER-negative contralateral invasive disease (high-grade NST type) initially presented with high-grade ER-positive DCIS.

4.6.3.3 The association between overall risk of developing a recurrent IBC event either ipsilateral or contralateral after primary diagnosis of DCIS and ER status

The 10-year risk of developing a recurrence episode either in the ipsilateral or contralateral breast was 17% (109/643), of which 69 events were invasive disease (11% of all cohort and 63% of all event). Within those 69 cases, the primary DCIS was ER-positive in 55 cases (80%). Most of the recurrent events after diagnosis of ER-positive DCIS showed positive ER expression, with few events recurring as ER-negative disease.

4.6.3.4 Overall survival

The ten and twenty-year overall BC specific death rate was 0.9% (6/643) and 1.3% (9/643), respectively. Those patients had median age of 66 years, initially presented high grade DCIS, with comedo necrosis and half of them were treated with BCS. The ER status was positive in 6 cases (67%). The recurrent episode was invasive carcinoma for all cases prior to distant metastasis and death. Thus, the overall death rate after primary diagnosis of ER-positive DCIS was less than 0.5% and 0.7% within 10 years and twenty years of the primary diagnosis of DCIS respectively. In addition, none of the patients initially presented with low grade DCIS died during the 20- year period of the study follow-up.

4.6.4 **Assessment of HER2 status**

In the pure DCIS group, 20% of cases were HER2 positive. IHC for HER2 was scored as 3+ in 9%, 2+ in 15% and 0 or 1+ in 76% (**Table *4-3***). All 3+ cases showed *HER2* amplification with CISH. 74% of 2+ cases showed *HER2* amplification (four cases in which CISH could not be assessed due to technical issues and were excluded). CISH confirmed high copy number of *HER2* gene in all IHC 3+ cases (**Figure 4-2**).

Table 4-3: HER2 status in pure DCIS cases using IHC and CISH

***HER2* CISH**	**HER2 IHC in pure DCIS**			
	0/1+ (n=493) (%)	2+ (n=98) (%)	3+ (n=56) (%)	Total (n=647) (%)
Amplified	1 (0.2)	72 (74)	56 (100)	129 (20)
Non-amplified	492 (99.8)	26 (26)	0 (0)	518 (80)

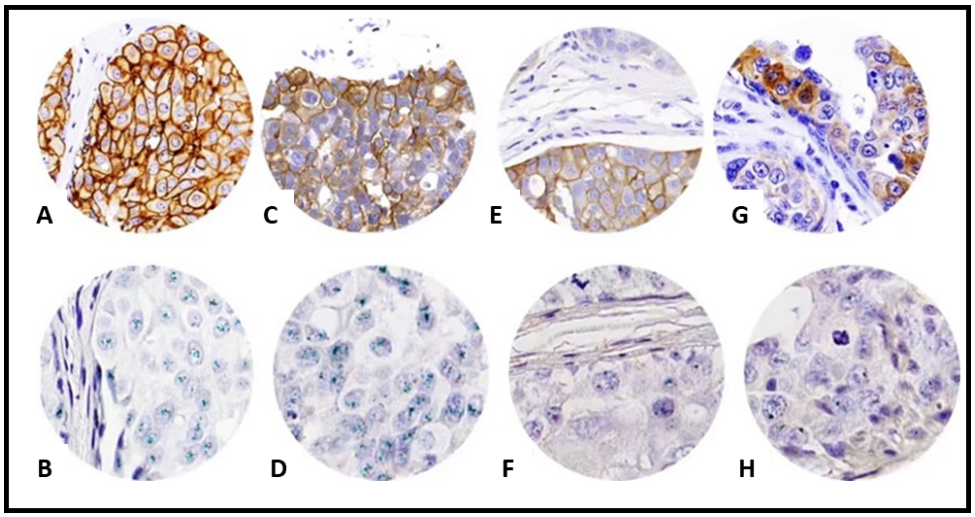

Figure 4-2: HER2 expression in pure DCIS cases
(A and B) DCIS showing HER2 3+ (A) confirmed by CISH (B), (C and D) HER2 2+ (C) showing gene amplification (D), (E and F) HER2 2+ (E) without amplified gene (F), and (G and H) HER2 1+ (G) showing no gene amplification (H)

Of the 493 cases with 0/1+ score using IHC, only one case showed *HER2* amplification. When IHC results were assessed with the exclusion of equivocal (2+) tumours, agreement between IHC and CISH in 0, 1+ and 3+ cases was 99.7% (Kappa coefficient = 0.9). Interestingly, when the overall rate of positivity was analysed over the period of the study, the frequency of positivity reduced from 30% in the 1990s to 20% in 2012 (**Figure 4-3**).

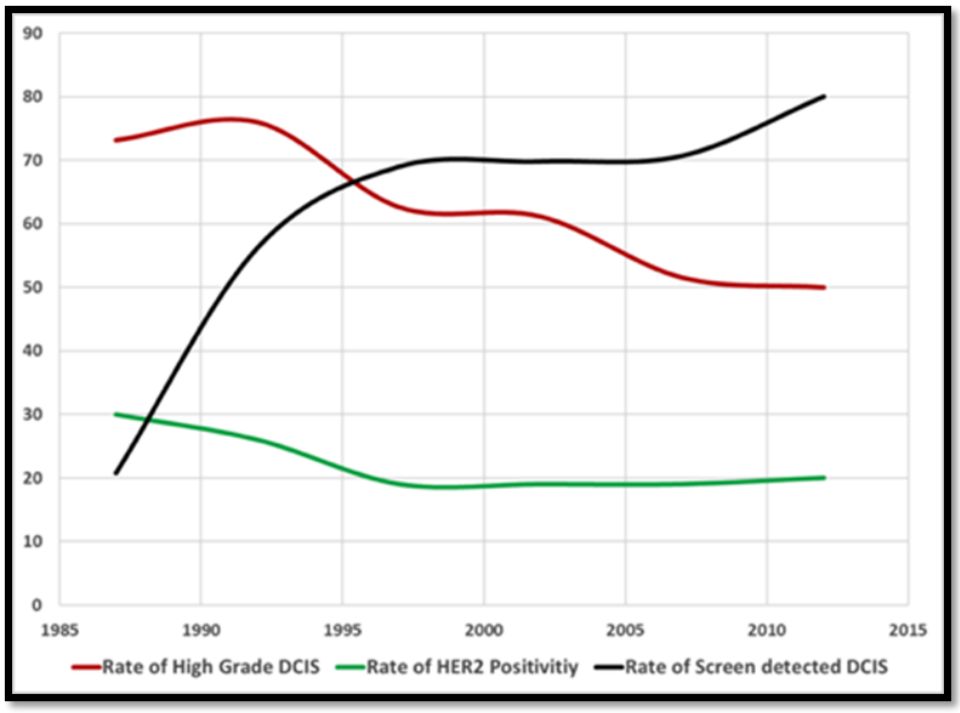

Figure 4-3: The rate of HER2 positivity over years

The graph shows that the rate of high-grade DCIS together with HER2 positivity declines over the years in contrast to the rate of screen detected DCIS

In mixed DCIS and invasive carcinoma cases, the DCIS component was HER2 positive in 15% and the invasive component in 12% (p=0.051, **Table 4-4** to **Table 4-10**). All 8 discordant cases had extensive DCIS; six of them were of high grade.

Table 4-4: HER2 status in DCIS cases mixed with invasion using IHC and CISH

CISH	HER2 IHC DCIS Component				HER2 IHC Invasive Component			
	1+	2+	3+	Total N. (%)	1+	2+	3+	Total N. (%)
Amplified	5	5	22	32 (15)	1	1	23	25 (12)
Non-amplified	180	5	0	185 (85)	191	1	0	192 (88)

Table 4-5: Final HER2 status of DCIS and invasive component of DCIS cases mixed with invasion

	Invasive		Total N. (%)
DCIS	**Positive**	**Negative**	
Negative	1	184	185 (85)
Positive	24	8	32 (15)
Total	25 (12)	192 (88)	217 (100)

Table 4-6: Comparison between HER2 status in pure DCIS cases using IHC and CISH

HER2 CISH	HER2 IHC in pure DCIS			
	0/1+ (n=493)(%)	**2+** (n=98)(%)	**3+** (n=56)(%)	Total (n=647) (%)
<4	489 (99)	26 (27)	0 (0)	515 (80)
4 to 6	3 (0.6)	3 (3)	1 (2)	7 (1)
>6	1 (0.4)	69 (70)	55 (98)	125 (19)

Table 4-7: HER2 status of DCIS cases mixed with invasion using IHC

	Invasive HER2 (IHC)			Total
DCIS HER2 (IHC)	**0/1+**	**2+**	**3+**	
0/1+	183	1	1	185 (85)
2+	7	0	3	10 (5)
3+	2	1	19	22 (10)
Total	192 (88)	2 (1)	23 (11)	217

Table 4-8: Comparison between HER2 status of the DCIS component in cases mixed with invasion using IHC and CISH

	DCIS *HER2* (CISH)			Total
DCIS HER2 (IHC)	**<4**	**4 to 6**	**>6**	
0/1+	179	1	5	185 (85)
2+	5	0	5	10 (5)
3+	0	0	22	22 (10)
Total	184 (85)	1 (1)	32 (14)	217

Table 4-9: Comparison between HER2 status of the invasive component in DCIS cases mixed with invasion using IHC and CISH

	Invasive *HER2* (CISH)			Total
Invasive HER2 (IHC)	**<4**	**4 to 6**	**>6**	
0/1+	190	1	1	192 (88)
2+	1	0	1	2 (1)
3+	0	0	23	23 (11)
Total	191 (88)	1 (1)	25 (11)	217

Table 4-10: HER2 status of DCIS and invasive component in DCIS cases mixed with invasion using CISH

	Invasive *HER2* (CISH)			Total
DCIS *HER2* (CISH)	**<4**	**4 to 6**	**>6**	
<4	182	1	1	184 (85)
4 To 6	1	0	0	1 (1)
>6	8	0	24	32 (15)
Total	191 (88)	1 (1)	25 (12)	217

4.6.5 Correlation with clinicopathological parameters and molecular biomarkers

In pure DCIS, HER2 positivity was associated with larger tumour size, high nuclear grade, comedo type DCIS, negative hormone receptor status and high Ki67 proliferation index (all $p<0.0001$) (**Table 4-11**).

4.6.6 Characteristics of DCIS by surrogate molecular subtypes

Five hundred and seventy-seven cases of the 651 DCIS cases classified into the surrogate molecular subtypes. Of the classified tumours, 348 were Luminal A (60%), 45 Luminal

B/HER2- (8%), 46 Luminal B/HER2+ (8%), 66 HER2+ (11%) and 72 Triple Negative (13%) (**Table 4-12**).

The HER2+, Luminal B/HER2+ and Triple Negative subtypes were more often of larger tumour size (>40mm), higher tumour grade and more often aggressively treated with mastectomy compared to Luminal A and Luminal B/HER2- tumours. Triple negative subtype was associated with presence of comedo necrosis, whereas Luminal A tumours were associated with cribriform and papillary DCIS.

Table 4-11: Association between final HER2 status and the clinicopathological parameters of pure DCIS cohort

Parameter	HER2 Status		
	Positive (n=128) n (%)	**Negative (n=518) n (%)**	**χ^2 (*p* value)**
Age, years			
<40	7 (5)	15 (3)	2.12
40 to 60	74 (58)	302 (58)	(0.347)
>60	47 (37)	201 (39)	
Presentation			
Screening	69 (54)	267 (52)	0.23
Symptomatic	59 (46)	251 (48)	(0.632)
DCIS Size (mm)			
<16	27 (21)	196 (38)	20.63
16 to 40	47 (38)	200 (39)	(**<0.0001**)
>40	52 (41)	119 (23)	
Nuclear Grade			
Low	0 (0)	87 (17)	58.58
Intermediate	13 (10)	153 (30)	(**<0.0001**)
High	115 (90)	278 (53)	
Comedo necrosis			
Yes	111 (87)	300 (58)	36.28
No	17 (13)	216 (42)	(**<0.0001**)
ER status			
Positive	45 (41)	381 (84)	88.86
Negative	66 (59)	74 (16)	(**<0.0001**)
PR status			
Positive	18 (14)	284 (55)	68.51
Negative	110 (86)	234 (45)	(**<0.0001**)
Ki67 Index			
High (≥14%)	46 (42)	62(17)	37.46
Low (<14%)	63 (58)	298 (83)	(**<0.0001**)

DCIS: Ductal carcinoma *in situ*; n: number; X^2: Chi square, ER: Oestrogen Receptor, PR: Progesterone Receptor
p value in **bold:** significant

Table 4-12: Characteristics of DCIS by surrogate molecular subtypes.

DCIS Characteristics	Luminal A (n=348), %	Luminal B/HER- (n=45), %	Luminal B/HER+ (n=46), %	HER2+ (n=66), %	Triple negative (n=72), %	χ^2 (p value)
Age, years						
<40	10 (3)	2 (4)	3 (6)	3 (5)	3 (4)	3.14
40 to 60	201 (58)	25 (56)	29 (64)	38 (58)	40 (56)	(0.925)
>60	137 (39)	18 (40)	14 (30)	25 (37)	29 (40)	
Presentation						
Screening	171 (49)	25 (56)	23 (50)	38 (58)	40 (56)	2.56
Symptomatic	177 (51)	20 (44)	23 (50)	28 (42)	32 (44)	(0.633)
DCIS Size (mm)						
<16	136 (39)	16 (36)	8 (18)	17 (26)	21 (29)	23.38
16 to 40	137 (39)	19 (42)	18 (40)	21 (32)	26 (36)	**(0.003)**
>40	75 (22)	10 (22)	19 (42)	27 (42)	25 (35)	
Nuclear Grade						
Low	71 (20)	3 (7)	0 (0)	0 (0)	5 (7)	112.26
Intermediate	128 (37)	11 (24)	5 (11)	5 (8)	5 (7)	(**<0.0001**)
High	149 (43)	31 (69)	41 (89)	61 (92)	62 (86)	
Comedo necrosis						
Yes	50 (14)	4 (9)	14 (30)	21 (32)	30 (42)	39.33
No	298 (86)	41 (91)	32 (70)	45 (68)	42 (58)	(**<0.0001**)
Solid DCIS						
Yes	167 (48)	29 (64)	26 (56)	36 (55)	34 (47)	5.78
No	181 (52)	16 (36)	20 (44)	30 (45)	38 (53)	(0.216)
Cribriform DCIS						
Yes	182 (52)	18 (40)	19 (41)	22 (33)	24 (33)	15.53
No	166 (48)	27 (60)	27 (52)	44 (67)	48 (67)	**(0.004)**
Papillary DCIS						
Yes	60 (17)	7 (16)	1 (2)	2 (3)	5 (7)	18.69
No	288 (83)	38 (84)	45 (98)	64 (97)	67 (93)	**(0.001)**
Micropapillary DCIS						
Yes	100 (29)	13 (29)	10 (22)	19 (29)	16 (22)	2.13
No	248 (71)	32 (71)	36 (78)	47 (71)	56 (78)	(0.710)

DCIS: Ductal carcinoma *in situ*; n: number; X^2: Chi square
***p* value in bold: significant**

4.6.7 **Associations with the outcome**

HER2 was associated with the development of local *in situ* recurrence (HR=2.51, 95%CI=2.11-11.45, *p*=0.03), but not invasive recurrence (**Table 4-13**). Patients with HER2+/Ki67-high DCIS had a high likelihood of developing local invasive recurrence (*p*=0.004). On multivariate analysis, patients with HER2+/Ki6-7-high DCIS had a Hazard Ratio (HR) of 2.5 (95%CI 1.7–55.0, *p*=0.006), compared to women with other profiles (**Table 4-14**).

Cox regression analyses showed no statistically significant differences between subtypes regarding local recurrence.

Table 4-13: Univariate analysis for predictors of local recurrence in pure DCIS patients treated with breast conserving surgery

Outcome	HR (95% CI)	***P*** value*
All local recurrence		
Tumour size	2.0 (1.3-3.3)	**0.004**
High tumour grade	1.7 (1.2-2.4)	**0.002**
Comedo necrosis	1.1 (0.6-1.6)	0.974
Margin width	2.5 (1.2-5.3)	**0.015**
Radiotherapy	0.5 (0.3-0.7)	**0.014**
ER status	1.09 (0.58-2.05)	0.777
HER2 status	0.89 (0.45-1.74)	0.734
Ki67 status	2.61 (0.33-5.01)	0.089
Invasive local recurrence		
Tumour size	2.3 (1.3-4.1)	**0.006**
High tumour grade	1.9 (1.2-3.0)	**0.003**
Comedo necrosis	1.49 (0.814-2.76)	0.194
Margin width	0.69 (0.43-2.47)	0.578
Radiotherapy	0.3 (0.2-0.8)	**0.008**
ER status	1.01 (0.45-2.65)	0.833
HER2 status	0.49 (0.17-1.41)	0.184
Ki67 status	1.28 (0.41-3.88)	0.668

HR: Hazard ratio, CI: Confidence Interval
DCIS: Ductal carcinoma in situ, ER: Oestrogen Receptor
P values in **bold** are significant

Table 4-14: Multivariate Cox proportional hazards for factors associated with local recurrence in pure ductal carcinoma in situ patients.

Variable	HR	95% CI	*p*-value
DCIS size	0.62	0.31-3.47	0.311
DCIS Grade	2.21	1.15-70.85	**0.031**
Comedo necrosis	0.32	0.12-0.87	**0.026**
Margin width	0.89	0.11-7.46	0.911
HER2+/Ki67-high group	1.52	1.64-60.74	**0.001**

HR: Hazard ratio, CI: Confidence Interval
DCIS: Ductal carcinoma in situ, ER: Oestrogen Receptor
P values in **bold** are significant

4.7 **Discussion**

DCIS is a heterogeneous disease, with molecular phenotypes seen in invasive cancer presenting in primary DCIS using IHC surrogate markers. These molecular phenotypes can be used to independently predict for both overall and, importantly, invasive recurrence [324]. There is no clinically established classification of DCIS that supports the prognosis for an individual woman [316]. In invasive cancer, molecular subtyping predicts prognosis [359, 360] but very little data has been published regarding DCIS [361].

The low recurrence rate, particularly in the luminal A DCIS, although not statistically significant, reflects a low risk of recurrence in the absence of RT and indicates a difference in the molecular phenotypes with regard to recurrence and RT sensitivity.

Optimal treatment of DCIS is still a controversial issue. Debate continues regarding potential overtreatment of DCIS; whether surgical excision is required for all cases, and the question as to whether adjuvant therapy, RT and/or ET can be avoided for low-risk subgroups [327]. Some multi-institutional, randomised trials are underway comparing active monitoring with standard treatment for DCIS [111, 362]. The LORIS (low-risk DCIS) trial, which started in 2014, is a randomised, non-

inferiority trial of comparing surgery versus active surveillance in low-risk DCIS patients. Patients with low- or intermediate-grade DCIS are randomised to either surgery or active surveillance with no hormonal treatment. The Comparison of Operative versus Medical Endocrine Therapy for Low-Risk DCIS (COMET) trial is currently occurring and randomises low- and intermediate-grade ER-positive and HER2-negative DCIS to either standard management versus active surveillance. ET use is encouraged in the active monitoring arm. The EORTC-sponsored LOw Risk DCIS (LORD) trial, is due to open, and this will randomise patients with low-grade DCIS to conventional treatment versus an active monitoring strategy. The principle objective of these trials is to avoid over treatment of low risk DCIS and to provide evidence that active surveillance is a management option for these patients.

Although prognosis following a diagnosis of DCIS is excellent, the goal of ET is to reduce recurrence, which is invasive in up to 50% of patients [327]. Two randomised studies of ET versus placebo have shown that ET significantly reduces BC recurrences [106, 332]: the NSABP B-24 reported that this benefit is limited to patients with ER-positive DCIS and reduces the recurrent events of both non-invasive and IBC in patients undergoing BCS. While both the NSABP B-24 [330] and the UK/ANZ [105], trials show a significant reduction in

BC recurrences (as discussed above), neither of these trials show an overall survival benefit from Tamoxifen. However, it is noted that these studies were not large enough nor were they designed to assess survival benefit. Importantly, the NSABP B-24 and UK/ANZ studies were on patients unselected by ER status. However as noted above, Allred *et al.* in a retrospective study in a sub-group of patients in NSABP B-24 reported that only patients with ER-positive DCIS showed a significant reduction in subsequent BC recurrence on receiving adjuvant Tamoxifen. There was no benefit from adjuvant Tamoxifen for patients with ER-negative DCIS. They concluded that the use of adjuvant Tamoxifen offered an additional therapeutic option for patients with ER-positive DCIS [105].

In the current study, our results showed that there is no significant association between ER status and the development of ipsilateral breast event over 5 or 10 years, either as DCIS or invasive recurrence. The current finding is similar to that of the sub-study of NSABP B-24 referred to above [105] and also of other studies [336, 363], where the recurrence rates in the placebo group were similar for both ER-positive and ER-negative DCIS. These results are clinically vital and concludes that ER assessment for DCIS might not be necessary in the clinical setting. In the current study, ER was also shown to not

be a contributing factor affecting the development of contralateral BC in DCIS patients.

The results in the current study showed that low risk DCIS treated with BCS, had excellent prognosis with 100% survival rate even after the invasive recurrence which was grade 1 invasive carcinoma in all cases. In addition, all ER positive DCIS that showed invasive recurrence with or without subsequent BC related mortality were of high grade, but they were treated with BCS only. We also showed that RT in general and RT offered to ER-positive DCIS cases have improved outcome after BCS. In ER negative DCIS, RT reduce the risk of recurrence from 28% (9/32) in patients who did not receive RT, to 19% (5/26) in patients who receive post- operative RT, however this difference was not statistically significant likely due to small number of ER negative cases included in the analysis. Therefore, the current results support NICE guidelines to provide ET for patients with high risk DCIS when RT cannot be given for any reason. Although the reasons for omitting RT in these patients is not known, they might get benefit if they were receiving ET. On the other hand, adjuvant ET for low risk DCIS might be controversial as in the current cohort, cases with low grade DCIS had good outcome even if they did not receive adjuvant Tamoxifen. In RTOG 9804, there are so few events at that time that the data could not support

or refute the role of Tamoxifen in the treatment of low risk DCIS [94]. This might allow for further discussion about the actual patient benefits of ET if they were diagnosed as low risk ER-positive DCIS and undergo surgery.

Routine application of NICE guidelines in clinical practice will have some potential implications on patients, pathologists and pathology services. While data regarding the benefits of Tamoxifen have continued to evolve in the last two decades, particularly the benefits of Tamoxifen for reducing second BC events, this needs to be balanced with the adverse effects; an increased risk of osteoporosis, cataract, endometrial cancer, stroke, deep vein thrombosis, pulmonary embolism, and potentially severe vasomotor and gynaecologic symptoms [364]. Therefore, the decision to give adjuvant anti-hormone therapy in DCIS is debateable particularly as it has no effect on the mortality. While BC recurrence can be a devastating event for patients who suffer it, the absence of an overall survival benefit highlights that the significant side effects of 5 years of ET on the quality of life have also to be considered in patients presenting with ER-positive DCIS who choose BCS [365]. A recent study has attempted to address this issue by utilising a 5mg Tamoxifen dosage [366]. This was a relatively small trial (n=500) of which only 346 had DCIS. No details are provided regarding the type of surgery patients received or

surgical margins which would impact on BC recurrence. In addition, while the BC events were reduced there was no breakdown whether this was in the DCIS sub-group or the high risk ADH / LCIS sub-group. Further better defined and larger studies are required before this approach can be supported but if in future it is shown to be effective and with a better side effect profile, this may then be considered a more acceptable option for the lower risk group.

The current study has some potential limitations. Firstly, all patients did not receive adjuvant ET and therefore evaluation of ET effect on DCIS was limited. Secondly, the study was conducted on DCIS cases spanning a long time period with potential bias regarding the availability of tumour tissue for ER assessment.

However, it can be concluded that recommending ET in those cases who do not receive RT is understandable, although often patients who refuse one treatment (i.e RT) may also refuse ET. Tumour grade is an essential factor to consider when assessing the risk of development of ipsilateral tumour recurrence following BCS treatment for DCIS patients. The routine management of all DCIS including the low risk group with ET should be carefully assessed and discussed with each patient. There is an urgent need for molecular biomarkers and

evidence-based guidelines to improve recurrence risk assessment and treatment decision-making in DCIS.

HER2 status is a known risk factor for recurrence in both IBC and DCIS. Some publications have shown an increased risk of non-invasive recurrence in HER2+ tumours and shown that the combination of HER2+ and high proliferation conferred an even higher risk of recurrence [31, 354]. The data presented in this chapter confirms a higher risk for local recurrence in HER2+ tumours.

HER2 status can be detected by analysing the number of gene copies or measuring the amount of protein expression. The most widely used methods at present are IHC, FISH and CISH due to their propensity in evaluating *HER2* in FFPE tissues in invasive carcinoma [367]. Most HER2 studies have been performed by IHC, which is widely accessible, easy to perform at a reasonable cost and is appropriate for initial HER2 assessment [368]. However, in cases with an IHC score of 2+, the inter-observer agreement is poor, and the predictive value is unsatisfactory for clinical use. This led to the recommendation of additional testing measuring *HER2* gene copy number status using an *in situ* hybridisation technique such as FISH or CISH to avoid inaccurate prognostication and inappropriate treatment [368, 369].

CISH is an alternative *in situ* hybridisation method to analyse gene amplification with more feasible technique and assessment method [370]. Furthermore, several studies have demonstrated good correlation between CISH and FISH results [371, 372].

In this study, similar to a previous study, but in invasive tumour [367], the concordance between 3+ IHC and CISH-amplified cases was 100%, denoting all HER2 over-expressing cases as having *HER2* gene amplification. In contrast, the proportion of 2+ IHC that were *HER2* amplified, as detected by CISH, was 73.5%, which is lower than previously reported (93%) [373]. The 26.5% (26/98) IHC-equivocal/*HER2* non-amplified tumours in this study, all of which had 2+ IHC scores, is higher than the result obtained by other studies on invasive tumours [374-376]. The concordance between 0/1+ IHC and *HER2* non-amplified tumours was 99.7%. A similar finding was reported by Zhao and colleagues where they considered that there is a small undetermined percentage of amplified *HER2* without protein over-expression [375]. The same study and other FISH studies on invasive carcinoma also report rare 3+ IHC tumours that are non-amplified [374-377], however, in this study no such cases were detected.

The low-amplified *HER2* category (≥4 to <6 CISH signals) was the most difficult to interpret, requiring an accurate enumeration of gene copy and addition of more tumour cells to assess the final status. This step was particularly important because these cases could either resolve as amplified (4/7) or non-amplified (3/7). Signal clustering, more probably a result of intra-chromosomal amplification of homogeneously staining regions, was immediately evident in highly amplified cases and was easily evaluated.

A lower HER2 expression was observed in DCIS compared to the previously published literature [321, 342]. This might be related to the increasing detection of low and intermediate grade DCIS by screening mammography. In support of this the HER2 positivity was higher (30%) in the earlier period of the study and declined over time to 20%.

The question of whether or not TMA cores are representative of whole tumours is frequently raised, as some tumours are heterogeneous and so a small sample of tissue may not always display the same biological characteristics as a larger section [378]. To increase the credibility of the TMA technique while reducing the probability of error associated with the difficulty of obtaining a representative sample, some studies use multiple cores from the same donor tissues as it has been

reported that only a few (up to four) cores are required to achieve a 100% agreement [379]. However, even when as many as 10 tissue cores are taken from a tumour, some disagreement may be noted [380, 381]. In the current study, 1 mm diameter cores were used to construct the TMA of the pure DCIS tumours, increasing the probability of accurate sampling by taking large TMA cores. In cases with multiple cores, the initial HER2 status was assessed at the protein level followed by confirmation with *in situ* hybridisation. The high agreement rate between IHC and CISH results suggests that it is possible to apply TMAs to DCIS research, with the caveat that, for HER2, the CISH results may be more reliable, countering the discrepancy that can be observed in IHC for either technical or biological reasons.

The subsequent goal of this chapter was to assess the role of HER2 in progression of DCIS. HER2 positive DCIS was associated with predictors of local recurrence including larger tumour size, high nuclear grade, comedo type DCIS, negative hormone receptor status and high Ki67 proliferation index, which was consistent with other studies [304, 337, 353, 382-384]. Local recurrence (invasive or DCIS) was associated with higher grade, comedo necrosis and margin status. DCIS local recurrence was associated with HER2 positivity and invasive local recurrence was associated with tumour size. Similar to

some studies, HER2 positive tumours were associated with DCIS local recurrence [354, 385].

DCIS patients with *HER2* amplification had higher nuclear grade lesions and therefore are probably at risk of relapse more frequently than the *HER2* unamplified group, but the prognostic role of *HER2* over-expression in DCIS is still not fully clarified. Some studies suggest that patients with *HER2* amplified DCIS are more frequently high nuclear grade and this aspect is related to an increased risk of relapse [386, 387]. In fact, some studies suggest that HER2 plays a major role in the transition from DCIS to IBC [324, 388], while others do not support this [344, 389]. In the current study, *HER2* amplification was more frequent in the pure DCIS cohort (20%) than in the mixed DCIS (15%) despite the more prevalent higher-grade DCIS in the mixed cases. HER2 positivity alone was not predictive of recurrence as a whole or as invasive disease but showed a trend to DCIS recurrence. This result is consistent with the observation that HER2 positive DCIS tend to extend within the ductal system and even in the epidermis (Paget's disease) than associated with invasive disease. It is a personal observation that when HER2 positive DCIS is associated with early invasion, that invasive disease may show aggressive features. Currently HER2 positive invasive tumours are treated more aggressively

regardless of its size [390]. This may suggest that HER2 positive DCIS tumour cells although highly proliferative are not highly invasive, whilst those that acquire invasive properties became aggressive and can metastasise.

In order to improve the risk stratification and therefore treatment recommendations, there is a need to identify potential predictors of invasive and/or non-invasive recurrence following BCS. HER2/Ki67 positivity was a predictor of recurrence, independent of other studied clinicopathological parameters such as nuclear grade and presence of comedo necrosis. In contrast to a previous study [31], the combination of ER status with HER2 and Ki67 further added additional predictive information. This difference may be due to the differences in patient populations, or to differences in the coding of HER2 positivity. The previous study coded DCIS lesions with equivocal immunostaining for HER2 (score of 2+) as positive whereas in the current study only equivocal cases with amplification were coded as HER2 positive.

In the present study, HER2 expression in the invasive component was seen less frequently as compared to the DCIS component adjacent to invasive carcinoma and pure DCIS although this was of borderline statistical significance. Similarly, other studies [387, 391] have observed that HER2

positivity is often in patients with pure DCIS compared to those with microinvasive or invasive carcinoma. As it has been reported that patients with HER2+ invasive cancer have a poorer prognosis than those whose tumours do not express HER2 [392], the higher incidence of expression found in DCIS may therefore seem paradoxical. It was postulated that HER2 expression happens during the process of ADH, and loss of HER2 expression occurs as DCIS develops into invasive disease. Another hypothesis is that *HER2* overexpression in invasive carcinoma does not develop from DCIS but from the associated ADH directly [393, 394]. Another theory explaining this phenomenon is that most invasive cancers develop from DCIS tumours which have low expression of HER2 but are highly proliferative [387]. Because such tumours progress rapidly, they are in the DCIS stage for only a short period and would therefore be under-represented in population samples [387].

In summary, CISH is a practical test that can be used in conjunction with IHC to determine *HER2* status in DCIS. IHC is easy to perform, relatively inexpensive, and able to detect a majority of BC patients whose tumours have negative (0 or 1+) or positive (3+) HER2 status. This IHC/CISH test stratification not only identifies the IHC borderline cases, but also keeps testing costs for HER2 status at a reasonable

minimum. As HER2 status is not currently routinely measured in clinical practice, the aim was to show statistically significant correlations between the development of local recurrence as well as poor prognostic pathological factors and HER2 positive DCIS which could alert clinicians. The results might suggest considering routine assessment of HER2 in DCIS, similar to IBC.

Also confirmed in this study is the suitability of TMAs for assessment of HER2 gene amplification status in tumours arising from different patients, while maintaining a representative tissue sample in each case, with good reproducibility and credible results.

To conclude, the frequency of HER2 positivity, driven by gene amplification, in DCIS is comparable to IBC and in combination with Ki67, is an independent predictor of recurrence. The results suggest the consideration of routine assessment of HER2 status for DCIS, as it is commonly done for IBC.

5 Chapter 5: The prognostic significance of tumour infiltrating lymphocytes in DCIS

5.1 **Introduction**

The higher rate of DCIS diagnosis together with increasing use of BCS for management have heightened the need for robust and reliable predictors of disease recurrence and progression, for risk stratification of patients. Comparison of DCIS recurrence rates and progression to invasive disease with the rates of mastectomies, surgical re-excisions or intense course of RT suggests overtreatment, stemming from a lack of accurate risk stratification [111]. Current application of molecular genetic signatures for DCIS categorisation to provide suitable individualised management remains challenging [78, 120, 178, 198, 231, 395].

5.2 **Tumour infiltrating lymphocytes**

TILs are indicators of the adaptive immune response against tumours and play a key role in cancer immunotherapy [132, 184]. In previous studies of IBC, dense TILs were shown to augment effect of chemotherapy providing better prognosis mainly in triple negative BC (TNBC) [396, 397]. Following demonstration of their prognostic significance in IBC and their potential clinical application, guideline recommendations for TILs evaluation have been published [133, 398] and update for TILs assessment in DCIS and other tumours has been

published in 2018 [399, 400]. However, the recommended method of TILs assessment in DCIS that relies mainly in the method followed in IBC may not be applicable in DCIS as not all stromal TILs are directly in contact with malignant ducts and identification of stromal area surrounding DCIS can be confusing and ill-defined. Despite the reported role of TILs in DCIS [178, 401], studies utilising the IBC guidelines for TILs assessment in the context of DCIS did not find any association with outcome [239, 398]. This is likely related to the difference in nature and distribution of TILs within DCIS compared to IBC and the sub-optimal method of their assessment.

5.2.1 TILs subpopulations and immune checkpoint proteins

Although the role of TME in disease behaviour is undeniable, incorporation of the microenvironmental factors with the clinicopathological and/or molecular signature for DCIS risk assessment is still limited. The tumour immune microenvironment undergoes several changes during carcinogenesis [402]. The triggering of an immune response in the form of infiltration of lymphocytes and other inflammatory mediators is a phenomenon known as "cancer immuno-editing" [403]. It is known that subtype, density and location of TILs play a role in cancer prognosis. Infiltration of

T lymphocytes extends an anti-tumour response through the CTLs while an immunosuppressive response occurs through Tregs [404, 405]. Similarly, CD20+ B lymphocytes are associated with a humoral anti-tumour response [406].

An important component of immuno-editing is the development of an immunosuppressive microenvironment mediated through the activation of the immune checkpoint pathway. The programmed cell death 1 (PD1) protein, a member of the B7/CD28 family of co-stimulatory receptors present mainly on T cells, sends inhibitory signals to T cells to suppress the anti-tumour response [139, 403]. PD1 functions mainly through its ligand PDL1, which is expressed on a variety of immune cells such as antigen presenting cells and activated T and B lymphocytes and tumour cells [407, 408]. Revolutionary results have been achieved from clinical trials involving monoclonal antibodies that target PD1 and block the PD1/PDL1 pathway in patients with non-small cell lung cancer, melanoma and renal cancer [409].

5.3 **Hypothesis and aims**

In view of the current debate arguing the role of TILs in progression of IBC, it is hypothesised that TILs play a similar role in DCIS progression to invasion. It is also hypothesised that TILs density is different between IBC and DCIS.

Moreover, we hypothesised that various immune cell subpopulations and the immune checkpoint proteins play roles in DCIS behaviour and this can be related to the underlying molecular prolife.

The aims of this chapter were to determine optimal method of TILs evaluation in DCIS in terms of reliability, reproducibility and prognostic significance with recurrence through utilisation of a large well-annotated DCIS cohort with long term follow. Additionally, the expression and the prognostic significance of T and B lymphocytes and immune checkpoint proteins PD1 and PDL1 were evaluated. The relationship between genomic copy number alteration and *TP53* variants (as measures of genomic instability) with immune cell infiltration in a subset of cases was also investigated.

5.4 Materials and methods

5.4.1 Evaluation of TILs and their prognostic significance

5.4.1.1 Study cohort

This retrospective study included 982 cases diagnosed from 1990 to 2012 at Nottingham City Hospital, Nottingham, UK. Following histological review of tumour slides of all cases and retrieval of tissue blocks, representative H&E stained sections from each case were prepared from 816 cases (684 pure DCIS

and 132 DCIS mixed with IBC). Representative sections were defined as those having the largest tumour burden. Clinicopathological data were collected as described in **Chapter 2**.

The cohort was split into two groups; a training set and a validation set (clinicopathological parameters of both sets are shown in **Table 5-1**)

5.4.1.1.1 Training set

The training set included 150 pure DCIS from patients >50 years of age with mixture of DCIS grades that was completely excised with free surgical margins, >10mm, to avoid the confounding effect of age or margin of excision on the outcome analyses. Within a median follow-up period of 161 months; 41 cases (27%) developed ipsilateral recurrence.

5.4.1.1.2 Validation set

The validation set (n=666) was further split into two subgroups; 1) Pure DCIS (n=534) which showed 63 ipsilateral local recurrence events (11.8%) within a median follow-up period of 109 months; 2) DCIS with co-existent IBC (DCIS/IBC) (n=132) to compare the pattern of TILs density between pure DCIS cases and cases wherein DCIS was associated with invasion. **Figure 5-1** shows the algorithm of the study cohorts.

Table 5-1: Clinicopathological characteristics of the training and validation sets for TILs assessment

Parameter	**Training set (*n*=150) Number of cases (%)**	**Validation set (*n*=534) Number of cases (%)**
Patient Age		
≤ 50 years	0 (0)	136 (25)
> 50 years	150 (100)	398 (75)
Presentation		
Symptomatic	78 (52)	254 (48)
Screening	72 (48)	280 (52)
DCIS Size		
≤ 20mm	78 (52)	232 (43)
>20mm	67 (45)	299 (56)
DCIS Grade		
Low	11 (8)	57 (11)
Intermediate	20 (13)	132 (25)
High	119 (79)	345 (64)
Comedo necrosis		
No	45 (30)	167 (31)
Yes	105 (70)	367 (69)
Paget's disease		
No	106 (71)	336 (63)
Yes	6 (4)	26 (5)
N/A	38 (25)	172 (32)
ER Status		
Positive	80 (64)	312 (73)
Negative	45 (36)	116 (27)
Surgical management		
Mastectomy	86 (57)	314 (59)
BCS)	64 (43)	219 (41)
Radiotherapy*		
No	127 (85)	139 (64)
Yes	23 (15)	80 (36)
Recurrence		
No	109 (73)	471 (88)
Yes	41 (27)	63 (12)

DCIS, ductal carcinoma in situ, ER, oestrogen receptor, BCS, breast-conserving surgery

**For patients treated with breast conserving surgery.

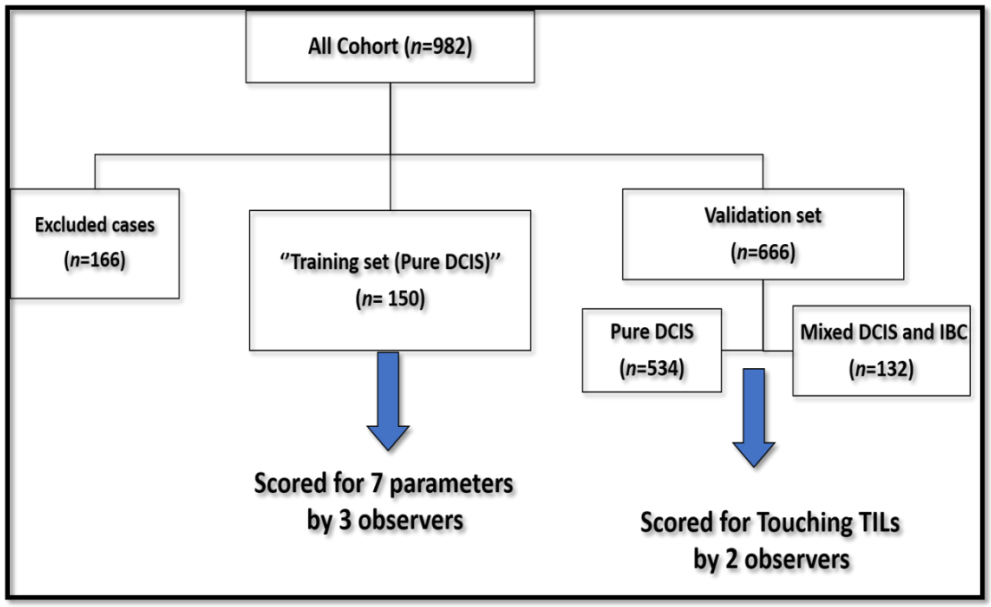

Figure 5-1: Schematic distribution of study cohorts

5.4.1.2 TILs scoring

Freshly stained H&E (4-5µm thick) full face sections were scanned using a high-resolution slide scanner (PANNORAMIC 250 FLASH III, 3D-HISTECH), followed by viewing the slides using ''Pannoramic Viewer Software program, version 1.15.4''. TILs were counted manually (eyeballing) using digital images. The International Working Group Recommendations for TILs assessment were modified and applied [398]. All recognisable mononuclear inflammatory cells including lymphocytes and plasma cells were counted (polymorphonuclear cells were excluded). TILs were assessed around all DCIS duct profiles up to 20 ducts (the average number of ducts within the training set). For cases with more than 20 malignant ducts, the section field was divided into four identical quadrants using

the Pannoramic Viewer software, and TILs were scored around five ducts in each quadrant in order to keep the scoring more representative especially in cases with heterogeneously distributed TILs. During scoring, very large (i.e., mass forming papillary carcinoma, branching or confluent DCIS ducts) or small (TDLUs involved by DCIS) ducts were not considered in TILs scoring to avoid skewing of the scores by the effect of extremes in duct sizes. Pure encapsulated papillary carcinomas, not associated with adjacent DCIS, were excluded from the scoring. Any type of circumferential TILs was considered, including minimal, partial, subtotal and total circumferential TILs distribution around ducts. TILs beyond the lesion limits, surrounding the adjacent or intermingled fat, normal ducts, associated LCIS, regressive hyalinosis or at crushing artefacts were excluded from the scoring.

In the training set, TILs were assessed using 7 different scoring methods (**Table 5-2**). These included: 1- Percentage of stromal TILs. The stromal area was defined as the area surrounding the DCIS duct within two high-power microscopic fields and used for evaluation of stromal TILs percentage [239, 398, 400]. In cases with numerous involved ducts, an evaluation of the area surrounding the whole lesion was performed, and percentage of stromal TILs in the total stromal area of all DCIS involved ducts was determined [178, 398,

410], 2-The mean number of touching TILs defined by TILs touching or within one lymphocyte cell thickness from the malignant ducts BM; 3-Mean number of TILs within 0.2mm distance from ducts' BM; 4- Mean number of TILs located within 0.5mm distance from ducts' BM; 5-Mean number of TILs located within 1mm from ducts' BM; 6-TILs hotspots defined as the largest number of lymphoid cells aggregates directly surrounding or located between DCIS ducts within the boundaries of the lesion; and 7-Assessment of lymphoid follicles with reactive germinal centres. Counting of TILs at different topographic areas was carried out manually with aid of the Panoramic Viewer Software program scale. Overlapping TILs between adjacent ducts in each topographic area were counted once. The detailed methods followed to assess TILs are summarised in **Table 5-2** and **Figure 5-2**.

Table 5-2: Methods and parameters of TILs assessment

Methods for evaluation of TILs in DCIS
1- TILs were assessed in H&E stained sections. Only full-face sections from surgically excised specimen were assessed. Lesions diagnosed on core biopsy were not included. 2- One representative section (4μm), per patient, which has the largest tumour burden, was selected for TILs assessment. 3- All mononuclear inflammatory cells apart from polymorphonuclear leukocytes were counted. 4- TILs within the boundaries of the DCIS were assessed. TILs beyond the tumour limits, surrounding normal ducts/lobules, adjacent fatty tissue, lobular carcinoma in situ, regressive hyalinosis, **crush** artefacts or sites of previous biopsy were excluded. 5- TILs within tumour cells (intra-tumour TILs) were not assessed. 6- TILs were assessed around all malignant ducts up to 20 ducts. For lesions with more than 20 malignant ducts, we assessed TILs surrounding 20 ducts (5 ducts from each quadrant of the lesion). 7- TILs were assessed around average sized ducts only (case specific). TILs around very large DCIS ducts such as mass forming papillary carcinoma, branching or confluent DCIS ducts or very small ducts such as terminal duct-lobular system involved by DCIS were excluded. 8- Any TILs around the ducts' circumference were considered. Overlapping TILs between adjacent ducts were counted once.
Parameters used for TILs assessment*
A- Estimation of stromal TILs • The stromal area was defined as the area surrounding the DCIS duct within two high power microscopic fields and used for evaluation of stromal TILs percentage **[239, 398, 400]**. In cases with numerous involved ducts, an evaluation of the area surrounding the whole lesion was performed, and

percentage of stromal TILs in the total stromal area of all DCIS involved ducts was determined **[178, 398, 410]**.

B-Estimation of periductal TILs (based on counting TILs around all DCIS duct profiles up to 20 ducts)

1- Evaluation of the mean number of TILs touching DCIS involved ducts (defined as TILs touching or within one lymphocyte cell thickness from ducts' BM).
2- Evaluation of the mean number of TILs within 0.2mm distance from the ducts
3- Evaluation of mean number of TILs within 0.5mm distance from the ducts
4- Evaluation of mean number of TILs with 1.0mm distance from the ducts
5- Evaluation of the TILs hotspot defined by largest number of lymphoid aggregates directly surrounding or located between DCIS ducts within the boundaries of the lesion
6- Evaluation of lymphoid follicles formations with reactive germinal centres in the stroma directly surrounding or located between DCIS ducts within the boundaries of the lesion.

*All parameters were assessed in the training set while touching and stromal TILs assessment were conducted to validation set.

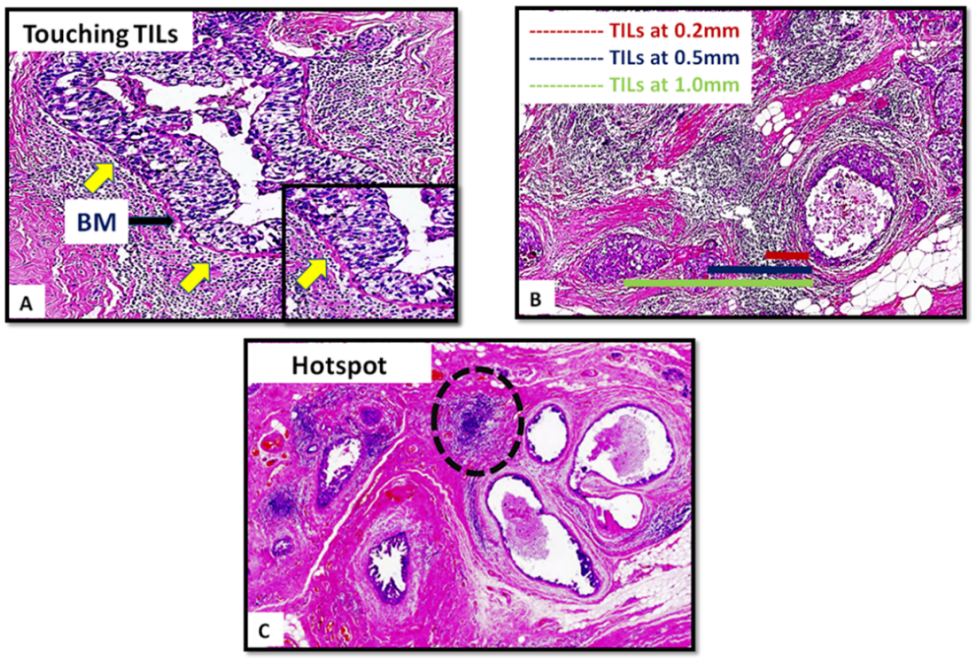

Figure 5-2: Parameters of TILs assessment

A) Touching lymphocytes (x40) defined by lymphocytes that touch the basement membrane (BM) or are located within one lymphocyte cell thickness distance from BM (yellow arrows); inset closer view for touching TILs, B) TILs assessment within 0.2mm, 0.5mm and 1.0mm distance from the involved ducts, and C) evaluation of hotspots (largest number of lymphoid cells aggregates within the lesion as shown in area surrounded by black dashed circle)

To check the reliability and reproducibility of the evaluation methods, the training set was scored using all the previous parameters by three observers. Two observers discussed the detailed methodology before starting their scoring, while the third observer scored the cases based on a written protocol without any verbal discussion. The optimal method for TILs assessment was determined based on the association with outcome and reproducibility in terms of inter-observer concordance as well as practicality, which was then applied to the validation set. The validation set, including the pure DCIS

and mixed DCIS/IBC cohorts, was scored for touching TILs by two observers to confirm reproducibility and prognostic significance. In DCIS/IBC cases, touching TILs were scored around the DCIS component only while TILs adjacent to invasive tumour were not considered in the scoring. TILs scoring carried out by the author were considered in the final statistical analysis. Other observers' scores were used to check the reproducibility and concordance rate.

As assessment of stromal TILs was the method used to evaluate TILs in DCIS in previous studies [239, 398, 400], stromal TILs was also evaluated in the pure DCIS validation set using the same criteria applied in training set.

5.4.2 Assessment of immune cell subpopulation and checkpoint proteins

5.4.2.1 IHC of immune cell markers and checkpoint proteins

TMAs from both cohorts as described in **Chapter 2** as well as 30 full face sections randomly selected from DCIS series were used to assess to reveal the infiltration pattern of various TILs subtypes and immune checkpoint proteins using IHC.

IHC was performed on TMA sections and full-face sections using a Novocastra Novolink TM Polymer Detection Systems Kit (Code: RE7280-K, Leica, Biosystems, UK) as detailed in

Chapter 2. Primary antibody specific for CD20 (mouse monoclonal, DAKO Clone L26/M0755), CD3 (rabbit monoclonal antibody [SP7], Abcam (ab16669)), CD8 (mouse monoclonal, DAKO Clone C8/144B), CD4 (rabbit monoclonal antibody [EPR6855], Abcam (ab133616)), FOXP3 (mouse monoclonal [236A/E7), Abcam (ab20034)), PD1 (Mouse monoclonal [EH33] Cell signalling (43248S)), PDL1 (Rabbit monoclonal antibody [E1L3N] Cell signalling (13684S)) were used to characterise TILs and immune checkpoint proteins. **Table 5-3** summarises the details of the antibodies used. Sections from normal tonsil were used as a positive control while a negative control was generated by omitting the primary antibodies.

Table 5-3: Different antibodies used for immune cells characterisation and their staining protocols

Abs	Clone	Source	Species	Antigen retrieval	Dilution	Incubation Time
CD3	SP7	Abcam	Rabbit monoclonal	Microwave in citrate PH6	1:300	24h
CD8	C8/144B	Dako	Mouse monoclonal	Microwave in citrate PH6	1:300	60min
FOXP3	236A/E7	Abcam	Mouse monoclonal	Microwave in citrate PH6	1:300	24h
CD20	L26	Dako	Mouse monoclonal	Microwave in citrate PH6	1:300	30min
CD4	EPR6855	Abcam	Rabbit monoclonal	Microwave in citrate PH6	1:500	24h
PD1	EH33	Cell signalling	Mouse monoclonal	Microwave in citrate PH6	1:75	24h
PDL1	E1L3N	Cell signalling	Rabbit monoclonal	EDTA PH9, water bath heating at 100c	1:25	24h

5.4.2.2 Immunoscoring

Stained slides were digitally scanned using a Nanozoomer (Hamamatsu Photonics), at 20X magnification high resolution images and viewed using the Aperio ImageScope Viewer software version 12.3.3 (developed by Leica Biosystems Imaging). All cases were scored visually using the digitised images for stromal expression of touching TILs [411], and for intratumour TILs. The average number of intratumour TILs per duct was counted for CD20, CD3, CD4, CD8, FOXP3 and PD1 to assess the intratumoural TILs. PDL1 expression in tumour epithelial cells was scored as percent of cells showing membranous and/or cytoplasmic staining, where cases with >1% positive cells were considered positive [398]. The pure DCIS and the *in-situ* component of mixed cases which clearly defined a demarcated tumour edge were assessed, separately. Average score was used as a final score for cases with multiple cores. All cases were scored independently by two observers blinded to patient histopathological data and clinical outcome. The average score was considered in discrepant cases between the two observers.

5.4.2.3 DNA extraction, targeted sequencing library preparation, enrichment, and sequencing

Sections from FFPE blocks from a subset of DCIS cases (n=58) were reviewed by two pathologists to select representative

sections. The cases were randomly selected based on tissue block availability and adequacy of tumour tissue for DNA extraction. Tumour epithelial cells were needle-microdissected from 10μm sections (8 – 20 slides) after haematoxylin staining and DNA was isolated using the AllPrep DNA/RNA FFPE kit (Qiagen, Hilden, Germany) according to the manufacturer's protocol. Targeted sequencing of tumour DNA was performed using an Agilent SureSelect XT Custom Panel (Agilent, Santa Clara, CA, USA) which targeted BC specific genes including *TP53*. Library preparation was performed from at least 80ng of tumour DNA using the KAPA Hyper system (Agilent). For samples with lower DNA yields available (≤10ng), library preparation was performed with the NEBNext® Ultra™ II DNA Library Prep Kit (New England BioLabs® Inc, Ipswich, MA, USA) and used for low-coverage whole-genome sequencing as described previously [412]. Illumina Nextseq500 (paired-end 75 bp reads) was used to run pooled, normalised, indexed libraries according to Illumina protocols. Average sequencing depth was 400X (SureSelect) and 1.3X low-coverage whole-genome sequencing.

DNA extraction, targeted sequencing library preparation and enrichment were performed externally in the Peter MacCallum Cancer Centre Lab (Melbourne, Australia).

5.4.2.4 Copy number and variant data analysis

Data was processed by an in-house bioinformatics pipeline at the Peter MacCallum Cancer Centre (Melbourne, Australia) to detect and filter for high confidence somatic variants. Paired-end sequence reads were aligned to the g1k v37 hg19 reference genome using BWA. Optical duplicate reads were removed using Picard and the Genome Analysis Tool Kit (GATK) was used to perform local realignment around indels and base quality score recalibration in accordance with the recommended best practice workflow [413]. Single nucleotide polymorphism (SNP) and indel variants were called using GATK Unified Genotyper, Platypus [414], and Varscan 2 [415]. Called variants were annotated using the Ensembl Variant Effect Predictor [416]. Somatic mutations were identified by removing previously available germline variant data for hereditary breast and ovarian cancer panel genes and by applying the following filters; canonical transcript; bidirectional read; quality ≥100; variants identified by at least two variant callers; minor allele frequency present at ≤0.0001 in ExAc (Version 0.3.1) [417], GnomAD (Version 2.0), EVS (Version ESP6500SI-V2-SSA137) [Exome Variant Server, available http://evs.gs.washington.edu/EVS/], and 1000 Genomes [418] databases.

Copy number profiles were obtained using the SureSelect panel off-target reads with CopywriteR [419] and Control-FREEC for low-coverage whole-genome sequencing reads [420]. A lymphocyte DNA control run (NA12878, Coriell Institute) in the same sequencing batch was used for baseline normalisation. Data were then imported to NEXUS Copy Number™ (software v9.0; BioDiscovery Inc, El Segundo, CA, USA), segmented using a FASST2 segmentation algorithm and visualised using a circular binary segmentation algorithm to determine gains and losses as described [421]. Fraction of the genome altered (FGA) was calculated as the percentage of base pairs with copy number gain or loss. Number of telomeric allelic imbalances (NTAI) was calculated as the count of telomeres (excluding chromosome Y) with a gain or loss [398]. Twenty cases showed deleterious/missense *TP53* variants annotated as described above.

5.4.2.5 Statistical analysis

The optimal cut-off point for TILs density against LRFI was defined using X-tile bioinformatics software (Yale University, version 3.6.1). TILs were classified into sparse and dense infiltrates depending on these cut-off points (**Table 5-4**). For consistency, the same cut-off point used in dichotomisation touching TILs in the training set into sparse and dense groups was applied in the validation set. Furthermore, to mimic the

three-tier prognostic classification system of TILs in melanoma [422] and based on the outcome analysis, TILs were further defined into three-groups; absent/very scanty (mean number of touching TILs/DCIS duct ≤5 cells), sparse (6-20 cells/DCIS duct) and dense (>20 cells/DCIS duct) TILs. This was based on counting TILs around DCIS ducts, in up to 20 ducts per case, and then the total number of TILs was divided by the number of DCIS ducts resulting in the mean TILs number. Inter-observer degree of agreement was assessed through inter-class correlation coefficient (ICC) for continuous data and Kappa test for categorical groups. Linear correlation between TILs densities within different topographic areas and touching TILs was analysed using Spearman's test which was used to correlate between the expression of different immune cells with each other, overall TILs and with the proliferation marker (Ki67), TP53 and HIF-1α. Chi square test was used to determine the association between different markers densities with other clinicopathological parameters. Expression of PDL1 within the tumour cells was not included in the analysis as the percentage of positive cases was very low (2% only). Mann-Whitney U test and Kruskal-Wallis test were used to compare between TILs densities and FGA, NTAI and *TP53* variants. Differential expression of various study markers between pure DCIS and DCIS coexisting with IBC was analysed using the

continuous score data and the Mann-Whitney U test. The association with LRFI was assessed in univariate analysis using Kaplan Meier curves and Log Rank Test. Cox regression was carried out for multivariate analysis to adjust for confounding by conventional prognostic factors. Survival analyses were confined to patients treated with BCS only as it was the highest group showing ipsilateral recurrence. For each test conducted, a two-tailed *p*-value of <0.05 was considered statistically significant.

Table 5-4: Cut-off points of mean TILs count/DCIS duct

Parameter	Definitions of TILs density	
	Sparse	Dense
Mean count of Touching TILs *	≤20 cells	>20 cells
Mean count of TILs within 0.2mm distance *	≤60 cells	>60 cells
Mean count of TILs within 0.5mm distance *	≤100 cells	>100 cells
Mean count of TILs within 1mm distance *	≤120 cells	>120 cells
Hotspots	Largest hotspot within the lesion's boundaries comprising 1200 cells or less	Largest hotspot within the lesion's boundaries compromising more than 1200 cells
Stromal TILs	TILs represent 5% or less of the total surrounding stromal area	TILs represent more than 5% of total surrounding stromal area

*Represent mean number of TILs count within a specified area/DCIS duct.

5.5 **Results**

5.5.1 **Training set**

The concordance rate of TILs assessment using different methods between the three observers is summarised in **Table 5-5** The highest degree of inter-observer agreement was observed in touching TILs (ICC=0.96) whereas the least concordance rate was found with the percentage of stromal TILs evaluation (ICC=0.79) which is the recommended method in IBC.

Table 5-5: TILs Inter-rater concordance results in the training set

Parameter	Intra-cluster correlation coefficient (ICC) between all observers
Mean TILs count Touching ducts	0.96
Mean TILs count within 0.2mm distance	0.89
Mean TILs count within 0.5mm distance	0.92
Mean TILs count within 1mm distance	0.90
Hotspots	0.89
Lymphoid follicles*	0.86
Stromal TILs percentage	0.79

*Performed using Kappa test between first and second observers.

Mean TILs count within different topographic areas around DCIS are summarised in **Table 5-6**. The mean count of TILs increased from 37 cells/DCIS duct at touching area to 482 cells/DCIS duct within 1mm distance. Largest hotspot density ranged from 20 to 6,000 cells while percentage of stromal TILs ranged from 1-65%. Mean TILs density increased by 4-fold between touching and within 0.2mm distance, while it increased only by 2-fold and 1.5-fold from 0.2mm to 0.5mm and from 0.5mm to 1mm distances, respectively. No cases with absent TILs were observed. Touching TILs showed positive linear correlation with TILs within the other topographic areas (**Table 5-7**). The highest correlation was observed between touching TILs and TILs counted at 0.2mm distance (Spearman's correlation=0.854, $p<0.0001$). Counting TILs in farer areas away from the ducts showed less correlation with touching TILs.

Table 5-6: Distribution of TILs in the training set

	Mean count of Touching TILs/DCIS duct	Mean count of TILs at 0.2mm distance /DCIS duct	Mean count of TILs at 0.5mm distance/DCIS duct	Mean count of TILs at 1.0mm distance/ DCIS duct	Hotspot *	Percentage of stromal TILs (%)
Mean	37	144	319	482	1010	13
Median	20	80	135	250	500	5
Minimum	4	10	20	50	20	1
Maximum	120	800	2000	3000	6000	65

*Defined as largest number of lymphoid cell aggregates within the boundaries of the DCIS.

Table 5-7: Correlation between Touching TILs and TILs at other topographic areas (training set)

Parameter	Spearman's correlation	*p* value
Mean TILs count within 0.2mm distance	0.85	**$1.0x10^{-13}$**
Mean TILs count within 0.5mm distance	0.75	**$1.0x10^{-13}$**
Mean TILs count within 1mm distance	0.69	**$1.0x10^{-13}$**
Hotspot	0.57	**$1.1x10^{-13}$**
Percentage of stromal TILs	0.69	**$1.0x10^{-13}$**

Percentage of the cases with dense TILs were 53%, 57%, 59% and 65% for touching TILs and within 0.2mm, 0.5mm and 1mm from DCIS ducts, respectively. Dense hotspots were observed in 31% of cases while dense stromal TILs were observed in 49% of cases. Lymphoid follicles were observed in 31 cases only (21%). The percentages of cases with dense and sparse TILs in context of each topographic area as well as the

percentage of cases that developed local recurrence within each category and their association with LRFI are summarised in **Table 5-8**. Examples of dense and sparse TILs are shown in **Figure 5-3**.

Table 5-8: Frequency of TILs density in different topographic areas and their association with recurrence in the training set

Parameter	TILs density (mean number of TILs/DCIS duct as cut-off)	Number of cases (%)	Recurrence (%)	*p*-value (Log rank test)
Touching TILs (Two-tier system)	Sparse (≤ 20) Dense (>20)	70 (47) 80 (53)	6 (15) 35 (85)	**$4.7x10^{-6}$**
Touching TILs (Three-tier system)	Absent/very scanty (≤5) Sparse (6-20) Dense (>20)	7 (5) 63 (42) 80 (53)	0 (0) 6 (15) 35 (85)	**$2.0x10^{-5}$**
TILs at 0.2mm distance	Sparse (≤ 60) Dense (> 60)	64 (43) 86 (57)	8 (20) 33 (80)	**0.001**
TILs at 0.5mm distance	Sparse (≤ 100) Dense (> 100)	61 (41) 89 (59)	8 (20) 33 (80)	**0.002**
TILs at 1.0mm distance	Sparse (≤ 120) Dense (> 120)	53 (35) 97 (65)	6 (15) 35 (85)	**0.001**
Hotspot	Sparse (≤ 1200) Dense (>1200)	103 (69) 47 (31)	33 (80) 8 (20)	0.089
Lymphoid follicles	No Yes	119 (79) 31 (21)	36 (88) 5 (12)	0.150
Percentage of Stromal TILs	Sparse (≤5%) Dense (>5%)	77 (51) 73 (49)	15 (37) 26 (63)	**0.020**

Significant *p* values are in **bold**

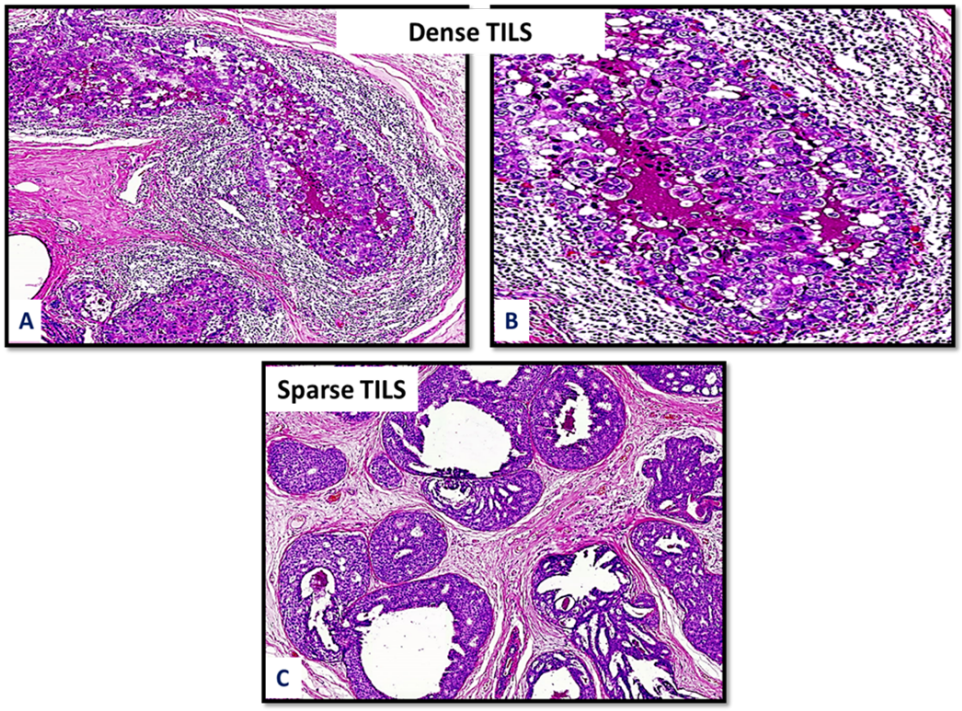

Figure 5-3: Touching TILs density around DCIS

A) Dense infiltrate where mean number of touching TILs is more than 20 cells/DCIS duct, B) High power view for dense touching TILs, and C) Sparse infiltrate where the mean number of touching TILs within the lesion is 20 cells or less/DCIS duct

More than 60% of DCIS cases that developed local recurrence showed dense TILs irrespective of the topographic area used for assessment (Touching, 0.2mm distance, 0.5mm, 1mm and % stromal TILs). Only five cases (12%) from those that developed local recurrence showed lymphoid follicle formations. Dense TILs infiltrate at different compartments showed statistically significant association with shorter LRFI (p=4.7x10^{-6}, p=0.001, p=0.002 and p=0.001 for touching TILs and TILs within 0.2mm, 0.5mm and 1mm distances, respectively). Stromal TILs density was also associated with shorter LRFI but with less statistical significance (p=0.02) than

dense TILs defined in context of circumferential distances from the malignant ducts. Neither hotspots nor lymphoid follicles formation showed significant association with recurrence (p=0.09 and p=0.15, respectively). Results of univariate survival analysis are detailed in **Table 5-8**. **Figure 5-4** shows Kaplan Meier survival curves for TILs density in different compartments and LRFI.

5.5.2 Validation set

The concordance rate between the two observers evaluated touching TILs in the validation set was comparable to the training set (ICC=0.95). Dichotomisation of touching TILs using 20 cells/DCIS duct as a cut-off point, showed that 239 cases (45%) had dense TILs infiltrate while 55% of cases showed sparse infiltrate.

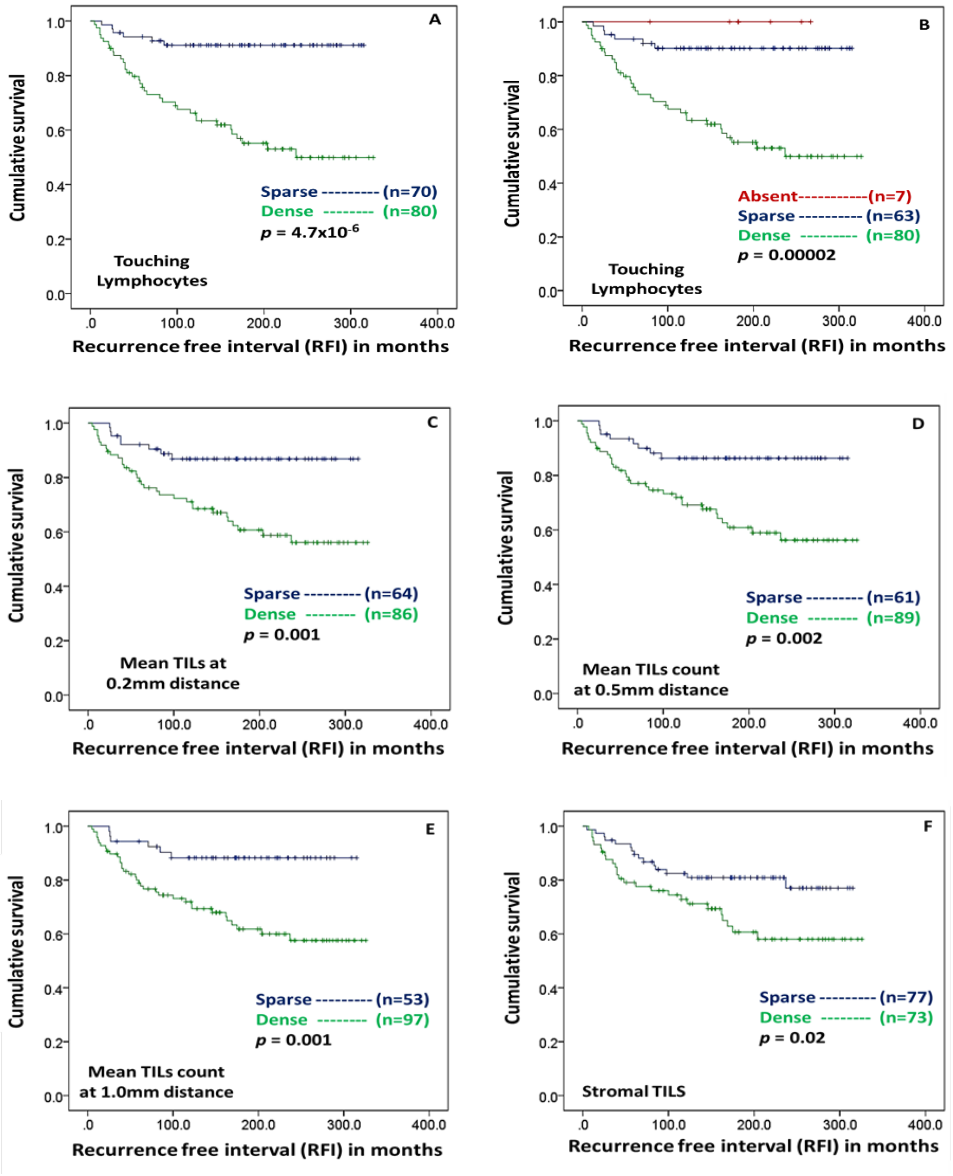

Figure 5-4: Kaplan-Meier curves showing association between TILs density within different topographic areas and LRFI in training set

(A) Touching TILs (two-tier), b) Touching TILs (three-tier), c) TILs within 0.2mm distance, d) TILs within 0.5mm distance, e) TILs within 1mm distance, and f) Stromal TILs

5.5.3 Association of TILs density with other clinicopathological parameters

Dense touching TILs were associated with parameters characteristic of aggressive tumour behaviour including

younger age, symptomatic presentation and larger tumour size. Only 8 cases (14%) of low nuclear grade lesions showed dense TILs in comparison with 33% and 54% of intermediate and high nuclear grade lesions, respectively (p<0.0001). Half of the cases (50%) associated with comedo necrosis harboured dense TILs while this was observed only in 32% of cases without comedo necrosis (p<0.0001). Approximately two thirds (69%) of DCIS cases associated with Paget's disease showed dense TILs infiltrate compared with 46% of patients without Paget's disease (p=0.025). 72% of ER negative DCIS showed dense TILs infiltrate while only 36% of ER positive cases showed high TILs density (p<0.0001).

Moreover, dense TILs were observed in 80% of DCIS mixed with IBC compared with 54% of pure grade-matched DCIS (χ^2=51.29, p<0.0001). This association was observed also when touching TILs was assessed as a continuous variable (p<0.0001). The association between TILs density and various clinicopathological parameters are summarised in **Table 5-9**.

Table 5-9: Correlation between TILs density and clinicopathological parameters in the validation set

Parameter	TILs density		Chi square (χ^2)	*p* value
	Dense N (%)	Sparse N (%)		
Patient age				
≤50 years	71 (52)	65 (48)	4.09	**0.043**
>50 years	168 (42)	230 (58)		
Presentation				
Screening	114 (41)	166 (59)	3.89	**0.049**
Symptomatic	125 (49)	129 (51)		
DCIS Size				
≤20mm	85 (37)	147 (63)	10.66	**0.001**
>20mm	152 (51)	147 (49)		
DCIS Grade				
Low	8 (14)	49 (86)	41.18	**<0.0001**
Moderate	44 (33)	88 (67)		
High	187 (54)	158 (46)		
Comedo type necrosis	185 (50)	182 (50)	15.16	**<0.0001**
Yes	54 (32)	113 (68)		
No				
Associated Paget's disease	18 (69)	8 (31)	5.03	**0.025**
Yes	156 (46)	180 (54)		
No				
Oestrogen receptor status	83 (72)	33 (28)	41.73	**<0.0001**
Negative	114 (36)	198 (64)		
Positive				
HER2 status				
Positive	83 (74)	29 (26)	51.67	**<0.0001**
Negative	126 (35)	230 (65)		
HIF**1a expression**	121 (43)	159 (57)	21.20	**<0.0001**
Low	64 (71)	26 (29)		
High				
Type of DCIS				
Mixed with invasion	105 (80)	27 (20)	51.29	**<0.0001**
Pure DCIS	239 (45)	295 (55)		

Significant *p* values are in **bold**
DCIS; ductal carcinoma in situ, HER2; Human epidermal growth factor receptor 2, HIF1a; hypoxia inducible factor 1 alpha

5.5.4 Outcome analysis

Ipsilateral local recurrence rate in the pure DCIS validation cohort was 11.8% (*n*=63). Recurrence occurred in 39/239 cases with dense TILs (62% from total recurrences), in comparison with 24/295 cases with sparse TILs (38% from total recurrences). Within patients treated with BCS, local recurrence was reported in 24/80 cases with dense TILs (56%) compared to 19/139 cases with sparse infiltrate (44%). When assessed based on ER status, there were 22 recurrent events among ER-positive DCIS with dense TILs (*n*=114) compared with 40 events among cases with sparse TILs (*n*=198). Among ER-negative DCIS cases, 14/83 cases with dense TILs had local recurrence while only 1/33 cases with sparse TILs experienced a recurrence.

When TILs were classified into three categories defined as; absent/very scanty TILs (mean number of touching TILs/DCIS duct ≤5 cells), sparse TILs (from 6-20 cells/DCIS duct) and dense TILs (>20 cells/DCIS duct), recurrence occurred in 1/37 patients (3% of the group, 1.5% of the total recurrences), 23/258 patients (9% of the group, 36.5% of the total recurrences) and 39/239 (16% of the group, 62% of the total recurrences); respectively.

In univariate survival analysis using two-tier classification system of TILs, dense TILs showed statistically significant association with shorter LRFI. This was observed when the analysis was conducted on the whole cohort (p=0.002) or confined to patients treated with BCS (p=0.001). In context of ER status, dense TILs infiltrate was associated with shorter RFI in both ER-positive (p=0.011) and ER-negative (p=0.025) DCIS. Supporting the reproducibility of touching TILs evaluation in outcome prediction, univariate analysis using the second observer's scoring showed significant association with recurrence in the whole cohort and in patients treated with BCS (p=0.0001 and p=0.004, respectively). Moreover, when the analysis was conducted using the average score between the two observers, it also showed significant association (p=0.002, p=0.01 for the whole cohort and for patients treated with BCS, respectively).

Similar findings were observed when the three-tier classification system was used in the univariate analysis where dense TILs infiltrate was associated with shorter LRFI in the whole cohort and BCS treated patients (p=0.005 and p=0.004; respectively), **Figure 5-5**. Interestingly, there was no statistically significant association between LRFI and TILs density when assessed based on the percentage of overall

stromal TILs (p=0.117 for the whole cohort and p=0.138 for patients treated with BCS).

Cox regression multivariate model with other clinicopathological parameters including patient's age, tumour size, nuclear grade, presence of comedo necrosis, adjuvant RT and ER status showed that dense touching TILs is the only independent predictor of shorter LRFI in patients treated with BCS (*HR*=2.6, 95% *CI*=1.4-4.7, p=0.002) (**Table 5-10**).

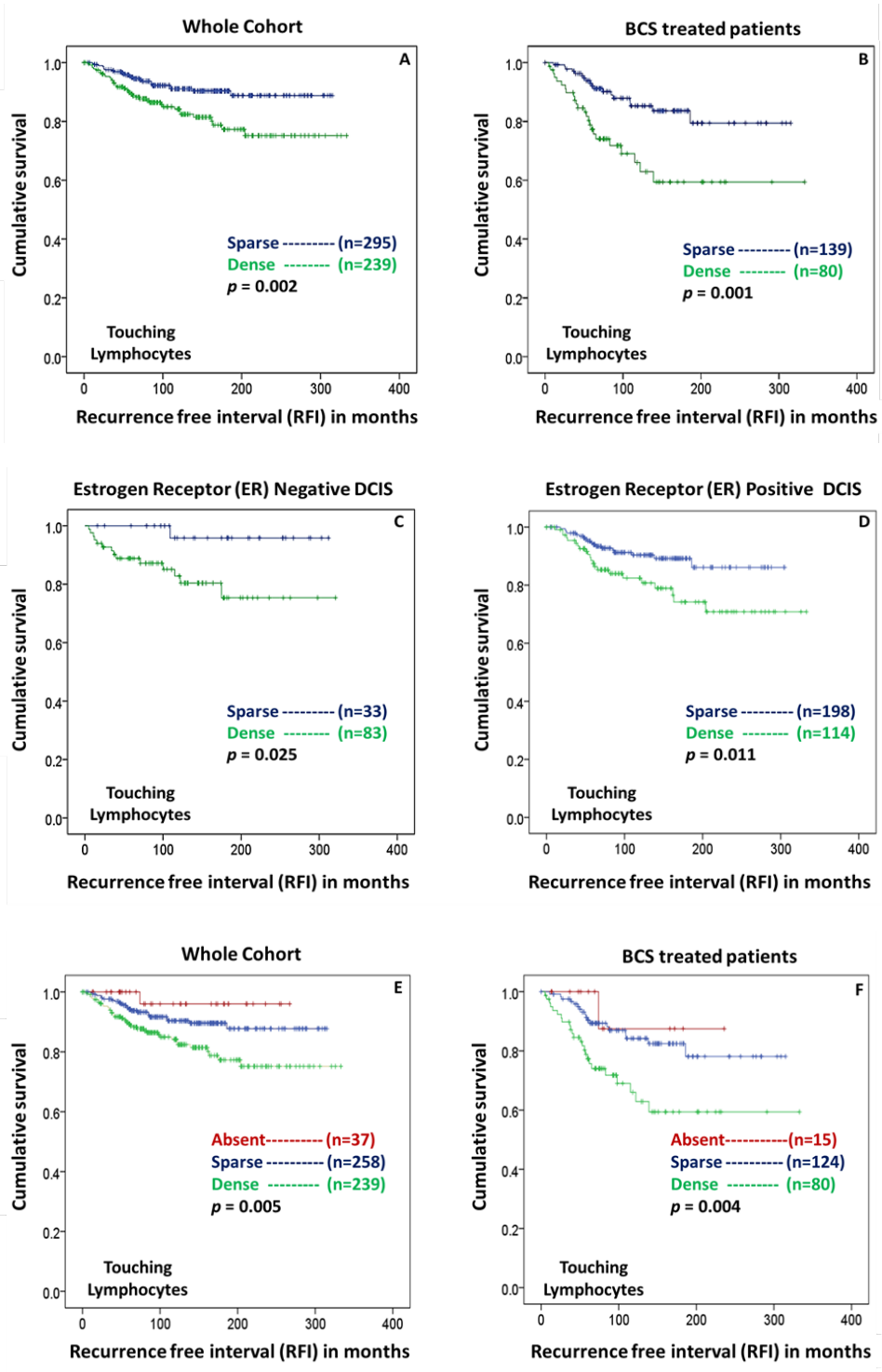

Figure 5-5: Association between touching TILs density with LRFI

A) all cases irrespective of surgical treatment, B) cases treated with breast conserving surgery (BCS), (C and D) according to Oestrogen Receptor (ER) status, as well as when TILs density defined as three-groups in; E) the whole cohort, and F) breast conserving surgery (BCS) treated patients

Table 5-10: Cox regression analysis of TILs association with LRFI*

Parameters	Hazard ratio (*HR*)	95.0% confident interval (*CI*)		*p*-value
		Lower	Upper	
Patient Age	0.599	0.318	1.127	0.112
DCIS Size	0.755	0.403	1.415	0.381
DCIS Grade	1.531	0.899	2.608	0.117
Comedo necrosis	0.639	0.341	1.197	0.162
Radiotherapy	0.423	0.172	1.037	0.060
Oestrogen receptor	0.934	0.477	1.829	0.841
Dense TILs	2.573	1.412	4.690	**0.002**

*Performed for patients treated with Breast conservative surgery (BCS) only.

5.5.5 Patterns of expression and distribution of various inflammatory cells and immune checkpoints

The assessment of the full-face sections revealed that TILs infiltration was comparable to the TMA sections thus justifying the representability of the TMA sections for immunoscoring both in the stromal and intratumoural compartments. Uninformative cores (lost, folded tissue or cores containing <15% tumour cells and/or stroma) were excluded from scoring. **Table 5-11** summarises the distribution of various types of lymphocytes as well as PD1 and PDL1 expression either in the stroma or intratumourally. The predominant lymphocytes in DCIS were CD3+ cells either intratumourally (median 1 cell/duct, range 0-50) or in the stroma (median 3 cells/duct, range 0-100) whereas CD4+ cells were the most

frequent subtype of T cells (range 0-60 in the stroma and 0-25 in the intratumoural compartment). Stromal FOXP3+ lymphocytes were the least frequent (median 0 cells/duct, range 0-25) while PD1+ cells were the lowest type intratumourally (median 0 cells/duct, range 0-15). Only 2% of pure DCIS cases showed positive expression for PDL1 within tumour cells. **Figure 5-6** and **Figure 5-7** show examples of dense TIL infiltrates in H&E and IHC stained sections with various markers demonstrating the distribution of immune cells and immune checkpoint protein in pure DCIS.

Table 5-11: Distribution of various TILs and immune check point proteins in the pure DCIS cohort

	sCD20	iCD20	sCD3	iCD3	sCD8	iCD8	sCD4	iCD4	sFOXP3	iFOXP3	sPD1	iPD1	sPDL1	tPDL1
Median	0	0	3	1	0	0	0	0	0	0	0	0	0	0
Minimum	0	0	0	0	0	0	0	0	0	0	0	0	0	0
Maximum	60	40	100	50	30	20	60	25	25	10	40	15	35	100
% Pure DCIS with high expression	**35**	**26**	**46**	**50**	**41**	**37**	**44**	**41**	**20**	**16**	**39**	**14**	**31**	**2**

Numbers represent average number of cells / duct except PDL1 in the tumour which represent the percentage of positive cells. s; stromal, i; intratumoural and t; tumour epithelial cells.

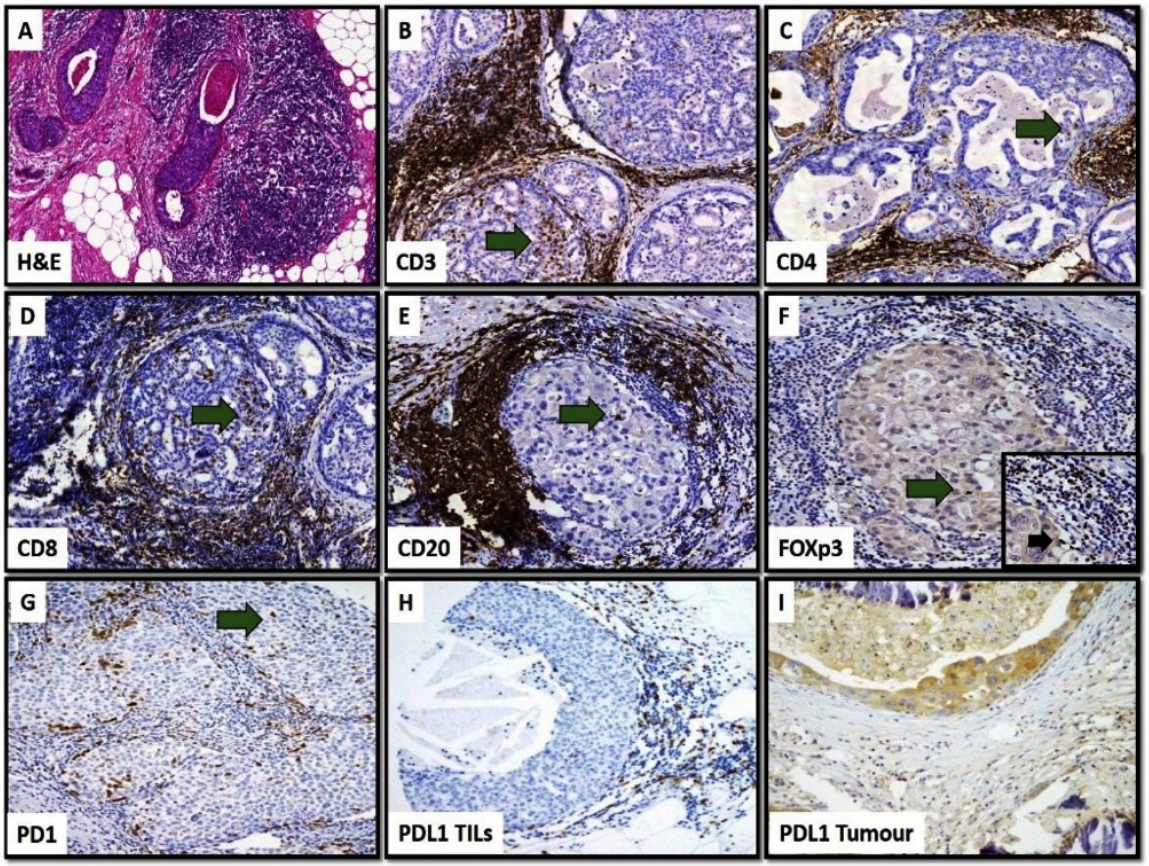

Figure 5-6: Photomicrograph for immune cells and checkpoint proteins in DCIS

A) Dense Overall TILs infiltration in H&E stained sections (20x). Dense stromal and intratumoural infiltration of various immune cell markers, B) CD3, C) CD4, D) CD8, E) CD20, F) FOXP3, G) PD1 and H) PDL1. Expression of PDL1 within the tumour epithelial cells is shown in (I). Green arrows highlight the intratumoural lymphocytes. Inset: higher magnification (40x) showing stromal FOXP3 positive cells

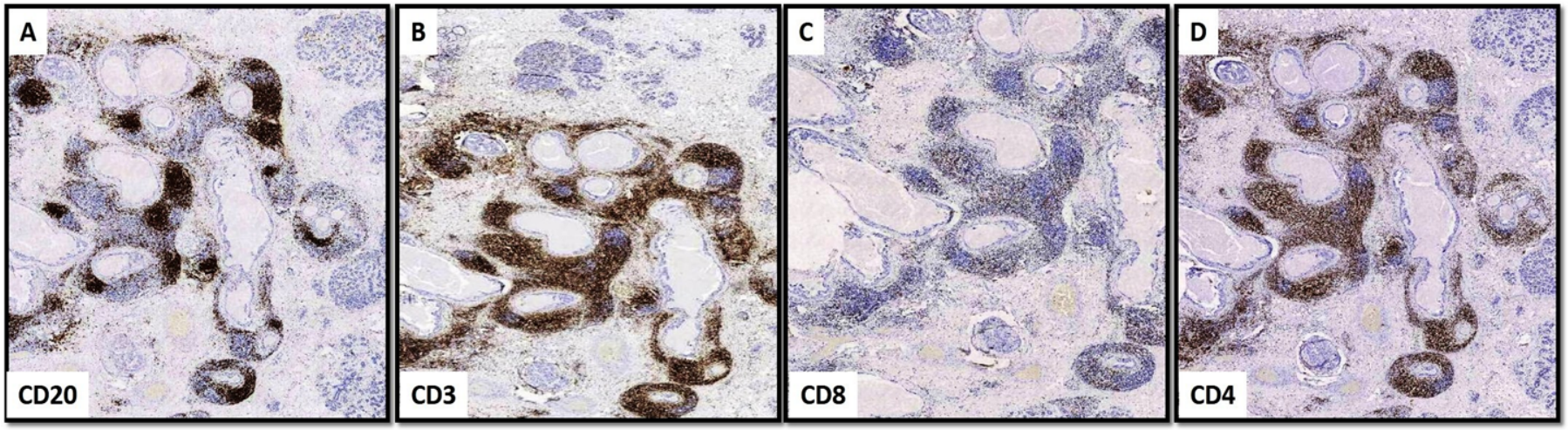

Figure 5-7: Distribution of CD20, CD3, CD4 and CD8 in DCIS

It is noticed that CD20 and CD3 are the most predominant subtypes. Also, CD4+ cells are more predominant T lymphocytes' subtype than CD8+ cells (4x)

Stromal CD3+, CD8+, CD4+, PDL1+ and PD1+ lymphocytes showed the highest correlation with overall TILs (all $r>0.4$, $p<0.0001$). The strongest correlation between various lymphocytes was observed with CD3+ and CD4+ lymphocytes ($r=0.96$, $p<0.0001$), followed by CD4+ and CD8+ cells ($r=0.94$, $p<0.0001$). **Figure 5-8**A shows a correlation matrix that summarises the associations between overall TILs, various immune cell subtypes, PD1, PDL1, hormonal receptors, Ki67, HIF-1α, CK5/6 and p53 protein.

Moreover, DCIS mixed with synchronous IBC harboured more dense stromal TILs, PD1, PDL1 and various subpopulation of lymphocytes within the stroma than pure DCIS, with the highest difference observed with stromal PD1+ ($Z=5.8$, $p<0.0001$) followed by stromal CD8+ ($Z=5.5$, $p<0.0001$). Only stromal CD4+ cells did not show a significant statistical difference between both groups. In the context of intratumoural immune cells, there was no difference in immune cells infiltrates between pure DCIS and DCIS mixed apart from intratumoural CD20 which was more prevalent in pure DCIS ($Z=2.7$, $p=0.007$) and PD1 which was more dense in DCIS associated with IBC ($Z=2.2$, $p=0.025$). **Figure 5-8**B and **Figure 5-9** demonstrate the differences in various immune cell markers between both groups.

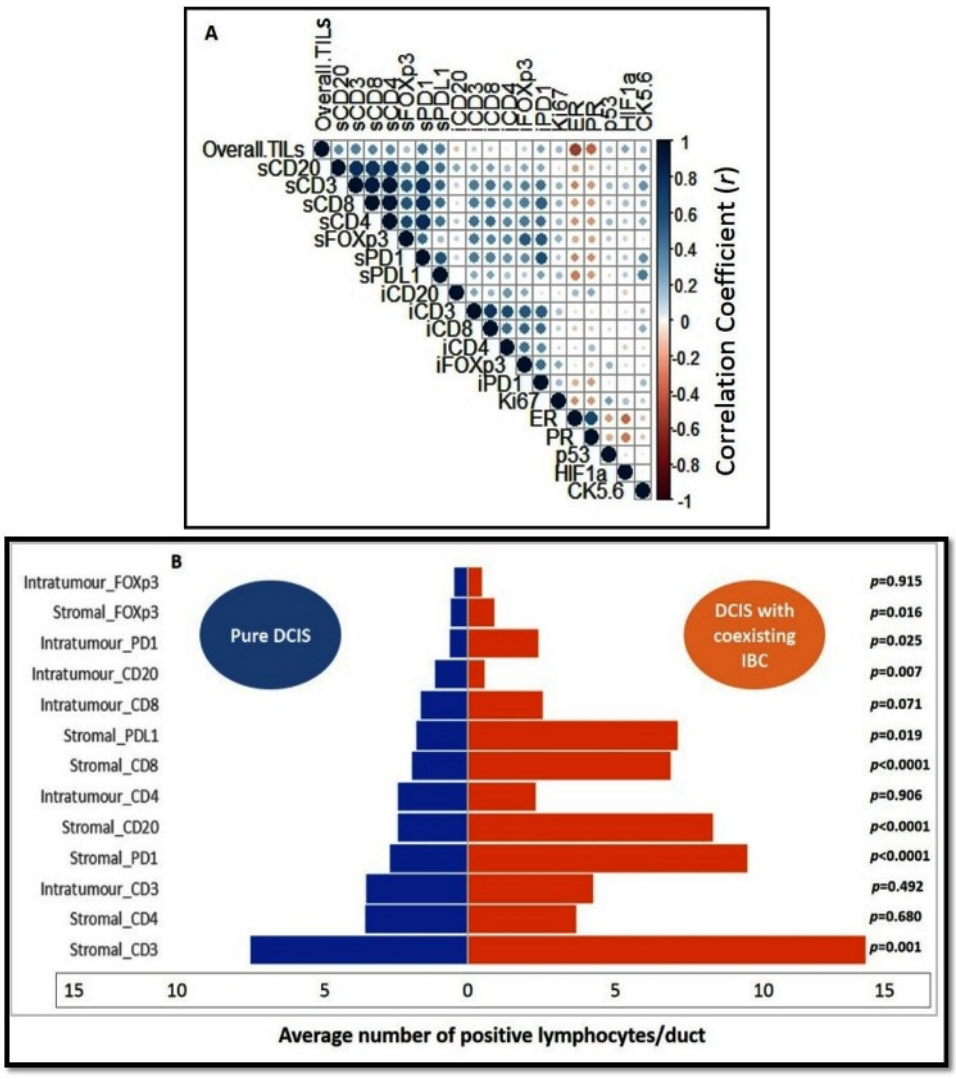

Figure 5-8: Correlation Matrix showing the correlation between TILs subtypes, overall TILs, and other associated biomarkers

Blue colour refers to positive correlation, while the red colour reflects negative correlations. The intensity of the colour propionate to the correlation coefficient. Lower image shows Tornado (Butterfly) plot showing the differential expression level of various lymphocytes between pure DCIS and DCIS mixed with synchronous invasive breast cancer (IBC) (s; stromal, i; intratumoural)

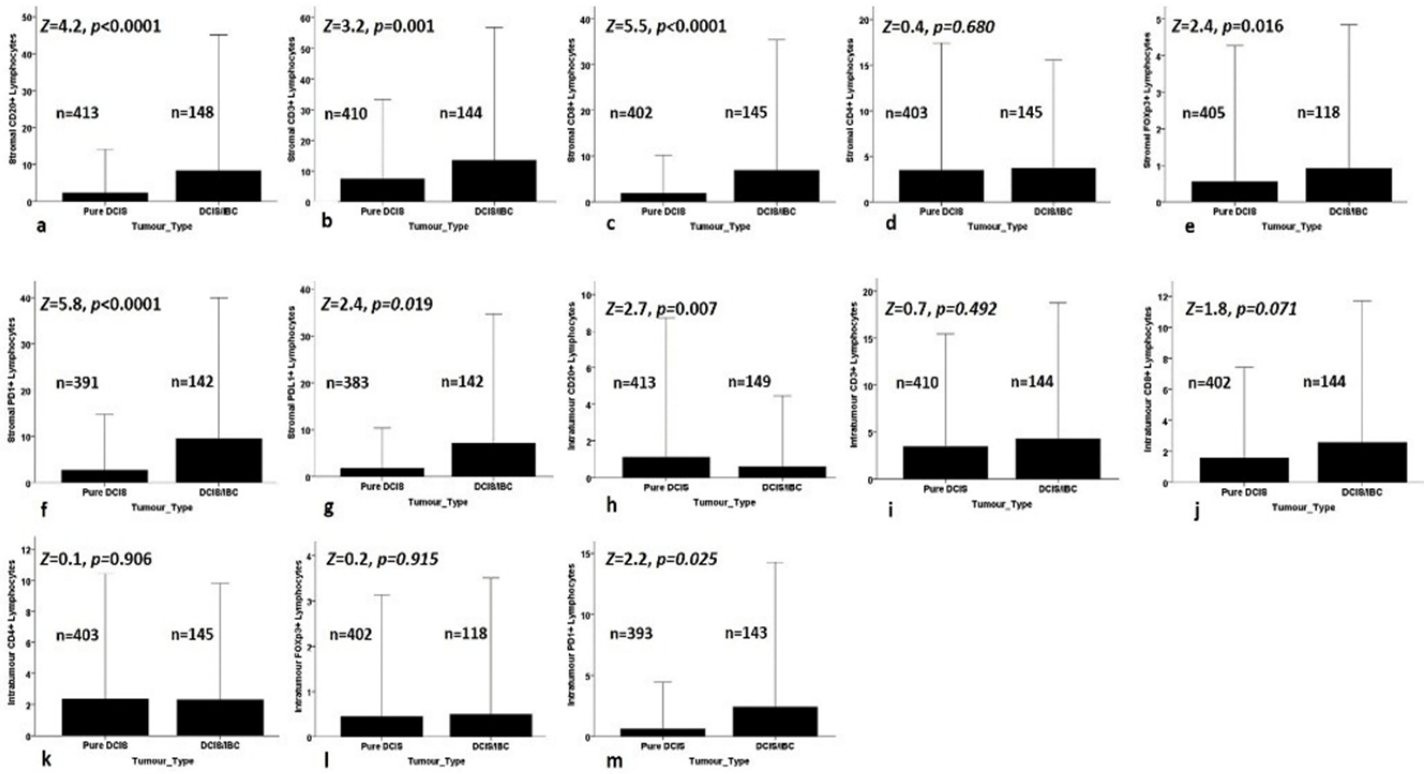

Figure 5-9: Bar charts showing the difference between expression of various immune cells and checkpoint proteins in pure DCIS and DCIS coexisting with invasive disease

a) stromal CD20+, b) stromal CD3+, c) stromal CD8+, d) stromal CD4+, e) stromal FOXP3+, f) stromal PD1+, g) stromal PDL1+, h) intratumoural CD20+, i) intratumoural CD3+, j) intratumoural CD8+, k) intratumoural CD4+, l) intratumoural FOXP3+ and m) intratumoural PD1+ lymphocytes. Error bars represent +2 standard deviation.

5.5.6 Association between immune cells subpopulations and other clinicopathological parameters

Higher expression of the majority of markers, either stromal or within the intratumoural comportment, was associated with hormonal receptor negativity. The exceptions were intratumoural CD20+ cells, which were associated with ER and PR positivity, and intratumoural CD3+, CD8+ and CD4+, which showed no association with ER or PR. High expression of all markers within the stroma, and intratumoural expression of PD1 and FOXP3, was associated with higher nuclear grade, HER2 positivity, and higher expression of HIF-1α. DCIS with smaller size and lower expression of HIF-1α showed higher expression of intratumoural CD20+ lymphocytes. It was also observed that dense infiltration of PD1, CD3, CD8, CD20 and FOXP3 in the stromal region was significantly associated with the presence of comedo-type necrosis. **Table 5-12** shows the correlation between various immune cells/checkpoint markers and the clinicopathological parameters in the pure DCIS cohort.

Table 5-12: Correlation between immune cell markers, immune checkpoints with the clinicopathological parameters in pure DCIS cohort

a) Parameters	Stromal CD20 +ve cells		χ^2 (*p*-value)	Intratumour CD20 +ve cells		χ^2 (*p*-value)	Stromal CD3 +ve cells		χ^2 (*p*-value)	Intratumour CD3 +ve cells		χ^2 (*p*-value)
	Low (N=268) N. (%)	High (n=145) N. (%)		Low (N=305) N. (%)	High (n=108) N. (%)		Low (N=207) N. (%)	High (n=203) N. (%)		Low (N=207) N. (%)	High (n=203) N. (%)	
Age												0.8
≤50 years	66 (25)	47 (32)	2.9	79 (26)	34 (31)	1.2	55 (25)	56 (30)	1.1	52 (25)	59 (29)	(0.369)
>50 years	202 (75)	98 (68)	(0.090)	226 (74)	74 (69)	(0.264)	165 (75)	134 (70)	(0.309)	155 (75)	144 (71)	
Presentation			1.2									
Screening	126 (47)	60 (41)	(0.272)	138 (45)	48 (44)	0.021	101 (50)	84 (44)	0.1	92 (44)	93 (46)	0.1
Symptomatic	142 (53)	85 (59)		167 (55)	60 (56)	(0.886)	119 (50)	106 (56)	(0.730)	115 (56)	110 (54)	(0.781)
DCIS Size						3.2						
≤20mm	109 (41)	59 (41)	0.1	116 (38)	52 (48)	(0.073)	92 (42)	75 (40)	0.2	74 (36)	93 (46)	4.3
>20mm	158 (59)	85 (59)	(0.977)	187 (62)	56 (52)		128 (58)	113 (60)	(0.694)	132 (64)	109 (54)	**(0.038)**
Nuclear Grade												0.7
Low	43 (15)	9 (6)	19.1	36 (12)	16 (15)	0.676	41 (18)	10 (5)	34.5	26 (13)	25 (12)	(0.711)
Moderate	81 (28)	27 (19)	**(<0.0001)**	81 (27)	27 (25)	(0.713)	71 (33)	35 (18)	**(<0.0001)**	57 (28)	49 (24)	
High	168 (57)	85 (75)		188 (61)	65 (60)		108 (49)	145 (77)		124 (59)	129 (64)	
Comedo necrosis			9.5			1.6						
Yes	163 (61)	110 (76)	**(0.002)**	207 (68)	66 (61)	(0.202)	132 (60)	139 (73)	7.9	140 (68)	131 (65)	0.4
No	105 (39)	35 (24)		98 (32)	42 (39)		88 (40)	51 (27)	**(0.005)**	67 (32)	72 (35)	(0.507)
Estrogen receptor												0.6
Negative	45 (19)	57 (44)	25.4	83 (32)	19 (19)	5.4	28 (15)	73 (42)	33.8	53 (30)	48 (26)	(0.433)
Positive	188 (81)	72 (56)	**(<0.0001)**	180 (68)	80 (81)	**(0.020)**	160 (85)	99 (58)	**(<0.0001)**	124 (70)	135 (74)	
Progesterone receptor												
Negative	87 (37)	79 (62)	21.3	132 (49)	34 (34)	6.6	62 (32)	103 (61)	29.5	86 (48)	79 (43)	0.8
Positive	151 (63)	49 (38)	**(<0.0001)**	135 (51)	65 (66)	**(0.010)**	131 (68)	67 (39)	**(<0.0001)**	94 (52)	104 (57)	(0.378)
HER2 status *						2.3						0.1
Negative	202 (80)	86 (65)	11.6	205 (73)	83 (81)	(0.126)	170 (83)	115 (65)	16.9	144 (75)	141 (75)	(0.930)
Positive	49 (20)	47 (35)	**(0.001)**	76 (27)	20 (19)		34 (17)	62 (35)	**(<0.0001)**	49 (25)	47 (25)	
Molecular classes			24.1			6.6			31.1			1.5
Luminal A	119 (58)	40 (34)	**(<0.0001)**	106 (46)	53 (57)	(0.086)	101 (62)	57 (35)	**(<0.0001)**	71 (46)	87 (52)	(0.674)
Luminal B	42 (20)	24 (20)		45 (19)	21 (23)		32 (20)	34 (21)		31 (20)	35 (21)	
HER2 Enriched	22 (11)	31 (26)		43 (19)	10 (12)		14 (9)	39 (24)		27 (18)	26 (15)	
Triple Negative	23 (11)	24 (20)		38 (16)	9 (10)		14 (9)	32 (20)		25 (16)	21 (12)	
HIF1a expression						6.3						0.1
Low	207 (83)	90 (63)	18.7	207 (72)	90 (84)	**(0.014)**	171 (84)	126 (66)	16.8	144 (75)	151 (76)	(0.771)
High	44 (17)	53 (37)	**(<0.0001)**	80 (28)	17 (16)		33 (16)	64 (34)	**(<0.0001)**	49 (25)	48 (24)	

b) Parameters	Stromal CD4 +ve cells		χ^2 (*p*-value)	Intratumour CD4 +ve cells		χ^2 (*p*-value)	Stromal CD8 +ve cells		χ^2 (*p*-value)	Intratumour CD8 +ve cells		χ^2 (*p*-value)
	Low (N=225) N. (%)	High (N=178) N. (%)		Low (N=233) N. (%)	High (N=170) N. (%)		Low (N=238) N. (%)	High (n=164) N. (%)		Low (N=253) N. (%)	High (n=149) N. (%)	
Age			0.1			1.3						
≤50 years	55 (24)	57 (32)	2.8	65 (28)	47 (28)	(0.956)	54 (23)	57 (35)	6.6	65 (26)	46 (31)	(0.262)
>50 years	170 (76)	121 (68)	(0.092)	168 (72)	123 (72)		184 (77)	107 (65)	**(0.010)**	188 (74)	103 (69)	
Presentation			0.9						2.3			
Screening	106 (47)	75 (42)	(0.363)	103 (44)	78 (46)	0.1	114 (48)	66 (40)	(0.129)	107 (42)	73 (49)	1.7
Symptomatic	119 (53)	103 (58)		130 (56)	92 (54)	(0.738)	124 (52)	98 (60)		146 (58)	76 (51)	(0.192)
DCIS Size												
≤20mm	88 (39)	75 (43)	0.6	83 (36)	80 (48)	5.8	94 (40)	67 (41)	0.1	92 (36)	69 (47)	4.3
>20mm	137 (61)	101 (57)	(0.424)	150 (64)	88 (52)	**(0.016)**	144 (60)	95 (59)	(0.773)	161 (64)	78 (53)	(0.038)
Nuclear Grade												5.8
Low	40 (18)	11 (6)	36.9	29 (12)	22 (13)	0.4	43 (19)	7 (4)	26.0	37 (15)	13 (9)	(0.055)
Moderate	75 (34)	29 (16)	**(<0.0001)**	63 (27)	41 (24)	(0.803)	71 (29)	35 (21)	**(<0.0001)**	72 (29)	34 (23)	
High	110 (48)	138 (78)		141 (61)	107 (63)		123 (52)	123 (75)		144 (56)	102 (68)	
Comedo necrosis						4.6						0.1
Yes	143 (63)	125 (70)	2.2	165 (71)	103 (61)	**(0.032)**	148 (63)	119 (73)	4.3	168 (66)	99 (66)	(0.993)
No	82 (37)	53 (30)	(0.134)	68 (29)	67 (39)		90 (37)	45 (27)	**(0.037)**	85 (34)	50 (34)	
Estrogen receptor						1.1						
Negative	28 (14)	73 (46)	44.8	61 (31)	40 (26)	(0.299)	38 (19)	62 (43)	25.1	54 (25)	46 (34)	3.5
Positive	168 (86)	86 (54)	**(<0.0001)**	138 (69)	116 (74)		173 (81)	82 (57)	**(<0.0001)**	165 (75)	90 (66)	(0.062)
Progesterone receptor						2.5						
Negative	66 (33)	96 (60)	25.0	101 (49)	61 (40)	(0.115)						3.3
Positive	132 (67)	64 (40)	**(<0.0001)**	106 (51)	90 (60)		77 (36)	85 (59)	19.0	93 (41)	69 (51)	(0.071)
							139 (64)	59 (41)	**(<0.0001)**	132 (59)	66 (49)	
HER2 status *						1.6						1.6
Negative	175 (83)	107 (65)	14.3	159 (73)	123 (78)	(0.205)	184 (82)	97 (64)	15.4	182 (77)	99 (71)	(0.203)
Positive	36 (17)	58 (35)	**(<0.0001)**	60 (27)	34 (22)		40 (18)	54 (36)	**(0.001)**	54 (23)	40 (29)	
Molecular classes			44.4			2.2			40.3			4.1
Luminal A	110 (65)	47 (31)	**(<0.0001)**	80 (45)	77 (53)	(0.527)	120 (63)	37 (28)	**(<0.0001)**	102 (54)	55 (42)	(0.260)
Luminal B	33 (19)	32 (21)		38 (22)	27 (19)		31 (16)	34 (26)		35 (18)	30 (23)	
HER2 Enriched	13 (8)	40 (27)		32 (18)	21 (15)		18 (10)	35 (27)		29 (15)	24 (19)	
Triple Negative	15 (8)	31 (21)		27 (15)	19 (13)		21 (11)	24 (19)		24 (13)	21 (16)	
HIF1a expression			24.1			0.2						
Low	180 (85)	112 (64)	**(<0.0001)**	168 (76)	124 (74)	(0.690)	196 (85)	97 (61)	29.1	188 (78)	105 (71)	2.4
High	33 (15)	63 (36)		53 (24)	43 (26)		32 (15)	62 (39)	**(<0.0001)**	52 (22)	42 (29)	(0.124)

c) Parameters	Stromal PD1 +ve cells		χ^2 (*p*-value)	Intratumour PD1 +ve cells		χ^2 (*p*-value)	Stromal PDL1 +ve cells		χ^2 (*p*-value)
	Low (N=241) N. (%)	High (n=152) N. (%)		Low (N=338) N. (%)	High (n=55) N. (%)		Low (N=264) N. (%)	High (n=119) N. (%)	
Age						0.1			
≤50 years	63 (26)	47 (31)	0.9	95 (28)	15 (27)	(0.898)	65 (25)	40 (34)	3.3
>50 years	178 (74)	105 (69)	(0.328)	243 (72)	40 (73)		199 (75)	79 (66)	(0.068)
Presentation			0.8			0.1			
Screening	114 (47)	64 (42)	(0.357)	154 (46)	24 (44)	(0.790)	128 (49)	45 (38)	3.8
Symptomatic	127 (53)	88 (58)		184 (54)	31 (56)		136 (51)	74 (62)	(0.052)
DCIS Size						0.742			
≤20mm	97 (41)	59 (39)	0.6	132 (39)	24 (45)	(0.389)	114 (43)	39 (33)	3.8
>20mm	144 (59)	91 (61)	(0.806)	206 (61)	29 (55)		150 (57)	79 (67)	(0.062)
Nuclear Grade						11.4			
Low	40 (17)	9 (6)	37.7	48 (14)	1 (2)	**(0.003)**	42 (16)	7 (6)	16.7
Moderate	83 (35)	22 (15)	**(<0.0001)**	95 (28)	10 (18)		79 (30)	22 (19)	**(<0.0001)**
High	118 (48)	121 (79)		195 (58)	44 (80)		143 (54)	90 (75)	
Comedo necrosis			11.7			0.9			
Yes	146 (60)	117 (77)	**(0.001)**	223 (66)	40 (73)	(0.324)	169 (64)	86 (72)	2.5
No	95 (40)	35 (23)		115 (34)	15 (27)		95 (36)	33 (28)	(0.113)
Estrogen receptor						6.2			
Negative	32 (15)	66 (46)	41.6	76 (25)	22 (42)	**(0.013)**	46 (20)	53 (49)	30.8
Positive	176 (85)	76 (54)	**(<0.0001)**	222 (75)	30 (58)		187 (80)	55 (51)	**(<0.0001)**
Progesterone receptor									
Negative	66 (30)	95 (67)	47.8	125 (41)	36 (71)	15.5	82 (35)	74 (68)	32.4
Positive	149 (70)	46 (33)	**(<0.0001)**	180 (59)	15 (29)	**(<0.0001)**	152 (65)	35 (32)	**(<0.0001)**
HER2 status *									
Negative	187 (84)	85 (60)	12.9	243 (77)	29 (56)	10.9	199 (82)	64 (58)	23.4
Positive	37 (16)	57 (40)	**(<0.0001)**	71 (23)	23 (44)	**(0.001)**	44 (18)	47 (42)	**(<0.0001)**
Molecular classes									
Luminal A	117 (64)	39 (29)	47.4	137 (51)	19 (38)	7.5	123 (60)	25 (25)	38.4
Luminal B	34 (19)	30 (23)	**(<0.0001)**	55 (21)	9 (18)	(0.057)	37 (18)	25 (25)	**(<0.0001)**
HER2 Enriched	14 (7)	40 (30)		39 (15)	15 (30)		23 (11)	30 (29)	
Triple Negative	18 (10)	24 (18)		35 (13)	7 (14)		21 (11)	22 (21)	
HIF1a expression									
Low	191 (85)	91 (61)	28.1	251 (78)	31 (57)	10.7	208 (85)	65 (55)	37.9
High	34 (15)	59 (39)	**(<0.0001)**	70 (22)	23 (43)	**(0.001)**	37 (15)	53 (45)	**(<0.0001)**

d) Parameters	Stromal FOXP3 +ve cells			Intratumour FOXP3 +ve cells		
	Low (N=327) N. (%)	High (N=79) N. (%)	χ^2 (*p*-value)	Low (N=330) N. (%)	High (N=66) N. (%)	χ^2 (*p*-value)
Age						
≤50 years	91 (28)	20 (25)	0.2	91 (27)	20 (30)	0.3
>50 years	236 (72)	59 (75)	(0.681)	239 (73)	46 (70)	(0.593)
Presentation						
Screening	143 (44)	39 (49)	0.7	156 (46)	26 (39)	1.1
Symptomatic	180 (56)	40 (51)	(0.405)	180 (54)	40 (61)	(0.294)
DCIS Size						
≤20mm	132 (41)	31 (40)	0.1	134 (40)	29 (45)	0.5
>20mm	191 (59)	46 (60)	(0.931)	201 (60)	36 (55)	(0.488)
Nuclear Grade						
Low	48 (15)	1 (1)		47 (14)	2 (3)	
Moderate	90 (28)	13 (17)	19.9	92 (27)	11 (16)	12.1
High	185 (57)	65 (82)	**(<0.0001)**	197 (59)	53 (81)	**(0.002)**
Comedo necrosis						
Yes	204 (63)	64 (19)	9.4	218 (65)	50 (76)	2.9
No	119 (37)	15 (81)	**(0.002)**	118 (35)	16 (24)	(0.087)
Estrogen receptor						
Negative	67 (24)	34 (53)	15.1	78 (27)	23 (38)	3.4
Positive	214 (76)	39 (47)	**(<0.0001)**	216 (73)	37 (62)	**(0.049)**
Progesterone receptor						
Negative	114 (40)	49 (69)	19.8	127 (42)	36 (61)	6.8
Positive	173 (60)	22 (31)	**(<0.0001)**	172 (53)	23 (39)	**(0.009)**
HER2 status *						
Negative	240 (80)	40 (58)	13.7	244 (78)	36 (59)	9.4
Positive	64 (20)	31 (42)	**(<0.0001)**	70 (22)	25 (41)	**(0.002)**
Molecular classes						
Luminal A	140 (55)	17 (25)		139 (53)	17 (29)	
Luminal B	48 (20)	17 (25)	24.6	46 (17)	18 (31)	12.3
HER2 Enriched	31 (12)	22 (33)	**(<0.0001)**	39 (15)	14 (24)	**(0.006)**
Triple Negative	35 (13)	11 (17)		37 (15)	9 (16)	
HIF1a expression						
Low	251 (81)	39 (50)	32.7	256 (80)	34 (52)	21.3
High	58 (19)	39 (50)	**(<0.0001)**	66 (20)	31 (48)	**(<0.0001)**

Significant *p* values are in **bold.**

DCIS; ductal carcinoma in situ, HER2; Human epidermal growth factor receptor 2, HIF1A; hypoxia inducible factor 1 alpha.

5.5.7 Copy number variation and *TP53* mutations

Higher FGA was associated with higher tumour grade (p=0.002), presence of comedo-type necrosis (p=0.0003), ER negativity (p=0.009), HER2 positivity (p=0.0003) and presence of at least one deleterious/missense *TP53* variant (p<0.0001); **(Figure 5-10).** Additionally, a higher NTAI was associated with high grade DCIS (p=0.008), presence of comedo-type necrosis (p=0.006), HER2 positivity (p=0.03), and with presence of deleterious/missense *TP53* variants (p=0.002). The median FGA in pure DCIS with dense TIL was 26% compared to 12% in cases with sparse TILs, however the difference was not statistically significant (p=0.08, **Figure 5-11**). Similar results were observed with stromal CD3 whereas median FGA in pure DCIS with dense CD3+ cells was 26% compared to 10% in cases with sparse CD3+ cells (p=0.07, **Figure 5-11**). No association between NTAI and TILs density nor immune cell/checkpoint proteins was observed. However, tumours carrying somatic deleterious/missense *TP53* variants showed higher counts of stromal CD3+ (p=0.031), CD4+ (p=0.04), and FOXP3+ (p=0.02); (**Figure 5-11**).

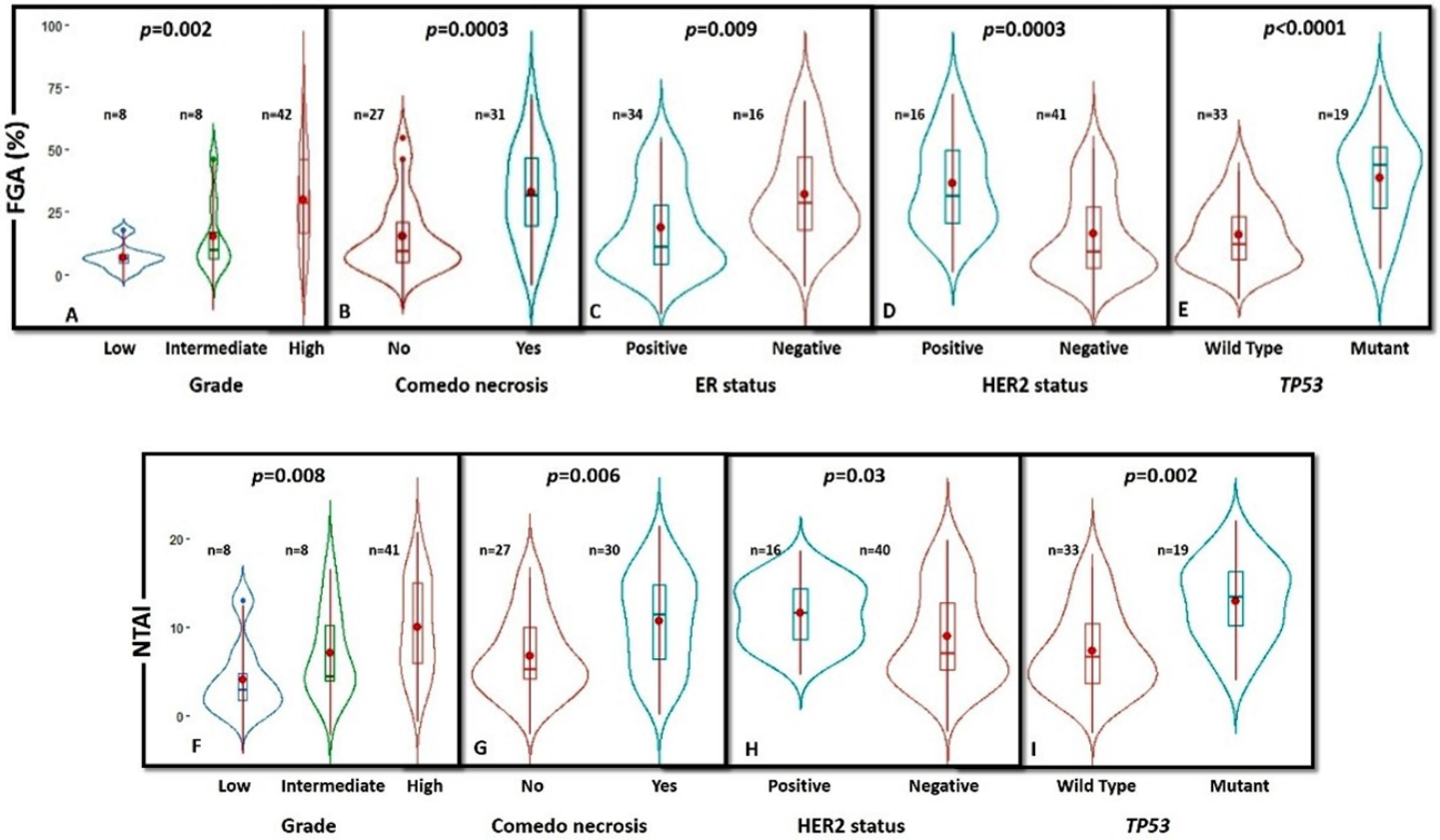

Figure 5-10: Violin plots showing the association between various clinicopathological parameters, *TP53* mutation with the fraction of genomic altered and with number of telomeric allelic imbalances

The central red dots represent the mean, boxes represent the interquartile range, central line represent the median and whiskers shows the 95% confidence interval

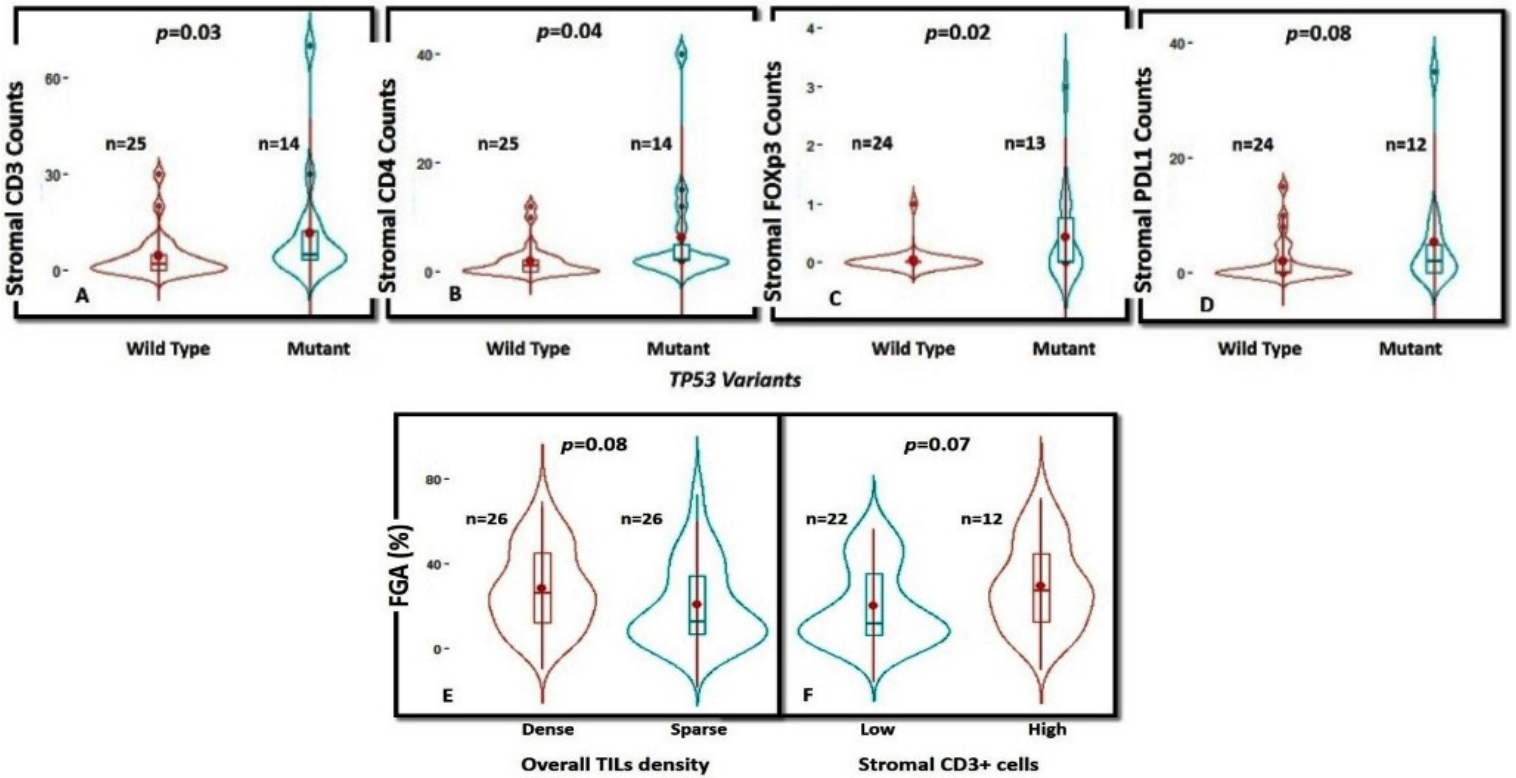

Figure 5-11: Violin plots showing the association between *TP53* variants TILS

(A) stromal CD3+ cells, (B) stromal CD4+ cells, (C) stromal FOXP3+ cells and (D) stromal PDL1+ TILs. The lower figures show the association between fraction of genome altered and (E) overall TILs density and (F) stromal CD3+ cells. The central red dots represent the mean, boxes represent the interquartile range, central line represent the median and whiskers shows the 95% confidence interval

5.5.8 Outcome analysis

High expression of stromal FOXP3+ and stromal PDL1+ were the sole markers associated with all recurrences in DCIS patients treated with BCS (*HR*=2.1, *95%CI*=1.1-3.7, *p*=0.025 and *HR*=4.4, *95%CI*=2.4-8.1, *p*<0.0001, respectively); **Figure 5-12**A and B. When analysis was restricted to invasive recurrences, only stromal PDL1 was associated with shorter LRFI (*HR*=2.4, *95%CI*=1.1-5.3, *p*=0.032), **Figure 5-12**C. No significant associations with recurrence were observed for the intratumoural infiltration of any immune cell marker with recurrence (**Table 5-13**). Outcome analysis in context of various intrinsic molecular subtypes revealed that high expression of stromal FOXP3 was associated with shorter LRFI in luminal A subtype (*HR*=2.9, *95%CI*=1.1-8.1, *p*=0.032) while higher PDL1 expression in stromal TILs was associated with shorter LRFI in luminal A (*HR*=7.1, *95%CI*=2.9-12.2, *p*<0.0001) and showing a trend of poor prognosis in luminal B (*HR*=3.2, *95%CI*=0.9-8.9, *p*=0.067) and HER2 enriched (*HR*=1.8, *95%CI*=0.5-7.5, *p*=0.080) subtypes. Other markers did not show association with outcome in different molecular classes.

In multivariate survival analysis, higher expression of stromal PDL1 was associated with shorter LRFI for all DCIS recurrences independent of other parameters of DCIS aggressiveness

including age at diagnosis, DCIS size, nuclear grade, presence of comedo-type necrosis and margin status (*HR*= 2.9, *95% CI*=1.4-6.1, *p*= 0.005). Interestingly, dense TILs was independently associated with DCIS recurrence either when included in a model comprising FOXP3+ and PDL1+ cells, or in a model where all immune cell markers associated with DCIS recurrence were incorporated with other DCIS clinicopathological parameters. A statistically significant result was obtained for all recurrences or when the analysis was confined to invasive recurrence only. **Table 5-14** summarises the various multivariate models analysed.

Moreover, high TILs density and higher stromal PDL1 expression could categorise high risk DCIS defined as high grade DCIS and >15mm in size into two distinct group with different outcome; whereas high TILs and stromal PDL1+ cells were associated with shorter LRFI in these patients (*HR*=3.2, *95%CI*=1.1-9.5, *p*=0.039, and *HR*=2.5, *95%CI*=1.1-6.3, *p*=0.044, respectively) (**Figure 5-13**)

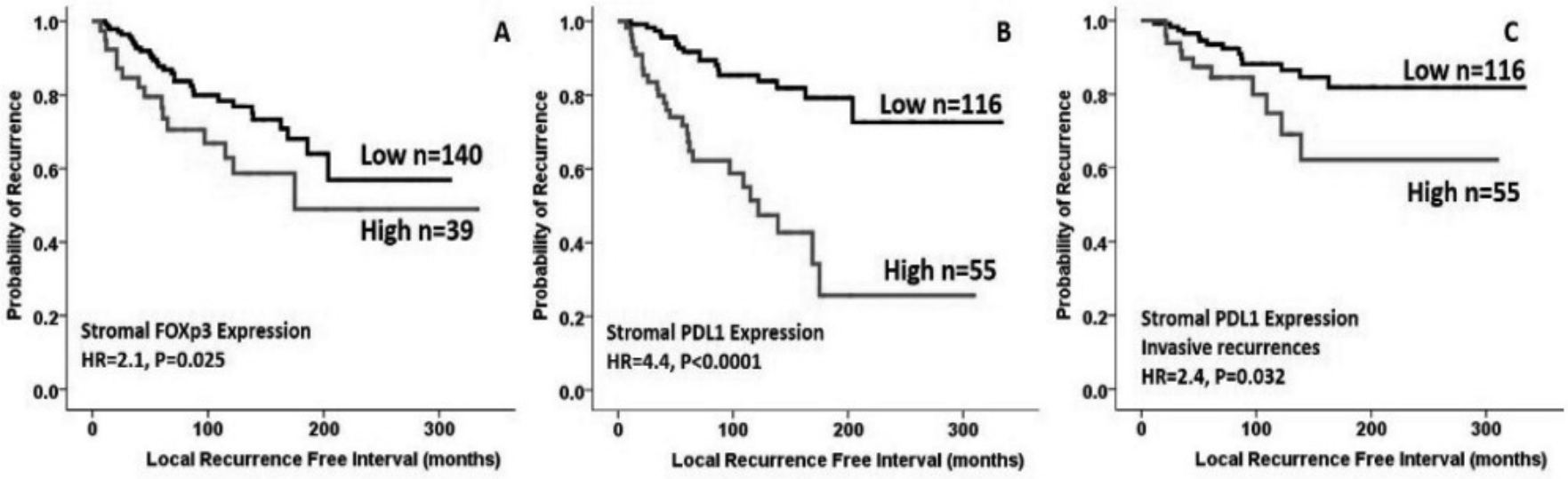

Figure 5-12: Kaplan Meier Curves showing the association between TILs and LRFI

Higher stromal FOXP3+ cells was associated with poor outcome for all DCIS recurrences (A), Dense stromal PDL1 expression was associated with shorter local recurrence free interval (LRFI) either for all recurrences (B), or invasive recurrences (C). All analyses were carried out on patients treated with breast conserving surgery alone

Table 5-13: Univariate survival analysis between overall TILs and various immune cell markers with the local recurrence free interval in DCIS patients treated with breast conserving surgery

Marker	All recurrences				Invasive recurrences			
	Hazard ratio	95% Confidence interval		p-value	Hazard ratio	95% Confidence interval		p-value
		Lower	Upper			Lower	Upper	
Overall TILs	2.9	1.7	5.0	**0.0001**	2.1	1.1	4.3	**0.040**
sCD20	0.9	0.5	1.7	0.793	0.9	0.4	1.9	0.770
sCD3	1.1	0.6	1.9	0.877	0.8	0.4	1.7	0.563
sCD8	0.9	0.5	1.8	0.992	0.5	0.2	1.2	0.109
sCD4	1.5	0.9	2.8	0.150	1.2	0.5	2.5	0.708
sFOXP3	2.1	1.1	3.7	**0.025**	1.1	0.4	2.6	0.895
sPD1	1.3	0.7	2.3	0.412	0.7	0.3	1.6	0.347
sPDL-1	4.4	2.4	8.1	**<0.0001**	2.4	1.1	5.3	**0.032**
iCD20	1.2	0.7	2.2	0.520	1.1	0.5	2.3	0.937
iCD3	1.2	0.7	2.2	0.522	0.9	0.5	2.1	0.979
iCD8	1.1	0.6	1.9	0.839	0.7	0.3	1.7	0.529
iCD4	1.2	0.7	2.1	0.572	1.1	0.5	2.2	0.985
iFOXP3	1.6	0.8	3.3	0.180	0.7	0.2	2.5	0.617
iPD1	0.9	0.4	2.1	0.766	0.7	0.2	2.5	0.652

s: Stromal, i: Intratumoral, Significant p values are in **bold**

Table 5-14: Multivariate survival analysis of variables (with and without immune cell markers) predicting outcome

Ipsilateral local all recurrences (A) and invasive recurrences (B) in patients treated by breast conserving surgery

A) All recurrences

Conventional clinicopathological parameters associated with high risk DCIS				
Parameters	Hazard ratio (HR)	95% confidence interval (CI)		p-value
		Lower	Upper	
Patient Age	0.4	0.2	0.8	**0.006**
DCIS presentation*	1.5	0.9	2.4	0.111
DCIS size	1.5	1.1	2.1	**0.040**
DCIS nuclear Grade	1.9	1.3	2.7	**0.001**
Comedo necrosis	0.6	0.4	0.9	**0.049**
Margin status	0.8	0.7	0.9	**0.004**
TILs density and other clinicopathological parameters				
Patient Age	0.4	0.1	0.8	**0.023**
DCIS presentation	1.5	0.9	3.8	0.395
DCIS size	0.8	0.4	1.6	0.498
DCIS nuclear Grade	1.2	0.6	2.4	0.662
Comedo necrosis	0.6	0.3	1.3	0.196
Margin status	0.9	0.9	1.1	0.637
Overall TILs density	7.0	2.8	1.2	**0.024**
Dense stromal FOXP3+ cells	1.7	0.7	0.3	0.453
Dense stromal PDL1+ cells	6.8	3.1	1.4	**0.004**
Overall TILs density with stromal FOXP3+ and stromal PDL1+ inflammatory cells				
Overall TILs density	3.5	1.5	8.2	**0.003**
Dense stromal FOXP3+ cells	0.8	0.4	1.7	0.554
Dense stromal PDL1+ cells	2.9	1.4	6.1	**0.005**

B) Invasive recurrence

Conventional clinicopathological parameters associated with high risk DCIS				
Parameters	Hazard ratio (HR)	95% confidence interval (CI)		p-value
		Lower	Upper	
Patient Age	0.5	0.2	1.3	0.156
DCIS presentation	1.4	0.8	2.6	0.245
DCIS size	1.8	1.1	2.4	**0.013**
DCIS nuclear Grade	1.9	1.1	3.0	**0.013**
Comedo necrosis	0.7	0.4	1.3	0.274
Margin status	0.9	0.8	1.1	0.075
TILs density and other clinicopathological parameters				
Patient Age	0.7	0.2	2.4	0.527
DCIS presentation	2.2	0.6	7.5	0.206
DCIS size	1.7	0.6	4.7	0.301
DCIS nuclear Grade	2.6	0.8	8.2	0.111
Comedo necrosis	0.7	0.2	2.0	0.497
Margin status	0.9	0.9	1.1	0.877
Overall TILs density	2.1	1.2	5.5	**0.029**
Dense stromal FOXP3+ cells	0.3	0.1	1.4	0.143
Dense stromal PDL1+ cells	1.7	0.6	5.1	0.307
Overall TILs density with stromal FOXP3+ and stromal PDL1+ inflammatory cells				
Overall TILs density	2.8	1.1	7.9	**0.045**
Dense stromal FOXP3+ cells	0.4	0.1	1.5	0.176
Dense stromal PDL1+ cells	1.7	0.6	4.8	0.318

Significant p values are in **bold**
* DCIS presentation refers to the method of DCIS diagnosis either through the mammography screening programme or symptomatic presentation.

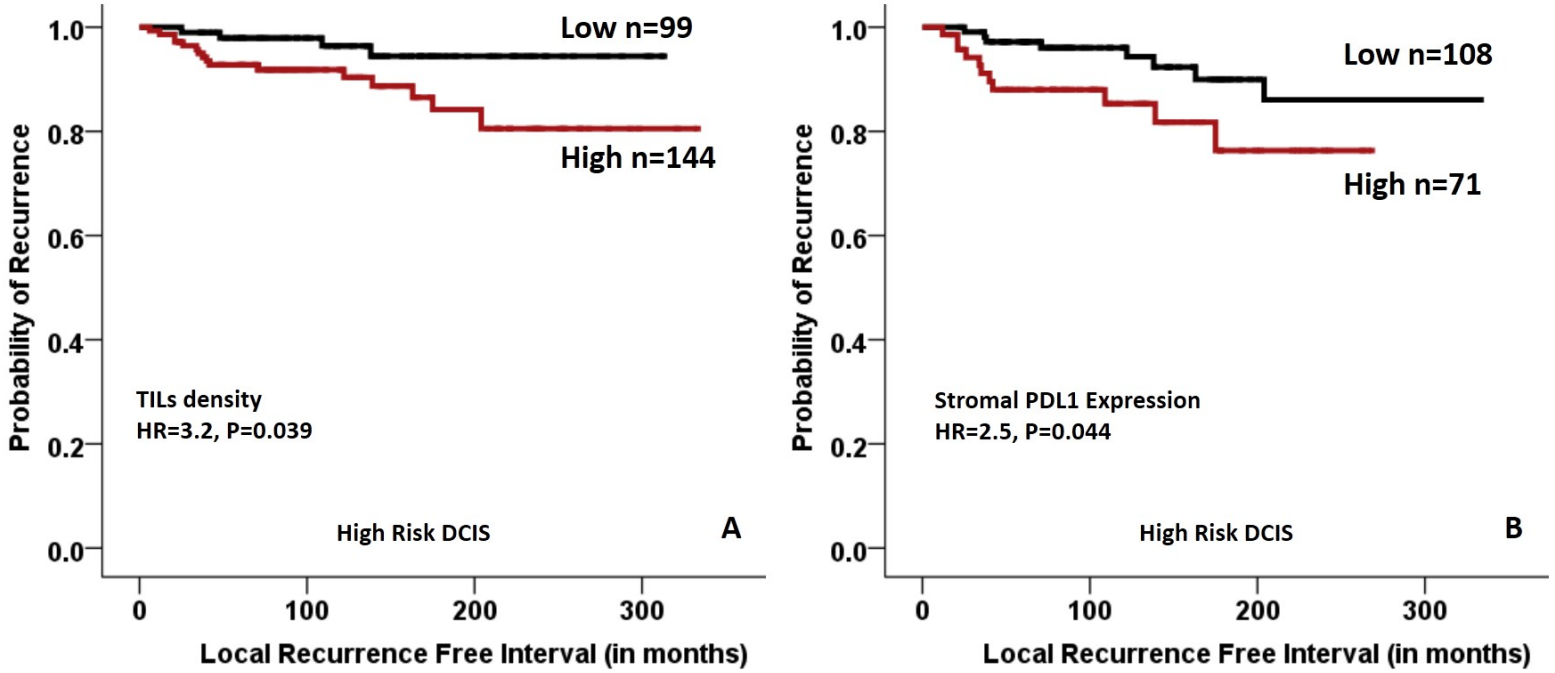

Figure 5-13: Kaplan Meier curves showing the association between TILs and PDL1 and local recurrence free interval

A) Higher TILs density is associated with shorter local recurrence free interval in high risk DCIS defined as high grade DCIS with size>1.5cm. B) High stromal PDL1 expression is associated with shorter local recurrence free interval (LRFI) in high risk DCIS

5.6 **Discussion**

Currently, clinicopathological parameters used for DCIS risk stratification such as age, nuclear grade, tumour size and associated comedo necrosis are still insufficient to accurately estimate recurrence risk associated with DCIS [7, 423]. TILs in DCIS are thought to have a role in tumour behaviour and progression; however, there are currently no consensus guidelines to evaluate TILs in clinical practice even after publishing the guidelines of TILs assessment [399, 400]. The lack of consensus about TILs assessment in DCIS was reflected in the new edition of the WHO classification of breast tumours which include methods of TILs assessment in IBC, but bot DCIS [53]. Previous studies of TILs evaluation in DCIS neither used clear or uniform definition of the stromal area surrounding DCIS for TILs assessment nor identified cut-off points that can prognostically stratify DCIS. Some studies used the International Working TILs Group guidelines [133] with modification to DCIS and assessed percentage of stromal TILs at the stroma within the boundaries of the whole lesion [178, 410]. Pruneri *et.al* [398] defined stromal TILs surrounding DCIS as those located at the area within two high power microscopic fields form the DCIS ducts and this method was adopted by other authors [239, 399, 400]. These studies

have reported lack of association between TILs density and DCIS recurrence. In the current study, TILs were assessed in a large cohort of DCIS with long-term follow-up data using various scoring methods to determine the most reproducible method that can additionally provide prognostic value. Prognostic stratification system has also been proposed to facilitate TILs application in DCIS in routine practice.

Assessment of TILs in the training set revealed that touching TILs is the optimal method for TILs scoring in DCIS. This conclusion was based on several criteria. Firstly, touching TILs had the highest concordance rate between the observers with or without prior methodology discussion. Secondly, they were positively correlated with TILs in the other topographic areas, hence representing TILs density within the whole lesion without requirement to assess TILs in wider areas around ducts which is time consuming. Thirdly, touching TILs assessment was the easiest and fastest method which can be performed without the need for accurate measurement of distance around ducts or adjustment of the scale and area's dimensions. Moreover, assessment of touching TILs avoids confusion/variability in scoring cells within overlapping areas between adjacent ducts. Lastly, touching TILs showed the strongest significant association with other prognostic clinicopathological parameters and DCIS outcome.

In this study, touching TILs showed significant association with LRFI in both training and validation cohorts as well as when the analysis was conducted using different observers' scores. Notably, dense touching TILs were associated with shorter LRFI when the analysis was performed either in the whole cohort or when confined only to patients treated with BCS. Importantly, touching TILs was an independent prognostic factor for DCIS recurrence in patients treated with BCS regardless of other known determinants of tumour behaviour [424-427].

Interestingly, the percentage of overall stromal TILs assessed using the same methods for TILs evaluation described in the previous studies [48, 139, 178, 262] and recommended by the International TILs Working Group [399] showed not only the least concordance rates but also variability in association with the outcome. Unlike stromal TILs evaluation in IBC, the low inter-observer and intra-observers' agreement may reflect the subjectivity of assessment of stromal TILs in DCIS, even with the use of predefined criteria of stromal area surrounding DCIS. Assessment of touching TILs provided an objective method for evaluation and could reflect the underlying interaction between TILs and DCIS progression as immune cells which are in direct contact with the BM might play the key role in its degradation and tumour cell invasion in contrast

to stromal TILs as not all stromal TILs are directly in contact with malignant ducts.

Studies of TILs in IBC reported associations between TILs and better prognosis especially in TNBC and supported their synergistic effect with chemotherapy [396, 397]. By contrast, the current study demonstrates that dense TILs in DCIS are associated not only with other potential risk factors for aggressive DCIS behaviour but also with increased risk of tumour recurrence and progression. Supporting our results, Pruneri *et al*. reported that dense TILs are correlated with more aggressive DCIS [398]. Hendry *et al*. have also reported dense TILs are associated with high grade, comedo type, ER negative and HER2 positive DCIS lesions [239]. Although both studies failed to find a significant association between TILs density and tumour outcome, this might be due to different assessment methodology. A recent molecular study showed that dense TILs were associated with aggressive DCIS. CNV in DCIS with dense TILs was shown to be more profound than lesions with low TILs density which might indicate the higher immunoediting capability of DCIS with dense TILs making them more likely to progress and recur [239]. In addition, dense TILs were associated with high DCIS Oncotype DX score [77], providing evidence to support our results that dense TILs are associated with poor outcomes in DCIS. Association

between dense TILs infiltrate and poor prognosis has also been reported in oral, colonic, prostatic and pancreatic preinvasive neoplasia [428, 429].

Interestingly, dense TILs were associated with shorter LRFI irrespective of ER expression in DCIS. This might indicate that the crosstalk between the immune microenvironment and tumour cells contributing to DCIS recurrence and/or progression is unrelated to ER pathway. Comparing TILs density in DCIS associated with IBC with pure DCIS indicates more TILs density in the former. This finding supports the hypothesised role of inflammatory cells in DCIS progression and aggressiveness [178, 215, 401, 430]. TILs density assessment and reporting in the routine practice for DCIS diagnosed by core biopsy may provide a predictive factor for presence of invasion in these lesions as previously observed [431, 432].

Through this study, it was aimed to characterise TIL subtypes and their potential prognostic role in DCIS. The dominance of CD3+ cells, including CD4+ and CD8+ subsets, indicates the immunologically active state of these early tumours, which could suggest an active chemokine secretion recruitment mechanism [433]. Apart from cell-mediated immunity, an active humoral immune response is also indicated with the

high expression of CD20+ cells. This result suggests that maturation of B lymphocytes may occur at an early stage of tumour development [434]. In comparison to pure DCIS, DCIS with synchronous IBC had notably increased levels of CD8+, CD20+, FOXP3+, PD1+ and PDL1+ cells. Since FOXP3 is the single most accurate marker of regulatory T cells (Tregs) [435], the high expression of FOXP3+ cells in a proportion of DCIS in addition to high expression of PDL1 suggests an immunosuppressive environment being created simultaneously in early tumour development, in concordance with previous studies [436-438]. A recent review by Chen *et al* summarised findings from previous work that support our study findings, such as high grade DCIS harbouring more TILs than low grade lesions and being associated with underlying genetic alterations [439].

It was observed that a significantly decreased recurrence-free survival in patients with a higher stromal infiltration of FOXP3. This suppressive environment appears to be particularly important for differentiating outcome in luminal A tumours, in which both FOXP3+ and PDL1+ were associated with poor outcome. FOXP3 was also described as an independent negative prognostic marker in IBC [440]. Higher infiltration of FOXP3+ cells also predicts poor overall survival in ovarian carcinoma where release of the chemokine CCL22 in the TME

by tumour associated macrophages facilitates the recruitment of FOXP3+ Tregs and hence, the suppression of cytotoxic T cells [441]. Another mechanism by which FOXP3 aids in tumour recurrence could be by binding to the upstream region of transcription start site of chemokines such as CCR7 and CXCR4.

The crucial role of the PD1/PDL1 pathway in the attenuation of T cell mediated immunity is well established [442]. We observed that high expression of stromal PDL1, but not PD1, was associated with a shorter recurrence free interval. High expression of PDL1 is associated with a poorer outcome in pancreatic cancer, renal cell carcinoma and BC [443-445]. Similarly, high expression of PD1 is associated with poorer outcome in renal cell carcinoma and BC [446, 447]. This association can be explained by the attenuation of the cytotoxic function of T lymphocytes in the presence of active PD1/PDL1 interactions thus aiding the tumour in its escape mechanisms [448, 449]. Another mechanism that might be at play is the upregulation of the PI3K pathway due to loss of *PTEN* or mutation of *PIK3CA* which ultimately leads to upregulation of PDL1 [450]. However, no association of *PIK3CA* mutations with PDL1 positivity was seen.

Despite the associations of an immunosuppressive microenvironment in DCIS with recurrence, in our multivariate analysis, overall TIL density was the strongest independent predictor for invasive recurrence. Since no significant associations of dense intratumoural infiltration of any immune cell with recurrence were observed, assessment of stromal infiltration of different subtypes of TILs was considered a better method of TILs evaluation for outcome analysis in DCIS [411]. It is similarly recommended to assess stromal TILs in IBC, but in IBC TILs are strongly associated with better outcome, particularly in TNBC [421]. The contradictory association of TILs as a good prognostic marker in IBC and as a poor prognostic marker in DCIS could support a hypothesis that direct contact between invasive tumour cells and immune cells leads to destruction of tumour cells and hence better prognosis, while in DCIS, a dense inflammatory reaction could provide a way for destruction of the surrounding myoepithelial layer [451] and BM. This facilitation of tumour cell infiltration to the surrounding stroma [401] would be enhanced by the immunosuppressive proteins produced by the tumour cells to escape destruction by host immunity and guarantee maintenance of the invasive tumour cells [438].

An alternative, and not necessarily exclusive, explanation could be that a heightened immune response in DCIS and its

association with poor prognosis reflects an underlying aggressive breast tumour biology. The findings regarding the significant association of the stromal immune markers with higher grade, HER2 positivity and hormone receptor negativity has been reported previously in DCIS [178] and IBC [421]. The ability to recruit more inflammatory cells through production of neoantigens and chemokines, as well as their ability to modulate the immunosuppressive microenvironment to evade the host immune response, combine to develop the immune resistance shown by these tumours and lead to still further aggressive behaviour [452]. ER negative DCIS are more proliferative and genomically unstable, hence stimulate a stronger attack from the immune cells. The association of dense infiltration in HER2+ tumours and TNBC can be best interpreted as a pro-tumourigenic function of TILs especially due to higher infiltration of Tregs [178, 453]. The findings regarding the association of PD1 and PDL1 in TILs with higher tumour grade, were supported by the findings of Muenst *et al.* [447]. This association with higher grade emphasises the role of PD1/PDL1 pathway adopted by DCIS to evade anti-tumour immunity and spread aggressively. Higher expression of PDL1 in TNBC has also been reported in other studies [184, 450]. The association of more proliferative tumours such as HER2 enriched, TNBC and basal-like tumours, with high expression

of PDL1 could be due to the increased immunogenicity of these tumours and increased presence of neoantigens.

All solid tumours elicit an inflammatory response that is critical for the recruitment of immune cells, tumour cell proliferation, survival, and angiogenesis. Tumours initiate these responses through several mechanisms including hypoxia and derived factors [454]. Hypoxia was reported to shape the immunosuppressive microenvironment of the tumour [455]. The positive correlation between HIF-1α and FOXP3 in this study supports such a hypothesis and shows the crosstalk between TME components in DCIS progression. This finding is supported other studies that showed tight interaction between hypoxia and the tumour inflammatory process [454, 456].

DCIS harbouring dense inflammatory cells was reported to have more copy number alteration [398] and higher Oncotype DX score [77] than those with low TILs density, which reflect the underlying biological association between TILs density and DCIS behaviour. As expected, in this study, high risk DCIS (high grade, comedo type necrosis, hormonal receptor negativity and HER2 positivity) showed a higher degree of genomic instability represented by an increased burden chromosomal gains and losses and the presence of deleterious/missense *TP53* mutations [457]. In general,

genomic instability leading to high risk DCIS lesions might promote T cell activation (CD3 and CD4) and recruitment of regulatory T cells (FOXP3) as suggested by our data. These findings are supported by Hendry *et al*, who concluded that tumour immune-editing and evasion of the immune system could be a key step in progression from DCIS into IBC [398]. Our data lacked sufficient numbers of cases analysed for mutation and CNVs to evaluate the interaction of these events with the immune context in terms of patient outcome.

Our findings could refine high risk DCIS into two distinct groups based on TILs density and stromal PDL1 expression, where high risk cases with dense TILs or higher stromal PDL1+ cells behaved more aggressively and had higher recurrence rate than high risk DCIS with lower TILs or stromal PDL1+. This observation reflects the role of immune microenvironment in DCIS risk stratification and management guidance. Implementation of TILs evaluation in clinical practice could avoid further management, i.e. unnecessary postoperative RT in a subgroup of patients.

In conclusion, using touching TILs as an assessment method for TILs in H&E-stained full-face DCIS sections is a reproducible and practical method to predict tumour behaviour and progression. Application of this method in routine practice

would aid in risk-stratification of DCIS for improved, individualised management. Moreover, this study highlights that the subsets of TILs, immune checkpoint proteins and their distribution should be carefully analysed for patient risk assessment. Since patient risk stratification has been difficult due to conflicting evidence regarding TILs affecting DCIS prognosis, this study provides a more uniform inference with the higher infiltration of FOXP3+ and PDL1 immune cells being associated with poor outcome.

However, there are some limitations of this study. It was conducted on TMA sections which may underestimate TILs infiltration although the distribution between TMA cores and full-face sections showed comparability. In addition, due to the small number of recurrence events in patients treated with RT or when the cohort was split by molecular class or risk groups (high vs. low risk DCIS), further studies of TILs in context of these limitations are recommended. Also, the role of ET is overlooked here as none of the study patients received such therapy. Data from genomic assessment was only available for a small subset of tumours limiting statistical power and the capability to conduct sub-group analysis (e.g. stratification by receptor status or grade), which might have weakened associations between TIL subtypes and genetic features.

6 Chapter 6: The role of extracellular matrix remodelling proteins in DCIS behaviour

6.1 **Introduction**

It is estimated that approximately half of all IBCs are associated with DCIS [90, 458], and it seems that in majority of these cases, the invasive component arises from the preceding DCIS, based on shared genetic changes and copy number profiles [54, 74, 87, 89, 222, 459-461]. It has been further reported that multiple genomic changes shared by ADH, DCIS and IDC exist, strengthening the argument for the linear progression model [460].

However, the linear model hypothesis has been argued against as only 20% to 50% of untreated DCIS later progress to invasive carcinoma [292, 462, 463]. This leads to the need to ask the question of when and whether DCIS will become invasive carcinoma. The percentage of IBC associated with DCIS also varies by the molecular subtype, with HER2-positive and luminal IDC more frequently associated with DCIS than basal-like BC [464]; however, neither molecular subtype nor histopathological features are consistent or reproducible predictors of DCIS behaviour [90]. Two schools of thought have thus arisen on the progression of DCIS to IDC, that is, DCIS becomes invasive as a result of intrinsic factors, namely genetic aberrations of the neoplastic cells or alternatively that extrinsic factors within the surrounding TME drive DCIS

progression, independent of or in conjunction with genetic changes within neoplastic cells [167].

6.2 Tumour cell intrinsic factors involved in DCIS progression

Logically, profound changes in cellular behaviour required for DCIS to overcome the barriers of the myoepithelium and BM necessitate *de novo* acquisition of equally profound genetic aberrations [54]. Accordingly, some research has been focused on understanding the genetic differences between *in situ* and invasive phenotypes, with the aim of defining predictive biomarkers and identifying novel therapeutic targets. More recently, studies of the different compartments of DCIS and IBC have shed further light on the process of malignant progression and highlighted avenues for future research [90]. So far, only a broad concept of IBC precursors has been established, and much remains unclear regarding the significance of the genomics of different cell types in tumour and stromal compartments in this process [465].

6.2.1 Molecular features of DCIS and its progression

Both DCIS and IBC are relatively similar on the genomic level [89, 466]. While some controversy remains around the definite interpretation of these studies, they suggest that the molecular

abnormalities required for the progression to an invasive phenotype likely exist at the premalignant stage [467].

In contrast to that theory, other studies suggest that such abnormalities required for progression occur at any stage particularly from *in situ* to invasive stage [76, 468]. According to this theory, distinct subclones with specific genetic changes are selected during the transition from DCIS to invasive disease. This leads to differences in the prevalence of specific mutations between neoplastic DCIS cells and their invasive counterparts [167, 469, 470].

Despite the absence of strong evidence supporting the mutation acquisition model of DCIS progression, there are some data that suggest a role of epigenetic changes such as DNA hypermethylation [471]. Aberrant hypermethylation of tumour suppressor genes occurs in both pure DCIS and the *in-situ* component of DCIS to IBC, triggering carcinogenesis and perhaps also progression of pure DCIS. Downregulation of expression of epithelial cell-related genes also suggests that hypermethylation of gene promoters may play a role in this step of DCIS progression [472]. In conclusion, these studies provide evidence of a general shared genetic susceptibility between DCIS and IBC, overlain with a degree of alteration to

DNA methylation patterns that might contribute to driving changes in gene expression that promote progression [458].

6.3 **Extrinsic factors and DCIS progression**

Recent studies have investigated tumour cell extrinsic factors in the local TME that might contribute to the invasive potential of DCIS that circumscribed by a dynamic layer of myoepithelium, exists within the context of a multicomponent stroma, accompanied by infiltrating immune cells (**Figure 6-1**).

Studies have recently revealed alterations to the biochemical and physical properties of the tumour associated ECM that promotes tumour progression and therapy resistance. These changes distort the normal ECM architecture which can adversely impact the functions of other stromal cell populations to favour tumour development [473]. Further studies on the earlier stages of BC initiation have revealed the importance of stromal factors in tumour emergence. Based on radiological findings, high-density breast stroma has been proposed to be one of the strongest risk factors for IBC, second only to germ line *BRCA* mutations [474, 475].

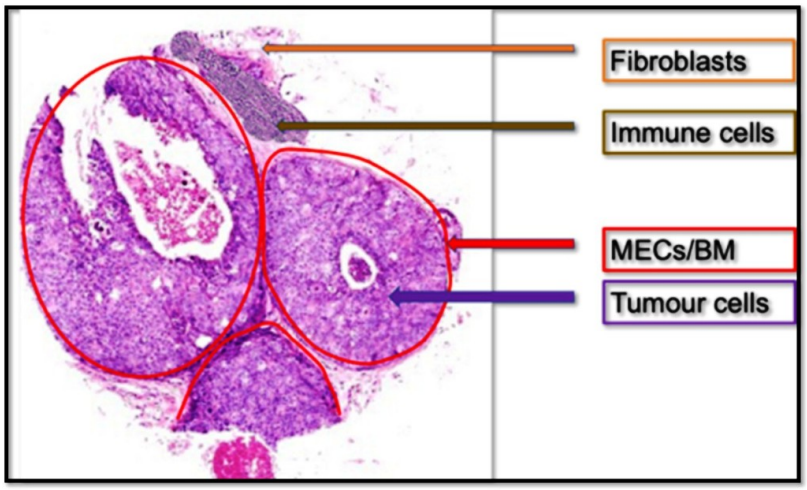

Figure 6-1: Factors contributing to the progression of DCIS to invasive cancer

The diagram illustration of DCIS shows the different factors that are involved in the progression to invasive breast carcinoma, including genetics of tumour cells, myoepithelial cells, BM, immune cells, fibroblasts and stroma

6.4 **Identification of progression drivers**

Although research has identified some genomic and transcriptomic changes within abnormal epithelial cells of DCIS together with altered microenvironment, none of these alterations have proven to be reliable indicators of *in situ* recurrence or invasive progression [476].

Although the role of the DCIS microenvironment and the crosstalk between intraductal malignant epithelial cells and the various components of the TME in the progression of DCIS to invasive disease is undeniable [178, 189, 230, 477, 478]. However, previous studies have indicated that the precise role of proteolytic enzymes in the ECM, such as MMPs, in predicting risk of development of local recurrence is unreliable and trials

for blocking these enzymes to limit tumour progression showed disappointing results [217, 479].

The approach that was used to identify the study biomarkers is illustrated in **Figure 6-2**. Briefly, the online resources and relevant literatures were mined and reviewed to identify the potential markers that could affect DCIS progression. In view of the study hypothesis and aims, the criteria that were used for identifying these biomarkers were: 1) Biomarkers related to ECM degradation, EMT and or remodelling, 2) Markers that showed previous association with BC either DCIS or IBC, 3) Markers that were reported to be differentially expressed between normal breast tissue and DCIS or DCIS and IBC either between epithelial cells or surrounding stromal tissue. The provisionally identified list contained more than 100 biomarkers with such criteria and potential candidate for the study. For further shortlisting and proper choosing of promising biomarkers, and in view of lacking robust transcriptomic available data for DCIS, the METABRIC data for IBC was used to rank the identified genes. It was hypothesised that biomarkers associated with lymph node metastasis and disease distant metastasis (DM) could be potentially associated with progression from DCIS to IBC through similar mechanisms. Taken together, the biomarkers were ranked and shortlisted based on their association with nodal stage and

then their association with DM free interval and overall survival. Further validation of the results was done using the publicly transcriptomic dataset "Breast Cancer Gene-Expression Miner v4.4 (bc-GenExMiner v4.4)" where the association between the biomarkers and DM was analysed. The top five biomarkers in the list were used in this thesis.

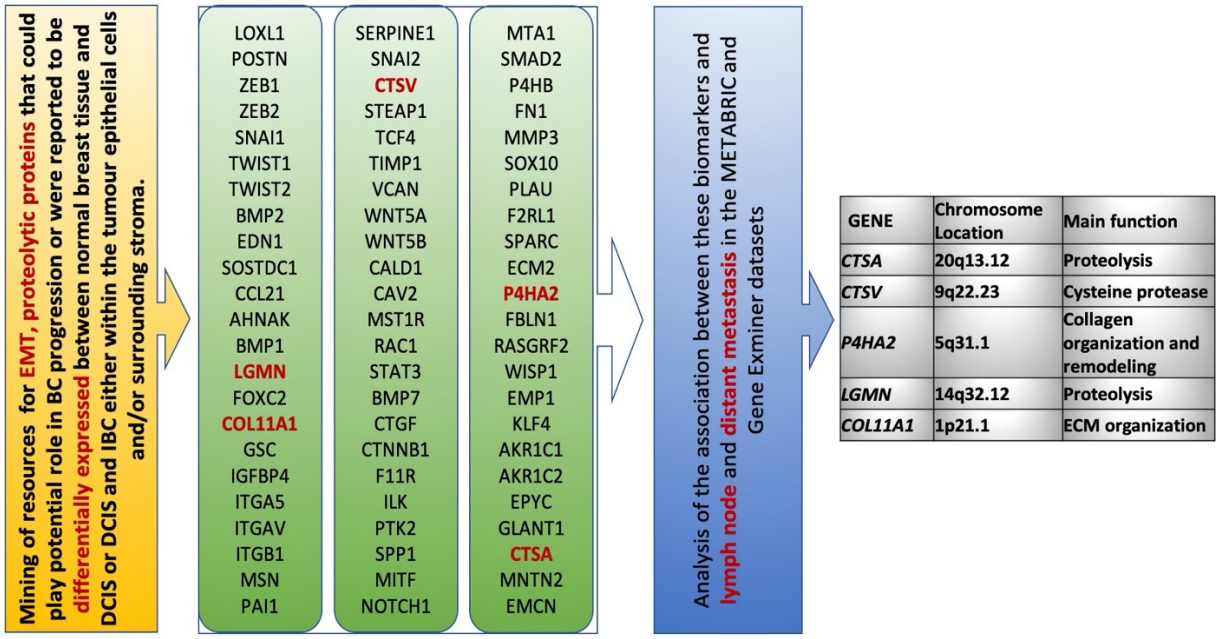

GENE	Chromosome Location	Main function
CTSA	20q13.12	Proteolysis
CTSV	9q22.23	Cysteine protease
P4HA2	5q31.1	Collagen organization and remodeling
LGMN	14q32.12	Proteolysis
COL11A1	1p21.1	ECM organization

Figure 6-2: Flowchart demonstrating the identification of the study biomarkers

Thus, we were interested in identifying novel proteins that play role in ECM remodelling and degradation and play role in DCIS progression. Among these proteins we studied: P4HA2, CTSA, CTSV, LGMN and COL11A1.

6.4.1 **Prolyl-4-Hydroxylase A Subunit 2**

Collagen is the main constituent of ECM and usually forms a network around tumour cells [196]. Collagen biosynthesis is a multistep process with several post-translational modifications. Prolyl-4-hydroxylases catalyse the formation of 4-hydroxyproline, which is essential for collagen triple helix formation and fibre stabilisation [480]. Increased P4HA2 expression has been detected in many solid tumours, including oral cavity squamous cell carcinoma [481], papillary thyroid cancer [482], and IBC [483]. P4HA2 is differentially expressed between normal breast tissue and IBC [484, 485]. However, to the best of our knowledge, no previous study has addressed the role of P4HA2 in DCIS progression and its prognostic impact.

6.4.2 **Lysosomal Protective Protein (Cathepsin A)**

Degradation and remodelling of the surrounding BM and stroma are fundamental steps in DCIS progression to invasive disease. The key role of MMPs in stromal degradation is undeniable, however, it is insufficient to explain DCIS progression to invasive disease depending solely on them. Blocking MMPs action did not show promising results in terms of prevention of disease progression [479].

Cathepsins are a family of lysosomal proteinases or endopeptidases that are highly expressed in numerous human cancers. Lysosomal protective protein/Cathepsin A (CTSA) is an acidic serine carboxypeptidase that has a proactive function towards β-D-galactosidase and N-acetyl-α-neuraminidase [486]. A deficiency in this multifunctional lysosomal protease can cause human lysosomal storage disease (galactosialidosis) [487]. CTSA is expressed in platelets [488], lymphocytes [489] and primary human antigen-presenting cells [490] and plays a role in primary and metastatic human melanocytic tumours [491]. Interestingly, *CTSA* is differentially expressed between IBC and DCIS at the mRNA level [189]. Moreover, while the role of different Cathepsins in BC has been studied before [492, 493], no previous study has addressed the role of CTSA in DCIS progression and its prognostic impact.

6.4.3 **Cathepsin V**

Cysteine proteinases (Cathepsins) are group of lysosomal proteolytic enzymes that play key roles in normal tissue homeostasis and participate in inflammatory and malignant conditions [494, 495]. Cathepsin V, known also as Cathepsin L2, (CTSV/CTSL2) is a cysteine proteinase secreted mainly by the thymus, cornea and testis [496, 497] and is associated with autoimmune diseases such as myasthenia gravis [498, 499] and type I diabetes mellitus [499]. CTSV is shown to be

overexpressed in some tumours including breast, colorectal, renal and ovarian carcinomas [216], and it was reported to be associated with poor prognosis in hepatocellular carcinoma [500]. However, studies about its prognostic significance in BC are lacking. *CTSV* is one of the genes included in the prognostic multigene assay (Oncotype DX) in IBC. The prognostic role of CTSV in DCIS has not been addressed yet. In context of the complexity of progression of DCIS into invasive disease that involves crosstalk between tumour epithelial cells and the surrounding microenvironment, we hypothesised that CTSV has a key role in DCIS aggressiveness.

6.4.4 **Legumain**

Identification of novel markers that play a role in DCIS invasiveness might help in better understanding of the disease biology and risk stratification.

LGMN is a cysteine endopeptidase belonging to the asparaginyl endopeptidase family encoded by the *LGMN* gene [246, 501]. LGMN activates zymogen gelatinase A by cleavage of pro-gelatinase A, which is an important mediator of ECM, thereby helping the tumour to invade and metastasise [502-504]. It also activates other proteases that are key in regulating angiogenesis, growth and other related functions in tumours [505]. LGMN is expressed at elevated levels in IBC [246, 506],

colorectal [507], prostate [508] and gastric carcinomas [501] and is related to poor prognosis [505]. Moreover, *LGMN* is differentially expressed between normal breast tissue and IBC [246], however the role of LGMN in DCIS has yet to be established. In this thesis, we aim to assess the pattern of LGMN expression and its prognostic significance in DCIS.

6.4.5 Collagen (XI) alpha-1 chain

ECM and its main constituent, collagen, plays a critical role in several biological processes in normal tissues. Collagen is aberrantly produced by CAFs, which reciprocally interact with tumour cells promoting the latter's proliferation, migration and differentiation and, therefore, aiding cancer development and progression [509].

Collagen11A1 (COL11A1) is a type of fibrillary collagen encoded by the *COL11A1* gene and is expressed mainly in cartilaginous tissue [510]. Its deficiency is associated with skeletal and chondroid disorders [511, 512]. It constitutes a minor component of the ECM and plays a role in its tensile strength. COL11A1 expression is associated with poor prognosis in non-small cell lung carcinoma and linked to its resistance to chemotherapy [513]. Moreover, COL11A1 promotes malignant cell proliferation and is associated with worse prognosis in many other types of cancer including

ovarian cancer, squamous cell carcinoma of the head and neck [514, 515], pancreatic [516], gastric [517], colorectal [518] carcinomas, and some sarcomas [519]. It is also associated with metastasis in IBC [520] and was previously described as a diagnostic marker to differentiate between invasive and non-IBC [521]. COL11A1 predicts invasive recurrence after primary diagnosis of breast intraductal papillomas [522], and is differentially expressed between IBC and DCIS [523]. However, the role of COL11A1 in DCIS and its prognostic significance has yet to be investigated.

6.5 **Hypothesis and aims**

It is hypothesised that a powerful way to discover key genes playing causal roles in progression from *in situ* to invasive carcinoma is to identify differentially expressed genes between them either in the tumour cells or the surrounding stroma. To confirm the effect of certain gene, detection of its protein expression is essential. Assessment of molecular markers can be used as surrogates of DCIS biology and behaviour and have the potential to predict patient outcome [70].

Therefore, it was hypothesised that some genes which play a role in ECM remodelling (P4HA2 and COL11A1), or degradation (CTSA, CTSV and LGMN) have a role in progression from DCIS

to invasive disease. This can be used as a tool to tailor treatment decisions of DCIS or have a therapeutic potential.

6.6 Patients and methods

6.6.1 Study cohort

This study was conducted on a consecutive series of primary pure DCIS cases and a series cases diagnosed as synchronous DCIS and invasive tumours (mixed DCIS and IBC) as a validation set, prepared as TMA (**Chapter 2**). In addition, a set of whole tissue sections from 10 randomly selected cases containing DCIS and invasive tumours were assessed to evaluate heterogeneity and the pattern of P4HA2, CTSA, CTSV, LGMN and COL11A1 expression in malignant breast lesions and adjacent stroma.

Demographic details, histopathological, management, RT and patient outcome data were collated as previously detailed in **Chapter 3**.

Additionally, data on different molecular classes, p53, Ki67 and HIF-1α was available for the cohort [524]. Ki67 high proliferation index was considered when more than or equal to 14% positively stained tumour cell nuclei were detected [525, 526]. Aberrant p53 staining was determined based on the percentage and the staining pattern in tumour cell nuclei, which has been shown to correlate with mutation of the gene

[245, 527]. HIF-1α was evaluated using IHC and was considered positive when >1% of tumour cells showed nuclear staining [528]. Tumours with an average number of 20 lymphocytes/duct or more was considered as dense tumour infiltrating lymphocytes in DCIS as described in **Chapter 5**. Validation of the studied antibodies was performed and highlighted in **Chapter 2**.

6.6.2 Analysis of biomarkers mRNA expression in breast cancer

To confirm the prognostic and clinical significance of the targets in IBC, and given the deficiency of data on the transcriptomic profiles of DCIS, normalised gene expression (mRNA) data were analysed using the Molecular Taxonomy of Breast Cancer International Consortium (METABRIC) dataset that comprises 1980 tumours with long term follow-up [529].

6.7 Results

6.7.1 Antibodies specificity

WB revealed that all the antibodies used in this study showed their specific band at the predicted molecular weight as listed by the supplying company (**Figure 6-3**).

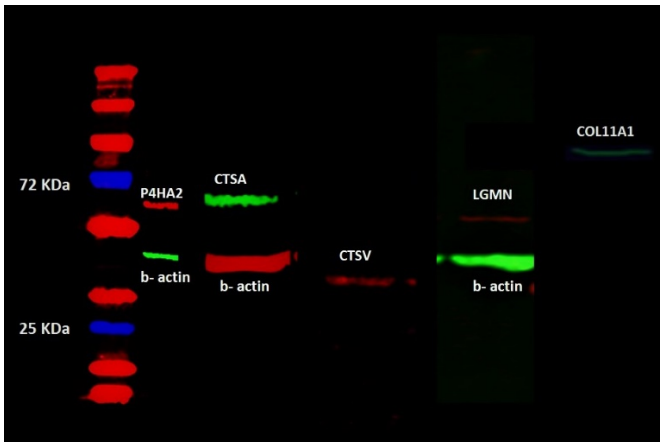

Figure 6-3: Western Blot of the antibodies used in the study

6.7.2 Biomarkers distribution and localisation

The evaluation of full-face tissue sections demonstrated a rather homogenous distribution of the expression of the studied biomarkers either within the tumour epithelial cells or the surrounding specialised stroma especially in cases with homogenous pattern and grade, indicating representability of TMAs to assess them. The final number of cores suitable for assessment various between markers after excluding of uninformative cores (they were randomly excluded due to loss of the cores during TMA construction or antigen retrieval, folded tissue during processing or cores containing <15% tumour cells).

6.7.2.1 P4HA2

Adjacent normal TDLUs showed negative or faint cytoplasmic staining of P4HA2. Occasional MECs and inflammatory cells in a few cores were also stained. When present, P4HA2 was

expressed in the cytoplasm of the epithelial tumour cells and surrounding fibroblasts.

The final number of cases suitable for scoring was 481 in pure DCIS and 196 in DCIS-mixed cohorts. The median H-score for P4HA2 expression was 40 in pure DCIS (range 0-250), 50 in the DCIS component of mixed cases (range 0-280), and 40 in IBC component of the latter (range 0-280). For stromal expression, the median percentage of positive stromal cells was 30% in pure DCIS (range 0-95), 55% in the DCIS component of mixed cases (range 0-95) and 80% in the invasive component of the latter (range 0-95). Within the pure DCIS cohort, high P4HA2 expression was observed in 247/481 (51%) and 121/481 (25%) in tumour epithelial and surrounding stromal cells; respectively. There was a positive linear correlation between expression of P4HA2 within the epithelial cells and surrounding fibroblasts (r=0.426, p<0.0001, Spearman's correlation).

The proportion of cases with high P4HA2 was greater in DCIS-mixed than pure DCIS, both within the tumour epithelial cells (54% of pure DCIS cases vs. 64% of DCIS mixed with IBC, χ2=8.6, p=0.003) and stromal cells (25% for pure DCIS vs. 50% of DCIS mixed with invasion, χ2=39.3, p<0.0001). Supporting this, similar observations results were observed

when the data had been analysed in a continuous scale (p=0.006 and p<0.0001, for tumour epithelial cells and stromal cells, respectively). Although there was no statistically significant difference between P4HA2 expression within the tumour epithelial cells of DCIS component and invasive component of DCIS-mixed cases (p=0.188), its expression within the stromal fibroblasts surrounding the invasive component was higher than those surrounding the DCIS component (p<0.0001). Different patterns of P4HA2 expression within the pure DCIS and DCIS-mixed cohorts are shown in **Figure 6-4**.

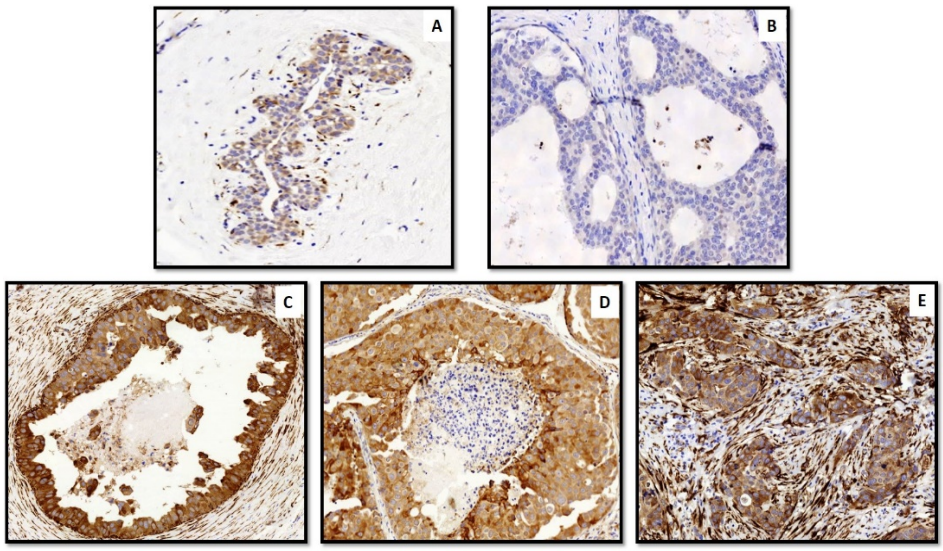

Figure 6-4: Patterns of P4HA2 expression

A) Normal breast duct (x20) shows faint cytoplasmic staining of P4HA2 in the normal epithelial cells. Occasional faint staining in the myoepithelial cells is also noticed, B) Negative P4HA2 expression (x40) in a pure DCIS case; C) strong expression of P4HA2 in tumour cells and surrounding fibroblasts (x20) in a pure DCIS case. D and E) Expression of P4HA2 in a mixed case (x40) showing almost the same intensity within the tumour cells of DCIS component (D) and invasive component (E) while expression within the surrounding stromal fibroblasts is higher in invasive component (E)

6.7.2.2 CTSA

Adjacent apparently normal TDLUs showed weak cytoplasmic staining. Occasional inflammatory cells and stromal fibroblasts were stained in a few cores in the pure DCIS cohort, while most cases in the mixed cohort showed stromal expression in addition to the expression within epithelial tumour cells. When present, CTSA was expressed in the cytoplasm of the epithelial tumour cells. In invasive cases, CTSA was expressed in epithelial tumour cells and surrounding fibroblasts (**Figure 6-5**).

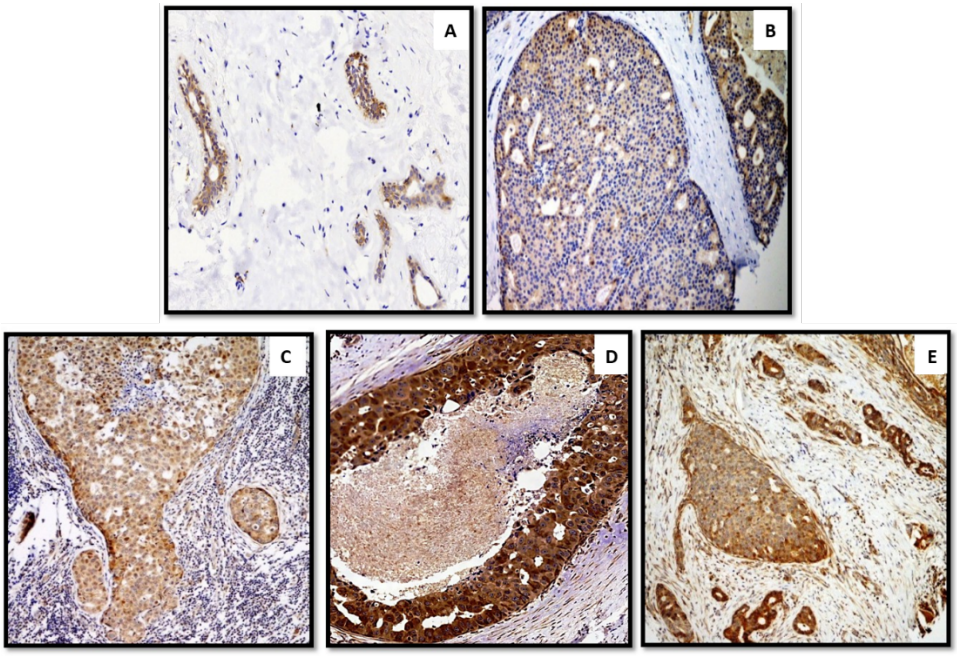

Figure 6-5: Patterns of CTSA expression

A) Normal breast duct (x20) shows weak cytoplasmic staining of CTSA in the normal epithelial cells. B) Weak CTSA expression (x40) in a pure low-grade DCIS case; C) stronger expression of CTSA in (x40) in a pure DCIS case. Note the dense inflammatory cells surrounding the DCIS. D) Strongest expression of CTSA (x40) in a pure high-grade DCIS case. E) Expression of CTSA in a mixed case (x20) showing higher intensity within the invasive tumour cells than the DCIS component. Stromal expression of CTSA is also noticed

After exclusion of uninformative cores, the final number of cases suitable for scoring was 527 and 204 cores in pure DCIS and DCIS-mixed cohorts, respectively. The median H-score was 75 in pure DCIS (range 0-250); which was similar to the cut-off point generated by X-tile, 90 in the DCIS component of mixed cases (range 0-200), and 110 in the IBC component of the latter (range 0-250). High CTSA expression was observed in 48% of pure DCIS.

The proportion of cases that showed high expression of CTSA was greater in DCIS-mixed than pure DCIS (48% of pure DCIS cases vs. 70% of DCIS with co-existence IBC, $\chi 2=3.0$, $p=0.04$). Similar results were observed when the score was analysed in a continuous scale ($p=0.0001$). Moreover, there was a statistically significant difference between CTSA expression within the tumour epithelial cells of the DCIS component and invasive component of the mixed cases ($Z=8.8$, $p<0.0001$).

6.7.2.3 CTSV

Adjacent apparently normal breast tissue did not show expression for CTSV. When expressed, CTSV was evident in the cytoplasm of the tumour epithelial cells and/or surrounding stromal fibroblasts (**Figure 6-6**).

After unbiased exclusion of the non-representative cores, 527 and 213 cases were suitable for assessment in the pure DCIS and DCIS-mixed cohorts, respectively. The median H-score for CTSV expression in tumour cells was 30 (range 0-140) in pure DCIS, 80 (range 0-180) in the DCIS component and 100 (range 20-180) in the invasive component of the DCIS-mixed group. The average percentage of positive fibroblasts surrounding the tumour was 20% in pure DCIS (range 0-100); and 20% (range 0-100) and 50% (range 0-100) in the DCIS and invasive components of the mixed cases, respectively. A total of 29% of pure DCIS had high tumour expression of CTSV (H-score >60) while high stromal expression (>65%) was detected in 20% of the pure DCIS cases.

The percentage of cases that showed overexpression of CTSV was higher in DCIS-mixed than pure DCIS either within the tumour epithelial cells (29% of pure DCIS cases vs. 71% of DCIS co-existing with IBC, $\chi 2=111.1$, $p<0.0001$) or surrounding stroma (20% in pure DCIS vs. 31% in DCIS-mixed cases, $\chi 2=10.8$, $p=0.001$). Comparable findings were gathered when the expression score was analysed using the continuous figures ($p<0.0001$ and 0.037 for tumour and stromal cell expression, respectively). Moreover, CTSV expression within the tumour cells and surrounding stroma of the invasive component was higher than the DCIS component

in the DCIS-mixed cases (Z=7.6, p<0.0001 and Z=5.9, p<0.0001), respectively (**Figure 6-7**).

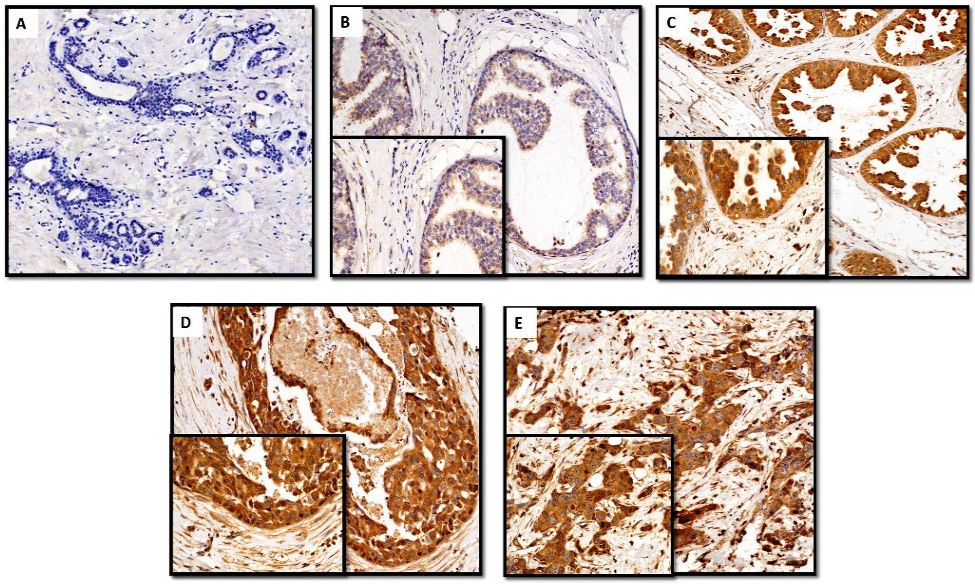

Figure 6-6: Patterns of CTSV expression

A) Normal breast duct (x20) shows negative staining of CTSV. B) Low tumour and stromal CTSV expression (x20) in a pure DCIS case; C) High expression of CTSV (x20) in the epithelial tumour cells and surrounding stroma of a pure DCIS case. D and E) Expression of CTSV in a mixed case showing lower expression of CTSV in the DCIS component (x20) (D), than the invasive component E) either within the tumour cells or the surrounding stroma (x20). All inset images are x40

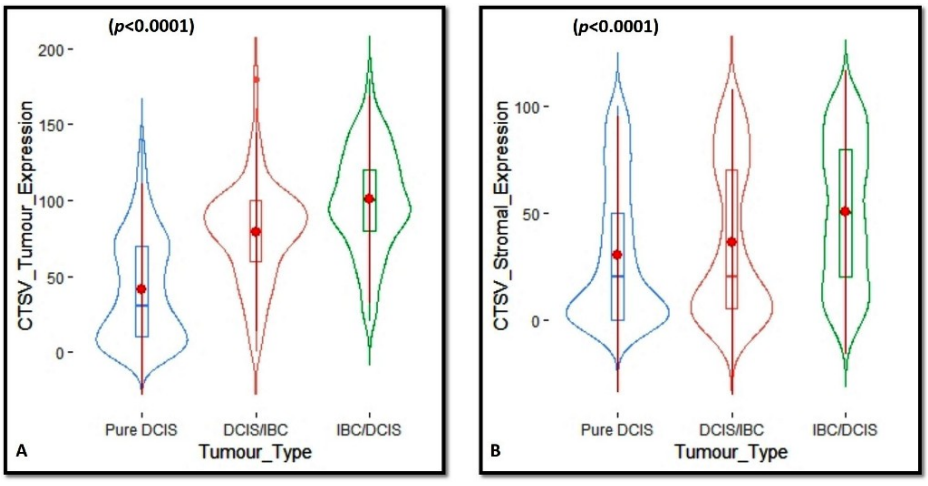

Figure 6-7: Violin plots show the difference between CTSV expression in pure DCIS, DCIS component in mixed cases and invasive component in mixed cases

Tumour epithelial cells (A) or surrounding stroma (B)

6.7.2.4 LGMN

Adjacent normal breast TDLUs showed negative or very faint cytoplasmic staining of LGMN. Occasional inflammatory and stromal cells were also stained in few cores. When present, LGMN was expressed in the cytoplasm of the epithelial tumour cells and surrounding fibroblasts (**Figure 6-8**).

The final number of cases suitable for scoring was 464 pure DCIS and 191 DCIS-mixed. The median percentage of positive tumour epithelial cells was 25% in pure DCIS, 30% in the DCIS component of mixed cases, and 60% in invasive component of the latter (all showed a range between 0-100%). For stromal expression, the median percentage of positive stromal cells was 5% in pure DCIS (range 0-80%), 70% in the DCIS component of mixed cases (range 0-80%) and 90% in the invasive component of the latter (range 0-90%). Within the pure DCIS cohort, high LGMN expression was observed in 23% and 44% in tumour epithelial and surrounding stromal cells; respectively. There was a positive linear correlation between expression of LGMN within the epithelial cells and surrounding fibroblasts (r=0.408, $p<0.0001$, Spearman's correlation).

The proportion of cases with high LGMN was greater in DCIS-mixed than pure DCIS, both within the tumour epithelial cells (23% of pure DCIS cases vs. 36% of DCIS mixed with IBC, $\chi2=11.7$, p=0.001) and stromal cells (44% for pure DCIS vs.

86% of DCIS mixed with invasion, $\chi 2=95.5$, $p<0.0001$). Similar results were observed when the data was analysed using a continuous scale ($p=0.049$ and $p<0.0001$, for tumour epithelial cells and stromal cells, respectively). Moreover, there was a statistically significant difference between LGMN expression within the tumour epithelial cells of the DCIS component and invasive component of DCIS-mixed cases ($p<0.0001$). Similarly, LGMN staining was more frequent in the stromal fibroblasts surrounding the invasive component than those surrounding the DCIS component ($p<0.0001$) (**Figure 6-9**).

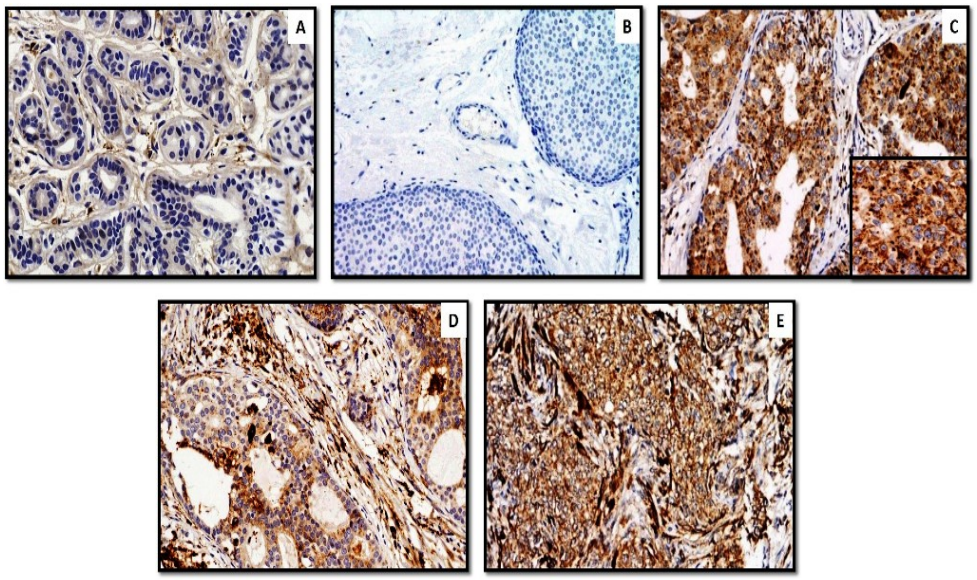

Figure 6-8: Patterns of LGMN expression

A) Normal breast ductolobular unit (x20) shows negative staining of legumain; B) Negative legumain expression (x20) in a pure DCIS case; C) strong expression of legumain in tumour cells and surrounding fibroblasts (x20) in a pure DCIS case (Inset: high power view showing the granular pattern of legumain expression). D) High expression of legumain in the fibroblasts surrounding DCIS case (x40). E) Expression of legumain in a mixed case (x40) showing strong staining in invasive component either within the tumour cells or surrounding stromal fibroblasts

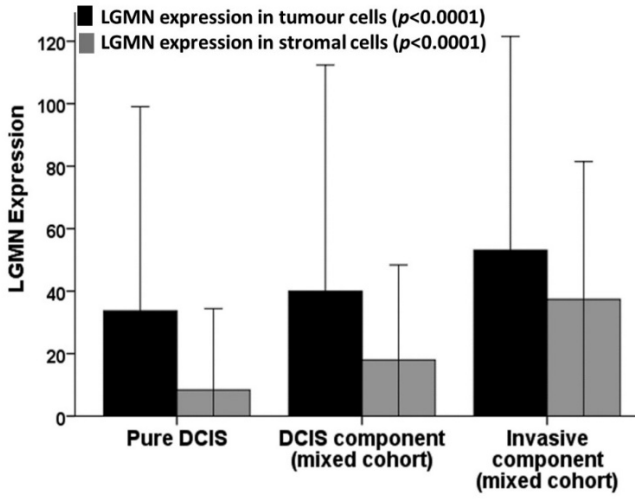

Figure 6-9: Bar chart showing differences of legumain expression between pure DCIS and DCIS-mixed both in tumour cells and surrounding stroma

6.7.2.5 COL11A1

Adjacent normal breast TDLUs showed negative or faint cytoplasmic staining. When present, COL11A1 was expressed in the cytoplasm of the epithelial tumour cells and/or surrounding fibroblasts (**Figure 6-10**). Higher stromal COL11A1 expression was observed around DCIS with periductal stromal reaction.

The final number of cases suitable for scoring was 488 pure DCIS and 184 DCIS-mixed. The median H-score of protein expression within the tumour was 100 in pure DCIS (range 0-160), 110 in the DCIS component of mixed cases (range 0-170), and 140 in invasive component of the latter (range 0-200). For stromal expression, the median percentage of positive stromal cells was 0% in pure DCIS (range 0-50%), 20% in the DCIS component of mixed cases (range 0-80%) and 40% in the invasive component of the latter (range 0-100%). Within the pure DCIS cohort, high COL11A1 expression was observed in 25% and 13% in tumour epithelial cells and surrounding fibroblasts; respectively. There was a positive linear correlation between expression of COL11A1 within the epithelial and surrounding stromal cells (r=0.3, p<0.0001, Spearman's correlation).

The proportion of cases with positive COL11A1 was significantly greater in DCIS-mixed than pure DCIS, both

within the tumour cells (25% of pure DCIS cases vs. 40% of DCIS mixed with invasive BC, $\chi 2=14.9$, $p<0.0001$) and stromal cells (13% for pure DCIS vs. 61% of DCIS mixed with invasion, $\chi 2=26.3$, $p<0.0001$). Similar results were observed when the data was analysed using a continuous scale ($p<0.0001$ for both tumour epithelial cells and stromal cells). Moreover, there was a statistically significant difference between COL11A1 expression within the tumour cells and surrounding stromal fibroblasts of the DCIS component and invasive component of DCIS-mixed cohort ($p<0.0001$ for both, using categorical and continuous data) (**Figure 6-11**).

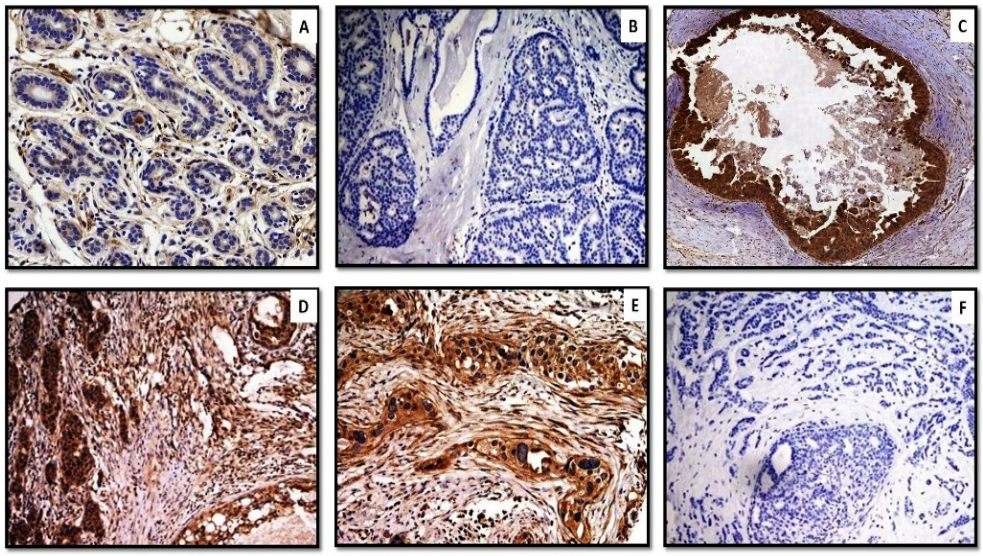

Figure 6-10: Patterns of COL11A1 expression

A) Normal breast ductolobular unit (x20) shows negative staining of COL11A1 in epithelial cells and occasional staining in the surrounding fibroblasts; B) Negative COL11A1 expression (x20) in a pure DCIS case; C) strong expression of COL11A1 in tumour cells and surrounding fibroblasts (x20) in a pure DCIS case; D and E) Expression of COL11A1 in a mixed case (x40) showing strong staining in invasive component within the tumour cells and/or surrounding stromal fibroblasts; and F) negative expression of COL11A1 in a mixed case (x20)

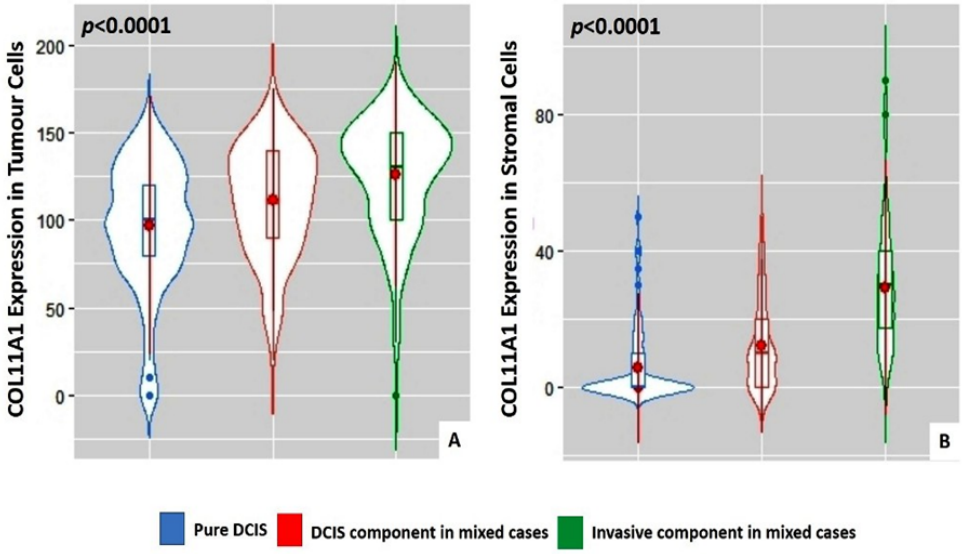

Figure 6-11: Violin plots showing differences of COL11A1 expression between pure DCIS and DCIS-mixed

Tumour cells (A) and surrounding stroma (B)

6.7.3 Association of the studied biomarkers and clinicopathological parameters

6.7.3.1 P4HA2

High expression of P4HA2 within the malignant epithelial cells and/or surrounding stromal fibroblasts in the pure DCIS was associated with various clinicopathological parameters characteristic of high risk DCIS (**Table 6-1**) including younger age at diagnosis, DCIS presented symptomatically, high nuclear grade, presence of comedo necrosis, ER negativity, PR negativity, HER2 positivity, and triple negative DCIS. Also, there was a positive association between high P4HA2 expression either within tumour epithelial cells or stromal cells and high HIF-1α expression. Analysis of continuous data of P4HA2 expression scores showed comparable results (**Table 6-2**).

Similar associations with aggressive clinicopathologic features were observed when evaluating *P4HA2* mRNA level in the IBC in the METABRIC series (n=1980), including high tumour grade (p=0.03), lymph node metastasis (p=0.028), ER negativity (p=0.0001), HER2 positivity (p<0.0001) (**Table 6-3**) in addition to shorter BC specific survival (BCSS) (HR=1.3, 95%CI=1.1-1.6, p=0.002).

Table 6-1: Correlation between P4HA2 expression with different clinicopathological parameters in the pure DCIS cohort

Parameters	**P4HA2 expression in tumour epithelial cells**		**χ^2 (*p*-value)**	**P4HA2 expression in stromal fibroblasts**		**χ^2 (*p*-value)**
	Low (N=234) N. (%)	High (N=247) N. (%)		Low (N=360) N. (%)	High (n=121) N. (%)	
Patient Age						
≤45 years	18 (8)	40 (16)	8.2	38 (11)	20 (17)	3.0
>45 years	216 (92)	207 (84)	**(0.004)**	322 (89)	101 (83)	(0.081)
DCIS Presentation						
Screening	126 (54)	112 (45)	3.5	189 (53)	49 (40)	5.2
Symptomatic	108 (46)	135 (55)	(0.062)	171 (47)	72 (60)	**(0.020)**
DCIS Size						
≤20mm	103 (44)	101 (41)	0.4	158 (44)	46 (38)	1.2
>20mm	130 (56)	144 (59)	(0.510)	200 (56)	74 (62)	(0.266)
DCIS Nuclear Grade						
Low	51 (22)	10 (4)	49.4	52 (14)	9 (7)	6.4
Moderate	73 (31)	52 (21)	**(<0.0001)**	98 (27)	27 (22)	**(0.04)**
High	110 (47)	185 (75)		210 (59)	85 (71)	
Comedo necrosis						10.1
Yes	130 (56)	191 (77)	25.6	226 (63)	95 (79)	**(0.001)**
No	104 (44)	56 (23)	**(<0.0001)**	134 (37)	26 (21)	
Oestrogen receptor						
Negative	24 (11)	93 (41)	50.9	75 (23)	42 (39)	10.9
Positive	190 (89)	132 (59)	**(<0.0001)**	256 (77)	66 (61)	**(0.001)**
Progesterone receptor						
Negative	65 (30)	121 (54)	25.0	127 (38)	59 (55)	8.7
Positive	149 (70)	103 (46)	**(<0.0001)**	203 (62)	49 (45)	**(0.003)**
HER2 status *						
Negative	164 (81)	156 (69)	8.4	245 (77)	75 (69)	2.2
Positive	38 (19)	70 (31)	**(0.004)**	75 (23)	33 (31)	(0.141)
Molecular classes			45.9			10.2
Luminal/HER2–	147 (76)	98 (47)	**(<0.0001)**	198 (65)	47 (48)	**(0.017)**
Luminal/HER2+	24 (12)	28 (13)		37 (12)	15 (15)	
ER-/HER2+	11 (6)	36 (17)		33 (11)	14 (14)	
Triple negative	11 (6)	48 (23)		37 (12)	22 (23)	

HIF1-a expression						
High	24 (15)	132 (66)	18.1	58 (21)	34 (36)	8.1
Low	141 (85)	68 (34)	**(<0.0001)**	213 (79)	60 (64)	**(0.004)**
DCIS Type**			8.6			39.3
Pure DCIS	234 (77)	247 (66)	**(0.003)**	360 (79)	121 (55)	**(<0.0001)**
DCIS with IBC	71 (23)	125 (34)		98 (21)	98 (45)	

Significant *p* values are in bold

P4HA2; prolyl-4-hydroxlase alpha subunit 2, DCIS; ductal carcinoma *in situ*, HER2; Human epidermal growth factor receptor 2, BCS; breast conserving surgery, IBC; invasive breast cancer, HIF1-a; hypoxia inducible factor 1 alpha.

*HER2 final status is achieved using combination of IHC and chromogenic *in situ* hybridisation (*CISH*).

**Including the cases in both cohorts; i.e. pure DCIS cohort (n=481)+ DCIS-mixed cohort (n=196).

Table 6-2: Correlation between P4HA2 expression with different clinicopathological parameters in the pure DCIS cohort using continuous data.

Parameters	Number of cases	P4HA2 expression in tumour epithelial cells (H-score)		P4HA2 expression in stromal fibroblasts (%)	
		Mean Rank	*p*-value	Mean Rank	*p*-value
Patient Age			**0.008**		**0.005**
≤45 years	58	286.0		288.3	
>45 years	423	234.8		234.5	
DCIS Presentation			**0.038**		**0.003**
Screening	238	227.8		222.1	
Symptomatic	243	253.9		259.5	
DCIS Size			0.098		0.136
≤20mm	204	227.5		228.7	
>20mm	274	248.5		247.5	
DCIS Nuclear Grade					**0.002**
Low	61	145.1	**<0.0001**	201.5	
Moderate	125	217.9		219.5	
High	295	270.6		258.3	
Comedo necrosis					
Yes	321	263.1	**<0.0001**	258.3	**<0.0001**
No	160	196.7		206.2	
Oestrogen receptor					
Negative	117	290.2	**<0.0001**	263.3	**<0.0001**
Positive	322	194.5		204.3	
Progesterone Receptor			**<0.0001**		**<0.0001**
Negative	186	258.2		248.8	
Positive	252	190.9		197.8	
HER2 status*					**0.011**
Negative	320	200.9	**<0.0001**	205.7	
Positive	108	254.6		240.5	
Molecular classes					
Luminal/HER2–	245	170.8	**<0.0001**	183.7	**<0.0001**
Luminal/HER2+	52	219.2		209.6	
ER-/HER2+	47	268.9		243.8	
Triple negative	59	263.2		238.4	
HIF1-a expression					
High	92	233.4	**<0.0001**	223.3	**<0.0001**
Low	273	166.0		169.4	
DCIS Type			**0.006**		
Pure DCIS	481	325.8		302.3	**<0.0001**
DCIS with IBC	196	371.4		429.0	

Significant *p* values are in bold

P4HA2; prolyl-4-hydroxlase alpha subunit 2, DCIS; ductal carcinoma *in situ*, HER2; Human epidermal growth factor receptor 2, BCS; breast conserving surgery, IBC; invasive breast cancer, HIF1-a; hypoxia inducible factor 1 alpha.

*HER2 final status is achieved using combination of IHC and chromogenic *in situ* hybridisation (*CISH*).

Table 6-3: Correlation between *P4HA2* mRNA level and the clinicopathologic parameters in the METABRIC series.

Parameter	Number of cases	Mean *P4HA2* mRNA level	*p*-value
Patient Age			0.336
<50 years	383	8.3	
≥50 years	1556	8.3	
Tumour Size			
≤20 mm	622	8.3	0.535
>20 mm	1331	8.3	
Histologic Grade			
1	170	8.2	
2	770	8.2	**0.034**
3	952	8.3	
Lymph node metastasis			
Negative	1035	8.2	**0.028**
Positive	938	8.3	
Oestrogen Receptor (ER) Status			
Positive	1506	8.2	**0.0001**
Negative	474	8.4	
HER2 Status			
Negative	1733	8.2	**<0.0001**
Positive	247	8.5	
PAM50 molecular classes			
Luminal A	718	8.2	
Luminal B	488	8.3	**0.005**
Basal-like	329	8.3	
HER2 enriched	240	8.4	
Normal like	199	8.2	

Significant *p* values are in bold
METABRIC: Molecular Taxonomy of Breast Cancer International Consortium

6.7.3.2 CTSA

Numerous clinicopathological parameters indicating poor DCIS prognosis were allied with high CTSA expression (**Table 6-4**). Comparable results were generated when the analysis was carried out using continuous data for CTSA expression (**Figure 6-12**).

In the METABRIC cohort, a higher level of *CTSA* mRNA was associated with adverse prognostic parameters including high tumour histological grade (p<0.0001), lymph node metastasis (p=0.001), ER negativity (p<0.0001), HER2 positivity (p<0.0001) (**Table 6-5**). *CTSA* was also associated with shorter BCSS (HR=1.5, 95%CI=1.1-1.5, p<0.0001).

Table 6-4: Correlation between CTSA expression with clinicopathological parameters in the pure DCIS cohort

Parameters	CTSA expression in tumour epithelial cells		χ^2 (*p*-value)
	Low (N=272) N. (%)	High (N=255) N. (%)	
Age (years)			
≤50	54 (20)	69 (27)	3.8
>50	218 (80)	186 (73)	**(0.045)**
DCIS Presentation			
Screening	144 (53)	115 (45)	3.2
Symptomatic	128 (47)	140 (55)	(0.071)
DCIS Size (mm)			
≤20	122 (45)	113 (45)	0.1
>20	150 (55)	139 (55)	(0.998)
DCIS Nuclear Grade			
Low	44 (16)	23 (9)	10.2
Moderate	79 (29)	60 (23)	**(0.006)**
High	149 (55)	172 (68)	
Comedo necrosis			
Yes	174 (64)	177 (69)	1.8
No	98 (36)	78 (31)	(0.18)
Oestrogen receptor status			
Negative	49 (20)	79 (34)	11.9
Positive	199 (80)	149 (66)	**(0.001)**
HER2 status			
Negative	219 (85)	169 (70)	17.2
Positive	37 (15)	72 (30)	**(<0.0001)**
Proliferation Index (Ki-67)			
High (≥14%)	41 (20)	58 (28)	3.7
Low (<14%)	168 (80)	152 (72)	(0.051)
Molecular classes			11.6
Luminal A	113 (59)	89 (43)	**(0.009)**
Luminal B	33 (17)	42 (20)	
HER2 enriched	19 (10)	40 (20)	
Triple negative	28 (14)	37 (17)	
Tumour infiltrating lymphocytes			
Dense	90 (44)	102 (53)	3.1
Sparse	116 (56)	92 (47)	(0.075)
Hypoxia inducible factor 1 alpha			
High	35 (18)	60 (32)	9.4
Low	159 (82)	130 (68)	**(0.002)**

Significant *p* values are in **bold**

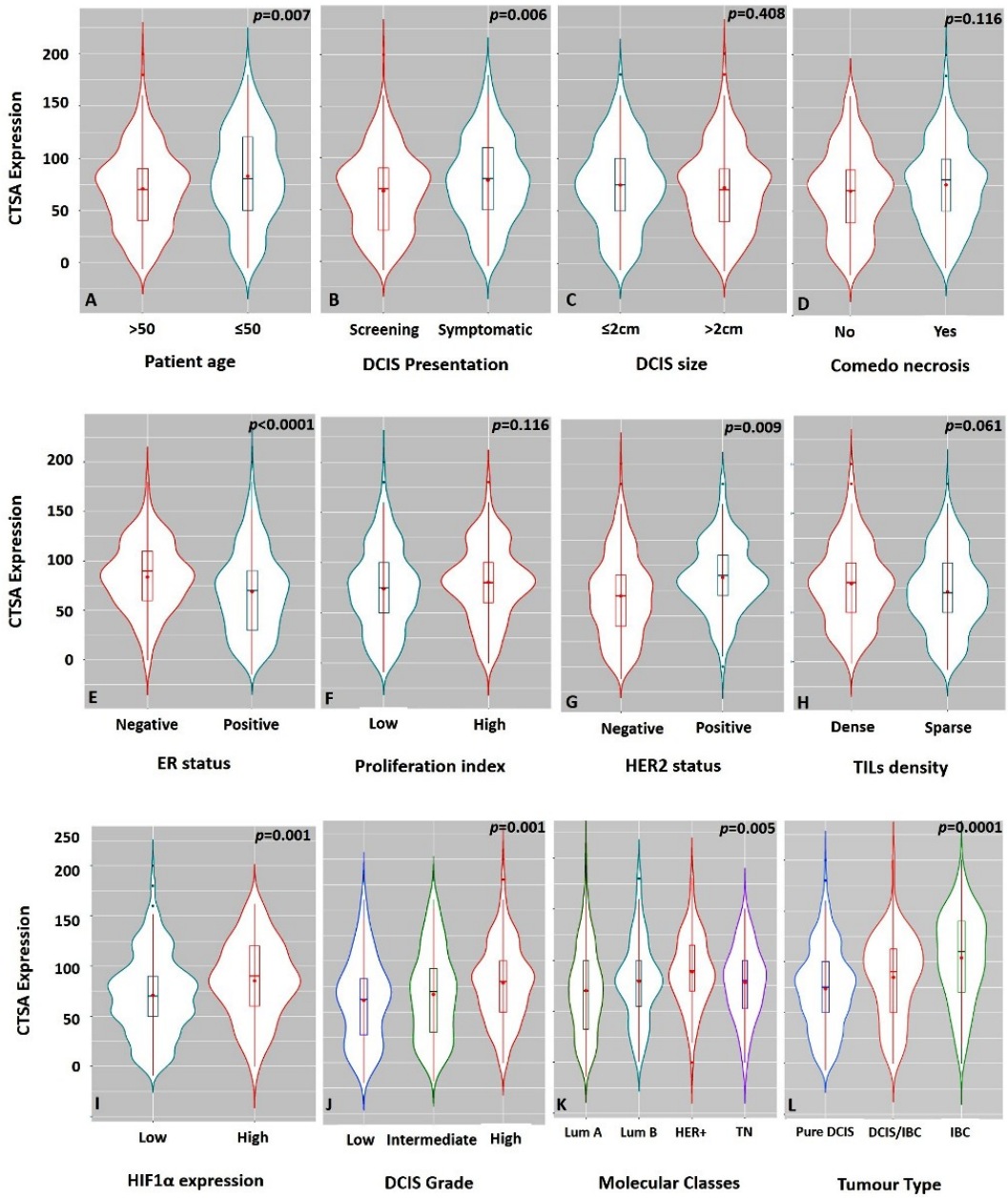

Figure 6-12: Violin plots showing the associations between CTSA expression and other clinicopathological parameters in pure DCIS cohort

(A-K) and the difference between CTSA expression in pure DCIS and DCIS mixed with invasive carcinoma (L), using continuous expression data. The central boxplot represents 95% confidence interval and the median while the red dot represents the mean. (TILs; tumour infiltrating lymphocytes, HIF1α; hypoxia inducible factor 1 alpha, Lum; luminal, TN; triple negative, DCIS; ductal carcinoma in situ, IBC; invasive breast cancer)

Table 6-5: Correlation between *CTSA* mRNA and the clinicopathologic parameters in the METABRIC series.

Parameter	Number of cases	Mean *CTSA* mRNA level	*p*-value
Patient Age (years)			0.452
<50	383	8.5	
≥50	1556	8.5	
Tumour Size (mm)			
≤20	622	8.4	**0.007**
>20	1331	8.5	
Histologic Grade			
1	170	8.3	
2	770	8.4	**<0.0001**
3	952	8.6	
Lymph node metastasis			
Negative	1035	8.4	**0.001**
Positive	938	8.5	
Oestrogen Receptor Status			
Positive	1506	8.4	**<0.0001**
Negative	474	8.6	
HER2 Status			
Negative	1733	8.4	**<0.0001**
Positive	247	8.6	
PAM50 molecular classes			
Luminal A	718	8.4	
Luminal B	488	8.6	**<0.0001**
Basal-like	329	8.6	
HER2 enriched	240	8.7	
Normal like	199	8.5	

p values in **bold**= significant
METABRIC: Molecular Taxonomy of Breast Cancer International Consortium

6.7.3.3 CTSV

Various clinical, morphological and pathological features determining high risk DCIS were aligned with CTSV protein overexpression (**Table 6-6**) including DCIS grade, negative hormonal receptors, HER2 positivity and HIF-1a overexpression for both CTSV tumoural and stromal expression. In addition, stromal expression was exclusively associated with larger DCIS size, comedo type necrosis, higher proliferation index (Ki67) and high TIL density. Similar results were observed when the continuous data for CTSV expression was used in the analysis (**Table 6-7**).

High levels of *CTSV* mRNA was associated with poor prognostic features, In the METABRIC cohort, such as younger age at diagnosis (p=0.005), large size of the tumour (p=0.0001), grade 3 tumours (p<0.0001), involvement of the lymph nodes (p=0.0001), negative ER expression (p<0.0001) and HER2 amplification (p<0.0001) (**Table 6-8**). *CTSV* was also associated with poor overall BCSS (HR=1.6, 95%CI=1.3-1.9, p<0.0001).

Table 6-6: Correlation between CTSV expression with clinicopathological parameters in the pure DCIS cohort.

Clinicopathological Parameters	CTSV expression in tumour epithelial cells		χ^2 (*p*-value)	CTSV expression in stromal fibroblasts		χ^2 (*p*-value)
	Low (N=373) N. (%)	High (N=154) N. (%)		Low (N=421) N. (%)	High (N=106) N. (%)	
Age (years)			3.1			0.5
≤50	97 (26)	29 (20)	(0.079)	98 (23)	28 (26)	(0.499)
>50	276 (74)	125 (80)		323 (77)	78 (74)	
Presentation						
Screening	189 (51)	72 (47)	0.7	212 (50)	49 (46)	0.6
Symptomatic	184 (49)	82 (53)	(0.413)	229 (50)	57 (54)	(0.447)
DCIS Size (mm)			0.1			5.1
≤20	166 (45)	70 (46)	(0.746)	199 (47)	37 (35)	**(0.025)**
>20	207 (56)	82 (54)		221 (53)	68 (65)	
Nuclear Grade						
Low	51 (14)	16 (10)	7.7	59 (14)	8 (8)	17.9
Moderate	111 (30)	31 (20)	**(0.021)**	127 (30)	15 (14)	**(<0.0001)**
High	211 (56)	107 (70)		235 (56)	83 (78)	
Comedo necrosis						9.0
Yes	235 (63)	107 (70)	2.1	260 (62)	82 (77)	**(0.003)**
No	137 (37)	47 (30)	(0.157)	161 (38)	24 (23)	
Oestrogen receptor						
Negative	68 (20)	54 (39)	17.3	68 (18)	56 (53)	50.6
Positive	267 (80)	86 (61)	**(<0.0001)**	305 (82)	48 (47)	**(<0.0001)**
Progesterone receptor						
Negative	126 (37)	72 (51)	7.7	131 (35)	67 (65)	30.2
Positive	211 (63)	69 (49)	**(0.006)**	244 (65)	36 (35)	**(<0.0001)**
HER2 status						
Negative	288 (82)	98 (68)	11.6	329 (84)	57 (56)	36.5
Positive	63 (18)	46 (32)	**(0.001)**	64 (16)	45 (44)	**(<0.0001)**
Proliferation index (Ki-67)						
High	66 (22)	37 (26)	0.7	64 (20)	36 (37)	12.2
Low	228 (78)	96 (74)	(0.407)	262 (80)	62 (63)	**(0.0001)**

Molecular classes			22.4			63.1
Luminal A	247 (73)	72 (51)	**(<0.0001)**	282 (75)	37 (37)	**(<0.0001)**
Luminal B	23 (7)	17 (12)		28 (8)	12 (12)	
HER2 Enriched	32 (10)	28 (20)		28 (7)	32 (32)	
Triple negative	34 (10)	23 (17)		37 (10)	20 (19)	
Tumour infiltrating lymphocytes			0.1			9.9
Dense	140 (48)	53 (47)	(0.934)	137 (44)	56 (62)	**(0.002)**
Sparse	153 (52)	59 (53)		178 (56)	34 (38)	
HIF1A expression						
High	60 (22)	37 (32)	4.1	58 (20)	39 (43)	20.8
Low	211 (78)	79 (68)	**(0.042)**	239 (80)	51 (57)	**(<0.0001)**

Significant *p* values are in bold.

CTSV; Cathepsin V, DCIS; ductal carcinoma in situ, HER2; Human epidermal growth factor receptor 2, HIF1A; hypoxia inducible factor 1 alpha

Table 6-7: Correlation between CTSV expression and clinicopathological parameters in the pure DCIS cohort using continuous data.

Clinicopathological Parameters	Number of cases	CTSV expression in tumour epithelial cells		CTSV expression in stromal fibroblasts	
		Mean Rank	*p*-value	Mean Rank	*p*-value
Age (years)					
≤50	126	244.1	0.090	265.4	0.904
>50	401	270.3		263.6	
Presentation					
Screening	261	256.9	0.285	255.7	0.213
Symptomatic	266	270.9		272.1	
DCIS Size (mm)					
≤20	236	263.2	0.975	247.6	**0.033**
>20	289	252.8		275.6	
Nuclear Grade					
Low	67	246.6	**0.001**	228.8	**0.001**
Moderate	142	228.1		235.1	
High	318	283.7		284.3	
Comedo necrosis					
Yes	342	274.5	**0.030**	281.2	**0.0003**
No	185	244.5		232.2	
Oestrogen receptor					
Negative	122	280.8	**<0.0001**	305.6	**0.002**
Positive	353	223.2		214.3	
Progesterone Receptor					
Negative	198	268.7	**<0.0001**	284.7	**<0.0001**
Positive	280	218.9		207.5	
HER2 status					
Negative	386	233.7	**<0.0001**	225.0	**<0.0001**
Positive	109	298.6		329.4	
Proliferation index (Ki-67)					
High	100	228.1	0.143	263.4	**<0.0001**
Low	324	207.7		196.8	
Molecular classes					
Luminal A	208	176.2		164.0	
Luminal B	76	218.9	**0.0001**	222.2	**<0.0001**
HER2 Enriched	60	237.1		278.7	
Triple negative	57	229.7		225.9	
Tumour infiltrating lymphocytes					
Dense	193	210.6	0.210	225.5	**0.0002**
Sparse	212	196.1		182.6	
HIF1A expression					
High	97	222.1	**0.004**	238.6	**<0.0001**
Low	290	184.6		179.1	

Significant *p* values are in bold.
CTSV; Cathepsin V, DCIS; ductal carcinoma in situ, HER2; Human epidermal growth factor receptor 2, HIF1A; hypoxia inducible factor 1 alpha.

Table 6-8: Correlation between *CTSV* mRNA level and the clinicopathological parameters in the METABRIC series

Clinicopathological parameters	Number of cases	Mean *CTSV* mRNA level	*p*-value
Patient Age (years)			**0.005**
<50	383	6.6	
≥50	1556	6.4	
Tumour Size (mm)			
≤20	622	6.4	**0.0001**
>20	1331	6.5	
Histologic Grade			
1	170	6.3	
2	770	6.4	**<0.0001**
3	952	6.6	
Lymph node metastasis			
Negative	1035	6.4	**0.0001**
Positive	938	6.6	
Oestrogen Receptor Status			
Positive	1506	6.4	**<0.0001**
Negative	474	6.8	
HER2 Status			
Negative	1733	6.7	**<0.0001**
Positive	247	6.5	
PAM50 molecular classes			
Luminal A	718	6.4	
Luminal B	488	6.6	**<0.0001**
Basal-like	329	6.6	
HER2 enriched	240	6.7	
Normal like	199	6.4	

Significant *p* values are in bold

METABRIC; Molecular Taxonomy of Breast Cancer International Consortium

6.7.3.4 LGMN

High expression of LGMN within the malignant epithelial cells and/or surrounding stromal fibroblasts in the pure DCIS was associated with clinicopathological parameters characteristic of poor prognosis (**Table 6-9**). Analysis of continuous data of LGMN expression scores showed similar results (**Table 6-10**).

Higher *LGMN* mRNA level in the METABRIC cohort was associated with high tumour grade (p=0.03), lymph node metastasis (p=0.04), estrogen receptor negativity (p=0.001), HER2 positivity (p=0.006) (**Table 6-11**) in addition to shorter BCSS (HR=1.3, 95% CI=1.1-1.5, p=0.007).

Table 6-9: Correlation between LGMN expression with different clinicopathological parameters in the pure DCIS cohort.

Clinicopathological Parameters	Legumain expression in tumour epithelial cells		χ^2 (*p*-value)	Legumain expression in stromal fibroblasts		χ^2 (*p*-value)
	Low (N=359) N. (%)	High (N=105) N. (%)		Low (N=259) N. (%)	High (N=205) N. (%)	
Age (years)			0.1			0.3
≤50	88 (25)	27 (24)	(0.802)	62 (24)	53 (26)	(0.635)
>50	271 (75)	78 (76)		197 (76)	152 (74)	
Presentation						
Screening	177 (49)	48 (46)	0.4	134 (51)	91 (44)	2.5
Symptomatic	182 (51)	57 (54)	(0.517)	125 (49)	114 (56)	(0.116)
DCIS Size (mm)			4.8			0.2
<16	112 (31)	22 (21)	(0.092)	77 (30)	57 (28)	(0.927)
16-40	148 (41)	45 (43)		107 (41)	86 (42)	
>40	98 (28)	37 (36)		75 (29)	60 (30)	
Nuclear Grade						
Low	51 (14)	8 (8)	19.2	39 (15)	20 (10)	12.6
Moderate	113 (32)	15 (14)	**(<0.0001)**	84 (32)	44 (21)	**(0.002)**
High	195 (54)	82 (78)		136 (53)	141 (69)	
Comedo necrosis						4.5
Yes	226 (63)	80 (76)	6.3	160 (62)	59 (30)	**(0.033)**
No	133 (37)	25 (23)	**(0.012)**	99 (38)	146 (70)	
Oestrogen receptor						
Negative	62 (19)	54 (54)	46.8	42 (18)	74 (39)	23.3
Positive	266 (81)	47 (46)	**(<0.0001)**	195 (82)	118 (62)	**(<0.0001)**
Progesterone receptor						
Negative	114 (34)	67 (66)	31.3	76 (32)	105 (55)	23.5
Positive	217 (66)	35 (34)	**(<0.0001)**	165 (68)	87 (45)	**(<0.0001)**
HER2 status						
Negative	256 (79)	60 (63)	9.9	190 (80)	126 (69)	6.6
Positive	68 (21)	35 (37)	**(0.002)**	47 (20)	56 (31)	**(0.010)**
Proliferation index (Ki-67)						
High	59 (20)	36 (37)	11.7	31 (33)	64 (61)	23.3
Low	240 (80)	62 (63)	**(0.001)**	184 (67)	118 (40)	**(<0.0001)**

Molecular classes			46.4			36.3
Luminal A	160 (58)	22 (24)	**(<0.0001)**	127 (63)	55 (33)	**(<0.0001)**
Luminal B	61 (22)	18 (20)		35 (18)	44 (26)	
HER2 Enriched	25 (9)	22 (25)		19 (10)	28 (17)	
Triple negative	29 (11)	28 (31)		18 (9)	39 (24)	
Tumour infiltrating lymphocytes			9.6			27.7
Dense	123 (44)	55 (63)	**(0.002)**	72 (36)	106 (63)	**(<0.0001)**
Sparse	159 (56)	33 (37)		130 (64)	62 (37)	
DCIS Type*						
Pure DCIS	359 (75)	105 (61)	11.7	259 (91)	205 (56)	95.6
DCIS with invasive breast cancer	123 (25)	68 (39)	**(0.001)**	27 (9)	164 (44)	**(<0.0001)**

Significant *p* values are in **bold**

DCIS; ductal carcinoma *in situ*, HER2; Human epidermal growth factor receptor 2, n; number

*Including the cases in both cohorts; i.e. pure DCIS cohort (n=464) + DCIS-mixed cohort (n=191).

Table 6-10: Correlation between LGMN expression and different clinicopathological parameters in the pure DCIS cohort using continuous data.

Clinicopathological Parameters	Number of cases	Legumain expression in tumour epithelial cells		Legumain expression in stromal fibroblasts	
		Mean Rank	*p*-value	Mean Rank	*p*-value
Age (years)					
≤50	115	225.1	0.488	243.4	0.276
>50	349	234.9		228.9	
Presentation					
Screening	225	228.8	0.563	221.7	0.070
Symptomatic	239	235.9		242.6	
DCIS Size (mm)					
<16	134	211.7	0.054	224.9	0.701
16-40	193	231.6		231.8	
>40	135	250.9		237.5	
Nuclear Grade					
Low	59	198.9	**<0.0001**	207.1	**0.002**
Moderate	128	201.1		208.5	
High	277	254.1		248.9	
Comedo necrosis					
Yes	306	247.4	**0.001**	242.5	**0.016**
No	158	203.5		213.1	
Oestrogen receptor					
Negative	116	277.5	**<0.0001**	262.9	**<0.0001**
Positive	313	191.9		197.3	
Progesterone Receptor					
Negative	181	259.9	**<0.0001**	250.7	**<0.0001**
Positive	252	186.2		192.8	
HER2 status					
Negative	316	195.9	**<0.0001**	200.9	**0.003**
Positive	103	253.1		238.0	
Proliferation index (Ki-67)					
High	95	245.3	**<0.0001**	244.2	**<0.0001**
Low	302	184.4		184.7	
Molecular classes					
Luminal A	182	146.3	**<0.0001**	151.9	**<0.0001**
Luminal B	79	195.4		201.6	
HER2 Enriched	47	237.4		214.3	
Triple negative	57	238.2		230.6	
Tumour infiltrating lymphocytes					
Dense	178	207.5	**<0.0001**	216.3	**<0.0001**
Sparse	192	165.1		156.9	
DCIS Type					
Pure DCIS	464	319.2	**0.049**	283.2	**<0.0001**
DCIS with invasive breast cancer	191	349.4		436.8	

Significant *p* values are in **bold**
DCIS; ductal carcinoma *in situ*, HER2; Human epidermal growth factor receptor 2

Table 6-11: Correlation between *LGMN* mRNA level and the clinicopathological parameters in the METABRIC series.

Clinicopathological parameters	**Number of cases**	**Mean *Legumain* mRNA level**	***p*-value**
Patient Age (years)			0.746
<50	383	8.7	
≥50	1556	8.6	
Tumour Size (mm)			
≤20	622	8.7	0.443
>20	1331	8.5	
Histologic Grade			
1	170	8.2	
2	770	8.2	**0.034**
3	952	8.3	
Lymph node metastasis			
Negative	1035	8.5	**0.040**
Positive	938	8.6	
Oestrogen Receptor Status			
Positive	1506	8.4	**0.001**
Negative	474	8.9	
HER2 Status			
Negative	1733	8.5	**0.006**
Positive	247	8.8	
PAM50 molecular classes			
Luminal A	718	8.4	
Luminal B	488	8.5	**<0.0001**
Basal-like	329	9.0	
HER2 enriched	240	8.7	
Normal like	199	8.9	

Significant *p* values are in **bold**
METABRIC; Molecular Taxonomy of Breast Cancer International Consortium

6.7.3.5 COL11A1

High expression of COL11A1 within the malignant epithelial cells and/or surrounding stromal fibroblasts in the pure DCIS was associated with hormonal receptor negativity, HER2 enriched and TNBC molecular subtypes. No association was observed between COL11A1 expression and the conventional clinicopathological parameters used in DCIS risk assessment such as age at diagnosis, tumour size, DCIS nuclear grade, and comedo necrosis (**Table 6-12**). Analysis of continuous data of COL11A1 expression showed similar results (**Table 6-13**). Moreover, there was a positive linear correlation between COL11A1 expression within tumour cells and surrounding fibroblasts with tumour proliferation fraction as assessed by Ki67 (r=0.3; $p<0.0001$, r=0.14; $p=0.01$, respectively), HIF-1α (r=0.15; $p=0.03$, r=0.13; $p=0.01$, respectively) and TILs (r=0.15; $p=0.009$, r=0.2; $p=0.001$, respectively).

Higher *COL11A1* mRNA level in the METABRIC cohort was associated with younger age ($p<0.0001$), lymph node metastasis ($p=0.001$), HER2 positivity ($p<0.0001$), HER2 enriched, triple negative and luminal B subtypes (**Table 6-14**) in addition to shorter BCSS (HR=1.2, 95% CI=1.02-1.4, $p=0.01$).

Table 6-12: Correlation between COL11A1 expression with different clinicopathological parameters in the pure DCIS cohort.

Clinicopathological Parameters	COL11A1 expression in tumour epithelial cells		χ^2 (*p*-value)	COL11A1 expression in stroma		χ^2 (*p*-value)
	Low (N=338) N. (%)	High (N=110) N. (%)		Low (N=391) N. (%)	High (N=57) N. (%)	
Age (years)			0.1			1.2
≤50	81 (24)	27 (25)	(0.902)	91 (23)	17 (30)	(0.280)
>50	257 (76)	83 (75)		300 (77)	40 (70)	
Presentation						
Screening	166 (49)	52 (47)	0.1	193 (49)	25 (44)	0.6
Symptomatic	172 (51)	58 (53)	(0.737)	198 (51)	32 (56)	(0.438)
DCIS Size (mm)						
≤20	147 (44)	51 (47)	0.4	163 (43)	30 (54)	2.6
>20	191 (56)	57 (53)	(0.497)	223 (57)	25 (46)	(0.106)
Nuclear Grade						
Low	40 (12)	13 (12)	0.2	49 (13)	4 (7)	1.6
Moderate	88 (26)	31 (28)	(0.903)	102 (26)	17 (30)	(0.457)
High	210 (62)	66 (60)		240 (61)	36 (63)	
Comedo necrosis						0.1
Yes	221 (65)	76 (69)	0.5	258 (66)	39 (68)	(0.716)
No	117 (35)	34 (31)	(0.475)	133 (34)	18 (32)	
Oestrogen receptor						
Negative	77 (25)	34 (33)	2.6	87 (24)	24 (44)	9.8
Positive	233 (75)	69 (67)	(0.105)	272 (76)	30 (56)	**(0.002)**
Progesterone receptor						
Negative	119 (38)	53 (52)	6.3	144 (40)	28 (55)	4.1
Positive	192 (62)	48 (48)	**(0.012)**	217 (60)	23 (45)	**(0.042)**
HER2 status						
Negative	231 (76)	75 (74)	0.2	289 (77)	39 (70)	1.5
Positive	74 (24)	27 (26)	(0.655)	85 (23)	17 (30)	(0.211)

Proliferation index (Ki-67)						
High	62 (23)	25 (24)	0.1	70 (22)	17 (34)	3.8
Low	210 (77)	78 (76)	(0.762)	255 (78)	33 (66)	**(0.049)**
Molecular classes			1.5			8.2
Luminal A	139 (54)	47 (48)	(0.685)	167 (54)	19 (38)	(0.041)
Luminal B	47 (18)	18 (18)		57 (18)	8 (16)	
HER2 Enriched	40 (15)	17 (17)		43 (14)	14 (28)	
Triple negative	34 (13)	17 (17)		42 (14)	9 (18)	
Tumour infiltrating lymphocytes			2.5			5.9
Dense	122 (47)	49 (57)	(0.113)	140 (47)	31 (66)	**(0.016)**
Sparse	137 (53)	37 (43)		158 (53)	16 (34)	
HIF1A expression						
High	58 (24)	26 (29)	1.1	63 (21)	21 (48)	13.8
Low	188 (76)	63 (71)	(0.293)	228 (78)	23 (52)	**(<0.0001)**

Significant *p* values are in **bold**

COL11A1; Collagen (XI) alpha-1 chain, DCIS; ductal carcinoma in situ, HER2; Human epidermal growth factor receptor 2, HIF1α; hypoxia-inducible factor 1 alpha.

Table 6-13: Correlation between COL11A1 expression and different clinicopathological parameters in the pure DCIS cohort using continuous data.

Clinicopathological Parameters	Number of cases	COL11A1 expression in tumor epithelial cells		COL11A1 expression in stroma	
		Mean Rank	*p*-value	Mean Rank	*p*-value
Age (years)			0.904		0.296
≤50	108	225.8		233.4	
>50	340	224.1		221.7	
Presentation			0.789		
Screening	218	222.8		219.5	0.312
Symptomatic	230	226.1		229.2	
DCIS Size (mm)			0.965		0.094
≤20	198	223.2		232.4	
>20	248	223.7		216.3	
Nuclear Grade			0.993		0.056
Low	53	223.1		201.6	
Moderate	119	224.0		214.8	
High	276	225.0		233.1	
Comedo necrosis			0.295		0.523
Yes	297	215.6		226.7	
No	151	229.1		220.2	
Oestrogen receptor			**<0.0001**		**<0.0001**
Negative	111	244.7		236.9	
Positive	302	193.15		196.0	
Progesterone Receptor			**<0.0001**		**0.004**
Negative	172	233.8		222.2	
Positive	240	186.9		195.3	
HER2 status			0.073		0.061
Negative	306	198.0		210.6	
Positive	101	222.1		231.4	
Proliferation index (Ki-67)			**0.006**		0.055
High	87	215.6		203.6	
Low	288	179.6		183.6	
Molecular classes			**0.014**		**0.004**
Luminal A	186	166.4		167.9	
Luminal B	65	179.1		177.4	
HER2 Enriched	57	215.8		212.7	
Triple negative	51	190.7		190.9	
Tumour infiltrating lymphocytes	171	189.1	**0.003**	187.1	**0.001**
Dense	174	157.1		159.1	
Sparse					
HIF1A expression			**0.008**		**0.001**
High	84	192.2		192.3	
Low	251	159.9		159.8	

Significant *p* values are in **bold**

COL11A1; Collagen (XI) alpha-1 chain, DCIS; ductal carcinoma in situ, HER2; Human epidermal growth factor receptor 2, HIF1α; hypoxia inducible factor 1 alpha.

Table 6-14: Correlation between *COL11A1* mRNA level and the clinicopathological parameters in the METABRIC series.

Clinicopathological parameters	Number of cases	Mean *COL11A1* mRNA level	*p*-value
Patient Age (years)			**<0.0001**
<50	383	8.7	
≥50	1556	8.8	
Tumour Size (mm)			
≤20	622	8.7	0.803
>20	1331	8.7	
Histologic Grade			
1	170	8.8	0.621
2	770	8.9	
3	952	8.9	
Lymph node Stage			
1	1035	8.7	**0.001**
2	622	8.9	
3	316	8.8	
Oestrogen Receptor Status			
Positive	1506	8.7	0.163
Negative	474	8.7	
HER2 Status			
Negative	1733	8.7	**<0.0001**
Positive	247	8.8	
PAM50 molecular classes			
Luminal A	718	8.7	
Luminal B	488	8.9	**<0.0001**
Basal-like	329	8.9	
HER2 enriched	240	8.7	
Normal like	199	8.5	

Significant *p* values are in **bold**
METABRIC; Molecular Taxonomy of Breast Cancer International Consortium

6.7.4 Association of the studied biomarkers and DCIS recurrence

6.7.4.1 P4HA2

High P4HA2 expression within tumour epithelial cells was associated with shorter LRFI in the whole cohort of pure DCIS (HR=2.3, 95%CI=1.3-4.1; *p*=0.003, **Figure 6-13**) and in the luminal ER-positive/HER2-negative subgroup (HR=3.3, 95%CI=1.1-5.2; *p*=0.001). Association with shorter LRFI was observed in patients treated with BCS without adjuvant RT (HR=3.6, 95%CI=1.9-7.1; *p*<0.0001), however; the significant association with poor outcome was not maintained in patients treated with either mastectomy or BCS followed by adjuvant RT (HR=0.9, 95%CI=0.2-4.8; *p*=0.9 and HR=1.8, 95%CI=0.3-9.1; *p*=0.5, respectively). Interestingly, there was an association between high P4HA2 expression and ipsilateral local recurrence as invasive disease in patients treated with BCS without post-operative adjuvant RT (HR=2.4, 95%CI=1.1-5.2; *p*=0.03) but this associated lost its significance in patients who were offered adjuvant RT (**Figure 6-13** and **Figure 6-14**).

To further evaluate the impact of P4HA2 on the outcome in the context of adjuvant RT response, the cohort of pure DCIS treated with BCS was stratified based on P4HA2 expression. In the high P4HA2 expression group, there was a statistically

significant association between adjuvant RT and longer LRFI (HR=0.3, 95%CI=0.1-0.8; *p*=0.01). In the low P4HA2 expression cohort, this association was lost (HR=0.6, 95%CI=0.1-2.8; *p*=0.5) (**Figure 6-15**). The interaction between the combined RT and P4HA2 expression and outcome in the Cox Regression model showed similar results, whereas RT*P4HA2 expression showed a significant association with outcome (HR=3.4, 95%CI=1.3-8.7, *p*=0.01).

Stromal expression of P4HA2 did not show any significant association with tumour recurrence. Forest plots illustrating the association between different clinicopathological parameters and ipsilateral local tumour recurrence are shown in **Figure 6-16**.

Multivariate survival analysis showed that tumour expression of P4HA2 is a poor prognostic factor for tumour recurrence in patients treated with BCS independent of known other determinants of DCIS aggressiveness including patient age, nuclear grade, tumour size, presence of comedo necrosis and RT in the model (HR=2.3, 95% CI=1.3-4.4; *p*=0.007) (**Table 6-15**).

Furthermore, when patients treated with BCS were stratified based on clinicopathological variables into high/intermediate (higher) risk and low risk groups, using the VNPI [62], the

ipsilateral local recurrence rate was comparable (12% and 10% for the higher and low risk groups; respectively). When P4HA2 expression was incorporated, the recurrence rate for the higher risk/high P4HA2 group (35% of the final cohort, i.e. 168/481 patients) was 16% but only 8% for the higher risk/low P4HA2 group. Interestingly, the low risk/high P4HA2 group (15% of the final cohort) showed a 13% ipsilateral local recurrence rate, while the low risk/low P4HA2 group had a recurrence rate of 6%. Further categorisation, in context of post-operative RT, showed that the recurrence rate in higher risk/high P4HA2 group with no RT is 25% compared to 6% for higher risk/high P4HA2 patients who received RT. Similarly, there was 19% ipsilateral local recurrence rate in low risk/high P4HA2 patients who did not receive RT compared to 5% in patients who offered adjuvant RT. The recurrence rate in low risk/low P4HA2 group with or without post-operative RT was comparable (3% and 4%, respectively).

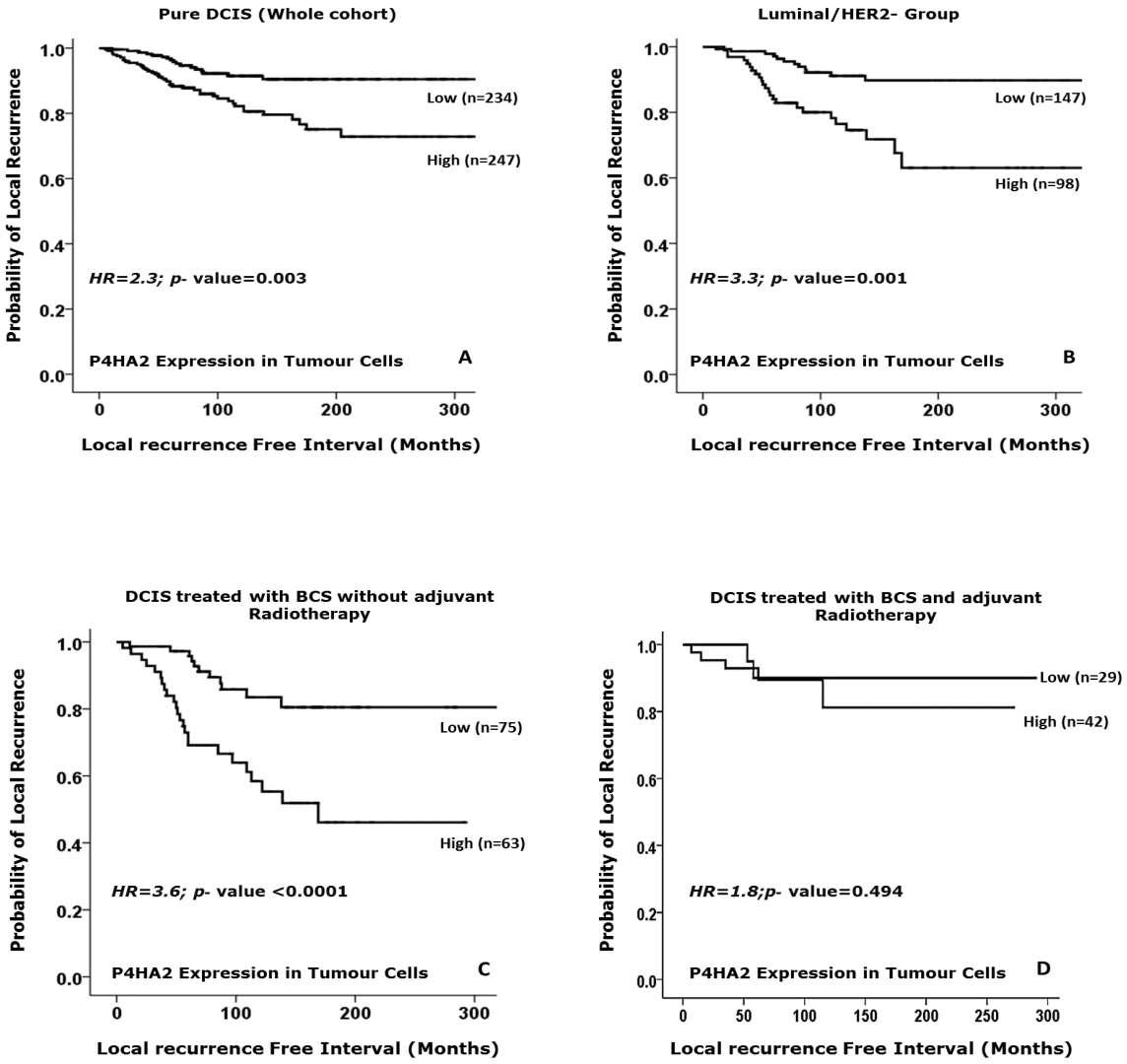

Figure 6-13: Kaplan Meier curves show the association between P4HA2 and outcome

High expression of P4HA2 within the tumour epithelial cells is associated with shorter ipsilateral local recurrence free interval (LRFI) in the whole series (A), and in luminal/HER2- subgroup (B). High expression also showed an association with shorter LRFI in patients treated with breast conserving surgery (BCS) without adjuvant radiotherapy (C) but not in patients treated with breast conserving surgery followed by adjuvant radiotherapy (D)

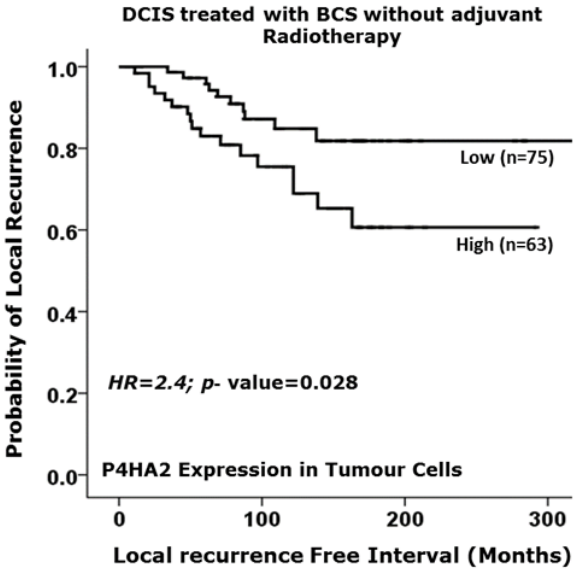

Figure 6-14: Kaplan Meier curve shows association between high P4HA2 expression and ipsilateral local invasive recurrences in BCS treated patients.

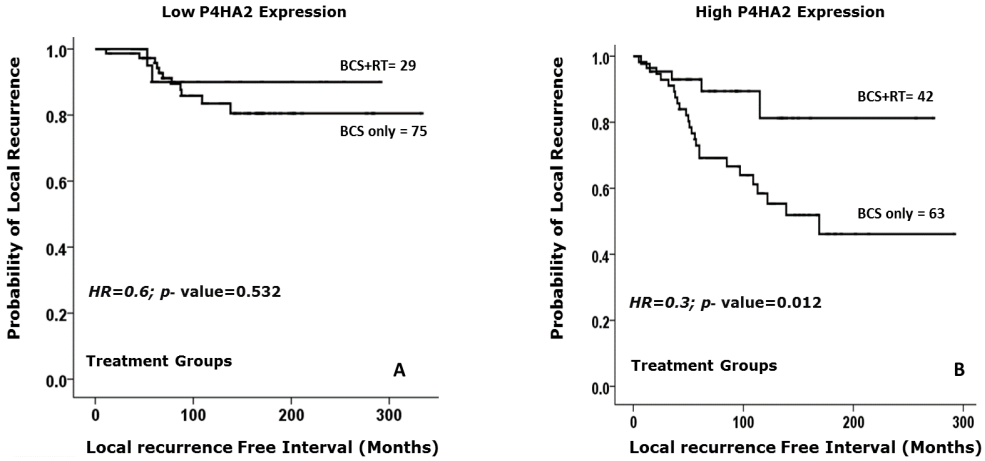

Figure 6-15: Kaplan Meier curves show association between post-operative adjuvant radiotherapy (RT) and recurrence within low and high P4HA2 expression groups

(A) in low P4HA2 expression group, (B) longer LRFI in patients treated with RT following breast conserving surgery (BCS) in high P4HA2 expression group.

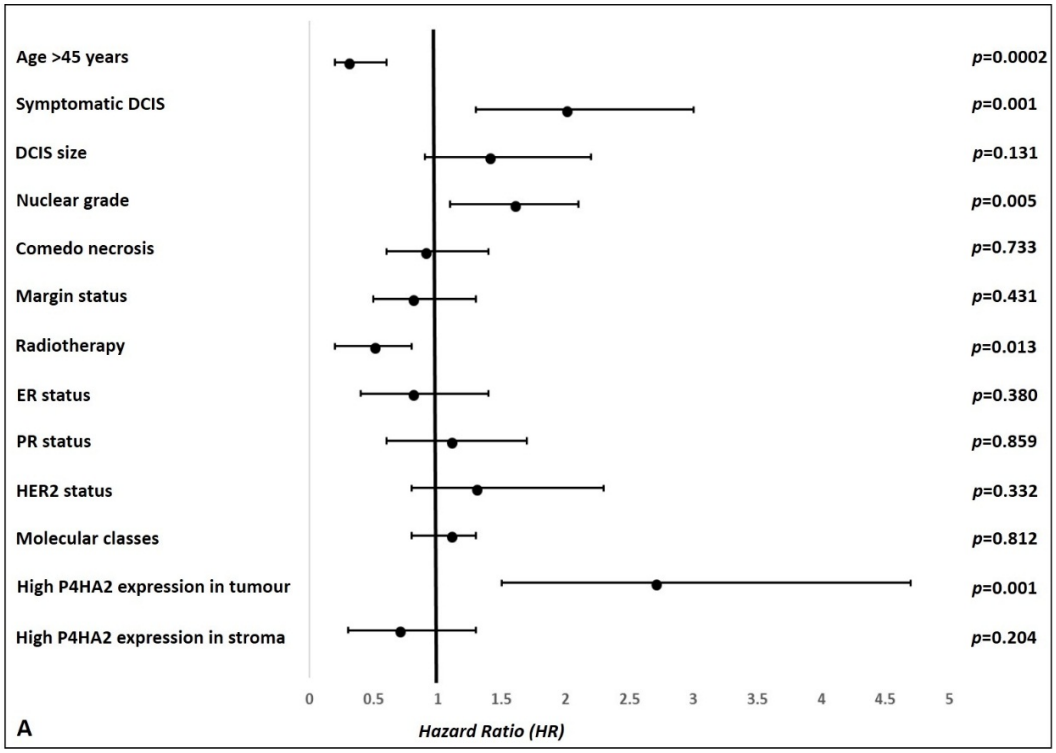

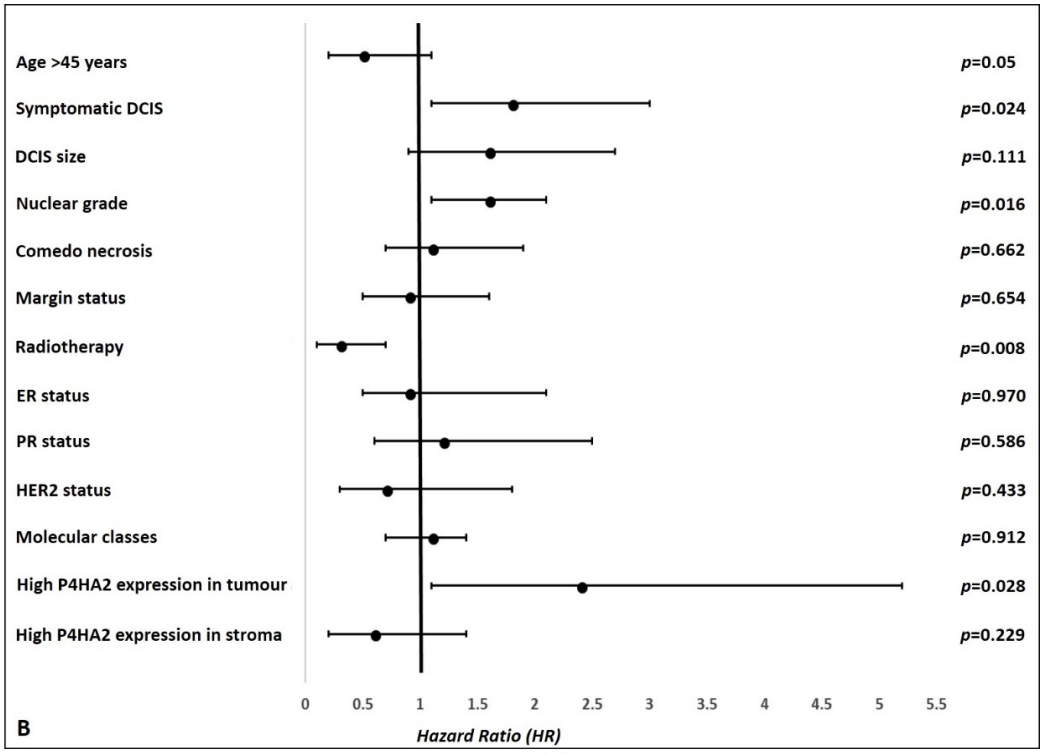

Figure 6-16: Forest plots showing the univariate analysis results of association between different clinicopathological parameters and ipsilateral tumour recurrence for patients treated with breast conserving surgery in pure DCIS cohort

A) all recurrences whether DCIS or invasive and B) for invasive recurrences only. High expression of P4HA2 in tumour epithelial cells is associated with higher recurrence risk in both groups

Table 6-15: Multivariate survival analysis of P4HA2 and other variables predicting ipsilateral local recurrence in patients treated by BCS in pure DCIS cohort

Parameters	**Hazard ratio (*HR*)**	**95.0% *confidence interval (CI)***		**Significance *p*-value**
		Lower	Upper	
High tumour P4HA2 expression	3.1	1.5	6.3	**0.002**
Patient Age	0.6	0.2	1.5	0.286
DCIS presentation	1.5	0.7	2.9	0.278
DCIS size	1.3	0.7	2.5	0.437
DCIS nuclear Grade	1.3	0.7	2.3	0.373
Comedo necrosis	1.1	0.5	2.1	0.895
Molecular classes	0.8	0.5	1.1	0.170
Radiotherapy	0.3	0.1	0.8	**0.015**
Margin status	0.8	0.5	1.4	0.510

Significant *p* values are in **bold**
P4HA2; prolyl-4-hydroxlase alpha subunit 2, DCIS; ductal carcinoma *in situ*.

6.7.4.2 CTSA

Higher expression of CTSA was correlated with shorter LRFI (all recurrences either as in situ or invasive disease) in the entire cohort of pure DCIS (HR=3.2, 95%CI=1.8-5.8; *p*=0.0001, **Figure 6-17**A. A similar result was seen in patients treated with BCS without any further treatment with adjuvant RT (HR=2.7, 95%CI=1.6-4.8; *p*=0.002, **Figure 6-17**B. However, there was no correlation between CTSA and outcome in patients treated with either mastectomy or BCS followed by adjuvant RT. In addition, there was a trend between high CTSA expression and occurrence of invasive recurrence (HR=1.8, 95%CI=0.9-4.6; *p*=0.07, **Figure 6-17**C.

Multivariate survival analysis revealed that high expression of CTSA is an independent poor prognostic factor for tumour recurrence after treatment with BCS (HR=2.5, 95% CI=1.2-5.3; *p*=0.015) regardless the other variables including patient age at diagnosis, DCIS size, mode of DCIS presentation, nuclear grade, presence of comedo necrosis, surgical margin width, different molecular classes and adjuvant RT (**Table 6-16**).

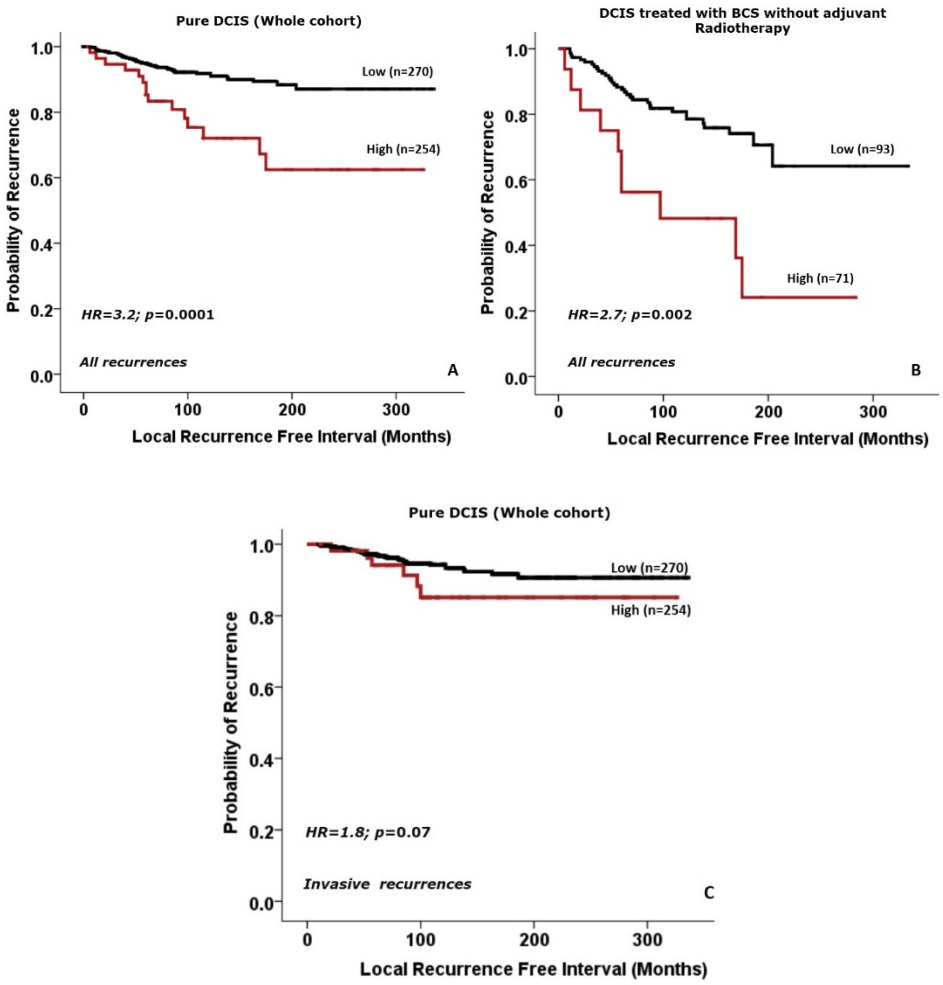

Figure 6-17: Kaplan Meier curves show the association between CTSA and outcome

High expression of CTSA is associated with shorter ipsilateral local recurrence free interval (LRFI) in the whole series (A), and in patients treated with breast conserving surgery (BCS) without adjuvant radiotherapy (B). (C) Showing the association between CTSA expression and invasive recurrences only in the whole cohort

Table 6-16: Multivariate survival analysis of CTSA and other variables predicting ipsilateral local recurrence in patients treated by BCS

Parameters	**Hazard ratio (*HR*)**	**95.0% *confidence interval (CI)***		**Significance *p*-value**
		Lower	Upper	
High CTSA expression	2.5	1.2	5.3	**0.015**
Patient Age	0.6	0.3	1.4	0.255
DCIS size	1.1	0.5	2.2	0.811
DCIS nuclear Grade	1.7	0.9	3.1	0.056
Comedo type necrosis	0.6	0.3	1.4	0.254
Radiotherapy	0.2	0.1	0.8	**0.019**
Surgical margins	0.8	0.4	1.4	0.381
Molecular classes	0.9	0.7	1.3	0.700
DCIS presentation	2.1	0.9	4.1	0.051

This model includes CTSA expression in tumour cells with other known parameters determining aggressive DCIS behaviour in the pure DCIS cohort.
p values in **bold** are significant

6.7.4.3 CTSV

High CTSV expression in the epithelial tumour cells was associated with shorter LRFI in the entire pure DCIS cohort (HR=1.9, 95%CI=1.1-3.1; *p*=0.013, **Figure 6-18**A. A similar result was observed in patients treated with BCS alone (HR=2.0, 95%CI=1.1-3.5; *p*=0.017, **Figure 6-18**B. There was no statistically significant association between CTSV and DCIS recurrence in patients treated with either mastectomy or those that received RT post BCS. Higher stromal expression of CTSV showed an association with higher rate of recurrence in the whole cohort as well as in patients treated solely with BCS. Higher CTSV stromal expression showed an association with all ipsilateral recurrence (HR=2.4, 95%CI=1.4-4.1; *p*=0.001, **Figure 6-19**A for whole cohort and HR=2.3, 95%CI=1.3-4.2; *p*=0.004, **Figure 6-19**C for BCS treated patients) and when the analysis was restricted to invasive recurrences only (HR=2.5, 95%CI=1.3-4.9; *p*=0.008, **Figure 6-19**B for whole cohort and HR=2.6, 95%CI=1.3-5.5; *p*=0.007, **Figure 6-19**D for BCS treated patients).

Multivariate survival analysis revealed that stromal CTSV was an independent prognostic factor for tumour recurrence after treatment with BCS for all recurrences (HR=2.7, 95% CI=1.5-4.8; *p*=0.001) and for invasive recurrences (HR=3.0, 95% CI=1.4-6.5; *p*=0.005) regardless of the other prognostic

variables included in the model. **Table 6-17** shows a Cox regression model of the multivariate analysis either without or with stromal CTSV overexpression for all recurrences or invasive recurrences.

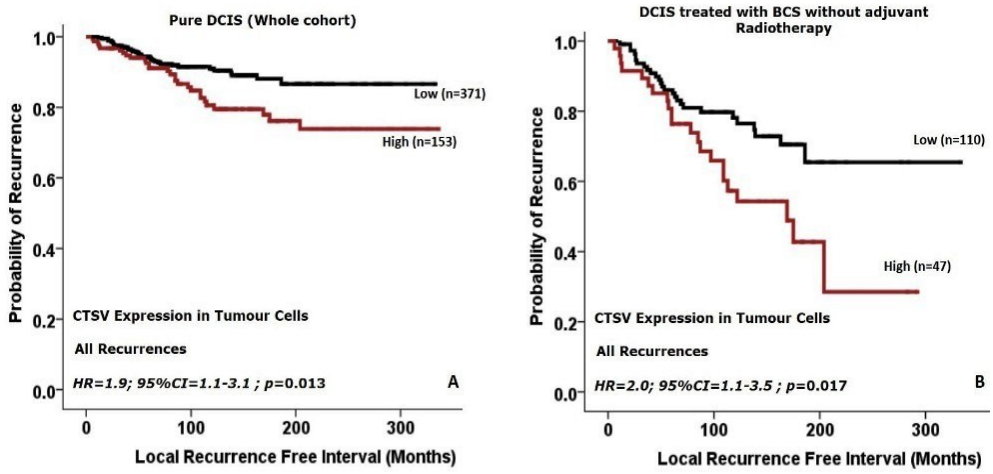

Figure 6-18: Kaplan Meier curves show the association between epithelial CTSV and outcome

High expression of CTSV in the tumour epithelial cells is associated with shorter ipsilateral local recurrence free interval (LRFI) in the whole series (A), and in patients treated with breast conserving surgery (BCS) without adjuvant radiotherapy (B)

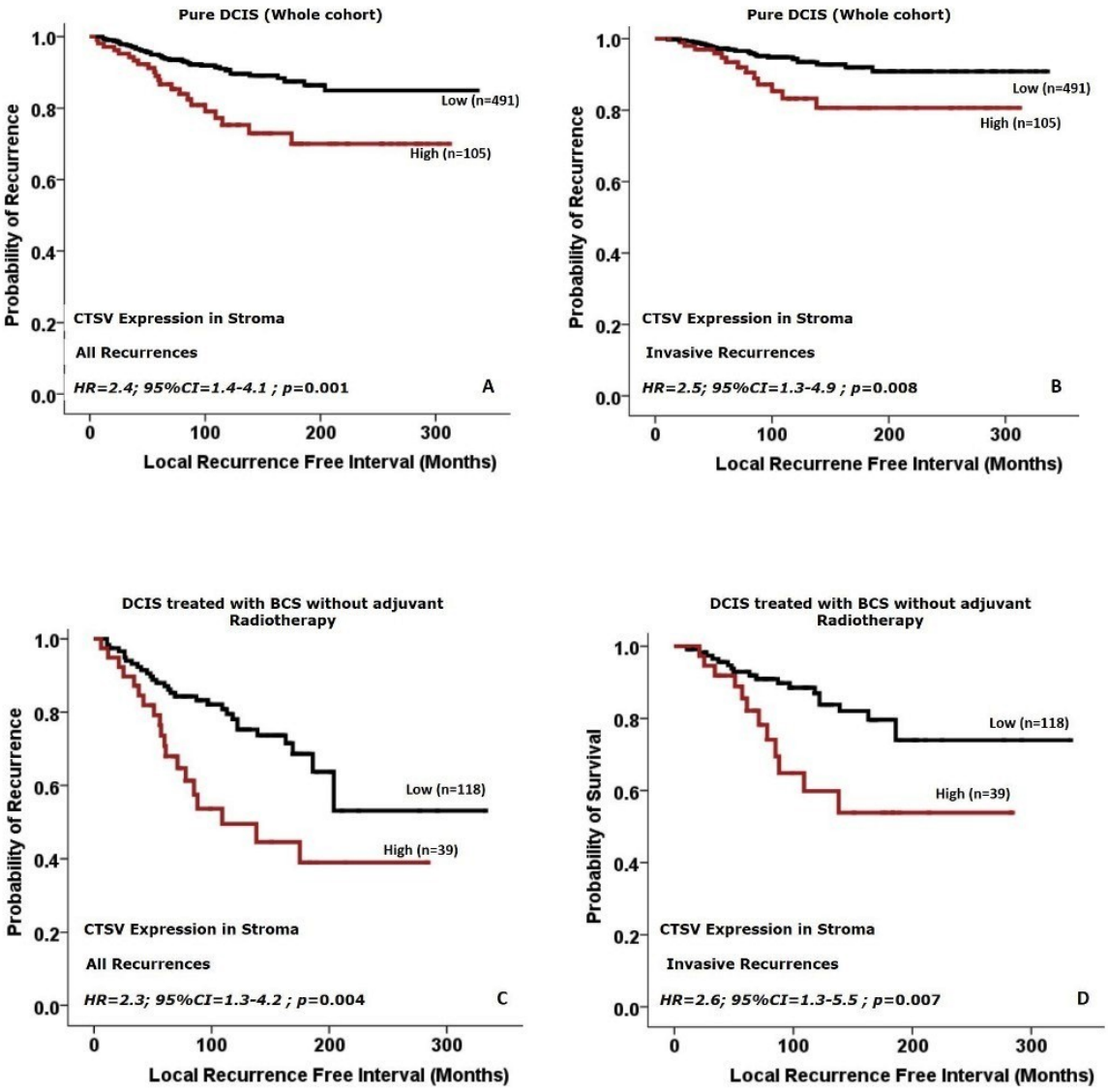

Figure 6-19: Kaplan Meier curves show the association between stromal CTSV and outcome

High expression of CTSV in the stroma is associated with shorter ipsilateral local recurrence free interval (LRFI) for al recurrences either in the whole series (A), and in patients treated with breast conserving surgery (BCS) without adjuvant radiotherapy (B). It was associated with higher rate of invasive recurrences in the whole cohort (C) or in patients treated solely with BCS (D)

Table 6-17: Multivariate survival analysis of CTSV and other variables predicting ipsilateral local recurrences in patients treated by BCS.

1. All recurrences

Conventional clinicopathological parameters associated with high risk DCIS				
Parameters	Hazard ratio (*HR*)	95% *confidence interval (CI)*		*p*-value
		Lower	Upper	
Patient Age	0.4	0.2	0.8	**0.006**
DCIS presentation	1.5	0.9	2.4	0.111
DCIS size	1.5	1.1	2.1	**0.040**
DCIS nuclear Grade	1.9	1.3	2.7	**0.001**
Comedo necrosis	0.6	0.4	0.9	**0.049**
Margin status	0.8	0.7	0.9	**0.004**
Stromal expression of CTSV and other clinicopathological parameters associated with high risk DCIS				
High stromal CTSV expression	2.7	1.5	4.8	**0.001**
Patient Age	0.6	0.3	1.1	0.101
DCIS presentation	1.5	0.8	2.8	0.168
DCIS size	0.8	0.4	1.6	0.578
DCIS nuclear Grade	1.8	1.1	2.8	**0.018**
Comedo necrosis	0.5	0.3	0.9	**0.026**
Margin status	0.9	0.9	1.0	0.336

Significant *p* values are in **bold**
CTSV; Cathepsin V, DCIS; ductal carcinoma in situ.

B) Invasive recurrence

Conventional clinicopathological parameters associated with high risk DCIS				
Parameters	Hazard ratio (*HR*)	95% *confidence interval (CI)*		*p*-value
		Lower	Upper	
Patient Age	0.5	0.2	1.3	0.156
DCIS presentation	1.4	0.8	2.6	0.245
DCIS size	1.8	1.1	2.4	**0.013**
DCIS nuclear Grade	1.9	1.1	3.0	**0.013**
Comedo necrosis	0.7	0.4	1.3	0.274
Margin status	0.9	0.8	1.1	0.075
Stromal expression of CTSV and other clinicopathological parameters associated with high risk DCIS				
High stromal CTSV expression	3.0	1.4	6.5	**0.005**
Patient Age	0.9	0.3	2.2	0.773
DCIS presentation	1.6	0.7	3.5	0.233
DCIS size	0.8	0.4	1.9	0.705
DCIS nuclear Grade	2.1	1.1	3.9	**0.028**
Comedo necrosis	0.5	0.2	1.1	0.101
Margin status	0.9	0.9	1.1	0.649

Significant *p* values are in **bold**
CTSV; Cathepsin V, DCIS; ductal carcinoma in situ

6.7.4.4 LGMN

High LGMN expression within tumour epithelial cells was associated with shorter LRFI (**Figure 6-20**) (all recurrences either as in situ or invasive disease) in pure DCIS (HR=2.7, 95% CI=1.6-4.8; p=0.0002). Association with shorter LRFI was observed in patients treated with BCS without adjuvant RT (HR=2.6, 95% CI=1.4-4.4; p=0.002) however; the significant association with poor outcome was not maintained in patients treated with either mastectomy (HR=0.9, 95% CI=0.1-8.8; p=0.9) or BCS followed by adjuvant RT (HR=2.4, 95% CI=0.8-10.4; p=0.08). Interestingly, there was an association between high LGMN expression and ipsilateral local recurrence as invasive disease (HR=3.1, 95% CI=1.5-6.5; p=0.001) particularly in patients treated with BCS without post-operative adjuvant RT (HR=3.3, 95% CI=1.5-7.3; p=0.004). Stromal expression of LGMN did not show any significant association with tumour recurrence.

Multivariate survival analysis showed that high expression of LGMN in tumour cells was a poor prognostic factor for tumour recurrence in patients treated with BCS independent of known other determinants of high risk DCIS including age at diagnosis, DCIS size, presentation, nuclear grade, comedo necrosis, margin status, molecular classes, and RT either for all recurrences (HR=3.5, 95% CI=1.8-4.9; p=0.0003) or when

the analysis was confined to invasive recurrences (HR=3.4, 95% CI=1.8-8.3; *p*=0.002) (**Figure 6-21**).

Interestingly, when LGMN expression in tumour cells was incorporated with the other determinants of DCIS risk described by VNPI [254], it provided better stratification for local recurrence risk, whereby high expression of LGMN was associated with worse outcome in all risk groups when compared to similar groups with low LGMN expression (**Figure 6-22**).

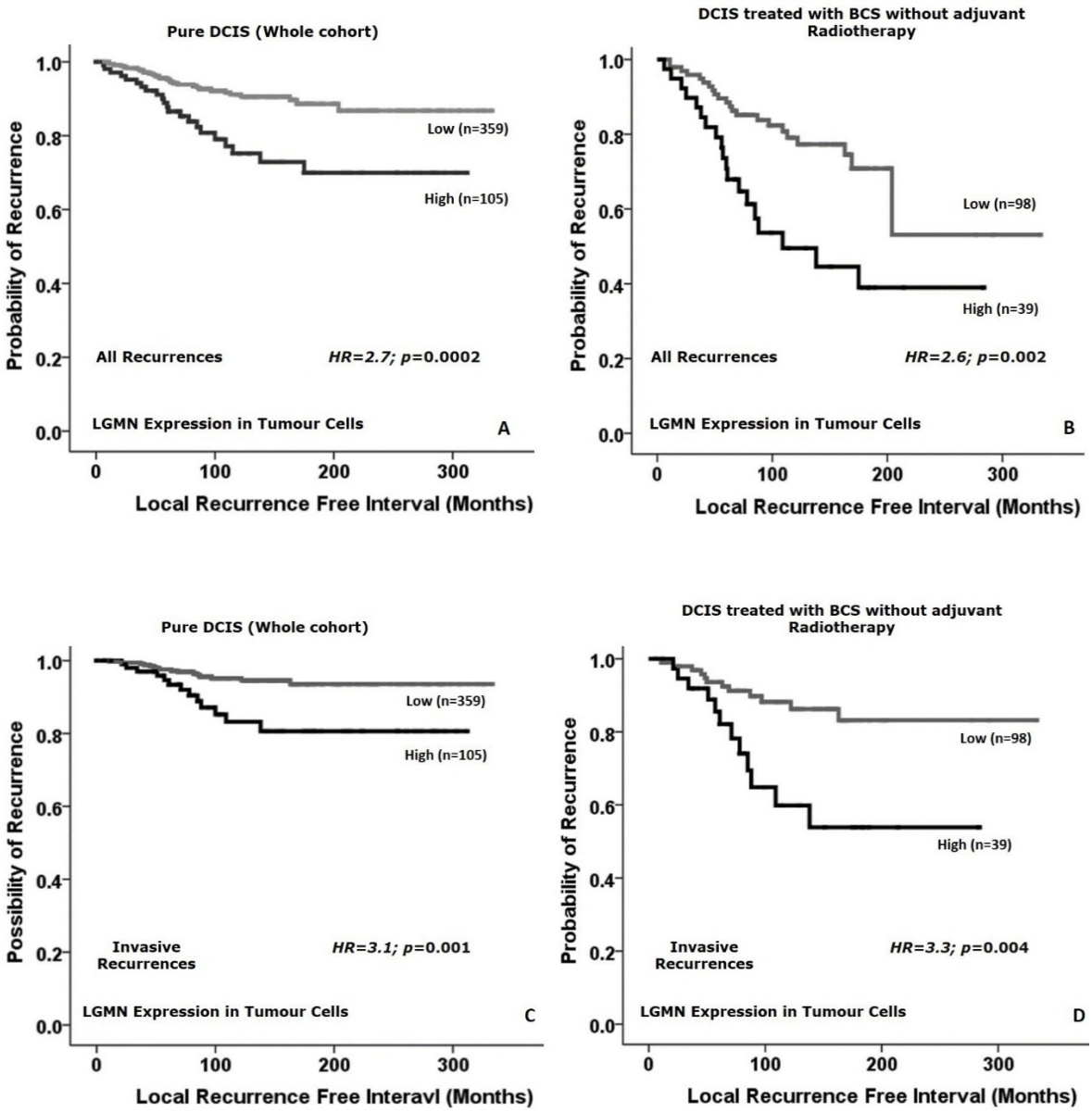

Figure 6-20: Kaplan Meier curves show the association between LGMN and outcome

High expression of legumain within the tumour epithelial cells is associated with shorter ipsilateral local recurrence free interval in the whole series (A), and in breast conserving surgery (BCS) without adjuvant radiotherapy (B). High expression also showed an association with shorter local recurrence free interval as invasive disease in the whole series (C) and in patients treated with breast conserving surgery without adjuvant radiotherapy (D)

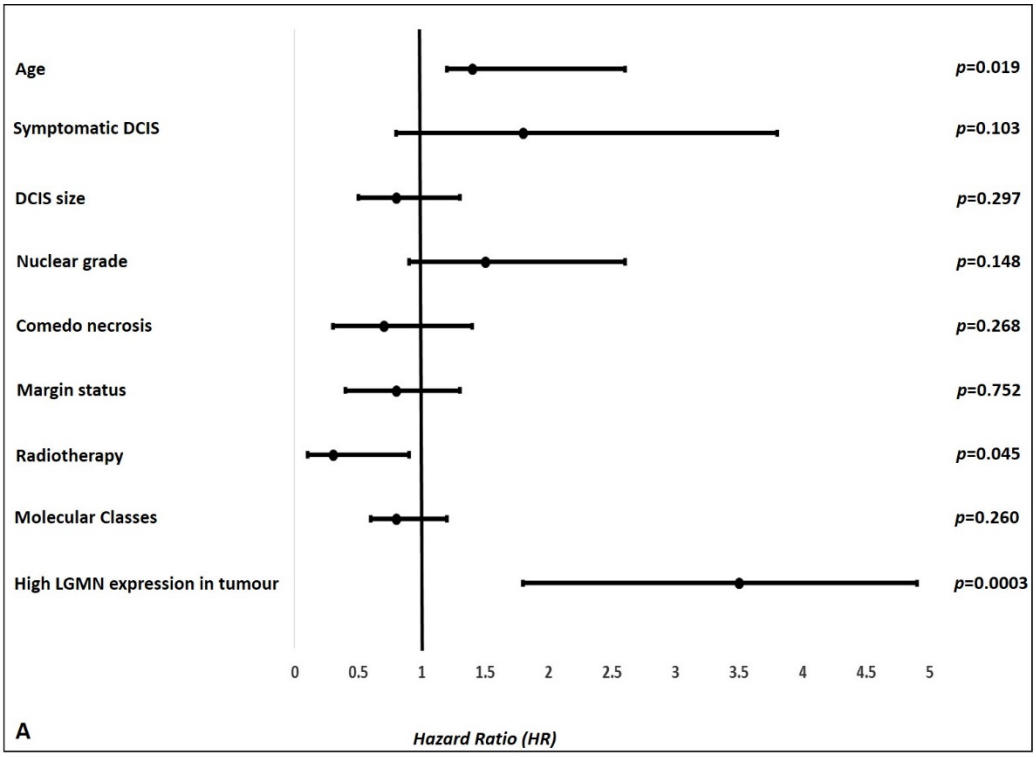

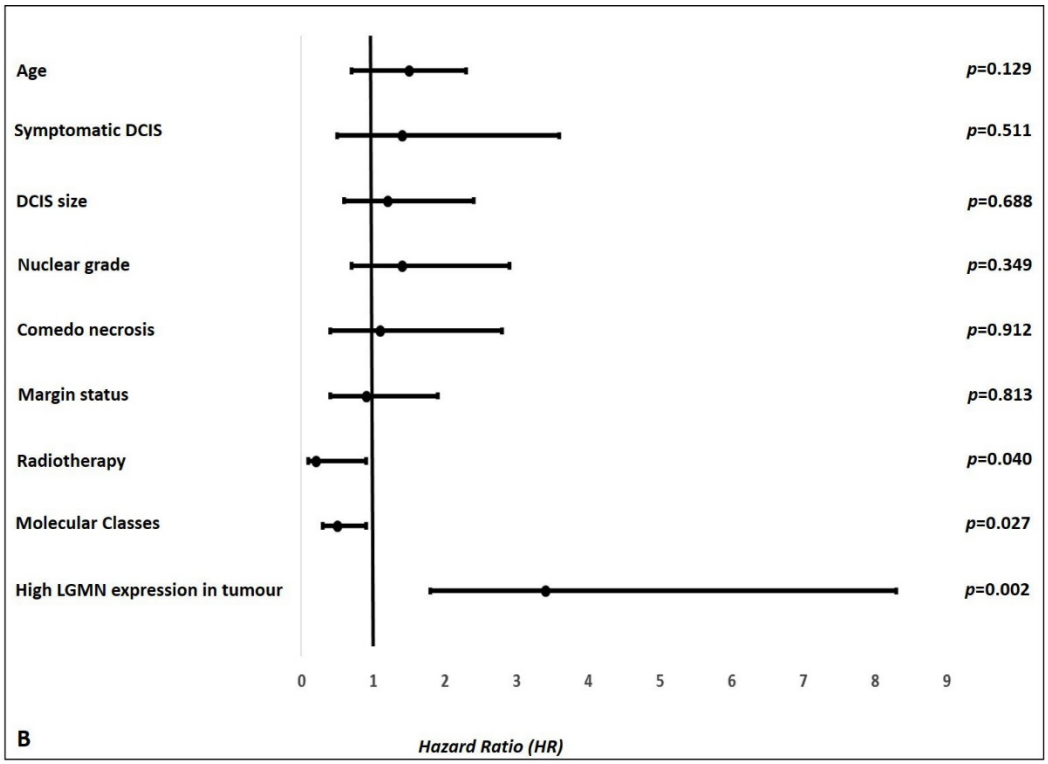

Figure 6-21: Forest plots showing the hazard ratio of the different clinicopathological parameters and ipsilateral tumour recurrence for patients treated with breast conserving surgery in pure DCIS cohort

A) all recurrences whether DCIS or invasive breast cancer and B) for invasive recurrences only

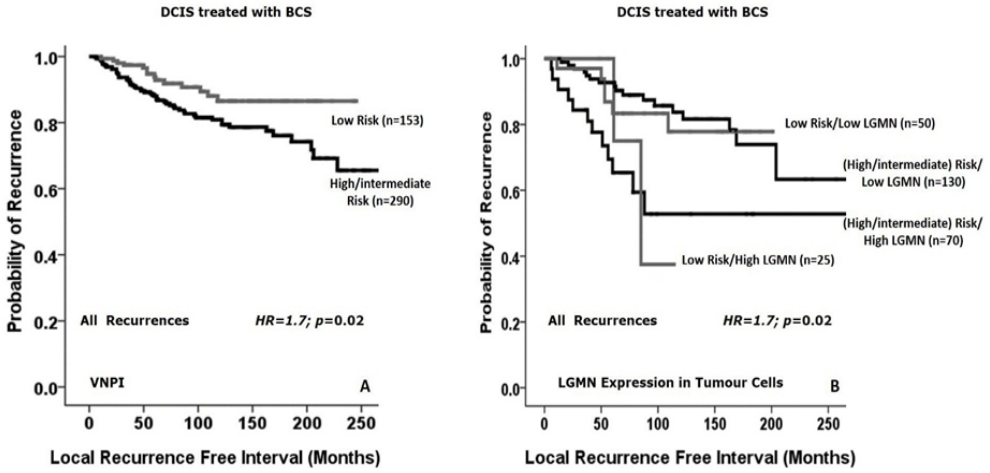

Figure 6-22: Kaplan Meier curves show the association between DCIS risk and local recurrence free interval in patients treated with breast conserving surgery

Van Nuys Prognostic Index alone (A), and when legumain was incorporated with the Van Nuys Prognostic Index (B)

6.7.4.5 COL11A1

Higher COL11A1 expression within the epithelial tumour cells was associated with shorter LRFI for all recurrences (DCIS and IBC) (HR=2.5; 95%CI=1.4-4.2, p=0.001) and showed a trend for invasive recurrences (HR=1.8; 95%CI=0.9-3.7, p=0.08) (**Figure 6-23**), while higher stromal expression was associated with shorter LRFI in the whole cohort for all recurrences and invasive recurrences (HR=15.9; 95%CI=9.1-27.5, p<0.0001 and (HR=12.1; 95%CI=6.1-24.0, p<0.0001, respectively) (**Figure 6-24**). Comparable results were obtained when the analysis was carried out with respect to different treatment groups (**Figure 6-24**). In the pure DCIS cohort, patients treated with BCS and followed by adjuvant RT showed better outcome than those treated with BCS only either for all recurrences (HR=0.5, 95%CI=0.3-0.9, p=0.014) or invasive recurrence (HR=0.3, 95%CI=0.2-0.8, p=0.008). Interestingly, when the cohort was stratified according to COL11A1 expression, RT did not improve the outcome in patients with high stromal COL11A1 either in all recurrences (HR=0.8, 95% CI=0.5-1.6, p=0.587) or for invasive recurrences (HR=0.6; 95% CI=0.2-1.8, p=0.225) compared to patients with low COL11A1 expression (HR=0.2; 95% CI=0.2-0.9, p=0.04 for all recurrences and HR=0.4; 95% CI=0.1-0.7, p=0.03 for invasive recurrences) (**Figure 6-25**).

Supporting this, evaluation of the interaction between high stromal COL11A1*RT using a Cox regression model showed significant association with shorter LRFI (HR=4.2, 95%CI=1.5-11.7, p=0.006). Furthermore, high COL11A1 expression within the stromal fibroblasts was associated with poorer outcome in all DCIS groups irrespective of the DCIS nuclear grade (low, intermediate and high) for all recurrences and for invasive recurrences (all p<0.0001).

Multivariate Cox proportional hazards analysis for the conventional clinicopathological parameters used to assess DCIS risk showed that patient's age at diagnosis, DCIS size, nuclear grade, presence of comedo type necrosis and surgical resection margins were independent prognostic factors for disease recurrence. However, when expression of COL11A1 in stromal fibroblasts was included in the model, it was solely the independent poor prognostic factor for tumour recurrence in patients treated with breast conserving surgery regardless of known other determinants of high risk DCIS; either for all recurrences (HR=13.2, 95%CI=6.9-25.4, p<0.0001) or when the analysis was confined to invasive recurrences (HR=11.2, 95%CI=4.9-25.8, p<0.0001), (**Table 6-18**).

Interestingly, when COL11A1 expression in the surrounding fibroblasts was incorporated with the other determinants of

DCIS risk described by VNPI [254], it provided better stratification for local recurrence risk, whereby high expression of stromal COL11A1 was associated with poorer outcome in all risk groups when compared to similar groups with low COL11A1 expression (HR=1.9, 95% CI=1.2-3.1; p=0.004) (**Figure 6-26**).

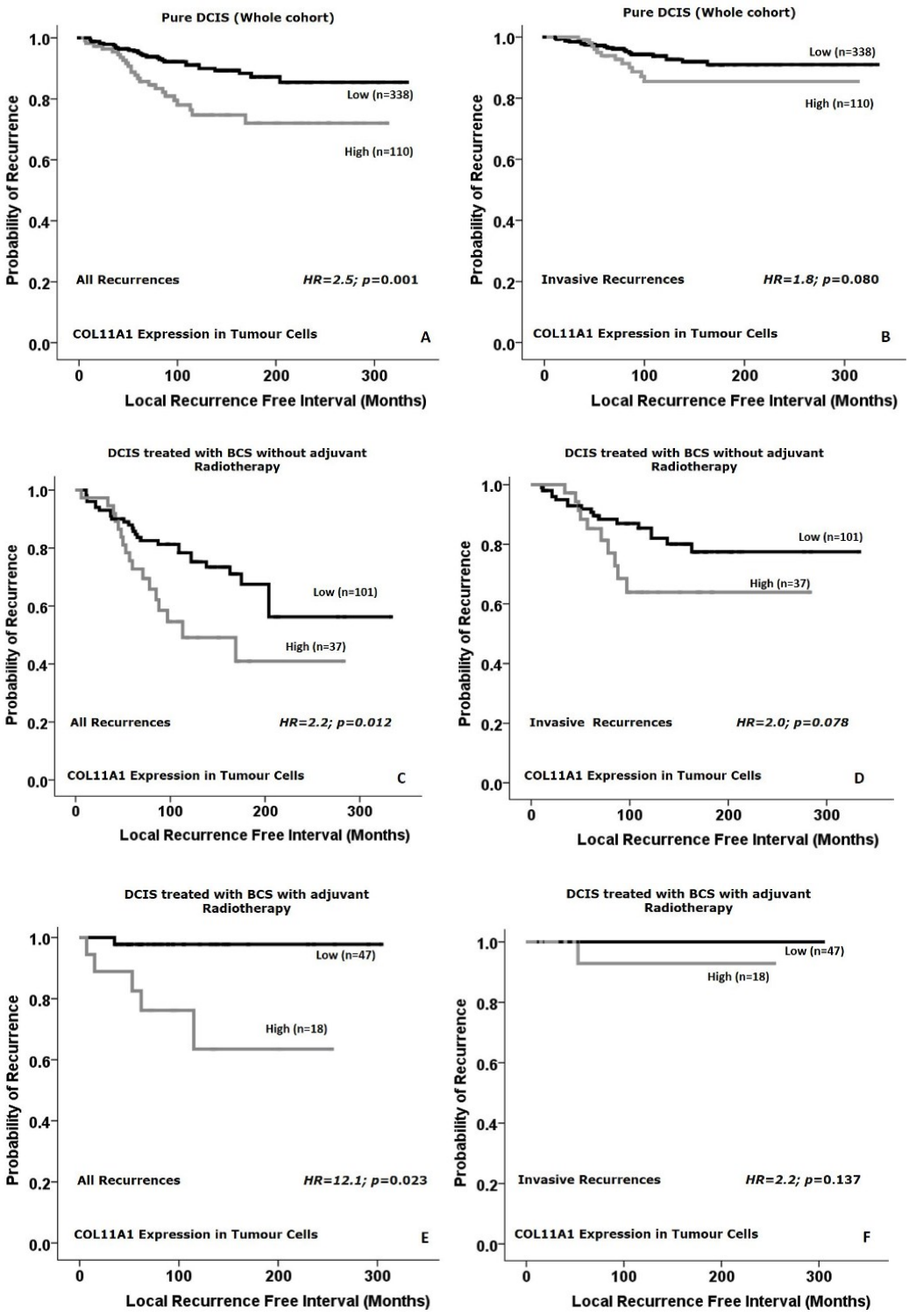

Figure 6-23: Kaplan Meier curves show the association between epithelial COL11A1 and outcome

High expression of COL11A1 within the tumour epithelial cells is associated with ipsilateral local recurrence free interval in the whole series either for all recurrences (A) or invasive recurrences (B), in breast conserving surgery without adjuvant radiotherapy (C; all recurrences and D; invasive recurrences) and in patients treated with breast conserving surgery followed by adjuvant radiotherapy (E; all recurrences and F; invasive recurrences)

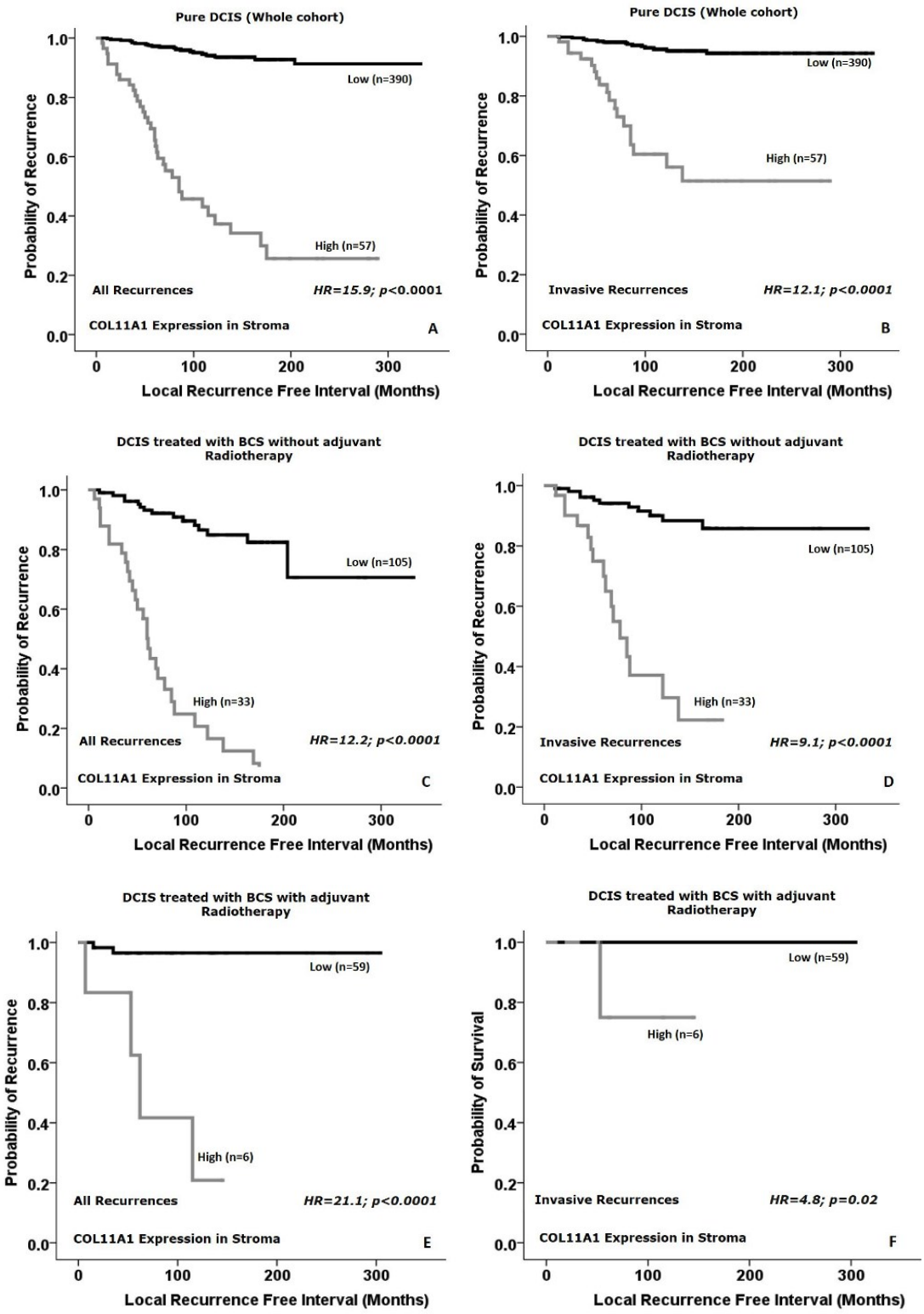

Figure 6-24: Kaplan Meier curves show the association between stromal COL11A1 and outcome

High expression of COL11A1 within the surrounding stromal fibroblast is associated with ipsilateral local recurrence free interval in the whole series either for all recurrences (A) or invasive recurrences (B), in breast conserving surgery without adjuvant radiotherapy (C; all recurrences and D; invasive recurrences) and in patients treated with breast conserving surgery followed by adjuvant radiotherapy (E; all recurrences and F; invasive recurrences)

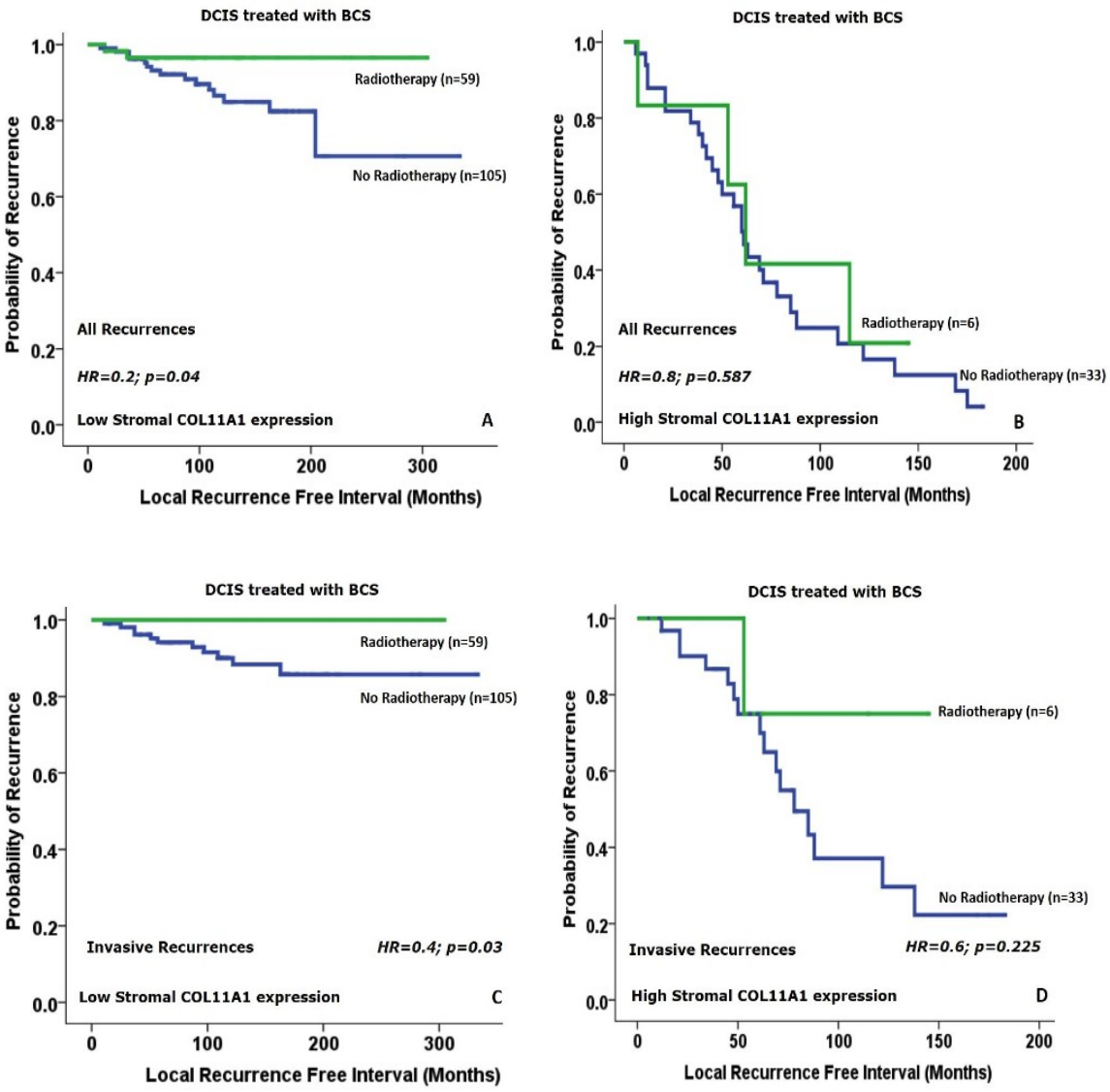

Figure 6-25: Kaplan Meier curves showing that radiotherapy is associated with better outcome in patients treated with breast conserving surgery and have low stromal COL11A1 expression

All recurrences (A), and invasive recurrences (C). While patients with high stromal expression of COL11A1 showed no difference in recurrence rate after radiotherapy for all recurrences (B), and for invasive recurrences (D)

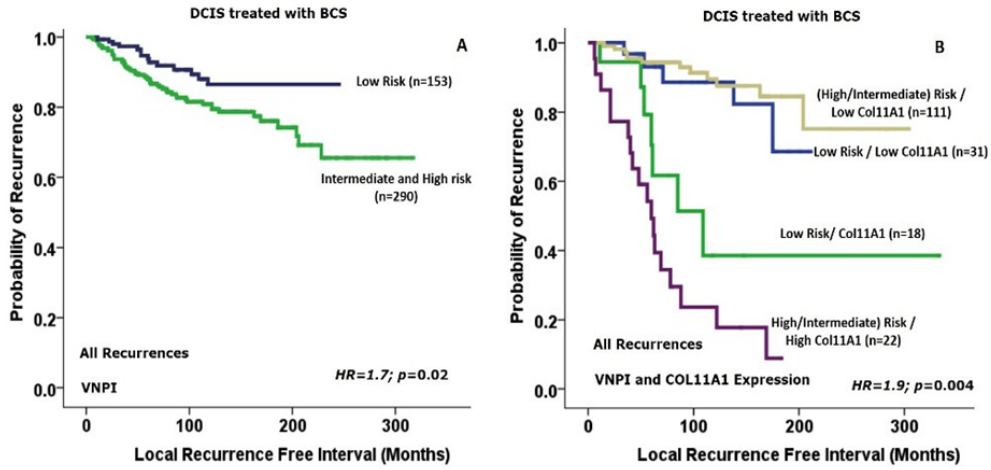

Figure 6-26: Kaplan Meier curves showing the association between DCIS risk and local recurrence free interval in patients treated with breast conserving surgery

Van Nuys Prognostic Index alone (A), and when COL11A1 was incorporated with the Van Nuys Prognostic Index (B)

Table 6-18: Multivariate survival analysis of COL11A and other variables predicting ipsilateral local recurrences in patients treated by BCS

1. All recurrences

Conventional clinicopathological parameters associated with high risk DCIS				
Parameters	Hazard ratio (*HR*)	95% *confidence interval (CI)*		*p*-value
		Lower	Upper	
Patient Age	0.4	0.2	0.8	**0.006**
DCIS presentation	1.5	0.9	2.4	0.111
DCIS size	1.5	1.1	2.1	**0.040**
DCIS nuclear Grade	1.9	1.3	2.7	**0.001**
Comedo necrosis	0.6	0.4	0.9	**0.049**
Margin status	0.8	0.7	0.9	**0.004**
COL11A1 and other clinicopathological parameters associated with high risk DCIS				
High stromal COL11A1 expression	13.2	6.9	25.4	**<0.0001**
Patient Age	0.6	0.3	1.4	0.261
DCIS presentation	1.9	0.9	3.9	0.084
DCIS size	1.1	0.7	1.9	0.609
DCIS nuclear Grade	1.6	0.9	3.1	0.123
Comedo necrosis	0.5	0.2	1.2	0.120
Margin status	1.0	0.9	1.1	0.728

Significant *p* values are in **bold**
COL11A1; Collagen (XI) alpha-1 chain, DCIS; ductal carcinoma in situ.

2. Invasive recurrence

Conventional clinicopathological parameters associated with high risk DCIS				
Parameters	Hazard ratio (*HR*)	95% *confidence interval (CI)*		*p*-value
		Lower	Upper	
Patient Age	0.5	0.2	1.3	0.156
DCIS presentation	1.4	0.8	2.6	0.245
DCIS size	1.8	1.1	2.4	**0.013**
DCIS nuclear Grade	1.9	1.1	3.0	**0.013**
Comedo necrosis	0.7	0.4	1.3	0.274
Margin status	0.9	0.8	1.1	0.075
COL11A1 and other clinicopathological parameters associated with high risk DCIS				
High stromal COL11A1 expression	11.2	4.9	25.8	**<0.0001**
Patient Age	0.9	0.3	3.3	0.974
DCIS presentation	2.0	0.8	5.2	0.156
DCIS size	1.5	0.7	2.9	0.258
DCIS nuclear Grade	1.9	0.8	4.4	0.119
Comedo necrosis	0.5	0.2	1.3	0.159
Margin status	1.1	0.9	1.2	0.386

Significant *p* values are in **bold**
COL11A1; Collagen (XI) alpha-1 chain, DCIS; ductal carcinoma in situ.

6.8 **Discussion**

The treatment of DCIS remains a challenge as the clinicopathologic features of the disease do not reliably stratify patients into distinct risk groups to tailor treatment decisions [530]. For this reason, some studies have attempted to risk stratify DCIS based on genetic and molecular factors including Oncotype Dx® DCIS score [78, 361, 531-533]. Although this score minimised the proportion of patients undergoing RT, the assay is expensive and not cost-effective [534], and shows inconsistent results and therefore needs further validation [77, 534]. None of the investigated parameters have been translated to clinical practice outside the US. Lack of robust prognostic markers is due to lack of adequately powered and methodologically sound studies (case-control, unbiased, comparison between DCIS that recur as invasive disease versus those do not). Therefore, there is a pressing need to identify robust and cost-effective biomarker(s) to predict outcome for DCIS patients.

DCIS progression is a complex process with interaction between tumour cells and TME. An explanation of disease progression based exclusively on intrinsic tumour cell factors is insufficient, as there is group of low grade DCIS with indolent appearance and low proliferation index that yet

carries progression potential to IBC [218]. In contrast, a considerable proportion of high-grade proliferating lesions remain as DCIS without progression. Laser-capture microdissection and microarray analysis show that whereas thousands of genes are differentially expressed in the epithelium during the transition from normal to DCIS, the majority of genes consistently showing differential expression from DCIS to IBC are associated with the stromal TME, highlighting its profound importance in the development of IBC [189, 211, 535-537]. It was reported that changes in the breast TME are often observed as early as the DCIS stage or even earlier, where hyperactive mitogenic signalling in epithelial cells results in secretion of many chemokines which modulate the surrounding tissues in a paracrine-like action [538, 539]. In turn, the stromal and epithelial cells participate in reciprocal and paracrine-acting signalling loops, which then remodel and condition the ECM and promote tumour cell proliferation, maintenance and invasion [189, 478, 540, 541].

Using the METABRIC cohort for robust molecular data in a large number of IBC showed associations between aggressive behaviour of IBC and higher levels of all chosen biomarkers in this study at the mRNA level. This observation supports our hypothesis that these markers are promising candidate

markers for evaluation as studies to decipher its role in DCIS behaviour and its association with disease progression have been lacking.

P4HA2 is one of the key regulator enzymes for collagen biosynthesis, stabilisation, ECM remodelling and stiffness [480] and has been reported to associate with poor outcome in many malignant tumours [481, 482, 485].

In this study, we evaluated the pattern of P4HA2 expression either within tumour epithelial cells or surrounding fibroblasts in a large annotated cohort of DCIS with long term follow up data. This is the first report of IHC staining for P4HA2 in any human breast tumour cohort to the best of our knowledge. High expression of P4HA2 was associated with other determinants of high-risk DCIS and poor outcome. These associations give insight for the potential role of P4HA2 in DCIS behaviour through its action in enhancing stromal stiffness and collagen deposition/alignment, which in turn might help in tumour aggressiveness [542]. Supporting this idea, our results showed that P4HA2 expression is higher in DCIS co-existing with invasive carcinoma than pure DCIS, and much higher in the stromal fibroblasts surrounding the invasive component. These findings are further supported by gene expression profiles that showed *P4HA2* mRNA level is

higher in IBC than DCIS [484, 485]. Stromal fibroblasts as well as tumour cells can produce P4HA2 and affect the surrounding ECM [483]. Our data showing strong tumour epithelial cell expression is entirely consistent with this report.

Importantly, the data showed association of higher P4HA2 expression with invasive recurrence. In concordance with the findings, thickening and linearisation of collagen fibres are often found in areas of active tissue invasion, suggesting their active role in facilitating cancer progression [196]. Indeed, studies using live imaging have shown that cancer cells migrate rapidly in areas enriched in collagen [195]. Gilkes *et al.*, reported that cancer cell invasion usually occurs with oriented collagen fibres at the tumour-stromal interface, and aligned collagen fibres can facilitate cell migration and invasion [483]. Moreover, in xenograft models a significant amount of aligned collagen fibres is detected in the tumours' invasion margins in a control group compared to the P4HA2-silenced group [485]. Taken together, DCIS with high P4HA2 expression may have a microenvironment supportive of tumour growth and therefore need to be managed properly to avoid progression or recurrence. This study shows that expression of P4HA2 in the tumour, but not stromal expression, is associated with recurrence a finding that might

reflect the potential epithelial cell-intrinsic role of early stage tumours in ECM remodelling that facilitates tumour progression and the dual role of tumour and stromal cells in progression and aggressiveness of advanced tumours. The latter interaction is supported by the dramatic increase of P4HA2 expression in stromal cells surrounding the invasive component compared to those surrounding the DCIS component in mixed cases or those surrounding pure DCIS. However, further functional studies are highly recommended to understand the underlying mechanisms of P4HA2 expression in carcinogenesis and tumour progression either from the tumour cells or the surrounding stroma. Interestingly, the results show that high P4HA2 expression is not associated with recurrence in patients treated with postoperative RT. Moreover, postoperative RT is associated with longer LRFI in patients with high P4HA2 than those with low P4HA2 expression. Taken together, P4HA2 is not only a marker to identify high-risk patients who need proper treatment with surgery followed by RT, but also suggest that adjuvant RT provides more benefit in DCIS expressing high levels of P4HA2, which needs further investigation to understand the underlying mechanisms.

Nonetheless, multivariate analysis shows that only RT and P4HA2 expression were significant prognostic factors, suggesting P4HA2 may be a more powerful marker of high risk than conventional features. Moreover, using the conventional clinicopathological features and the previously described Van Nuys Prognostic Index [62] could not provide a proper DCIS risk stratification, which supports the contention that more robust criteria for DCIS risk determination is required. Incorporation of P4HA2 with the other clinicopathological factors provided a better identification of different risk groups. These findings indicate that P4HA2 is a promising marker for better definition of high-risk DCIS as well as identification of a group of patients with lower risk where RT could be omitted.

Although the exact mechanism of how P4HA2 overexpression and subsequent ECM remodelling helps in tumour progression is unclear, there are many hints from existing data. Deregulation of ECM dynamics can facilitate cellular dedifferentiation and cancer stem cell expansion [543, 544]. Additionally, it disrupts tissue polarity and promotes cellular motility and tissue invasion [545]. As a result, epithelial cells are directly affected by deregulated ECM dynamics, leading to cellular transformation and metastasis [543, 545-547]. Collagen fibre alignment plays a critical role in directing the

migration of tumour cells in vivo [548]. Moreover, increased stromal stiffness in BC facilitates integrin clustering to promote focal adhesions between tumour cells and surrounding stroma, which drive invasion [549]. Also, it has been shown in xenograft studies that P4HA2 regulates tumour growth. Silencing of P4HA2 expression or treatment with a P4HA inhibitor significantly inhibited cell proliferation and suppressed aggressive phenotypes of BC cells in 3D culture, accompanied by reduced deposition of collagen I and IV [485].

A key driver of P4HA2 and other ECM remodelling proteins is hypoxia and related factors, mainly HIF1a [550], supporting our finding that high P4HA2 expression is associated with higher levels of HIF-1α. P4HA2 has been reported to co-localise with HIF-1α in peri-necrotic, i.e. hypoxic, areas within tumours [550, 551]. The hypoxia pathway has a complex role in tumour progression through enhancing angiogenesis, tumour proliferation, secretion of growth factors and other proteolytic enzymes [551]. Therefore, P4HA2 overexpression might be a consequence of hypoxia related changes. In addition, hypoxia is associated with overexpression of lysyl oxidases, proteins known to promote cell invasion by increasing tissue tension and ECM rigidity [485]. These results

indicate that the ECM microenvironment remodelled by cancer cells is critical for cancer progression.

Cathepsins are a superfamily of proteins expressed in various types and stages of human cancers [552]. Each member of this family has different functions compared to each other under normal and cancerous conditions. Several cathepsins have been studied and linked to poor prognosis in BC [553]. The transcriptomic analysis showed *CTSA* is differentially expressed between DCIS and IBC [189]. *CTSV* is one of the gene including in the Oncotype DX® of IBC as a marker of invasiveness. These findings rationalise studying their role in DCIS behaviour. However, there is lack in studies assessing the prognostic role of CTSA and CTSV at the protein level in BC and particularly in the pre-invasive tumours. To date, this is the first IHC based study assessing their expression in BC, in the epithelial tumour cells and surrounding stroma. The results here showed that both pure DCIS and the DCIS component of mixed tumours had significantly less CTSA and CTSV staining than IBC both within the tumour cells and in the surrounding stromal fibroblasts. Fibroblasts have previously been reported to be an additional source of CTSA activity [554, 555]. These results reflect the interactive role between tumour cells and surrounding tissues in tumour aggressiveness.

Analysis of both Cathepsin A and V in a large well characterised cohort of DCIS supported the hypothesis that these proteins would be associated with features of high-risk DCIS. In addition, the poor prognostic significance of higher CTSA and higher stromal CTSV expression expressions was shown to be independent from other clinical and morphological features. Stromal CTSV was particularly correlated with recurrence as invasive disease, which reflects the important role of the surrounding microenvironment in tumour progression to IBC.

Despite the direct role of CTSA and CTSV in the BM and ECM degradation that helps in tumour invasion, there are other mechanisms by which they might contribute to tumour aggressiveness. For instance, an increase in CTSA chymotrypsin-like activity was documented to induce the degradation effect of tumour suppressor proteins leading to greater resistance to apoptosis, which would result in more aggressive cancer behaviour [489]. Another mechanism by which CTSA participates in tumour growth is by regulating chaperone-mediated autophagy, which is reported to be essential for cancer cell proliferation [556]. CTSV plays a role in tumour growth through loop connection with the surrounding inflammatory cells [140]. Finally, like all cysteine proteases, activation of CTSA and CTSV, requires a low pH

acidic environment [497]. The observation of an association between high CTSA and CTSV with HIF-1α, which usually is accompanied by lower pH, supports the elevated expression as a mechanism of surviving acidic hypoxic environments and more aggressive behaviour. Altogether, these findings support a role in disease progression for the crosstalk and interactions between various factors within the DCIS tumour cells and the surrounding microenvironment.

The role of CTSA in inflammatory processes and in antigen presenting cell function was previously studied [490]. Moreover, overexpression of CTSA in tumour associated macrophages and lymphocytes of the surrounding tissues has been reported [490, 557]. Similarly, CTSV has a role in inflammatory conditions and autoimmune diseases mainly through modulating antigen presenting cell function [140, 495, 498]. Here, there was a tendency for high CTSA and CTSV expression in DCIS harbouring dense lymphocytic infiltration that may be associated with an inflammatory function or tumour associated immunity role for CTSA. Further studies are highly warranted to decipher the possible underlying biological interaction and its significance.

The lysosomal cysteine protease LGMN is a proteolytic enzyme and plays role in autoimmunity and cancer [505, 558].

Overexpression of LGMN is linked with poor prognosis in different tumour s including IBC [501, 506-508, 559, 560]. Its action depends mainly on increasing the invasive and metastatic potential of the tumour via its proteolytic properties and stromal degradation [561]. Comparing LGMN expression between normal, borderline and invasive ovarian tissues reveals that it has a role not only in tumour migration and invasion but also in tumour development [559]. However, similar studies are lacking in BC to assess the role of LGMN in DCIS. It was reported that *LGMN* is differentially expressed between normal breast tissue and IBC [558]. These observations support our hypothesis that LGMN is a promising candidate marker that requires additional studies to decipher its role in DCIS behaviour.

Interestingly, high LGMN expression was associated with other features of high-risk DCIS. These findings support the role of LGMN in DCIS progression. Supporting this, our results showed that LGMN expression is higher in DCIS co-existing with invasive carcinoma than pure DCIS, and much higher in the invasive component either within the tumour cells or in the surrounding stromal fibroblasts.

The poor prognostic value of LGMN was shown with a shorter LRFI in patients with high levels of LGMN expression

independently from other clinicopathological factors. These findings were consistent for all recurrent events, either DCIS or IBC or when the analysis was confined to invasive recurrences only, which provides more evidence that LGMN plays a key role in DCIS progression to invasive disease. The study shows that expression of LGMN in tumour epithelial cells, but not stromal cells, is associated with recurrence; a finding that might reflect the potential epithelial cell-intrinsic role of early stage tumours in ECM degradation that facilitates tumour progression and the dual role of tumour and stromal cells in progression and aggressiveness of advanced tumours. The latter interaction is supported by the dramatic increase of LGMN expression in stromal cells surrounding the invasive component compared to those surrounding the DCIS component in mixed cases or those surrounding pure DCIS.

Incorporation of LGMN with the other clinicopathological factors provided a better identification of different risk groups. These findings indicate that LGMN is a promising marker for better definition of high-risk DCIS as well as for the identification of patients with lower risk where RT could be omitted.

Thus far, little is known about the biological processes which involve LGMN in cancer progression. However, a correlation

was observed between tumour invasion and metastasis and the presence of cysteine endopeptidases, such as cathepsins B and L [492]. Protease zymogen cathepsins B and L may also be activated by LGMN-mediated hydrolysis of asparaginyl bonds. LGMN acts as an asparaginyl endopeptidase in regulation of ECM remodelling through the activation of zymogen progelatinase A, which is an important mediator of ECM degradation, or the degradation of fibronectin, which is a main component of the ECM [562, 563]. Animal tumour models generated with cells overexpressing LGMN demonstrated an in vivo behaviour that is vigorous with more invasive growth and metastasis [246, 505, 558]. This phenotype is proposed to result from the proteolytic function of LGMN to activate other protease zymogens. The inhibitory effect of cystatins on tumour cells is consistent with the involvement of LGMN, and perhaps other cysteine proteases, in tumour invasion and metastasis. Whether the tumour suppressing effect is mediated through inhibition of LGMN catalytic activity or other cysteine proteases is presently unknown [562].

LGMN is present intracellularly in a pro-active form [558, 561] and one of the activating mechanisms is low pH. Interestingly, our findings showed that LGMN is associated with presence of

comedo-type necrosis, which is consistent with low pH and supports our findings. LGMN is usually overexpressed in cells adjacent to necrosis [558], which was observed in our study as well where central cells facing the comedo necrosis showed higher LGMN expression than the peripheral cells within the ducts.

The role of LGMN in tumour aggressiveness is not related solely to its proteolytic activity but also to its proliferation activation mechanisms. This may be related to decreased apoptotic activity of cells and increased calcium influx into cells [505, 564]. Supporting this possibility, our study showed that LGMN was expressed in highly proliferative DCIS, which may further augment the adverse action of LGMN in the context of disease outcome.

The role of LGMN in autoimmune disease and inflammatory process is undeniable [561]. LGMN functions in antigen presentation to inflammatory cells may be a cause for such phenomenon. Overexpression of LGMN in tumour associated macrophages and endothelial cells of the surrounding tissues has been reported [560]. Accordingly, the link between LGMN and dense inflammatory cell infiltrates is warranted to be investigated. There was a striking association of high stromal LGMN and a dense lymphocytic infiltrate in pure DCIS that

may be associated with an inflammatory function for LGMN. Taken together, LGMN may interact with the inflammatory cascade and affect DCIS behaviour.

COL11A1 is a minor fibrillary collagen present mainly in cartilage, but it is produced at varying levels by other normal tissues as well as and under some pathological conditions. Interestingly, several studies reported that overexpression of COL11A1 by tumour cells and/or the surrounding CAFs is linked with tumour progression and poorer prognosis in a variety of cancers including IBC [513-515, 517, 518, 565]. Moreover, in IBC, some authors reported that COL11A1 is exclusively produced by invasive tumours [521], while others showed that it is expressed in normal, preinvasive and invasive tumours at different levels [565]. *COL11A1* is differentially expressed between IBC and DCIS [523], however there is no previous study investigating its role in DCIS progression and its potential prognostic significance. These observations support our hypothesis that COL11A1 is a promising potential protein that could provide additional knowledge to DCIS behaviour and might help in the stratification of disease risk.

High COL11A1 expression was associated with some features of high-risk DCIS. Additionally, the data showed that COL11A1

expression was higher in DCIS co-existing with IBC than pure DCIS, and much higher in the invasive component both within the tumour cells and in the surrounding stroma.

The prognostic value of COL11A1 was shown with a shorter LRFI in patients with higher levels of COL11A1 expression, particularly stromal expression, independently from other clinicopathological factors. These findings were consistent for all recurrent events including DCIS and IBC, and also when the analysis was confined to invasive recurrences only, which provides more evidence that COL11A1 could play a key role in DCIS progression to invasive disease. Although it was thought that COL11A1 is exclusively produced by CAFs, other studies showed that COL11A1 was expressed in tumour cells as well as the surrounding stroma [523, 565]. This study showed that expression of COL11A1 in tumour epithelial and stromal cells is associated with disease recurrence; a finding that might reflect the epithelial-stromal interaction and its role in progression of DCIS. This interaction is supported by the obvious increase of COL11A1 expression in stromal and epithelial cells surrounding the invasive component compared to those surrounding the DCIS component in mixed cases or those surrounding pure DCIS. It was observed that higher expression COL11A1 is associated with periductal stromal

reaction around DCIS, a finding that was reported to be associated with invasive recurrence in DCIS [566]. However, further functional studies are highly recommended to understand the underlying mechanisms and functions of COL11A1 expression in carcinogenesis and tumour progression either from the tumour cells or the surrounding stroma.

Multiple authors have noted a group of low grade DCIS with indolent appearance and low proliferation index that yet carries progression potential to IBC [167, 189, 567]. An explanation of disease progression based exclusively on intrinsic epithelial tumour cell-related factors is inadequate and identifying other candidate potential markers that could explain progression of different phenotypes and hence better risk stratification is highly warranted. The findings showed that there was no association between high COL11A1 expression and other conventional clinicopathological factors that are described as a surrogate for high risk DCIS such as younger age at diagnosis, high grade DCIS, comedo-type necrosis and mode of presentation. In addition, high expression of stromal COL11A1 showed an association with recurrence regardless the grade of the DCIS or method of therapy. These findings show that COL11A1 is a very promising protein for better DCIS

risk stratification and understanding of the disease biology. Moreover, incorporation of COL11A1 with the other clinicopathological factors described in the VNPI provided a better stratification of different risk groups. These findings indicate that COL11A1 is a marker that could be used to better define high-risk DCIS and identify of patients who need more radical treatment e.g. BCS with wider excision margins or mastectomy.

Although the effect of RT in reduction of DCIS recurrence in undeniable [93, 98, 285, 289], there is still a considerable proportion of patients treated with BCS and followed by adjuvant RT who develop disease recurrence. There are no data available for DCIS patients at higher susceptibility to show poor outcome after adjuvant RT management. Our findings showed that high expression of stromal COL11A1 is associated with higher rate of recurrence even with RT compared to DCIS with lower levels of expression, which indicates that COL11A1 could provide a signature for RT resistance in DCIS. However, the number of cases with recurrence after RT, especially invasive recurrence, is low, and this finding needs to be assessed in an independent cohort. Studies showed that dense stroma is associated with poor response to RT in cancer treatment [568, 569] which might

provide a similar explanation in DCIS. These findings warrant more validation and mechanistic studies to decipher the underlying mechanisms and biology.

The data supports a key role for COL11A1 in progression to invasive disease and yet high levels of COL11A1 were highly significantly related to invasive recurrence. Thus far, understanding of the biological processes which involve COL11A1 in cancer progression is lacking, although we hypothesise that high stromal COL11A1 may in some way enable individual tumour cell invasion and/or remnant cell survival beyond the surgical margin, leading to invasive recurrence. Collagen provides a scaffold for the tumour cells and helps in tumour growth, angiogenesis and invasion [509]. These findings are supported by the association between COL11A1 and proliferation and hypoxia related proteins in our cohort. The link between hypoxia and increased collagen deposition and remodelling through P4HA2 and lysyl oxidase enzymes is well studied even in DCIS [483, 570, 571]. One of the potential mechanisms that COL11A1 could use in promoting cellular proliferation is its association with the Smad signalling pathway via binding to integrin [513]. In addition, it was thought that collagen acts as a barrier against tumour invasion, but now it is proven that it has multifaceted roles

and could promote tumour progression. Increased collagen deposition promotes tumour progression through destabilisation of cell polarity and cell-cell adhesion, and enhancement of growth factor signalling. Tissue tension regulates the EMT through crosslink between tumour cells and stromal cells [572, 573].

The five novel biomarkers presented in this chapter are assessed separately. The author tried to put them all into a multivariate analysis model to see if they are independent of each other or if they interact, or to develop an index or signature that could predict DCIS recurrence based on clustering of these proteins. The different final number of cases included in the analysis of each biomarker was a limiting factor to perform this clustering analysis due to missing values. Multivariate analysis was not reliable because of loss of power due to low number of cases with complete data for all markers. Expansion of the cohort or applying statistical methods for handling missing data are possibilities to create a protentional prognostic DCIS index based on these biomarkers. Exploring these solutions is highly warranted.

In conclusion, the difficulty in implementing predictive markers for DCIS remains the availability of large cohorts with consistent treatment for validation, and this study is an

exception. ECM remodelling and degradation are essential steps for DCIS progression. P4HA2, CTSA, CTSV, LGMN and COL11A1 are independent prognostic factors in DCIS which require further functional studies to extensively validate the role of these biomarkers as predictors of progression to invasive disease.

7 Chapter 7: Geometric characteristics of collagen in DCIS

7.1 Introduction

The key difference between IBC and DCIS is the destruction of the surrounding BM and invasion of the malignant cells into the surrounding stroma accompanied by desmoplastic reaction. However, studies have shown that changes in the surrounding TME including TILs, stromal cells and ECM composition occurs early in carcinogenesis much before malignant cells invade the surrounding stroma [178, 222, 230, 574, 575]. More so, these changes may provide a surrogate to predict tumour behaviour and potential outcomes [178, 411, 576]. One of the major limitations of currently available clinicopathological indices and molecular signatures to predict risk of recurrence in DCIS patients is the underestimated role of microenvironmental factors. Therefore, despite advances in management modalities, a considerable percentage of DCIS are either over- or under-treated. In addition, most molecular studies that have compared the genetic profiles of DCIS and IBC report a high degree of similarity [35, 218], creating a compelling need to decipher the role of the TME in DCIS behaviour.

7.1.1 Collagen

Collagen is the main constituent of ECM and plays a crucial role in tissues homeostasis [571]. There are many types of

collagen with varied localisations and functions in normal and pathological conditions [571, 574]. The role of collagen in cancer development is not solely related to its chemical composition or signalling interaction but is mainly linked to its physical properties and geometric characteristics in relation to the tumour cells [195, 196, 575, 577]. Recent advances in imaging techniques and specific histochemical staining of collagen have spurred an increased interest to discover its physical roles and biological functions [577-580]. In invasive cancers including BC, studies have shown that densely aligned collagen is associated with poor outcome and various TACS have been described to assess the collagen organisation surrounding IBC [195]. There is a dearth of studies deciphering the role of collagen in DCIS; hence more investigations are needed to evaluate its prognostic significance. While an earlier study has shown association of aligned collagen with other determinants of DCIS aggressive behaviour, no statistically significant association with disease recurrence or progression has been reported [576].

7.2 **Hypothesis and aims**

In this chapter, it was hypothesised that collagen re-organisation surrounding DCIS is linked to aggressive behaviour and that an imaged-based Collagen Prognostic

Index (CPI) that relies on three factors: the directionality of collagen fibre relative to DCIS boundary, collagen density and dispersion could be used for prognostication.

7.3 Patients and methods

7.3.1 Study cohort

This retrospective study was conducted on a consecutive series of primary pure DCIS cases and a series of cases diagnosed as synchronous DCIS and invasive tumours (mixed DCIS and IBC) as a validation set, prepared as TMA (**Chapter 2**).

Demographic details, histopathological, management, RT and patient outcome data were collated as previously described (**Chapter 3**).

7.3.2 Histochemical collagen staining

Picrosirius red (PSR) solution was prepared by mixing 0.5g of Sirius Red [Direct red 80, Cat#365548, Sigma-Aldrich, Darmstadt, Germany] with 500ml of saturated aqueous solution of picric acid [Cat# P6744-1GA, Sigma-Aldrich, Darmstadt, Germany]. TMA sections (4μm) were deparaffinised and rehydrated and immersed in PSR solution for 60 minutes. Physical removal of excess stain was carried out by vigorous slide shaking followed by gentle blotting

against soft filter paper. Slides were washed in two changes of acidified water, dehydrate in three changes of 100% ethanol 3 minutes each, cleared in xylene twice for 5 minutes each, mounted and cover slipped. Using light microscopy, epithelial cells were stained yellow while the collagen fibres stained red.

7.3.3 Image acquisition

The stained TMA sections were scanned using a high-resolution digital scanner (NanoZoomer; Hamamatsu Photonics, Welwyn Garden City, UK), at 20× magnification. For obtaining the images for subsequent analysis, individual tissue spots were exported as Joint Photographic Experts Group format (JPEG) (8-bit) files at ×20 magnification (1368 × 768 pixels). Multiple spots were exported for each core to represent the whole tissue. To improve the reliability of the study, cores with less than 15% area of stroma were excluded from the analysis. All excluded cases were unbiased with respect to clinicopathological features.

7.3.4 Image analysis

The image analysis was carried out by the author using the Fiji package of ImageJ (NIHR public domain) which is available for free download at (https://imagej.nih.gov/ij/download.html). Individual tissue spot JPEG files were imported into ImageJ and was split into RBG (Red, Blue, Green) channels. The image

segmentation of tumour from stroma was carried out on the green colour space; the red and blue channels were discarded. The segmentation to identify objects of interest was carried out by adjusting the greyscale data to a binary image with foreground pixels of interest set to red (pixel signal intensity of 0) and background pixels set to white (maximum 8-bit intensity of 255). The pixel intensity threshold for classifying all pixels as either foreground or background was defined automatically using the ImageJ histogram thresholding feature. To decease background noise, all images were adjusted to threshold of 150. Fields of interest (specialised stromal collagen surrounding DCIS ducts) [239] were identified by manually delineating of multiple squares, 400x400μm each in dimension (i.e. equivalent to two high power fields of the surrounding collagen), with their bases touching and parallel/tangential to the duct boundary at the area of contact. Several non-overlapping areas were marked per image to segment the surrounding stroma resulting in >100 fields (average 120 fields) of interest were delineated per each core. Features were extracted by measuring the pixel numbers for any particles in the final image using the automated built-in tools in ImageJ. Features extracted included the directionality of collagen fibres, i.e. the angle of the adjacent collagen fibres in each square relative to the

angle of the tangent (duct boundary); collagen fibres dispersion, i.e. the arrangement of fibres relative to each other; and solidity representing the collagen density. Data were recorded in degree (°) for directionality and dispersion while pixels were used for solidity measurement. Each field of interest was analysed separately and the average reading for each tissue core was considered as the final score for analysis. Moreover, cases with multiple cores were scored and the average of the final scores for each core were used for the analysis. **Figure 7-1** and **Figure 7-2** show a schematic representation of the image analysis process.

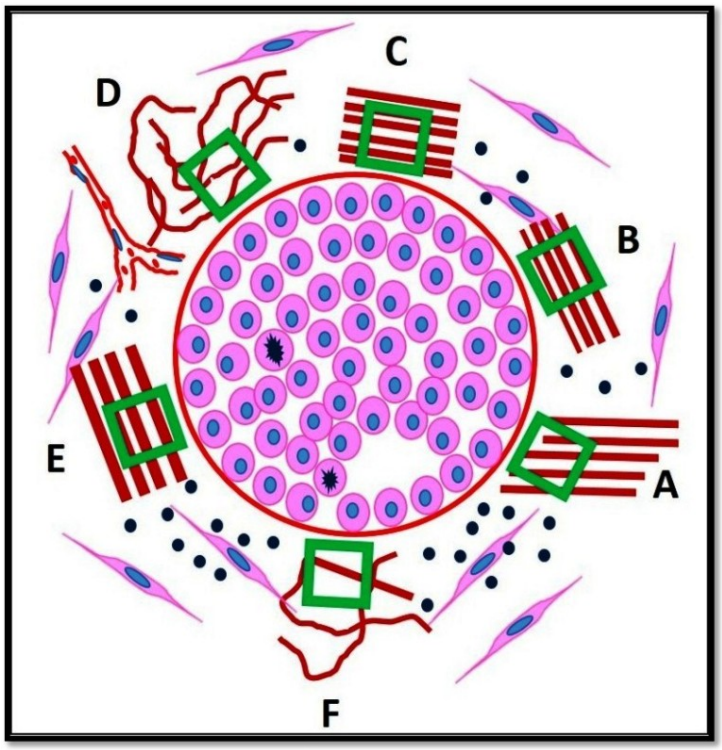

Figure 7-1: Diagram shows the different parameters assessed to evaluate the collagen characteristics surrounding DCIS

Green squares refer to the fields of interest for analysis (400x400μm surrounding the DCIS boundary and note that all squares are aligned touching and parallel to imaginary tangential line to the duct boundary. A) Perpendicularly arranged collagen fibres relative to duct boundary, B) Parallel arranged fibres towards the duct boundary, C) Collagen fibres arranged parallel to each other (lower dispersion) while D) randomly arranged fibres (higher dispersion). E) Dense collagen fibres and F) scanty collagen fibres. During the analysis the three parameters were assessed per each field of interest (square) and the final average value was used in the analysis

7.3.5 **Calculation of Collagen Prognostic Index score**

Each parameter was categorised into three scores (1, 2 and 3) using cut-offs generated from X-tile bioinformatics software (Yale University, version 3.6.1) [240] based on LRFI in the pure DCIS cohort (**Table 7-1**). Score 3 directionality indicated more perpendicular collagen fibres to duct boundary, score 3

solidity related to dense collagen fibres while score 3 dispersion referred to lower degree of collagen fibre dispersion i.e. collagen fibres parallel to each other. Collagen prognostic index was calculated according to the following equation;

Collagen prognostic index (CPI)=collagen directionality score (1-3) + collagen solidity score (1-3) + collagen dispersion score (1-3)

The generated score range was 3-9, and was divided into three prognostic groups based on X-tile software whereby a score of 3 or 4 is the good prognostic group, 5-7 for intermediate and score 8 or 9 indicates the poor prognostic group (**Table 7-1**).

Table 7-1: Scores of collagen directionality, dispersion, density and collagen prognostic index

	Collagen Directionality			**Collagen Dispersion**			**Collagen Solidity**		
Score	1	2	3	1	2	3	1	2	3
Thres hold	<13.6	13.6 - 19.6	>19.6	>15.8	12.3- 15.8	<12.3	<0.2	0.2- 0.6	>0.6

Collagen prognostic index (CPI) = Collagen directionality score + collagen solidity score + collagen dispersion score

Collagen prognostic index groups:

- Good prognostic group: Scores 3 or 4
- Moderate prognostic group: Scores 5, 6 or 7
- Poor prognostic group: Scores 8 or 9

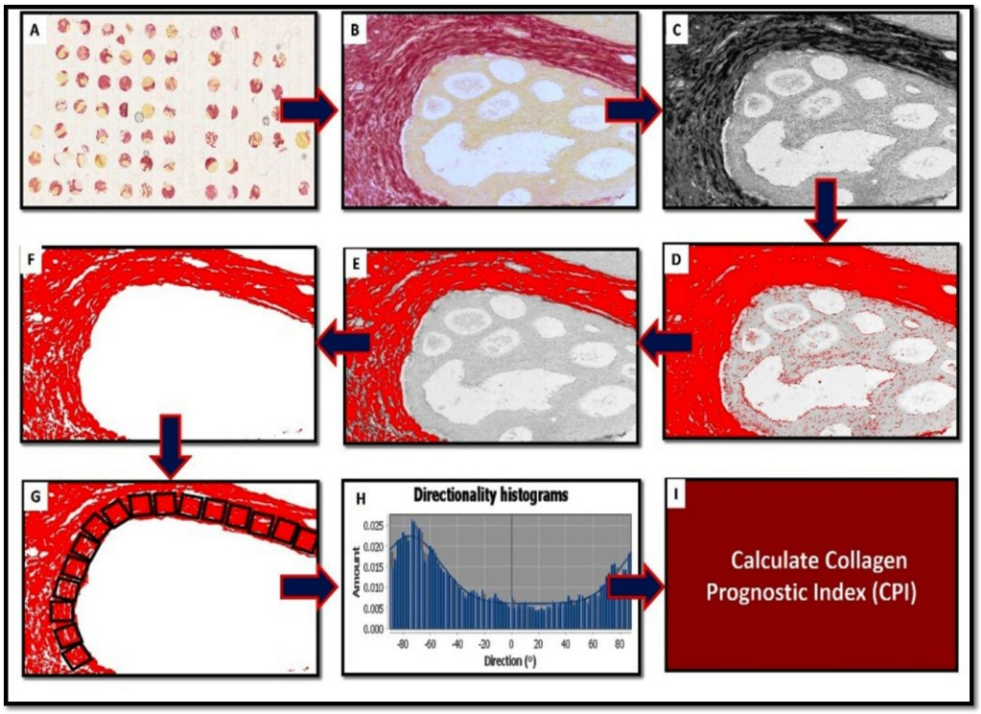

Figure 7-2: Schematic representation of evaluation of collagen around DCIS ducts

A) Scanned TMA section stained with PSR visualised by Imagescope software. B) Magnification of spot of interest 20x and exporting the image as JPEG format into ImageJ software. C) Splitting the colour channel using ImageJ built-in function and selection of the green channel. D) Visualisation of collagen fibres by adjusting the red pixels and the threshold at 150 to decrease the background noise. E,F) Segmentation of collagen fibres from other tissue components i.e. tumour cells, inflammatory cells in the stroma, red blood cells etc. G) Annotation of collagen at the specialised stroma surrounding DCIS by drawing a 400x400µm squares all over the area surrounding DCIS whereby the base of each square faces the duct boundary and is parallel to its tangential imaginary line. H) Run measurement for collagen dispersion, directionality and solidity using the ImageJ in built functionality. The final score used in the analysis is the average of the scores obtained from all images. I) Assessment of collagen prognostic index through sum of the scores of the 3 evaluated parameters.

7.4 **Results**

7.4.1 **Distribution of CPI**

The final number of cases suitable for scoring was 424 pure DCIS and 149 DCIS co-existing with IBC after unbiased exclusion of uninformative cores (lost, folded and those

containing <15% stroma area). The distribution of CPI and the three collagen geometric parameters are summarised in **Table 7-2.** The median directionality and dispersion angles in the pure DCIS were 19.6° (range 1-85) and 16.7° (range 5-58), respectively, while the median solidity was 0.5 (range 0.001-0.9) and the median CPI score was 6 (range 3-9). The distribution of all parameters was unimodal. The poor CPI group represented 24% of the cohort with a similar percentage of DCIS in the good prognostic group (23%). **Figure 7-3** shows various patterns of collagen arrangement surrounding DCIS. A positive linear correlation between high collagen solidity and perpendicular or oblique collagen arrangement related to the DCIS ducts' boundary was found (r=0.5, p<0.0001, Spearman's correlation). However, the degree of collagen dispersion showed a negative linear correlation with both collagen solidity (r=-0.3, p<0.0001, Spearman's correlation) and directionality (r=-0.3, p<0.0001, Spearman's correlation).

Table 7-2: Distribution of CPI and its parameters scores

	Collagen Directionality	**Collagen Dispersion**	**Collagen Solidity**	**CPI**
Mean ± SD	23.6 ± 17.2	17.8 ± 6.8	0.5 ± 0.3	6 ± 1.8
Median	19.6	16.7	0.5	6
Minimum	1.0	5.1	0.001	3
Maximum	85.0	58.1	0.9	9

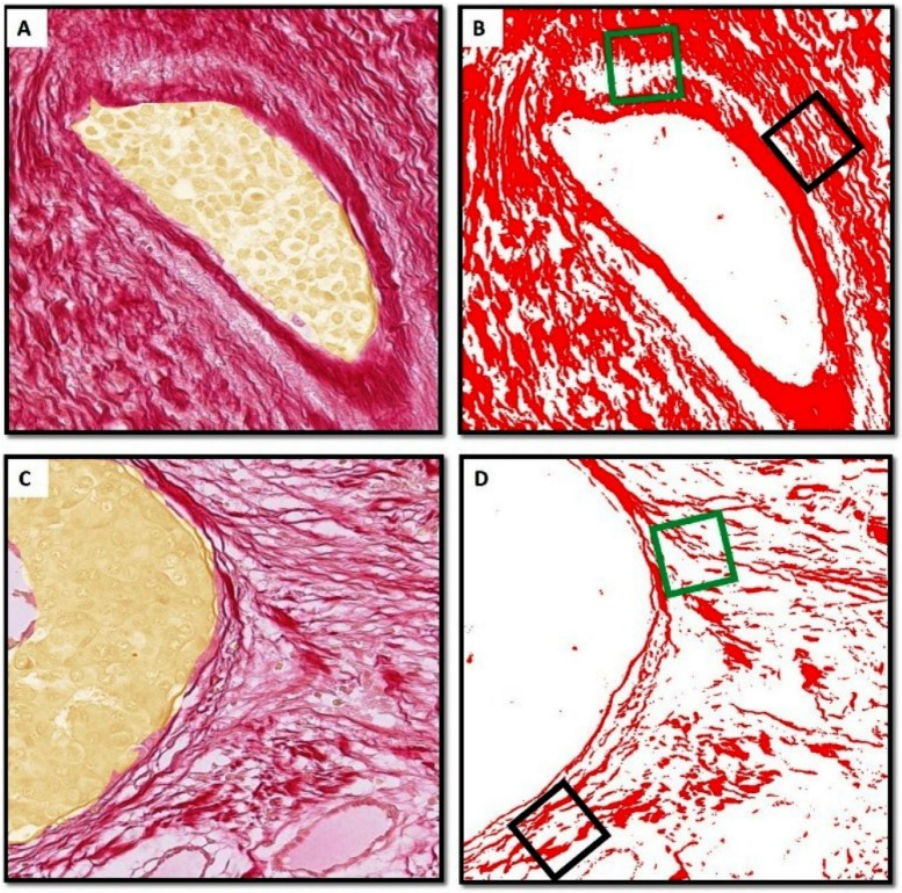

Figure 7-3: Example of collagen fibre arrangement

A and B represent DCIS case surrounded by dense collagen with lower dispersion (parallelly arranged collagen fibres all over the duct perimetry) and different directionalities, where collagen fibres delineated in (B) with black square show parallel arrangement relative to duct boundary (The tangential line), the fibres in the green square show more perpendicular arrangement relative to the tangential line touching the duct boundary. C and D represent DCIS surrounded by scanty randomly distributed collagen fibres with varied directionality relative to tangential line to the duct boundary. (A and C are DCIS sections stained with picrosirius red, while B and D are the images generated from ImageJ software)

The proportion of cases with a high CPI score (poor prognostic group) was higher in DCIS co-existing with IBC than pure DCIS (38% and 24% respectively; $\chi 2=36.5$, $p<0.0001$) (**Table 7-3**). Similar results were observed when the score was analysed using a numerical scale ($p<0.0001$) (**Table 7-4**). Comparable results were observed for all index parameters whereby DCIS co-existing with invasive carcinoma showed a higher extent of perpendicular collagen fibres in relation to DCIS boundaries and with collagen fibres more often arranged in parallel (lower dispersion) than pure DCIS either in categorical groups or using the numerical scores (**Table 7-5** and **Table 7-6**). The proportion of DCIS co-existing with IBC showed denser collagen fibres was slightly higher than pure DCIS (58% Vs. 50%) which was not statistically significant ($p=0.364$). **Figure 7-4** illustrates the distribution of CPI parameters within pure DCIS and DCIS-IBC cohorts.

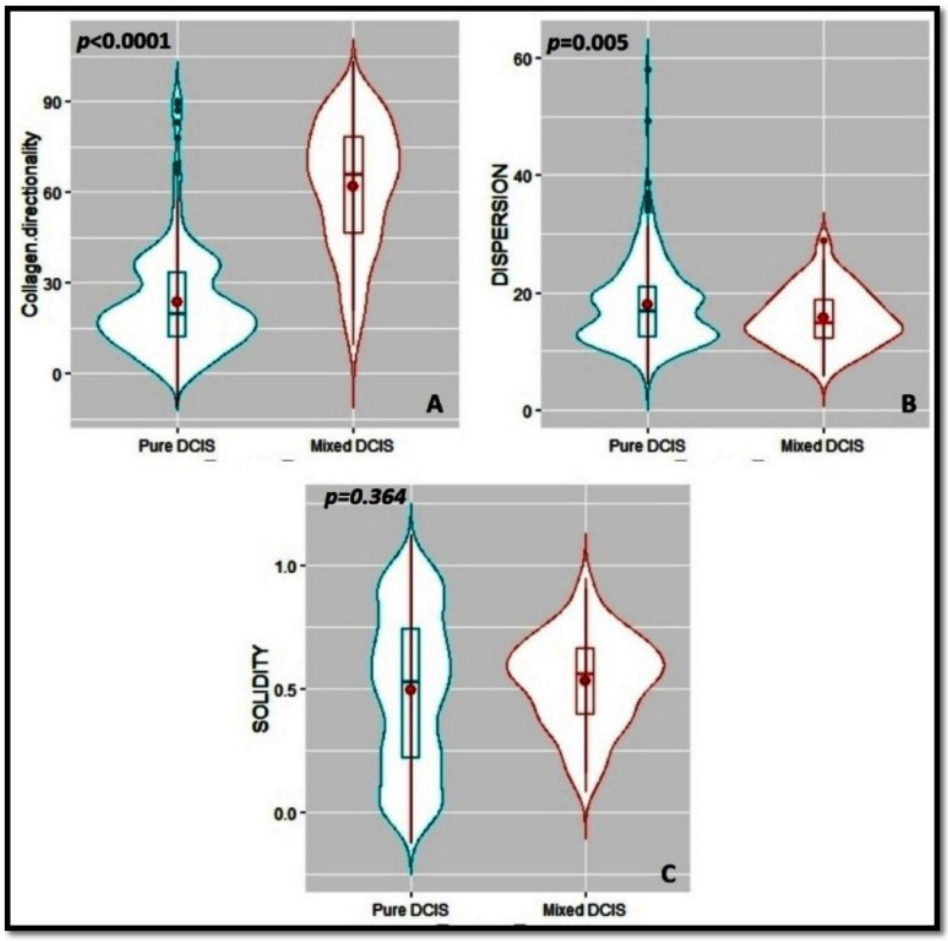

Figure 7-4: Violin plots comparing the distribution of CPI parameters between pure DCIS and DCIS co-existing with invasive carcinoma

Obviously, DCIS mixed showed higher angle of directionality and lower dispersion degree than pure DCIS. No statistically significant difference between collagen density between pure and mixed DCIS. Central line in the boxplot represents the median while the error bars represent the standard deviation

7.4.2 Significance of CPI

Poor CPI was associated with other clinicopathological determinants of poor prognosis in DCIS (**Table 7-3**) including higher nuclear grade (p<0.0001), presence of comedo type necrosis (p<0.0001), hormonal receptor negativity (p=0.032, p=0.029 for ER and PR, respectively) and HER2 positivity

(p=0.003). Luminal A DCIS had lower CPI scores where 67% of cases belonged to good prognostic group (p=0.037). Moreover, poor CPI was associated with other microenvironmental and stromal factors associated with poor DCIS prognosis such as dense TILs (p=0.016) and high levels of P4HA2 expression (p<0.0001. The results were validated by analysing the numeric CPI scores which gave comparable results (**Table 7-4**). Furthermore, collagen directionality, dispersion and solidity scores were analysed individually with other clinicopathological parameters and the results are summarised in **Table 7-5** (for categorical groups) and **Table 7-6** (for continuous scores).

Table 7-3: Correlation between CPI and clinicopathological parameters

Clinicopathological Parameters	Collagen prognostic index groups			χ^2 (*p*-value)
	Good (n=96)	Moderate (n=128)	Poor (n=100)	
Age (years)				
≤50	26 (27)	52 (23)	30 (30)	2.1
>50	70 (73)	176 (77)	70 (70)	(0.356)
Presentation				
Screening	45 (47)	115 (50)	60 (60)	3.7
Symptomatic	51 (53)	113 (50)	40 (40)	(0.150)
DCIS Size (mm)				
≤20	45 (47)	90 (40)	45 (45)	1.7
>20	51 (53)	137 (60)	55 (55)	(0.414)
Nuclear Grade				
Low	39 (41)	7 (3)	0 (0)	155.6
Moderate	35 (37)	64 (28)	9 (9)	**(<0.0001)**
High	22 (22)	157 (69)	91 (91)	
Comedo necrosis				
Yes	41 (43)	168 (74)	83 (83)	42.4
No	55 (57)	60 (26)	17 (17)	**(<0.0001)**
Oestrogen receptor status				
Negative	15 (17)	59 (28)	32 (34)	6.8
Positive	73 (83)	154 (72)	62 (66)	**(0.032)**
Progesterone receptor				
Negative	28 (32)	99 (46)	47 (49)	7.1
Positive	61 (69)	115 (54)	49 (51)	**(0.029)**
HER2 status				
Negative	79 (86)	163 (75)	63 (64)	11.8
Positive	13 (14)	54 (25)	35 (36)	**(0.003)**
Proliferation index (Ki-67)				
High	13 (16)	49 (24)	29 (31)	5.4
Low	68 (84)	156 (76)	64 (69)	(0.066)
Molecular classes				13.4
Luminal A	51 (67)	95 (49)	34 (40)	**(0.037)**
Luminal B	11 (14)	40 (21)	20 (24)	
HER2 Enriched	6 (8)	32 (17)	19 (22)	
Triple negative	8 (11)	25 (13)	12 (14)	
Tumour infiltrating lymphocytes				8.2
Dense	27 (39)	96 (50)	53 (62)	**(0.016)**
Sparse	43 (61)	96 (50)	33 (38)	
P4HA2 expression				19.2
High	28 (34)	127 (62)	52 (60)	**(<0.0001)**
Low	54 (66)	78 (38)	35 (40)	
HIF-1α expression				
High	11 (15)	45 (25)	23 (30)	4.7
Low	62 (85)	137 (75)	54 (70)	0.094
Tumour Type*				
Pure DCIS	96 (97)	228 (72)	100 (64)	36.5
DCIS associated with IBC	3 (3)	89 (28)	57 (36)	**(<0.0001)**

*Including pure DCIS (n=424) and DCIS coexisting with IBC (n=149)
Significant p values are in **bold**
DCIS; ductal carcinoma in situ, HER2; human epidermal growth factor receptor 2, P4HA2; prolyl-4-hydroxylase alpha subunit 2, HIF-1α; hypoxia inducible factor-1 alpha, IBC; invasive breast cancer.

Table 7-4: Correlation between CPI scores (continuous values) and different clinicopathological parameters

Clinicopathological Parameters	Number of cases	collagen prognostic index score	
		Mean Rank	*p*-value
Age (years)			0.657
≤50	108	216.9	
>50	316	210.9	
Presentation			**0.042**
Screening	220	224.0	
Symptomatic	204	200.0	
DCIS Size (mm)			0.742
≤20	180	214.2	
>20	243	210.3	
Nuclear Grade			**<0.0001**
Low	46	65.8	
Moderate	108	155.3	
High	270	260.4	
Comedo necrosis			**<0.0001**
Yes	292	237.7	
No	132	156.9	
Oestrogen receptor			**0.013**
Negative	106	221.2	
Positive	289	189.5	
Progesterone Receptor			**0.015**
Negative	174	215.7	
Positive	225	187.8	
HER2 status			**0.003**
Negative	305	193.9	
Positive	102	234.0	
Proliferation index (Ki-67)			**0.004**
High	91	218.1	
Low	288	18611	
Molecular classes			**0.017**
Luminal A	180	160.4	
Luminal B	71	192.4	
HER2 Enriched	57	198.6	
Triple negative	45	191.8	
Tumour infiltrating lymphocytes			
Dense	176	185.1	**0.044**
Sparse	172	163.7	
P4HA2 expression			**0.0001**
High	207	206.4	
Low	167	164.2	
HIF-1α expression			**0.017**
High	79	188.1	
Low	253	159.5	
Tumour Type*			**<0.0001**
Pure DCIS	424	262.9	
DCIS associated with IBC	149	355.6	

*Including pure DCIS (n=424) and DCIS coexisting with IBC (n=149)
Significant p values are in **bold**
DCIS; ductal carcinoma in situ, HER2; human epidermal growth factor receptor 2, P4HA2; prolyl-4-hydroxylase alpha subunit 2, HIF-1α; hypoxia inducible factor-1 alpha, IBC; invasive breast cancer

Table 7-5: Correlation between CPI parameters and different clinicopathological parameters

Clinicopathological Parameters	Collagen Directionality (n=424)			X^2 (*p*-value)	Collagen Solidity (n=424)			X^2 (*p*-value)	Collagen Dispersion (n=424)			X^2 (*p*-value)
	Score 1	Score 2	Score 3		Score 1	Score 2	Score 3		Score 1	Score 2	Score 3	
Age (years)												
≤50	33 (26)	25 (28)	50 (24)	0.6	25 (26)	43 (28)	40 (23)	0.9	54 (23)	21 (22)	33 (34)	4.9
>50	92 (74)	64 (72)	160 (76)	(0.710)	72 (74)	111 (72)	133 (77)	(0.608)	179 (77)	73 (78)	64 (66)	(0.088)
Presentation				8.3								2.1
Screening	60 (48)	37 (42)	123 (59)	**(0.016)**	42 (43)	82 (53)	96 (56)	3.8	116 (50)	55 (58)	49 (51)	(0.343)
Symptomatic	65 (52)	52 (59)	87 (41)		55 (57)	72 (47)	77 (44)	(0.144)	117 (50)	39 (42)	48 (49)	
DCIS Size (mm)												0.9
≤20	54 (44)	31 (35)	95 (45)	2.8	45 (46)	65 (43)	70 (41)	0.8	95 (41)	44 (47)	41 (43)	(0.607)
>20	70 (56)	58 (65)	115 (55)	(0.242)	52 (54)	88 (57)	103 (59)	(0.639)	138 (59)	50 (53)	55 (57)	
Nuclear Grade				54.5								47.3
Low	30 (24)	15 (17)	1 (1)	**(<0.0001)**	46 (47)	0 (0)	0 (0)		32 (14)	11 (12)	3 (3)	**(<0.0001**
Moderate	36 (29)	16 (18)	56 (27)		44 (44)	50 (33)	14 (8)	164.2	84 (36)	15 (16)	9 (9)	)
High	59 (47)	58 (65)	153 (72)		7 (7)	104 (67)	159 (92)	**(<0.0001)**	117 (50)	68 (72)	85 (88)	
Comedo necrosis												12.8
Yes	73 (58)	62 (70)	157 (75)	9.8	32 (33)	114 (74)	146 (84)	79.6	144 (62)	70 (75)	78 (80)	(**0.002**)
No	52 (42)	27 (30)	53 (25)	**(0.007)**	65 (67)	40 (26)	27 (16)	**(<0.0001)**	89 (38)	24 (25)	19 (20)	
Oestrogen receptor status				4.3								7.7
Negative	27 (24)	30 (36)	49 (25)	(0.114)	8 (9)	48 (33)	50 (31)	19.8	48 (22)	23 (26)	35 (38)	**(0.022)**
Positive	87 (76)	54 (64)	148 (75)		83 (91)	96 (67)	110 (69)	**(0.0001)**	166 (78)	65 (74)	58 (62)	
Progesterone receptor												**7.3**
Negative	48 (41)	47 (56)	79 (40)	6.7	20 (22)	73 (50)	81 (50)	23.3	82 (38)	41 (47)	51 (54)	**(0.025)**
Positive	68 (59)	37 (44)	120 (60)	**(0.036)**	72 (78)	72 (50)	81 (50)	**(<0.0001)**	135 (62)	46 (53)	44 (46)	
HER2 status				2.9				26.4				5.9
Negative	93 (78)	57 (68)	155 (76)	**(0.237)**	88 (95)	107 (72)	110 (66)	**(<0.0001)**	175 (79)	67 (74)	63 (66)	(0.051)
Positive	27 (22)	27 (32)	48 (24)		5 (5)	41 (28)	56 (34)		46 (21)	24 (26)	32 (34)	
Proliferation index (Ki-67)				0.7				7.2				9.1
High	23 (21)	19 (25)	49 (25)	(0.696)	11 (13)	35 (25)	45 (29)	**(0.027)**	37 (18)	23 (28)	31 (33)	(0.011)
Low	86 (79)	58 (75)	144 (75)		71 (87)	107 (75)	110 (71)		167 (82)	59 (72)	62 (67)	
Molecular classes				7.2								8.8
Luminal A	58 (56)	31 (42)	91 (52)	(0.303)	59 (76)	61 (47)	60 (41)	32.1	108 (56)	36 (48)	36 (42)	(0.185)
Luminal B	19 (18)	15 (20)	37 (21)		10 (13)	22 (17)	39 (26)	**(<0.0001)**	37 (19)	17 (23)	17 (20)	
HER2 Enriched	16 (16)	18 (24)	23 (13)		2 (3)	27 (21)	28 (19)		23 (12)	13 (17)	21 (24)	
Triple negative	10 (10)	10 (14)	25 (14)		6 (8)	19 (15)	20 (14)		24 (13)	9 (12)	12 (14)	
TILs				0.3				6.8				
Dense	49 (50)	41 (53)	86 (50)	(0.867)	28 (38)	64 (51)	84 (56)	**(0.033)**	85 (46)	39 (49)	52 (62)	5.8
Sparse	49 (50)	36 (47)	87 (50)		46 (62)	61 (49)	65 (44)		99 (54)	41 (51)	32 (38)	(0.054)

P4HA2 expression				5.6				24.7				
High	50 (46)	48 (58)	109 (60)	(0.060)	27 (32)	89 (63)	91 (62)	(<0.0001)	99 (49)	50 (58)	58 (67)	7.8
Low	59 (54)	34 (42)	74 (40)		58 (68)	53 (37)	56 (38)		102 (51)	36 (42)	29 (33)	**(0.020)**
HIF-1α expression				0.9				14.2				
High	23 (24)	20 (28)	36 (22)	(0.608)	9 (12)	26 (21)	44 (34)	(0.001)	38 (20)	16 (22)	25 (34)	5.7
Low	72 (76)	52 (72)	129 (78)		69 (88)	98 (79)	86 (66)		149 (80)	56 (78)	48 (66)	(0.057)
Tumour Type*												
Pure DCIS	125 (98)	89 (95)	210 (60)	97.8	97 (91)	154 (65)	173 (75)	26.4	233 (78)	94 (67)	97 (72)	6.8
DCIS associated with IBC	2 (2)	5 (5)	142 (40)	(<0.0001)	9 (9)	82 (35)	58 (25)	(<0.0001)	65 (22)	47 (33)	37 (27)	**(0.033)**

*Including pure DCIS (n=424) and DCIS coexisting with IBC (n=149)
Significant p values are in **bold**
DCIS; ductal carcinoma in situ, HER2; human epidermal growth factor receptor 2, P4HA2; prolyl-4-hydroxylase alpha subunit 2, HIF-1α; hypoxia inducible factor-1 alpha, IBC; invasive breast cancer.

Table 7-6: Correlation between different CPI parameters and clinicopathological parameters using continuous data.

Clinicopathological Parameters	Number of cases	Collagen Directionality		Collagen Solidity		Collagen Dispersion	
		Mean Rank	*p*-value	Mean Rank	*p*-value	Mean Rank	*p*-value
Age (years)			0.822		0.286		0.162
≤50	108	210.2		201.7		198.3	
>50	316	213.3		216.2		217.4	
Presentation			**0.029**				
Screening	220	225.0		225.2	**0.027**	211.4	0.840
Symptomatic	204	199.0		198.8		213.8	
DCIS Size (mm)			0.482		0.489		0.801
≤20	180	216.9		207.2		213.7	
>20	243	208.4		215.5		210.7	
Nuclear Grade			**<0.0001**		**<0.0001**		**<0.0001**
Low	46	83.0		31.4		249.1	
Moderate	108	192.2		134.2		264.2	
High	270	242.7		274.7		185.6	
Comedo necrosis			**0.0002**		**<0.0001**		**0.014**
Yes	292	227.0		244.8		202.7	
No	132	180.4		140.9		234.2	
Oestrogen receptor			0.776		**0.001**		**0.019**
Negative	106	200.7		230.4		175.7	
Positive	289	197.0		186.1		206.2	
Progesterone Receptor			0.722		**<0.0001**		**0.029**
Negative	174	197.7		226.3		185.7	
Positive	225	201.8		179.6		211.1	
HER2 status			0.183		**<0.0001**		0.055
Negative	305	199.5		189.2		210.5	
Positive	102	217.4		248.3		184.6	
Proliferation index (Ki-67)			0.290		**0.029**		**0.005**
High	91	200.6		211.8		161.7	
Low	288	186.7		183.1		198.9	
Molecular classes			0.694		**0.0001**		0.109
Luminal A	180	171.5		153.9		186.6	
Luminal B	71	186.4		198.8		176.8	
HER2 Enriched	57	175.8		208.2		148.6	
Triple negative	45	185.6		195.5		174.7	
Tumour infiltrating lymphocytes							
Dense	176	175.2	0.892	187.3	**0.016**	165.1	0.075
Sparse	172	173.7		163.3		184.2	
P4HA2 expression			**0.048**		**<0.0001**		**0.015**
High	207	197.4		205.6		175.3	
Low	167	175.2		165.1		202.7	
HIF-1α expression			0.865		**0.001**		**0.038**
High	79	168.1		198.9		146.9	
Low	253	166.0		156.4		172.6	
Tumour Type*			**<0.0001**		0.364		**0.005**
Pure DCIS	424	225.8		283.3		298.6	
DCIS associated with IBC	149	461.3		297.6		254.0	

*Including pure DCIS (n=424) and DCIS coexisting with IBC (n=149)
Significant p values are in **bold**
DCIS; ductal carcinoma in situ, HER2; human epidermal growth factor receptor 2, P4HA2; prolyl-4-hydroxylase alpha subunit 2, HIF-1α; hypoxia inducible factor-1 alpha, IBC; invasive breast cancer.

7.4.3 **Outcome analysis**

High CPI was associated with shorter DCIS LRFI either for all recurrences (DCIS or IBC) (*HR*=2.0*; 95%CI*=1.3-3.1*; p*=0.002) and for invasive recurrences alone (*HR*=3.1*; 95%CI*=1.6-5.5*; p*=0.0003) (**Figure 7-5**). When analysis was confined to patients treated with BCS, similar results were obtained where poor CPI was associated with worse outcome for all recurrences (*HR*=2.1*; 95%CI*=1.4-3.1*; p*=0.001) and for invasive recurrences (*HR*=3.0*; 95%CI*=1.6-5.4*; p*=0.0003) (**Figure 7-5**). CPI was associated with poor outcome regardless of the DCIS nuclear grade, whereby poor CPI was associated with shorter LRFI either for all recurrences or invasive recurrences only (**Figure 7-6**) for both high grade DCIS and non-high grade DCIS (low and intermediate DCIS were combined together due to the small number of events in the former group). Moreover, evaluation of the interaction between CPI and RT (CPI*RT) using a Cox regression model showed that higher CPI was significantly associated with shorter LRFI even with RT (*HR*=1.8, 95%*CI*=1.3-2.3, *p*=0.0001). Analysis of the individual index parameters (collagen directionality, dispersion and solidity), showed significant associations with disease recurrence (**Figure 7-7**). Forest plots for univariate analysis of other clinicopathological

parameters and CPI groups and their association with DCIS recurrence are shown in **Figure 7-8**.

Multivariate survival analysis including the conventional determinants of DCIS risk showed that age at diagnosis, nuclear grade, DCIS size, margin status and comedo type necrosis are independent prognostic factors for DCIS recurrence. However, when CPI was incorporated in the model it was the only independent poor prognostic factor for DCIS recurrence in patients treated with BCS regardless of other known determinants of high-risk DCIS either for all recurrences (*HR*=2.3, 95% *CI*=1.3-4.2; *p*=0.005) or invasive recurrences only (*HR*=3.4, 95% *CI*=1.5-7.6; *p*=0.003) (**Table 7-7**).

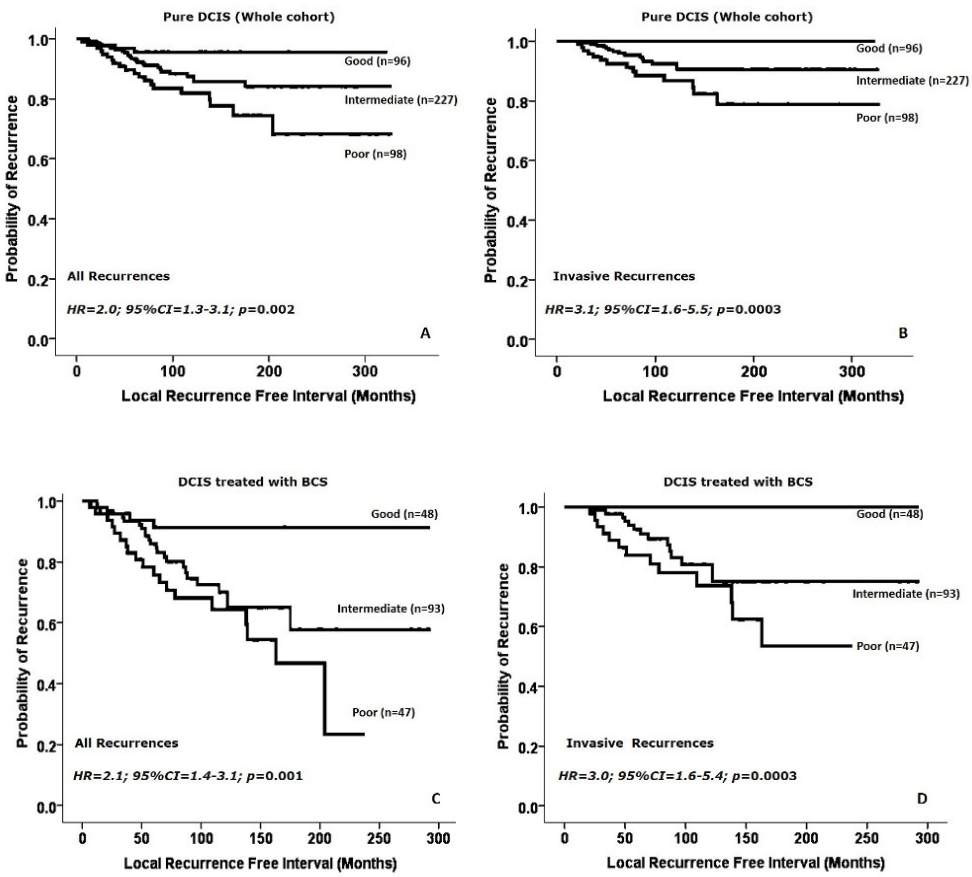

Figure 7-5: Kaplan Meier curves show that the poor collagen prognostic index group is associated with shorter ipsilateral local recurrence free interval

For all recurrences (A) and invasive recurrences (B) in the whole series as well as in the breast conserving surgery treated group (C; for all recurrences and D; for invasive recurrences)

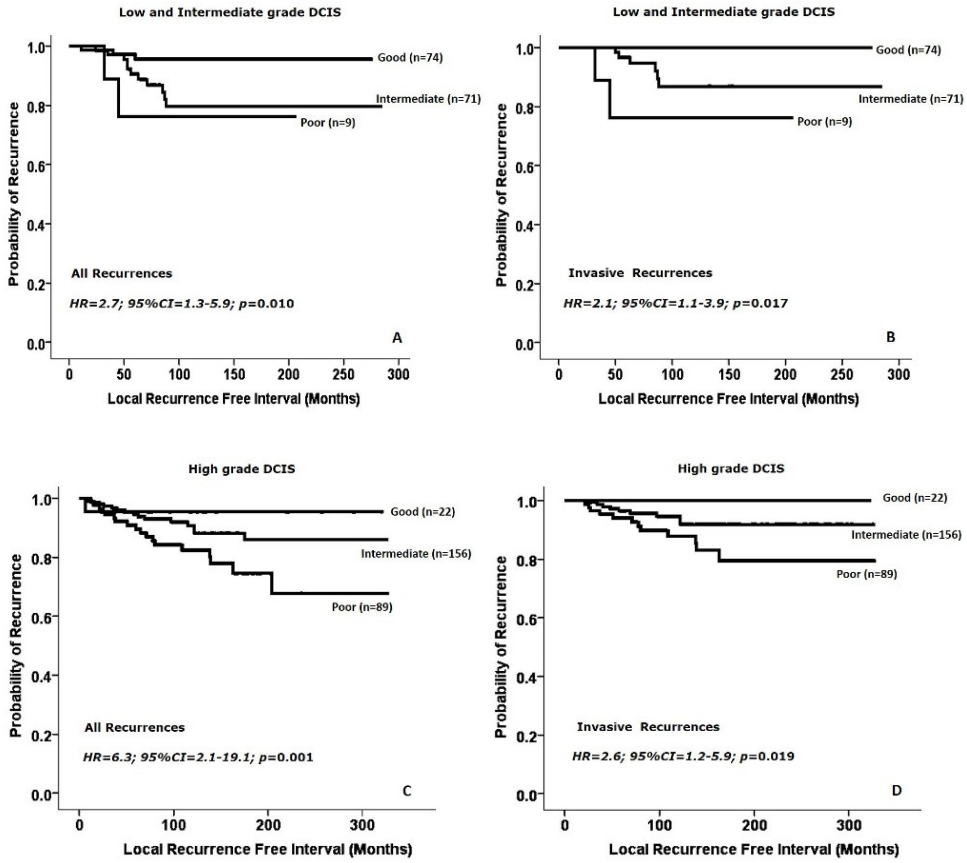

Figure 7-6: Kaplan Meier curves show that poor collagen prognostic index group is associated with shorter ipsilateral local recurrence free interval

For all recurrences (A) and invasive recurrences (B) in non-high grade DCIS as well as in high grade DCIS (C; for all recurrences and D; for invasive recurrences)

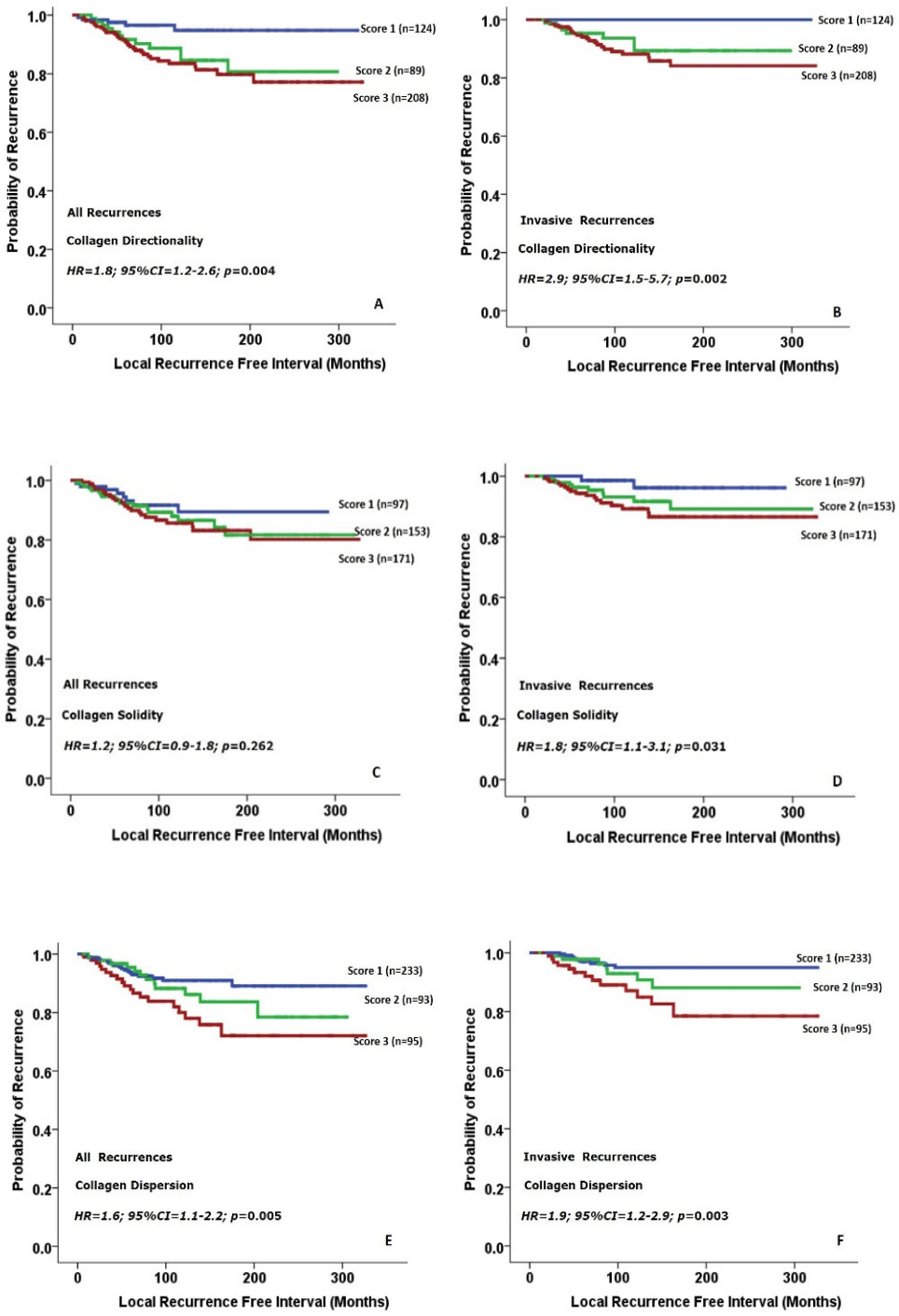

Figure 7-7: Kaplan Meier curves show the association between collagen geometrics and outcome

Collagen directionality (A, B), solidity (C, D) and dispersion (E, F) with DCIS recurrence, either all recurrences or invasive recurrences (In the whole DCIS cohort)

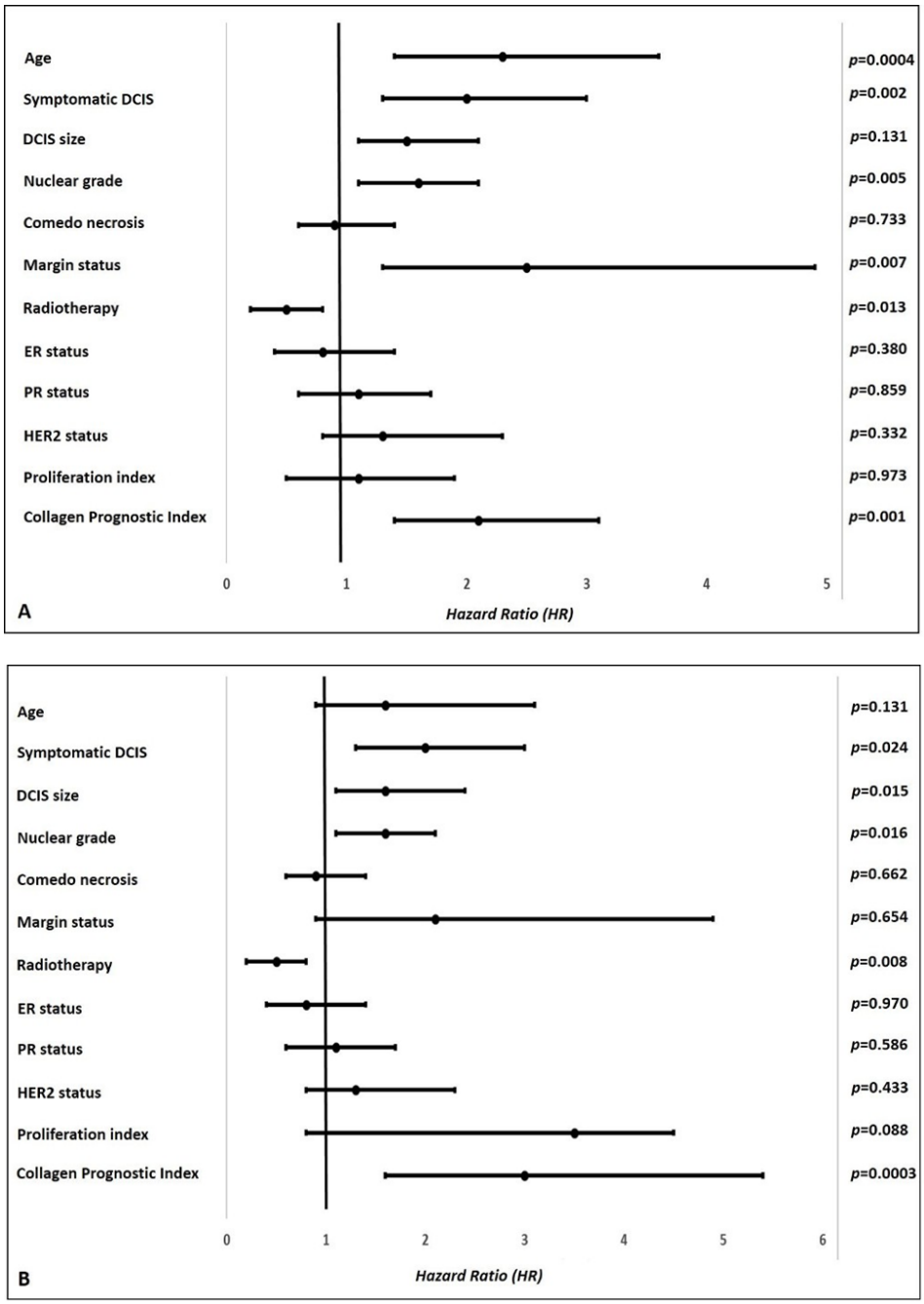

Figure 7-8: Forest plots showing the univariate analysis results of association between different clinicopathological parameters and the ipsilateral tumour recurrence

A) All recurrences whether DCIS or invasive and B) for invasive recurrences only

Table 7-7: Multivariate survival analysis of CPI and other variables predicting ipsilateral local recurrence

A) All recurrences

Conventional clinicopathological parameters associated with high risk DCIS				
Parameters	Hazard ratio (*HR*)	95% *confidence interval (CI)*		*p*-value
		Lower	Upper	
Patient Age	0.4	0.2	0.8	**0.006**
DCIS presentation	1.5	0.9	2.4	0.111
DCIS size	1.5	1.1	2.1	**0.040**
DCIS nuclear Grade	1.9	1.3	2.7	**0.001**
Comedo necrosis	0.6	0.4	0.9	**0.049**
Margin status	0.8	0.7	0.9	**0.004**
CPI and other clinicopathological parameters associated with high risk DCIS				
Collagen prognostic index	2.3	1.3	4.2	**0.005**
Patient Age	0.5	0.2	1.1	0.072
DCIS presentation	2.1	0.9	4.3	0.052
DCIS size	0.9	0.5	1.6	0.760
DCIS nuclear Grade	1.1	0.5	1.9	0.994
Comedo necrosis	0.8	0.4	1.6	0.559
Margin status	0.9	0.8	1.1	0.236

Significant *p* values are in **bold**

B) Invasive recurrence

Conventional clinicopathological parameters associated with high risk DCIS				
Parameters	Hazard ratio (*HR*)	95% *confidence interval (CI)*		*p*-value
		Lower	Upper	
Patient Age	0.5	0.2	1.3	0.156
DCIS presentation	1.4	0.8	2.6	0.245
DCIS size	1.8	1.1	2.4	**0.013**
DCIS nuclear Grade	1.9	1.1	3.0	**0.013**
Comedo necrosis	0.7	0.4	1.3	0.274
Margin status	0.9	0.8	1.1	0.075
CPI and other clinicopathological parameters associated with high risk DCIS				
Collagen prognostic index	3.4	1.5	7.6	**0.003**
Patient Age	1.2	0.4	3.7	0.697
DCIS presentation	3.0	1.2	7.9	**0.025**
DCIS size	1.3	0.7	2.7	0.412
DCIS nuclear Grade	0.9	0.4	2.3	0.909
Comedo necrosis	0.9	0.4	2.1	0.786
Margin status	0.9	0.8	1.1	0.838

Significant *p* values are in **bold**

7.5 **Discussion**

Precise assessment of DCIS risk is still challenging despite advances in high throughput molecular techniques. None of the currently available clinicopathological based nomograms and indices [120, 296, 297, 581] or molecular signatures such as Oncotype DX DCIS [78] provide a reliable and clinically valid tool to predict DCIS risk of progression and/or recurrence to improve personalised management. The biological and clinical heterogeneity of DCIS coupled with underestimation of the important role of the TME in disease behaviour are potential reasons for this lack of accuracy. Cancer is not exclusively a disease of malignant cells, but also involves crosstalk between tumour, stromal cells and other components of the surrounding TME. Thus, studying the role of DCIS microenvironment and its interaction with the tumour cells could resolve the DCIS management dilemma and provide an adequate and reliable risk stratification model [90, 178, 211, 230, 551].

ECM and its main constituent, collagen, plays a key role in normal mammary gland development [582]. Interestingly, increased breast tissue density, caused mainly by increased collagen deposition, is a strong risk factor for BC development with high breast density carrying a two- to six-fold increase in

BC risk compared to women with normal breast density [575, 583]. It is reported that DCIS arises more commonly in dense regions of the breast [21, 575]. Whilst it was thought that collagen provided a natural physiological barrier against tumour invasion, recent studies have provided concrete evidence on the key role of collagen dynamic changes (collagen deposition, degradation, re-organisation and remodelling) in carcinogenesis, tumour maintenance and progression through its role in cellular adhesion, proliferation, migration, invasion and angiogenesis [584]. A recent genetic study showed that ECM re-organisation and response to cellular stress are key factors in BC progression [585]. Several studies on IBC and other types of cancer using second harmonic generation microscopy or multiphoton laser scanning showed that organisation of collagen around malignant tissues provides a tumour associated collagen signature that is associated with tumour behaviour and patients' outcome [196, 574, 575]. Given that, the role of collagen remodelling in DCIS behaviour is relatively understudied, the collagen fibre organisation surrounding DCIS and its prognostic significance was evaluated. A novel imaging method, to the best of my knowledge, was used to assess collagen characteristics in a large cohort of DCIS and

develop a CPI to predict the risk of DCIS recurrence and progression.

In this study, the density and arrangement of collagen relative to each other and the boundary of DCIS was examined. Interestingly, higher CPI was associated with features of high-risk DCIS including higher nuclear grade, comedo type necrosis, hormonal receptor negativity and HER2 positivity, supporting its role in DCIS progression. Additionally, the data showed that CPI was higher in DCIS co-existing with IBC than pure DCIS. Taken together, collagen re-organisation is a potential factor for high risk DCIS. The poor prognostic value of collagen rearrangement was shown with a shorter LRFI in patients with higher levels of CPI independently from other clinicopathological factors. These findings were consistent for all recurrent events, either DCIS or IBC or when the analysis was confined to invasive recurrences only, which provides more evidence that collagen rearrangement and deposition could play a key role in DCIS progression to invasive disease. CPI could predict the risk of recurrence in non-high-grade DCIS, which is a group at risk of under-treatment due to the lack of accurate predictors of recurrence in this group, although genetic studies showed that the DCIS are the precursors of low-grade IBC. Hence, CPI could drive the

management decision is these patients. The poor prognostic group of non-high-grade DCIS had a 22% risk of invasive recurrence within 10 years, compared to zero invasive recurrences in the good prognostic group.

Although the effect of RT in reduction of DCIS recurrence is undeniable [93, 98, 285, 289], there is still a considerable percentage of patients treated with BCS and followed by adjuvant RT that develop disease recurrence. There is no data available for DCIS patients at higher susceptibility for poor response to RT. Our findings showed that DCIS with a high CPI is associated with poor outcome even when RT was offered. This index could provide a signature for RT resistance in DCIS. It is reported that dense stroma is associated with poor response to RT in cancer treatment [568] which might provide a similar explanation in DCIS. These findings need mechanistic studies for validation.

Although the mechanisms that lead to collagen changes and how these changes affect tumour behaviour are not fully understood, several explanations are available. Tumour cells could secrete factors that realign a random collagen matrix into a radially arranged collagen to facilitate local invasion [196]. The role of hypoxia and collagen remodelling proteins such as P4HA2 and lysyl oxidase are obvious in developing

collagen signatures as shown from previous studies and the findings in the current study [483, 571]. As a reciprocal effect, collagen density can affect tumour growth even in tumour harbouring scanty stroma. Cells cultured within low-density matrices form well-differentiated acini structures, while colonies that formed within high-density matrices are larger, more proliferative and less organised structures indicating that increasing collagen matrix density can directly promote epithelial cell proliferation [575].

Stiffer ECM due to increased collagen deposition results in high local mechanical loads and higher resistance to cellular contractility [575]. Such changes in the physical microenvironment lead to loss of cellular adhesion, increase tumour cell proliferation and promotes a transformed phenotype. These findings are supported from our results where higher collagen solidity and lower collagen dispersion were associated with a higher proliferation index. Moreover, stromal fibroblasts can regulate epithelial cells in part through secretion of specific soluble growth factors and chemokines such as TGF-β that has been associated with reactive stroma and fibrosis, while studies indicate that the epidermal growth factors/receptors (i.e.HER2) are important not only in the normal mammary gland but also during tumorigenesis and

metastasis [192, 586]. These findings are supported from the results wherein higher CPI was associated with HER2 overexpression and higher proliferation index.

Mechanical forces can induce EMT leading to tumour invasion [574]. With the tumour mass increasing, stress on ECM increases correspondingly until reaching a critical point, the biomechanical trigger, which can be sensed by mechanical receptors in both tumour and stromal cells. In turn these cells exert cytoskeletal-dependent traction forces on the ECM [196, 587, 588]. Eventually, tumour and stromal cells deform as consequences of the altered tissue tension [589, 590], the expanding tumour mass [591], matrix stiffening [592], and increased interstitial pressure due to a leaky vasculature and poor lymphatic drainage, initiating EMT [593]. These deformed cells acquire a more spindle-like fibroblastic morphology, lower adhesive properties, enhanced motility and invasive behaviour. Studies show that local invasion in stroma rich areas is due an intrinsic property of tumour cells arising in a collagen-dense stroma rather than being a simple reflection of increased local collagen that facilitates invasion. Tumour cells isolated from collagen-dense tissues were in fact innately more migratory, indicating that the ease of invasiveness facilitated by certain collagen structures is likely not the sole

cause for increased metastasis but that the tumour cells themselves are more invasive [575]. Moreover, aligned collagen provides an adhesive scaffold that support tumour cells in their invasion and migratory process [195, 196, 576, 577, 580]. Mechanical forces also activate sites on collagen to recruit monocytes leading to a cascade of innate immuno-inflammatory reactions [574]. Results showed that dense collagen is associated with denser TILs than lesions with scanty and randomly distributed stromal collagen. The underlying biology warrants an investigation, given the previous report that dense TILs have poor prognostic significance in DCIS, a reverse phenomenon to that in invasive disease for which the underlying mechanisms are unclear [411].

This study has been carried out on TMA without including full face sections, which might underestimate the role of DCIS heterogeneity. However, all cases in our cohort were histologically reviewed before TMA construction and multiple cores were used for cases with heterogeneous grade or morphological patterns. Also, our cohort did not include patients treated with ET.

In conclusion, CPI could provide a signature for prediction of DCIS recurrence risk. Collagen deposition and re-organisation

around DCIS plays a role in tumour progression and recurrence. Collagen features are stable and robust, persisting even when tissues have not been properly fixed, and these features are maintained under various tissue-processing approaches. Thus, PSR staining of collagen and subsequent image analysis to assess CPI could readily be used in clinical practice and could drive DCIS management decisions.

8 Chapter 8: Hypoxia Driven Centrosome Amplification in DCIS

8.1 Introduction

Current predictors of recurrence risk for DCIS such as the VNPI [594] and the Memorial Sloan Kettering DCIS nomogram [120] are based on routinely-used clinicopathological parameters but lack consistency and reproducibility in risk prediction [254]. In addition, these tools do not integrate prognostically-informative molecular predictors, and do not consider DCIS heterogeneity. While Oncotype Dx DCIS has some value in predicting DCIS behaviour, it has only been validated in two cohorts (ECOG E5194 and Ontario DCIS). The poor stratification of high/intermediate-risk patients in these two cohorts has called into question the prognostic value of this tool [78, 309].

8.1.1 Role of centrosome amplification in carcinogenesis

Amplified centrosomes that underlie erroneous mitoses and fuel chromosomal instability (CIN) is a well-recognised driver of tumour development and tumour heterogeneity [595, 596]. Although normal cells have one centrosome pre- S-phase and two centrosomes post- S-phase, cancer cells invariably display centrosome amplification (CA); an abnormal increase in the number (i.e., numerical amplification) and/or volume (i.e., structural amplification) of centrosomes [597]. Semi-

quantitative studies have shown that CA correlates with higher tumour grade, larger tumour size, disease recurrence and/or distant metastasis in various malignancies [598]. Moreover, CA occurs within precancerous and preinvasive lesions including DCIS, suggesting that CA is an early event in tumourigenesis [599, 600]. TME plays role in such centrosomal aberrations mainly through hypoxia and related factors [246]. **Figure 8-1** shows the underlying mechanisms and pathways through which hypoxia can leads to CA [601].

In the present study, it was postulated that recurrent and non-recurrent DCIS cases might differ in the extent and/or type of CA. The prognostic value of CA has remained unexplored for clinical application, as there is no methodology available for the rigorous quantitation of CA phenotypes. Also, it is unclear whether the prognostic value of CA lies in numerical and/or structural CA. It is unknown which of the two features of CA-frequency (i.e., percentage of cells showing amplified centrosomes), and/or severity (i.e., how abnormal the number/volume of centrosomes is in a given sample), is prognostically informative.

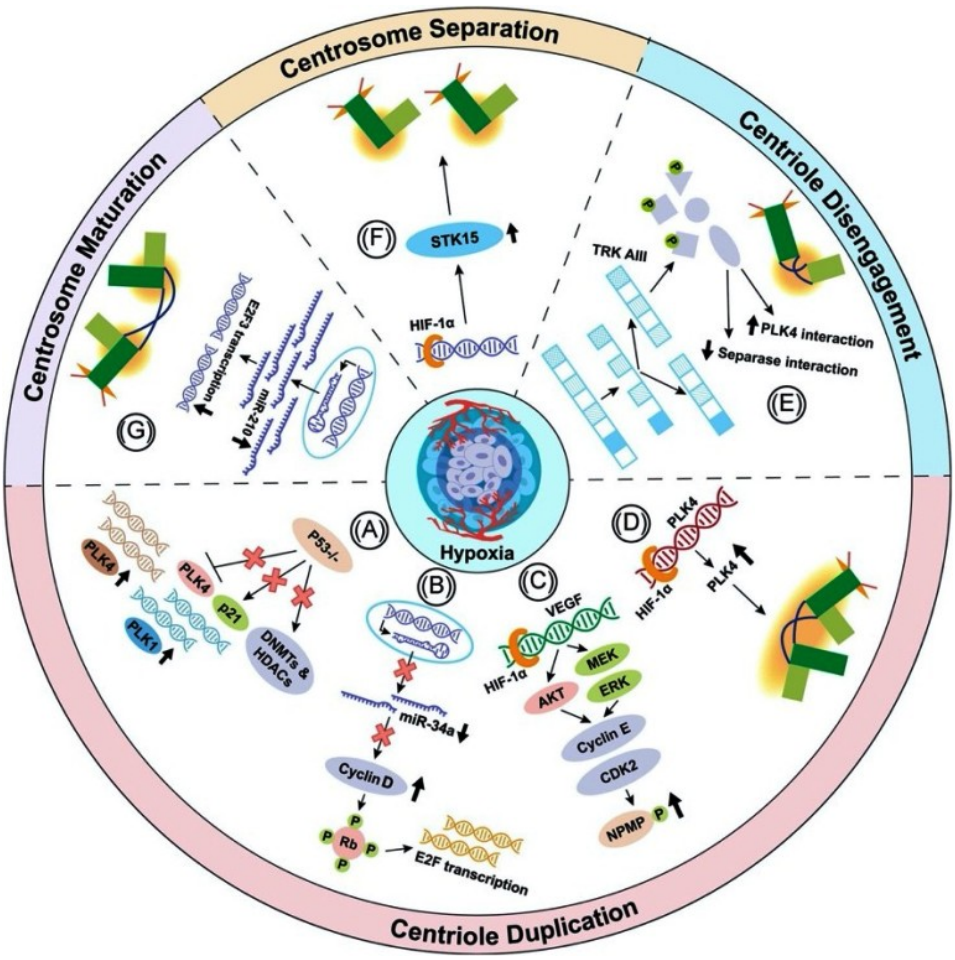

Figure 8-1: A schematic summarising the role of hypoxia in CA at different stages of the centrosome cycle.

(A) Hypoxia in the TP53 null cell lines epigenetically regulates expression of PLK4 protein levels. (**B**) HIF-1α downregulates expression of mir-34a which results in increased expression of cyclin D1 expression. (**C**) VEGF, through either MEK/ERK or AKT increases cyclin E/Cdk2 activity by regulating the expression of cyclin E. (**D**) HIF-1α transcriptionally regulates expression of PLK4. (**E**) hypoxia-regulated alternative TrkAIII splice variant differentially phosphorylates several centrosome-associated components resulting in increased centrosome interaction with PLK4 and decreased centrosome interaction with separase. (**F**) HIF-1α transcriptionally regulates expression of STK15, and **(G)** HIF-1α upregulates expression of mir-210 which results in a decrease in E2F3 transcription which results in increased Cyclin E/CDK2 activity. CA, centrosome amplification; HIF-1α, hypoxia-inducible factor 1α; VEGF, vascular endothelial growth factor [601].

8.2 **Hypothesis and aims**

It was hypothesised that CA driven by hypoxia plays role in DCIS behaviour and outcome. The aim of this study was to

develop a new methodology for centrosomal phenotyping to quantitate both numerical and structural centrosomal aberrations in clinical tissue samples.

8.3 **Materials and methods**

8.3.1 **Study cohort**

This study was carried out as a collaborative work with Georgia State University, USA. The study design, DCIS samples, histological review and relevant clinical data were provided by the author. The experimental work including immunofluorescence staining, assessment of CA and development of CA score evaluation algorithm was carried out by Georgia University researchers. The author identified the regions of interest (ROIs) in tissue sections that were used to run the algorithm and estimate the various components of CA. The basic statistical analysis was carried out by the authors; however, the advanced statistics and graphs were created by Georgia University team.

This was a retrospective study of FFPE tissue sections of primary pure DCIS as described in **Chapter 2**. To calculate the sample size a pilot study which included 50 samples was performed (these samples were later included in the discovery cohort, **Table 8-1**) and based upon the findings, the proposed sample size of 116 for each cohort was expected to yield a

power of 80% with an alpha of 0.05. The discovery cohort (DC) (n=133) and validation cohort (VC) (N=119) comprised of consecutive pure DCIS patients with available tissue samples that showed free surgical margins >2mm (to avoid the effect of this confounder on the study outcome) and underwent BCS or mastectomy with or without adjuvant RT (**Figure 8-2**). Median age of these patients was 56 years, and the median follow-up was 121 months. In addition, survival analysis was initially performed to show the effect of standard prognostic factors like age at diagnosis, tumour size, RT and comedo necrosis on recurrence for the whole dataset (DC and VC, n=252) (**Figure 8-3**).

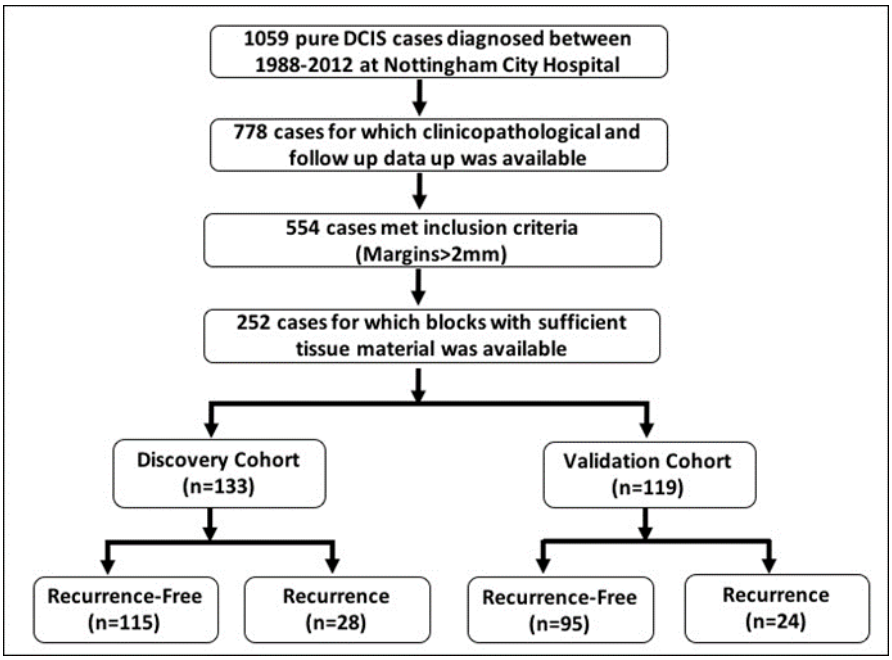

Figure 8-2: Diagram describing the flow of patients through the study

Table 8-1: Clinicopathological features of study cohort

Parameter	Discovery Cohort		Validation Cohort	
	Recurrence free	With Recurrence	Recurrence free	With Recurrence
Age (years)				
≤50	18 (17)	6 (21)	27 (28)	12 (50)
>50	87 (83)	22 (79)	68 (72)	12 (50)
DCIS Size (mm)				
≤16	54 (51)	13 (46)	14 (15)	15 (62)
>16	51 (49)	15 (54)	81 (85)	9 (38)
Nuclear Grade				
Low and Moderate	8 (8)	7 (25)	48 (51)	12 (50)
High	97 (92)	21 (75)	47 (49)	12 (50)
Comedo necrosis				
Yes	91 (87)	20 (71)	58 (61)	16 (67)
No	14 (13)	8 (29)	37 (39)	8 (33)
Radiotherapy				
No	57 (54)	21 (75)	83 (87)	22 (92)
Yes	48 (46)	7 (25)	12 (13)	2 (8)

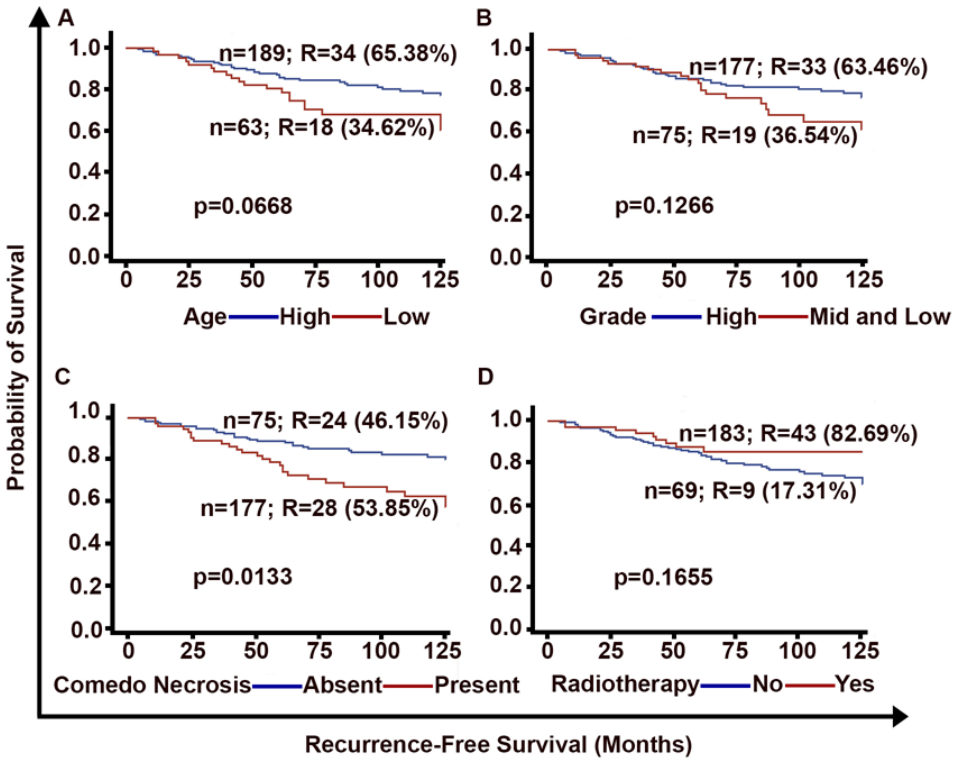

Figure 8-3: Association between conventional clinicopathological parameters and DCIS recurrence in the whole study cohort

Kaplan Meier survival curves representing the LRFI of patients in the DC and VC combined cohort (n=252) stratified into high and low groups based on (A) age at diagnosis, (B) DCIS grade, (C) presence of comedo necrosis, and (D) radiotherapy. n: total number of patients in each group; R: number of patients who developed LR.

A third cohort of full-face sections from resection samples from patients with DCIS and synchronous IBC (n=87), was also used (as described in **Chapter 2**).

To determine normal volumes of the centrosomes, full-face sections of normal breast tissue from reduction mammoplasties (n=40) and breast tumours with extensive regions of adjacent uninvolved tissues (n=40) were obtained from Stavanger University Hospital, Norway, and Nottingham City Hospital, UK, and West Georgia Hospital, GA, USA. All

study aspects were (a) approved by every Institutional Review Board, and (b) in compliance with guidelines in material transfer and data use agreements for all involved institutions, and Georgia State University where this study was mainly carried out.

8.3.2 Immunofluorescence staining and imaging

Centrosomes were immunofluorescently stained for ɣ-tubulin (red) in FFPF of the samples. Images of the stained samples were acquired with a Zeiss LSM 700 confocal microscope (using 63x oil immersion lens with a numerical aperture of 1.4 at 1.5x optical zoom). For optimal results, laser power was adjusted to the minimum level wherein fluorophore emission was saturated. For detector saturation, the gain (master) was adjusted such that the detector registers the target fluorophores in each channel within full range of detector settings (8-bit, 12-bit, 16-bit) to prevent over- and under-saturation and maximise accuracy. The offset was adjusted to minimise the background in the sample. Normal, DCIS and IBC areas pre-marked were imaged to obtain at least 10 ROIs each containing 20-30 nuclei and associated centrosomes (**Figure 8-4**).

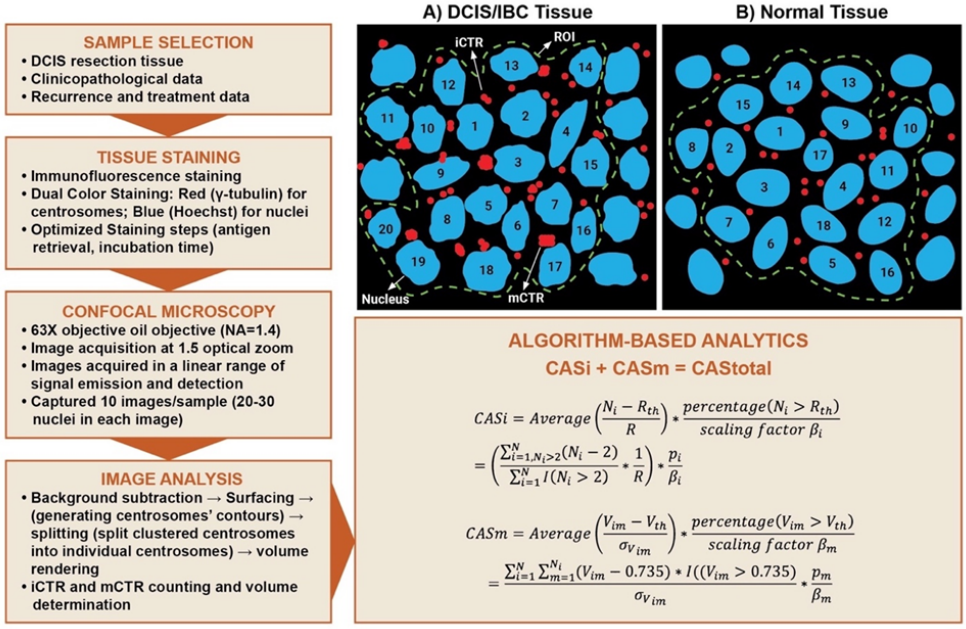

Figure 8-4: Schematic depicting semi-automated workflow to quantify CA

8.3.3 Centrosome scoring

Raw 3D image data were processed using IMARIS Biplane 8.2 3D volume rendering software to determine the volume of each centrosome within each ROI. "Volume rendering" refers to transforming a 2D image stack for 3D visualisation and subsequent analysis. To exclude non-specific signals, a common background subtraction was applied to all images. This parameter was derived by first measuring the average diameter of ~100 centrosomes in 10 ROIs (**Figure 8-4**), and then using the background corresponding to this average diameter as the background subtraction threshold. Finally, data from all optical sections were ordered to enable volume measurement for each centrosome. The final data of volumes

of all centrosomes were then compared to a maximum intensity projection image and centrosomes for each cell were quantified based on proximity to their associated nuclei. The number and volume of all centrosomes associated with each nucleus in the tumour area were recorded.

8.3.4 Centrosomes categorisation

Centrosomes in breast tissue (normal, DCIS or IBC) were categorised into individually distinguishable centrosomes (iCTRs) and megacentrosomes (mCTRs). iCTRs were defined as centrosomes that stain positive for γ-tubulin; iCTR numbers and boundaries were clearly distinguishable, and their volumes lay within the range of centrosome volumes found in normal breast tissue stained for γ-tubulin. The volume range for a normal centrosome was determined by analysing volumes of centrosomes from both adjacent uninvolved tissue from cancer patients and normal breast tissue from disease-free individuals (**Figure 8-5**).

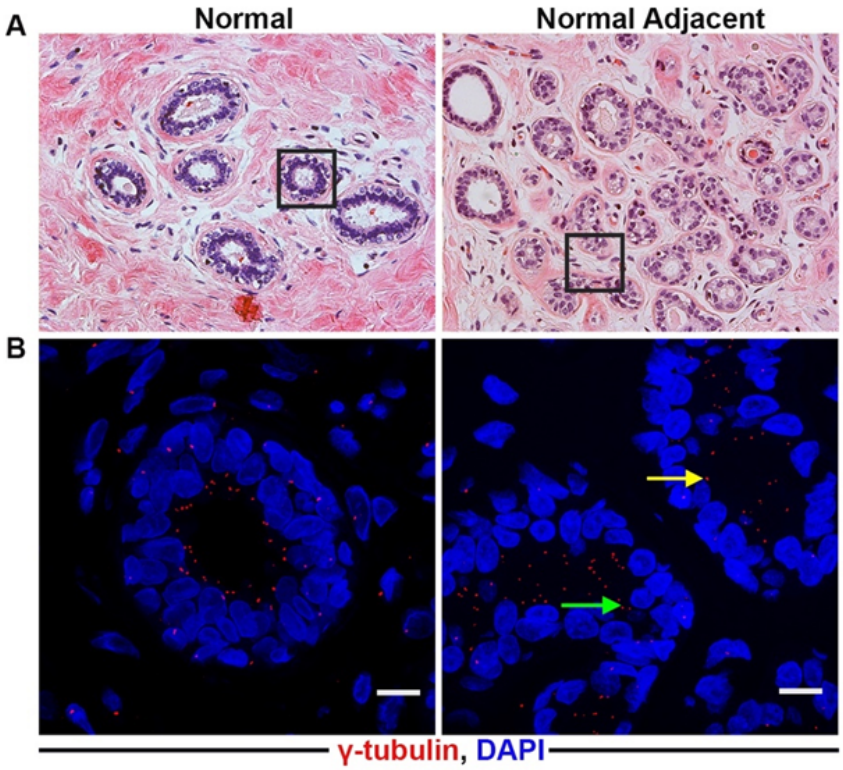

Figure 8-5: Representative immunographs of normal and normal adjacent breast tissue sections for centrosomes

(A) Representative H&E images of the ducts of the normal and normal adjacent breast tissue sections. (Images were captured at 20x magnification). (B) Confocal micrographs showing numerical and structural centrosomal aberrations in normal adjacent breast tissue sections

The mean centrosome volume for the adjacent uninvolved tissue sections was higher relative to the normal tissue from reduction mammoplasty. Thus, the smallest and largest values for individual centrosome volume from normal tissue as the "normal centrosome volume range" for breast tissue were chosen. The mean volume of centrosomes in normal breast epithelial cells ranged from 0.20-0.74μm^3. Centrosomes with volumes >0.74μm^3 were categorised as mCTRs. All centrosomes in each ROI were thus categorised as iCTRs or

mCTRs. In other words, mCTRs are centrosomes with aberrantly large volumes and are considered to represent structurally amplified centrosomes. The numbers and volumes of each iCTR and mCTR associated with each nucleus in an ROI were recorded.

8.3.5 Algorithm-based analytics

A computed algorithm [602] was modified and used to evaluate the CAS. For each sample, a cumulative CAS (CAStotal) was computed based on the formula: CAStotal =CASi + CASm, where CASi and CASm are scores that describe numerical and structural CA phenotypes, respectively.

8.3.5.1 Quantitation of numerical CA

For CASi, equation 1 represents how an aggregate value reflecting both frequency and severity of numerical CA was derived for each sample:

$$CASi = Average\left(\frac{N_i - R_{th}}{R}\right) * \frac{percentage(N_i > R_{th})}{scaling\ factor\ \beta_i}$$

$$= \left(\frac{\sum_{i=1,N_i>2}^{N}(N_i - 2)}{\sum_{i=1}^{N} I(N_i > 2)} * \frac{1}{R}\right) * \frac{p_i}{\beta_i}$$

where:

Rth is the highest number of centrosomes present in a normal breast cell, i.e., 2. Ni is the number of iCTRs in a cell that contains more than 2 iCTRs; Thus, (Ni- Rth) indicates the number of excess centrosomes present in a cell with numerical CA; R is the range of values for number of centrosomes present in a normal cell, which is 2 here; pi is the percentage of cells with >2 iCTRs; ßi is a scaling factor to ensure that both CASi (numerical) and CASm (structural) are assigned equal weight in the formula for CAStotal; N is the total number of cells analysed in the sample; Ni depicts the average number of cells with numerical CA.

The "severity" component of CASi, (i.e., $Average\ \left(\frac{N_i - R_{th}}{R}\right)$ quantifies how "severe" the numerical CA is [i.e., the extent to which the numerical CA exceeds the baseline value of 2 in cells that carry three or more iCTRs (i.e., $N_i > 2$)] (**Figure 8-6**).

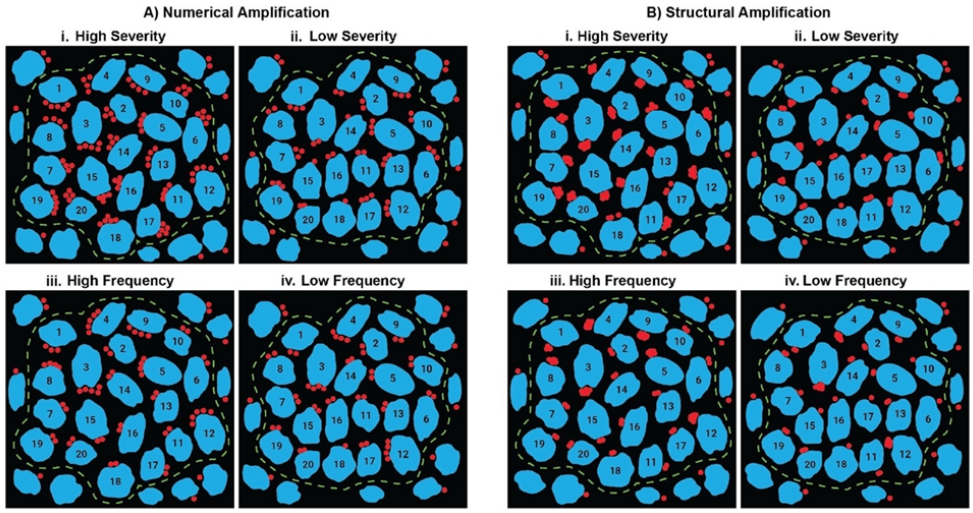

Figure 8-6: Schematic depicting the high and low severity and frequency of numerical and structural centrosome amplification.

Therefore, cancer cells with 1 or 2 iCTRs do not contribute to this component. Since cells with larger numbers of iCTRs

represent severe numerical CA, a linear measurement was implemented to provide a measure of the number of iCTRs (above the baseline value of 2) in a given cell by computing the score (N_i - 2) for each cell. Finally, an average of all these scores is determined. The "frequency" component of the CASi score (i.e., $p_i/ß_i$) provides the scaled frequency of numerical CA in the sample (**Figure 8-6**). The value of CASi scaling factor β_i used here is 0.1 for breast tissue.

8.3.5.2 Quantitation of structural CA

Equation 2 for CASm represents how an aggregate value reflecting both frequency and severity of structural CA is derived for the sample:

$$CASm = Average\left(\frac{V_{im} - V_{th}}{\sigma_{V\,im}}\right) * \frac{percentage(V_{im} > V_{th})}{scaling\ factor\ \beta_m}$$

$$= \frac{\sum_{i=1}^{N}\sum_{m=1}^{N_i}(V_{im} - 0.735) * I((V_{im} > 0.735)}{\sigma_{V\,im}} * \frac{p_m}{\beta_m}$$

where:

$V_{im}$is the volume of the m_{th} mCTR in the i_{th} nucleus; $p_m$is the percentage of cells with mCTRs; where a mCTR is defined as a centrosome whose volume exceeds the V_{th} critical for that tissue; V_{th} critical for a given tissue is the maximum volume of a normal centrosome in that tissue, which is 0.735 µm3 for breast tissue; $\beta_m$is a scaling factor used to ensure that both CASi and CASm contribute equally towards CAStotal. Value of $\beta_m$used here is 0.148. $\sigma_{V\,im}$ is the standard deviation of the volume of mCTRs.

For each mCTR, a z-score was computed based on the formula below, reflecting the extent to which the volume of that mCTR exceeded the maximal normal value (i.e., the value for V_{im} –

V_{th}critical is computed) relative to the baseline (achieved by dividing by the $\sigma_{V\,im}$ the standard deviation):

$$z = \frac{V_{im} - V_{th}}{\sigma_{V\,im}}$$

Next, this value was multiplied by the number of mCTRs per nucleus. Finally, all values were averaged to obtain the severity score for structural CA (**Figure 8-6**). The frequency component of CASm has essentially the same overall mathematical formula as the corresponding term in the CASi component (**Figure 8-6**). The components, CASi and CASm, contribute equally to the CAStotal score.

Next, 15 high-grade DCIS samples we co-immunolabeled for both centrosomes (using anti ɣ-tubulin antibody) and centrioles (using anti-centrin-2 antibody) and generated CAStotal. In all samples, ɣ-tubulin foci invariably overlapped with centrin-2 foci, confirming that both structurally and numerically amplified centrosomes are bona fide centrosomes and not simply aggregates of pericentriolar material. It was also observed that none of the mCTRs had >2 centrin-2 foci, suggesting that enlarged γ-tubulin foci represent structurally augmented centrosomes and not supernumerary centrosomes that are tightly clustered to be indistinguishable (**Figure 8-7**).

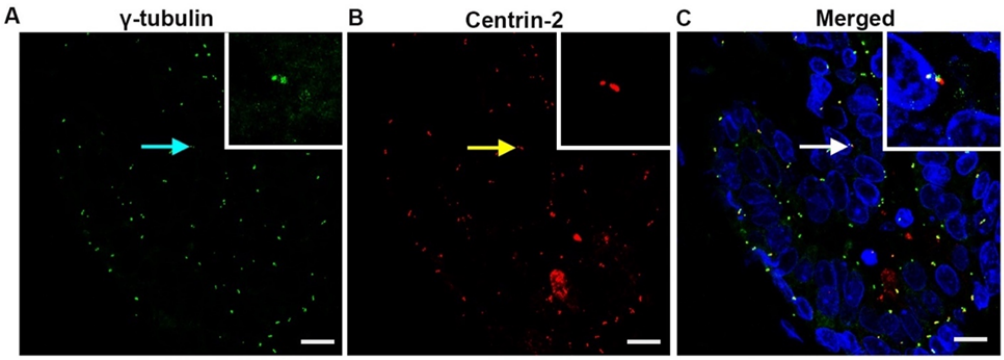

Figure 8-7: Representative confocal micrographs of DCIS tissue sections immunolabeled for centrin-2 (red), γ-tubulin (green) and nuclei (blue) in split form

8.3.6 **Statistical analysis**

Statistical analysis was accomplished with SAS 9.4 software (Cary, NC, USA), and the R-project version 3.4.3 (R Foundation for Statistical Computing, Vienna, Austria, https://www.R-project.org/). Raw CA volume data were converted to CASi, CASm and CAStotal according to the algorithm. Scaling factors recommended were used to normalise score of CASi and CASm in the range 0–3. The tests of group mean differences shown in Box Plots were based on nonparametric Wilcoxon Rank Sum Tests and Kruskal-Wallis tests. LRFI was used as the endpoint for the survival analysis (restricted to 10 years). The optimal cut-off (threshold used to categorise patients into high-or low-risk of local recurrence subgroups) of the CAStotal value was selected based on the results of 133 log-rank tests. We simply set each possible CAStotal value from 133 cases in the DC as cut-off and then constructed Kaplan-Meier survival estimators

for cases classified into high-risk and low-risk groups. The value 1.436 was finalised since it minimised the log-rank *p*-value. The same CAStotal cut-off was then used for the 119 cases from the VC to validate the model's effectiveness. Both univariate and multivariable Cox proportional hazard models, with age, grade, comedo necrosis, and RT, were built to estimate HR and 95%CI between high vs. low CAStotal groups. A non-zero slope was detected in a generalised linear regression of the scaled Schoenfeld residuals on functions of time, which satisfied of the proportional hazards' assumption (**Figure 8-8**). A 2X2 confusion matrix and performance metrics was used for sensitivity analysis. The fitted Cox models were also used to predict the approximate 10-year recurrence rate using SAS PROC PHREG module. For all tests $p<0.05$ was considered to be statistically significant. All Graphs and illustrations were produced by Georgia State University team.

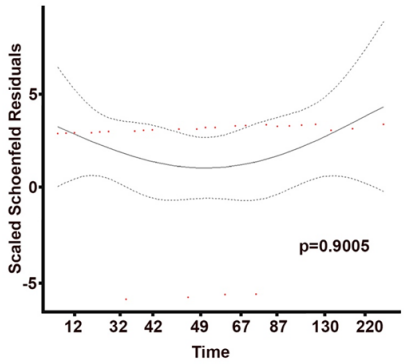

Figure 8-8: Graphical checks of the proportional hazard assumption

Scaled Schoenfeld residuals against time plotted for CAStotal in the proportional hazards Cox model

8.4 **Results**

8.4.1 **CAS and DCIS recurrence**

Centrosome numbers and volumes evaluated and scored for CASi and CASm were integrated using our algorithm to generate a composite CAStotal value for each sample of the DC. Interestingly, DCIS patients that developed local recurrence within 10 years showed significantly higher CASi relative to recurrence free patients (p=<0.0001). Recurrent cases showed greater CASi severity (p=0.025) and higher CASi frequency (p<0.0001) of numerical CA. Analysis of structural CA revealed that CASm was significantly higher (p=0.04) for in the recurrence group. DCIS with recurrence exhibited greater CASm severity (p=0.01) and CASm frequency (p=0.08) of structural CA. CAStotal was significantly higher for DCIS patients with recurrence relative to recurrence-free patients regardless of grade.

Employing the same methodology for the VC, the CAS was calculated and found that irrespective of grade, DCIS cases with recurrence exhibited higher CAStotal (p<0.0001). Further, similar trends were seen for other CAS subcomponents as observed in the DC; the ranked mean values of CASi (p<0.0001) and CASm (p<0.0001), including their severity (CASi severity p=0.0014; CASm severity

p=0.014) and frequency (CASi frequency p<0.0001, CASm frequency p<0.0001) components, were higher in the patient subgroup with recurrence than in recurrence-free subgroup. **Figure 8-9** to **Figure 8-11** summarise these results.

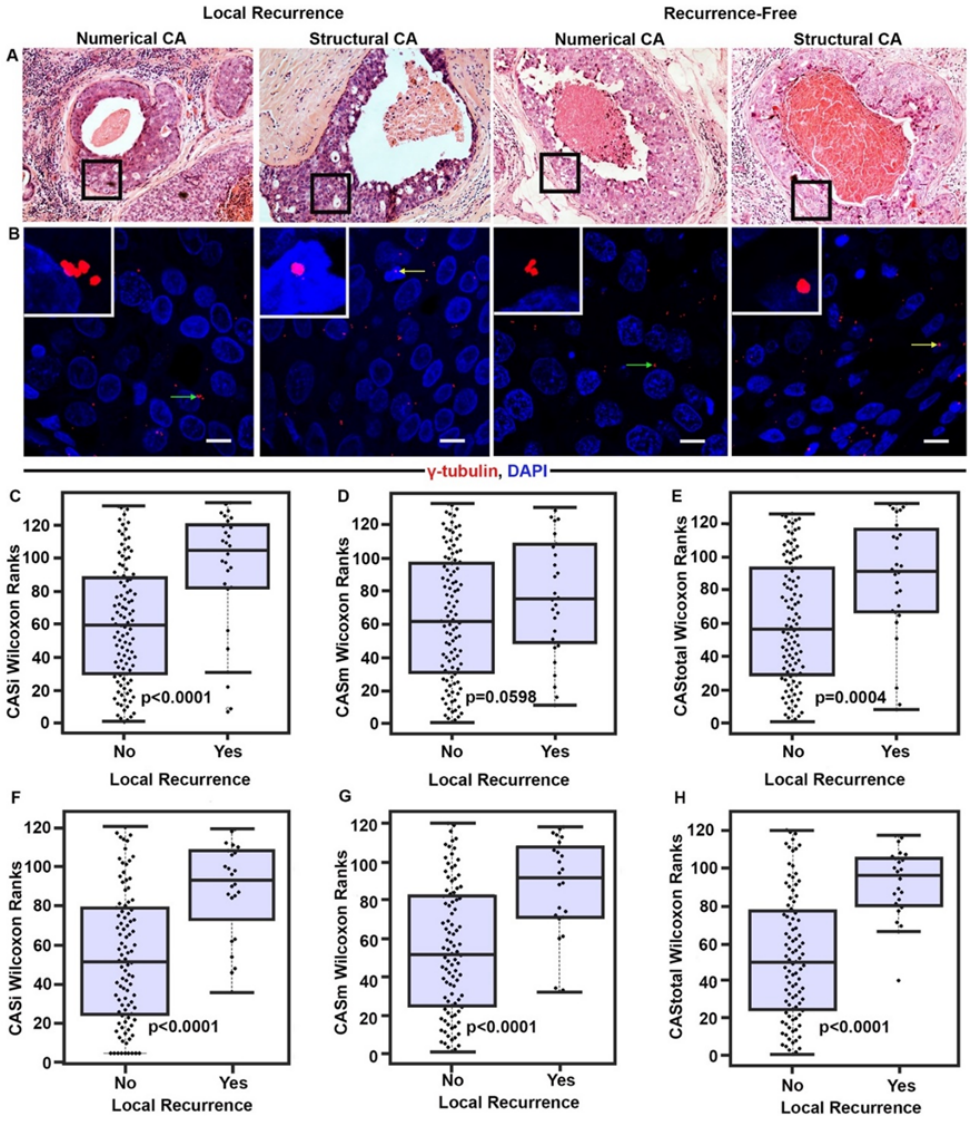

Figure 8-9: DCIS cases in the DC with ipsilateral recurrence exhibit higher CAS than recurrence-free cases

(A) Representative H&E images (20x magnification) of the ducts from DCIS with and without local recurrence. (B) Confocal micrographs showing numerical (green arrows) and structural (yellow arrows) CA in DCIS with or without recurrence. Scale bar (white), 20μm. Beeswarm box plots showing Wilcoxon ranks for pure DCIS cases with local recurrence and without recurrence in DC. (C) CASi (D) CASm (E) CAStotal. p<0.05 was considered statistically significant. Beeswarm box plots showing Wilcoxon ranks for pure DCIS cases with local recurrence and recurrence-free cases in VC (F) CASi, (G) CASm, and (H) CAStotal

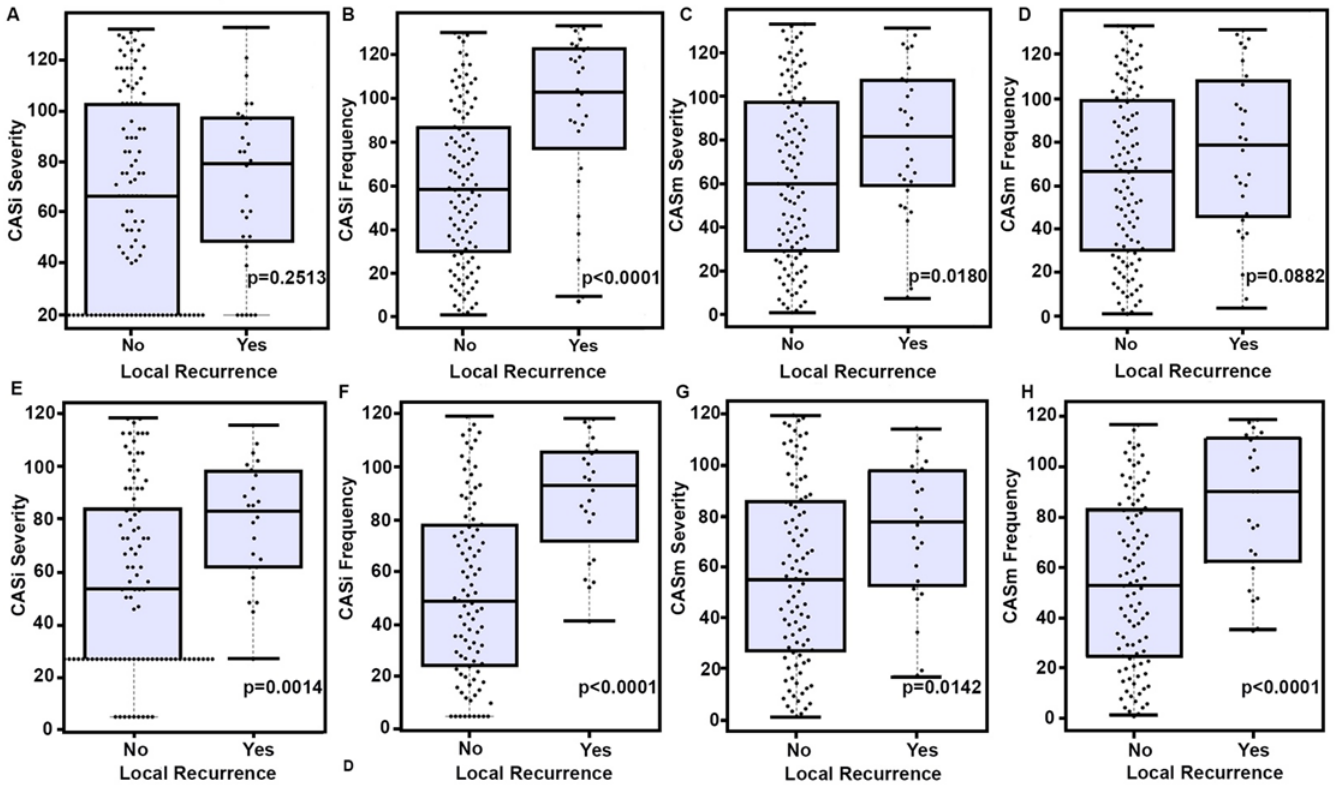

Figure 8-10: DCIS cases in the DC with local recurrence exhibit higher frequency and severity of both numerical and structural CA

Beeswarm box plots showing Wilcoxon ranks for different CASs in pure DCIS cases with recurrence and without recurrence in DC and in VC . (A) CASi severity, (B) CASi frequency, C) CASm severity, D) CASm frequency. E) CASi severity, F) CASi frequency, G) CASm severity, D) CASm frequency

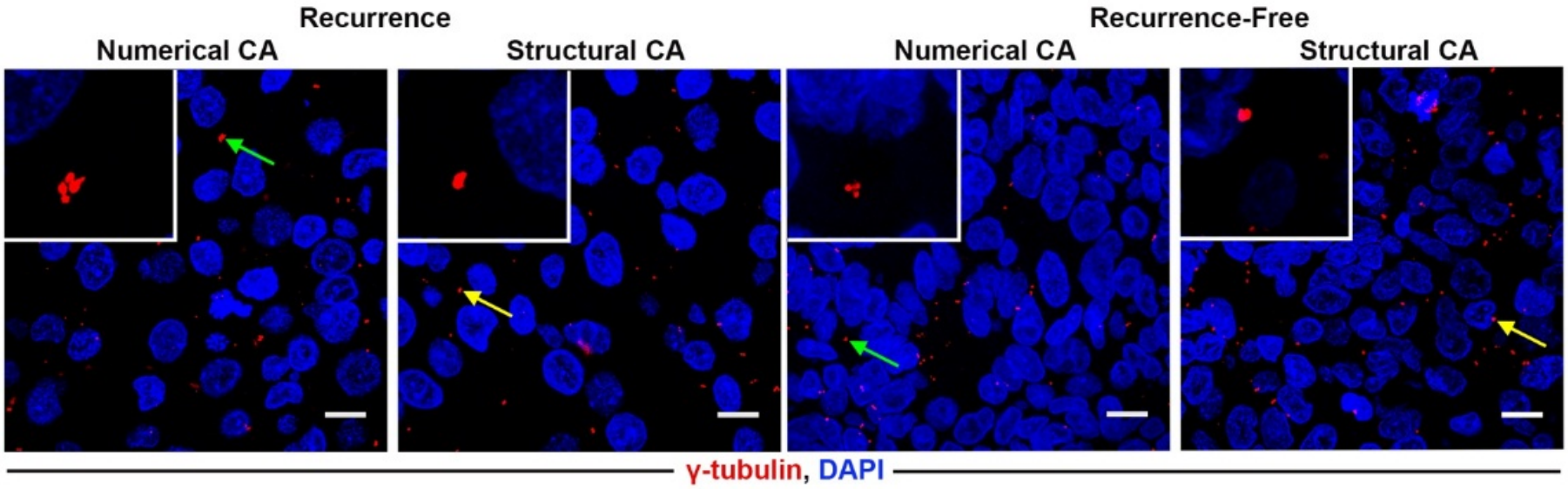

Figure 8-11: Representative confocal micrographs of DCIS tissue sections from VC immunolabeled for γ-tubulin (red) and Hoechst (blue) in recurrence and recurrence free samples

Similar findings were evident for grade-matched patients in DC and VC (**Figure 8-12**) and patients that were treated with BCS (**Figure 8-13**). Collectively, the data strongly suggest a stark difference in CA between DCIS tumours of patients with and without local recurrence.

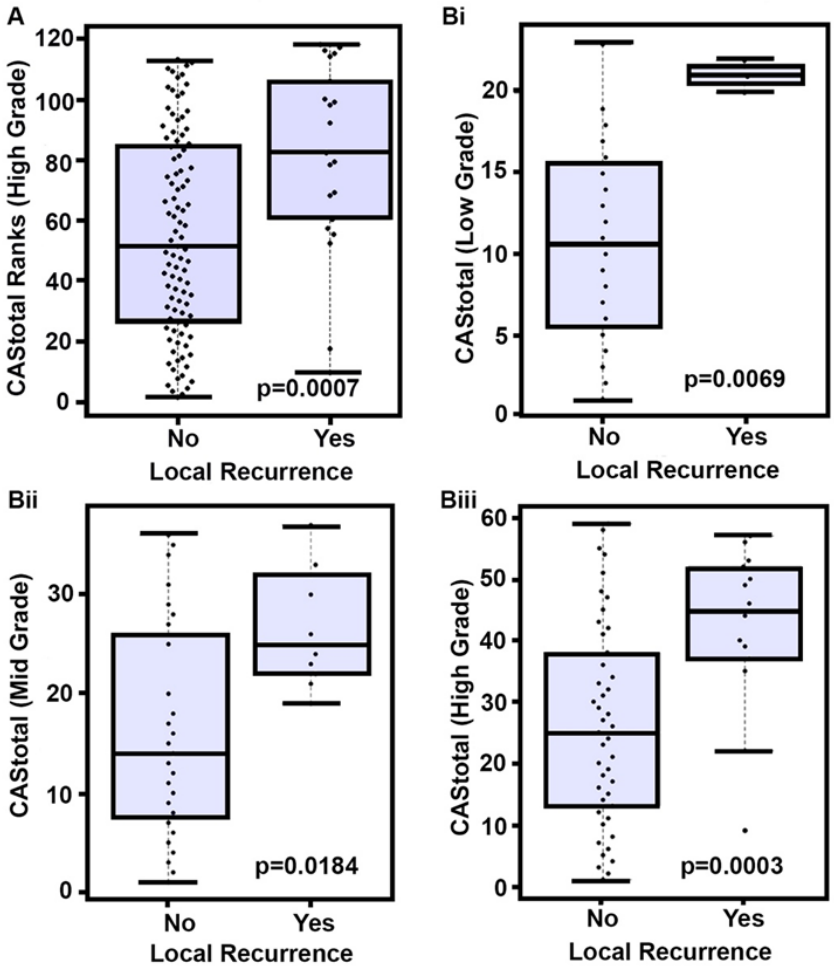

Figure 8-12: Grade matched DCIS cases with local recurrence exhibit higher CAS than grade-matched cases without recurrence

Beeswarm box plots showing CAStotal Wilcoxon ranks for pure, high-grade DCIS with local recurrence and without recurrence. Beeswarm box plots showing CAStotal Wilcoxon ranks for low-grade pure DCIS cases with recurrence and without recurrence in VC. (B) Beeswarm box plots showing CAStotal Wilcoxon ranks for intermediate-grade DCIS. (C) Beeswarm box plots showing CAStotal Wilcoxon ranks for high-grade DCIS

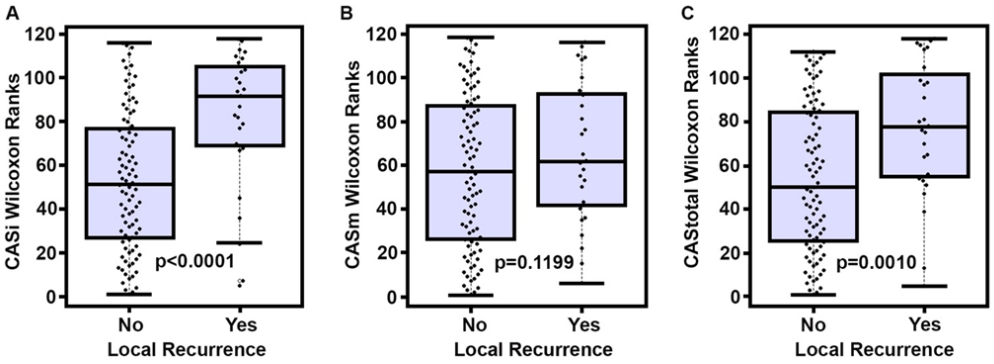

Figure 8-13: Recurrent DCIS cases treated with BCS in the DC exhibit higher CAS than recurrence-free cases

Upon stratification of all DC patients into low- and high-CAS groups, DCIS patients with high CASi were associated with poorer LRFI (p<0.0001, HR=4.80) relative to those with low CASi. Similarly, high CASm was associated with poorer LRFI (p=0.04, HR=2.396) compared to low CASm. CAStotal stratified the high-risk and low-risk DCIS patients with high significance (p<0.0001, HR= 6.3). A total of 86% of patients with local recurrence were in the high CAStotal group. This association with CAStotal remained significant (p<0.0001, HR=7.4) even after accounting for potential confounders, including comedo necrosis, tumour grade, age and RT. Although presence of comedo necrosis and CAStotal were associated with LRFI in univariate analyses, only CAStotal remained significantly associated with LRFI in multivariable analyses (p<0.0001, HR=5.5). Furthermore, when similar Cox regression univariate and multivariate analysis was performed

for CASi and CASm separately CASi and CASm was the strongest and most significant independent predictor of LRFI, (p<0.0001, HR=6.8 for CASi) and (p=0.002, HR=4.2, for CASm). Similar results were evident for the cases that were treated only with BCS. To verify whether CAStotal, CASi, and CASm could be used to stratify patients in the VC, pre-determined CAS cut-offs from the DC were used. High CASi, CASm and CAStotal were associated with poorer LRFI compared to low CASi, CASm and CAStotal, respectively. Of the patients with recurrence, 75% were classified into the high CASi group and ~67% of those patients were classified into the high CAStotal subgroups. Of the patients in the recurrence-free group, 87% were classified in the low CASm group. These results are illustrated in **Figure 8-14**, **Figure 8-15** and **Figure 8-16**. In both univariate and multivariate analyses after adjusting for potentially confounding effects of factors like age, grade and RT and CAStotal and comedo necrosis were the strongest and most significant independent predictor of LRFI. Similar to DC it was observed that CASi and CASm also independently predicted the LRFI.

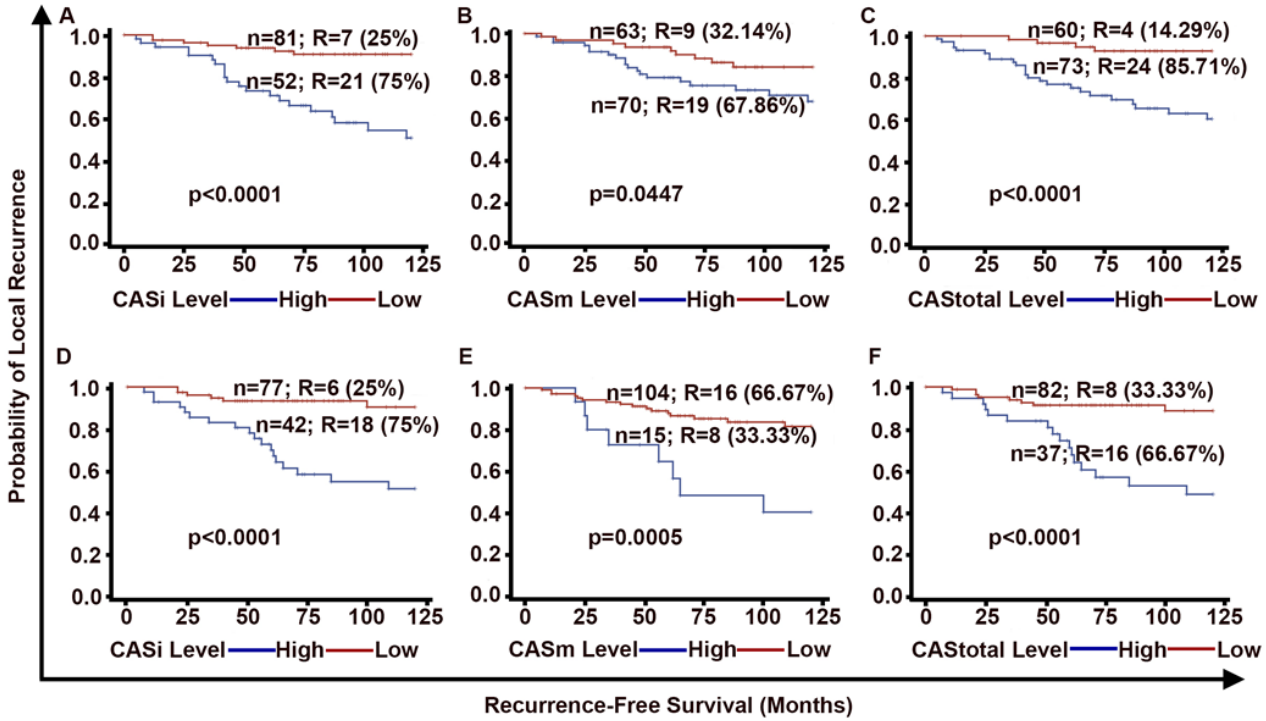

Figure 8-14: In the DC and VC, higher CAS is associated with poorer LRFI

Kaplan Meier survival curves representing the LRFI of patients in the DC stratified into (A) CASi high and low groups, (B) CASm high and low groups, (C) CAStotal high and low groups. Kaplan Meier curves representing the LRFI of DCIS patients in the VC stratified into (D) CASi high and low groups, (E) CASm high and low groups, and (F) CAStotal high and low groups. N: total number of patients in each group; R: number of patients who developed local recurrence

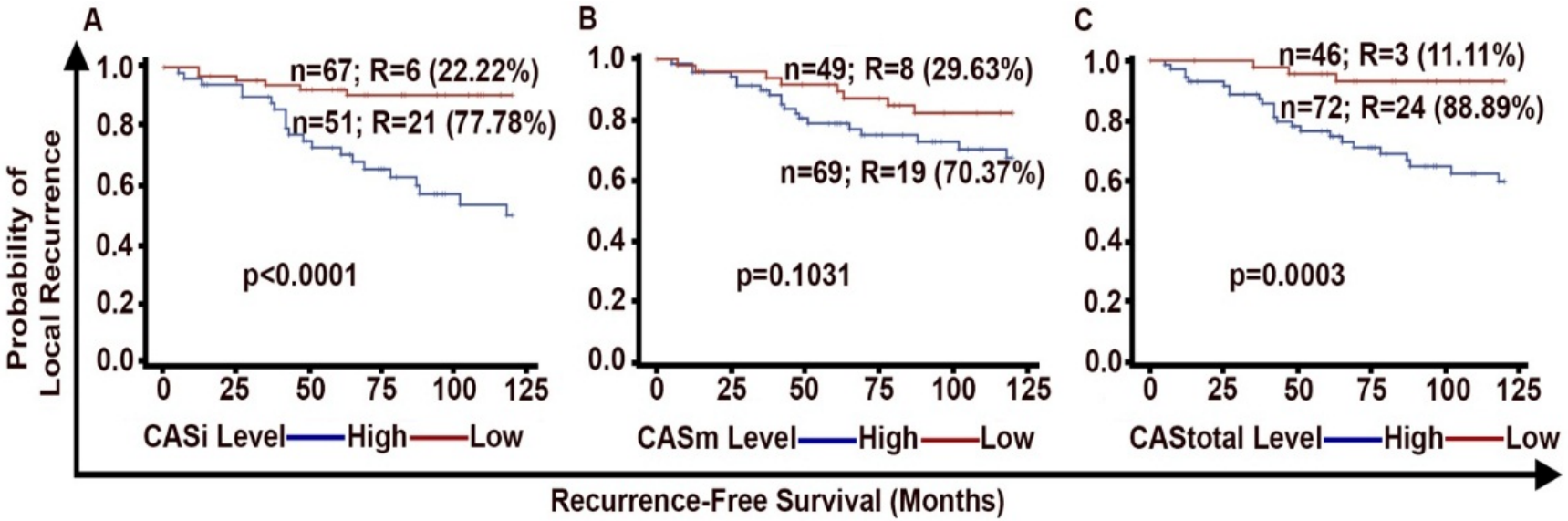

Figure 8-15: Higher CAS is associated with poorer LRFI for DCIS patients treated with BCS in the DC

Kaplan Meier survival curves representing the LRFI of patients in the DC stratified into: (A) CASi high and low groups, (B) CASm high and low groups, (C) CAStotal high and low groups. N: total number of patients in each group; R: number of patients who developed recurrence

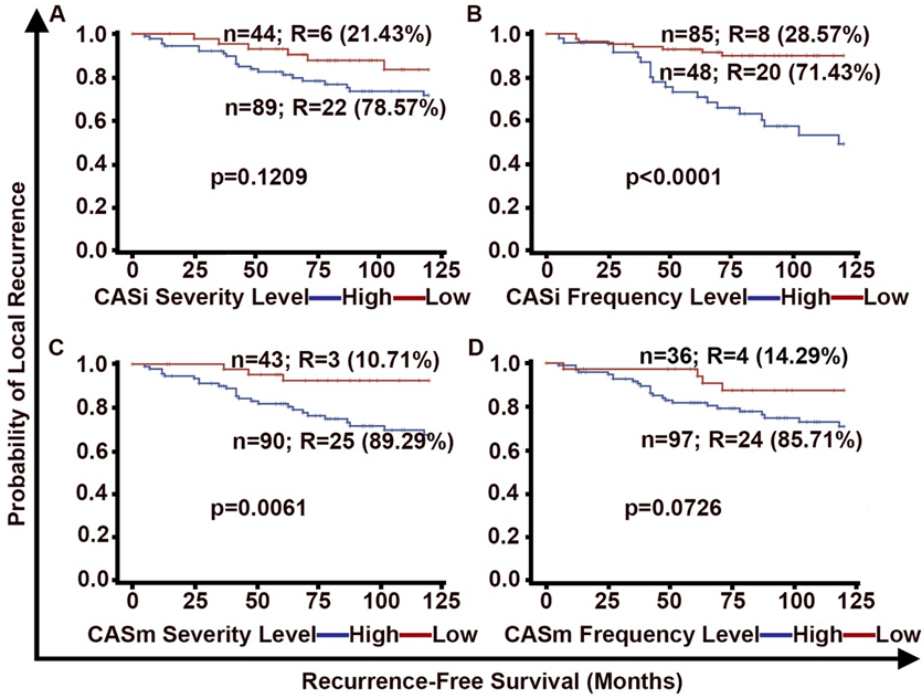

Figure 8-16: Higher severity and frequency of numerical and structural CA are associated with poor LRFI in the DC

Kaplan-Meier survival curves representing the LRFI of patients in: (A) high and low groups based on the severity component of numerical CA, (B) high and low groups based on the frequency component of numerical CA, (C) high and low groups based on the severity component of structural CA, (D) high and low groups based on the frequency component of structural CA. N: total number of patients in each group; R: number of patients who showed local recurrence

In addition a bootstrap analysis for the COX regression univariate and multivariate models on the combined (DC+VC=252) dataset was performed and it was observed that mean HR for the univariate analysis was 5.22 and the multivariate analysis conditional on all other variables is 6.58 (p<0.0001) (**Figure 8-17**). Also, CAStotal was able to identify patients for both DCIS (**Figure 8-18**) and invasive recurrence even after adjusting for potentially confounding effects of factors (**Figure 8-18**) in both DC and VC.

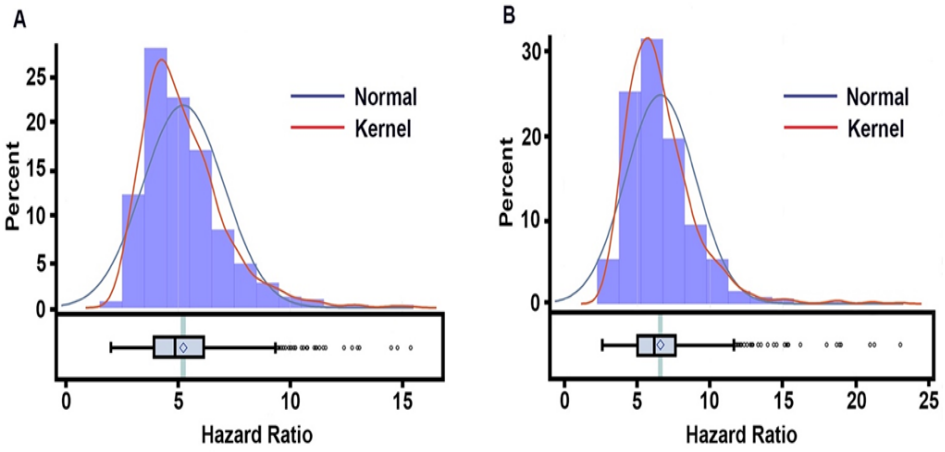

Figure 8-17: Fitted normal and kernel density curves on the histogram are estimated based on the bootstrap sample mean and standard deviation

They show that 1000 hazard ratios are nearly normally distributed with light skewness. A) Univariate analysis, and B) multivariate analysis

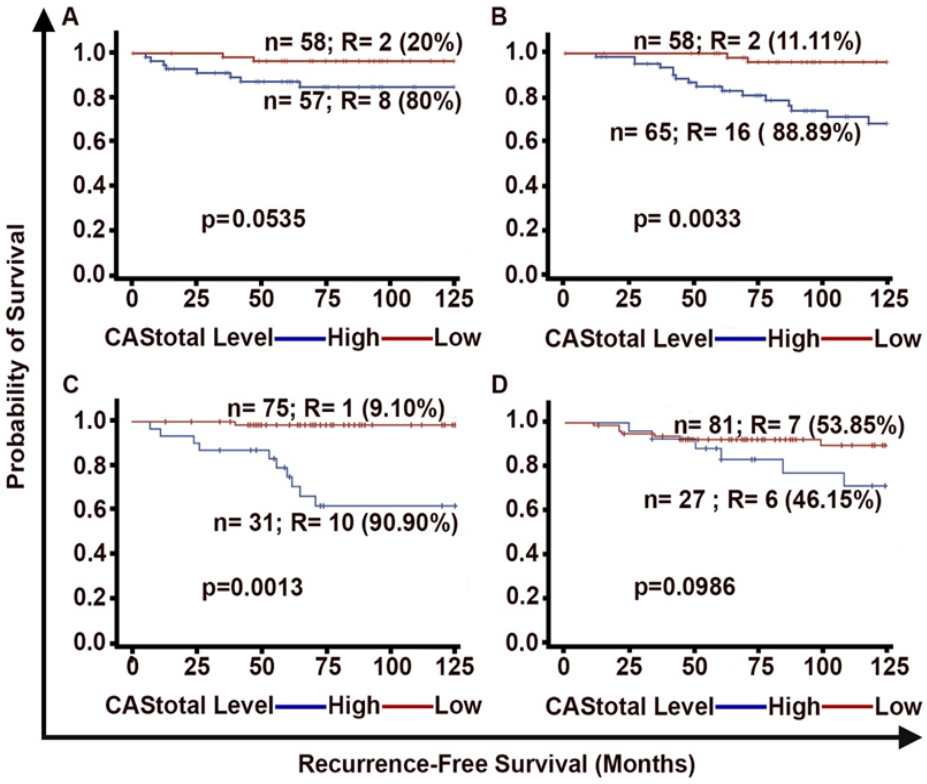

Figure 8-18: Higher CAStotal is associated with LRFI

Kaplan Meier survival curves representing the LRFI of patients in the DC stratified into CAStotal high and low groups in, (A) DC where recurrence was in DCIS form, (B) DC where recurrence was in invasive form (C) VC where recurrence was in DCIS form (D) VC where recurrence was in invasive form. N: total number of patients in each group; R: number of percentage/proportion of patients with local recurrence out of the total number of patients with recurrence in both groups combined

Further, in both the DC and VC, the 10-year estimated risk of ipsilateral local recurrence increased continuously as the CAStotal increased (**Figure 8-19**).

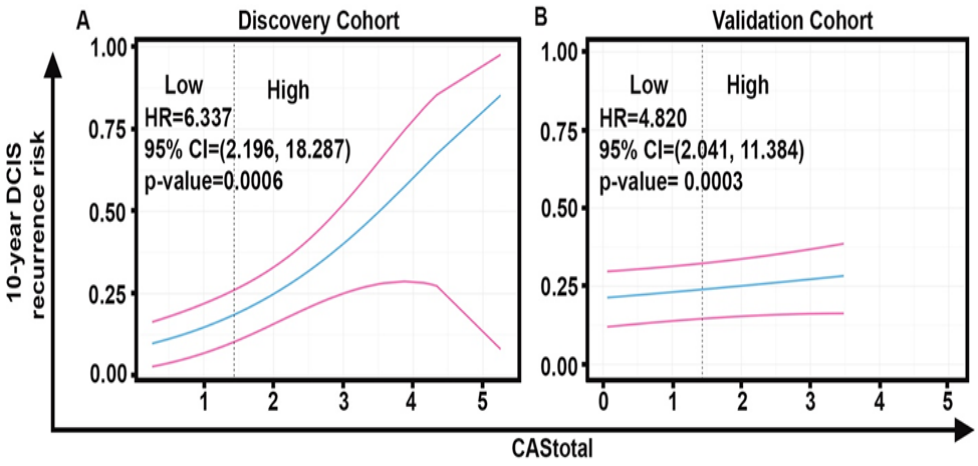

Figure 8-19: Estimated 10-year risk of local recurrence as a continuous function using CAStotal

Next, it was determined if the survival model had high predictive accuracy using the Harrell's concordance index. The higher the concordance index, the better the survival model discriminates between patients who experienced recurrence versus those who have not. The results indicated that any patient with a shorter LRFI had a 73% probability of being in the high CAStotal group. Also, a 2x2 confusion matrix performance metrics was created to show the accuracy of CAStotal to predict 10-year recurrence. To do so, the sensitivity, specificity, positive predictive value (PPV), negative predictive value (NPV) of CAStotal and odds ratio

(OR) were calculated, for both cohorts to compare the performance of CAStotal with that of the traditional clinicopathological variables. The results showed that CAStotal provided an accuracy (0.60), sensitivity (0.85), specificity (0.53), PPV (0.32), NPV (0.93), and OR (6.8). Additionally, select clinical variables (age, grade, tumour size and RT) neither improved the overall model nor added any prognostic relevance individually. These results indicate that CAStotal, in both cohorts, shows a relatively superior specificity, PPV, NPV, and OR compared to the other clinicopathological variables.

8.4.2 CAS and RT benefit

In the DC, CAStotal stratified DCIS patients treated with surgery (mastectomy/BCS) or BCS alone (**Figure 8-20**) into subgroups with high and low local recurrence risks with greater significance relative to patients treated with surgery (mastectomy/BCS) and post-operative RT (HR=11.6, $p<0.0001$ for surgery alone; HR=17.05, $p=0.0005$ for BCS alone, and HR=2.4, $p=0.3589$ for BCS+RT). Similarly, in the VC, CAS stratified DCIS patients treated with surgery only (**Figure 8-21**) into subgroups with high and low recurrence risks with higher significance compared to patients treated with surgery (mastectomy or BCS) and post-operative adjuvant RT (BCS+RT) (HR=3.97, $p=0.049$ for surgery alone

and HR=1.4, p=0.109 for BCS+RT). These data suggest that CAStotal can identify patients who might benefit from adjuvant RT. In addition, it was observed that DCIS patients who recurred as IBC exhibited higher CAStotal (p=0.07) compared to the patients who recurred as DCIS (**Figure 8-22**) in the DC.

8.4.3 Clinical significance of CAS total

The clinical significance of CAS was evaluated by examining the associations of CAS with traditionally employed clinicopathological variables i.e., age, grade, tumour size, comedo necrosis, and RT (**Figure 8-23** and **Figure 8-24**). The data shows that CAStotal provides clinically relevant prognostic information over and beyond what is provided by current clinicopathologic parameters alone. Given that high CA is associated with more aggressive disease phenotypes, we not only observed the association of high CAStotal with higher recurrence rates, but also found that CAStotal segments patient subgroups more deeply than traditional clinicopathologic parameters. The forest plot (**Figure 8-25**) for high grade DCIS patients in the DC showed that patients with comedo necrosis (red), are at high risk of recurrence (0.59) compared to the overall recurrence rate for patients (0.33), regardless of the CAStotal. When we further stratified

these DCIS patients with comedo necrosis into high (green) and low (blue) CAS groups, it was observed that the recurrence rate for the high CAS group (green) was 0.83 and the rate for the low CAS subgroup (blue) was 0.10. Similar results were observed for VC (**Figure 8-25**). Thus, CAS was able to more deeply segment the patients with comedo necrosis into high and low risk groups. Similar trends were evident for tumour size, RT, and age.

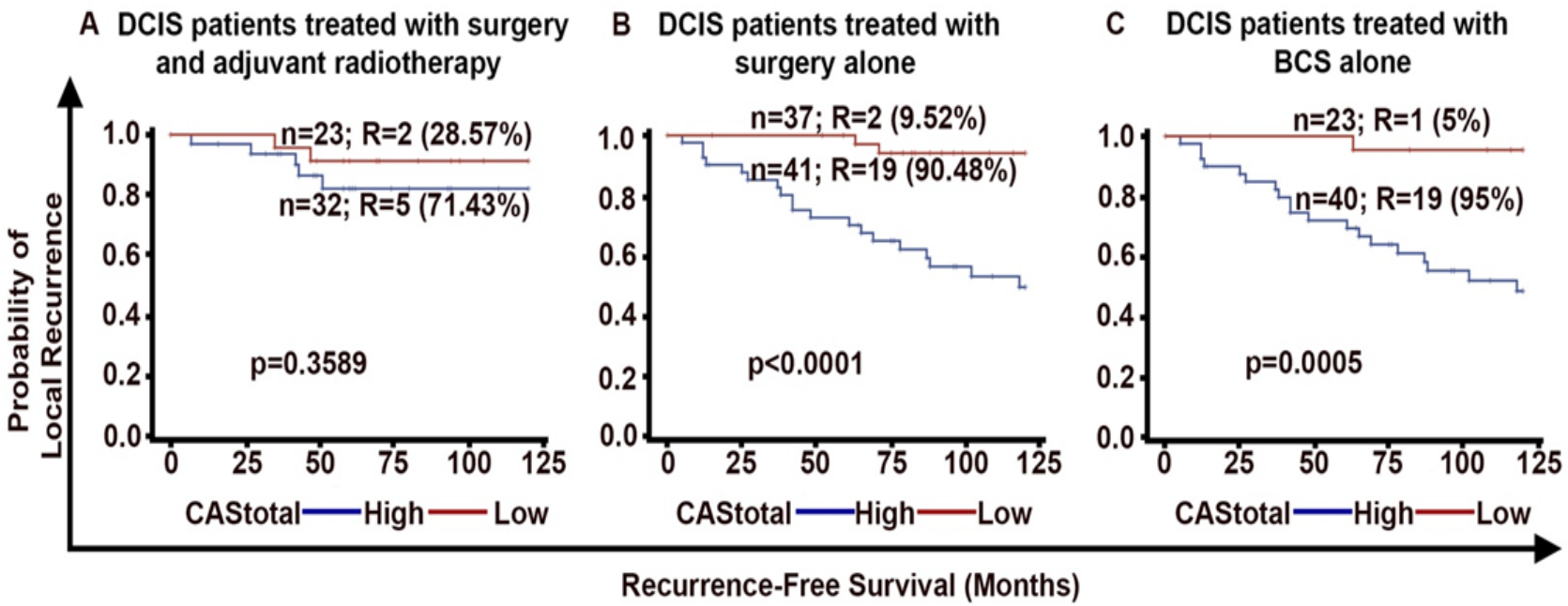

Figure 8-20: Higher CAS is associated with poor LRFI for DCIS patients treated with surgery

Kaplan Meier survival curves representing LRFI of the DCIS patient subgroups stratified based on high vs. low CAStotal: (A) DCIS patients treated with surgery and adjuvant RT (mastectomy/BCS+RT), (B) DCIS patients treated with surgery alone (mastectomy/BCS), (C) DCIS patients treated with BCS alone. N: total number of patients in each group; R: number of patients who showed local recurrence

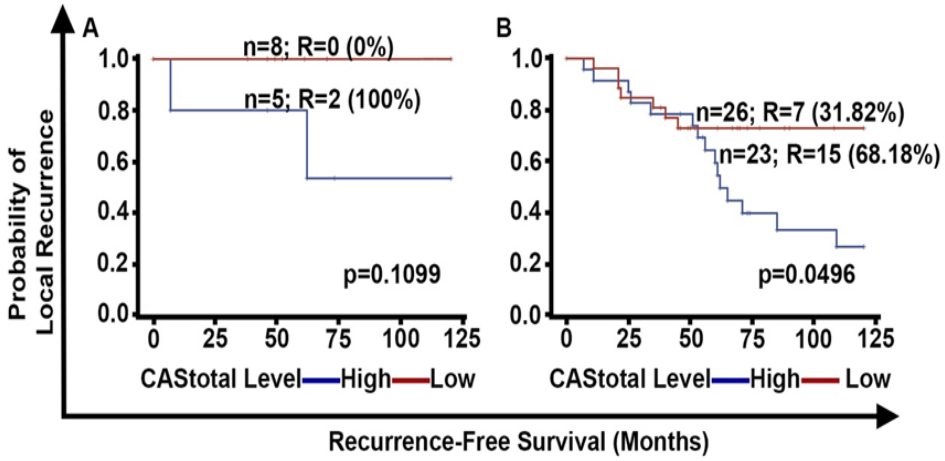

Figure 8-21: Higher CAS is associated with poor LRFI for DCIS patients in the VC treated with surgery alone

Kaplan Meier survival curves representing the LRFI of the DCIS patient subgroups stratified based on high vs. low CAStotal. (A) DCIS patients treated with surgery (BCS/mastectomy) and adjuvant RT (surgery+RT), (B) DCIS patients treated with surgery alone. N: total number of patients in each group; R: number of patients who showed Local recurrence

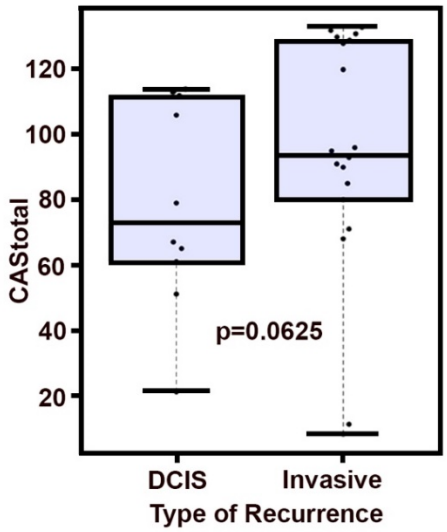

Figure 8-22: DCIS cases who recurred as IBC exhibited higher CAStotal compared to the patients who recurred as DCIS

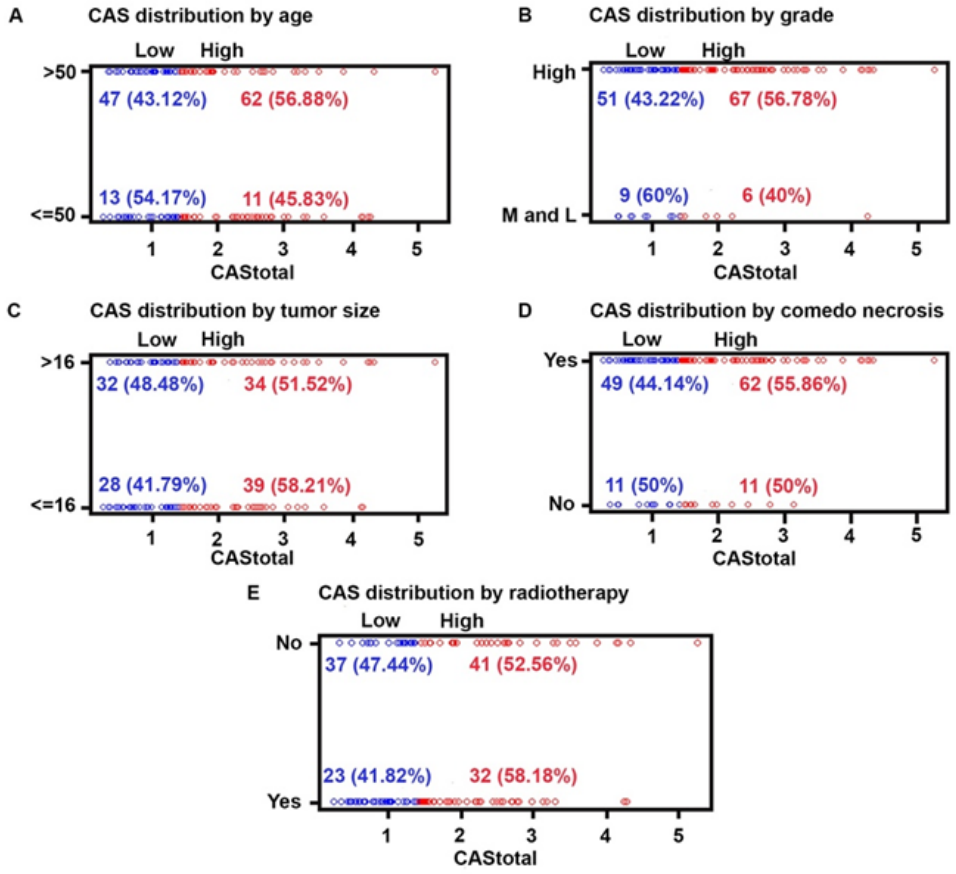

Figure 8-23: Distribution of the CAStotal according to clinical and pathologic characteristics in DC

Distribution of CAStotal according to (A) age, (B) grade, (C) tumor size, (D) comedo necrosis, and (E)RT. Blue: number and percentage of patients in the low-CAStotal subgroup; Red: Number and percentage of patients in the high-CAStotal subgroup

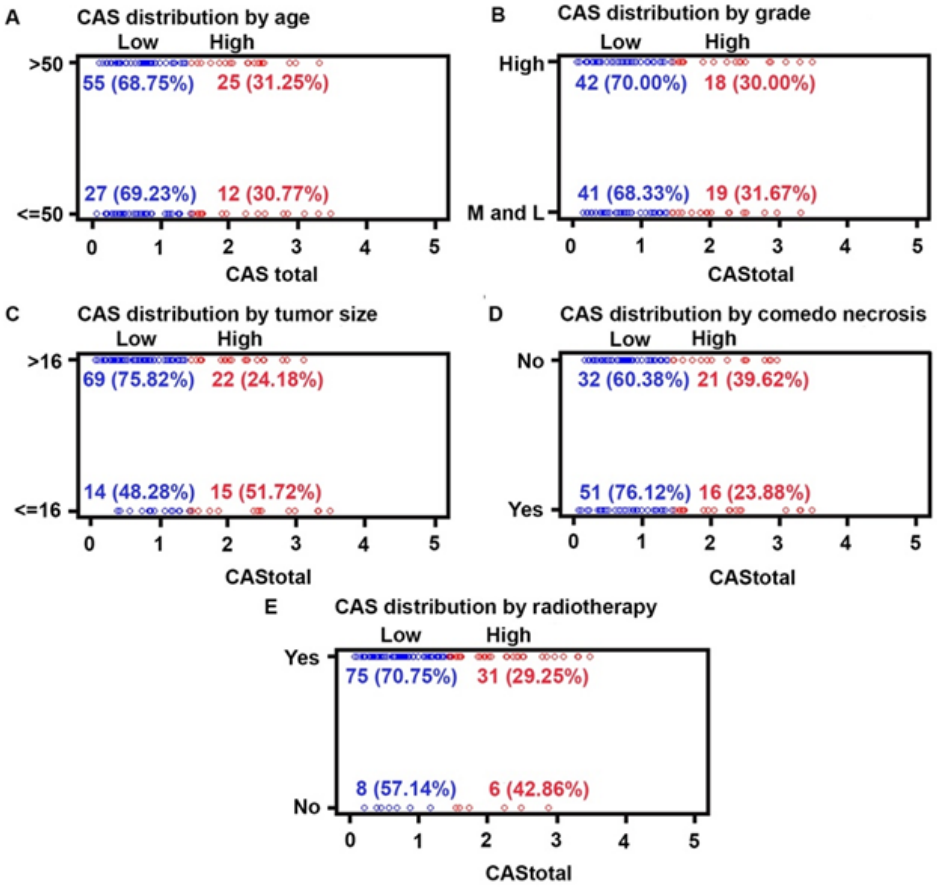

Figure 8-24: Distribution of the CAStotal according to clinical and pathologic characteristics in VC

Distribution of CAStotal according to (A) age, (B) grade, (C) tumor size, (D) comedo necrosis, and (E) RT

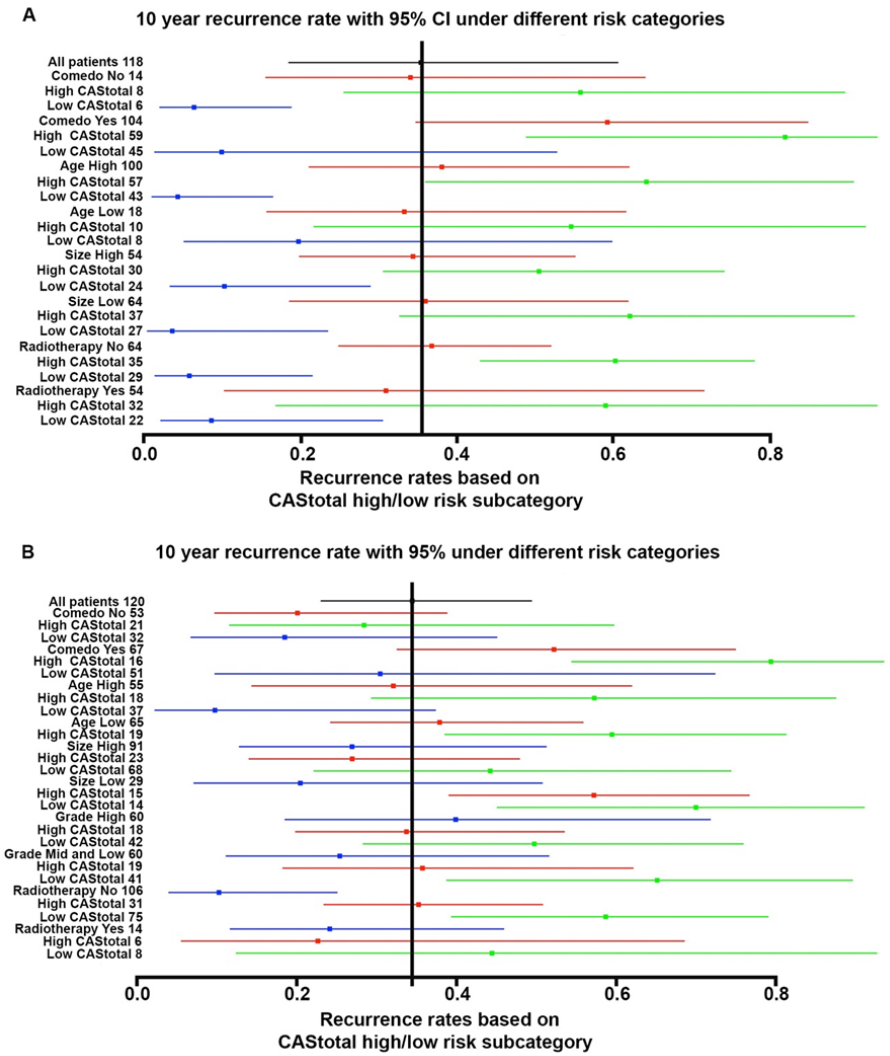

Figure 8-25: Forest plot representing estimates of 10-year recurrence rates within high grade DCIS patient subgroups

(A) CAStotal allows deeper stratification of patient subgroups than traditional clinicopathologic parameters alone in the high grade DCIS patient subgroups from the DC. Forest plot representing estimates of 10-year risk ratio (with 95% CIs) within high grade DCIS in the DC defined by clinical parameters alone, or within the CAStotal high and low risk subpopulations within these subgroups. The CAStotal cutpoint used here was that used for the whole DC patient population and not the optimal cutpoint for the patient subgroup. The black box represents the overall risk ratio. The red boxes represents the risk ratio observed among the patients in the specific subgroup defined by the clinical parameter (regardless of their CAStotal). The green boxes represents the risk ratio in the high CAStotal sub-population and the blue boxes represents the risk ratio in the low CAStotal sub-population within each subgroup. **(B)** CAStotal enables deeper stratification of patient subgroups than traditional clinicopathologic parameters alone in the VC. Forest plot representing estimates of 10-year risk ratio (with 95% CIs) within DCIS subgroups (from VC) defined by clinical parameters alone, or within the CAStotal high- and low-risk subpopulations. The CAStotal cutpoint used here was the cutpoint used for the entire DC. The black box represents the overall risk ratio observed for the DCIS patients in the VC. The red boxes represents the risk ratio observed for the patients in the specific subgroup defined by the clinical parameter (and regardless of their CAStotal). The green boxes represent the risk ratio in the high CAStotal sub-population, and the blue box represent the risk ratio in the low CAStotal sub-population within each subgroup.

8.4.4 Comparison between CAS and VNPI in recurrence prediction

The performance of VNPI and CAStotal in cases combined from both DC and VC (n=164) was assessed (**Figure 8-26**) using univariate and Kaplan Meier survival analyses. Higher VNPI was not significantly associated with poorer LRFI and VNPI did not significantly stratify patients as high and low risk subgroups. By contrast, CAStotal stratified patients into subgroups of high and low risk of local recurrence (CAStotal HR=5.6 vs. VNPI HR=0.70). Multivariable analyses adjusted for other potentially confounding factors, revealed that CAStotal showed the highest association with LRFI.

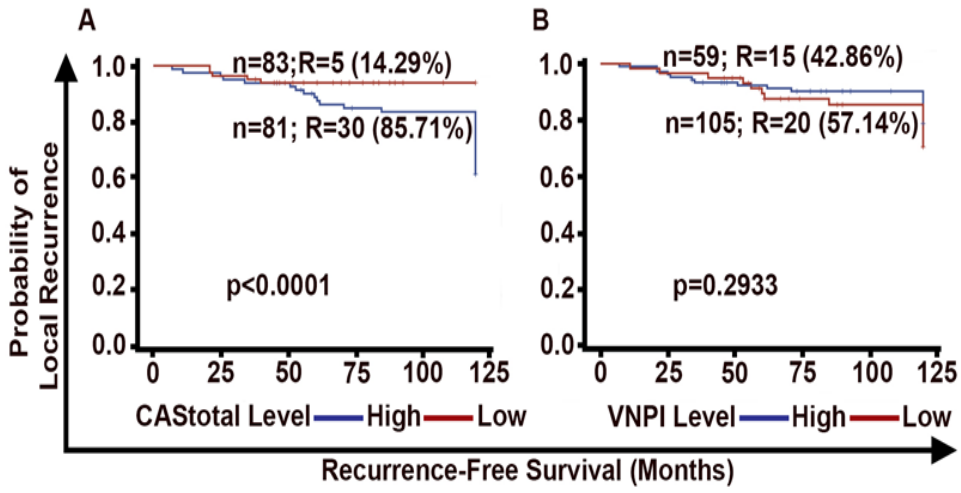

Figure 8-26: Comparison of the stratification of DCIS patients by CAStotal and VNPI

Kaplan Meier survival curves representing the LRFI of DCIS patients stratified by (A) CAStotal, and (B) VNPI. N: total number of patients in each group; R: number of patients who showed local recurrence

8.4.5 Comparison between CAS in pure DCIS and DCIS co-exist with IBC

DCIS regions within the mixed DCIS samples showed significantly higher CASi (p=0.0043), CASm (p=0.0006) and CAStotal (p<0.0001) when compared to the corresponding cores for pure DCIS cases (**Figure 8-27**).

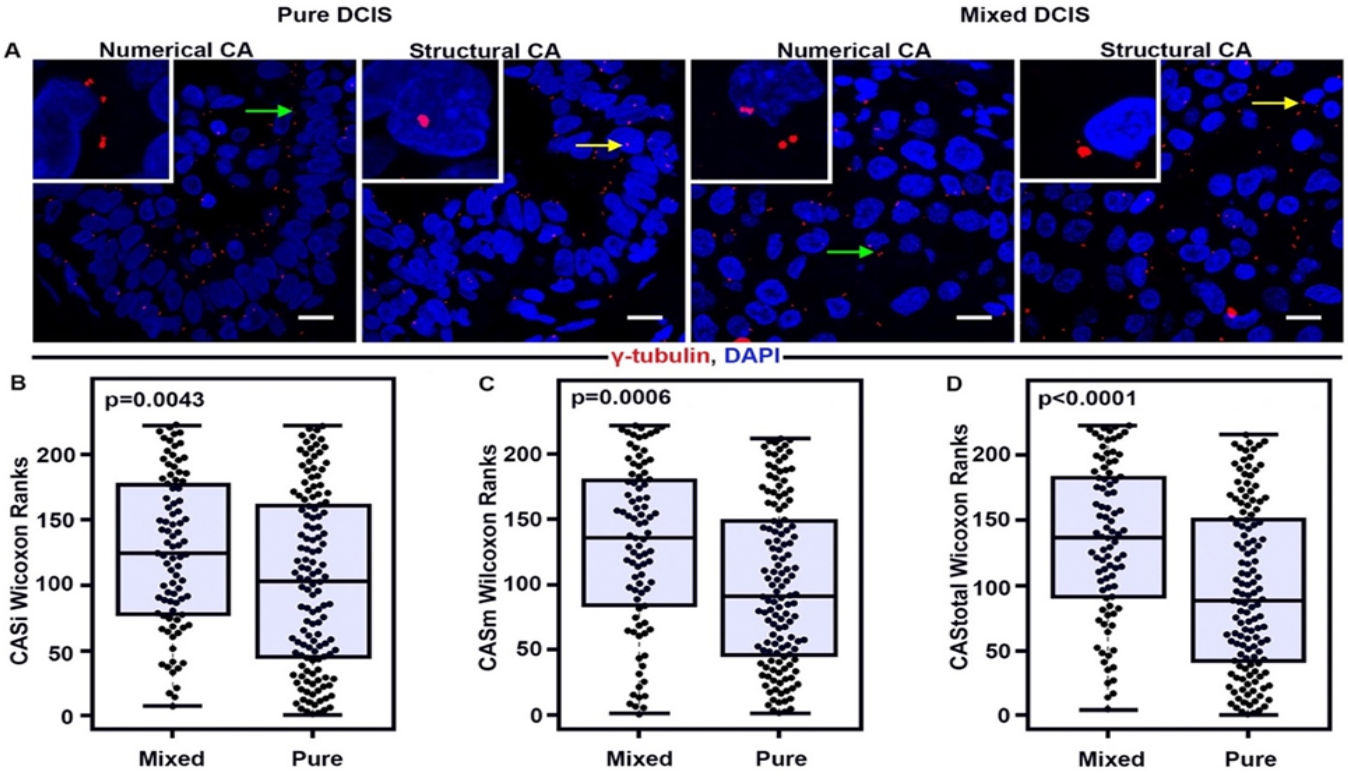

Figure 8-27: DCIS cases in the mixed DCIS cohort exhibit higher CAS when compared with CAS of pure DCIS samples

Beeswarm box-whisker plots showing (A) CASi, (B) CASm, and (C) CAStotal Wilcoxon ranks for the mixed DCIS (n=87) and pure DCIS (n=133) cases

8.5 **Discussion**

DCIS exhibits considerable inter-patient heterogeneity and has a poorly understood natural history. A lack of accurate models for prediction of recurrence risk results in over- and under-treatment, complicated by the variable prognostic evidence of patient age, tumour margins, DCIS grade, and size. CA is a hallmark of cancers and is observable in >80% of breast tumours including pre-invasive lesions, and is associated with high grade in DCIS and IBC [598, 599]. Amplified centrosomes are present in premalignant cells and increase as the disease progresses to dysplasia, highlighting the potential involvement of CA in neoplastic transformation and progression [603].

Although studies have reported that BC exhibit structurally amplified centrosomes, they have not yet established its prognostic value [604]. This may be due, in part, to the 2D (i.e., cross-sectional) approaches used in these studies, which have limitations to accurately capture the 3D size of the centrosome. Moreover, studies examining CA in BC have not rigorously evaluated the confounding effects of other clinicopathological variables on the prognostic value of CA [605].

The new semi-automated methodology uses quantitative centrosomal phenotyping and an algorithm to measure both numerical and structural centrosomal aberrations in DCIS. For each sample, a continuous CAS was computed that categorised patients as having a high or low 10-year risk of recurrence. Findings from this retrospective study showed that patients with local recurrence within 10 years exhibited higher CAStotal relative to recurrence-free patients. This study is the first to show that organellar-level differences distinguish high from low risk DCIS patients, and that high levels of both numerical and structural CA are associated with increased 10-year risk of local recurrence in DCIS. The results suggest that aberrant centrosomal homeostasis in DCIS drives pathophysiological alterations that potentially facilitates disease progression through CIN-dependent as well as CIN-independent mechanisms. While CA may drive intra-tumour heterogeneity through CIN, an increased centrosome complement may, via modulation of the microtubule cytoskeleton, enhance directional migration and invasion of malignant cells [606]. This has further demonstrated that CAStotal is significantly and independently associated with shorter LRFI, and upon inclusion of both CAStotal and VNPI into multivariable models, where it was found that CAStotal outperforms VNPI in recurrence predicting. In DCIS subsets,

defined based on their clinical and histopathological parameters, stratification by CAStotal prognostically augmented several clinicopathologic parameters in determining rate of recurrence. Among subsets of DCIS patients treated with BCS or those receiving adjuvant RT, CAStotal identified patients with high risk of local recurrence. Thus, CAStotal can be used as a clinical tool to identify patients who can be safely treated with BCS alone, and those who will benefit from the inclusion of RT. This centrosomal profiling methodology, which dichotomises DCIS into high- and low-risk categories, enables clear go/no-go therapeutic decision making, and can substantially augment individualised management of DCIS based upon risk conferred by the patient's centrosomal complement.

CAS, as the linear expression of the severity and frequency of numerical and structural CA, may serve as an indirect measure of tumour heterogeneity in DCIS. This study, the first to robustly quantify CA in both pure and mixed DCIS samples, has contributed evidence supporting a model of CA-driven DCIS progression into IBC. These findings concur with previous studies wherein others observed that TNBC, the most aggressive subtype of BC, exhibits highest CA among all BC subtypes [607, 608]. Centrosome profiling can complement

clinicopathologic and genomic evaluation to provide a comprehensive portrait of disease status. An exciting avenue for future research is to profile CA in all the stages of tumour progression starting from atypical hyperplasia to invasive and metastatic disease to evaluate if CA can function as a biomarker for tumour evolution.

The gene signature that comprises the basis of the Oncotype DX DCIS score consists mainly of proliferation-related genes. CA is a phenotypic biomarker that serves as a readout of hundreds of deregulated signalling pathways that culminate in numerical and/or structural CA, including dysregulated proliferation-related signalling cascades. Thus, this methodology captures prognostic information from a broader swathe of biological pathways that are deregulated in and drive the biology of DCIS.

This chapter provided evidence that TME, namely the hypoxia associated factors, plays a key role in genomic instability and abnormal cellular division that could explain tumour heterogeneity and resistance to therapy. Although the clinical applicability of CAS score in routine practice could be limited especially in DCIS, this study added a basic research supported evidence about the role of hypoxia-CA axis in tumour progression that can be used for development target

therapies to be applied to more aggressive tumours such as IBC to stop this axis, hence avoid resistance to therapy, tumour aggressiveness and progression.

However, the study has a few limitations. There are imbalances in the DC and VC of the study, which has resulted in slightly better results in the former. Wherein, DC has more high-grade patients and VC has an equal number of high, intermediate and low-grade patients. High grade patients tend to present invasive recurrence and there are a higher number of patients recurred as invasive in DC which limited the performance of the CAS to predict the type of recurrence and better performance of model in the DC when compared to the VC. These imbalances in the DC and VC lead to variable performance of CAS in DC and VC.

9 Chapter 9: General Discussion

The current study demonstrated the importance of constellation of different clinicopathological factors, proteomics, TME and genetics in prediction of DCIS behaviour in terms of development of local recurrence and disease progression.

9.1 **Background**

Incidence of DCIS has increased as screening programmes are widely implemented [7]. Given the increasing proportion of screening-detected tumours, clinicians are encountering DCIS with size of <1 cm more often than in the past [609]. A number of clinicopathological factors have been suggested to predict the risk of recurrence and therefore help individualise treatment in DCIS [610] although these remain inefficient for patients' risk stratification.

Our inability to elucidate DCIS lesions which will progress to invasion and which will remain indolent culminate in recommendations that women with DCIS undergo treatment [611]. Most women are treated by BCS followed by adjuvant whole breast RT, which has been postulated to lower the risk of local recurrence by 50% [318]. Some women will derive little or no absolute benefit from RT, resulting in unnecessary exposure to radiation and its potential toxicities (over-

treatment), while in others the omission of RT may result in a higher risk of DCIS or invasive recurrence that might have been avoided by treatment (under-treatment) [126]. To reduce over- or under-treatment of DCIS, ascertainment of more precise estimates of individualised recurrence risk after BCS is advised to help clinicians and patients more accurately assess the risks of local recurrence with potential absolute benefits of treatment [611].

Despite the widely accepted notion that DCIS is a non-obligate precursor of IBC, no reliable biomarkers or clinical tests are available to predict which DCIS cases are most likely to progress [458].

In addition, neither molecular subtype nor histological features/grades are consistent or reproducible predictors of DCIS behaviour. For this reason, it is hypothesised that DCIS becomes invasive as a result of either intrinsic factors (genetic aberrations of the neoplastic cells) or extrinsic factors within the TME, independent of, or in association with genetic changes within the tumour cells [167].

It is widely accepted that the engagement between histopathological classification, assessment of molecular prognostic biomarkers; ER, PR and HER2 status remains the mainstay of BC management and is currently contributing to

DCIS management [612]. HER2 and ER are important pathways involved in BC development and it is well known that HER2 is an oncogenic factor that is responsible for driving adverse DCIS prognosis [612]. *HER2* amplification in primary DCIS is identified more frequently in younger patients and it is hypothesised that high risk of recurrence in HER2-positive DCIS is related to histopathological predictors of overall relapse such as high nuclear grade, high Ki67 expression, low ER and PR levels, and other identified clinicopathological factors [324].

Different pathways have been recognised to have interactions with HER2, ER, Ki67 and/or p53 including proliferation [613], oncogenes such as kinases [614] and tumour suppressor genes [615]. Evidence whether HER2 or ER can overwhelm the driving effect on different proteins especially when both are co-expressed and the potential effect on therapeutic response is insufficient and needs further investigation.

9.2 **Hypothesis, aims and methods of the study**

In this thesis, it was hypothesised that DCIS progression and/or recurrence after BCS is a complex process where the TME plays a fundamental role. The progression of DCIS and the development of ipsilateral recurrence particularly invasive

recurrence after BCS is multifactorial and it is unlikely that a single marker will act as a prognostic determinant, rather, a panel of synergistic molecular tissue markers that can be used in synergism with each other.

A set of aims were put forward to explore the hypotheses and identify biological markers or molecular predictors within the surrounding TME for local recurrence able to stratify women with DCIS into high- and low-risk populations and improve risk stratification and treatment recommendations for DCIS patients.

Therefore, this thesis aimed to determine the clinicopathological and molecular characteristics associated with recurrence in women with DCIS after treatment with BCS. This was achieved through assessment of a large cohort of DCIS cases treated in a single institution with attached all relevant clinical information together with a comparator set of cases mixed with invasive disease and construction of a TMA. This was followed by characterisation of the pure DCIS cohort via IHC and CISH for molecular markers. Studying the expression pattern of a proposed biomarker panel of adverse clinical outcome in DCIS was done by selecting of markers spanning important biological changes responsible for ECM remodelling and immune microenvironment changes that

reflect DCIS progression upon their deregulation. Also, the role of hypoxia and the associated changes within the centrosomal integrity of the tumour cells was studied.

9.3 Cardinal findings of the study

9.3.1 Clinical characterisation of DCIS

In Nottingham, approximately two thirds of DCIS patients were treated with BCS in particular those with screen detected lesions. However, mastectomy was the choice for symptomatic patients, with features of aggressive tumour behaviour as high tumour grade with comedo necrosis and large lesion size. The improvement in imaging quality, better evaluation of DCIS size and extent, surgery quality and adjuvant RT contributed to the reduction in mastectomy, re-excision after BCS and local recurrence rates.

Despite the surgical margin being adopted as an essential factor in determining the rate of re-excision and recurrence afterwards, the current study showed that the change in surgical margin width to narrow (2mm) in BCS treated patients in fact did not affect the recurrence rate. Therefore, it is proposed that better risk assessment, rational use of RT and individualised patient management based on constellation of different clinicopathological factors are essential to tailor DCIS treatment.

This study reported a comparable incidence of local recurrence to previous studies and this rate was associated with high grade tumours involving more than one breast quadrant and where RT was not an option for treatment.

In addition, it was shown that VNPI was a reasonable risk index for determining the treatment modalities but might not be the best index to predict tumour recurrence.

Therefore, certain clinicopathological factors for DCIS patients remain important in assessment of patients and determining the treatment modality.

9.3.2 Molecular Taxonomy of DCIS

This study demonstrated that cases of luminal A DCIS subtype showed lower recurrence rate in absence of RT which suggests that the differences in the molecular subtypes are contributing to DCIS behaviour. Conversely, HER2 positive tumours which showed high proliferation rate were associated with increased risk of recurrence. HER2 expression was higher in DCIS compared with invasive tumours but at a lower level than the published literature [344, 354].

The current study postulated that high HER2 detection rate might be related to increased detection of DCIS by imaging which was shown in the earlier period of the study and declined over time. It therefore suggests a potential role of

HER2 as a prognostic marker that needs further studies to prove its precise role as it was previously addressed by other studies [344, 616].

The current study suggested the need to identify potential predictors of recurrence, as the identification of molecular predictors in DCIS is challenging because the number of recurrences is low, and the expression levels of molecular biomarkers are often correlated, but this study has shown that combined HER2/Ki67 positivity was a predictor of local recurrence.

The current study showed that assessment of *HER2* gene amplification was complementary to protein expression as HER2 2+ cases required to be confirmed of their status and CISH was a robust technique for such cases.

9.3.3 Effect of ECM changes

It was hypothesised that the progression of DCIS to invasion is multifactorial and requires the interplay between genetic factors within tumour cells and the surrounding microenvironment, some identified aberrated genes were studied in terms of their protein expression. In this study, some genes were selected based on the gene expression data for IBC due to the lack of DCIS datasets. These genes have distinct role in ECM remodelling and degradation in IBC

progression and correlated with adverse outcome, so they were of interest to study their role in DCIS progression.

In this thesis, P4HA2 and COL11A1 were shown to have a role in progression of DCIS to IBC confirming previous studies. P4HA2 and COL11A1 play role in ECM remodelling and collagen deposition that increase the stromal density which lead to tumour initiation and progression.

CTSA, CTSV and LGMN are proteolytic enzymes that are produced by tumour epithelial cells and surrounding fibroblasts and lead to ECM degradation which help in tumour cell invasion. They were reported to have differential expression pattern between normal breast tissue, DCIS and invasive disease. Studying the geometric characteristics of collagen surrounding DCIS ducts with the novel image analysis methodology support these findings and that these changes are associated with worse outcome in DCIS patients and can provide a potential tool for precise risk stratification.

9.3.4 Prognostic significance of TILs

As the TME is an important contributing factor to DCIS progression, it is important to study TILs as major component of the microenvironment. This thesis has explored the detailed optimal methodology for TILs assessment in DCIS and concluded that touching TILs was the most robust type of TILs

in predicting patient outcome as well as being the easiest, fastest and most accurate method without the need to measure the distance around the ducts. The current results also showed a significant association between dense TILs and shorter LRFI as well as potential risk factors for aggressive DCIS behaviour, in contrary to the previous results shown in invasive carcinoma [397]. This finding might be attributed to the more profound copy number changes in DCIS with dense TILs than lesions with low TILs density making them more aggressive in behaviour [400]. In addition, it is reported that dense TILs are associated with high Oncotype DX DCIS score [77], supporting the current results of association between dense TILs and poor outcome in DCIS.

A subset of TILs; T and B lymphocytes as well as the immune checkpoint proteins were studied in this thesis and results were similar to whole TILs in terms of their association with aggressive tumour behaviour. The immune suppressors proteins including FOXP3 and PDL1 showed association with tumour recurrence, that reflect the cornerstone role of such mechanism in DCIS progression.

9.3.5 Centrosome amplification and recurrence

The results showed that the structural and numerical changes with the tumour cells' centrosomes are associated with high

risk DCIS and higher rate of tumour progression and recurrences. The association between hypoxia and centrosomal aberrations reflects the role of the microenvironmental changes in DCIS behaviour and progression.

9.4 **Tumour microenvironment and DCIS progression**

This thesis highlighted the various roles of TME components and the interactions between these components between each other and with the tumour cells. The results showed that TILs have a potential direct role in DCIS progression through BM degradation, and indirect roles through immunosuppression mechanisms, crosstalk with the epithelial cells and surrounding fibroblasts to produce matrix degradation proteins and collagen remodelling biomarkers. Collagen stiffens and increase mechanical force surrounding DCIS lead to disease progression and also activate inflammatory reaction. Both inflammatory reaction and dense stroma are activator for tissue hypoxia. Hypoxia seems to be a playmaker in TME orchestra where it affects tumour cells directly leading to genomic instability and abnormal cell division through CA that lead to accumulation of further mutations which are

reflected in tumour heterogeneity and resistance to therapy. Also, hypoxia is the factor that links between the immune response associated with DCIS, surrounding tumour associated fibroblasts, collagen remodelling and activation of the proteolytic proteins. **Figure 9-1** illustrates the interactions between TME components and DCIS tumour cells and eliciting their roles in disease behaviour. The graph was created by the author using publicly available image creation software (https://biorender.com).

9.5 **Clinical applicability**

The findings from this thesis can be applied clinically for better characterisation of DCIS patient risk. Prior to this, validation studies using different sources' cohorts are recommended to assess the reproducibility and reliability of the findings. In the fasting growing era of digital pathology (DP) and using Artificial Intelligence (AI) in pathology, algorithms for objective and fast TILs count and CPI evaluation can be created which will allow to implement these parameters in DCIS reporting and to help in patient risk stratification and personalised management.

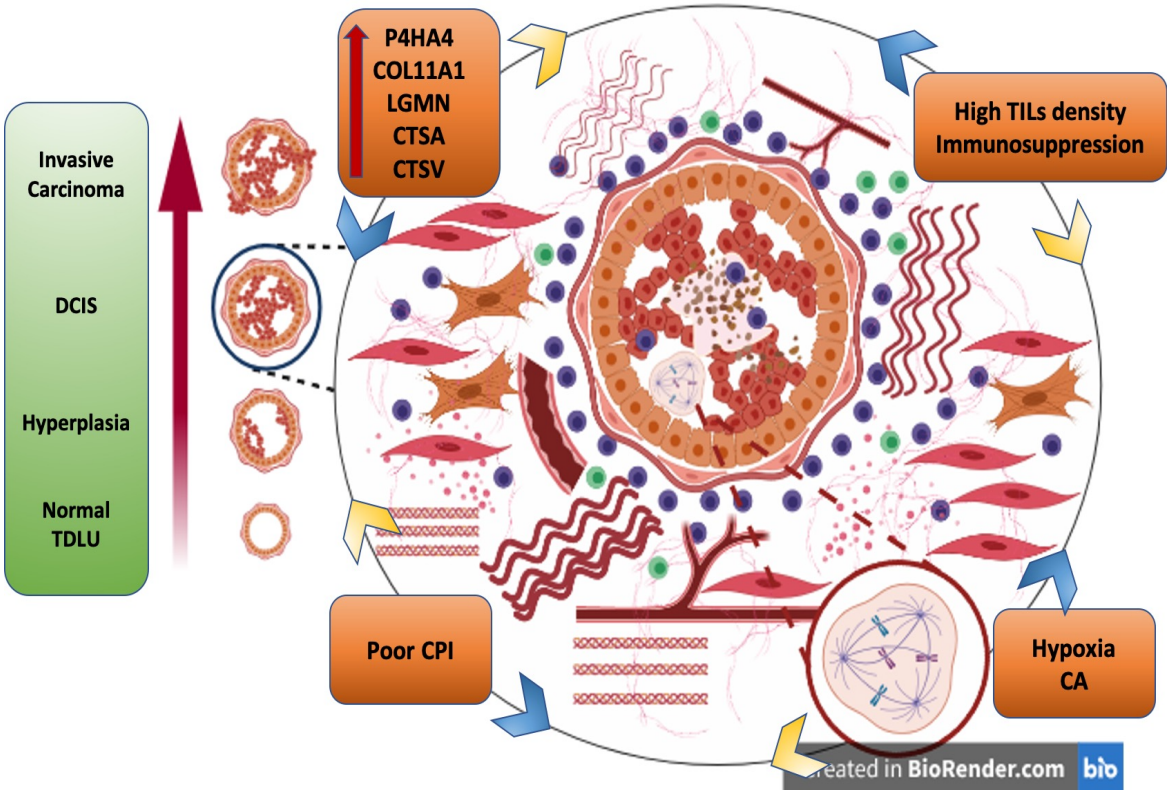

Figure 9-1: The tumour microenvironment orchestra and DCIS progression

The left side of the figure shows the model of breast cancer initiation and progression from normal terminal duct lobular unit (TDLU) to invasive disease going through ductal hypoplasia and ductal carcinoma *in situ*. Looking closer to the DCIS and surrounding tumour microenvironment, it is observed that the crosstalk between various comments and each other and with the tumour cells lease to tumour progression. There are harmony and orchestrion between Tumour associated hypoxia and its direct association with centrosomal aberration and abnormal cellular division, tumour associated fibroblasts, collagen remodelling proteins (P4HA2 and COL11A1), high collagen prognostic index (CPI) which reflects stromal rigidity and collagen fibres dispersion and directions in relation to the DCIS axis, stromal degradation proteins (CTSA, CTSV and LGMN), tumour infiltrating lymphocytes (TILs) especially cells associated with immunosuppressive microenvironment such as FOXP3 and PDL1 positive lymphocytes. All components with the tumour cells affect each other for tumour support and progression.

Large duct in the centre of the image represents DCIS with central necrosis, one cell is in abnormal mitosis due to multiple centrosomes. Spiral lines represent collagen fibres with various densities and arrangements. Trihelix structures represent collagen formation and remodelling by the effect of various components. Plump red spindle cells are fibroblasts, while large oranges stellate shaped cells represent myofibroblasts. Blue round cells are lymphocytes while the green cells refer to immunosuppressive lymphocytes. Vascular structures represent the blood vessel that provide the tumour and microenvironment with required nutrient and energy sources which could be insufficient to meet the tumour demands and hence lead to more hypoxia. Yellow and blue arrows show that the crosstalk between the microenvironment components is bidirectional and how they affect each other.

9.6 **Final conclusions**

DCIS progression is a result of constellation of different phenotypic and genotypic factors including the clinicopathological, tumour cell and microenvironment factors. The availability of large cohort of cases was the mainstay of obtaining robust results and in risk stratifying DCIS patients and predicting disease behaviour. IHC assessment of the cellular and molecular derangements is cost-effective, reproducible and clinically applicable, therefore targeting these molecular allies, through specific therapies could halt DCIS progression particularly those targeting specific proteins such as P4HA2, CTSA, CTSV, LGMN and COL11A1. Also, the results show a role of immune microenvironment in DCIS behaviour could provide a rational for using immunotherapy in DCIS treatment. Characterisation of DCIS using similar classification system to IBC via well characterised biomarkers such as ER, PR and HER2 would clarify the biology of DCIS.

9.7 **Strengths of the study**

1- The study was designed to use a large cohort of DCIS patients. In addition, clinicopathological and outcome data was individually collected, validated and prospectively maintained. Therefore, findings of different

studied tissue markers were linked to the robust clinical outcome and IHC defined intrinsic biological subtypes.

2- In the current study, antibodies were used with positive and negative controls in addition to WB for some of the studied antibodies. In addition, for adequate staining interpretation and statistical correlations, strict adherence to published guidelines of prognostic marker studies was followed throughout [617, 618].

3- The use of different statistical approaches in determination of the optimal cut-off points of staining positivity of the used markers, rather than using arbitrarily chosen ones.

4- The use of data as both continuous and categorical was helpful in confirmation of the results.

5- Validation of the semi-qualitative results of HER2 protein expression by using CISH which confirms HER2 status in HER2 2+ cases.

6- Using the pathologist's eye approach in markers expression scoring rather than using automated image analysis methods. An important concern is that automated methods might count *in situ* lesions or some foci of normal mammary epithelial cells entrapped in some tissue cores as hyperplasia, whereas a pathologist's

score/count would more likely exclude this potential error.

9.8 **Potential limitations and weakness**

1- This study could have possible limitations, for instance, the subjectivity of staining interpretation and qualitative results of IHC detection of marker expression [619]. However, a standard approach to keep these to the minimum was followed. Inter- and intra-observer agreement in staining interpretation was calculated with excellent concordance achieved.

2- The data were only assessed in one centre and no multicentre validation was considered except for the CA study which is aimed to be in collaboration with another research group in USA.

3- To facilitate studying tissue markers in large cohorts of samples, the biomarker panel was trained on subsets of full-face sections and studied on TMAs, which has been shown to have specific technical limitations such as core loss. However, TMA results have repeatedly been reported to show excellent concordance with full face sections of cancer tissues including BC. In addition, previous studies have validated the use of one TMA core to study the expression of tumour marker.

4- For this historical patient cohort, relatively old paraffin blocks were used to study tissue marker expression which might have exhausted/consumed some blocks. Moreover, therapeutic methods used at the time when patients of this study were treated tended to be different from those currently in practice and many modalities are continually evolving.

9.9 **Suggestions and future investigations**

1- Assessment of a subset of prospective cases of DCIS in addition to the current series would be of value as a comparator set. This would be regarding different clinicopathological factors particularly patient age, presentation, tumour size, grade, operative procedure and margin assessment together with hormone receptor and HER2 status.

2- Multicentre assessment of the DCIS cases will be more robust as this will provide the opportunity to rely on the obtained results if deemed parallel with the possibility for their clinical application.

3- Using additional cohort or statistical methods to compensate the missing values of various biomarkers to be suitable for powerful clustering to developed a TME based index or signature for DCIS recurrence that can be

applied in the routine practice to predict invasive recurrence risk after primary diagnosis of DCIS and hence aid in patient management without over or under treatment.

4- Further functional studies are required to validate the protein expression results. These could include, in vitro cell line and tissue culture studies using DCIS cell lines (such as MCF10DCIS) either using moncellular culture or more preferable 3D cultures with stroma and myoepithelial cells co-culture, to mimic the normal breast tissue environment. In vitro knockdown of the identified genes particularly the oncogenes would be of value to explore the practicality of therapeutic consideration of the target genes. Animal models also can be prepared to induce DCIS lesions and study the effect of various TME component to understand the underlying mechanisms.

5- To highlight the role of subcellular localisation, measuring different cellular components separately, known as subcellular fractionation, is warranted.

6- Using multiple cores per case in the TMA could be more beneficial for better assessment to overcome the core loss and the heterogeneity if there is any. Ideally, a core from each quadrant of the lesion should be obtained.

7- Apply DP, AI and machine learning techniques for assessing and validation of the thesis results regarding TILs and CPI assessment. Beside their validation utility, DP and AI could provide an objective and fast method to assess these features and incorporate them in the clinical practice for DCIS reporting.

References

1. Bane, A., *Ductal carcinoma in situ: what the pathologist needs to know and why.* Int J Breast Cancer, 2013. **2013**: p. 914053.

2. Cheatle, G.L., *Cysts, and primary cancer in cysts, of the breast.* British Journal of Surgery, 1920. **8**(30): p. 149-166.

3. BLOODGOOD, J.C., *THE PATHOLOGY OF CHRONIC CYSTIC MASTITIS OF THE FEMALE BREAST: WITH SPECIAL CONSIDERATION OF THE BLUE-DOMED CYST.* JAMA Surgery, 1921. **3**(3): p. 445-542.

4. Rosner, D., et al., *Noninvasive Breast Carcinoma: Results of a National Survey by the American College of Surgeons.* Annals of Surgery, 1980. **192**(2): p. 139-147.

5. Smart, C.R., M.H. Myers, and L.A. Gloeckler, *Implications from SEER data on breast cancer management.* Cancer, 1978. **41**(3): p. 787-9.

6. Ernster, V.L., et al., *Incidence of and treatment for ductal carcinoma in situ of the breast.* Jama, 1996. **275**(12): p. 913-8.

7. Virnig, B.A., et al., *Ductal carcinoma in situ of the breast: a systematic review of incidence, treatment, and outcomes.* J Natl Cancer Inst, 2010. **102**(3): p. 170-8.

8. DeSantis, C.E., et al., *Breast cancer statistics, 2019.* CA Cancer J Clin, 2019.

9. Szynglarewicz, B., et al., *Screen-detected ductal carcinoma in situ found on stereotactic vacuum-assisted biopsy of suspicious microcalcifications without mass: radiological-histological correlation.* Radiol Oncol, 2016. **50**(2): p. 145-52.

10. Adams-Cameron, M., et al., *Trends in incidence and treatment for ductal carcinoma in situ in Hispanic, American Indian, and non-Hispanic white women in New Mexico, 1973-1994.* Cancer, 1999. **85**(5): p. 1084-90.

11. Ciatto, S., et al., *Intraductal breast carcinoma. Review of a multicenter series of 350 cases. Coordinating Center and Writing Committee of FONCAM (National Task Force for Breast Cancer), Italy.* Tumori, 1990. **76**(6): p. 552-4.

12. Bellamy, C.O., et al., *Noninvasive ductal carcinoma of the breast: the relevance of histologic categorization.* Hum Pathol, 1993. **24**(1): p. 16-23.

13. Silverstein, M.J., et al., *Intraductal carcinoma of the breast (208 cases). Clinical factors influencing treatment choice.* Cancer, 1990. **66**(1): p. 102-8.

14. Kerlikowske, K., *Epidemiology of ductal carcinoma in situ.* J Natl Cancer Inst Monogr, 2010. **2010**(41): p. 139-41.

15. Tunon-de-Lara, C., et al., *Ductal carcinoma in situ of the breast in younger women: a subgroup of patients at high risk.* Eur J Surg Oncol, 2010. **36**(12): p. 1165-71.

16. Perez, A.A., et al., *Ductal carcinoma in situ of the breast: correlation between histopathological features and age of patients.* Diagn Pathol, 2014. **9**: p. 227.

17. Tunon-de-Lara, C., et al., *Ductal carcinoma in situ of the breast: influence of age on diagnostic, therapeutic, and prognostic features. Retrospective study of 812 patients.* Ann Surg Oncol, 2011. **18**(5): p. 1372-9.

18. Lertsithichai, P., et al., *Effect of young age, positive margins, and triple negative status on disease recurrence after breast conserving therapy.* Gland Surg, 2016. **5**(1): p. 15-23.

19. Reinier, K.S., P.M. Vacek, and B.M. Geller, *Risk factors for breast carcinoma in situ versus invasive breast cancer in a prospective study of pre- and post-menopausal women.* Breast Cancer Res Treat, 2007. **103**(3): p. 343-8.

20. Gill, J.K., et al., *The association of mammographic density with ductal carcinoma in situof the breast: the Multiethnic Cohort.* Breast Cancer Research, 2006. **8**(3): p. R30.

21. MacKenzie, T.A., et al., *Breast density in relation to risk of ductal carcinoma in situ of the breast in women undergoing screening mammography.* Cancer Causes Control, 2007. **18**(9): p. 939-45.

22. Yang, R.L., et al., *DCIS in BRCA1 and BRCA2 mutation carriers: prevalence, phenotype, and expression of oncodrivers C-MET and HER3.* J Transl Med, 2015. **13**: p. 335.

23. Moelans, C.B., A.H. Verschuur-Maes, and P.J. van Diest, *Frequent promoter hypermethylation of BRCA2, CDH13, MSH6, PAX5, PAX6 and WT1 in ductal carcinoma in situ and invasive breast cancer.* J Pathol, 2011. **225**(2): p. 222-31.

24. Frank, T.S., et al., *Clinical characteristics of individuals with germline mutations in BRCA1 and BRCA2: analysis of 10,000 individuals.* J Clin Oncol, 2002. **20**(6): p. 1480-90.

25. Vaidya, Y., P. Vaidya, and T. Vaidya, *Ductal Carcinoma In Situ of the Breast.* Indian J Surg, 2015. **77**(2): p. 141-6.

26. O'Connell, P., et al., *Analysis of loss of heterozygosity in 399 premalignant breast lesions at 15 genetic loci.* J Natl Cancer Inst, 1998. **90**(9): p. 697-703.

27. Aasmundstad, T.A. and O.A. Haugen, *DNA ploidy in intraductal breast carcinomas.* European Journal of Cancer and Clinical Oncology, 1990. **26**(9): p. 956-959.

28. Killeen, J.L. and H. Namiki, *DNA analysis of ductal carcinoma in situ of the breast. A comparison with histologic features.* Cancer, 1991. **68**(12): p. 2602-7.

29. Liu, E., et al., *The HER2 (c-erbB-2) oncogene is frequently amplified in in situ carcinomas of the breast.* Oncogene, 1992. **7**(5): p. 1027-32.

30. Ho, G.H., et al., *In microdissected ductal carcinoma in situ, HER-2/neu amplification, but not p53 mutation, is associated with high nuclear grade and comedo histology.* Cancer, 2000. **89**(11): p. 2153-60.

31. Kerlikowske, K., et al., *Biomarker expression and risk of subsequent tumors after initial ductal carcinoma in situ diagnosis.* J Natl Cancer Inst, 2010. **102**(9): p. 627-37.

32. Radford, D.M., et al., *Allelic loss on a chromosome 17 in ductal carcinoma in situ of the breast.* Cancer Res, 1993. **53**(13): p. 2947-9.

33. Lichy, J.H., et al., *Loss of heterozygosity on chromosome 11p15 during histological progression in microdissected ductal carcinoma of the breast.* Am J Pathol, 1998. **153**(1): p. 271-8.

34. Chen, T., A. Sahin, and C.M. Aldaz, *Deletion map of chromosome 16q in ductal carcinoma in situ of the breast: refining a putative tumor suppressor gene region.* Cancer Res, 1996. **56**(24): p. 5605-9.

35. Lee, S., et al., *Differentially expressed genes regulating the progression of ductal carcinoma in situ to invasive breast cancer.* Cancer Res, 2012. **72**(17): p. 4574-86.

36. Barsky, S.H., Z.M. Shao, and S. Bose, *Should DCIS Be Renamed Carcinoma of the Ductal System?* Breast J, 1999. **5**(1): p. 70-72.

37. Ernster, V.L., et al., *Detection of ductal carcinoma in situ in women undergoing screening mammography.* J Natl Cancer Inst, 2002. **94**(20): p. 1546-54.

38. Downing, A. and R. Corsetti, *Palpable ductal carcinoma in situ of the breast.* Ochsner J, 2014. **14**(3): p. 438-40.

39. Venkatesan, A., et al., *Positive predictive value of specific mammographic findings according to reader and patient variables.* Radiology, 2009. **250**(3): p. 648-57.

40. Holland, R., et al., *Extent, distribution, and mammographic/ histological correlations of breast ductal carcinoma in situ.* The Lancet, 1990. **335**(8688): p. 519-522.

41. Carlson, K.L., et al., *Relationship between mammographic screening intervals and size and histology of ductal carcinoma in situ.* AJR Am J Roentgenol, 1999. **172**(2): p. 313-7.

42. Stomper, P.C., et al., *Clinically occult ductal carcinoma in situ detected with mammography: analysis of 100 cases with radiologic-pathologic correlation.* Radiology, 1989. **172**(1): p. 235-41.

43. Reiff, D.B., et al., *Ductal carcinoma in situ presenting as a stellate lesion on mammography.* Clin Radiol, 1994. **49**(6): p. 396-9.

44. Menell, J.H., et al., *Determination of the presence and extent of pure ductal carcinoma in situ by mammography and magnetic resonance imaging.* Breast J, 2005. **11**(6): p. 382-90.

45. Lagios, M.D., P.R. Westdahl, and M.R. Rose, *The concept and implications of multicentricity in breast carcinoma.* Pathol Annu, 1981. **16**(Pt 2): p. 83-102.

46. Schwartz, G.F., et al., *Nonpalpable in situ ductal carcinoma of the breast. Predictors of multicentricity and microinvasion and implications for treatment.* Arch Surg, 1989. **124**(1): p. 29-32.

47. Ashikari, R., A.G. Huvos, and R.E. Snyder, *Prospective study of non-infiltrating carcinoma of the breast.* Cancer, 1977. **39**(2): p. 435-9.

48. Fisher, E.R., et al., *Pathologic findings from the National Surgical Adjuvant Breast Project (NSABP) Protocol B-17. Intraductal carcinoma (ductal carcinoma in situ). The National Surgical Adjuvant Breast and Bowel Project Collaborating Investigators.* Cancer, 1995. **75**(6): p. 1310-9.

49. Silverstein, M.J., et al., *Duct carcinoma in situ: 227 cases without microinvasion.* Eur J Cancer, 1992. **28**(2-3): p. 630-4.

50. Poller, D.N., *Pathology of ductal carcinoma in situ of the breast: current status.* Eur J Surg Oncol, 2001. **27**(5): p. 498-503.

51. Allred, D.C., *Ductal carcinoma in situ: terminology, classification, and natural history.* J Natl Cancer Inst Monogr, 2010. **2010**(41): p. 134-8.

52. Poller, D.N., et al., *Ideas in pathology. Ductal carcinoma in situ of the breast: a proposal for a new simplified histological classification association between cellular proliferation and c-erbB-2 protein expression.* Mod Pathol, 1994. **7**(2): p. 257-62.

53. (WHO)., W.H.O., *WHO classification of tumours of the breast.* 5th Edition ed. 2019, Lyon: International Agency for Research on Cancer (IARC).

54. Carraro, Dirce M., Eliana V. Elias, and Victor P. Andrade, *Ductal carcinoma in situ of the breast: morphological and molecular features implicated in progression.* Biosci Rep, 2014. **34**(1).

55. Rakha, E.A., et al., *Encapsulated papillary carcinoma of the breast: an invasive tumor with excellent prognosis.* Am J Surg Pathol, 2011. **35**(8): p. 1093-103.

56. Guerry, P., R.A. Erlandson, and P.P. Rosen, *Cystic hypersecretory hyperplasia and cystic hypersecretory duct carcinoma of the breast. Pathology, therapy, and follow-up of 39 patients.* Cancer, 1988. **61**(8): p. 1611-20.

57. Scott, M.A., et al., *Ductal carcinoma in situ of the breast: reproducibility of histological subtype analysis.* Hum Pathol, 1997. **28**(8): p. 967-73.

58. O'Malley, F.P. and A. Bane, *An update on apocrine lesions of the breast.* Histopathology, 2008. **52**(1): p. 3-10.

59. Farshid, G., et al., *Spindle cell ductal carcinoma in situ. An unusual variant of ductal intra-epithelial neoplasia that simulates ductal hyperplasia or a myoepithelial proliferation.* Virchows Arch, 2001. **439**(1): p. 70-7.

60. Wang, L., et al., *Clinicopathologic characteristics and molecular subtypes of microinvasive carcinoma of the breast.* Tumour Biol, 2015. **36**(4): p. 2241-8.

61. Orzalesi, L., et al., *Microinvasive breast cancer: pathological parameters, cancer subtypes distribution, and correlation with axillary lymph nodes invasion. Results of a large single-institution series.* Breast Cancer, 2015.

62. Silverstein, M.J., *The University of Southern California/Van Nuys prognostic index for ductal carcinoma in situ of the breast.* Am J Surg, 2003. **186**(4): p. 337-43.

63. Group, N.P.C.-o. *Pathology Reporting of Breast Disease.* NHS BSP Publication 2005.

64. *Consensus Conference on the classification of ductal carcinoma in situ. The Consensus Conference Committee.* Cancer, 1997. **80**(9): p. 1798-802.

65. Lester, S.C., et al., *Protocol for the examination of specimens from patients with ductal carcinoma in situ of the breast.* Arch Pathol Lab Med, 2009. **133**(1): p. 15-25.

66. Rakha, E.A., et al., *Prognostic significance of Nottingham histologic grade in invasive breast carcinoma.* J Clin Oncol, 2008. **26**(19): p. 3153-8.

67. Pinder, S.E., et al., *A new pathological system for grading DCIS with improved prediction of local recurrence: results from the UKCCCR/ANZ DCIS trial.* Br J Cancer, 2010. **103**(1): p. 94-100.

68. Stasik, C.J., et al., *Grading ductal carcinoma in situ of the breast using an automated proliferation index.* Ann Clin Lab Sci, 2011. **41**(2): p. 122-30.

69. Wells, W.A., et al., *Pathologists' agreement with experts and reproducibility of breast ductal carcinoma-in-situ classification schemes.* Am J Surg Pathol, 2000. **24**(5): p. 651-9.

70. Gorringe, K.L., et al., *Copy number analysis of ductal carcinoma in situ with and without recurrence.* Mod Pathol, 2015. **28**(9): p. 1174-84.

71. Tavassoli, T. and P. Devilee, *Pathology&Genetics. Tumours of the Breast and Female Genital Organs.* 2003, IARC Press, Lyon, France,.

72. Vuong, D., et al., *Molecular classification of breast cancer.* Virchows Archiv, 2014. **465**(1): p. 1-14.

73. Selvi, R., *Molecular Classification of Breast Cancers*, in *Breast Diseases: Imaging and Clinical Management*. 2015, Springer India: New Delhi. p. 247-249.

74. Vincent-Salomon, A., et al., *Integrated genomic and transcriptomic analysis of ductal carcinoma in situ of the breast.* Clin Cancer Res, 2008. **14**(7): p. 1956-65.

75. Chin, K., et al., *Genomic and transcriptional aberrations linked to breast cancer pathophysiologies.* Cancer Cell, 2006. **10**(6): p. 529-41.

76. Heselmeyer-Haddad, K., et al., *Single-cell genetic analysis of ductal carcinoma in situ and invasive breast cancer reveals enormous tumor heterogeneity yet conserved genomic imbalances and gain of MYC during progression.* Am J Pathol, 2012. **181**(5): p. 1807-22.

77. Knopfelmacher, A., et al., *Correlation of histopathologic features of ductal carcinoma in situ of the breast with the*

oncotype DX DCIS score. Mod Pathol, 2015. **28**(9): p. 1167-73.

78. Solin, L.J., et al., *A multigene expression assay to predict local recurrence risk for ductal carcinoma in situ of the breast.* J Natl Cancer Inst, 2013. **105**(10): p. 701-10.

79. Mardekian, S.K., A. Bombonati, and J.P. Palazzo, *Ductal carcinoma in situ of the breast: the importance of morphologic and molecular interactions.* Hum Pathol, 2016. **49**: p. 114-23.

80. Lopez-Garcia, M., et al., *Breast cancer precursors revisited: molecular features and progression pathways.* Histopathology, 2010. **57**: p. 171 - 92.

81. Wellings, S.R. and H.M. Jensen, *On the origin and progression of ductal carcinoma in the human breast.* J Natl Cancer Inst, 1973. **50**(5): p. 1111-8.

82. Simpson, P.T., et al., *Molecular evolution of breast cancer.* J Pathol, 2005. **205**(2): p. 248-54.

83. Sotiriou, C. and L. Pusztai, *Gene-expression signatures in breast cancer.* N Engl J Med, 2009. **360**(8): p. 790-800.

84. Weigelt, B. and J.S. Reis-Filho, *Histological and molecular types of breast cancer: is there a unifying taxonomy?* Nat Rev Clin Oncol, 2009. **6**(12): p. 718-30.

85. Allred, D.C., et al., *Ductal carcinoma in situ and the emergence of diversity during breast cancer evolution.* Clin Cancer Res, 2008. **14**(2): p. 370-8.

86. Ma, X.J., et al., *Gene expression profiles of human breast cancer progression.* Proc Natl Acad Sci U S A, 2003. **100**(10): p. 5974-9.

87. Johnson, C.E., et al., *Identification of copy number alterations associated with the progression of DCIS to invasive ductal carcinoma.* Breast Cancer Res Treat, 2012. **133**(3): p. 889-98.

88. Hu, M., et al., *Distinct epigenetic changes in the stromal cells of breast cancers.* Nat Genet, 2005. **37**(8): p. 899-905.

89. Doebar, S.C., et al., *Extent of ductal carcinoma in situ according to breast cancer subtypes: a population-based cohort study.* Breast Cancer Res Treat, 2016. **158**(1): p. 179-87.

90. Yeong, J., et al., *Identifying progression predictors of breast ductal carcinoma in situ.* J Clin Pathol, 2017. **70**(2): p. 102-108.

91. Rutter, C.E., et al., *Growing Use of Mastectomy for Ductal Carcinoma-In Situ of the Breast Among Young Women in the United States.* Ann Surg Oncol, 2015. **22**(7): p. 2378-86.

92. Holmberg, L., et al., *Absolute risk reductions for local recurrence after postoperative radiotherapy after sector resection for ductal carcinoma in situ of the breast.* J Clin Oncol, 2008. **26**(8): p. 1247-52.

93. Donker, M., et al., *Breast-conserving treatment with or without radiotherapy in ductal carcinoma In Situ: 15-year recurrence rates and outcome after a recurrence, from the EORTC 10853 randomized phase III trial.* J Clin Oncol, 2013. **31**(32): p. 4054-9.

94. McCormick, B., et al., *RTOG 9804: a prospective randomized trial for good-risk ductal carcinoma in situ comparing radiotherapy with observation.* J Clin Oncol, 2015. **33**(7): p. 709-15.

95. Emdin, S.O., et al., *SweDCIS: Radiotherapy after sector resection for ductal carcinoma in situ of the breast. Results of a randomised trial in a population offered mammography screening.* Acta Oncol, 2006. **45**(5): p. 536-43.

96. Wapnir, I.L., et al., *Long-term outcomes of invasive ipsilateral breast tumor recurrences after lumpectomy in NSABP B-17 and B-24 randomized clinical trials for DCIS.* J Natl Cancer Inst, 2011. **103**(6): p. 478-88.

97. Rampaul, R.S., et al., *Wide local excision with 10 mm clearance without radiotherapy for DCIS.* European Journal of Cancer, 2001. **37**: p. 15.

98. Dodwell, D., et al., *Radiotherapy following breast-conserving surgery for screen-detected ductal carcinoma in situ: indications and utilisation in the UK. Interim findings from the Sloane Project.* Br J Cancer, 2007. **97**(6): p. 725-9.

99. Kim, T., et al., *Is radiotherapy necessary for intermediate risk ductal carcinoma in situ after breast conserving surgery?* Springerplus, 2014. **3**: p. 405.

100. Farante, G., et al., *Are all patients with ductal carcinoma in situ of the breast candidates for radiotherapy after breast conservative treatment? Institute of European Oncology Guidelines.* Breast J, 2014. **20**(4): p. 431-3.

101. Toss, M.S., et al., *Breast conservation in ductal carcinoma in situ (DCIS): what defines optimal margins?* Histopathology, 2016.

102. Morrow, M., et al., *Society of Surgical Oncology-American Society for Radiation Oncology-American Society of Clinical Oncology Consensus Guideline on Margins for Breast-Conserving Surgery With Whole-Breast Irradiation in Ductal Carcinoma in Situ.* Practical Radiation Oncology, 2016. **6**(5): p. 287-295.

103. Guerrieri-Gonzaga, A., et al., *Benefit of low dose tamoxifen in a large observational cohort of high risk ER positive breast DCIS.* Int J Cancer, 2016.

104. Cutuli, B., et al., *Breast-conserving treatment for ductal carcinoma in situ: Impact of boost and tamoxifen on local recurrences.* Cancer Radiother, 2016.

105. Allred, D.C., et al., *Adjuvant tamoxifen reduces subsequent breast cancer in women with estrogen receptor-positive ductal carcinoma in situ: a study based on NSABP protocol B-24.* J Clin Oncol, 2012. **30**(12): p. 1268-73.

106. Cuzick, J., et al., *Effect of tamoxifen and radiotherapy in women with locally excised ductal carcinoma in situ: long-term results from the UK/ANZ DCIS trial.* Lancet Oncol, 2011. **12**(1): p. 21-9.

107. Staley, H., I. McCallum, and J. Bruce, *Postoperative Tamoxifen for ductal carcinoma in situ: Cochrane systematic review and meta-analysis.* Breast, 2014. **23**(5): p. 546-51.

108. Margolese, R.G., et al., *Anastrozole versus tamoxifen in postmenopausal women with ductal carcinoma in situ undergoing lumpectomy plus radiotherapy (NSABP B-35): a randomised, double-blind, phase 3 clinical trial.* Lancet, 2016. **387**(10021): p. 849-56.

109. Daly, M.B., et al., *NCCN Guidelines Insights: Genetic/Familial High-Risk Assessment: Breast and Ovarian, Version 2.2017.* J Natl Compr Canc Netw, 2017. **15**(1): p. 9-20.

110. Hancock, M.J., *Appraisal of Clinical Practice Guideline: Early and locally advanced breast cancer: diagnosis and management. NICE guideline [NG101].* J Physiother, 2019. **65**(1): p. 57.

111. Francis, A., et al., *Addressing overtreatment of screen detected DCIS; the LORIS trial.* Eur J Cancer, 2015. **51**(16): p. 2296-303.

112. Elshof, L.E., et al., *Feasibility of a prospective, randomised, open-label, international multicentre, phase III, non-inferiority trial to assess the safety of active surveillance for low risk ductal carcinoma in situ - The LORD study.* Eur J Cancer, 2015. **51**(12): p. 1497-510.

113. Lippey, J., A. Spillane, and C. Saunders, *Not all ductal carcinoma in situ is created equal: can we avoid surgery for low-risk ductal carcinoma in situ?* ANZ Journal of Surgery, 2016. **86**(11): p. 859-860.

114. Zhang, X., et al., *Predictors for local invasive recurrence of ductal carcinoma in situ of the breast: a meta-analysis.* Eur J Cancer Prev, 2016. **25**(1): p. 19-28.

115. Shamliyan, T., et al., *Association between patient and tumor characteristics with clinical outcomes in women with ductal carcinoma in situ.* J Natl Cancer Inst Monogr, 2010. **2010**(41): p. 121-9.

116. Wang, S.Y., et al., *Tumor characteristics as predictors of local recurrence after treatment of ductal carcinoma in situ: a meta-analysis.* Breast Cancer Res Treat, 2011. **127**(1): p. 1-14.

117. Habel, L.A., et al., *Mammographic density and breast cancer after ductal carcinoma in situ.* J Natl Cancer Inst, 2004. **96**.

118. Di Saverio, S., et al., *259 Patients with DCIS of the breast applying USC/Van Nuys prognostic index: a retrospective review with long term follow up.* Breast Cancer Res Treat, 2008. **109**(3): p. 405-16.

119. MacAusland, S.G., et al., *An attempt to independently verify the utility of the Van Nuys Prognostic Index for ductal carcinoma in situ.* Cancer, 2007. **110**(12): p. 2648-53.

120. Rudloff, U., et al., *Nomogram for predicting the risk of local recurrence after breast-conserving surgery for ductal carcinoma in situ.* J Clin Oncol, 2010. **28**(23): p. 3762-9.

121. Sweldens, C., et al., *Local relapse after breast-conserving therapy for ductal carcinoma in situ: a European single-center experience and external validation of the Memorial Sloan-Kettering Cancer Center DCIS nomogram.* Cancer J, 2014. **20**(1): p. 1-7.

122. Pang, J.M., K.L. Gorringe, and S.B. Fox, *Ductal carcinoma in situ - update on risk assessment and management.* Histopathology, 2016. **68**(1): p. 96-109.

123. Erbas, B., et al., *The natural history of ductal carcinoma in situ of the breast: a review.* Breast Cancer Res Treat, 2006. **97**(2): p. 135-44.

124. Sanders, M.E., et al., *The natural history of low-grade ductal carcinoma in situ of the breast in women treated by biopsy only revealed over 30 years of long-term follow-up.* Cancer, 2005. **103**(12): p. 2481-4.

125. Adler, E.H., et al., *Predictors of disease progression in ductal carcinoma in situ of the breast and vascular patterns.* Hum Pathol, 2012. **43**(4): p. 550-6.

126. Rakovitch, E., et al., *Can we select individuals with low risk ductal carcinoma in situ (DCIS)? A population-based outcomes analysis.* Breast Cancer Res Treat, 2013. **138**(2): p. 581-90.

127. Quail, D.F. and J.A. Joyce, *Microenvironmental regulation of tumor progression and metastasis.* Nat Med, 2013. **19**(11): p. 1423-37.

128. Mao, Y., et al., *Stromal cells in tumor microenvironment and breast cancer.* Cancer Metastasis Rev, 2013. **32**(1-2): p. 303-15.

129. Grivennikov, S.I., F.R. Greten, and M. Karin, *Immunity, inflammation, and cancer.* Cell, 2010. **140**(6): p. 883-99.

130. de Martel, C., et al., *Global burden of cancers attributable to infections in 2008: a review and synthetic analysis.* The Lancet Oncology, 2008. **13**(6): p. 607-615.

131. Vinay Kumar, A.K.A., Jon C. Aster, *Robbins basic pathology*. 9th ed. 2013, Canada ELSEVIER.

132. Pardoll, D.M., *The blockade of immune checkpoints in cancer immunotherapy.* Nat Rev Cancer, 2012. **12**(4): p. 252-264.

133. Salgado, R., et al., *The evaluation of tumor-infiltrating lymphocytes (TILs) in breast cancer: recommendations by an International TILs Working Group 2014.* Ann Oncol, 2015. **26**(2): p. 259-71.

134. Velcheti, V., et al., *Programmed death ligand-1 expression in non-small cell lung cancer.* Lab Invest, 2014. **94**(1): p. 107-116.

135. Mittal, D., et al., *New insights into cancer immunoediting and its three component phases--elimination, equilibrium and escape.* Curr Opin Immunol, 2014. **27**: p. 16-25.

136. Taube, J.M., et al., *Association of PD-1, PD-1 ligands, and other features of the tumor immune microenvironment with response to anti-PD-1 therapy.* Clin Cancer Res, 2014. **20**(19): p. 5064-74.

137. Qian, B.Z. and J.W. Pollard, *Macrophage diversity enhances tumor progression and metastasis.* Cell, 2010. **141**(1): p. 39-51.

138. Condeelis, J. and J.W. Pollard, *Macrophages: obligate partners for tumor cell migration, invasion, and metastasis.* Cell, 2006. **124**(2): p. 263-6.

139. Coniglio, S.J., et al., *Microglial stimulation of glioblastoma invasion involves epidermal growth factor receptor (EGFR) and colony stimulating factor 1 receptor (CSF-1R) signaling.* Mol Med, 2012. **18**: p. 519-27.

140. Gocheva, V., et al., *IL-4 induces cathepsin protease activity in tumor-associated macrophages to promote cancer growth and invasion.* Genes Dev, 2010. **24**(3): p. 241-55.

141. Mosser, D.M. and J.P. Edwards, *Exploring the full spectrum of macrophage activation.* Nat Rev Immunol, 2008. **8**(12): p. 958-969.

142. Lewis, C. and C. Murdoch, *Macrophage responses to hypoxia: implications for tumor progression and anti-cancer therapies.* Am J Pathol, 2005. **167**(3): p. 627-35.

143. Talmadge, J.E. and D.I. Gabrilovich, *History of myeloid-derived suppressor cells.* Nat Rev Cancer, 2013. **13**(10): p. 739-752.

144. Mazzoni, A., et al., *Myeloid suppressor lines inhibit T cell responses by an NO-dependent mechanism.* J Immunol, 2002. **168**(2): p. 689-95.

145. Gabrilovich, D.I., et al., *Mechanism of immune dysfunction in cancer mediated by immature Gr-1+ myeloid cells.* J Immunol, 2001. **166**(9): p. 5398-406.

146. Liu, C., et al., *Expansion of spleen myeloid suppressor cells represses NK cell cytotoxicity in tumor-bearing host.* Blood, 2007. **109**(10): p. 4336-42.

147. Whiteside, T.L., P. Schuler, and B. Schilling, *Induced and natural regulatory T cells in human cancer.* Expert opinion on biological therapy, 2012. **12**(10): p. 1383-1397.

148. Bates, G.J., et al., *Quantification of regulatory T cells enables the identification of high-risk breast cancer patients and those at risk of late relapse.* J Clin Oncol, 2006. **24**(34): p. 5373-80.

149. Fu, J., et al., *Increased regulatory T cells correlate with CD8 T-cell impairment and poor survival in hepatocellular carcinoma patients.* Gastroenterology, 2007. **132**(7): p. 2328-39.

150. Frey, D.M., et al., *High frequency of tumor-infiltrating FOXP3(+) regulatory T cells predicts improved survival in mismatch repair-proficient colorectal cancer patients.* Int J Cancer, 2010. **126**(11): p. 2635-43.

151. von Boehmer, H. and C. Daniel, *Therapeutic opportunities for manipulating T(Reg) cells in autoimmunity and cancer.* Nat Rev Drug Discov, 2013. **12**(1): p. 51-63.

152. Tomasek, J.J., et al., *Myofibroblasts and mechano-regulation of connective tissue remodelling.* Nat Rev Mol Cell Biol, 2002. **3**(5): p. 349-63.

153. Kalluri, R. and M. Zeisberg, *Fibroblasts in cancer.* Nat Rev Cancer, 2006. **6**(5): p. 392-401.

154. Olumi, A.F., et al., *Carcinoma-associated fibroblasts direct tumor progression of initiated human prostatic epithelium.* Cancer Res, 1999. **59**(19): p. 5002-11.

155. Zeisberg, E.M., et al., *Discovery of endothelial to mesenchymal transition as a source for carcinoma-associated fibroblasts.* Cancer Res, 2007. **67**(21): p. 10123-8.

156. Petersen, O.W., et al., *Epithelial to mesenchymal transition in human breast cancer can provide a nonmalignant stroma.* Am J Pathol, 2003. **162**(2): p. 391-402.

157. Fukumura, D., et al., *Tumor induction of VEGF promoter activity in stromal cells.* Cell, 1998. **94**(6): p. 715-25.

158. Erez, N., et al., *Cancer-Associated Fibroblasts Are Activated in Incipient Neoplasia to Orchestrate Tumor-Promoting Inflammation in an NF-kappaB-Dependent Manner.* Cancer Cell, 2010. **17**(2): p. 135-47.

159. Bergamaschi, A., et al., *Extracellular matrix signature identifies breast cancer subgroups with different clinical outcome.* J Pathol, 2008. **214**(3): p. 357-67.

160. Naba, A., et al., *The matrisome: in silico definition and in vivo characterization by proteomics of normal and tumor*

extracellular matrices. Mol Cell Proteomics, 2012. **11**(4): p. M111.014647.

161. Hanahan, D. and Robert A. Weinberg, *Hallmarks of Cancer: The Next Generation.* Cell, 2011. **144**(5): p. 646-674.

162. Weis, S.M. and D.A. Cheresh, *Tumor angiogenesis: molecular pathways and therapeutic targets.* Nat Med, 2011. **17**(11): p. 1359-1370.

163. Semenza, G.L., *Cancer-stromal cell interactions mediated by hypoxia-inducible factors promote angiogenesis, lymphangiogenesis, and metastasis.* Oncogene, 2013. **32**(35): p. 4057-63.

164. Cuiffo, B.G. and A.E. Karnoub, *Mesenchymal stem cells in tumor development: emerging roles and concepts.* Cell Adh Migr, 2012. **6**(3): p. 220-30.

165. Alitalo, A. and M. Detmar, *Interaction of tumor cells and lymphatic vessels in cancer progression.* Oncogene, 2012. **31**(42): p. 4499-508.

166. Schoppmann, S.F., et al., *Tumor-associated macrophages express lymphatic endothelial growth factors and are related to peritumoral lymphangiogenesis.* Am J Pathol, 2002. **161**(3): p. 947-56.

167. Cowell, C.F., et al., *Progression from ductal carcinoma in situ to invasive breast cancer: revisited.* Mol Oncol, 2013. **7**(5): p. 859-69.

168. Goswami, S., et al., *Macrophages promote the invasion of breast carcinoma cells via a colony-stimulating factor-1/epidermal growth factor paracrine loop.* Cancer Res, 2005. **65**(12): p. 5278-83.

169. Huober, J., et al., *Prognosis of medullary breast cancer: analysis of 13 International Breast Cancer Study Group (IBCSG) trials.* Ann Oncol, 2012. **23**(11): p. 2843-51.

170. Mahmoud, S.M., et al., *Tumor-infiltrating CD8+ lymphocytes predict clinical outcome in breast cancer.* J Clin Oncol, 2011. **29**(15): p. 1949-55.

171. Teschendorff, A.E., et al., *Improved prognostic classification of breast cancer defined by antagonistic activation patterns of immune response pathway modules.* BMC Cancer, 2010. **10**: p. 604.

172. Gu-Trantien, C., et al., *CD4+ follicular helper T cell infiltration predicts breast cancer survival.* The Journal of Clinical Investigation, 2013. **123**(7): p. 2873-2892.

173. Gobert, M., et al., *Regulatory T cells recruited through CCL22/CCR4 are selectively activated in lymphoid infiltrates*

surrounding primary breast tumors and lead to an adverse clinical outcome. Cancer Res, 2009. **69**(5): p. 2000-9.

174. West, N.R., et al., *Tumour-infiltrating FOXP3(+) lymphocytes are associated with cytotoxic immune responses and good clinical outcome in oestrogen receptor-negative breast cancer.* British Journal of Cancer, 2013. **108**(1): p. 155-162.

175. Qi, W., X. Huang, and J. Wang, *Correlation between Th17 cells and tumor microenvironment.* Cell Immunol, 2013. **285**(1-2): p. 18-22.

176. Mahmoud, S.M., et al., *The prognostic significance of B lymphocytes in invasive carcinoma of the breast.* Breast Cancer Res Treat, 2012. **132**(2): p. 545-53.

177. Sikandar, B., et al., *Differential immune cell densities in ductal carcinoma In-Situ and invasive breast cancer: Possible role of leukocytes in early stages of carcinogenesis.* Pak J Med Sci, 2015. **31**(2): p. 274-9.

178. Thompson, E., et al., *The immune microenvironment of breast ductal carcinoma in situ.* Mod Pathol, 2016. **29**(3): p. 249-58.

179. Cimino-Mathews, A., et al., *PD-L1 (B7-H1) expression and the immune tumor microenvironment in primary and*

metastatic breast carcinomas. Hum Pathol, 2016. **47**(1): p. 52-63.

180. Ghaderi, A., et al., *Cytotoxic T lymphocyte antigen-4 gene in breast cancer.* Breast Cancer Res Treat, 2004. **86**(1): p. 1-7.

181. Sun, W.Y., Y.K. Lee, and J.S. Koo, *Expression of PD-L1 in triple-negative breast cancer based on different immunohistochemical antibodies.* J Transl Med, 2016. **14**(1): p. 173.

182. Soliman, H., F. Khalil, and S. Antonia, *PD-L1 expression is increased in a subset of basal type breast cancer cells.* PLoS One, 2014. **9**(2): p. e88557.

183. Ali, H.R., et al., *PD-L1 protein expression in breast cancer is rare, enriched in basal-like tumours and associated with infiltrating lymphocytes.* Ann Oncol, 2015. **26**(7): p. 1488-93.

184. Sabatier, R., et al., *Prognostic and predictive value of PDL1 expression in breast cancer.* Oncotarget, 2015. **6**(7): p. 5449-64.

185. Yeong, J., et al., *Identifying progression predictors of breast ductal carcinoma in situ.* J Clin Pathol, 2016.

186. Dumont, N., et al., *Breast Fibroblasts Modulate Early Dissemination, Tumorigenesis, and Metastasis through*

Alteration of Extracellular Matrix Characteristics. Neoplasia, 2013. **15**(3): p. 249-IN7.

187. Xu, K., et al., *The fibroblast Tiam1-osteopontin pathway modulates breast cancer invasion and metastasis.* Breast Cancer Research : BCR, 2016. **18**: p. 14.

188. Liao, D., et al., *Cancer associated fibroblasts promote tumor growth and metastasis by modulating the tumor immune microenvironment in a 4T1 murine breast cancer model.* PLoS One, 2009. **4**(11): p. e7965.

189. Ma, X.J., et al., *Gene expression profiling of the tumor microenvironment during breast cancer progression.* Breast Cancer Res, 2009. **11**(1): p. R7.

190. Bauer, M., et al., *Heterogeneity of gene expression in stromal fibroblasts of human breast carcinomas and normal breast.* Oncogene, 2010. **29**(12): p. 1732-40.

191. Osuala, K.O., et al., *Il-6 signaling between ductal carcinoma in situ cells and carcinoma-associated fibroblasts mediates tumor cell growth and migration.* BMC Cancer, 2015. **15**: p. 584.

192. Orimo, A., et al., *Stromal fibroblasts present in invasive human breast carcinomas promote tumor growth and*

angiogenesis through elevated SDF-1/CXCL12 secretion. Cell, 2005. **121**(3): p. 335-48.

193. Levental, K.R., et al., *Matrix crosslinking forces tumor progression by enhancing integrin signaling.* Cell, 2009. **139**(5): p. 891-906.

194. Giussani, M., et al., *Tumor-extracellular matrix interactions: Identification of tools associated with breast cancer progression.* Semin Cancer Biol, 2015. **35**: p. 3-10.

195. Conklin, M.W., et al., *Aligned collagen is a prognostic signature for survival in human breast carcinoma.* Am J Pathol, 2011. **178**(3): p. 1221-32.

196. Provenzano, P.P., et al., *Collagen reorganization at the tumor-stromal interface facilitates local invasion.* BMC Med, 2006. **4**(1): p. 38.

197. Van Bockstal, M., et al., *The Baader-Meinhof phenomenon in ductal carcinoma in situ of the breast.* Histopathology, 2016.

198. Van Bockstal, M., et al., *Stromal architecture and periductal decorin are potential prognostic markers for ipsilateral locoregional recurrence in ductal carcinoma in situ of the breast.* Histopathology, 2013. **63**(4): p. 520-33.

199. Dudley, A.C., *Tumor endothelial cells.* Cold Spring Harb Perspect Med, 2012. **2**(3): p. a006536.

200. Hoeben, A., et al., *Vascular endothelial growth factor and angiogenesis.* Pharmacol Rev, 2004. **56**(4): p. 549-80.

201. Emerman, J.T. and A.W. Vogl, *Cell size and shape changes in the myoepithelium of the mammary gland during differentiation.* Anat Rec, 1986. **216**(3): p. 405-15.

202. Barcellos-Hoff, M.H., et al., *Functional differentiation and alveolar morphogenesis of primary mammary cultures on reconstituted basement membrane.* Development, 1989. **105**(2): p. 223-35.

203. Bergstraesser, L.M., et al., *Expression of hemidesmosomes and component proteins is lost by invasive breast cancer cells.* Am J Pathol, 1995. **147**(6): p. 1823-39.

204. Allen, M.D., J.F. Marshall, and J.L. Jones, *avβ6 Expression in Myoepithelial Cells: A Novel Marker for Predicting DCIS Progression with Therapeutic Potential.* Cancer Res, 2014. **74**(21): p. 5942-5947.

205. Adriance, M.C., et al., *Myoepithelial cells: good fences make good neighbors.* Breast Cancer Res, 2005. **7**(5): p. 190-7.

206. Sternlicht, M.D., et al., *The human myoepithelial cell is a natural tumor suppressor.* Clin Cancer Res, 1997. **3**(11): p. 1949-58.

207. Sternlicht, M.D., et al., *Characterizations of the extracellular matrix and proteinase inhibitor content of human myoepithelial tumors.* Lab Invest, 1996. **74**(4): p. 781-96.

208. Bissell, M.J. and D. Radisky, *Putting tumours in context.* Nat Rev Cancer, 2001. **1**(1): p. 46-54.

209. Shao, Z.M., et al., *The human myoepithelial cell exerts antiproliferative effects on breast carcinoma cells characterized by p21WAF1/CIP1 induction, G2/M arrest, and apoptosis.* Exp Cell Res, 1998. **241**(2): p. 394-403.

210. Zou, Z., et al., *Maspin, a serpin with tumor-suppressing activity in human mammary epithelial cells.* Science, 1994. **263**(5146): p. 526-9.

211. Allinen, M., et al., *Molecular characterization of the tumor microenvironment in breast cancer.* Cancer Cell, 2004. **6**(1): p. 17-32.

212. Smith, M.C., et al., *CXCR4 regulates growth of both primary and metastatic breast cancer.* Cancer Res, 2004. **64**(23): p. 8604-12.

213. Gudjonsson, T., et al., *Normal and tumor-derived myoepithelial cells differ in their ability to interact with luminal breast epithelial cells for polarity and basement membrane deposition.* J Cell Sci, 2002. **115**(Pt 1): p. 39-50.

214. Pandey, P.R., J. Saidou, and K. Watabe, *Role of myoepithelial cells in breast tumor progression.* Frontiers in bioscience : a journal and virtual library, 2010. **15**: p. 226-236.

215. Man, Y.-g., et al., *Cell clusters overlying focally disrupted mammary myoepithelial cell layers and adjacent cells within the same duct display different immunohistochemical and genetic features: implications for tumor progression and invasion.* Breast Cancer Research, 2003. **5**(6): p. R231-R241.

216. Santamaria, I., et al., *Cathepsin L2, a novel human cysteine proteinase produced by breast and colorectal carcinomas.* Cancer Res, 1998. **58**(8): p. 1624-30.

217. Kim, H.J., et al., *Expression of MT-1 MMP, MMP2, MMP9 and TIMP2 mRNAs in ductal carcinoma in situ and invasive ductal carcinoma of the breast.* Yonsei Med J, 2006. **47**(3): p. 333-42.

218. Afghahi, A., et al., *Chromosomal copy number alterations for associations of ductal carcinoma in situ with invasive breast cancer.* Breast Cancer Res, 2015. **17**: p. 108.

219. Liao, S., et al., *Differential copy number aberrations in novel candidate genes associated with progression from in situ to invasive ductal carcinoma of the breast.* Genes Chromosomes Cancer, 2012. **51**(12): p. 1067-78.

220. Pan, A., et al., *Detection of gene copy number alterations in DCIS and invasive breast cancer by QM-FISH.* Am J Transl Res, 2016. **8**(11): p. 4994-5004.

221. Diepenbruck, M. and G. Christofori, *Epithelial-mesenchymal transition (EMT) and metastasis: yes, no, maybe?* Curr Opin Cell Biol, 2016. **43**: p. 7-13.

222. Knudsen, E.S., et al., *Progression of ductal carcinoma in situ to invasive breast cancer is associated with gene expression programs of EMT and myoepithelia.* Breast Cancer Res Treat, 2012. **133**(3): p. 1009-24.

223. Mathew, J., et al., *Factors influencing local control in patients undergoing breast conservation surgery for ductal carcinoma in situ.* Breast, 2017. **31**: p. 181-185.

224. Ilyas, M., et al., *Guidelines and considerations for conducting experiments using tissue microarrays.* Histopathology, 2013. **62**(6): p. 827-39.

225. Dancau, A.M., et al., *Tissue microarrays.* Methods Mol Biol, 2010. **576**: p. 49-60.

226. Shergill, I.S. and M. Arya, *Tissue microarrays.* Expert Rev Mol Diagn, 2004. **4**(4): p. 421-3.

227. Jawhar, N.M.T., *Tissue Microarray: A rapidly evolving diagnostic and research tool.* Annals of Saudi Medicine, 2009. **29**(2): p. 123-127.

228. Dancau, A.M., et al., *Tissue Microarrays.* Methods Mol Biol, 2016. **1381**: p. 53-65.

229. Lacombe, A., et al., *Re-Punching Tissue Microarrays Is Possible: Why Can This Be Useful and How to Do It.* Microarrays (Basel), 2015. **4**(2): p. 245-54.

230. Allen, M.D., et al., *Altered microenvironment promotes progression of preinvasive breast cancer: myoepithelial expression of alphavbeta6 integrin in DCIS identifies high-risk patients and predicts recurrence.* Clin Cancer Res, 2014. **20**(2): p. 344-57.

231. Carraro, D.M., E.V. Elias, and V.P. Andrade, *Ductal carcinoma in situ of the breast: morphological and molecular features implicated in progression.* Biosci Rep, 2013.

232. Clamp, M., et al., *Distinguishing protein-coding and noncoding genes in the human genome.* Proc Natl Acad Sci U S A, 2007. **104**(49): p. 19428-33.

233. Stuart, D. and W.R. Sellers, *Linking somatic genetic alterations in cancer to therapeutics.* Curr Opin Cell Biol, 2009. **21**(2): p. 304-10.

234. Futreal, P.A., et al., *A census of human cancer genes.* Nat Rev Cancer, 2004. **4**(3): p. 177-83.

235. Baudis, M., *Genomic imbalances in 5918 malignant epithelial tumors: an explorative meta-analysis of chromosomal CGH data.* BMC Cancer, 2007. **7**: p. 226.

236. Beroukhim, R., et al., *The landscape of somatic copy-number alteration across human cancers.* Nature, 2010. **463**(7283): p. 899-905.

237. Torhorst, J., et al., *Tissue microarrays for rapid linking of molecular changes to clinical endpoints.* Am J Pathol, 2001. **159**(6): p. 2249-56.

238. McCarty, K.S., Jr., et al., *Estrogen receptor analyses. Correlation of biochemical and immunohistochemical methods using monoclonal antireceptor antibodies.* Arch Pathol Lab Med, 1985. **109**(8): p. 716-21.

239. Hendry, S., et al., *Relationship of the Breast Ductal Carcinoma In Situ Immune Microenvironment with Clinicopathological and Genetic Features.* Clin Cancer Res, 2017. **23**(17): p. 5210-5217.

240. Camp, R.L., M. Dolled-Filhart, and D.L. Rimm, *X-tile: a new bio-informatics tool for biomarker assessment and outcome-based cut-point optimization.* Clin Cancer Res, 2004. **10**(21): p. 7252-9.

241. Dolled-Filhart, M., et al., *Quantitative in situ analysis of beta-catenin expression in breast cancer shows decreased expression is associated with poor outcome.* Cancer Res, 2006. **66**(10): p. 5487-94.

242. Hammond, M.E., et al., *American society of clinical oncology/college of american pathologists guideline recommendations for immunohistochemical testing of estrogen and progesterone receptors in breast cancer.* J Oncol Pract, 2010. **6**(4): p. 195-7.

243. Wolff, A.C., et al., *American Society of Clinical Oncology/College of American Pathologists guideline recommendations for human epidermal growth factor receptor 2 testing in breast cancer.* Arch Pathol Lab Med, 2007. **131**(1): p. 18-43.

244. Cheang, M.C., et al., *Ki67 index, HER2 status, and prognosis of patients with luminal B breast cancer.* J Natl Cancer Inst, 2009. **101**(10): p. 736-50.

245. Kobel, M., et al., *The biological and clinical value of p53 expression in pelvic high-grade serous carcinomas.* J Pathol, 2010. **222**(2): p. 191-8.

246. Gawenda, J., et al., *Legumain expression as a prognostic factor in breast cancer patients.* Breast Cancer Res Treat, 2007. **102**(1): p. 1-6.

247. Rothman, K.J., *No adjustments are needed for multiple comparisons.* Epidemiology, 1990. **1**(1): p. 43-6.

248. Saville, D.J., *Multiple Comparison Procedures: The Practical Solution.* The American Statistician, 1990. **44**(2): p. 174-180.

249. Sakorafas, G.H., D.R. Farley, and G. Peros, *Recent advances and current controversies in the management of DCIS of the breast.* Cancer Treat Rev, 2008. **34**(6): p. 483-97.

250. Fallowfield, L., A. Francis, and A.M. Thompson, *EFfects of standard treatments for ductal carcinoma in situ—making informed choices.* JAMA Oncology, 2016. **2**(3): p. 396-397.

251. *Surgical guidelines for the management of breast cancer.* Eur J Surg Oncol, 2009. **35 Suppl 1**: p. 1-22.

252. Van Zee, K.J., et al., *Relationship Between Margin Width and Recurrence of Ductal Carcinoma In Situ: Analysis of 2996*

Women Treated With Breast-conserving Surgery for 30 Years. Ann Surg, 2015. **262**(4): p. 623-31.

253. Silverstein, M.J., *Current controversies in ductal carcinoma in situ of the breast: summary from the Lynn Sage Breast Cancer Symposium.* J Am Coll Surg, 2003. **197**(1): p. 115-8.

254. Boland, G.P., et al., *Value of the Van Nuys Prognostic Index in prediction of recurrence of ductal carcinoma in situ after breast-conserving surgery.* Br J Surg, 2003. **90**(4): p. 426-32.

255. Holland, P.A., et al., *The importance of complete excision in the prevention of local recurrence of ductal carcinoma in situ.* Br J Cancer, 1998. **77**(1): p. 110-4.

256. Dillon, M.F., et al., *Factors affecting successful breast conservation for ductal carcinoma in situ.* Ann Surg Oncol, 2007. **14**(5): p. 1618-28.

257. Wei, S., et al., *Factors associated with residual disease after initial breast-conserving surgery for ductal carcinoma in situ.* Hum Pathol, 2012. **43**(7): p. 986-93.

258. report, T.n.i.b.c., NCIN 2007.

259. Ernster, V.L., et al., *Incidence of and treatment for ductal carcinoma in situof the breast.* JAMA, 1996. **275**.

260. Torres-Mejia, G., et al., *Mammographic features and subsequent risk of breast cancer: a comparison of qualitative and quantitative evaluations in the Guernsey prospective studies.* Cancer Epidemiol Biomarkers Prev, 2005. **14**.

261. Lyman, G.H., et al., *Sentinel lymph node biopsy for patients with early-stage breast cancer: American Society of Clinical Oncology clinical practice guideline update.* J Clin Oncol, 2014. **32**(13): p. 1365-83.

262. Claus, E.B., M. Stowe, and D. Carter, *Breast carcinoma in situ: risk factors and screening patterns.* J Natl Cancer Inst, 2001. **93**.

263. *Cancer Facts and Figures 2005*. 2005, Atlanta, GA: American Cancer Society, Inc.

264. Shiyanbola, O.O., et al., *Emerging trends in surgical and adjuvant radiation therapies among women diagnosed with ductal carcinoma in situ.* Cancer, 2016. **15**(122(18)): p. 2810-8.

265. Thomas, J., et al., *Radiological and pathological size estimations of pure ductal carcinoma in situ of the breast, specimen handling and the influence on the success of breast conservation surgery: a review of 2564 cases from the Sloane Project.* Br J Cancer, 2010. **102**(2): p. 285-93.

266. Gapstur, S.M., M. Morrow, and T.A. Sellers, *Hormone replacement therapy and risk of breast cancer with a favorable histology: results of the Iowa Women's Health Study.* JAMA, 1999. **281**.

267. Jeevan, R., et al., *Reoperation rates after breast conserving surgery for breast cancer among women in England: retrospective study of hospital episode statistics.* BMJ, 2012. **345**: p. e4505.

268. Bernstein, L., *The epidemiology of breast carcinoma in situ*, in *Ductal Carcinoma In Situ of the Breast*, M.J. Silverstein, A. Recht, and M.D. Lagios, Editors. 2002, Lippincott, Williams and Wilkins: Philadelphia.

269. Lambe, M., et al., *Parity, age at first birth and the risk of carcinoma in situof the breast.* Int J Cancer, 1998. **77**.

270. Jacobson, A.F., et al., *Do additional shaved margins at the time of lumpectomy eliminate the need for re-excision?* Am J Surg, 2008. **196**(4): p. 556-8.

271. Guidroz, J.A., et al., *Sampling of secondary margins decreases the need for re-excision after partial mastectomy.* Surgery, 2011. **150**(4): p. 802-9.

272. Gurdal, S.O., et al., *Positive or close margins in breast conserving surgery: is re-excision always necessary?* Eur J Surg Oncol, 2012. **38**(5): p. 399-406.

273. McCahill, L.E., et al., *Variability in reexcision following breast conservation surgery.* JAMA, 2012. **307**(5): p. 467-75.

274. Merrill, A.L., et al., *Implications of New Lumpectomy Margin Guidelines for Breast-Conserving Surgery: Changes in Reexcision Rates and Predicted Rates of Residual Tumor.* Ann Surg Oncol, 2016. **23**(3): p. 729-34.

275. Pilewskie, M., et al., *Do LORIS Trial Eligibility Criteria Identify a Ductal Carcinoma In Situ Patient Population at Low Risk of Upgrade to Invasive Carcinoma?* Ann Surg Oncol, 2016. **23**(11): p. 3487-93.

276. Margenthaler, J.A., F. Gao, and V.S. Klimberg, *Margin index: a new method for prediction of residual disease after breast-conserving surgery.* Ann Surg Oncol, 2010. **17**(10): p. 2696-701.

277. Fisher, C.S., et al., *Margin index is not a reliable tool for predicting residual disease after breast-conserving surgery for DCIS.* Ann Surg Oncol, 2011. **18**(11): p. 3155-9.

278. Moran, M.S., et al., *Society of Surgical Oncology-American Society for Radiation Oncology consensus guideline*

on margins for breast-conserving surgery with whole-breast irradiation in stages I and II invasive breast cancer. J Clin Oncol, 2014. **32**(14): p. 1507-15.

279. Singletary, S.E., *Surgical margins in patients with early-stage breast cancer treated with breast conservation therapy.* Am J Surg, 2002. **184**(5): p. 383-93.

280. Kell, M.R. and M. Morrow, *An adequate margin of excision in ductal carcinoma in situ.* BMJ, 2005. **331**(7520): p. 789-90.

281. Morrow, M., *Breast conservation and negative margins: how much is enough?* Breast, 2009. **18 Suppl 3**: p. S84-6.

282. Azu, M., et al., *What is an adequate margin for breast-conserving surgery? Surgeon attitudes and correlates.* Ann Surg Oncol, 2010. **17**(2): p. 558-63.

283. National Institute for Health and Care Excellence, *Early and locally advanced breast cancer: diagnosis and management, [A] Evidence reviews for surgery to the breast, NICE guideline NG101.* 2018.

284. Schulman, A.M., et al., *Reexcision Surgery for Breast Cancer: An Analysis of the American Society of Breast Surgeons (ASBrS) MasterySM Database Following the SSO-ASTRO "No Ink on Tumor" Guidelines.* Annals of Surgical Oncology, 2017. **24**(1): p. 52-58.

285. Ben-David, M.A., et al., *Long-term results of conservative surgery and radiotherapy for ductal carcinoma in situ using lung density correction: the University of Michigan experience.* Breast J, 2007. **13**(4): p. 392-400.

286. Ward, E.M., et al., *Cancer statistics: Breast cancer in situ.* CA Cancer J Clin, 2015. **65**(6): p. 481-95.

287. Wadsten, C., et al., *A validation of DCIS registration in a population-based breast cancer quality register and a study of treatment and prognosis for DCIS during 20 years.* Acta Oncol, 2016. **55**(11): p. 1338-1343.

288. Silverstein, M.J., et al., *The influence of margin width on local control of ductal carcinoma in situ of the breast.* N Engl J Med, 1999. **340**(19): p. 1455-61.

289. Bijker, N., et al., *Breast-conserving treatment with or without radiotherapy in ductal carcinoma-in-situ: ten-year results of European Organisation for Research and Treatment of Cancer randomized phase III trial 10853--a study by the EORTC Breast Cancer Cooperative Group and EORTC Radiotherapy Group.* J Clin Oncol, 2006. **24**(21): p. 3381-7.

290. Fisher, B., et al., *Prevention of invasive breast cancer in women with ductal carcinoma in situ: an update of the National Surgical Adjuvant Breast and Bowel Project experience.* Semin Oncol, 2001. **28**(4): p. 400-18.

291. Ringberg, A., et al., *Histopathological risk factors for ipsilateral breast events after breast conserving treatment for ductal carcinoma in situ of the breast--results from the Swedish randomised trial.* Eur J Cancer, 2007. **43**(2): p. 291-8.

292. Sanders, M.E., et al., *The natural history of low-grade ductal carcinoma in situ of the breast in women treated by biopsy only revealed over 30 years of long-term follow-up.* Cancer, 2005. **103**.

293. Boxer, M.M., G.P. Delaney, and B.H. Chua, *A review of the management of ductal carcinoma in situ following breast conserving surgery.* Breast, 2013. **22**(6): p. 1019-25.

294. Bijker, N., et al., *Risk factors for recurrence and metastasis after breast-conserving therapy for ductal carcinoma-in-situ: analysis of European Organization for Research and Treatment of Cancer Trial 10853.* J Clin Oncol, 2001. **19**(8): p. 2263-71.

295. Asjoe, F.T., et al., *The value of the Van Nuys Prognostic Index in ductal carcinoma in situ of the breast: a retrospective analysis.* Breast J, 2007. **13**(4): p. 359-67.

296. Mazouni, C., et al., *Nomogram for risk of relapse after breast-conserving surgery in ductal carcinoma in situ.* J Clin Oncol, 2011. **29**(2): p. e44; author reply e45-6.

297. Lee, S.K., et al., *Nomogram for predicting invasion in patients with a preoperative diagnosis of ductal carcinoma in situ of the breast.* Br J Surg, 2013. **100**(13): p. 1756-63.

298. Clark, G.M., et al., *Prognostic factors: rationale and methods of analysis and integration.* Breast Cancer Res Treat, 1994. **32**(1): p. 105-12.

299. Lee, A.H. and I.O. Ellis, *The Nottingham prognostic index for invasive carcinoma of the breast.* Pathol Oncol Res, 2008. **14**(2): p. 113-5.

300. Mauriac, L., M. Debled, and G. MacGrogan, *When will more useful predictive factors be ready for use?* Breast, 2005. **14**(6): p. 617-23.

301. Yamashiro, H. and M. Toi, *Update of evidence in chemotherapy for breast cancer.* Int J Clin Oncol, 2008. **13**(1): p. 3-7.

302. Nofech-Mozes, S., et al., *Prognostic and predictive molecular markers in DCIS: a review.* Adv Anat Pathol, 2005. **12**(5): p. 256-64.

303. Benson, J.R. and G.C. Wishart, *Predictors of recurrence for ductal carcinoma in situ after breast-conserving surgery.* Lancet Oncol, 2013. **14**(9): p. e348-57.

304. Holmes, P., et al., *Prognostic markers and long-term outcomes in ductal carcinoma in situ of the breast treated with excision alone.* Cancer, 2011. **117**(16): p. 3650-7.

305. Kantor, O. and D.J. Winchester, *Breast conserving therapy for DCIS--does size matter?* J Surg Oncol, 2014. **110**(1): p. 75-81.

306. Wong, J.S., et al., *Eight-year update of a prospective study of wide excision alone for small low- or intermediate-grade ductal carcinoma in situ (DCIS).* Breast Cancer Res Treat, 2014. **143**(2): p. 343-50.

307. Berman, H.K., M.L. Gauthier, and T.D. Tlsty, *Premalignant breast neoplasia: a paradigm of interlesional and intralesional molecular heterogeneity and its biological and clinical ramifications.* Cancer Prev Res (Phila), 2010. **3**(5): p. 579-87.

308. Yi, M., et al., *Evaluation of a breast cancer nomogram for predicting risk of ipsilateral breast tumor recurrences in patients with ductal carcinoma in situ after local excision.* J Clin Oncol, 2012. **30**(6): p. 600-7.

309. Rakovitch, E., et al., *A population-based validation study of the DCIS Score predicting recurrence risk in individuals treated by breast-conserving surgery alone.* Breast cancer research and treatment, 2015. **152**(2): p. 389-398.

310. Siziopikou, K.P., *Ductal Carcinoma In Situ of the Breast: Current Concepts and Future Directions.* Archives of Pathology & Laboratory Medicine, 2013. **137**(4): p. 462-466.

311. Sorlie, T., et al., *Gene expression patterns of breast carcinomas distinguish tumor subclasses with clinical implications.* Proc Natl Acad Sci U S A, 2001. **98**(19): p. 10869-74.

312. Weigelt, B. and J.S. Reis-Filho, *Molecular profiling currently offers no more than tumour morphology and basic immunohistochemistry.* Breast Cancer Res, 2010. **12 Suppl 4**: p. S5.

313. Vuong, D., et al., *Molecular classification of breast cancer.* Virchows Arch, 2014. **465**(1): p. 1-14.

314. Goldhirsch, A., et al., *Strategies for subtypes--dealing with the diversity of breast cancer: highlights of the St. Gallen International Expert Consensus on the Primary Therapy of Early Breast Cancer 2011.* Ann Oncol, 2011. **22**(8): p. 1736-47.

315. Perou, C.M., et al., *Molecular portraits of human breast tumours.* Nature, 2000. **406**(6797): p. 747-52.

316. Zhou, W., et al., *Molecular subtypes in ductal carcinoma in situ of the breast and their relation to prognosis: a*

population-based cohort study. BMC Cancer, 2013. **13**: p. 512.

317. Goldhirsch, A., et al., *Personalizing the treatment of women with early breast cancer: highlights of the St Gallen International Expert Consensus on the Primary Therapy of Early Breast Cancer 2013.* Ann Oncol, 2013. **24**(9): p. 2206-23.

318. Correa, C., et al., *Overview of the randomized trials of radiotherapy in ductal carcinoma in situ of the breast.* J Natl Cancer Inst Monogr, 2010. **2010**(41): p. 162-77.

319. Rakha, E.A., J.S. Reis-Filho, and I.O. Ellis, *Combinatorial biomarker expression in breast cancer.* Breast Cancer Res Treat, 2010. **120**(2): p. 293-308.

320. Jensen, E.V. and V.C. Jordan, *The estrogen receptor: a model for molecular medicine.* Clin Cancer Res, 2003. **9**(6): p. 1980-9.

321. Lari, S.A. and H.M. Kuerer, *Biological Markers in DCIS and Risk of Breast Recurrence: A Systematic Review.* J Cancer, 2011. **2**: p. 232-61.

322. Meijnen, P., et al., *Immunohistochemical categorisation of ductal carcinoma in situ of the breast.* Br J Cancer, 2008. **98**(1): p. 137-42.

323. Altintas, S., et al., *Prognostic significance of oncogenic markers in ductal carcinoma in situ of the breast: a clinicopathologic study.* Breast J, 2009. **15**(2): p. 120-32.

324. Williams, K.E., et al., *Molecular phenotypes of DCIS predict overall and invasive recurrence.* Ann Oncol, 2015. **26**(5): p. 1019-25.

325. Narod, S.A., et al., *Breast cancer mortality after a diagnosis of ductal carcinoma in situ.* JAMA Oncol, 2015. **1**.

326. Mitchell, K.B. and H. Kuerer, *Ductal Carcinoma In Situ: Treatment Update and Current Trends.* Curr Oncol Rep, 2015. **17**(11): p. 48.

327. Nguyen, T.T., et al., *Factors Influencing Use of Hormone Therapy for Ductal Carcinoma In Situ: A National Cancer Database Study.* Ann Surg Oncol, 2017. **24**(10): p. 2989-2998.

328. Meattini, I., et al., *Impact of hormonal status on outcome of ductal carcinoma in situ treated with breast-conserving surgery plus radiotherapy: Long-term experience from two large-institutional series.* Breast, 2017. **33**: p. 139-144.

329. Forbes, J.F., et al., *Anastrozole versus tamoxifen for the prevention of locoregional and contralateral breast cancer in postmenopausal women with locally excised ductal carcinoma*

in situ (IBIS-II DCIS): a double-blind, randomised controlled trial. Lancet, 2016. **387**(10021): p. 866-73.

330. Fisher, B., et al., *Tamoxifen in treatment of intraductal breast cancer: National Surgical Adjuvant Breast and Bowel Project B-24 randomised controlled trial.* Lancet, 1999. **353**(9169): p. 1993-2000.

331. Allison, K.H., et al., *Estrogen and Progesterone Receptor Testing in Breast Cancer: ASCO/CAP Guideline Update.* J Clin Oncol, 2020: p. Jco1902309.

332. Houghton, J., et al., *Radiotherapy and tamoxifen in women with completely excised ductal carcinoma in situ of the breast in the UK, Australia, and New Zealand: randomised controlled trial.* Lancet, 2003. **362**(9378): p. 95-102.

333. Cuzick, J., et al., *Tamoxifen for prevention of breast cancer: extended long-term follow-up of the IBIS-I breast cancer prevention trial.* Lancet Oncol, 2015. **16**(1): p. 67-75.

334. Cuzick, J., et al., *Anastrozole for prevention of breast cancer in high-risk postmenopausal women (IBIS-II): an international, double-blind, randomised placebo-controlled trial.* Lancet, 2014. **383**(9922): p. 1041-8.

335. Goss, P.E., et al., *Exemestane for breast-cancer prevention in postmenopausal women.* N Engl J Med, 2011. **364**(25): p. 2381-91.

336. Guerrieri-Gonzaga, A., et al., *Benefit of low-dose tamoxifen in a large observational cohort of high risk ER positive breast DCIS.* Int J Cancer, 2016. **139**(9): p. 2127-34.

337. Lebeau, A., et al., *EGFR, HER-2/neu, cyclin D1, p21 and p53 in correlation to cell proliferation and steroid hormone receptor status in ductal carcinoma in situ of the breast.* Breast Cancer Res Treat, 2003. **79**(2): p. 187-98.

338. Hanley, K., et al., *Lack of expression of androgen receptor may play a critical role in transformation from in situ to invasive basal subtype of high-grade ductal carcinoma of the breast.* Hum Pathol, 2008. **39**(3): p. 386-92.

339. Kulkarni, S., et al., *COX-2 and PPARgamma expression are potential markers of recurrence risk in mammary duct carcinoma in-situ.* BMC Cancer, 2008. **8**: p. 36.

340. Ringberg, A., et al., *Cell biological factors in ductal carcinoma in situ (DCIS) of the breast-relationship to ipsilateral local recurrence and histopathological characteristics.* Eur J Cancer, 2001. **37**(12): p. 1514-22.

341. Provenzano, E., et al., *Biological markers that predict clinical recurrence in ductal carcinoma in situ of the breast.* Eur J Cancer, 2003. **39**(5): p. 622-30.

342. Roses, R.E., et al., *HER-2/neu overexpression as a predictor for the transition from in situ to invasive breast cancer.* Cancer Epidemiol Biomarkers Prev, 2009. **18**(5): p. 1386-9.

343. Wilson, C.A., et al., *HER-2 overexpression differentially alters transforming growth factor-beta responses in luminal versus mesenchymal human breast cancer cells.* Breast Cancer Res, 2005. **7**(6): p. R1058-79.

344. Borgquist, S., et al., *The prognostic role of HER2 expression in ductal breast carcinoma in situ (DCIS); a population-based cohort study.* BMC Cancer, 2015. **15**: p. 468.

345. Hanna, W., H.J. Kahn, and M. Trudeau, *Evaluation of HER-2/neu (erbB-2) status in breast cancer: from bench to bedside.* Mod Pathol, 1999. **12**(8): p. 827-34.

346. Jimenez, R.E., et al., *Determination of Her-2/Neu status in breast carcinoma: comparative analysis of immunohistochemistry and fluorescent in situ hybridization.* Mod Pathol, 2000. **13**(1): p. 37-45.

347. Pothos, A., et al., *Comparison of chromogenic in situ hybridisation with fluorescence in situ hybridisation and immunohistochemistry for the assessment of her-2/neu oncogene in archival material of breast carcinoma.* Acta Histochem Cytochem, 2008. **41**(3): p. 59-64.

348. Penault-Llorca, F., et al., *Emerging technologies for assessing HER2 amplification.* Am J Clin Pathol, 2009. **132**(4): p. 539-48.

349. Gerdes, J., et al., *Production of a mouse monoclonal antibody reactive with a human nuclear antigen associated with cell proliferation.* Int J Cancer, 1983. **31**(1): p. 13-20.

350. Colozza, M., et al., *Proliferative markers as prognostic and predictive tools in early breast cancer: where are we now?* Ann Oncol, 2005. **16**(11): p. 1723-39.

351. Park, D., et al., *Ki-67 expression in primary breast carcinomas and their axillary lymph node metastases: clinical implications.* Virchows Arch, 2007. **451**(1): p. 11-8.

352. de Azambuja, E., et al., *Ki-67 as prognostic marker in early breast cancer: a meta-analysis of published studies involving 12,155 patients.* Br J Cancer, 2007. **96**(10): p. 1504-13.

353. Kuerer, H.M., et al., *Biologic and immunologic effects of preoperative trastuzumab for ductal carcinoma in situ of the breast.* Cancer, 2011. **117**(1): p. 39-47.

354. Rakovitch, E., et al., *HER2/neu and Ki-67 expression predict non-invasive recurrence following breast-conserving therapy for ductal carcinoma in situ.* British Journal of Cancer, 2012. **106**(6): p. 1160-1165.

355. Wilson, G.R., et al., *Activated c-SRC in ductal carcinoma in situ correlates with high tumour grade, high proliferation and HER2 positivity.* Br J Cancer, 2006. **95**(10): p. 1410-4.

356. Rakha, E.A., et al., *Updated UK Recommendations for HER2 assessment in breast cancer.* J Clin Pathol, 2015. **68**(2): p. 93-9.

357. Wolff, A.C., et al., *Recommendations for human epidermal growth factor receptor 2 testing in breast cancer: American Society of Clinical Oncology/College of American Pathologists clinical practice guideline update.* J Clin Oncol, 2013. **31**(31): p. 3997-4013.

358. Hammond, M.E., et al., *American Society of Clinical Oncology/College of American Pathologists guideline recommendations for immunohistochemical testing of estrogen and progesterone receptors in breast cancer*

(unabridged version). Arch Pathol Lab Med, 2010. **134**(7): p. e48-72.

359. Normanno, N., et al., *Prognostic applications of gene expression signatures in breast cancer.* Oncology, 2009. **77 Suppl 1**: p. 2-8.

360. Su, Y., et al., *Distinct distribution and prognostic significance of molecular subtypes of breast cancer in Chinese women: a population-based cohort study.* BMC Cancer, 2011. **11**: p. 292.

361. Zhou, W., et al., *Long-term survival of women with basal-like ductal carcinoma in situ of the breast: a population-based cohort study.* BMC Cancer, 2010. **10**: p. 653.

362. Hwang, E.S., et al., *The COMET (Comparison of Operative versus Monitoring and Endocrine Therapy) trial: a phase III randomised controlled clinical trial for low-risk ductal carcinoma in situ (DCIS).* BMJ Open, 2019. **9**(3): p. e026797.

363. Stout, N.K., et al., *Estrogen-receptor status and risk of contralateral breast cancer following DCIS.* Breast Cancer Res Treat, 2018. **171**(3): p. 777-781.

364. Freedman, A.N., et al., *Benefit/risk assessment for breast cancer chemoprevention with raloxifene or tamoxifen for*

women age 50 years or older. J Clin Oncol, 2011. **29**(17): p. 2327-33.

365. Ganz, P.A., et al., *Patient-reported outcomes with anastrozole versus tamoxifen for postmenopausal patients with ductal carcinoma in situ treated with lumpectomy plus radiotherapy (NSABP B-35): a randomised, double-blind, phase 3 clinical trial.* Lancet, 2016. **387**(10021): p. 857-65.

366. DeCensi, A., et al., *Randomized Placebo Controlled Trial of Low-Dose Tamoxifen to Prevent Local and Contralateral Recurrence in Breast Intraepithelial Neoplasia.* J Clin Oncol, 2019. **37**(19): p. 1629-1637.

367. Madrid, M.A. and R.W. Lo, *Chromogenic in situ hybridization (CISH): a novel alternative in screening archival breast cancer tissue samples for HER-2/neu status.* Breast Cancer Res, 2004. **6**(5): p. R593-600.

368. Kakar, S., et al., *HER-2/neu assessment in breast cancer by immunohistochemistry and fluorescence in situ hybridization: comparison of results and correlation with survival.* Mol Diagn, 2000. **5**(3): p. 199-207.

369. Thomson, T.A., et al., *HER-2/neu in breast cancer: interobserver variability and performance of immunohistochemistry with 4 antibodies compared with*

fluorescent in situ hybridization. Mod Pathol, 2001. **14**(11): p. 1079-86.

370. Tabarestani, S., S.M. Ghaderian, and H. Rezvani, *Detection of Gene Amplification by Multiplex Ligation-Dependent Probe Amplification in Comparison with In Situ Hybridization and Immunohistochemistry.* Asian Pac J Cancer Prev, 2015. **16**(17): p. 7997-8002.

371. Gong, Y., et al., *Chromogenic in situ hybridization is a reliable method for detecting HER2 gene status in breast cancer: a multicenter study using conventional scoring criteria and the new ASCO/CAP recommendations.* Am J Clin Pathol, 2009. **131**(4): p. 490-7.

372. Garcia-Caballero, T., et al., *Determination of HER2 amplification in primary breast cancer using dual-colour chromogenic in situ hybridization is comparable to fluorescence in situ hybridization: a European multicentre study involving 168 specimens.* Histopathology, 2010. **56**(4): p. 472-80.

373. Arnould, L., et al., *Agreement between chromogenic in situ hybridisation (CISH) and FISH in the determination of HER2 status in breast cancer.* Br J Cancer, 2003. **88**(10): p. 1587-91.

374. Tubbs, R.R., et al., *Discrepancies in clinical laboratory testing of eligibility for trastuzumab therapy: apparent immunohistochemical false-positives do not get the message.* J Clin Oncol, 2001. **19**(10): p. 2714-21.

375. Zhao, J., et al., *Determination of HER2 gene amplification by chromogenic in situ hybridization (CISH) in archival breast carcinoma.* Mod Pathol, 2002. **15**(6): p. 657-65.

376. Bartlett, J.M., F.M. Campbell, and E.A. Mallon, *Determination of HER2 amplification by in situ hybridization: when should chromosome 17 also be determined?* Am J Clin Pathol, 2008. **130**(6): p. 920-6.

377. Sapino, A., et al., *Which breast carcinomas need HER-2/neu gene study after immunohistochemical analysis? Results of combined use of antibodies against different c-erbB2 protein domains.* Histopathology, 2003. **43**(4): p. 354-62.

378. Malicka-Durczak, A., K. Korski, and M. Ibbs, *Comparison of in situ hybridization methods for the assessment of HER-2/neu gene amplification status in breast cancer using a tissue microarray.* Rep Pract Oncol Radiother, 2012. **17**(1): p. 44-9.

379. Jourdan, F., et al., *Tissue microarray technology: validation in colorectal carcinoma and analysis of p53, hMLH1,*

and hMSH2 immunohistochemical expression. Virchows Arch, 2003. **443**(2): p. 115-21.

380. Camp, R.L., L.A. Charette, and D.L. Rimm, *Validation of tissue microarray technology in breast carcinoma.* Lab Invest, 2000. **80**(12): p. 1943-9.

381. Mulrane, L., W.M. Gallagher, and D.P. O'Connor, *Assessment of Significance of Novel Proteins in Breast Cancer Using Tissue Microarray Technology.* Methods Mol Biol, 2017. **1501**: p. 311-325.

382. Claus, E.B., et al., *Pathobiologic findings in DCIS of the breast: morphologic features, angiogenesis, HER-2/neu and hormone receptors.* Exp Mol Pathol, 2001. **70**(3): p. 303-16.

383. DiGiovanna, M.P., et al., *Active signaling by HER-2/neu in a subpopulation of HER-2/neu-overexpressing ductal carcinoma in situ: clinicopathological correlates.* Cancer Res, 2002. **62**(22): p. 6667-73.

384. Latta, E.K., et al., *The role of HER2/neu overexpression/amplification in the progression of ductal carcinoma in situ to invasive carcinoma of the breast.* Mod Pathol, 2002. **15**(12): p. 1318-25.

385. Han, K., et al., *Expression of HER2neu in ductal carcinoma in situ is associated with local recurrence.* Clin Oncol (R Coll Radiol), 2012. **24**(3): p. 183-9.

386. Millis, R.R., L.G. Bobrow, and D.M. Barnes, *Immunohistochemical evaluation of biological markers in mammary carcinoma in situ: correlation with morphological features and recently proposed schemes for histological classification.* Breast, 1996. **14**(6).

387. Rohilla, M., et al., *Prediction of heterogeneity in breast cancer immunophenotype at ductal carcinoma in situ stage?* J Cancer Res Ther, 2016. **12**(4): p. 1249-1256.

388. Burkhardt, L., et al., *Gene amplification in ductal carcinoma in situ of the breast.* Breast Cancer Res Treat, 2010. **123**(3): p. 757-65.

389. Kim, J.Y., et al., *Predictors of Recurrent Ductal Carcinoma In Situ after Breast-Conserving Surgery.* J Breast Cancer, 2016. **19**(2): p. 185-90.

390. Joerger, M., B. Thurlimann, and J. Huober, *Small HER2-positive, node-negative breast cancer: who should receive systemic adjuvant treatment?* Ann Oncol, 2011. **22**(1): p. 17-23.

391. Park, K., et al., *HER2 status in pure ductal carcinoma in situ and in the intraductal and invasive components of invasive ductal carcinoma determined by fluorescence in situ hybridization and immunohistochemistry.* Histopathology, 2006. **48**(6): p. 702-7.

392. Rom, J., et al., *Association of HER2 Overexpression and Prognosis in Small (T1N0) Primary Breast Cancers.* Breast Care (Basel), 2013. **8**(3): p. 208-14.

393. Hoque, A., et al., *Her-2/neu gene amplification in ductal carcinoma in situ of the breast.* Cancer Epidemiol Biomarkers Prev, 2002. **11**(6): p. 587-90.

394. Mylonas, I., et al., *Expression of Her2/neu, steroid receptors (ER and PR), Ki67 and p53 in invasive mammary ductal carcinoma associated with ductal carcinoma In Situ (DCIS) Versus invasive breast cancer alone.* Anticancer Res, 2005. **25**(3a): p. 1719-23.

395. Muggerud, A.A., et al., *Molecular diversity in ductal carcinoma in situ (DCIS) and early invasive breast cancer.* Mol Oncol, 2010. **4**(4): p. 357-68.

396. Adams, S., et al., *Prognostic value of tumor-infiltrating lymphocytes in triple-negative breast cancers from two phase III randomized adjuvant breast cancer trials: ECOG 2197 and ECOG 1199.* J Clin Oncol, 2014. **32**(27): p. 2959-66.

397. Ibrahim, E.M., et al., *The prognostic value of tumor-infiltrating lymphocytes in triple-negative breast cancer: a meta-analysis.* Breast Cancer Res Treat, 2014. **148**(3): p. 467-76.

398. Pruneri, G., et al., *The prevalence and clinical relevance of tumor-infiltrating lymphocytes (TILs) in ductal carcinoma in situ of the breast.* Annals of oncology : official journal of the European Society for Medical Oncology, 2017. **28**(2): p. 321-328.

399. Dieci, M.V., et al., *Update on tumor-infiltrating lymphocytes (TILs) in breast cancer, including recommendations to assess TILs in residual disease after neoadjuvant therapy and in carcinoma in situ: A report of the International Immuno-Oncology Biomarker Working Group on Breast Cancer.* Semin Cancer Biol, 2018. **52**(Pt 2): p. 16-25.

400. Hendry, S., et al., *Assessing Tumor-infiltrating Lymphocytes in Solid Tumors: A Practical Review for Pathologists and Proposal for a Standardized Method From the International Immunooncology Biomarkers Working Group: Part 1: Assessing the Host Immune Response, TILs in Invasive Breast Carcinoma and Ductal Carcinoma In Situ, Metastatic Tumor Deposits and Areas for Further Research.* Adv Anat Pathol, 2017. **24**(5): p. 235-251.

401. Man, Y.G., et al., *Tumor-infiltrating immune cells promoting tumor invasion and metastasis: existing theories.* J Cancer, 2013. **4**(1): p. 84-95.

402. Artacho-Cordón, A., et al., *Tumor microenvironment and breast cancer progression: A complex scenario.* Cancer Biology and Therapy, 2012. **13**: p. 4-35.

403. Schreiber, R.D., L.J. Old, and M.J. Smyth, *Cancer immunoediting: integrating immunity's roles in cancer suppression and promotion.* Science, 2011. **331**(6024): p. 1565-70.

404. Emens, L.A., *Breast cancer immunobiology driving immunotherapy: vaccines and immune checkpoint blockade*, in *Expert review of anticancer therapy*. 2012. p. 1597-1611.

405. Cruz-merino, L.D., et al., *New Insights into the Role of the Immune Microenvironment in Breast Carcinoma.* 2013. **2013**.

406. Nelson, B.H., *CD20+ B cells: the other tumor-infiltrating lymphocytes.* (1550-6606 (Electronic)).

407. Keir, M.E., et al., *Tissue expression of PD-L1 mediates peripheral T cell tolerance.* J Exp Med, 2006. **203**(4): p. 883-95.

408. Wang, X., et al., *PD-L1 expression in human cancers and its association with clinical outcomes.* Onco Targets Ther, 2016. **9**: p. 5023-39.

409. Topalian, S.L., et al., *Safety, activity, and immune correlates of anti-PD-1 antibody in cancer.* N Engl J Med, 2012. **366**(26): p. 2443-54.

410. Campbell, M.J., et al., *Characterizing the immune microenvironment in high-risk ductal carcinoma in situ of the breast.* Breast Cancer Res Treat, 2017. **161**(1): p. 17-28.

411. Toss, M.S., et al., *Prognostic significance of tumor-infiltrating lymphocytes in ductal carcinoma in situ of the breast.* Mod Pathol, 2018. **31**(8): p. 1226-1236.

412. Kader, T., et al., *Copy number analysis by low coverage whole genome sequencing using ultra low-input DNA from formalin-fixed paraffin embedded tumor tissue.* Genome Med, 2016. **8**(1): p. 121.

413. Van der Auwera, G.A., et al., *From FastQ data to high confidence variant calls: the Genome Analysis Toolkit best practices pipeline.* Curr Protoc Bioinformatics, 2013. **43**: p. 11.10.1-11.10.33.

414. Rimmer, A., et al., *Integrating mapping-, assembly- and haplotype-based approaches for calling variants in clinical sequencing applications.* Nat Genet, 2014. **46**(8): p. 912-918.

415. Koboldt, D.C., et al., *VarScan 2: somatic mutation and copy number alteration discovery in cancer by exome sequencing.* Genome Res, 2012. **22**(3): p. 568-76.

416. McLaren, W., et al., *The Ensembl Variant Effect Predictor.* Genome Biol, 2016. **17**(1): p. 122.

417. Lek, M., et al., *Analysis of protein-coding genetic variation in 60,706 humans.* Nature, 2016. **536**(7616): p. 285-91.

418. Auton, A., et al., *A global reference for human genetic variation.* Nature, 2015. **526**(7571): p. 68-74.

419. Kuilman, T., et al., *CopywriteR: DNA copy number detection from off-target sequence data.* Genome Biol, 2015. **16**: p. 49.

420. Boeva, V., et al., *Control-FREEC: a tool for assessing copy number and allelic content using next-generation sequencing data.* Bioinformatics, 2012. **28**(3): p. 423-5.

421. Rathore, A.S., et al., *CD3+, CD4+ & CD8+ tumour infiltrating lymphocytes (TILs) are predictors of favourable*

survival outcome in infiltrating ductal carcinoma of breast. Indian J Med Res, 2014. **140**(3): p. 361-9.

422. Lee, N., et al., *Tumour-infiltrating lymphocytes in melanoma prognosis and cancer immunotherapy.* Pathology, 2016. **48**(2): p. 177-87.

423. Furnival, C., *Ductal carcinoma in situ of the breast: present and future.* ANZ J Surg, 2006. **76**(1-2): p. 4-5.

424. Kong, I., et al., *Age at diagnosis predicts local recurrence in women treated with breast-conserving surgery and postoperative radiation therapy for ductal carcinoma in situ: a population-based outcomes analysis.* Curr Oncol, 2014. **21**(1): p. e96-e104.

425. Kerlikowske, K., et al., *Characteristics associated with recurrence among women with ductal carcinoma in situ treated by lumpectomy.* J Natl Cancer Inst, 2003. **95**(22): p. 1692-702.

426. Stallard, S., et al., *Ductal carcinoma in situ of the breast -- among factors predicting for recurrence, distance from the nipple is important.* Eur J Surg Oncol, 2001. **27**(4): p. 373-7.

427. Mechera, R., C.T. Viehl, and D. Oertli, *Factors predicting in-breast tumor recurrence after breast-conserving surgery.* Breast Cancer Res Treat, 2009. **116**(1): p. 171-7.

428. Gannot, G., et al., *Increase in immune cell infiltration with progression of oral epithelium from hyperkeratosis to dysplasia and carcinoma.* Br J Cancer, 2002. **86**(9): p. 1444-8.

429. Hiraoka, N., et al., *Prevalence of FOXP3+ regulatory T cells increases during the progression of pancreatic ductal adenocarcinoma and its premalignant lesions.* Clin Cancer Res, 2006. **12**(18): p. 5423-34.

430. Jiang, B., et al., *Tumor-infiltrating immune cells: triggers for tumor capsule disruption and tumor progression?* Int J Med Sci, 2013. **10**(5): p. 475-97.

431. Doebar, S.C., et al., *Ductal carcinoma in situ diagnosed by breast needle biopsy: Predictors of invasion in the excision specimen.* Breast, 2016. **27**: p. 15-21.

432. Lee, A.H., et al., *Different patterns of inflammation and prognosis in invasive carcinoma of the breast.* Histopathology, 2006. **48**(6): p. 692-701.

433. Kristensen, V.N., et al., *Integrated molecular profiles of invasive breast tumors and ductal carcinoma in situ (DCIS) reveal differential vascular and interleukin signaling.* Proc Natl Acad Sci U S A, 2012. **109**(8): p. 2802-7.

434. Miligy, I., et al., *Prognostic significance of tumour infiltrating B lymphocytes in breast ductal carcinoma in situ.* 2017: p. 1-11.

435. Mahmoud, S.M.A., et al., *An evaluation of the clinical significance of FOXP3 + infiltrating cells in human breast cancer.* 2011: p. 99-108.

436. Bates, G.J., et al., *Quantification of Regulatory T Cells Enables the Identification of High-Risk Breast Cancer Patients and Those at Risk of Late Relapse.* 2018. **24**: p. 5373-5380.

437. Lal, A., et al., *FOXP3-positive regulatory T lymphocytes and epithelial FOXP3 expression in synchronous normal , ductal carcinoma in situ , and invasive cancer of the breast.* 2013: p. 381-390.

438. Gil Del Alcazar, C.R., et al., *Immune Escape in Breast Cancer During In Situ to Invasive Carcinoma Transition.* Cancer Discov, 2017. **7**(10): p. 1098-1115.

439. Chen, X.Y., et al., *Prognostic role of immune infiltrates in breast ductal carcinoma in situ.* Breast Cancer Res Treat, 2019. **177**(1): p. 17-27.

440. Merlo, A., et al., *FOXP3 expression and overall survival in breast cancer.* J Clin Oncol, 2009. **27**(11): p. 1746-52.

441. Curiel, T.J., et al., *Specific recruitment of regulatory T cells in ovarian carcinoma fosters immune privilege and predicts reduced survival.* Nat Med, 2004. **10**(9): p. 942-9.

442. Dermani, F.K., et al., *PD-1/PD-L1 immune checkpoint: Potential target for cancer therapy.* J Cell Physiol, 2019. **234**(2): p. 1313-1325.

443. Nomi, T., et al., *Clinical Significance and Therapeutic Potential of the Programmed Death-1 Ligand/Programmed Death-1 Pathway in Human Pancreatic Cancer.* Clinical Cancer Research, 2007. **13**(7): p. 2151.

444. Thompson, R.H., et al., *Costimulatory B7-H1 in renal cell carcinoma patients: Indicator of tumor aggressiveness and potential therapeutic target.* (0027-8424 (Print)).

445. Trella, E., et al., *Expression of programmed death ligand 1 (PD-L1) is associated with poor prognosis in human breast cancer.* 2014. **1**.

446. Thompson, R.H., et al., *PD-1 is expressed by tumor-infiltrating immune cells and is associated with poor outcome for patients with renal cell carcinoma.* (1078-0432 (Print)).

447. Muenst, S., et al., *The presence of programmed death 1 (PD-1)-positive tumor-infiltrating lymphocytes is associated*

with poor prognosis in human breast cancer, in *Breast cancer research and treatment*. 2013.

448. Schalper, K.A., et al., *In Situ Tumor PD-L1 mRNA Expression Is Associated with Increased TILs and Better Outcome in Breast Carcinomas.* 2014: p. 2773-2783.

449. Freeman, G.J., et al., *Engagement of the PD-1 immunoinhibitory receptor by a novel B7 family member leads to negative regulation of lymphocyte activation.* (0022-1007 (Print)).

450. Mittendorf, E.A., et al., *PD-L1 Expression in Triple-Negative Breast Cancer.* Cancer Immunology Research, 2014. **2**: p. 361-370.

451. Man, Y.G. and Q.X. Sang, *The significance of focal myoepithelial cell layer disruptions in human breast tumor invasion: a paradigm shift from the "protease-centered" hypothesis.* Exp Cell Res, 2004. **301**(2): p. 103-18.

452. Ma, X.-J., et al., *Gene expression profiling of the tumor microenvironment during breast cancer progression.* Breast Cancer Research, 2009. **11**: p. R7.

453. Loi, S., et al., *Tumor infiltrating lymphocytes are prognostic in triple negative breast cancer and predictive for trastuzumab benefit in early breast cancer: results from the*

FinHER trial. Annals of oncology : official journal of the European Society for Medical Oncology, 2014. **25**: p. 1544-1550.

454. Triner, D. and Y.M. Shah, *Hypoxia-inducible factors: a central link between inflammation and cancer.* J Clin Invest, 2016. **126**(10): p. 3689-3698.

455. Chouaib, S., V. Umansky, and C. Kieda, *The role of hypoxia in shaping the recruitment of proangiogenic and immunosuppressive cells in the tumor microenvironment.* Contemp Oncol (Pozn), 2018. **22**(1a): p. 7-13.

456. Sitkovsky, M. and D. Lukashev, *Regulation of immune cells by local-tissue oxygen tension: HIF1 alpha and adenosine receptors.* Nat Rev Immunol, 2005. **5**(9): p. 712-21.

457. Kastenhuber, E.R. and S.W. Lowe, *Putting p53 in Context.* Cell, 2017. **170**(6): p. 1062-1078.

458. Doebar, S.C., et al., *Progression of ductal carcinoma in situ to invasive breast cancer: comparative genomic sequencing.* Virchows Arch, 2018.

459. Damonte, P., et al., *Mammary carcinoma behavior is programmed in the precancer stem cell.* Breast Cancer Res, 2008. **10**(3): p. R50.

460. Gao, Y., et al., *Genetic changes at specific stages of breast cancer progression detected by comparative genomic hybridization.* J Mol Med (Berl), 2009. **87**(2): p. 145-52.

461. Schnitt, S.J., *The transition from ductal carcinoma in situ to invasive breast cancer: the other side of the coin.* Breast Cancer Res, 2009. **11**(1): p. 101.

462. Page, D.L., et al., *Intraductal carcinoma of the breast: follow-up after biopsy only.* Cancer, 1982. **49**(4): p. 751-8.

463. Page, D.L., et al., *Continued local recurrence of carcinoma 15-25 years after a diagnosis of low grade ductal carcinoma in situ of the breast treated only by biopsy.* Cancer, 1995. **76**(7): p. 1197-200.

464. Xu, K., et al., *The fibroblast Tiam1-osteopontin pathway modulates breast cancer invasion and metastasis.* Breast Cancer Res, 2016. **18**(1): p. 14.

465. Kitamura, M., et al., *Progression Potential of Ductal Carcinoma in situ Assessed by Genomic Copy Number Profiling.* Pathobiology, 2018: p. 1-10.

466. Sonoda, A., et al., *Genetic lineages of undifferentiated-type gastric carcinomas analysed by unsupervised clustering of genomic DNA microarray data.* BMC Med Genomics, 2013. **6**: p. 25.

467. Petridis, C., et al., *Genetic predisposition to ductal carcinoma in situ of the breast.* Breast Cancer Res, 2016. **18**(1): p. 22.

468. Hernandez, L., et al., *Genomic and mutational profiling of ductal carcinomas in situ and matched adjacent invasive breast cancers reveals intra-tumour genetic heterogeneity and clonal selection.* J Pathol, 2012. **227**(1): p. 42-52.

469. Turner, N.C. and J.S. Reis-Filho, *Genetic heterogeneity and cancer drug resistance.* Lancet Oncol, 2012. **13**(4): p. e178-85.

470. Yap, T.A., et al., *Intratumor heterogeneity: seeing the wood for the trees.* Sci Transl Med, 2012. **4**(127): p. 127ps10.

471. Baylin, S.B., et al., *Aberrant patterns of DNA methylation, chromatin formation and gene expression in cancer.* Hum Mol Genet, 2001. **10**(7): p. 687-92.

472. Castro, N.P., et al., *Evidence that molecular changes in cells occur before morphological alterations during the progression of breast ductal carcinoma.* Breast Cancer Res, 2008. **10**(5): p. R87.

473. Shiga, K., et al., *Cancer-Associated Fibroblasts: Their Characteristics and Their Roles in Tumor Growth.* Cancers (Basel), 2015. **7**(4): p. 2443-58.

474. Hwang, E.S., et al., *Association between breast density and subsequent breast cancer following treatment for ductal carcinoma in situ.* Cancer Epidemiol Biomarkers Prev, 2007. **16**(12): p. 2587-93.

475. Acerbi, I., et al., *Human breast cancer invasion and aggression correlates with ECM stiffening and immune cell infiltration.* Integr Biol (Camb), 2015. **7**(10): p. 1120-34.

476. Dossus, L. and P.R. Benusiglio, *Lobular breast cancer: incidence and genetic and non-genetic risk factors.* Breast Cancer Res, 2015. **17**: p. 37.

477. Boudreau, A., L.J. van't Veer, and M.J. Bissell, *An "elite hacker": breast tumors exploit the normal microenvironment program to instruct their progression and biological diversity.* Cell Adh Migr, 2012. **6**(3): p. 236-48.

478. Bissell, M.J. and W.C. Hines, *Why don't we get more cancer? A proposed role of the microenvironment in restraining cancer progression.* Nat Med, 2011. **17**.

479. Coussens, L.M., B. Fingleton, and L.M. Matrisian, *Matrix metalloproteinase inhibitors and cancer: trials and tribulations.* Science, 2002. **295**(5564): p. 2387-92.

480. Myllyharju, J., *Prolyl 4-hydroxylases, the key enzymes of collagen biosynthesis.* Matrix Biol, 2003. **22**.

481. Chang, K.P., et al., *Identification of PRDX4 and P4HA2 as metastasis-associated proteins in oral cavity squamous cell carcinoma by comparative tissue proteomics of microdissected specimens using iTRAQ technology.* J Proteome Res, 2011. **10**(11): p. 4935-47.

482. Jarząb, B., et al., *Gene Expression Profile of Papillary Thyroid Cancer: Sources of Variability and Diagnostic Implications.* Cancer Research, 2005. **65**(4): p. 1587-1597.

483. Gilkes, D.M., et al., *Collagen prolyl hydroxylases are essential for breast cancer metastasis.* Cancer Res, 2013. **73**(11): p. 3285-96.

484. Pan, P.W., et al., *Profiling and comparative analysis of glycoproteins in Hs578BST and Hs578T and investigation of prolyl 4-hydroxylase alpha polypeptide II expression and influence in breast cancer cells.* Biochemistry (Mosc), 2012. **77**(5): p. 539-45.

485. Xiong, G., et al., *Prolyl-4-hydroxylase α subunit 2 promotes breast cancer progression and metastasis by regulating collagen deposition.* BMC Cancer, 2014. **14**(1): p. 1.

486. Timur, Z.K., S. Akyildiz Demir, and V. Seyrantepe, *Lysosomal Cathepsin A Plays a Significant Role in the*

Processing of Endogenous Bioactive Peptides. Frontiers in molecular biosciences, 2016. **3**: p. 68-68.

487. Kolli, N. and S.C. Garman, *Proteolytic activation of human cathepsin A.* The Journal of biological chemistry, 2014. **289**(17): p. 11592-11600.

488. Jackman, H.L., et al., *A peptidase in human platelets that deamidates tachykinins. Probable identity with the lysosomal "protective protein".* J Biol Chem, 1990. **265**(19): p. 11265-72.

489. Hanna, W.L., et al., *Dominant chymotrypsin-like esterase activity in human lymphocyte granules is mediated by the serine carboxypeptidase called cathepsin A-like protective protein.* Journal of immunology (Baltimore, Md. : 1950), 1994. **153**(10): p. 4663-4672.

490. Villadangos, J.A., *Presentation of antigens by MHC class II molecules: getting the most out of them.* Mol Immunol, 2001. **38**(5): p. 329-46.

491. Kozlowski, L., M.Z. Wojtukiewicz, and H. Ostrowska, *Cathepsin A activity in primary and metastatic human melanocytic tumors.* Arch Dermatol Res, 2000. **292**(2-3): p. 68-71.

492. Duivenvoorden, H.M., et al., *Myoepithelial cell-specific expression of stefin A as a suppressor of early breast cancer invasion.* J Pathol, 2017. **243**(4): p. 496-509.

493. Rochefort, H., *Cathepsin D in breast cancer: a tissue marker associated with metastasis.* Eur J Cancer, 1992. **28a**(11): p. 1780-3.

494. Duffy, M.J., *The role of proteolytic enzymes in cancer invasion and metastasis.* Clin Exp Metastasis, 1992. **10**(3): p. 145-55.

495. Yasuda, Y., et al., *Cathepsin V, a novel and potent elastolytic activity expressed in activated macrophages.* J Biol Chem, 2004. **279**(35): p. 36761-70.

496. Adachi, W., et al., *Isolation and characterization of human cathepsin V: a major proteinase in corneal epithelium.* Invest Ophthalmol Vis Sci, 1998. **39**(10): p. 1789-96.

497. Bromme, D., et al., *Human cathepsin V functional expression, tissue distribution, electrostatic surface potential, enzymatic characterization, and chromosomal localization.* Biochemistry, 1999. **38**(8): p. 2377-85.

498. Tolosa, E., et al., *Cathepsin V is involved in the degradation of invariant chain in human thymus and is*

overexpressed in myasthenia gravis. J Clin Invest, 2003. **112**(4): p. 517-26.

499. Viken, M.K., et al., *Polymorphisms in the cathepsin L2 (CTSL2) gene show association with type 1 diabetes and early-onset myasthenia gravis.* Hum Immunol, 2007. **68**(9): p. 748-55.

500. Jing, J., et al., *Elevated CTSL2 expression is associated with an adverse prognosis in hepatocellular carcinoma.* Int J Clin Exp Pathol, 2018. **11**(8): p. 4035-4043.

501. Guo, P., et al., *Expression of legumain correlates with prognosis and metastasis in gastric carcinoma.* PLoS One, 2013. **8**(9): p. e73090.

502. Chen, J., et al., *Activation of progelatinase A by mammalian legumain, a recently discovered cysteine proteinase.* Biol. Chem., 2001. **382**(5): p. 777-783.

503. Mai, J., et al., *Human procathepsin B interacts with the annexin II tetramer on the surface of tumor cells.* The Journal of biological chemistry, 2000. **275**(17): p. 12806.

504. Stern, L., et al., *A novel antitumor prodrug platform designed to be cleaved by the endoprotease legumain.* Bioconjugate chemistry, 2009. **20**(3): p. 500.

505. Zhen, Y., et al., *Clinicopathologic significance of legumain overexpression in cancer: a systematic review and meta-analysis.* Sci Rep, 2015. **5**: p. 16599.

506. Wu, M., et al., *Legumain protein as a potential predictive biomarker for Asian patients with breast carcinoma.* Asian Pac J Cancer Prev, 2014. **15**(24): p. 10773-7.

507. Murthy, R.V., et al., *Legumain expression in relation to clinicopathologic and biological variables in colorectal cancer.* Clin Cancer Res, 2005. **11**(6): p. 2293-9.

508. Ohno, Y., et al., *Association of legumain expression pattern with prostate cancer invasiveness and aggressiveness.* World J Urol, 2013. **31**(2): p. 359-64.

509. Prockop, D.J., et al., *The biosynthesis of collagen and its disorders (first of two parts).* N Engl J Med, 1979. **301**(1): p. 13-23.

510. Bernard, M., et al., *Cloning and sequencing of pro-alpha 1 (XI) collagen cDNA demonstrates that type XI belongs to the fibrillar class of collagens and reveals that the expression of the gene is not restricted to cartilagenous tissue.* J Biol Chem, 1988. **263**(32): p. 17159-66.

511. Tompson, S.W., et al., *Fibrochondrogenesis results from mutations in the COL11A1 type XI collagen gene.* Am J Hum Genet, 2010. **87**(5): p. 708-12.

512. Khalifa, O., et al., *A recessive form of Marshall syndrome is caused by a mutation in the COL11A1 gene.* J Med Genet, 2012. **49**(4): p. 246-8.

513. Shen, L., et al., *COL11A1 is overexpressed in recurrent non-small cell lung cancer and promotes cell proliferation, migration, invasion and drug resistance.* Oncol Rep, 2016. **36**(2): p. 877-85.

514. Wu, Y.H., et al., *COL11A1 promotes tumor progression and predicts poor clinical outcome in ovarian cancer.* Oncogene, 2014. **33**(26): p. 3432-40.

515. Sok, J.C., et al., *Collagen type XI alpha1 facilitates head and neck squamous cell cancer growth and invasion.* Br J Cancer, 2013. **109**(12): p. 3049-56.

516. Erkan, M., et al., *Organ-, inflammation- and cancer specific transcriptional fingerprints of pancreatic and hepatic stellate cells.* Mol Cancer, 2010. **9**: p. 88.

517. Zhao, Y., et al., *A potential role of collagens expression in distinguishing between premalignant and malignant lesions in stomach.* Anat Rec (Hoboken), 2009. **292**(5): p. 692-700.

518. Fischer, H., et al., *Colorectal carcinogenesis is associated with stromal expression of COL11A1 and COL5A2.* Carcinogenesis, 2001. **22**(6): p. 875-8.

519. Kleman, J.P., et al., *The human rhabdomyosarcoma cell line A204 lays down a highly insoluble matrix composed mainly of alpha 1 type-XI and alpha 2 type-V collagen chains.* Eur J Biochem, 1992. **210**(1): p. 329-35.

520. Ellsworth, R.E., et al., *A gene expression signature that defines breast cancer metastases.* Clin Exp Metastasis, 2009. **26**(3): p. 205-13.

521. Freire, J., et al., *Collagen, type XI, alpha 1: an accurate marker for differential diagnosis of breast carcinoma invasiveness in core needle biopsies.* Pathol Res Pract, 2014. **210**(12): p. 879-84.

522. Freire, J., et al., *Collagen Type XI Alpha 1 Expression in Intraductal Papillomas Predicts Malignant Recurrence.* Biomed Res Int, 2015. **2015**: p. 812027.

523. Vargas, A.C., et al., *Gene expression profiling of tumour epithelial and stromal compartments during breast cancer progression.* Breast Cancer Res Treat, 2012. **135**(1): p. 153-65.

524. Miligy, I.M., et al., *Thioredoxin-interacting protein is an independent risk stratifier for breast ductal carcinoma in situ.* Mod Pathol, 2018.

525. Ohara, M., et al., *Prognostic value of Ki67 and p53 in patients with estrogen receptor-positive and human epidermal growth factor receptor 2-negative breast cancer: Validation of the cut-off value of the Ki67 labeling index as a predictive factor.* Mol Clin Oncol, 2016. **4**(4): p. 648-654.

526. Fulawka, L. and A. Halon, *Ki-67 evaluation in breast cancer: The daily diagnostic practice.* Indian J Pathol Microbiol, 2017. **60**(2): p. 177-184.

527. Kobel, M., et al., *Optimized p53 immunohistochemistry is an accurate predictor of TP53 mutation in ovarian carcinoma.* J Pathol Clin Res, 2016. **2**(4): p. 247-258.

528. van der Groep, P., et al., *HIF-1alpha overexpression in ductal carcinoma in situ of the breast in BRCA1 and BRCA2 mutation carriers.* PLoS One, 2013. **8**(2): p. e56055.

529. Curtis, C., et al., *The genomic and transcriptomic architecture of 2,000 breast tumours reveals novel subgroups.* Nature, 2012. **486**(7403): p. 346-52.

530. Allegra, C.J., et al., *National Institutes of Health State-of-the-Science Conference statement: Diagnosis and*

Management of Ductal Carcinoma In Situ September 22-24, 2009. J Natl Cancer Inst, 2010. **102**(3): p. 161-9.

531. Gauthier, M.L., et al., *Abrogated response to cellular stress identifies DCIS associated with subsequent tumor events and defines basal-like breast tumors.* Cancer Cell, 2007. **12**(5): p. 479-91.

532. Bartova, M., et al., *COX-2, p16 and Ki67 expression in DCIS, microinvasive and early invasive breast carcinoma with extensive intraductal component.* Bratisl Lek Listy, 2014. **115**(7): p. 445-51.

533. Perez, A.A., et al., *Co-Expression of p16, Ki67 and COX-2 Is Associated with Basal Phenotype in High-Grade Ductal Carcinoma In Situ of the Breast.* J Histochem Cytochem, 2015. **63**(6): p. 408-16.

534. Raldow, A.C., et al., *Cost Effectiveness of the Oncotype DX DCIS Score for Guiding Treatment of Patients With Ductal Carcinoma In Situ.* J Clin Oncol, 2016.

535. Gorringe, K.L. and S.B. Fox, *Ductal Carcinoma In Situ Biology, Biomarkers, and Diagnosis.* Frontiers in Oncology, 2017. **7**: p. 248.

536. Hu, M., et al., *Regulation of in situ to invasive breast carcinoma transition.* Cancer Cell, 2008. **13**(5): p. 394-406.

537. Unsworth, A., R. Anderson, and K. Britt, *Stromal fibroblasts and the immune microenvironment: partners in mammary gland biology and pathology?* J Mammary Gland Biol Neoplasia, 2014. **19**(2): p. 169-82.

538. Liu, S., et al., *Breast cancer stem cells are regulated by mesenchymal stem cells through cytokine networks.* Cancer Res, 2011. **71**(2): p. 614-24.

539. Rattigan, Y., et al., *Interleukin 6 mediated recruitment of mesenchymal stem cells to the hypoxic tumor milieu.* Exp Cell Res, 2010. **316**(20): p. 3417-24.

540. Hanahan, D. and R.A. Weinberg, *Hallmarks of cancer: the next generation.* Cell, 2011. **144**(5): p. 646-74.

541. Karnoub, A.E., et al., *Mesenchymal stem cells within tumour stroma promote breast cancer metastasis.* Nature, 2007. **449**(7162): p. 557-63.

542. Lu, P., V.M. Weaver, and Z. Werb, *The extracellular matrix: a dynamic niche in cancer progression.* J Cell Biol, 2012. **196**(4): p. 395-406.

543. Raymond, K., et al., *Adhesion within the stem cell niches.* Curr Opin Cell Biol, 2009. **21**(5): p. 623-9.

544. Shen, Q., et al., *Adult SVZ stem cells lie in a vascular niche: a quantitative analysis of niche cell-cell interactions.* Cell Stem Cell, 2008. **3**(3): p. 289-300.

545. Feigin, M.E. and S.K. Muthuswamy, *Polarity proteins regulate mammalian cell-cell junctions and cancer pathogenesis.* Curr Opin Cell Biol, 2009. **21**(5): p. 694-700.

546. Condeelis, J. and J.E. Segall, *Intravital imaging of cell movement in tumours.* Nat Rev Cancer, 2003. **3**(12): p. 921-30.

547. Wang, W., et al., *Single cell behavior in metastatic primary mammary tumors correlated with gene expression patterns revealed by molecular profiling.* Cancer Res, 2002. **62**(21): p. 6278-88.

548. Provenzano, P.P., K.W. Eliceiri, and P.J. Keely, *Shining new light on 3D cell motility and the metastatic process.* Trends Cell Biol, 2009. **19**(11): p. 638-48.

549. Keely, P.J., et al., *Alteration of collagen-dependent adhesion, motility, and morphogenesis by the expression of antisense alpha 2 integrin mRNA in mammary cells.* J Cell Sci, 1995. **108 (Pt 2)**: p. 595-607.

550. Gilkes, D.M., et al., *Hypoxia-inducible factor 1 (HIF-1) promotes extracellular matrix remodeling under hypoxic*

conditions by inducing P4HA1, P4HA2, and PLOD2 expression in fibroblasts. J Biol Chem, 2013. **288**.

551. Semenza, G.L., *The hypoxic tumor microenvironment: A driving force for breast cancer progression.* Biochim Biophys Acta, 2016. **1863**(3): p. 382-91.

552. Jedeszko, C. and B.F. Sloane, *Cysteine cathepsins in human cancer.* Biol Chem, 2004. **385**(11): p. 1017-27.

553. Sun, T., et al., *Expression profile of cathepsins indicates the potential of cathepsins B and D as prognostic factors in breast cancer patients.* Oncology letters, 2016. **11**(1): p. 575-583.

554. Willemsen, R., et al., *Immunoelectron microscopical localization of lysosomal beta-galactosidase and its precursor forms in normal and mutant human fibroblasts.* Eur J Cell Biol, 1986. **40**(1): p. 9-15.

555. Nanba, E., et al., *Galactosialidosis: a direct evidence that a 46-kilodalton protein restores deficient enzyme activities in fibroblasts.* Biochem Biophys Res Commun, 1987. **144**(1): p. 138-42.

556. Kon, M., et al., *Chaperone-mediated autophagy is required for tumor growth.* Sci Transl Med, 2011. **3**(109): p. 109ra117.

557. Jackman, H.L., et al., *Plasma membrane-bound and lysosomal peptidases in human alveolar macrophages.* Am J Respir Cell Mol Biol, 1995. **13**(2): p. 196-204.

558. Liu, C., et al., *Overexpression of legumain in tumors is significant for invasion/metastasis and a candidate enzymatic target for prodrug therapy.* Cancer Res, 2003. **63**(11): p. 2957-64.

559. Wang, L., et al., *Legumain: a biomarker for diagnosis and prognosis of human ovarian cancer.* J Cell Biochem, 2012. **113**(8): p. 2679-86.

560. Luo, Y., et al., *Targeting tumor-associated macrophages as a novel strategy against breast cancer.* J Clin Invest, 2006. **116**(8): p. 2132-2141.

561. Dall, E. and H. Brandstetter, *Activation of legumain involves proteolytic and conformational events, resulting in a context- and substrate-dependent activity profile.* Acta Crystallogr Sect F Struct Biol Cryst Commun, 2012. **68**(Pt 1): p. 24-31.

562. Cheng, T., et al., *Cystatin M/E is a high affinity inhibitor of cathepsin V and cathepsin L by a reactive site that is distinct from the legumain-binding site. A novel clue for the role of cystatin M/E in epidermal cornification.* J Biol Chem, 2006. **281**(23): p. 15893-9.

563. Chen, J.M., et al., *Activation of progelatinase A by mammalian legumain, a recently discovered cysteine proteinase.* Biol Chem, 2001. **382**(5): p. 777-83.

564. Andrade, V., et al., *Nucleoplasmic calcium regulates cell proliferation through legumain.* J Hepatol, 2011. **55**(3): p. 626-635.

565. Halsted, K.C., et al., *Collagen alpha1(XI) in normal and malignant breast tissue.* Mod Pathol, 2008. **21**(10): p. 1246-54.

566. Bosman, F.T. and I. Stamenkovic, *Functional structure and composition of the extracellular matrix.* J Pathol, 2003. **200**(4): p. 423-8.

567. Doebar, S.C., et al., *Progression of ductal carcinoma in situ to invasive breast cancer: comparative genomic sequencing.* Virchows Arch, 2019. **474**(2): p. 247-251.

568. Barker, H.E., et al., *The tumour microenvironment after radiotherapy: mechanisms of resistance and recurrence.* Nature reviews. Cancer, 2015. **15**(7): p. 409-425.

569. Park, C.C., et al., *High mammographic breast density is independent predictor of local but not distant recurrence after lumpectomy and radiotherapy for invasive breast cancer.* Int J Radiat Oncol Biol Phys, 2009. **73**(1): p. 75-9.

570. Bos, R., et al., *Hypoxia-inducible factor-1alpha is associated with angiogenesis, and expression of bFGF, PDGF-BB, and EGFR in invasive breast cancer.* Histopathology, 2005. **46**(1): p. 31-6.

571. Toss, M.S., et al., *Prolyl-4-hydroxylase Alpha subunit 2 (P4HA2) expression is a predictor of poor outcome in breast ductal carcinoma in situ (DCIS).* Br J Cancer, 2018. **119**(12): p. 1518-1526.

572. Wolf, K., et al., *Multi-step pericellular proteolysis controls the transition from individual to collective cancer cell invasion.* Nat Cell Biol, 2007. **9**(8): p. 893-904.

573. Motrescu, E.R., et al., *Matrix metalloproteinase-11/stromelysin-3 exhibits collagenolytic function against collagen VI under normal and malignant conditions.* Oncogene, 2008. **27**(49): p. 6347-55.

574. Fang, M., et al., *Collagen as a double-edged sword in tumor progression.* Tumour Biol, 2014. **35**(4): p. 2871-82.

575. Provenzano, P.P., et al., *Collagen density promotes mammary tumor initiation and progression.* BMC Med, 2008. **6**: p. 11.

576. Conklin, M.W., et al., *Collagen Alignment as a Predictor of Recurrence after Ductal Carcinoma In Situ.* Cancer Epidemiol Biomarkers Prev, 2018. **27**(2): p. 138-145.

577. Drifka, C.R., et al., *Periductal stromal collagen topology of pancreatic ductal adenocarcinoma differs from that of normal and chronic pancreatitis.* Mod Pathol, 2015. **28**(11): p. 1470-80.

578. Vogel, B., et al., *Determination of collagen content within picrosirius red stained paraffin-embedded tissue sections using fluorescence microscopy.* MethodsX, 2015. **2**: p. 124-34.

579. Whittaker, P., et al., *Quantitative assessment of myocardial collagen with picrosirius red staining and circularly polarized light.* Basic Res Cardiol, 1994. **89**(5): p. 397-410.

580. Liu, Z., et al., *3D organizational mapping of collagen fibers elucidates matrix remodeling in a hormone-sensitive 3D breast tissue model.* Biomaterials, 2018. **179**: p. 96-108.

581. Silverstein, M.J., et al., *A prognostic index for ductal carcinoma in situ of the breast.* Cancer, 1996. **77**(11): p. 2267-74.

582. Hu, G., L. Li, and W. Xu, *Extracellular matrix in mammary gland development and breast cancer progression.* Frontiers in Laboratory Medicine, 2017. **1**(1): p. 36-39.

583. Wolfe, J.N., *Risk for breast cancer development determined by mammographic parenchymal pattern.* Cancer, 1976. **37**(5): p. 2486-92.

584. Maragoudakis, M.E., et al., *Basement membrane biosynthesis as a target for developing inhibitors of angiogenesis with anti-tumor properties.* Kidney Int, 1993. **43**(1): p. 147-50.

585. Kothari, C., et al., *Identification of a gene signature for different stages of breast cancer development that could be used for early diagnosis and specific therapy.* Oncotarget, 2018. **9**(100): p. 37407-37420.

586. Bavik, C., et al., *The gene expression program of prostate fibroblast senescence modulates neoplastic epithelial cell proliferation through paracrine mechanisms.* Cancer Res, 2006. **66**(2): p. 794-802.

587. Roth, J.M., et al., *Inhibition of experimental metastasis by targeting the HUIV26 cryptic epitope in collagen.* Am J Pathol, 2006. **168**(5): p. 1576-86.

588. Meyaard, L., *The inhibitory collagen receptor LAIR-1 (CD305).* J Leukoc Biol, 2008. **83**(4): p. 799-803.

589. Provenzano, P.P., et al., *Intrinsic fibroblast-mediated remodeling of damaged collagenous matrices in vivo.* Matrix Biol, 2005. **23**(8): p. 543-55.

590. Suresh, S., *Biomechanics and biophysics of cancer cells.* Acta Biomater, 2007. **3**(4): p. 413-38.

591. Paszek, M.J. and V.M. Weaver, *The tension mounts: mechanics meets morphogenesis and malignancy.* J Mammary Gland Biol Neoplasia, 2004. **9**(4): p. 325-42.

592. Paszek, M.J., et al., *Tensional homeostasis and the malignant phenotype.* Cancer Cell, 2005. **8**(3): p. 241-54.

593. Netti, P.A., et al., *Role of extracellular matrix assembly in interstitial transport in solid tumors.* Cancer Res, 2000. **60**(9): p. 2497-503.

594. Silverstein, M.J. and M.D. Lagios, *Treatment selection for patients with ductal carcinoma in situ (DCIS) of the breast using the University of Southern California/Van Nuys (USC/VNPI) prognostic index.* Breast J, 2015. **21**(2): p. 127-32.

595. Godinho, S.A. and D. Pellman, *Causes and consequences of centrosome abnormalities in cancer.* Philos Trans R Soc Lond B Biol Sci, 2014. **369**(1650).

596. McBride, M., P.C. Rida, and R. Aneja, *Turning the headlights on novel cancer biomarkers: Inspection of mechanics underlying intratumor heterogeneity.* Mol Aspects Med, 2015. **45**: p. 3-13.

597. Nigg, E.A., *Centrosome duplication: of rules and licenses.* Trends Cell Biol, 2007. **17**(5): p. 215-21.

598. Chan, J.Y., *A clinical overview of centrosome amplification in human cancers.* Int J Biol Sci, 2011. **7**(8): p. 1122-44.

599. D'Assoro, A.B., W.L. Lingle, and J.L. Salisbury, *Centrosome amplification and the development of cancer.* Oncogene, 2002. **21**(40): p. 6146-53.

600. Fukasawa, K., *Centrosome amplification, chromosome instability and cancer development.* Cancer Lett, 2005. **230**(1): p. 6-19.

601. Mittal, K. and R. Aneja, *Spotlighting the hypoxia-centrosome amplification axis.* Med Res Rev, 2020.

602. Mittal, K., et al., *Amplified centrosomes and mitotic index display poor concordance between patient tumors and cultured cancer cells.* Scientific Reports, 2017. **7**(1): p. 43984.

603. Lopes, C.A.M., et al., *Centrosome amplification arises before neoplasia and increases upon p53 loss in tumorigenesis.* J Cell Biol, 2018. **217**(7): p. 2353-2363.

604. Guo, H.Q., et al., *Analysis of the cellular centrosome in fine-needle aspirations of the breast.* Breast Cancer Res, 2007. **9**(4): p. R48.

605. D'Assoro, A.B., et al., *Amplified centrosomes in breast cancer: a potential indicator of tumor aggressiveness.* Breast Cancer Res Treat, 2002. **75**(1): p. 25-34.

606. Ogden, A., P.C. Rida, and R. Aneja, *Heading off with the herd: how cancer cells might maneuver supernumerary centrosomes for directional migration.* Cancer Metastasis Rev, 2013. **32**(1-2): p. 269-87.

607. Pannu, V., et al., *Rampant centrosome amplification underlies more aggressive disease course of triple negative breast cancers.* Oncotarget, 2015. **6**(12): p. 10487-97.

608. Denu, R.A., et al., *Centrosome amplification induces high grade features and is prognostic of worse outcomes in breast cancer.* BMC Cancer, 2016. **16**: p. 47.

609. Cho, W.K., et al., *Adjuvant radiation therapy in small ductal carcinoma in situ.* Breast, 2018. **43**: p. 55-58.

610. Sagara, Y., et al., *Patient Prognostic Score and Associations With Survival Improvement Offered by Radiotherapy After Breast-Conserving Surgery for Ductal Carcinoma In Situ: A Population-Based Longitudinal Cohort Study.* J Clin Oncol, 2016. **34**(11): p. 1190-6.

611. Rakovitch, E., et al., *Refined estimates of local recurrence risks by DCIS score adjusting for clinicopathological features: a combined analysis of ECOG-ACRIN E5194 and Ontario DCIS cohort studies.* Breast Cancer Res Treat, 2018. **169**(2): p. 359-369.

612. Di Cesare, P., et al., *The Relationships between HER2 Overexpression and DCIS Characteristics.* Breast J, 2017. **23**(3): p. 307-314.

613. Lesurf, R., et al., *Molecular Features of Subtype-Specific Progression from Ductal Carcinoma In Situ to Invasive Breast Cancer.* Cell Rep, 2016. **16**(4): p. 1166-79.

614. Finn, R.S., *Targeting Src in breast cancer.* Ann Oncol, 2008. **19**(8): p. 1379-86.

615. Nie, W., et al., *TXNIP interaction with the Her-1/2 pathway contributes to overall survival in breast cancer.* Oncotarget, 2015. **6**(5): p. 3003-12.

616. Mustafa, R.E., et al., *Evaluating the Risk of Upstaging HER2-Positive DCIS to Invasive Breast Cancer.* Ann Surg Oncol, 2017. **24**(10): p. 2999-3003.

617. McShane, L.M., et al., *REporting recommendations for tumor MARKer prognostic studies (REMARK).* Breast Cancer Res Treat, 2006. **100**(2): p. 229-35.

618. Sauerbrei, W., et al., *Reporting Recommendations for Tumor Marker Prognostic Studies (REMARK): An Abridged Explanation and Elaboration.* J Natl Cancer Inst, 2018. **110**(8): p. 803-811.

619. Oyama, T., et al., *The effects of fixation, processing and evaluation criteria on immunohistochemical detection of hormone receptors in breast cancer.* Breast Cancer, 2007. **14**(2): p. 182-8.